DANUBE ADRIA ASSOCIATION FOR AUTOMATION & MANUFACTURING
DAAAM International Vienna
DAAAM Baltic

PROCEEDINGS

OF THE 9TH INTERNATIONAL CONFERENCE OF DAAAM BALTIC
INDUSTRIAL ENGINEERING
24-26th APRIL 2014, TALLINN, ESTONIA

ORGANIZED UNDER THE AUSPICES
OF DAAAM INTERNATIONAL VIENNA

in co-operation with:
BALTECH Consortium
Estonian Academy of Sciences
Federation of Estonian Engineering Industry
Association of Estonian Mechanical Engineers
Innovative Manufacturing Engineering Systems Competence Centre IMECC
Tallinn City Enterprise Board
Eesti Energia
MECTORY

EDITED BY
T. OTTO

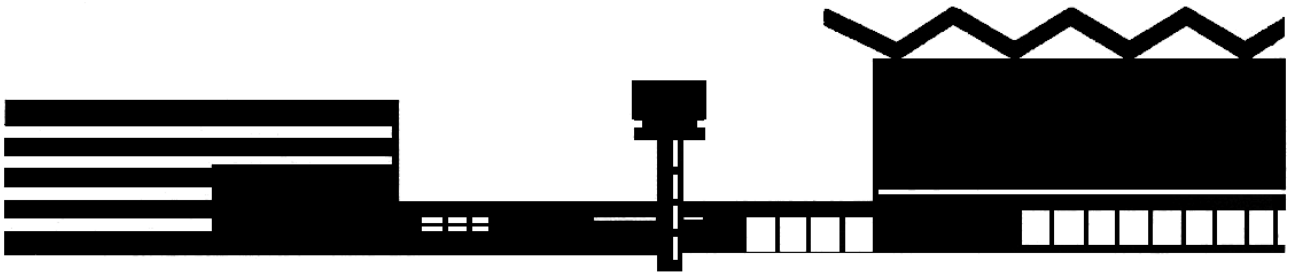

TALLINN UNIVERSITY OF TECHNOLOGY

The Chairman of DAAAM Baltic Scientific Committee expresses special personal thanks to Professor Branko Katalinic for encouraging to organise and for advising during the preparation of the conference. Also special thanks for the support during the organising the conference to the following persons: A. Hermaste, R. Kulbas, K. Karjust.

EDITORS' NOTE

This publication was reproduced by the photo process, using the soft copies supplied by their authors. The editor and the DAAAM Baltic are not responsible either for the statements or for the opinion expressed in this publication.

Proceedings of 9th International Conference of DAAAM Baltic INDUSTRIAL ENGINEERING
Editor T. Otto
24–26 April 2014, Tallinn, Estonia

ISBN 978-9949-23-620-6
ISSN 2346-612X

Layout & Design copyright: B. Katalinic, R. Kyttner, T. Otto

Additional copies can be obtained from the publisher:
DAAAM Baltic, Tallinn University of Technology, Ehitajate tee 5, 19086 Tallinn
Estonia

Phone: +372 620 3257
Fax: +372 620 3250
E-mail: daaam@ttu.ee

Foreword

Over the past years, DAAAM-Baltic has been an international forum for researchers and engineers to present their research results in the areas of industrial engineering, manufacturing and automation. It provides an avenue for discussion and exchange of new ideas addressing new techniques and methods for product development and manufacturing engineering.

This DAAAM-Baltic-2014 conference in the DAAAM-Baltic Conference series will continue the mission of the DAAAM, which is to give for young and active scientists of the Baltic Sea region an opportunity to introduce their works and find partners.

The main idea of starting DAAAM-Baltic meetings was to organize regional conferences of DAAAM International events (DAAAM – Danube-Adrian Association for Automation & Manufacturing). DAAAM International is association for international scientific and academic cooperation in the fields of intelligent automation and modern production. This year DAAAM International celebrates its 25th anniversary and is proved to be sustainable network and family of scientists, scholars, students and engineers. DAAAM-Baltic is organized in Estonia every second year. Estonia has been represented as a member of International DAAAM Committee since 1994. In year 2014 we have 9th Conference of DAAAM-Baltic and 18 years of history of publishing the Proceedings. The Proceedings of DAAAM-Baltic have been included in Web of Science of Thomson Reuters since 2004.

The Conference addresses the issues of managing globalization in the internet age. Its scope ranges from design engineering, production engineering, production management, materials engineering to mechatronics and system engineering, with an emphasis on innovative practices, to ensure that the focus of the conference is on learning, networking and generating new ideas. We emphasize importance of European initiatives towards Factories of the Future and technology platform Manufuture, and hope to give our contribution by bringing scientists, entrepreneurs and industry specialists together for exchange of future visions based on scientific research and case studies.

In 2014 we received over hundred proposals from 13 countries. About ninety participants from 11 countries take part in the Conference. All proposals have been carefully selected and full texts of presentations peer-reviewed to address key topics of the conference. About sixty papers were selected to present orally. Part of proposals were rejected on the grounds of either not being appropriate for the areas that DAAAM-Baltic covers or being of rather narrow and specialized nature.

We wish to thank all authors, referees, members of the Organizing Committee and Program Committee, as well as supportive organizations for their efforts which made this conference possible. DAAAM-Baltic would not be possible without contributions from members of the scientific community of the Baltic-Sea region.

We look forward to a very exciting and stimulating conference, and hope that you will join us in next DAAAM-Baltic in 2016.

Tallinn; April 2014

Tauno Otto
Chairman of the Scientific Committee DAAAM-Baltic 2014

Steering Committee

Tauno Otto - *chair*

Kristo Karjust

Rein Küttner

Aadu Paist

Leo Mõtus

Mart Tamre

Renno Veinthal

International Program Committee

M.Airila (FIN)

J.Balic (SLV)

F.Boór (HUN)

S.Bockus (LIT)

J.Brnić (CRO)

M.Eerme (EST)

L.Hagman (SWE)

H.Jähn (GER)

T.Karaulova (EST)

B.Katalinic (AUT)

T.Kjellberg (SWE)

K. Korbe (EST)

P.Kulu (EST)

P.Kuosmanen (FIN)

T. Kübarsepp (EST)

J. Lavrentjev (EST)

J.Martikainen (FIN)

W. Maass (GER)

V.Mironov (LAT)

S. Ottosson (SWE)

J.-G.Persson (SWE)

P.Pukk (SWE)

J.Riives (EST)

A.Schulz (LAT)

F.Sergejev (EST)

A.Siirde (EST)

T. Torims (LAT)

M.Veveris (UK)

A.Voet (BEL)

A.Zawada-Tomkiewicz (POL)

CONTENTS

I DESIGN ENGINEERING 9

Aan A., Heinloo M., Allas J.
Design of a radial cam for the cam-follower mechanism…….…….11

Harf, M. & Grossschmidt, G.
Multi-pole modeling and intelligent simulation of control valves of fluid power systems (1).17

Harf, M. & Grossschmidt, G.
Multi-pole modeling and intelligent simulation of control valves of fluid power systems (2).23

Kabral, R., Auriemma, F., Knutsson, M., Åbom, M.
A new type of compact silencer for high frequency noise……....29

Koskinen, H.; Isomaa, T.; Lehto, J.; Stark, T.; Salmela, J.; Liukkonen, J.; Kiviluoma, P.; Widmaier, T. & Kuosmanen, P.
Device for continuous cellulose yarn drying and forming……36

Källo, R.; Eerme, M. & Reedik, V.
On chaos control in hierarchical multi-agent systems……..…41

Luppin, J. & Auriemma, F.
Acoustic studies on porous sintered powder metals……..……47

Moon, G. & Park, S.
Balancing completion times for multi-vehicle delivery with time various vehicle speeds…...53

Pabut, O., Allikas, G., Herranen, H., Talalaev, R. & Vene, K.
Load sensitivity analysis of a large diameter permanent magnet generator for wind turbines.59

Shvartsman, B.S., Majak, J. & Kirs, M.
Numerical method for stability analysis of functionally graded columns……...…65

Sivitski, A; Põdra, P.
Finite element method and its usable applications in wear models design……...71

II PRODUCTION ENGINEERING & MANAGEMENT.....77

Bashkite, V.& Karaulova, T.
Green framework development for used industrial equipment…….....79

Eiskop, T.; Snatkin, A. & Kõrgesaar, K., Søren, J.
Development and application of a holistic production monitoring system……...85

Hermaste, A.; Riives, J.; Sonk, K., Sarkans, M.
Design principles of flexible manufacturing systems……...92

Kaganski, S.; Paavel, M. & Lavin, J.
Selecting key performance indicators with support of enterprise analyze model…….97

Katalinic, B.; Kukushkin, I. & Haskovic, D.
Bionic assembly system cloud: functions, information flow and behavior……103

Kromanis, A.; Pikurs, G., Muiznieks G., Kravalis K. & Gutakovskis, V.
Design of internally cooled tools for dry cutting…….……109

Kuhi, K.; Kõrbe Kaare, K. & Koppel, O.
Performance measurement in network industries: example of power distribution and road networks……..……115

Kõrgesaar, K.; Eiskop, T. & Snatkin, A.
Overview about person monitoring possibilities in workplace performance evaluation……...121

Lavin, J., Riives, J., Kaganski S; Paavel, M.
The model for improving the company's productivity and efficiency……127

Leemet, T.; Allas, J. & Adoberg, E.
Tool wear investigations by direct and indirect methods in end milling……133

Lemmik, R.; Otto, T.; Küttner, R.
Knowledge management systems for service desk environment……....139

Maceika, A. & Jančiauskas, B.
Engineering change and organizational behaviour of the enterprise……..145

Maceika, A. & Zabielavičienė, I.
Development of innovation team creative abilities…….151

Paavel, M.; Kaganski, S.; Lavin, J.; Sonk, K.
Optimizing PLM implementation from vision to real implementation in Estonian SME`s...157

Polyantchikov, I.; Shevtshenko, E.
Partner selection criteria for virtual organization forming……..163

Randmaa, M. & Otto, T
Centeric business: an in-depth analysis of one case company.....169

Rimašauskas, M.; Rimašauskienė, R.; Balevičius, G.
Development of the intelligent forecasting model for manufacturing cost estimation in polyjet process…….175

Sahno, J. & Shevtshenko, E.
Quality improvement methodologies for continuous improvement of production processes and product quality and their evolution…….181

Sarkans, M.; Pikner, H.; Sell, R.; Sonk, K.
Energy efficiency monitoring system for technology mapping driven by fof concept……...187

Serg, R.; Aruväli, T.; Otto, T.
Power consumption based online condition monitoring in milling machine ……193

Snatkin, A.; Eiskop, T. & Kõrgesaar, K.
Production monitoring system concept development…….198

Sonk, K.; Sarkans, M.; Hermaste, A. & Paavel, M.
Optimizing production technology selection process with functional requirements……..204

Tammaru, T. & Kiitam, A.
Customisation of excellence models and assessment schemes, considering sectoral specifics……...207

Vaezipour, A.; Kangilaski, T
Business and it alignment in enterprise considering the partner network's constraints…….213

III MECHATRONICS AND SYSTEM ENGINEERING.....219

Dhoska, K.; Kübarsepp, T. & Hermaste, A.
Uncertainty evaluation of angle measurements by using 3d coordinate measuring machine.221

Gorordo, I.; Mäntylä, J.; Popkov, A.; Saastamoinen, J.; Sepponen, R.; Kiviluoma, P. & Kuosmanen, P.
Device for muscle coordination improvement……226

Hemming, B., T. Widmaier, I. Palosuo, V-P Esala, P. Laukkanen, L. Lillepea, K. Simson, D. Brabandt, J. Haikio
Traceability for roundness measurements of rolls - European Metrology Research Programme, project No. IND62.....232

Karu, M.; Henno, E.; Veskimeister, V.; Tamre, M.; Juurma, M.; Hiiemaa, M.
Technology for rapid foot support making……...…238

Kulderknup, E.; Pandis, A.
Autocorrelation influence by geometrical deviations measurement……...243

Lees, Ü.; Hudjakov, R.; Tamre, M.
Development of virtual reality interface for remote robot control……...…247

Liukkonen, J.; Knuuttila, P.; Nguyen, T.; Ingale, S.; Kiviluoma, P.; Korkiala-Tanttu, L. & Kuosmanen, P.
Automation of an excavator boom movement in 3-dimensions…….251

Logins, A.; Torims, T.; Gutierrez Rubert, S. C.; Rosado Castellano, P.; Torres, R.
Influence of the high-speed milling strategy on 3d surface roughness parameters……256

Lohani, V.; Sandström, V.; Shekh, A.; Teinonen, H.; Korkolainen, P.; Kiviluoma, P.; Widmaier, T.; Sandler, N. and Kuosmanen, P.
Development of dual head inkjet dispenser for pharmaceuticals……262

Praks, T.; Romot, C.; Sillat, M.-L.; Soomänd, K.; Hiiemaa, M.; Tamre, M. & Juurmaa, M.
Gesture controlled human machine interface for future machines……..…..268

Põlder, A.; Juurma, M.; Tamre, M.
Optimal use of spectral information for waste paper detection……..273

Rayat, H.; Pulkkinen, V.; Johansson, M.; Nyfors, V.; Partanen, J.; Kiviluoma, P. & Kuosmanen, P.
The effects of minituarisation of projection stereolithography equipment on printing quality……..278

Roosileht, I.; Lentsius, M.; Mets, O; Heering, S; Hiiemaa, M. & Tamre, M.
Automated inspection system of electric motor stator and rotor sheets…….…….283

Shvarts, D., Tamre, M.
Bulk material volume estimation method and system for logistic applications……..…289

Simson, K.; Lillepea, L.; Hemming, B.; Widmaier, T.
Traceable in-process dimensional measurement – European Metrology Research Programme, project No. IND62…….……..295

Zhigailov, S. ;. Musalimov, V.; Aryassov, G.
Design of experimental stand for human gait imitation…….300

Vauhkonen, N.; Liljeström, J.; Maharjan, D.; Mahat, C.; Sainio, P.; Kiviluoma, P. & Kuosmanen, P.
Electrification of excavator…….…….305

Vu Triu Minh
Predictive control for controlling and driving autonomous vehicles……..311

Vuorio, J.; Nikkilä, V.; Teivastenaho, V.; Peltola, J.; Partanen, J.; Kiviluoma, P. & Kuosmanen P.
Additive manufacturing with uv light cured……...317

IV MATERIALS ENGINEERING.....323

Aruniit, A., Kers, J.; Krumme, A. & Peetsalu, P.
Particle size and proportion influence to impact properties of particulate polymer composite….325

Dobris, J.; Luts, A.; Meier, P. & Kers, J.
Analysis of the twisted and fluted birch dowel joints…….331

Drozdova, M., Ivanov, R., Aghayan, M., Hussainova, I., Dong, M., Rodríguez, M. A.
Fabrication of alumina nanocomposites reinforced by a novel type of alumina nanofiber and graphene coated alumina nanofiber……337

Gonca, V.; Polukoshko, S.
Theoretical and experimental studies of stiffness properties of laminated elastomeric structures…….342

Ivanov, R., Aghayan, M., Hussainova, I., Petrov, M.
Graphene coated alumina nanofibers as zirconia reinforcement……348

Kommel, L. Pardis, N. & Kimmari, E.
Micromechanical properties and electrical conductivity of CU and CU-0.7WT% CR alloy.354

Kovalska, A.; Eiduks, M.
Investigation of composite repair of pipelines with volumetric surface defect……..360

Kängsepp K., Poltimäe, T., Liimand K., Kallakas H., Süld, T.-M., Repeshova I., Goljandin D., Kers, J.
The effect of wood flour fraction size on the properties of wood-plastic composites……366

Kärner, K.; Elomaa, M. & Kallavus, U.
Lignin and outer cell wall removal from aspen pulp fibres by using supercritical CO_2 extraction……..…372

Lille, H.; Ryabchikov, A.; Lind, L.; Sergejev, F.; Adoberg, E. & Peetsalu, P.
On determination of residual stresses in some pvd coatings by the curvature method……...378

Pirso, J.; Juhani, K.; Tarraste, M.; Viljus, M. & Letunovitš, S.
The effect of VC, TIC and CR3C2 on the microstructure and properties of WC-15CO hardmetals fabricated by the reactive sintering……...383

Priss, J.; Klevtsov, I. & Dedov, A., Antonov, M
Investigation of boiler materials with relation to corrosion and wear: review……...389

Ridzon, M.; Bilik, J. & Kosik, M.
Effect of reducing on the mechanical properties of cold drawn tubes……..……..395

Saar, K.; Kers, J.; Luga, Ü. & Reiska, A.
Mechanical properties of connecting fittings for plywood furniture……..399

I DESIGN ENGINEERING

9th International DAAAM Baltic Conference
"INDUSTRIAL ENGINEERING"
24 – 26th April 2014, Tallinn, Estonia

DESIGN OF A RADIAL CAM FOR THE CAM-FOLLOWER MECHANISM

Aan A., Heinloo M., Allas J.

Abstract: *This paper presents a method for designing of a radial cam on the worksheet of Mathcad including the calculation of follower's displacements, values of its velocities and accelerations, the optimization of the contour of a cam by choosing the eccentricity of follower and the radius of base circle of cam and the simulation of the working process of the cam mechanism. The optimal coordinates the contour of the cam were calculated. Finally, practical information for exporting cam contour data from Mathcad environment in data format necessary for CNC part program generation is discussed, considering CNC controllers using the most widespread ISO type program format and contouring with linear interpolation.*
Key words: cam mechanism, design, optimization, visualization.

1. INTRODUCTION

Cam mechanisms consisting of only two elements, the cam as mechanical driver element and the follower as driven element, are widely used in technical applications due to reduced constructive complexity. Any functional motion of follower due to the movement of cam can be produced [1].
Cam mechanism can be classified in several ways: by follower motion (translating, rotating), by type of cam (radial, cylindrical), by joint closure, by follower (flat, rolling, mushroom), by cam curves [2].
Alaci et al. [3] have showed some aspects concerning the design of cam mechanisms with oscillating flat faced follower by using computer software. They also have generated figures of cam profiles as envelopes of the straight lines paths on the Mathcad worksheet.
In the study of Ahmet Shala and Ramë Likaj [4] an analytical method for synthesis of cam mechanism is presented. They use Mathcad for displacement, velocity and acceleration calculation of the follower.
This paper presents the method and the results of numerical analysis of the radial cam, with translating follower on the worksheet of Mathcad. The visualization of the cam and follower and the simulation of working process of cam-follower mechanism are presented. The coordinates of the visualized cam contour coordinates can be used in the CNC milling machine for the production of the real cam.

2. MATERIALS AND METHODS

2.1 The scheme of cam-follower mechanism

Fig 1 shows the scheme of a cam-follower mechanism

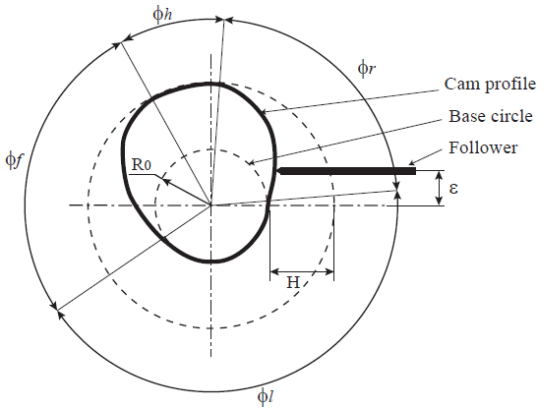

Fig. 1. The scheme cam mechanism, where ϕ_f is the rise angle, ϕ_h – the high dwell angle, ϕ_f – the fall angle, ϕ_l – the low dwell angle, ε – the eccentricity, H – the follower stroke

Let us consider the cam-follower mechanism by the following parameters: the rise angle of the follower $\phi_r = 60°$; the high dwell angle of the follower $\phi_h = 60°$; the fall (return) angle of the follower $\phi_f = 60°$; the stroke of the follower $H = 0.005m$; the offset of the follower ε; the radius of the base circle of the cam R_0; the number of positions of cam in computations $N = 360$; angular velocity of the cam $\omega = 10rad/s$.

2.2 Follower's displacement

According to [2] let us describe the displacement of the follower in the rise by the law:

$$s_1(\varphi) = H\left[35\left(\frac{\varphi}{\phi_r}\right)^4 - 84\left(\frac{\varphi}{\phi_r}\right)^5 + 70\left(\frac{\varphi}{\phi_r}\right)^6 - 20\left(\frac{\varphi}{\phi_r}\right)^7\right] \quad (1)$$

and in the fall by the law

$$s_2(\varphi) = H - H\left[35\left(\frac{\varphi-\phi_r-\phi_h}{\phi_f}\right)^4 - 84\left(\frac{\varphi-\phi_r-\phi_h}{\phi_f}\right)^5 + 70\left(\frac{\varphi-\phi_r-\phi_h}{\phi_f}\right)^6 - 20\left(\frac{\varphi-\phi_r-\phi_h}{\phi_f}\right)^7\right]. \quad (2)$$

In (1), (2) φ is the rotation angle of a cam from the initial position.

The displacement of a follower in one cycle of cam's rotation can be determined by the following program on the worksheet of the Mathcad (Fig. 2)

$$s(\varphi) = \begin{cases} s_1(\varphi) & \text{if } 0 \le \varphi \le \phi_r \\ s_1(\phi_e) & \text{if } \phi_r < \varphi \le \phi_r + \phi_h \\ s_2(\varphi) & \text{if } \phi_r + \phi_h < \varphi \le \phi_r + \phi_h + \phi_f \\ 0 & \text{otherwise} \end{cases}$$

Fig. 2. Program for determination of the follower displacement

Accordingly to program (Fig. 2) we get follower displacement on fig. 3.

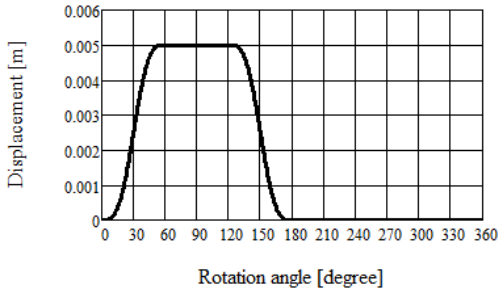

Fig. 3. The dependence of the displacement of the follower on rotation angle φ of the cam

2.3 Follower's velocity

The first derivative from equations (1) and (2) gives the velocity analogue functions:

$$v_1(\varphi) = \frac{d}{d\varphi}s_1(\varphi), \quad (3)$$

$$v_2(\varphi) = \frac{d}{d\varphi}s_2(\varphi). \quad (4)$$

The velocity analogue in one cycle of cam's motion can be determined by the program on the figure 4.

$$v(\varphi) = \begin{cases} v_1(\varphi) & \text{if } 0 \le \varphi \le \phi_r \\ 0 & \text{if } \phi_r < \varphi \le \phi_r + \phi_h \\ v_2(\varphi) & \text{if } \phi_r + \phi_h < \varphi \le \phi_r + \phi_h + \phi_f \\ 0 & \text{otherwise} \end{cases}$$

Fig. 4. Program for determination of the follower velocity analogue

The program in fig. 4 computes the analogue of the follower's velocity in the dependence on the rotation angle φ of the cam. To determine follower's real velocity (fig. 5) the velocity analogue were multiplied by the angular velocity ω of the cam.

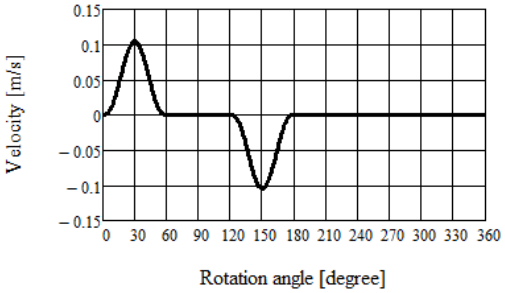

Fig. 5. The dependence of the follower velocity on the rotation angle φ of the cam

2.4 Follower's acceleration

The second derivative from equations (1) and (2) gives the acceleration analogue functions:

$$a_1(\varphi) = \frac{d^2}{d\varphi^2} s_1(\varphi), \qquad (5)$$

$$a_2(\varphi) = \frac{d^2}{d\varphi^2} s_2(\varphi). \qquad (6)$$

The acceleration analogue for one cycle of cam's motion can be determined by the program on the fig. 6.

$$a(\varphi) = \begin{cases} a_1(\varphi) \text{ if } 0 \le \varphi \le \phi_r \\ 0 \text{ if } \phi_r < \varphi \le \phi_r + \phi_h \\ a_2(\varphi) \text{ if } \phi_r + \phi_h < \varphi \le \phi_r + \phi_h + \phi_f \\ 0 \text{ otherwise} \end{cases}$$

Fig. 6. Program for determination of the follower acceleration analogue

The program in fig. 6 computes the follower's acceleration analogue in the dependence on the rotation angle φ of the cam. To determine follower's acceleration (fig. 7) the acceleration analogue were multiplied by the square of the cam angular velocity ω^2.

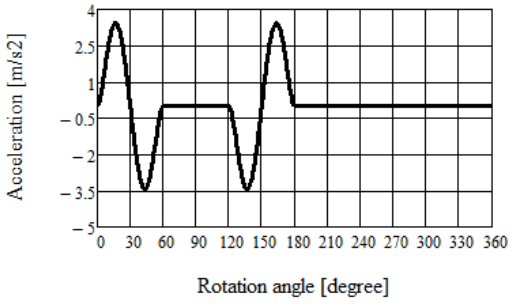

Fig. 7. The dependence of the follower acceleration on the rotation angle φ of the cam

2.5 Optimization of the eccentricity and the radius of the base circle

The pressure angle α (fig. 8) is one of the limiting criteria's for cam design. Accordingly to Norton [2] the pressure angle must be between 0 to ± 30 degrees. Pressure angle value can be adjusted by the values of the eccentricity ε and radius R_0 of base circle.

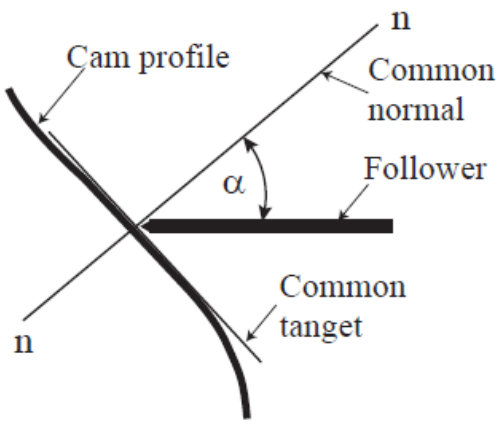

Fig. 8. The pressure angle α between the cam and the follower

According to [2] the pressure angle α of the cam determines the following formula:

$$\alpha(\varphi, R_0, \varepsilon) = arctan\left(\frac{v(\varphi)-\varepsilon}{s(\varphi)+\sqrt{R_0^2-\varepsilon^2}}\right). \quad (7)$$

Base circle radius and eccentricity cannot be solved conveniently directly. To find proper R_0 and ε Norton [2] suggest to use special cam design program Dynacam or some equation solvers such as Matlab, TKSolver or Mathcad.

To determine the radius of base circle R_0 and eccentricity ε let us formulate the following problem of optimization:

find such values for R_0 and ε that guarantee satisfaction of the restriction

$$\alpha(\varphi, R_0, \varepsilon) = \propto_e \qquad (8)$$

in the rise and the restriction

$$\alpha(\varphi, R_0, \varepsilon) = \propto_n \qquad (9)$$

in the fall.

With lower accuracy the solution of system of equations (8) and (9) can be obtained also by hand [2], changing the values of R_0 and ε from initial values step by step. Doing so it is useful to know that the change of value ε moves the graph of the function $\alpha(\varphi, R_0, \varepsilon)$ upwards or downwards without changing it shape and the change of value R_0 increases or decreases the external values of the function $\alpha(\varphi, R_0, \varepsilon)$. In such way the solution for system of equations (8) and (9) by low accuracy can be obtained relatively quickly satisfying the need of teaching process.

The solution method of high accuracy for the system of equations (8) and (9) with respect to R_0 and ε by the help of Mathcad will be developed in future.

Let us consider an example with the maximal value of the pressure angle $\alpha(\varphi, R_0, \varepsilon)$ $a_e = 20^o$ (in rise) and minimal value of the pressure angle $a_n = -24^o$ (in fall). Let´s take the initial values $R_0 = 20mm$ and $\varepsilon = 0mm$. In this case the curve of the function $\alpha(\varphi, R_0, \varepsilon)$ is presented in fig. 9, showing the pressure angle curve crossing the values of $a_e = 20^o$ and $a_n = -24^o$. This means that the system of equations (8) and (9) is not satisfied.

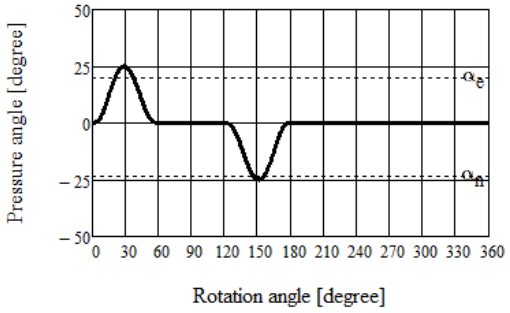

Fig. 9 Cam mechanism pressure angle, $R_0 = 20\text{mm}$ and $\varepsilon = 0$

By changing the values of R_0 and ε step by step one can visually observe the change of the graph of function $\alpha(\varphi, R_0, \varepsilon)$ and quickly obtain the position of this graph, shown in fig. 10. This means that the system of equations (8) and (9) is satisfied with some compromise of accuracy. The case in fig. 10 corresponds approximately to $R_0 = 31mm$ and $\varepsilon = -1.5mm$.

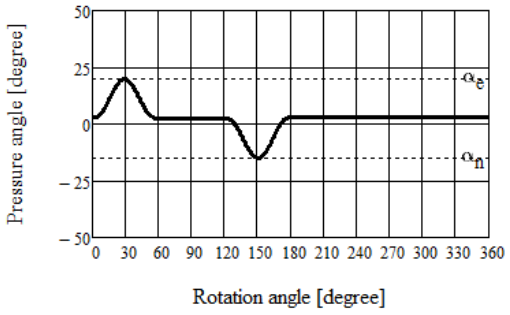

Fig. 10 Cam mechanism pressure angle, $R_0 = 31\text{mm}$ and $\varepsilon = -1.5\text{mm}$

2.6 Visualization of the cam and simulation of the working process of cam-follower mechanism

The polar coordinates $\beta(\varphi), R(\varphi)$ of contact point of the follower and the cam are

$$R(\varphi) = \sqrt{s(\varphi)^2 + R_0^2 + 2 \cdot s(\varphi)\sqrt{R_0^2 - \varepsilon^2}}, \quad (10)$$

$$\beta(\varphi) = \varphi - \left(\operatorname{asin}\left(\frac{\varepsilon}{R(\varphi)}\right) - \operatorname{asin}\left(\frac{\varepsilon}{R_0}\right)\right), \quad (11)$$

where $R(\varphi)$ is the polar radius and $\beta(\varphi)$ – the polar angle of the contour point in dependence of angle of cam's rotation φ.

To visualize the contour of the cam let us assume that the cam is not rotating but the follower rotates around the centre of the cam with angle of rotation φ. Then the contact point with polar coordinates $\beta(\varphi), R(\varphi)$ draws the contour of the cam. Fig. 11 visualizes the initial position of the cam in the case $R_0 = 31mm$ and $\varepsilon = -1.5mm$.

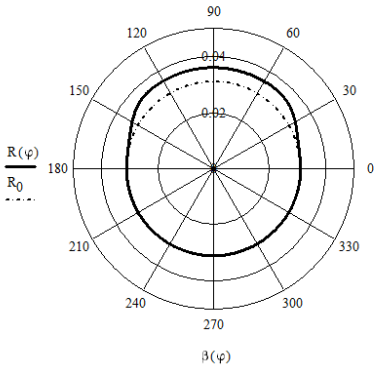

Fig. 11 Cam contour in the polar coordinates $\beta(\varphi), R(\varphi)$

The Cartesian coordinates of the cam contour at the initial position are

$$x(\varphi) = R(\varphi)\cos(\beta(\varphi)), \quad (12)$$

$$y(\varphi) = R(\varphi)\sin(\beta(\varphi)). \quad (13)$$

To simulate the working process of the cam-follower mechanism the cam in fig. 11 [5] is rotated by the angle $\theta = \omega t$, where ω is the angular velocity and t – the time. Equations

$$x_1(\varphi) = x(\varphi) \cdot G(\theta), \quad (14)$$

$$y(\varphi)_1 = y(\varphi) \cdot G(\theta), \quad (15)$$

where

$$G(\theta) = \begin{pmatrix} \cos\theta & \sin\theta \\ -\sin\theta & \cos\theta \end{pmatrix}$$

determine the contour of the cam, turned around the centre of cam by the angle θ counter clockwise.

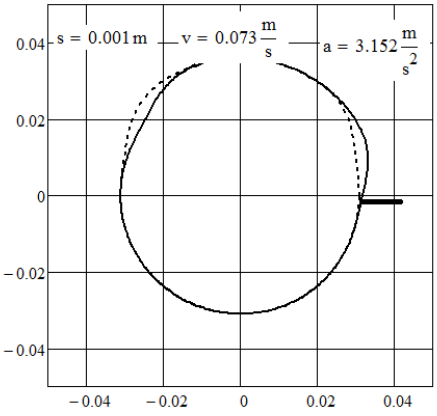

Fig. 12 A frame from video clip [5]

3. PRODUCTION OF CAM

Nowadays any part despite of its complicated shape can be machined on modern industrial CNC machine tools with geometrical accuracy of at least 15 microns, so the machining of the modelled geometrical shape of a cam can be accomplished quite easily with great precision. An ordinary radial cam can be produced in CNC machining centre by contour cutting with a square end mill of suitable type according to cam material and dimensions. Cam geometry points in Cartesian coordinates can be calculated with required accuracy according to equations (12) and (13) (fig. 13) by changing the angular increment of calculations.

x(φ) =		y(φ) =	
31	mm	0	mm
30.999		0.271	
30.995		0.541	
30.989		0.811	
30.981		1.082	
30.971		1.352	
30.958		1.622	
30.944		1.893	
...		...	

Fig. 13 Contour coordinates of optimal cam

Different geometrical interpolation techniques for connecting the calculated contour points of cam can be available and used in CNC machine tools depending on the machine tool control options. As discussed by Norton [2], circular and spline fitting interpolation techniques are superior to linear interpolation in terms of vibratory noise in acceleration measurements. Still, on most CNC controllers in everyday use only linear or circular tool movement interpolation is available, so the geometrical accuracy of a machined cam (so called "chordal deviation") compared to mathematical model must be regulated by selecting appropriate angular increment for contour points calculation.
Coordinate values on the fig. 13 can be exported from Mathcad to another different file formats (for example to Microsoft Excel or Notepad) for converting exported data into file format suitable for direct usage in CNC machine tool part program. Majority of CNC part programs are composed in the form of a simple ASCII text file. Widespread CNC controllers using ISO or similar program format accept the input of contour point values for linear interpolation in the form of successive lines of type
X…Y… ,
characters X and Y hereby representing the machine tool axes followed by numerical coordinate value, for example (numerical values taken from fig.13)
…
X30.989Y0.811
X30.981Y1.082
X30.971Y1.352 .

Coordinate output in showed format can be accomplished from Mathcad calculations.
As the cutting tool centre must be offset from cam contour by the radius value of the cutter, CNC controller's cutter radius compensation function must be used in process of machining. The optimal method for bringing the tool into cut for closed contours is to approach the contour tangentially, which helps to avoid contouring mistakes caused by tool deflection, so the tangent line direction for the starting point of

contour cutting must be known. Considering the fact the type of cam contour studied in this work is an arc between rotation angles φ=180...360, we can assume that the tangent line for contour point φ=0=360 is parallel to Y axis (fig. 14). As the machining of contour is started and finished in point φ=0, additional tool moves parallel to X and Y axis can be manually added to program for smooth tool transition into and out of the cut.

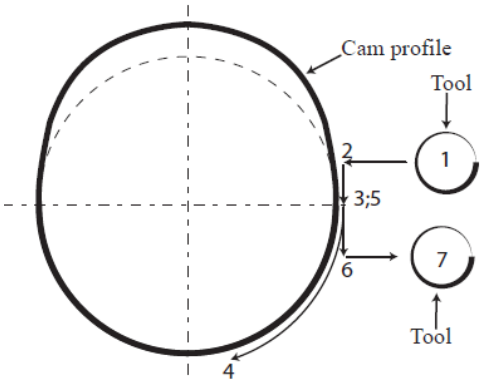

Fig. 14 Tool movement steps: 1 – initial position, 2 – beginning of contour start point tangent line, 3 – starting point of contour cutting, 4 - contour cutting, 5 – end point of contour cutting, 6 – end of contour end point tangent line, 7 – end position

In general the contours are milled using climb cutting, although conventional cutting may give better results in some special cases. The choice between climb and conventional cutting affects the machining direction of a contour, which are accordingly clockwise or counter clockwise for external contours. However, the choice between cutting direction can be easily taken into account while exporting coordinate data from Mathcad. Defining the rotation angle range φ to change clockwise (from 360 to 0 instead) results in contour point coordinates output in clockwise direction and vice versa.

4. CONCLUSION

1. The Computer Package Mathcad can be considered as a convenient tool for design of cams.
2. Mathcad allows the simulation of motion of virtual models of cam mechanisms.
3. Mathcad can be used to compute cam contour coordinates, which can be used for CNC part program.
4. The method presented in this paper can be used in the teaching process of engineering subjects and also by engineers in their work.

5. REFERENCES

1. Shin, J.-H., Kwon, S.-M. & Nam, H. A hybrid approach for cam shape design and profile machining of general plate cam mechanisms, *International Journal of Precision Engineering and Manufacturing.* 2010, **11**(3), 419-472.
2. Norton, R. L. *Cam design and manufacturing handbook.* 2009, Industrial Press Inc., new York.
3. Alaci, S., Ciornei, F. C., Amarandei, D., Filote, C., Patras-Ciceu, S., Prodas, D. *Some aspects regarding computer aided design of cam mechanism with flat face oscillating follower*. Fiability & Durability, 2011, **1**(7).
4. Shala, A., Likaj, R. *Analytical method for synthesis of cam mechanism*. International Journal of Current Engineering and Technology, 2013, **3**(2).
5. Aan, A. Simulation the working process of c*am-follower mechanism*. 2013. https://www.youtube.com/watch?v=c43JIq7-rvc

6. ADDITIONAL DATA

MSc (Eng Sc) Aan, Aare (author)
e-mail: aare.aan@emu.ee.
Dr (math) Heinloo, Mati (co-author)
e-mail: mati.heinloo@emu.ee.
MSc (Engn Sc) Allas, Jaanus (co-author)
e-mail: jaanus.allas@emu.ee.

Institute of Technology,
Estonian University of Life Sciences,
Kreutzwaldi 56, 51014, Tartu, Estonia

9th International DAAAM Baltic Conference
"INDUSTRIAL ENGINEERING"
24-26 April 2014, Tallinn, Estonia

MULTI-POLE MODELING AND INTELLIGENT SIMULATION OF CONTROL VALVES OF FLUID POWER SYSTEMS (PART 1)

Harf, M. & Grossschmidt, G.

Abstract: *Composing of multi-pole models and simulation of pressure control valves and flow regulating valves used in fluid power systems is considered in the paper.*
Part 1 of the paper discusses methodology of modeling and simulation. Multi-pole mathematical models of pressure control valves are presented. An intelligent simulation environment CoCoViLa supporting declarative programming in a high-level language and automatic program synthesis is used as a tool. Simulation examples of pressure control valves are presented and discussed.
In Part 2 multi-pole mathematical models of flow regulating valves are described. Simulation examples of flow regulating valves are presented and discussed.
Key words: *multi-pole model, pressure control valve, intelligent programming environment, simulation.*

1. INTRODUCTION

When composing models of complex fluid power systems usually models of components of different levels are used. Components of the lowest level are hydraulic resistors, tubes, hydraulic interface elements, main valves, pilot valves, etc. Hydraulic control valves of different types are used as components of the medium level. In this way models of complex systems can be built up hierarchically.
Hydraulic control valves [1-5] are quite complex devices containing low level components, including internal feedbacks and having possibilities for adjusting.
Modeling and simulation tools in existence, their characteristics and disadvantages have been discussed in [6-8].
Using mainly two-pole models for describing hydraulic control valves [3-5] is not adequate, as components of such systems exert feedback actions. Obtained large equation systems usually need checking and correcting to guarantee solvability.
In the current paper an approach is proposed, which is based on using multi-pole models with different oriented causalities [6].
A special technique is used that allows avoid solving large equation systems during simulations [7]. Therefore, multi-pole models of large systems do not need considerable simplification.

2. MULTI-POLE MODELS

In general a multi-pole model represents mathematical relations between several input and output values (poles).
In hydraulic and mechanical systems variables are usually considered in pairs (effort and flow variable). Multi-pole models enable to express both direct actions and feedbacks.
Each component of the system is represented as a multi-pole model having its own structure including inner variables, outer variables (poles) and relations between variables.
Using multi-pole models allows describe models of required complexity for each component. For example, a component model can enclose nonlinear dependences, inner iterations, logic functions and own

integration procedures. Multi-pole models of system components can be connected together using only poles. It is possible directly simulate statics or steady state conditions without using differential equation systems.

3. SIMULATION ENVIRONMENT

CoCoViLa is a flexible Java-based simulation environment that includes both continuous-time and discrete event simulation engines and is intended for applications in a variety of domains [9]. The environment supports visual and model-based software development and uses structural synthesis of programs [10] for translating declarative specifications of simulation problems into executable code. Designer do not need to deal with programming, he can use the models with prepared calculating codes. It is convenient to describe simulation tasks visually, using prepared images of multi-pole models with their input and output poles.

4. PRESSURE CONTROL VALVES

Here we consider pressure control valves that are types of valves used to limit (safety valve) or control (relief valve) pressure in a fluid power system.
Two types of pressure control valves: direct operated and pilot operated are under consideration.

4.1 Direct Operated Pressure Control Valve

Direct operated pressure control valve under consideration is shown in Fig.1.

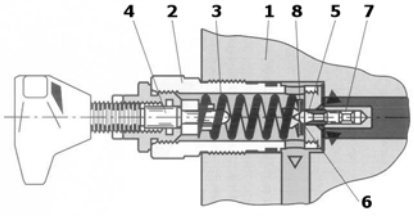

Fig. 1. Direct operated pressure control valve (Mannesmann Rexroth)

The valve consists of housing 1, sleeve 2, spring 3, advance mechanism 4, poppet with cushioning spool 5, hardened seat 6, spool sleeve 7 and spring retainer of a special shape 8 (used to compensate fluid jet force).
If the valve is used as safety valve, pressure is considered as input. If the valve is used as relief valve, volumetric flow is considered as input.

Simulation task for dynamics on a direct operated safety valve model is shown in Fig.2.

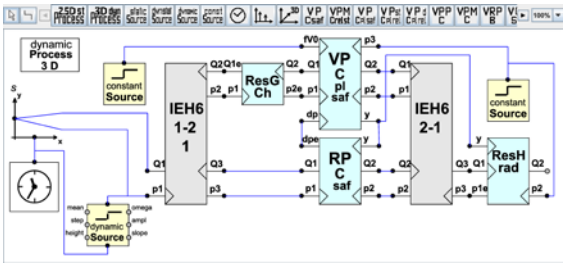

Fig.2. Simulation task of a direct operated safety valve dynamics

Multi-pole models: VPCplsaf – poppet with spool and spring, RPCsaf – flow through slot of poppet valve, ResHrad – spring retainer as resistor, ResGCh – cushioning resistor, IEH6-1-2-1, IEH6-2-1 – interface elements.
Inputs: pressure p1, spring preliminary compressibility fV0, outlet pressures p2, p3.
Outputs: volumetric flows Q1 and Q2.
Simulation manager*:*dynamic Process 3D.

4.1.1 Mathematical Models

Poppet with spool and spring VPCplsaf
Inputs: pressures p1, p2, p3, spring preliminary compressibility fV0, pressure drop in flow-through slot of poppet valve dp.
Outputs: volumetric flows Q1, Q2, displacement of poppet valve y.

Force acting to spring retainer:

$$Fr = \pi * (dr^2 - d1^2)/4 * (p2+p3)/2,$$

where
dr diameter of spring retainer,
d1 diameter of spool sleeve,
p2 pressure after poppet valve,
p3 outlet pressure.

Lifting force to the poppet valve:

$$F1 = \pi * d1^2 * p1/4 + \pi * (d2^2 - d1^2) * (p1 - p2)/8 * \sin(\beta * \pi/180) + Fr,$$

where
d1 diameter of spool sleeve,
d2 outer diameter of poppet seat,
p1 input pressure,

p2 pressure after poppet valve,
β half of cone angle,
Fr force acting to spring retainer.

Opposite force to the poppet valve:

$$F2 = \pi * dr^2 * p3 / 4,$$

where
dr diameter of spring retainer,
p3 outlet pressure.

Stiffness of the spring:

$$c = G * ds^4 / (Ds^3 * n * 8),$$

where
G shear modulus,
ds diameter of spring wire,
Ds diameter of spring,
n number of turns of the spring.

Displacement of the poppet valve:

$$y = (F1 - F2) / c - fV0,$$

where
F1 lifting force to the poppet valve,
F2 opposite force to the poppet valve,
fV0 spring preliminary compressibility.

Volumetric flows:

$$Q1 = 0, \quad Q2 = 0.$$

Difference of valve velocity used in Runge-Kutta method for integration for dynamics:

$$dv = (\Delta t / m) * (F1 - F2 - (y + fV0) * c - (Ff0 + kfr * (p1 + p2)/2) * sign(v, 0.001) - hv * v),$$

where
Δt time step,
m mass,
Ff0 constant part of friction force,
kfr coefficient of friction force,
v velocity of valve,
hv damping coefficient.

Difference of valve displacement:

$$dy = \Delta t * v.$$

Effective area of valve:

$$A = \pi * d1^2 / 4.$$

Volumetric flows:

$$Q1 = A * v, \quad Q2 = Q1.$$

Poppet valve slot RPCsaf

Inputs: pressures p1, p2, displacement of poppet valve y.
Outputs: volumetric flows Q1, Q2, pressure drop in poppet valve slot dpe.

Area of the poppet valve slot:

$$Ad = \mu * \pi * (d1 + d2)/2 * y * \sin(\beta * \pi / 180),$$

where
μ discharge coefficient,
d1 diameter of spool sleeve,
d2 outer diameter of poppet seat,
y displacement of the poppet valve,
β half of cone angle.

Pressure drop in poppet valve slot:

$$dp = p1 - p2.$$

Volumetric flows:

$$Q1 = Ad * (2 * abs(dp) / \rho)^{1/2}, \quad Q2 = Q1,$$

where
ρ fluid density.

4.1.2 Simulations

The following parameter values are used in the simulations under consideration.

Basic parameters for the fluid HLP46: kinematic viscosity at temperature 40^0C ν_{40} = 46e–6 m^2/s, density at temperature 15^0C ρ_{15} = 875 kg/m^3, basic compressibility factor of fluid at temperature 20^0C β_{F20} = 1/18.4e8 m^2/N , relative content of undissolvable air in fluid *vol* = 0.02 and temperature $\theta = 40^0$C.

For VPCplsaf: d1=0.0048 m, d2=0.005 m, dr=0.014 m, β=15 deg, ds=0.0025 m, Ds=0.016 m, n=6, G=8e11 N/m, m=0.04 kg, kfr=0 N/Pa, Ff0=0 N, hv=0 Ns/m.

For RPCsaf: d1=0.0048 m, d2=0.005 m, μ=0.8, β=15 deg.

For ResHrad: dr=0.014 m, d1= 0.0048 m.

For ResGCh: diameter d=0.0005 m, length l=0.02 m.

Results of direct operated safety valve statics simulation are shown in Fig.3.

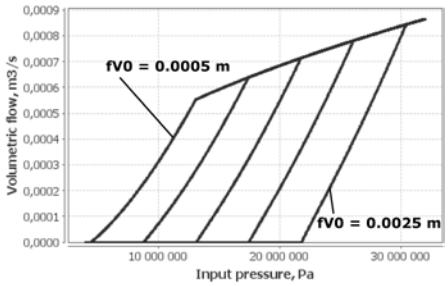

Fig.3. Direct operated safety valve statics

Graphs of volumetric flow through the valve depending on the input pressure for 5 different values of spring preliminary compressibility fV0 from 0.0005 m to 0.0025 m are presented. The valve opens correspondingly at pressures 5e6 Pa to 22e6 Pa depending on fV0. The value of

volumetric flow is defined by restricted displacement value 1e-3 m of the poppet valve.

Results of direct operated safety valve dynamics simulation are shown in Fig.4.

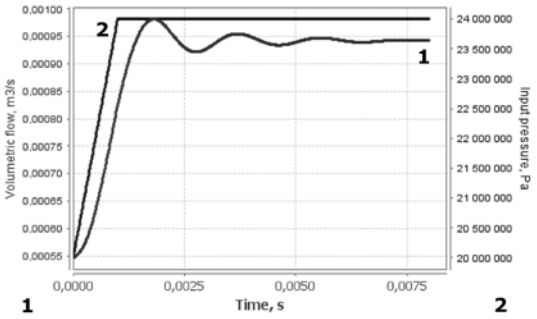

Fig.4. Direct operated safety valve dynamics

A step disturbance 4e6 Pa of pressure p1 at the left port during 0.001 s is applied as input (graph 2). The volumetric flow (1) follows the change of the input pressure, oscillations damp in 0.008 s.

Results of direct operated relief valve statics simulation are shown in Fig.5.

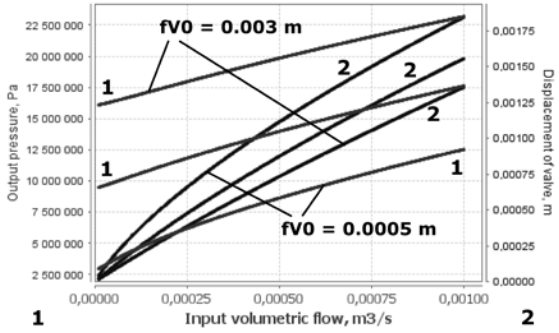

Fig.5. Direct operated relief valve statics

Graphs of output pressure (1) and displacement of the valve (2) depending on the input volumetric flow for three different values of spring preliminary compressibility fV0 from 0.0005 m to 0.003 m are presented. Some dependence of output pressure from input volumetric flow can be observed.

Results of direct operated relief valve dynamics simulation are shown in Fig.6. A step disturbance 1e-4 m^3/s of volumetric flow during 0.001 s at the left port is applied as input (2).

Displacement of the valve (3) almost follows change of the input volumetric flow. Damped oscillating output pressure (1) increases from initial to new higher level.

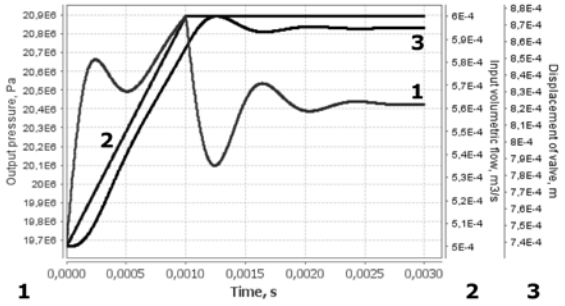

Fig.6. Direct operated relief valve dynamics

4.2 Pilot Operated Pressure Control Valve

Pilot operated pressure control valve under consideration is shown in Fig.7.

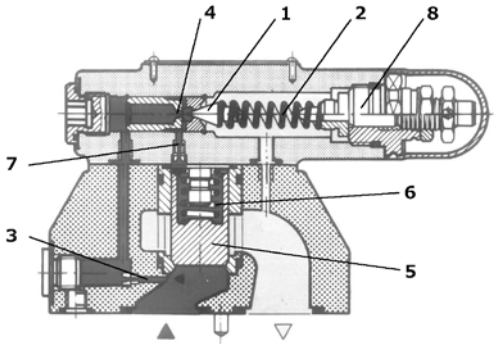

Fig.7. Pilot operated pressure control valve (Mannesmann Rexroth)

The valve contains pilot poppet valve 1, pilot valve spring 2, pilot control line resistors 3 and 4, main valve 5, main valve spring 6, main valve cushioning resistor 7 and advance mechanism 8.

If the valve is used as safety valve, pressure is considered as input. If the valve is used as relief valve, volumetric flow is considered as input.

Simulation task for dynamics on a pilot operated safety valve model is shown in Fig.8.

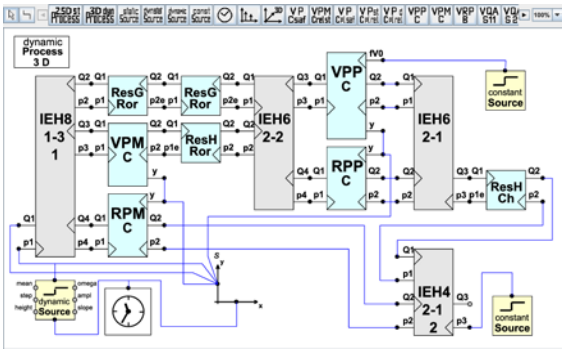

Fig.8. Simulation task of a pilot operated safety valve dynamics

Multi-pole models: VPPC – pilot poppet valve with spring, RPPC – pilot poppet valve slot, VPMC – main poppet valve with spring, RPMC – main poppet valve slot, ResGRor – pilot control line resistors, ResHRor – main poppet valve cushioning resistor, ResHCh – outlet resistor, IEH8-1-3-1, IEH6-2-2, IEH6-2-1, IEH4-2-1-2 – interface elements.
Inputs: pressure p1, spring preliminary compressibility fV0, outlet pressure p3.
Outputs: volumetric flows Q1 and Q2.
Simulation manager*:* dynamic Process 3D.

The following parameter values are used in the simulations.

For VPPC: d1=0.0048 m, d2=0.005 m, dr=0.014 m, β=15 deg, ds=0.0015 m, Ds=0.008 m, n=8, G=8e11 N/m, m=0.02 kg, kfr=2e-9 N/Pa, Ff0=0 N, hv=50 Ns/m.

For RPPC: d1=0.0048 m, d2=0.005 m, μ=0.8, β=15 deg.

For VPMC: d1=0.021m, d2=0.022m, β=45 deg, ds=0.0008 m, Ds=0.016 m, n=8, G= 8e11 N/m, m=0.05 kg, kfr=2e-9 N/Pa, Ff0=2 N, hv=5 Ns/m.

For RPMC: d1=0.021 m, d2=0.022 m, μ=0.8, β=45 deg.

For ResGRor: d=0.001 m and 0.002 m, l=0.005 m.

For ResHRor: d=0.001 m, l=0.005 m.

For ResHCh: d=0.002 m, l=0.03 m.

Results of pilot operated safety valve statics simulation are shown in Fig.9.

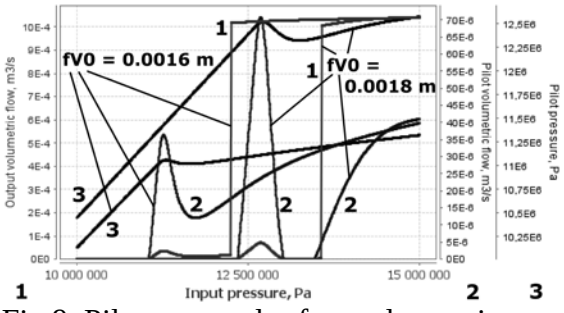

Fig.9. Pilot operated safety valve statics

Graphs of main volumetric flow (1), pilot volumetric flow (2) and pilot pressure (3) depending on the input pressure for two different values of preliminary compressibility fV0 = 0.0016 m and 0.0018 m of the pilot valve spring are presented.
If fV0 = 0.0016 m pilot valve opens rapidly at pressure 11e6 Pa then closes a bit and opens more later. If fV0 = 0.0018 m pilot valve opens rapidly at pressure 12.3e6 Pa then closes and reopens later.
The main valve reacts slightly to opening of the pilot valve and opens rapidly correspondingly at pressures 12.2e6 Pa and 13.6e6 Pa depending on the value of fV0.
Results of pilot operated safety valve dynamics simulation are shown in Fig.10.

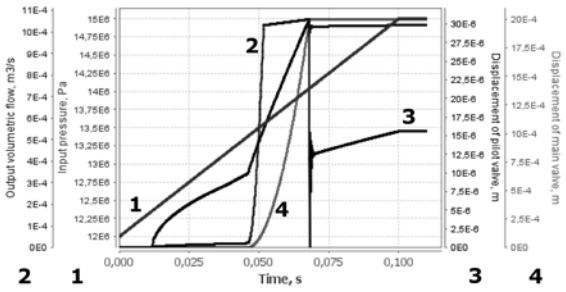

Fig.10. Pilot operated safety valve dynamics

A step disturbance 3e6 Pa of pressure p1 during 0.1 s at the left port is applied as input (1). Pilot valve (3) begins to open at input pressure 12.3e6 Pa. At input pressure 13.4e6 Pa main valve (4) begins to open. At the same time output volumetric flow (2) rapidly increases to maximum. Main valve shift (4) to maximum 20e-4 m causes additional flow through pilot valve and its additional shift (3). When the main valve stops at the maximum displacement the additional flow through pilot valve disappears and pilot valve partly closes.

Results of pilot operated relief valve statics simulation are shown in Fig.11.

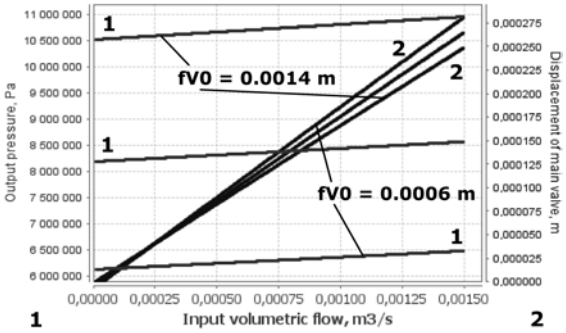

Fig.11. Pilot operated relief valve statics

Graphs of output pressure (1) and displacement of the main valve (2) depending on the input volumetric flow for three values of preliminary compressibility fV0 from 0.0006 m to 0.0014 m of pilot valve spring are presented. Slight dependence of output pressure on input

volumetric flow can be observed.

Results of pilot operated relief valve dynamics simulation are shown in Fig.12.

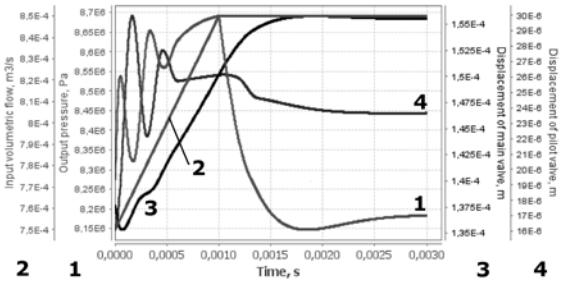

Fig.12. Pilot operated relief valve dynamics

A step disturbance 1e-4 m^3/s of volumetric flow during 0.001 s at the left port is applied as input (2). Displacement of the main valve (3) follows the input volumetric flow with a little delay.

Both the pilot valve (4) and the output pressure (1) oscillate and reach the new level during 0.003 s.

5. CONCLUSION

In the paper modeling and simulation of hydraulic pressure valves of fluid power systems were considered. Multi-pole models are used that enable adequately describe physical processes in hydraulic systems. Both direct actions and feedbacks can be expressed in component models.

Simulations are performed using an intelligent programming environment CoCoViLa with feature of automatic synthesis of programs from the knowledge available in visual model.

6. ACKNOWLEDGEMENTS

This research has been partially supported by the *European Regional Development Fund* (ERDF) through:

- Estonian Centre of Excellence in Computer Science (EXCS).
- The project no 3.2.1201.13-0026 „Model-based Java software development technology“.
- The project no 3.2.1101.12-0012 „Smart composites - design and manufacturing“.

7. REFERENCES

1. Schmitt, A. *The Hydraulic Trainer, **Vol. 1**, Instruction and Information on Oil Hydraulics*, RE 00 301, Rexroth GmbH, Lohr am Main.

2. *Eaton Hydraulics Training Services*, Industrial Hydraulics Manual, 5th Ed., 2008.

3. Murrenhoff, H. *Grundlagen der Fluid-technik, Teil 1: Hydraulik*, 4. neu überarbeitete Auflage. Institut für fluidtechnische Antriebe und Steuerungen, Aachen, 2005.

4. Manring, N. D. *Hydraulic Control Systems*. John Wiley & Sons, Inc. Hoboken, 2005.

5. Gebhardt, N., Will, D. and Nollau, R. *Hydraulik: Grundlagen, Komponenten, Schaltungen*, 5. Neubearb. Auflage, Springer Verlag Berlin Heidelberg, 2011.

6. Grossschmidt, G. and Harf, M. “COCO-SIM - Object-oriented Multi-pole Modeling and Simulation Environment for Fluid Power Systems, Part 1: Fundamentals”. *International Journal of Fluid Power*, **10(2)**, 2009, 91 – 100.

7. Harf, M. and Grossschmidt G. “Modeling and simulation of an electro-hydraulic servo-valve in an intelligent programming environ-ment.” In: *ASME 2012 11th Biennal Conference on Engineering Systems Design and Analysis (ESDA 2012), July 2-4, 2012*. Nantes, France, [Proceedings]. New York, ASME, 2012, 1-9.

8. Grossschmidt, G. and Harf, M. Modeling and simulation of an electro-hydraulic servo-system in an intelligent programming environ-ment. In: *The 13th Mechatronics Forum Inte-rnational Conference: Proceedings **Vol.3/3**, September 17-19, 2012, Johannes Kepler Uni-versity Linz, Austria*, (Scheidl, R. and Jakoby, B., eds.). Linz: Trauner, 2012, 939 - 946.

9. Kotkas, V., Ojamaa A., Grigorenko P., Maigre R., Harf M. and Tyugu E. “CoCoViLa as a multifunctional simulation platvorm“, In: *SIMUTOOLS 2011 - 4th International ICST Conference on Simulation Tools and Techniques, March 21–25, Barcelona, Spain:* Brussels, ICST, 2011, 1-8.

10. Matskin, M. and Tyugu, E.. Strategies of structural synthesis of programs and its extensions, *Computing and Informatics, **Vol. 20**,* 2001, 1-25.

9th International DAAAM Baltic Conference
"INDUSTRIAL ENGINEERING"
24-26 April 2014, Tallinn, Estonia

MULTI-POLE MODELING AND INTELLIGENT SIMULATION OF CONTROL VALVES OF FLUID POWER SYSTEMS (PART 2)

Harf, M. & Grossschmidt, G.

Abstract: *The paper is a continuation of the Part 1. All the general aspects and a simulation tool used were considered in the Part 1.*
Here multi-pole mathematical models for flow regulating valves of three types are described. Mathematical models of a two-directional flow regulating valve are presented. Examples of simulations of flow regulating valves are presented and discussed.
Key words: *multi-pole model, flow regulating valve, simulation.*

1. INTRODUCTION

In the paper, modeling and simulation of flow regulating valves used in fluid power systems are considered. Methodology, multi-pole mathematical models and simulation environment have been discussed in the Part 1 of the paper.

2. FLOW REGULATING VALVES

In flow regulating valves [1-7] the flow is not related to the pressure drop between the valve input and output. This means that the fluid flow set remains constant, even with pressure deviations. Flow regulating valves are used when the working speed should remain fixed in spite of different loads at the user.
Flow regulating valve contains adjustable throttle and pressure compensator ensuring constant pressure drop in the throttle.
Flow regulating valves of three main types exist:

1. Two-directional valve where throttle is located after pressure compensator.
2. Two-directional valve where throttle is located before pressure compensator.
3. Three-directional valve where throttle and pressure compensator are connected in parallel way.

Functional schemes of the flow regulating valves of three types are shown in Fig.1.

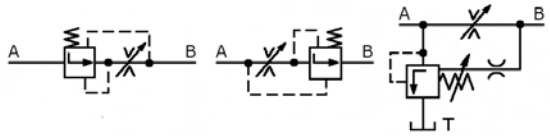

Fig. 1. Functional schemes of flow regulating valves

2.1 Two-directional Flow Regulating Valve (type 1)

Two-directional flow regulating valve (type 1) is shown in Fig.2.

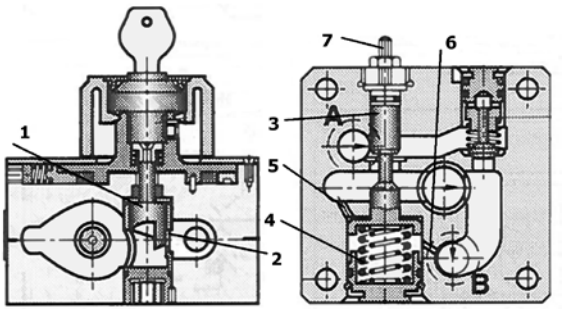

Fig. 2. Two-directional flow regulating valve (type 1) (Mannesmann Rexroth)

The valve consists of throttle pin 1 with orifice 2, normally open control spool 3 with two springs 4, bores 5, 6 to the spool surfaces and stroke limiter 7.

Simulation task for dynamics on a two-directional flow regulating valve model (type 1) is shown in Fig.2.

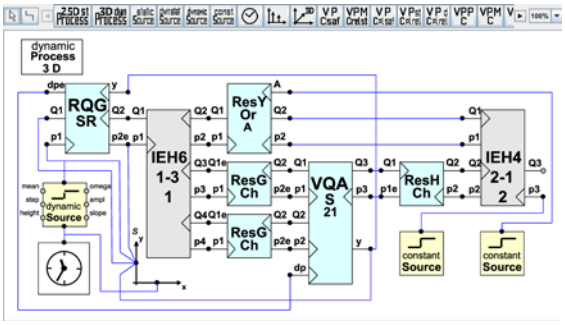

Fig.3. Simulation task of a two-directional flow regulating valve dynamics (type 1)

Multi-pole models: RQGSR – pressure compensator slots, ResYOrA – regulating spool slot, VQAS21 – pressure compensator spool, ResGCh, ResHCh – cushioning resistors, IEH6-1-3-1, IEH4-2-1-2 – interface elements.
Inputs: pressure p1, regulating slot area A, outlet pressure p3.
Outputs: volumetric flows Q1 and Q3.
Simulation manager: dynamic Process 3D.

2.1.1 Mathematical Models

Pressure compensator slots RQGSR

Inputs: pressure p1, volumetric flow Q2, displacement of the pressure compensator spool y.
Outputs: pressure p2e, volumetric flow Q1, pressure drop dpe.

Spool conical part length:

$$a = (d1-d2)/2/\tan(\beta * \pi /180),$$

where
d1 diameter of spool sleeve,
d2 diameter of the end of the cone,
β half angle of the cone.

Displacement of the spool corresponding to switching point from one model to another:

$$h = a/(\cos^2(\beta * \pi /180)).$$

If y >= h:

width of the spool slot

$$x = ((y-a)^2+(d1-d2)^2/4)^{1/2},$$

median diameter of the spool slot

$$dx = (d1 + d2)/2.$$

If y < h:

$$x = y*\sin(\beta * \pi /180),$$

$$d1x = (d1 - 2*x*\cos(\beta * \pi /180)),$$

$$dx = (d1 + d1x)/2.$$

Pressure compensator slot area:

$$A = \mu * \pi *dx*x,$$

where
μ discharge coefficient.

Output pressure:

$$p2e = p1 - Q2^2/A^2*\rho /2,$$

where
ρ fluid density.

Output volumetric flow:

$$Q1 = Q2.$$

Output pressure drop:

$$dpe = p1 - p2.$$

Pressure compensator spool VQAS21

Inputs: pressures p1, p2, p3, pressure drop dp in poppet valve flow-through slot.
Outputs: volumetric flows Q1, Q2, Q3, displacement of poppet valve y.

Pressure compensator spool areas:

$$A1 = \pi * d1^2/ 4,$$

$$A2 = \pi * (d2^2- d1^2) / 4,$$

$$A3 = \pi * d2^2/ 4,$$

where
d1 diameter of the spool sleeve,
d2 diameter of the spool sleeve head.

Force to pressure compensator spool:

$$F = A1*p1+A2*p2-A3*p3.$$

Coefficient of fluid jet force:

$$B = \mu*\pi*d1*2*dp*(\cos(\beta *\pi/180))*$$
$$\sin(\beta*\pi/180)/c.$$

Stiffness of springs:

$$c1 = G * ds1^4 / (Ds1^3 * n1 * 8),$$

$$c2 = G * ds2^4/ (Ds2^3* n2 * 8),$$

where
G shear modulus,
ds1, ds2 diameters of spring wires,
Ds1, Ds2 diameters of springs,
n1, n2 numbers of turns of springs.

Sum of spring stiffnesses:

$$c = c1 + c2.$$

Displacement of the pressure compensator spool:

$$y1 = 1/(1-B)*(F/c-fV0),$$

where
fV0 spring preliminary compressibility.

Pressure compensator spool slot width:

$$y = y0 - y1,$$

where
y0 initial spool slot width.

Differences of spool velocity and spool displacement used for dynamics are calculated using the similar procedure as for difference of valve velocity and spool displacement in the direct operated pressure control valve in Part 1 of the paper. Here difference dv is calculated by formula:

$$dv=(\Delta t/m)*(F-(y1*(1-B)+fV0)*c-(Ff0+kfr*(p1+p2)/2)*sign(v,0.001)-hv*v).$$

Volumetric flows:

$$Q1 = A1*v,\ Q2 = A2*v,\ Q3 = A3*v.$$

Regulating throttle orifice ResYOrA

Inputs: pressures p1, p2, area of the regulating throttle orifice A.
Outputs: volumetric flows Q1, Q2.

Volumetric flows:

$$Q1 = \mu*A*(2*(p1-p2)/\rho)^{1/2},\quad Q2=Q1.$$

2.1.2 Simulations

The following parameter values are used in the simulations.

The fluid HLP46 is used. Basic parameters of the fluid have been described in the Part 1 of the paper.

For RQGSR: d1=0.012 m, d2=0.01 m, μ =0.8, β=30 deg.

For VQAS21: d1=0.01 m, d2=0.03 m, y0=0.0023 m, μ=0.8, β=30 deg, ds1=0.0028 m, Ds1=0.022 m, n1=5, ds2=0.0017 m, Ds2=0.014 m, n2=4, G= 8e11 N/m, m=0.04 kg, kfr=2e-9 N/Pa, Ff0=0.3 N, hv=0 Ns/m.

For ResYOrA: μ =0.8, A=1.7e-5 m^2.

For ResGCh: diameters d=0.0015 m, lengths l=0.02 m and 0.01 m.

For ResHCh: d=0.0025 m, l= 0.01 m.

Results of two-directional flow regulating valve (type 1) statics simulation are shown in Fig.4.
Graphs of volumetric flow (graph 1), regulated pressure (2) and displacement of the valve (3) depending on the input pressure for two different values of the area of regulating throttle orifice A = 1.7e-5 m^2 and 3e-5 m^2 are presented. As it can be seen, the valve operates normally at input pressures higher than 2e6 Pa. Output volumetric flow (1) slightly drops if input pressure increases.

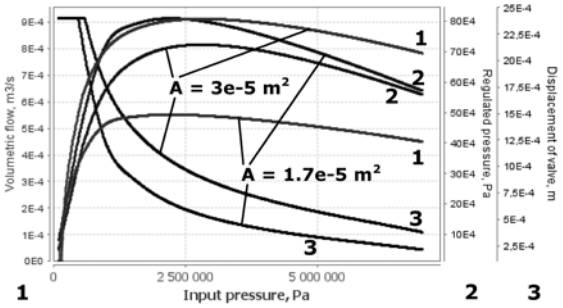

Fig.4. Two-directional flow regulating valve statics (type 1)

Results of two-directional flow regulating valve (type 1) dynamics simulation are shown in Fig.5.

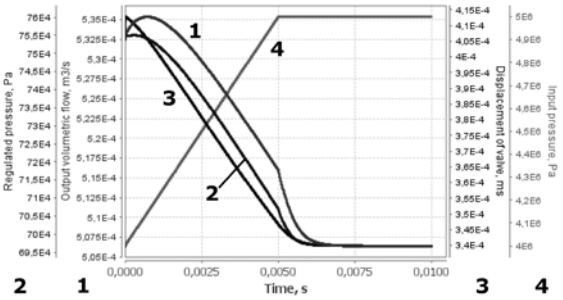

Fig.5. Two-directional flow regulating valve (type 1) dynamics

A step disturbance 1e6 Pa of pressure p1 during 0.005 s at the left port is applied as input (4). Step change of the input pressure causes regulated pressure (2) change. Regulated pressure causes valve shift (3). Valve shift together with regulated pressure cause output volumetric flow (1) to achieve a new level.

2.2 Two-directional Flow Regulating Valve (type 2)

Two-directional flow regulating valve (type 2) is shown in Fig.6.

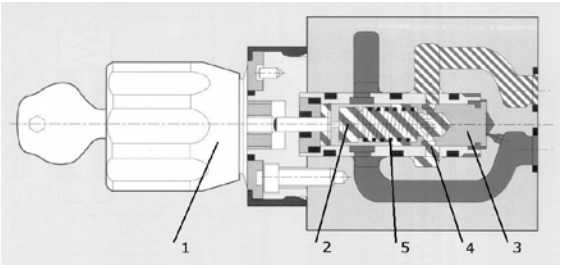

Fig. 6. Two-directional flow regulating valve (type 2) (Mannesmann Rexroth)

The flow regulating valve consists of adjustment device 1, triangle shape regulating slots 2, pressure compensator spool 3, pressure compensator round slots 4 and spring 5. Simulation task for dynamics on a two-directional flow regulating valve model (type 2) is shown in Fig.7.

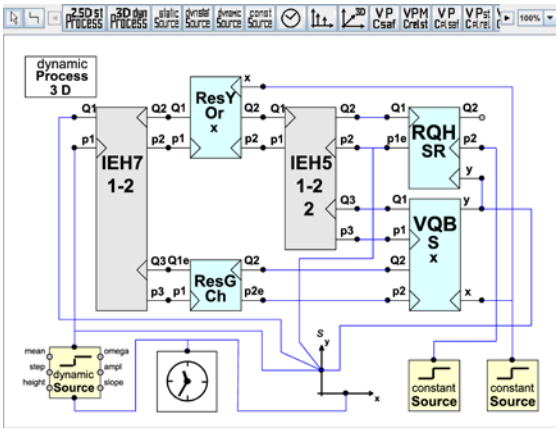

Fig.7. Simulation task of a two-directional flow regulating valve dynamics (type 2)

Multi-pole models: ResYOrx – triangle shape regulating slots, RQHSR – pressure compensator round slots, VQBSx – pressure compensator spool, ResGCh – cushioning resistor, IEH7-1-2, IEH5-1-2-2 – interface elements.
Inputs: pressure p1, triangle shape regulating slot displacement x, outlet pressure p2.
Outputs: volumetric flows Q1 and Q2.
Simulation manager*:* dynamic Process 3D.

The following parameter values are used in the simulations.

For ResYOrx: μ=0.8, x=1.75e-6 m.

For RQHSR: d=0.012 m, μ=0.8, y0=0.0022 m, pressure compensator slot radius r=0.002m.

For VQBSx: d=0.012m, y0=0.0022m, ds=0.0017 m, Ds=0.008 m, n=6, G= 8e11 N/m, fV0=0.0005 m, Ff0=0.05 N, kfr=2e-9 N/Pa, m=0.03 kg, hv=20 Ns/m.

For ResGCh: diameter d=0.00065 m, length l=0.003 m.

Results of two-directional flow regulating valve (type 2) statics simulation are shown in Fig.8.

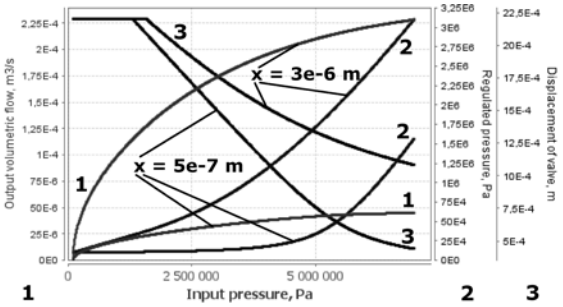

Fig.8. Two-directional flow regulating valve (type 2) statics

Graphs of volumetric flow (graphs 1), regulated pressure (2) and displacement of the valve (3) depending on the input pressure for two different values of the triangle shape regulating slot displacement x = 5e-7 m and 3e-6 m are presented. As it can be seen, the valve operates better at smaller displacements of triangle shape regulating slot.

Results of two-directional flow regulating valve (type 2) dynamics simulation are shown in Fig.9.

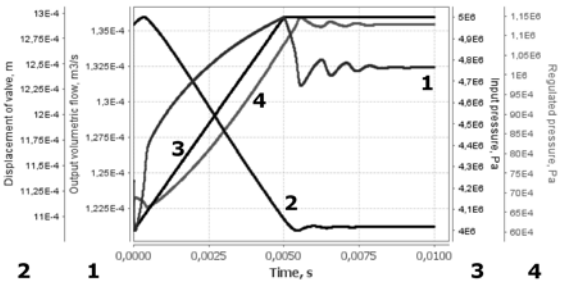

Fig.9. Two-directional flow regulating valve (type 2) dynamics

A step disturbance 1e6 Pa of pressure p1 during 0.005 s at the left port is applied as input (3).Step change of the input pressure causes valve shift (2). Valve shift causes regulated pressure (4) change. Regulated pressure together with input pressure cause output volumetric flow (1) to take a new level through damped oscillations.

2.3 Three-directional Flow Regulating Valve

Three-directional flow regulating valve is shown in Fig.10.

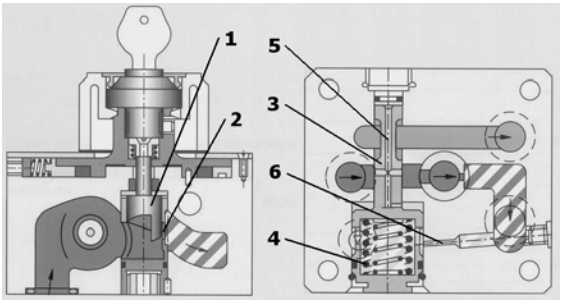

Fig. 10. Three-directional flow regulating valve (Mannesmann Rexroth)

The valve consists of the throttle pin 1 with orifice 2, normally closed control spool 3 with two springs 4, bores 5 and 6 to the spool surfaces.

Simulation task for dynamics on a three-directional flow regulating valve model is shown in Fig.11.

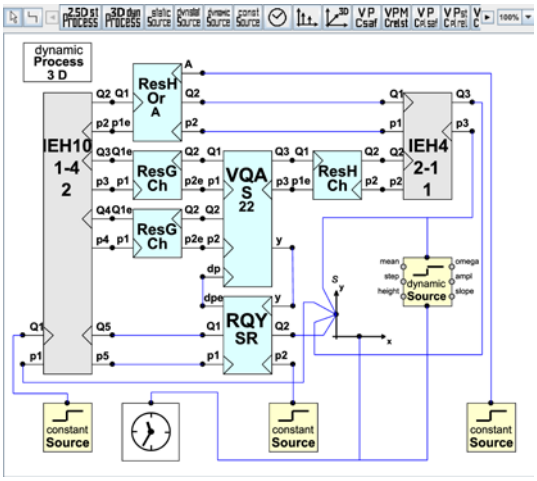

Fig.11. Simulation task of a three-directional flow regulating valve dynamics

Multi-pole models: ResHOrA – regulating orifice, VQAS22 – pressure compensator spool, RQYSR – pressure compensator slots, ResGCh, ResHCh – cushioning resistors, IEH10-1-4-2, IEH4-2-1-1 – interface elements.
Inputs: outlet pressure p3, volumetric flow Q1, regulating orifice area A, outlet pressure p2.
Outputs: inlet pressure p1, volumetric flows Q2 and Q3.
Simulation manager: dynamic Process 3D.

The following parameter values are used in the simulations.

For **ResHOrA:** μ=0.8, A=2e-6 m^2.

For **VQAS22:** d1=0.008 m, d2=0.02 m, μ=0.8, β=30 deg, ds1=0.0035 m, Ds1=0.014 m, n1=5, ds2=0.0025 m, Ds2=0.01 m, n2=4, G=8e11 N/m, m=0.04 kg, kfr=2e-9 N/Pa, Ff0=0.3 N, hv=5 Ns/m.

For **RQYSR:** d1=0.008 m, d2=0.006 m, μ=0.8, β=30 deg.

For ResGCh: d=0.0015 m, l=0.02 m.

For ResHCh: d=0.001 m, l= 0.02 m.

Results of three-directional flow regulating valve statics simulation are shown in Fig.12.

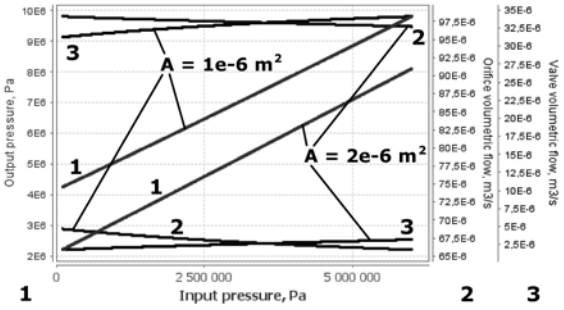

Fig.12. Three-directional flow regulating valve statics

Graphs of output pressure of the right port (graphs 1), regulating orifice volumetric flow (2) and valve volumetric flow (3) depending on the input pressure for two different values of the area of regulating orifice A = 1e-6 m^2 and 2e-6 m^2 are presented. Output pressure linearly depends on input pressure. Sum of valve volumetric flow and regulating orifice volumetric flow equals to input volumetric flow Q1 = 1e-4 m^3/s. If A=1e-6 m^2 the output pressure is constantly 4e6 Pa higher of the input pressure. If A=2e-6 m^2 the output pressure is constantly 2e6 Pa higher of the input pressure.

Results of three-directional flow regulating valve dynamics simulation are shown in Fig.13.

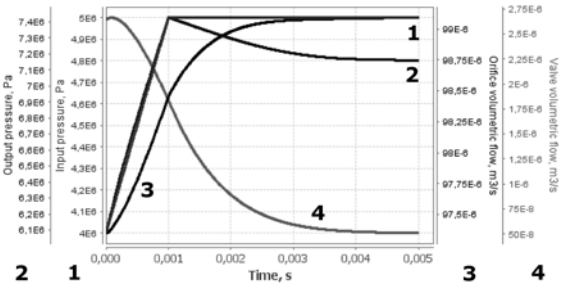

Fig.13. Three-directional flow regulating valve dynamics

A step disturbance of pressure p3 1e6 Pa at the right port during 0.001 s is applied as input (graph 1). Step change of the input pressure causes valve shift. Valve shift causes valve volumetric flow (4) change. Difference of input volumetric flow Q1 and valve volumetric flow equals to regulating orifice volumetric flow (3). Output pressure (2) is defined by input pressure, area of regulating orifice and orifice volumetric flow. Transient responses take 0.005 s.

3. CONCLUSION

In the paper modeling and simulation of hydraulic flow regulating valves of fluid power systems was considered.

The results of static simulations of both hydraulic pressure and flow regulating valves considered in Part 1 and Part 2 are in accordance with Mannesmann Rexroth and Eaton-Vickers catalogue performance characteristics.

Dynamic simulations for valves of both types are performed and results are shown.

Models and results of dynamics simulation could be useful for describing dynamic behaviour of control valves and representing their dynamic performance characteristics in catalogues.

Proposed pressure and flow regulating valve models can be used as subsystems when simulating complex fluid power systems.

4. ACKNOWLEDGEMENTS

This research has been partially supported by The *European Regional Development Fund* (ERDF) through:

- Estonian Centre of Excellence in Computer Science (EXCS).
- The project no 3.2.1201.13-0026 „Model-based Java software development technology“.
- The project no 3.2.1101.12-0012 „Smart composites - design and manufacturing“.

5. REFERENCES

1. *Industrieventile und Zubehör*, Mannesmann Rexroth, RD 00 101709.92, Rexroth GmbH, Lohr am Main.

2. Eaton-Vickers. *Industrial Hydraulics Manual*. 5th Ed., 2nd Printing, Eaton Hydraulics Training, 2001.

3. Murrenhoff, H. *Grundlagen der Fluidtechnik, Teil 1: Hydraulik*, 4. neu überarbeitete Auflage. Institut für fluidtechnische Antriebe und Steuerungen, Aachen, 2005.

4. Schmitt, A. *The Hydraulic Trainer, **Vol. 1**, Instruction and Information on Oil Hydraulics*, RE 00 301, Rexroth GmbH, Lohr am Main.

5. Parr, A. *Hydraulics and Pneumatics.* A technicians and Engineer's Guide, Third Edition, Elsevier Ltd, 2011.

6. Watton, J. *Fundamentals of Fluid Power Control.* Cambridge University Press, New York, 2009.

7. Gebhardt, N., Will, D. and Nollau, R. *Hydraulik: Grundlagen, Komponenten, Schaltungen*, 5. Neubearb. Auflage, Springer Verlag Berlin Heidelberg, 2011.

9th International DAAAM Baltic Conference
"INDUSTRIAL ENGINEERING -
24-26 April 2014, Tallinn, Estonia

A NEW TYPE OF COMPACT SILENCER FOR HIGH FREQUENCY NOISE

Kabral, R., Auriemma, F., Knutsson, M., Åbom, M.

Abstract: *In modern IC engine design super-chargers are utilized to increase the fuel conversion efficiency. Nevertheless, these components are also recognized as strong high frequency noise sources in the engine compartment. For installations under such limited space and high sound pressure conditions innovative noise control concepts are essential.*
To reduce this type of noise a new type of silencer based on micro-perforated plates and optimized using the so called Cremer's acoustic impedance is proposed and investigated experimentally. The experimental data is also used to validate modelling done on the new silencer.
Key words: Compact silencer, Micro-perforated, Acoustic impedance, Super-Charger.

1. INTRODUCTION

Since 2015 the vehicle manufacturers have been obliged to implement engines complying the Euro 6 emission standard [1]. To this aim, the super-charging of the engine is almost un-avoidable, as it increases the indicated fuel conversion efficiency. On the other hand, additional concerns related with high frequency noise generation, will arise from compressors.
Traditional solutions to reduce intake noise of the IC engine are based on the well-known Helmholtz resonator, which reflects sound generated back to the source. Moreover, sound reflections also occur at the opening of the duct termination (See e.g. [2] or [3]). Therefore, in such solutions, the noise dissipation relies on the source ability to absorb the reflected noise.
To overcome this dependence, and to design a robust noise control solution, the sound has to be dissipated by properly designed absorptive elements.
Traditionally, dissipative silencers are based on fibrous materials, which pollute the medium and, when integrated to the air inlet, can cause failure of the IC unit.
Therefore, producing acoustic absorption with non-fibrous materials is of interest.
The idea of producing acoustic resistance in room applications by employing the viscosity in circular small apertures (in order of acoustic boundary layer) is originated from D. Y. Maa [4]. Usually, producing such acoustic elements is a time consuming and expensive process. These issues can be overcome by using mass produced sound absorbing panels called Acustimet™ [5].
These panels were studied also as one possible noise control solution in vehicle applications (See e.g. [6]). In addition, a new type of silencer based on the micro-perforated panels (MPP) was proposed and studied by Allam and Åbom in [7]. In order to eliminate the drawback of having transmission loss minima at half-wave length multiples, the locally reacting limit was formulated by Åbom and Allam in [8]. The proposed design consists of straight-flow channel made of MPP that is adjoined to locally reacting cavity, thus resulting in a locally reacting surface.
Kabral et. al. proposed the optimization technique for such compact silencer in the [9]. The essence of the method is matching the acoustic wall impedance with the Cremer optimum impedance [10]. The latter was derived to obtain the highest sound damping in an infinite channel. The

concept was developed further by Tester in [11], who derived the expression for the circular cross-section, and also added the plug-flow correction as follows:

$$Z_{Cc} = (0.88 - 0.38i)\frac{kr}{\pi(1+M)^2}\ , (1)$$

Z_{Cc} – the norm. surface impedance for theor. maximum sound damping in a circular duct;
k – the wave number, m^{-1};
r – the radius of the channel, m;
M – the Mach number.

The investigation in [9] was carried out by employing simplified FEM model where the cavity and perforation of the compact silencer were defined as an acoustic impedance boundary condition. The model was been validated with hi-resistance configuration under no flow conditions.
The results indicated that, by implementing this optimization technique, very high controlled sound damping is achievable.
In the present work, a systematic validation of the modelling, and a detailed investigation of the sound damping mechanisms, will be performed. The same prototype cavity, used in [9], will be implemented in configuration with three different Acustimet™ MPPs (see Fig. 1). In addition, the same simplified FEM model is employed to compute acoustic quantities corresponding to the Cremer's optimum.

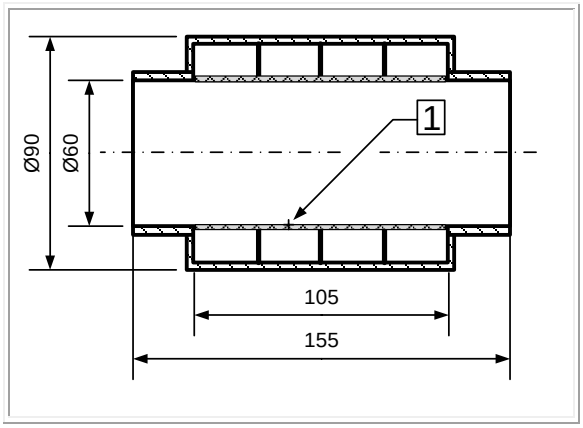

Fig.1. The sketch of the prototype silencer [9] with indicated MPP in field no. 1.

2. METHOD

In order to evaluate if the MPP and cavity combination is optimal, the acoustic impedance of the absorbing surface has to be determined and compared to the Cremer's optimum. In the compact silencer this impedance is formed by contributions from MPP and the locally reacting cavity as

$$Z_{surf} = Z_{MPP} + Z_{cav}\ , \qquad (2)$$

where
Z_{surf} – a normalized surface impedance;
Z_{MPP} – the normalized MPP impedance;
Z_{cav} – the normalized cavity impedance.

The geometrical parameters are known in case of two of the three MPP Acustimet included in the investigation (Tab. 1). As a consequence, the acoustic transfer impedance can be determined by means of existing semi-empirical models. On the other hand, exact parameters of the Acustimet panel with largest apertures are unknown, except the thickness, which is 1mm for all the panels. Therefore, the acoustic transfer impedance of this panel will be determined experimentally.

Name	Perforation Ratio	Slit width [mm]
Res. 0.05	Unknown	Unknown
Res. 0.25	6.5	0.240
Res. 1.50	4.3	0.095

Table 1. Geometrical parameters of Acustimet MPP's.

2.1 Acoustic impedance models

The comprehensive overview of the existing semi-empirical models for MPP transfer impedance has been given by Guo et. al. in [6]. The resulting model of slit type MPP, utilized also herein, was validated experimentally by testing different Acustimet™ panels.
The acoustic resistance *Re(Z)* and reactance *Im(Z)* of Acustimet MPP is being computed as:

$$r_s = \mathrm{Re}\left\{\frac{i\omega t}{\sigma c}\left[1 - \frac{\tanh\left(k\sqrt{i}\right)}{k\sqrt{i}}\right]^{-1}\right\} + \\ + \frac{4R_s}{\sigma\rho c} + \frac{|u_h|}{\sigma c} + \beta\frac{M}{\sigma} \quad (3)$$

and

$$x_s = \mathrm{Im}\left\{\frac{i\omega t}{\sigma c}\left[1 - \frac{tanh\left(k\sqrt{i}\right)}{k\sqrt{i}}\right]^{-1}\right\}, \quad (4)$$

where

ω – a radial frequency, s^{-1};
ρ – the density of the medium, kg/m^3;
k – shear wave number, m^{-1};
t – the thickness of perforated panel, m;
σ – the porosity of the perf. surface;
β – a factor for grazing flow effects;
u_h – peak particle velocity in apertures, m/s; and
R_s – surface resistance, Pas/m.

The shear wave number which is used to relate the acoustic boundary layer thickness with the dimensions of the aperture, is defined as:

$$k = d\sqrt{\frac{\omega}{4v}}, \quad (5)$$

where

d – the slit width, m; and
v – the kinematic viscosity of medium,m^2/s.

The consequence of the oscillating motion of the fluid on the perforated surface is the increase of the acoustic resistance, which contribution is given by [6]:

$$R_s = \frac{1}{2}\sqrt{2\rho\omega\eta}\,, \quad (6)$$

where

η – the dynamic viscosity of the medium, kgm2/s.

The equation for cavity impedance, implemented herein, was derived in [8] as:

$$Z_{cav} = \\ = \frac{i\left[H_0^{(1)}(k_a r) - \frac{H_1^{(1)}(k_a R)}{H_1^{(2)}(k_a R)}H_0^{(2)}(k_a r)\right]}{H_1^{(1)}(k_a r) - \frac{H_1^{(1)}(k_a R)}{H_1^{(2)}(k_a R)}H_1^{(2)}(k_a r)}, \quad (7)$$

where

k_a – the axial wave number, m^{-1};
R – the radius of the expansion chamber, m;
r – the radius of main duct, m;
$H_m^{(n)}$ – the Hankel function of n:th kind and m:th order.

2.2 Experiments

The experimental procedures in the present work is considering plane wave 0th duct mode and assuming time dependency of *exp(iωt)*. Consequently, the well-known acoustic two-port model [12] for flow-duct elements is appropriate for the investigation.

Depending on the selection of acoustic state variables, the linear relation of the states between the ports are given though either acoustic scattering (Eq. 8) or transfer matrix (Eq. 9) [12]:

$$\begin{bmatrix} p_{a+}^I & p_{a+}^{II} \\ p_{b+}^I & p_{b+}^{II} \end{bmatrix} = \begin{bmatrix} R_a & T_b \\ T_a & R_b \end{bmatrix}\begin{bmatrix} p_{a-}^I & p_{a-}^{II} \\ p_{b-}^I & p_{b-}^{II} \end{bmatrix}, \quad (8)$$

$$\begin{bmatrix} p_a^I & p_a^{II} \\ q_a^I & q_a^{II} \end{bmatrix} = \begin{bmatrix} T_{11} & T_{12} \\ T_{21} & T_{22} \end{bmatrix}\begin{bmatrix} p_b^I & p_b^{II} \\ q_b^I & q_b^{II} \end{bmatrix}, \quad (9)$$

where p_{a+}^I and p_{b-}^{II} are complex acoustic pressure wave amplitudes at port a and b of the first and second set of state variables. The subscript + and – indicate the propagation direction; *R* and *T* are complex reflection and transmission coefficients.

p_a^I and q_b^{II} are total acoustic pressure and acoustic volume flow at port a and b of first and second set of state variables.

By considering the number of unknowns in these matrixes, and by assuming not

symmetric setup, two sets of linearly independent state vectors have to be experimentally determined.
While the elements of scattering matrix are straightforward description of the wave interaction problem, the transfer matrix formulation is more appropriate for estimation of transfer properties, e.g. acoustic impedance. Moreover, one can be obtained from the other one by linear transformation of the state vectors.
In order to determine the necessary state vectors of two-port, the acoustic pressures at both branches are measured with duct wall mounted microphones. Finally, the wave decomposition is carried out according to technique described in [13].
For perforated elements, whose thickens is much smaller than the acoustic wave length, the air inside the apertures can be considered as lumped mass. In this case it can be shown that the transfer matrix elements (Eq. 9) become $T_{11} = 1$, $T_{21} = 0$, $T_{22} = 1$ and $T_{12} = Z_{MPP}\rho_0 c/A$.

2.2 Performance parameters

The most common quantity used to evaluate the acoustic performance of a silencer is sound transmission loss (TL). The TL can be interpreted as the loss of acoustic power in sound transmission through the two-port element. This can be obtained from the transmission elements of the scattering matrix (Eq. 8) according to:

$$TL = 10\log_{10}\left(\frac{1}{|T|^2}\right), \qquad (10)$$

The Eq. 10 is valid in case of same cross-sectional area in both ports (*a* and *b*), negligible flow pressure loss and temperature gradient.
The transmission loss is produced by the absorption and reflection of incident waves.
The latter is not favorable, in terms of robust noise control solution, since it relies on the ability of the source to absorb the reflected waves. Hence, the TL alone is not sufficient to evaluate the silencers acoustic performance.
In addition to the TL, the absorption coefficient spectra are commonly studied to evaluate the silencer ability to absorb sound. This can be computed by utilizing the scattering matrix elements and normalizing the input sound power to 1W as:

$$A = 1 - |R|^2\frac{(1-M)^2}{(1+M)^2} - |T|^2, \qquad (11)$$

The absorption coefficient provides insight of how much incident sound power is absorbed. This is not adequate to evaluate the performance of the absorbing element of the silencer as soon as *R* becomes not negligible. In addition, the absorption coefficient is computed in linear domain while the sound perceived by the receiving person is in logarithmic scale.
Therefore, for optimization purposes, the sound actually entering the silencer has to be considered. This can be done by computing sound absorption (SA) instead of absorption coefficient as:

$$SA = 10\log_{10}\left[\frac{1 - |R|^2\frac{(1-M)^2}{(1+M)^2}}{|T|^2}\right], \qquad (12)$$

Also the sound reflected can be obtained in similar fashion as:

$$SR = -10\log_{10}\left[1 - |R|^2\frac{(1-M)^2}{(1+M)^2}\right], \qquad (13)$$

The set of TL, SA and SR will give detailed description of the silencer acoustic performance and quantification of dampened, absorbed and reflected sound power. Hence, the set of these logarithmic quantities is adequate to evaluate the goodness of the optimized silencer.

3. RESULTS

The normalized acoustic resistance and reactance of locally reacting surface inside the compact silencer prototype has been computed by means of Eq. 3, 4 and 7 for Res. 0.25 and Res 1.50 MPPs (See Tab. 1).

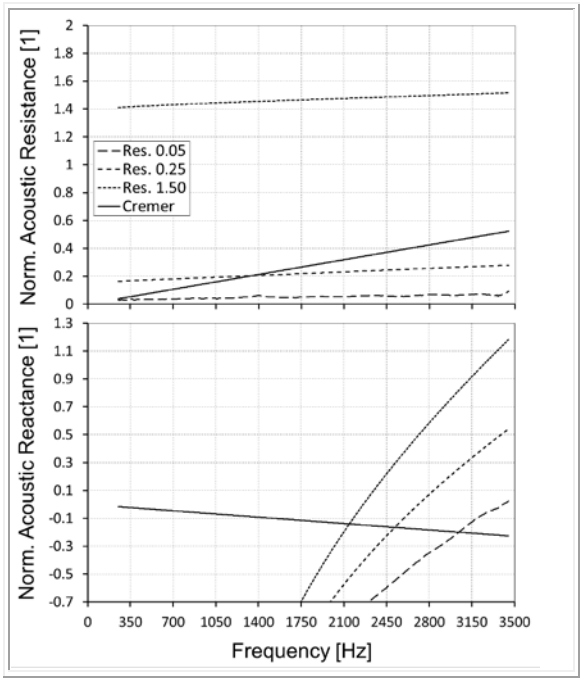

Fig. 2. Acoustic Impedance of the locally reacting surface inside the compact silencer prototype for no mean flow case.

The respective quantities of Res. 0.05 MPP are obtained by combining the experimentally determined transfer impedance with the Eq. 7 according to Eq. 2. These results are plotted in the comparison with the Cremer's optimum for no mean flow case in the Fig. 2.

In the Fig. 2 one can observe that, for none of the configurations, the total (Eq. 2) acoustic impedance is not matching exactly the Cremer's optimum. Nevertheless, the prototype provided with the MPP of Res. 0.25 is matching the above optimum at around 2.5 kHz, since the delivered normalized resistance is only 0.1 lower.

However, as the grazing flow on the surface of MPP generates additional contribution to the resistance (See Eq. 3), it is expected to match the Cremer condition even better when a mean flow through the silencer is introduced.

In the Fig. 3 the acoustic surface impedance of the configuration with the Res. 0.25 MPP is computed and compared to the Cremer optimum in case of 0.05 Mach mean flow condition.

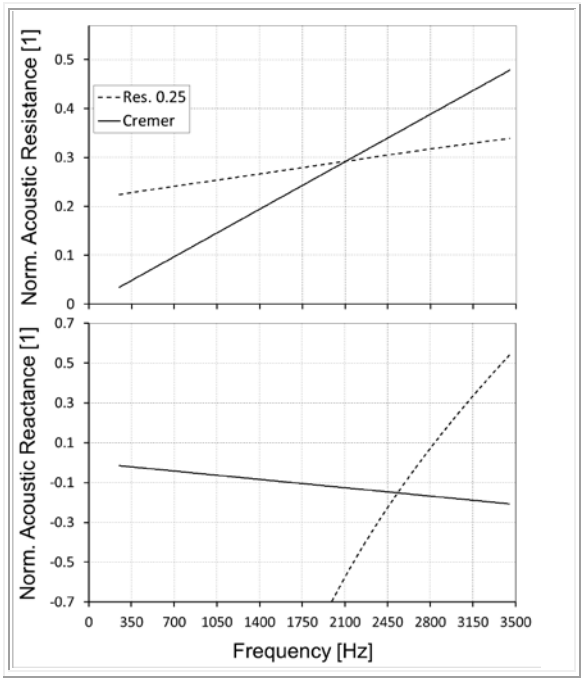

Fig. 3. Acoustic Impedance of the locally reacting surface inside the compact silencer prototype for 0.05 Mach mean flow case.

It can be seen in the plot (Fig. 3) that, in case of 0.05 Mach mean flow, the Cremer condition is closely fulfilled.

In the following figure (Fig. 4) the set of acoustic performance quantities (See Eq. 12 and 13) are plotted for the three compact silencer configurations in no mean flow conditions.

The wide and low TL peak of Res. 1.50 configuration in Fig. 4 indicates the absorptive type of damping which can be confirmed by observing the SA curve of the same configuration. In this setup the acoustic resistance is too large, i.e. the access to the cavity is restricted and, therefore, the cavity is not efficiently utilized.

Although this type of low reflection behavior (See the SR curve in the Fig. 4) is desirable in anechoic terminations, it is not

optimum in perspective of space, and hence it will not be considered further.

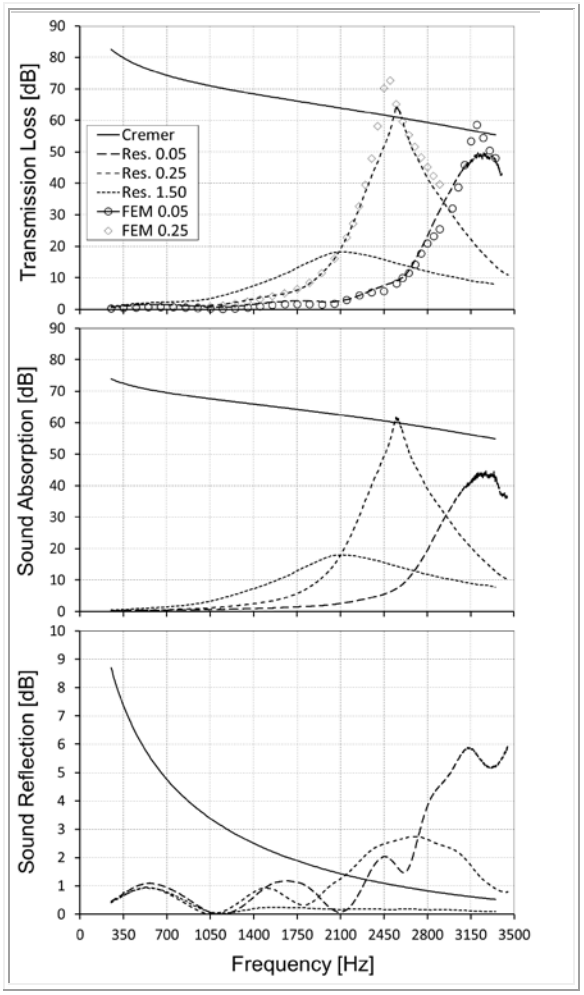

Fig. 4. Acoustic performance quantities under no mean flow conditions.

The other configurations in Fig. 4 have both high TL peaks. For this reason, by looking only at the TL spectrums, it would be hard prefer one over another. Nevertheless, by studying the SA an SR spectrums, the mechanism on sound damping is revealed. One has to note that the cut-off of the peak of the configuration Res. 0.05 is believed related with the experimental difficulties to realize the completely sealed cavities. This means that even higher reflection properties are expected.

The transfer impedance of the MPPs has been determined for planar elements, whereas the plates inside prototype are bended to tubular shape. Nevertheless, the numerical results of simplified FEM model presented in [9] are validated reasonably well for both configurations in the Fig. 4.

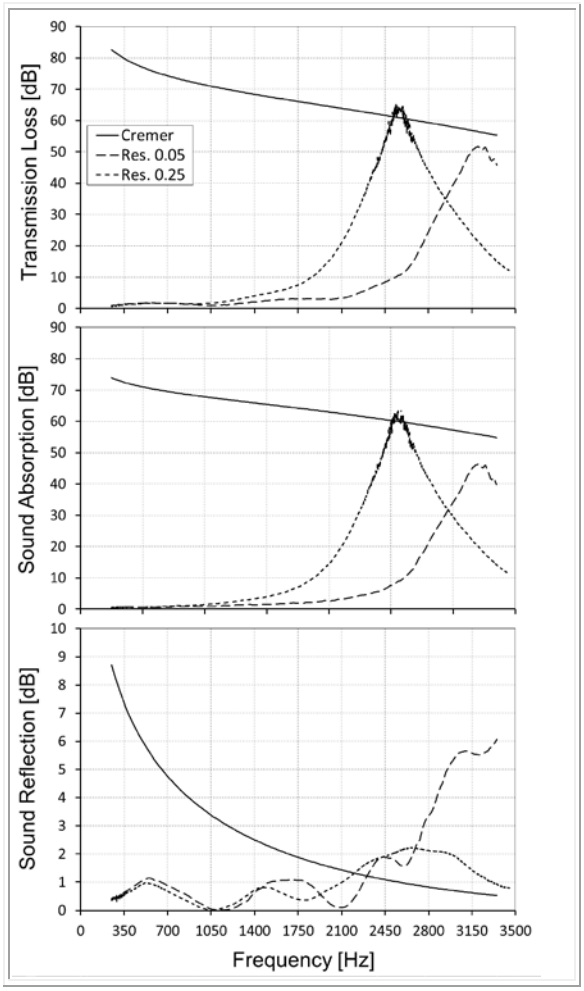

Fig. 5. Acoustic performance quantities under 0.05 Mach mean flow conditions.

Accordingly, this modelling technique can be efficiently utilized in the optimization process.

In the Fig. 5 it is observable that the absorption properties of the prototype configurations are unaffected and the reflection of sound has been reduced further at the resonance frequency.

4. CONCLUSIONS

In the present work a new type of compact silencer was proposed and experimentally investigated. In addition, the numerical model of this silencer has been validated.

It was shown that the sound transmission loss is not adequate for the acoustic performance assessment of the compact silencer.
To get better insight of the sound damping mechanism, another set of quantities, describing the sound power distribution, were derived and analyzed.
This enabled to evaluate whether in a certain configuration the absorption is optimal.
It was confirmed experimentally that the proposed compact silencer, optimized according to the Cremer's impedance, is a very effective solution for noise control.

5. REFERENCES

1. Regulation (EC) No 715/2007 of the European Parliament and of the Council, Official Journal of the European Union L171, 2007.
2. Rämmal, H.; Lavrentjev, J. "Sound reflection at an open end of a circular duct exhausting hot gas", Noise Control Engineering Journal, 2008, 56(2), 107-114.
3. Tiikoja, H.; Lavrentjev, J.; Rämmal, H.; Åbom, M. "Experimental Investigations of Sound Reflection from Hot and Subsonic Flow Duct Termination", Journal of Sound and Vibration, 2014, 333(3), 788 - 800.
4. Maa, D.-Y., "Theory and design of micro perforated-panel sound-absorbing construction," Science China Mathematics 1975, XVIII:55-71.
5. Knipstein, D., "Soundabsorbing element and procedure for manufacture of this element and use of this element", European Patent No. EP0876539, 23.01.1997.
6. Guo, Y., Allam, S., Åbom, M., "Microperforated plates for vehicle applications", Proceedings of Inter-Noise, 2008.
7. Allam, S., Åbom, M., "A New Type of Muffler Based on Microperforated Tubes", Journal of Vibration and Acoustics, 2011, 133(03):1005.
8. Åbom, M., Allam, S., "Dissipative Silencers Based on Micro-Perforated Plates", SAE Technical Paper Series, 2013, 2013-24-0071.
9. Kabral, R., Du, L., Åbom, M., Knutsson, M., "A Compact Silencer for the Control of Compressor Noise", SAE Technical Paper Series, 2014, 2014-01-2060.
10. Cremer, L., "Theory regarding the attenuation of sound transmitted by air in a rectangular duct…," Acustica, 1953, 3:249-263.
11. Tester, B. J., "The propagation and attenuation of sound in lined ducts containing uniform or "plug" flow," Journal of Sound and Vibration, 1973, 28(2):151-203.
12. Åbom, M., "Measurement of the Scattering-Matrix of Acoustical Two-Ports", Mechanical Systems and Signal Processing, 1991, 5(2):89-104.
13. Seybert, A., F., Ross, D., F., "Experimental Determination of Acoustic Properties Using a Two-Microphone Random-Excitation Technique", Journal of Acoustical Society of America, 1977, 61(5):1362-1370.

6. ADDITIONAL DATA ABOUT AUTHORS

Raimo Kabral, KTH, Tallinn University of Technology, kabral@kth.se.
Fabio Auriemma, Tallinn University of Technology.
Magnus Knutsson, Volvo Car Corporation.
Mats Åbom, MWL KTH Royal Institute of Technology.

7. ACKNOWLEDGMENTS

The financial support from European Union (7th Framework program) through Marie Curie actions initial training network FlowAirS (www.flowairs.eu) is greatly acknowledged.
The financial support of the ERMOS programme (Co-funded by Marie Curie Actions) is acknowledged too.

9th International DAAAM Baltic Conference
"INDUSTRIAL ENGINEERING"
24 - 26 April 2014, Tallinn, Estonia

DEVICE FOR CONTINUOUS CELLULOSE YARN DRYING AND FORMING

Koskinen, H.; Isomaa, T.; Lehto, J.; Stark, T.; Salmela, J.; Liukkonen, J.; Kiviluoma, P.; Widmaier, T. & Kuosmanen, P.

Abstract: *Cotton fibres are widely used for manufacturing of fabrics but cotton farming requires heavy use of agrochemicals and irrigation. However, it is possible to produce yarn directly from pulp fibres with no dissolution or disintegration process. This research describes design, manufacture and testing for a device which is used to dry and form continuously flowing pulp fibre suspension into yarn. The developed device described in this paper was capable of continuous manufacturing of fibre yarn and it established solid basis for future research.*
Key words: cellulose, fibre, yarn, cotton, wire, rayon

1. INTRODUCTION

Cotton farming covers 5 % of worlds farming area but it uses 11 % of all agrochemicals. Intensive farming of cotton has caused pollution to the waters, wear of the soil and it has changed the animal population. In the future highly pollutant cotton can be replaced by cellulose based materials. There are already alternatives to cotton. Rayon is a material produced from cellulose fibers but it still requires heavy chemical treatments [1].

One of the main motivations for this research was finding a method for taking advantage of new material by forming it mechanically into a yarn and enable of producing environmentally friendly material which can substitute for cotton and rayon.[1],[2] New method described later to produce cellulose based yarn is cleaner to the environment and it can use harvesting surplus. Finland's harvesting surplus alone could replace 20 % of the world's cotton demand [3].

Starting point for this research was the invention of new method for the manufacture of fibrous yarn [3,8]. The method was invented in Technical Research Centre of Finland (VTT). In previous research VTT has successfully manufactured short samples of the yarn. [4]

Target of this research was to develop a device that can produce cellulose based yarn continuously. Main function of this device is forming of the cellulose yarn. Based on experiences from laboratory scale manufacturing excess water must be compressed out while the yarn is simultaneously twisted to maintain the round cross section during the pressing (Figure 1).

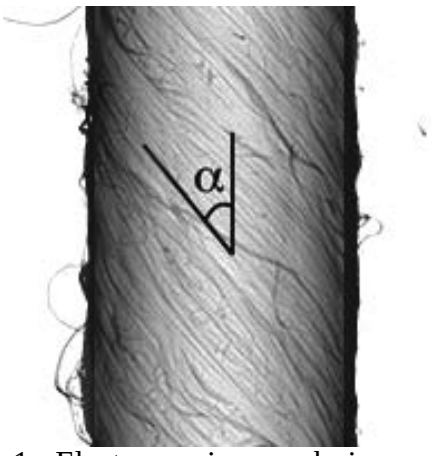

Fig. 1. Electron micrograph image of a rotated yarn where α is the turning angle of the yarn. [5]. Example is not from fibre yarn.

Research hypothesis was that if the pulp fibre suspension is extruded between two angled wires the compression will dewater the yarn and angular force element will twist the yarn and it will achieve its final form. The final result would resemble ordinary cotton yarn. [6]

This paper describes how the main functions of the process have been solved and how they are technically implemented. Part of this research was also seeking the proper parameters for producing the yarn and find out how speed, pressure and rotating angle affect to the quality and properties of the yarn in this case. [7]

2. MATERIALS AND METHODS

VTT has invented and patented a completely new method for producing cellulose based yarn [8]. The results from earlier experiments show that material properties of this new type of cellulose yarn are promising and good quality yarn has already been made. Previous experiments are made in laboratory scale and produced yarns have not been long enough for making e.g. fabric out of them.[4]

Initial shape of the yarn is achieved through fast suspension crosslinking right after the special nozzle before hitting the wire. In the nozzle rheology modifiers prevent clocking and the fibres are oriented with the flow [8]. Different compounds are pumped through the nozzle with synchronized speeds and as they get mixed the crosslinking prevents further mixing and initial dewatering with gravity. Figure 2 schematically illustrates the process in the nozzle.

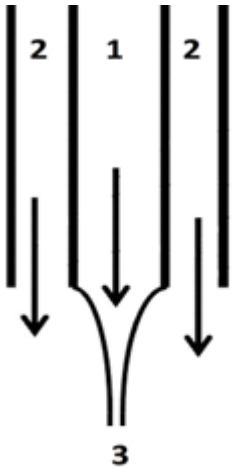

Fig. 2. Schematic illustration of the nozzle. Fiber suspension with rheology modifiers (1) salt water (2) gel yarn (3). [8]

Wet gel yarn is extruded directly to the lower wire which conveys the material between upper and lower wires. When the yarn encounters the upper wire the water begin to be compressed out of it. The diameter of yarn decreases when it moves along between the wires. Wires are aligned so that the gap between them decreases when approaching the output point and wire angle difference in X-Y direction maintains the yarn rotation while pressing.

All free water is removed by pressing the yarn between the wires. At this point the strength of the yarn is sufficient for reeling and the final drying takes place there. In the future also drying is included to this device.

Angular adjusting of the wires is implemented by two-pieced frame. Lower frame part is solid and upper frame can be rotated. Upper frame rotates along two conductors and it is lockable. Conductors permit slight movements also in horizontal plane.

Frame of the device is designed to be easy to adjust and maintain. The final construction is seen on the Figure 3.

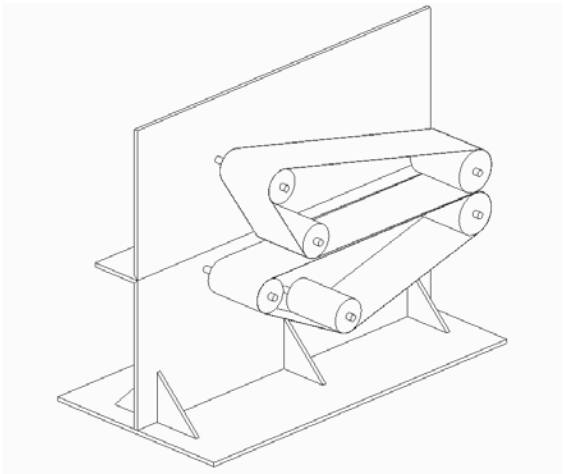

Fig. 3. Basic layout of frame and wire arrangement.

The frame of the device is required to have high stiffness because rollers are attached only from one end and they must stay well aligned to get the yarn to uniform quality. Adding features and modifying the placement of the rollers for possible upcoming needs should be easy.
The speed of the wires must be accurately adjustable to get the operating speed synchronized with the pump that is feeding the material. The operation of wires is done individually with two PC controlled AC servo motors. The velocities can be automatically synchronized to each other by giving the amount of deviation in angularity of wires.
In the first operating tests the device is being used for drying woolen yarn that has been soaked into water. With this kind of yarn different parameters can be tested to get the yarn to go nicely between the wires while getting its shape.

3. RESULTS

As a result of this project a fully functional and highly adjustable device for drying and forming cellulose yarn is designed and manufactured. The device can handle yarn speeds up to 10 m/s. The preliminary tests were performed with speed of 1 m/s. At low speed it is possible to optimize nozzle position and relations of wire speeds.

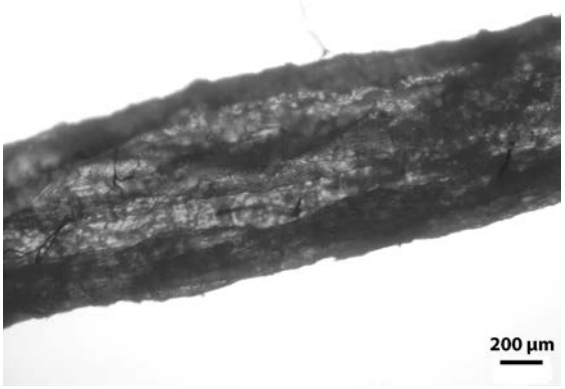

Fig. 4. Optical microscopic image of fibre yarn manufactured by the developed device.

Main production parameters were chosen by experimental tests, where effect of each parameter on the form of yarn was studied. The final parameters were wire speed, rotating angle and space between the upper and the lower wire. By changing the wire angle in X-Y plane the force rotating the yarn at horizontal plane is changed. Gap between the wires affect the compression pressure and it can also change the yarn rotation by changing friction force.
Rough adjusting for these parameters was based on results of visual inspection of the yarn (Figure 4). The main goal at this point was to produce yarn continuously. The specific properties of yarn (constant diameter, tensile strength) were minor issues. The results of the preliminary tests were promising and established solid basis for future research.

4. DISCUSSION

The purpose of this project was to develop a device to continuously produce yarn directly from pulp suspension. The way of turning fibre suspension into a yarn is completely new and the developed device is first of its kind. Achieved results were compared to manually manufactured cellulose yarn and commercial yarn made from cotton. The yarn produced by the device has very similar properties compared to untreated cotton yarn.
The device can be easily adjusted for future

needs. For example operating speed and reliability needs to be improved before commercial use. Upcoming needs have been taken into account when choosing materials and actuators. In the future this machine can produce cellulose yarn continuously at very high speeds. Even higher speeds than 10 m/s are possible but then at least motors and drive pulleys needs to be changed.

The results are giving a good basis for the further research and development. In this project goal was to find rough parameters for the speed and position of the wires. Correct wire speeds and positions make continuous process possible. Even if the device and process are still under development, the basic concept of the machine is fully working and adjustable.

The studies in the future can focus on improving the quality of the yarn when the parameters affecting yarn quality are more precisely defined. If the angle and distance of the wires could be accurately adjustable by computer while the process is ongoing even longer and better shape yarn could be manufactured.

With similar treatments as used with cotton yarn, cellulose yarn can reach comparable properties to cotton and can be utilized in fabrics. Raw cellulose material costs less than cotton which makes it also economically interesting. In addition, cellulose yarn is environmentally friendly. Raw material for cellulose can be gathered for example from harvesting surplus.

5. AUTHORS

CORRESPONDING ADDRESS

Panu Kiviluoma, D.Sc. (Tech.)
Aalto University School of Engineering, Department of Engineering Design and Production
P.O. Box 14100
00076 Aalto, Finland
Phone: +358 50 433 8661
E-mail: panu.kiviluoma@aalto.fi
http://edp.aalto.fi/en/

ADDITIONAL DATA ABOUT AUTHORS

Isomaa, Tuomas
E-mail: tuomas.isomaa@aalto.fi

Koskinen, Hans
E-mail: hans.koskinen@aalto.fi

Lehto, Jyri
E-mail: jyri.lehto@aalto.fi

Stark, Tuomas
E-mail: tuomas.stark@aalto.fi

Salmela, Juha, M.Sc.
E-mail: juha.salmela@vtt.fi

Liukkonen, Johanna, M.Sc.
E-mail: johanna.liukkonen@vtt.fi

Widmaier, Thomas, D.Sc. (Tech.)
E-mail: thomas.widmaier@aalto.fi

Kuosmanen, Petri, D.Sc. (Tech.), Professor
E-mail: petri.kuosmanen@aalto.fi

6. REFERENCES

1. Smet, E., Lens, P., & Van Langenhove, H., Treatment of Waste Gases Contaminated with Odorous Sulfur Compounds, Critical Reviews in Environmental Science and Technology, 1998, 28:1, 89-117.

2. Qiu, X., Zhu, T., Li, J., Pan, H., Li, Q., Miao, G. & Gong, J. Organochlorine Pesticides in the Airaround the Taihu Lake, China, Environmental Science and Technology, 2004, 5:1, 1368-1374.

3. Finland to lead the way as a designer of cellulose-based products, VTT internet article, URL: http://www.vtt.fi/news/2013/02102013_DDWoC.jsp?lang=en (22.3.2014)

4. Harlin, A., Joint research into forest-based Biomaterials - Industrial

Biomaterials Spearhead Programme, 2009 Wood and Fiber Product Seminar, 2009, 263, 6-12.

5. Carbon nanotubes give artificial muscles a new twist, Royal Society of Chemistry, internet article, Referred in 11st of May 2014, URL: http://www.rsc.org/chemistryworld/News/2011/October/13101104.asp (22.3.2014)

6. Balasubramanian, N., Rotor Spinning – influence of fibre properties, yarn quality compared to ring spinning, preparatory and post spinning, Asian Textile Journal, 2013, 22:7, 67-74.

7. Hashemi, S.J., Crotogino, R.H., & Douglas, W.J.M., Effect of Papermaking Parameters on Through Drying of Semi-Permeable Paper, Drying Technology: An International Journal, 2007, 15:2, 371-397

8. WO2013034814, Method for the manufacture of fibrous yarn, fibrous yarn and use of the fibrous yarn, VTT, Jyväskylä, Finland, (Salmela, J. Kiiskinen, H. Oksanen, A.), WO2012FI50877 20120910, 14.03.2013, 18 p.

9th International DAAAM Baltic Conference
"INDUSTRIAL ENGINEERING"
24-26 April 2014, Tallinn, Estonia

ON CHAOS CONTROL IN HIERARCHICAL MULTI-AGENT SYSTEMS

Källo, R.; Eerme, M. & Reedik, V.

Abstract: *The present paper is focused on the problems of chaos control in multi-agent hierarchical systems similar to the environment of the realization of automated factory projects. The basis for this research is a unique database of empirical studies of human faults and mistakes at the design and commissioning of factory automation systems. It is shown that for primary chaos control it is appropriate to use Design Structure Matrix (DSM) technology tools, enabling to describe synergistic relations between all teams' members on the basis of the frequency and amount of information interchange. For further chaos control an effective system is proposed to track and hinder different human shortcomings spreading in the hierarchical teamwork system. As a basis for it an advanced simulation technique - discrete event modelling is used. The proposed methodology of suppressing the influence of human shortcomings allows us to increase the synergy in teamwork and to substantially reduce the losses of resources at starting-up new factories.*
Key words: chaos control, factory automation, control systems design, teamwork management, synergy deployment.

1. INTRODUCTION

The losses of resources at the start-up of new automated factories caused by human shortcomings reach up to 5-10% of whole labour costs and tend to increase with the growing complexity of control systems. That is without any doubt too much, thus requiring the reasons for the misspent resources to be cleared up.

It is a reality that from the engineering side automation systems have become more and more complex. At the same time the amount of data and variables circulating in these systems have enormously increased. Therefore, the need for systems engineering is growing owing to a steady increase in systems complexity [1, 2, 3]. The described above technical background has paved the way for a substantial increase of the role of engineering competence and human shortcomings [4]. This situation has initiated a new wave of research into human shortcomings at the beginning of the present century [5].

The firm basis of any research in the field of the effectiveness of human cooperation is its reality database concerning empirical studies of human shortcomings. The existence of such a unique database gives confidence about "bad" engineering and authenticity of the results attained by theoretical research, developed on this basis. During the last 20 years, the authors' research activities have been focussed on the empirical research into human shortcomings in the field of the quality of engineering design activities.

At first, a service database for non-safety-critical mechatronic office equipment was completed on the basis of which the concept of negative and positive synergy was developed [6]. Next a human shortcomings database was developed for factory automation design and commissioning, for the design of pneumatic and hydraulic control systems

for industrial equipment and the design and production of serial light fittings. All these efforts were integrated into the fifth database of human shortcomings in quality management [7]. At the same time it has been the starting platform for the present research which was initiated with compiling a new advanced database of human shortcomings in factory automation systems design and commissioning. This database covers 26 automated factories on three continents, including pulp and paper mills, chemical and petrochemical plants and power stations [8].

The experience of the research group has shown that human shortcomings can be treated as a result of negative synergy in mutual or inner communication of team members and due to the lack of competence or inability in managing the teamwork in highly competitive environment [4]. In this context it is appropriate to define the concept of synergy which is used in the present paper. According to Oxford Dictionary the word *synergy* or *synergism* refers to the integration or cooperation of two or more drugs, agents, organizations, etc. to produce a new or enhanced effect compared to their separate effects. However, synergy has a qualitative and a quantitative side. Changing the input parameters of the system may result in dramatic changes in the system's behaviour [9]. Qualitative changes in synergy have enabled using it in lattice dynamics, laser technology, superconductivity etc. Quantitative synergy effects have also been used successfully in business and engineering. Despite the wide existence of synergy effects in nature and artefacts, the real deployment of synergy in engineering is often hidden behind the terms of optimization, rationalization, effectiveness, etc.

For the better integration of all these matters the synergy-based approach is used in the present research, which aims to compensate mutual weaknesses and to boost the beneficial features at joining technologies and human activities. The synergy-based approach to the start-up difficulties of factory automation systems is comparatively new, providing a real opportunity to analyze the reasons of human-based start-up impediments and to plan the measures to avoid them [10].

2. CHAOTIC BEHAVIOUR IN HIERARCHICAL MULTI-AGENT DECISION MAKING SYSTEMS

In the calendar plan the process of automated factory design covers the drafting of the general description of the system, detailed task description for system configuration and a factory acceptance test, followed by commissioning. First of all, the owner names responsible persons in his team to keep watch on the progress of building a new production plant and to transfer his own requirements and necessary competence from the already existing production. Next, to run the project a consultant company is hired to integrate all efforts of project and commissioning groups. The task of the consultancy group is to forward the owner's requirements to the process supplier(s). After that, it is necessary to collect the resound data from the process supplier(s), convert them into the required format, get approval from the owner and give this input information to the automation supplier. Then the automation supplier starts system configuration, including application software programming, human-machine interface and process interface configuration. After the configuration is complete and the automation system is tested in the workshop of the automation supplier (Factory Acceptance Test), it is delivered to the factory and integrated with the process supplier's equipment. The activities continue with commissioning, where a lot of additional specialists are involved in the project team. A separate commissioning team is formed which includes members from project teams.

Also, the end users are part of commissioning, getting trained to run the plant at the same time.

The described above system is a hierarchy where the information of completed tasks is transferred from one team to another within the scheduled time. Such a multi-agent distributed artificial intelligence system is very sensitive to tainted information transfer [11; 12]. It is inevitable that an agent's decision also depends on the decisions made by another agent upper in information flow. This obstacle makes the whole system extremely complicated and nonlinear. If agents use tainted or imperfect information, they tend to make poor decisions. In summary, it leads to the chaotic behaviour of downward agents and downgrading the performance of the whole system. In such a way human shortcomings may cause real chaos in automated factory design and commissioning.

For the present research a detailed database of human shortcomings in factory automation system design and commissioning for the years 2006-2013 was compiled. The newly introduced advanced classification of human shortcomings is shown in Fig. 1.

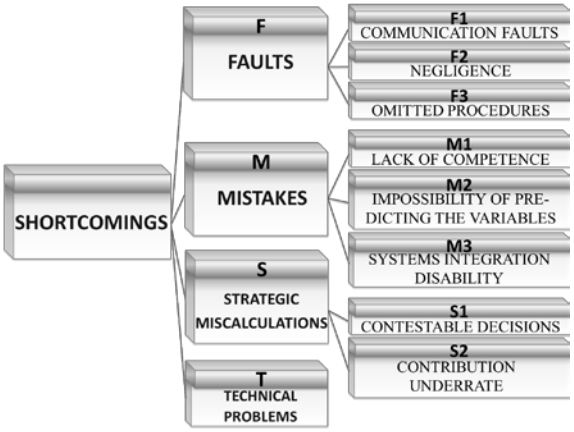

Fig. 1. Advanced classification of human Shortcomings

In this new database human shortcomings are divided into three main categories – faults, mistakes and strategic miscalculations. The faults class **F1** includes all misunderstandings in communication between the client, consultant and the design teams or between design team members. **F2** joins together all shortcomings connected with negligence. All transfers of unsuitable or late information and documentation in the design process are classified into the faults class **F3**.

Mistakes have a far more complicated nature. To this category belong wrong decisions **M1**, caused by lack of core competence. Mistakes **M2** are conditional and are caused by the impossibility of predicting the production process characteristics at the moment of design and they may be resolved in the course of further projects activities. The third class **M3** includes mistakes caused by system integration disability that leads to the situation where technologies cannot be integrated due to their different level of development. A new differentiated category of human shortcomings is strategic miscalculations **S**. Contestable decisions **S1** may be made due to the temptation to use cheaper or simple technical solutions that are not able to grant the necessary operating ability and quality. Contribution underrate **S2** is a very spread phenomenon in a highly competitive society when under market pressure unreal obligations are accepted. A special category here is that of technical problems **T** which involve classical reliability problems.

In Fig. 2 the statistics of shortcomings for factory automation system design and commissioning is presented. For obvious reasons the factories involved are confidential.

As there are data included about 26 factories it is possible to presume the probability of any human shortcoming during the ongoing project. The impacts of shortcomings in the project for teams involved in automation design and commissioning are in average between 1500 and 3000 working hours. Additionally, there are losses of profit caused by the late start of production. The

real number and impact of shortcomings depends on the competence of the project team and also on the complexity of the task. As any of the shortcomings may lead to chaos its control is extremely important.

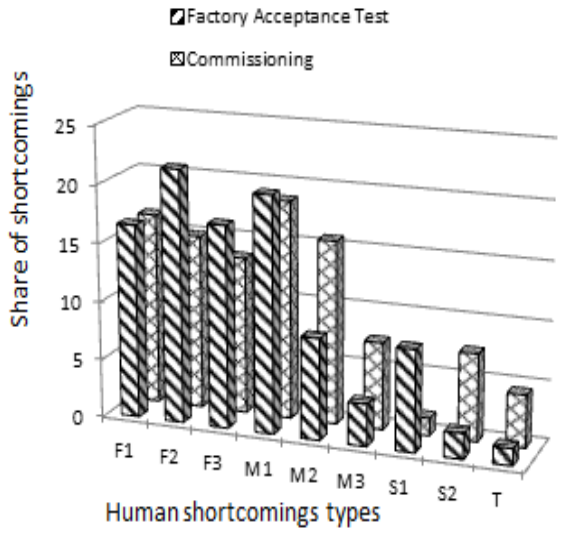

Fig. 2. Statistics of shortcomings for the design and commissioning the automated factories

Classical solutions for chaos control [11] do not apply to the present specific hierarchical task and it is necessary to find a new strategic approach to solve the problem. In the present research a two-step approach is proposed. At first an exhaustive synergistic information transfer system should be created suppressing the development of chaos from the very beginning. And finally inhibitive chaos control for the spreading of human shortcomings must be developed.

The search for a powerful tool for describing human relations and grouping them on the basis of their cooperation tasks resulted in proving the Design Structure Matrix (DSM) technology to be the most suitable [5]. The additional value of DSM technology is the wide choice of mathematical tools to exploit the information concentrated in the DSM matrix. The mathematical treatment of DSM matrixes enables us to form the most capable teams, to schedule and evaluate their activities, to create an optimal communication and cooperation scheme where the competences and capabilities of the teams and their members can be entirely exploited [13].

3. BASIC CONCEPTS FOR INHIBITIVE CHAOS CONTROL

The above described discussions have led to the understanding that the best way to cut losses of resources at automated factory design and commissioning caused by human shortcomings is to create an effective system to track and hinder the different human shortcomings spreading in the hierarchical teamwork system. In Fig. 3 the structure of the proposed system is presented.

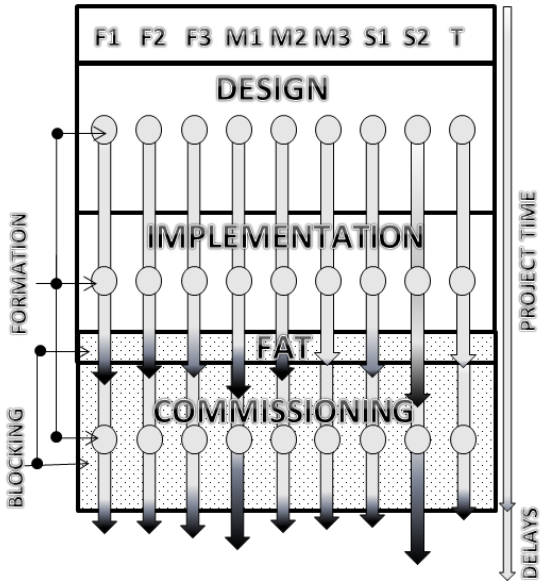

Fig. 3. Impact of shortcomings on the whole project time

The formation zones of shortcomings are shown as integrated ones taking into account that origination of the human fault or mistake may happen at any moment on the time-scale. The same applies to the blocking zones of shortcomings. Behind the arrows of shortcomings impacts are the real working hours spent on the correction of the specific shortcoming impact. The overrun of the longest arrows on the time-

scale is conditional as it depends on how many human resources with necessary competence can be concentrated on eliminating the impact of shortcomings. As it is seen in Fig.3 the most dramatic losses can be caused by lack of competence (M1) and contribution underrate (S2). The project time depends on the complexity and novelty of the designed factory. The simplest projects last about 0.5 and the more complicated ones up to 4 years, having the average duration of 1...1.5 years.

The formation of human faults and mistakes is fully accidental and therefore project activities are more or less chaotic. However, the chaotic nature of designing and commissioning automated factory projects never results in a catastrophe where the project has to be stopped. During commissioning all the impacts of shortcomings will be removed and production will be launched. The profitability and competitiveness of a new factory is another question.

Planning the duration of a project has presumably a probabilistic nature leading to the field of soft computing. It is a very complicated area as at iterations the new or corrected information can appear at any moment of the process of rework. At the same time the amount of repetitive work is reducing according to the learning curve. On the basis of the probabilistic analysis of the wrong actions of decision-making agents special tracking maps can be completed enabling us to evaluate the probabilistic dangerousness of the different types of faults and mistakes. These maps are completed by integrating the synergy-based approach into information management with the use of an advanced simulation technique - discrete event modelling. This approach allows computing probability distribution of lead-time in the project network where iterations take place among sequential, parallel and overlapped tasks. So we reach the complete treatment of the evaluation of the time losses due to the faults and mistakes in information transfer taking into account necessary iterations, reworks and learning curves [14].

In Fig.4 the typical result of discrete event modelling is shown giving an idea of the probabilistic nature of any arrow in Fig. 3.

Finalizing the results of the present research it is possible to aver that the full picture about the formation of human shortcomings, their impact and blocking activities has been attained. It is proved that the most powerful effect on the neutralization of human shortcomings is achieved by increasing synergistic information transfer procedures between all project teams and their members. As a result, a concept for the probabilistic evaluation of project duration is proposed, which is of great importance in project planning stage.

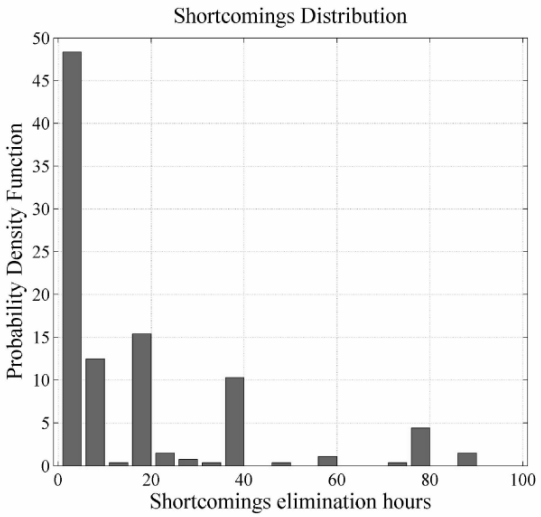

Fig. 4 Example of the probabilistic prediction of the time for shortcoming results removal

4. CONCLUSIONS

The research efforts in the area of automated factory design and commissioning have given sufficient evidence that most of the troubles with quality are caused by shortcomings in human activities.

It is shown that a capable tool for suppressing human shortcomings is Design

Structure Matrix (DSM) technology enabling us to visualize the synergy relations in information interchange between both development projects working groups and between the group members. The DSM technology allows us to form the most capable teams and to schedule their activities and predict the time necessary to complete the project. The proposed methodology of tracking and hindering human shortcomings at automated factory design and commissioning presents an opportunity to increase synergy in teamwork and so to substantially reduce the losses of start-up new factories.

5. REFERENCES

1. Seilonen, I., Pirtioja, I., Koskinen, K. Extending Process Automation Systems with Multi-Agent Techniques. *Engineering Applications of Artificial Intelligence,* 2009, **22**, 1056-1067.
2. Samad,T., McLaughlin, P., Lu.J. System Architecture for Process Automation: Review and Trends. *Journal of Process Control*, 2007, **17** , 191–201.
3. Jämsä–Jounela, S.-L. Future Trends in Process Automation. *Annual Reviews in Control*, 2007, **31,** 211–220.
4. Kaljas, F., Källo, R., Reedik, V. Human Aspects at Design of Mechatronic Systems. *Proceedings of the 9th Mechatronic Forum International Conference*. Ankara, Turkey, Atilim University Publications, 2004, 147-157.
5. Eppinger, S.D. A Planning Method for Integration of Large-Scale Engineering Systems. In *Proceedings of the International Conference on Engineering Design ICED'1997*. Tampere, 1997, 19-21.
6. Tähemaa T., Reedik, V. Positive and Negative Synergy at mechatronic Systems Design. In *Proceedings of International Conference Nord Design 2000*, DTU Publications, Copenhagen, Denmark, 2000, 35-44.
7. Hindreus, T., Reedik, V. Synergy-Based Approach to Quality Assurance, *Estonian Journal of Engineering,* 2009, **15,** 87-98.
8. Källo, R., Eerme, M., Reedik, V. Ways of Increasing Synergy in Automated Factory Design and Commissioning Teamwork, *Journal of Material Science and Engineering B,* 3 (9), 2013, 597-604
9. Haken, H. *Synergetics*. Springer-Verlag, Berlin, 2004.
10. Hindreus,T., Kaljas, F., Källo, R., Martin, A. Tähemaa,T. and Reedik, V. On Synergy Deployment in Engineering Design. *Journal of Material Science and Engineering B,* 2(6), 2012, 408-413
11. Ivancevic, V.G., Ivancevic, T.T. *Complex Nonlinearity: Chaos, Phase Transitions, Topology Change and Path Integrals*. Springer-Verlag, Berlin, 2008.
12. Mikhailov, A.S., Calenbuhr, V. *From Cells to Societies: Models of Complex Coherent Action.* Springer-Verlag, Berlin, 2002.
13**.** Eppinger, S. D. and Browning, T. *Design Structure Matrix Methods and Applications.* Massachusetts Institute of Technology. Cambridge, MA., USA, 2012.
14. Cho, S.H., Eppinger, S.D. Product Development Process Modelling Using Advanced Simulation. In *Proceedings of ASME Design Engineering Technical Conference DETC'01*. Pittsburg, Pensilvania, USA, 2001, 1-10.

6. CORRESPONDING AUTHOR

Ph. D. Student Rommi Källo,
TUT, Department of Machinery
Ehitajate tee 5, 19086 Tallinn, Estonia
Phone: +3725096788
Fax:
E-mail: rommi.kallo@hecc.ee

9th International DAAAM Baltic Conference
"INDUSTRIAL ENGINEERING"
24-26 April 2014, Tallinn, Estonia

ACOUSTIC STUDIES ON POROUS SINTERED POWDER METALS

Luppin, J. & Auriemma, F.

Abstract: *In response to strict environmental noise regulations the development of novel types of silencing materials is essential.*

The composition of the porous sintered powder metals (PSPMs) studied in this paper is based on the formation of sintered powder particles providing internal micro-paths (tunnels and pores) and cavities.

In the micro-path the energy dissipation of the acoustic waves is primarily originated by thermal and viscous losses.

The transfer impedance and absorption as the key parameters are presented and analysed for the PSPM samples designed. In order to study the influence of loudness on the acoustic performance the test samples are exposed to a variety of sound excitation levels during the experiments.

Key words: Porous sintered metals, acoustic properties, scattering matrix, sound absorption, excitation levels.

1. INTRODUCTION

1.1 Acoustic materials for noise control

Once noise and vibration sources of machinery have been identified, the sound field around the receiver can be modified to achieve satisfying solution. The typical engineering solutions applicable for noise control are the vibration isolators, sound barriers, acoustic absorbing elements, or enclosures around noise sources for the protection of passengers in vehicles. Today, sound-absorbing materials are increasingly implemented in aircraft, spacecraft and ship structures, especially around the major noise sources – the engines. As the development of vehicles is accounting for higher load capacity, reliability, ergonomics, fuel economy and cost effectiveness, the solutions with low weight and well tuned noise cancellation properties are endeavoured.

In this paper the development of novel sound absorbing materials is in focus. Challenging to achieve an acoustic material, which provides high sound absorption in a desired frequency range while being technologically cost effective and lightweight, a number of solutions have been presented by various authors [1-9] during the recent decades.

Traditional porous materials, like fibres, wools and foams, have been the most commonly utilized materials in duct acoustics for almost a century [10]. Nowadays environmental issues have redirected the interest of the market towards absorptive elements where fibres and wools are typically avoided. The primary concerns associated with those porous materials are the non-renewability, the deterioration of the performance over time and the possible separation of small particles that pollute the surrounding media [6, 9]. One of the recent trends in acoustic panels (including aero engine liners) is the introduction of various solutions where the noise cancellation effect is originating from the viscous friction that occurs inside a number of micro-paths (e.g. in micro-perforated or micro grooved elements [2-9]. Such an absorption principle is also applied in the design of the PSPM's presented in this paper. Naturally, the absorbing materials absorb most of the acoustic energy affecting them and reflect little.

These materials are used in a variety of locations, usually in the vicinity of the noise sources (e.g. engines), in various paths (barriers), and in some situations close to a receiver (inside earmuffs) [11]. Recent advances in material science, chemistry, and nanotechnologies have made a contribution in development of the design, production and acoustic performance of absorbing materials. These novel solutions [11] include the use of natural fibres, bio-based polymers, recycled and surplus materials, new composites, smart materials and the porous metals treated in this paper (see section 2.1).

1.2 Acoustics of porous materials

A porous absorbing material is a solid that contains cavities, channels or interstices, which sound waves can enter or pass through. A schematic representation of a porous solid material layer is shown in Fig. 1.

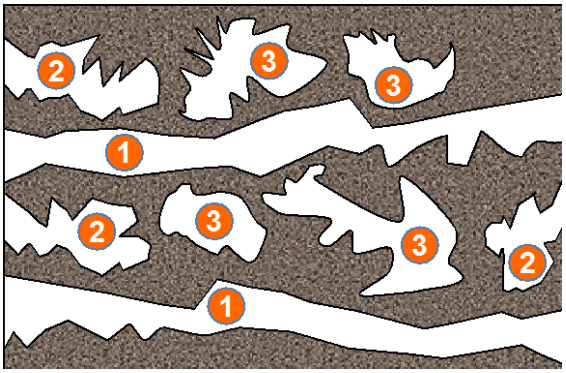

Fig. 1. A simplified schematic representation of cross-section of the porous material layer. 1-pores open at two ends (channels), 1-pores open at one end, 3-closed pores. According to [11] the pores that are totally isolated from their neighbours have an effect on some macroscopic properties of the material such as its bulk density, mechanical strength and thermal conductivity. Regarding he absorption of sound the closed pores are substantially less efficient than the open pores as the open pores "communicate" with the external surface of the material, and therefore have more influence. Based on [11] the open pores can be distinguished as "blind" (open only at one end) or "through" (open at two ends). A practical convention is used to make a distinction between porosity and roughness, which assumes that a rough surface is not porous unless it has irregularities that are deeper than they are wide [11]. Porous absorbing materials can be classified as cellular, fibrous, or granular as studied in this paper. This is based on their microscopic configurations.

To influence the surrounding sound field and to provide desired noise cancellation the characteristic surface of the porous materials allows the sound waves to enter the material through a number of small holes or openings [12-14]. When such porous material is exposed to incident sound waves, the air molecules at the surface of the material and within the pores of the material are forced to vibrate. This process naturally involves the thermal and viscous losses inside the pores (see Fig. 1) where part of the acoustic energy is converted into heat and consequently the absorption of sound takes place.

2. EXPERIMENTAL STUDY

2.1 Powder metal samples tested

The experiments were carried out on two planar PSPM samples developed (see Fig. 2 and Table 1). The samples were manufactured by Materials Engineering Department in Tallinn University of Technology (TUT), following a powder metallurgical process described hereafter.

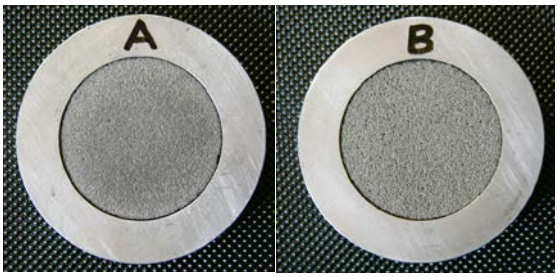

Fig. 2. Photos of the PSPM samples A and B (left and right) fitted in Aluminium rings for mounting into test-rig.

sample mark	diameter (mm)	height (mm)	granule size (mm)	porosity (%)
PSPM-A	42	7.1	0.16	76
PSPM-B	42	3.7	0.16	81

Table 1. Characteristic data of the PSPM samples tested.

A stainless steel alloy with Cr and Ni content (X18H15-160-24, an analogue to AISI 316L) [15] powdered to granular size of 0,16mm was used. The material was sintered in vacuum, by following a constant temperature rise of 10 °C/min up to 1200 °C. The temperature and pressure conditions achieved were maintained for 30min after which the compound was cooled down 8…10 °C/min. Recovering the atmospheric conditions the samples were removed and prepared for the acoustic investigation. In order to mount the samples in a measurement section of the acoustic two-port test facility, described in [8 - 9], the circular PSPM samples were fitted into aluminium rings, as shown in Fig 2.

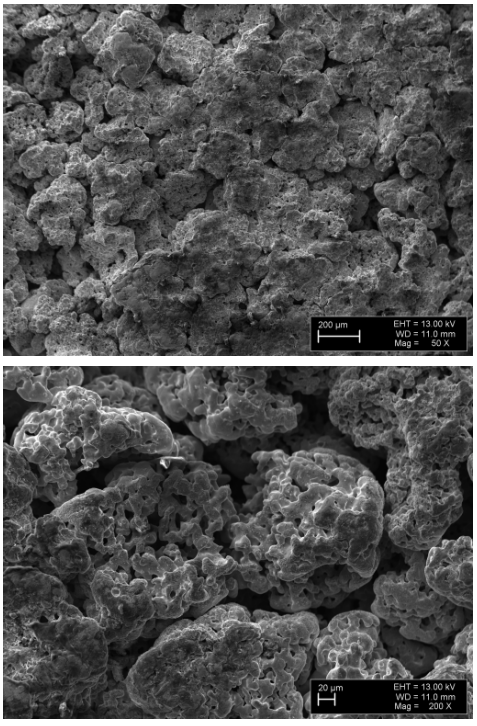

Fig. 3. Microscope images of the surface of the PSPM sample A. Magnification 50X, distance marking 200 µm (above) and 200X, distance marking 20 µm (below).

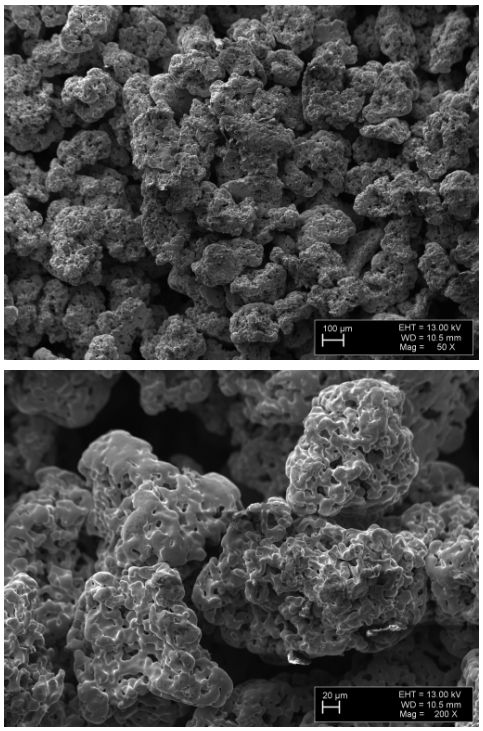

Fig. 4. Microscope images of the surface of the PSPM sample B. Magnification 50X, distance marking 100 µm (above) and 200X, distance marking 20 µm (below).

A scanning electron microscopy (SEM) was performed to observe the composition of the PSPM materials developed. The images captured at the surfaces of the samples A and B are shown in Fig. 3 and 4.

2.2 Comparison material samples tested

Additionally to the PSPM samples, a recently introduced solution a micro-grooved (MG) element [6, 9] and a sample made of commercially available absorptive wool (density 550 kg/m^3, glass fibre Ø8…19µm, see Fig. 3) were included as reference materials for comparison.

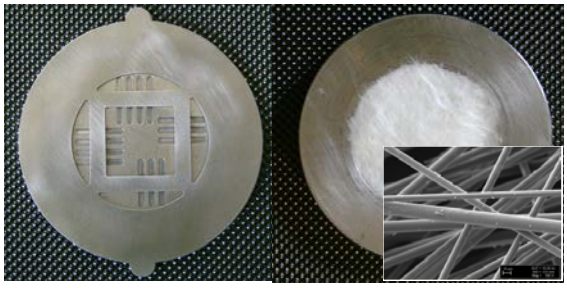

Fig. 3. Photos of the MG element sample (left) and the wool sample (right, including a 500X magnified SEM image).

2.3 Experimental procedures

Experiments have been performed in the acoustic laboratory of Tallinn University of Technology (TUT), which is equipped with a dedicated test facility for the characterization of acoustic one- and two-ports in a variety of operating conditions, described in details in [8, 9, 16, 17]. All tests performed with planar elements have been carried out in the absence of mean flow by using the classical two-port method [10].

2.4 Determination of the acoustic parameters

In this paper the transfer impedances together with the absorption coefficients of the samples, coupled with a 27 mm back cavity, have been determined experimentally. The transfer impedance, also known as separation impedance, is believably the most suitable parameter for the characterization of the performance of permeable materials. It represents the ratio between acoustic pressure drop Δp through the material and the normal particle velocity [1, 9, 10].

Let p_a and p_b represent the respective sound pressures upstream and downstream of the acoustic element and u_a and u_b the respective particle velocities.

For acoustically thin samples, i.e. for samples with thickness much smaller than the wavelength, it is reasonable to assume a single particle velocity across the material, i.e. $u = u_a = u_b$.

The transfer impedance can be then defined as: $Z_{tr} = (p_b - p_a)/u$. The normalized transfer impedance, z_{tr} is $z_{tr} = Z_{tr}/(\rho c)$, where ρ is the air density and c is the speed of sound.

In this work, the transfer matrix **T** of PSPM samples [18] has been computed in order to determine the transfer impedance associated.

In particular **T** relates the acoustic pressures p_a and p_b with the volume velocities q_a and q_b (where $q_a = u_a*A$, $q_b = u_b*A$ and A is the sample area) according to the following relationship:

$$\begin{pmatrix} p_b \\ q_b \end{pmatrix} = \begin{bmatrix} T_{11} & T_{12} \\ T_{21} & T_{22} \end{bmatrix} \begin{pmatrix} p_a \\ q_a \end{pmatrix} \quad (1)$$

It can be shown that, under the assumption of constant particle velocity across the sample, $T_{11}=1$, $T_{21}=0$, $T_{22}=1$ and $T_{12}=(p_1-p_2)/q$, where $q=q_a=q_b$. By multiplying T_{12} with the sample area A, the transfer impedance is computed.

Once the transfer impedance is known, the absorption coefficient (α) of the element can be determined as shown in [9].

In particular, when a thin acoustic element is coupled with a back cavity, the transfer impedance of the panel and the cavity impedance (Z_{cav}) form a series (Z_{tot}): $Z_{tot} = Z_{tr} + Z_{cav}$. Whereas the cavity impedance [19] can be expressed as $Z_{cav} = -j\cot(w_l l)$ in which w_l is the wavelength and l is the cavity length.

As a consequence, once the reflection coefficient (R) has been computed, for example by using the equation:

$$R = \frac{Z_{tr} - 1}{Z_{tr} + 1}, \quad (2)$$

the absorption coefficient of the coupled system can be obtained as follows:

$$\alpha = 1 - |R|^2 \quad (3)$$

In this work, the parameters characterizing the acoustic performance of the PSPM samples and materials in comparison have been experimentally determined in the absence of mean flow, in 60 – 4000 Hz frequency range. Three different sound excitation levels (110 dB, 130 dB and 140 dB inside the test section) have been used to study the influence on the acoustic performance of the samples.

3. RESULTS AND DISCUSSION

The absorption coefficients of the elements tested have been obtained by considering a back cavity with 27mm length. In Fig. 4

the experimentally determined transfer impedance for all the acoustic elements treated is presented.

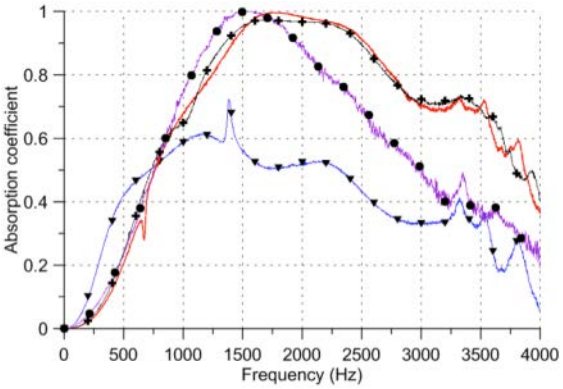

Fig. 4. Absorption coefficients of the acoustic elements tested, coupled to a 27 mm back cavity. PSPM A - blue line with triangles, MG element - magenta line with circles, Glass wool – black line with diamonds, PSPM B – red line.

As can be noticed the absorption coefficient of the thinner PSPM element (sample B) is almost identical to the one of the glass wool. In this respect the performance of the PSPM-B is remarkable, as the glass wool sample taken for reference here is one of the highly efficient fibrous absorbers commercially available. Regarding the absorption (Fig. 4), the thinner PSPM-B element outperforms the thicker PSPM-A and also the modern MG element in almost entire frequency range.

In Figs. 5 and 6 the experimentally determined transfer impedance (resistance in Fig. 5 and reactance in Fig. 6) for the acoustic elements is presented. It can be observed that the resistance of the samples except the PSPM-A is close to unity. One should highlight here that the unitary normalized transfer resistance and negligible transfer reactance are considered as the desired acoustic properties for an absorbing material [10]. In this respect the closest to that condition are the PSPM-B and expectedly also the glass wool.

Regarding the excitation levels the results indicate that the acoustic characteristics of both the PSPM and the glass wool samples are not affected by the loudness of the sound field. Thus, the PSPMs can be effectively applied to a wide variety of noise cancellation applications, irrespective of the loudness.

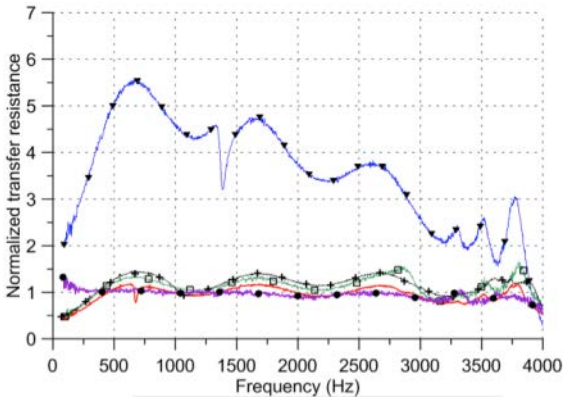

Fig. 5. The real part of the transfer impedance of the acoustic elements tested. PSPM A - blue line with triangles, MG element (140 dB) - magenta line with circles, MG element (130 dB) – green line with rectangles, Glass wool – black line with diamonds, PSPM B – red line.

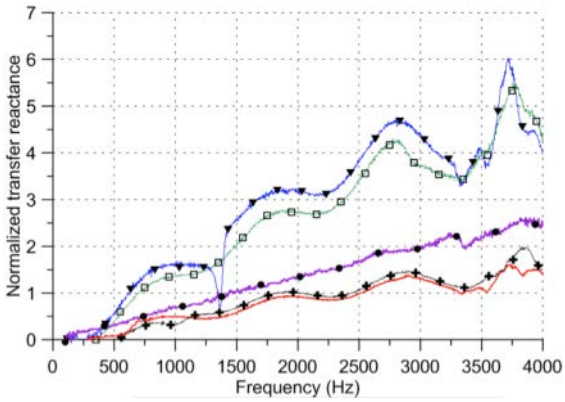

Fig. 6. The imaginary part of the transfer impedance of the acoustic elements tested. PSPM A - blue line with triangles, MG element (140 dB) - magenta line with circles, MG element (130 dB) – green line with rectangles, Glass wool – black line with diamonds, PSPM B – red line.

As concluded in the earlier papers, e.g. in [9] the performance of the MG elements was found to be dependent on the excitation level, improving at higher levels.

4. CONCLUSIONS

Innovative porous sintered powder metal samples have been developed and acoustically tested in this paper. The absorption coefficient and transfer acoustic impedance have been determined successfully and the results exhibit a good potential for the PSPMs in the noise control applications. Regarding the future research, investigations for the reliability and performance in practical applications, e.g. in silencers and aero engine liners, are aimed.

5. REFERENCES

1. Crocker, M. J., Ed., Handbook of Noise and Vibration Control, John Wiley and Sons, New York, 2007.
2. Maa, D. Y. Micro perforated panel wide band absorbers, Noise Control Engineering Journal, 29(3), pp. 77–84, 1987.
3. Herrin D., Liu J., Seybert A. Properties and applications of microperforated panels, Sound and vibration magazine, July 2011.
4. Knipstein, D.M. Soundabsorbing element and procedure for manufacture of this element and use of this element, European Patent Office, patent number EP0876539B1.
5. Randeberg, R. T. Perforated Panel Absorbers with Viscous Energy Dissipation Enhanced Design, Doctoral thesis, Trondheim, June 2000.
6. F. Auriemma. Elemento fonoassorbente costituito da strati con scavi passanti e solchi dissipativi superficiali, Patent number NA2012A000012.
7. Allam, S., and Åbom, M. Experimental Characterization of Acoustic Liners With Extended Reaction," The 14th AIAA/CEAS Conference 2008, p. 3074.
8. Kabral R., Auriemma, F., Rämmal, H., et al. Acoustic Studies on Small Engine Silencer Elements, SAE Technical Paper 2011-32-0514, 2011.
9. Auriemma, F., Rämmal, H., Lavrentiev, J. Micro-Grooved Elements - A Novel Solution for Noise Control, SAE International Journal of Material and Manufacturing, June 2013, 6:599-610; doi:10.4271/2013-01-1941, p. 599-610.
10. Boden, H., Carlsson, U., Glav, R., Wallin, H. P., Abom, M. Sound and Vibration, Course Book. MWL, KTH, The Royal Institute of Technology, Stockholm, ISSN 1651-7660.
11. Arenas, J. P., Crocker, M. J. Recent Trends in Porous Sound-Absorbing Materials, Sound & Vibration, July, 2010.
12. Rouquerol, J., et al. Recommendations for the Characterization of Porous Solids, Pure & Applied Chemistry, Vol. 66, No. 8, pp. 1739-1758, 1994.
13. Magrini, U., and Ricciardi, P. Surface Sound Acoustical Absorption and Application of Panels Composed of Granular Porous Materials, Proceedings of Inter-Noise 2000, pp. 27-30, Nice, France, 2000.
14. Asdrubali, F., Horoshenkov, K. The Acoustic Properties of Expanded Clay Granulates, *Building Acoustics*, Vol. 9, No 2, pp. 85-98, 2002.
15. Martin, J. J. W. Materials for Engineering, Maney publishing, ISBN: 1902653505, 9781902653501, 2002.
16. Tiikoja, H., Lavrentjev, J., Rämmal, et al. Experimental investigations of sound reflection from hot and subsonic flow duct termination, J. of Sound and Vibration, 333 (2014), pp. 788-800.
17. Rämmal, H., Lavrentjev, J. Sound reflection at an open end of a circular duct exhausting hot gas. Noise Control Eng. J. 56 (2), 2008.
18. Munjal M. L. Acoustics of Ducts and mufflers, John Wiley and Sons, New York, 1987.
19. Allard J.F, Atalla N. Propagation of sound in porous media – Modelling sound absorbing materials, John Wiley & Sons, Ltd publication, 2009, ISBN: 978-0-470-746615-0.

6. CORRESPONDING ADDRESS

MSc. Janek Luppin,
Dept. of Machinery, TUT, Ehitajate tee 5, 19086 Tallinn, Estonia.
Phone: 372 56475490,
E-mail: janek.luppin@lettore.ee

7. ACKNOWLEDGMENTS

The research has been carried out in TUT, with the financial support of the project "Optimal design of composite and functional material structures, products and manufacturing processes" (SF0140035s12). Dept. of Materials Eng. (TUT) is acknowledged for valuable consultations and assistance in development of the PSPM samples. The investigations have also been supported by the ERMOS programme (ERMOS153). The design of new test section for rig was provided by Risto Kõiv (Wisefab).

9th International DAAAM Baltic Conference
"INDUSTRIAL ENGINEERING -
24-26 April 2014, Tallinn, Estonia

BALANCING COMPLETION TIMES FOR MULTI-VEHICLE DELIVERY WITH TIME VARIOUS VEHICLE SPEEDS

Moon, G. & Park, S.

Abstract: *An efficient heuristic to balance two vehicle delivery completion times is developed in this research. Vehicle moving speeds are assumed to be unsymmetrical between two points and time various. Delivery area divisions for each vehicle are made by modified sweep algorithm by adding two-stage reassignment procedure to resolve a possible unbalance of two vehicle delivery completion times. Three different size of common area are examined to determine the optimum size of common area. Vehicle delivery route is constructed by the 4-time-zone heuristic to avoid time various vehicle moving speeds situations efficiently.*
Key words: multi-vehicle, sweep algorithm, VRP, combinatorial optimization

1. INTRODUCTION

Vehicle routing problems are studied by many researchers in operations research and management science area due to the combinatorial optimization features. Many solution methods are suggested so far, but most of them are not good enough for real life applications such as door-to-door delivery system in metropolitan area. There are always traffic jams in certain area during rush hours. Also, vehicle moving speeds are changing time to time along moving directions. These limitations make VRPs (vehicle routing problems) really hard to solve.

In this research, such VRPs of traffic congestions during rush hours and various vehicle moving speeds are studied. It is extremely hard to design a good solution methodology for multi-vehicle delivery problems. A modified sweep algorithm is designed and applied to assign delivery area for each vehicle. The procedure consists of two stages such as initial solution search stage and an improvement stage. Improvements are made with common area to reassign them to balance delivery completion times.

Many of related researches are found in the literature. Malandraki and Daski [4] developed a heuristic for time dependent VRPs. Cordeau et al [3] studied on multi-vehicle delivery area assignment using Euclidean distance. Baker and Ayechew [1] used Genetic algorithm as well as sweep algorithm and assignment approach. Barreto et al [2] worked on five depots and fifty cities to visit with capacity limitation. They used 3-opt local search method to improve the routes found by an exact algorithm.

2. PROBLEM STATEMENTS

The model studied in this research is the same one as in Park and Moon [7]. The main objective of the research is to minimize the delivery completion time of both vehicles. It is assumed that the minimum completion time for all vehicles can be achieved by balancing delivery loads for all vehicles. If one vehicle loaded too much while less loads for the other, then the completion time will be very long due to the more loaded vehicle's delayed completion time.

There are no vehicle capacity limits, neither of delivery completion time limits. The delivery will be over after finishing all assigned parcels delivered for the day.

Problems descriptions and assumptions are summarized as follows:

① There are one depot and two delivery vehicles
② Each delivery points are known in advance and visited by vehicle exactly once
③ Each vehicle starts delivery from the depot and comes back to the depot after finishing delivery.
④ Final delivery completion time for each vehicle is the arrival time to depot after finishing all the parcels assigned
⑤ Vehicle moving speeds between to points of i and j are known.
⑥ The vehicle speeds for from i to j and from j to i can be different.
⑦ Required time to move from i to j is calculated by dividing distance with vehicle moving speed.
⑧ The location of depot is assumed to be not located inside of delivery area. It is assumed to be located somewhere on the boundary of whole delivery area

3. SUGGESTED HEURICTIC

3.1 Resolving Time Various Speeds

The vehicle moving speeds are changing every hour based on the surveys. The hourly moving speeds can be obtained from local government surveys. In this research a special heuristic is designed to make very complicated vehicle routing problems easy to solve. All vehicles moving speeds are analysed and then 4 stable moving speed hours are defined in Moon and Park [6]. Vehicle moving speeds in time zone “a” is stable for three hours from 10:00 am to 12:59, “b” for five hours from 1:00pm to 5:59, “c” for one hour from 6:00pm to 6:59, “d” from 7:00pm and rests as shown in Fig. 1. Therefore, it is possible to solve even a complicated VRP as a simple TSP (travelling salesman problem) with stable distance between two points within a time zone.

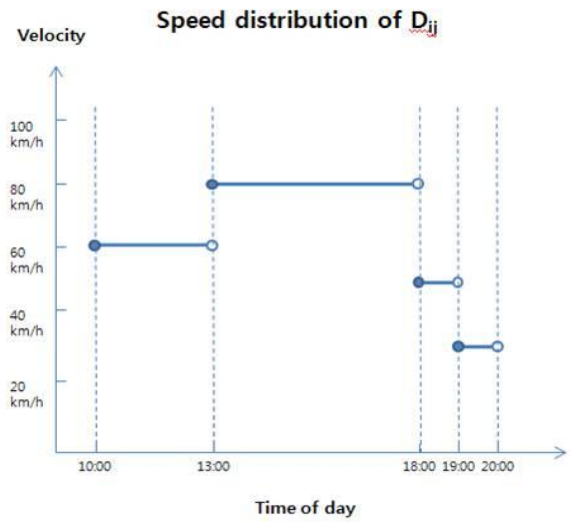

Fig. 1 Four different time zones

All delivery points are equally divided into 10 blocks as shown in Fig. 2. And then bind them again based on the numbers in a specific time zone. For example, three blocks are bind together for the time zone “a”. Now, it is possible to assume that the moving speeds are not changing in a time zone. A delivery route can be constructed from the depot and other points in the time zone “a” easily. And then zone “b” and so on as in Fig. 3.

It is necessary to improve the constructed initial delivery route by pair-wise exchange method. Refer the detailed explanations at Moon and Park [8]. This routing heuristic is good for one depot and one vehicle problem.

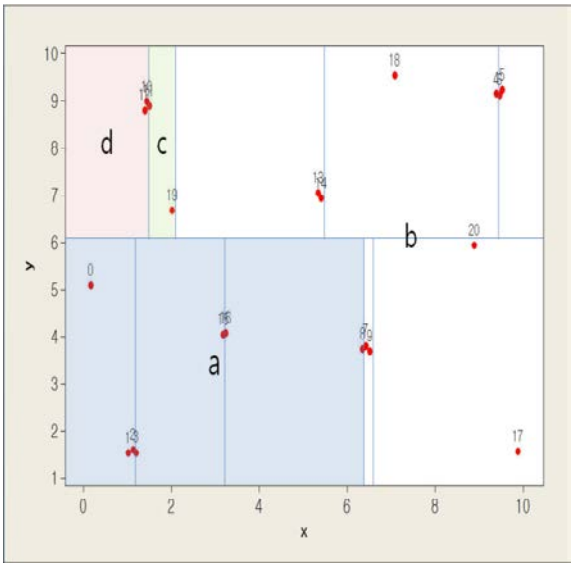

Fig. 2 Four time zone division

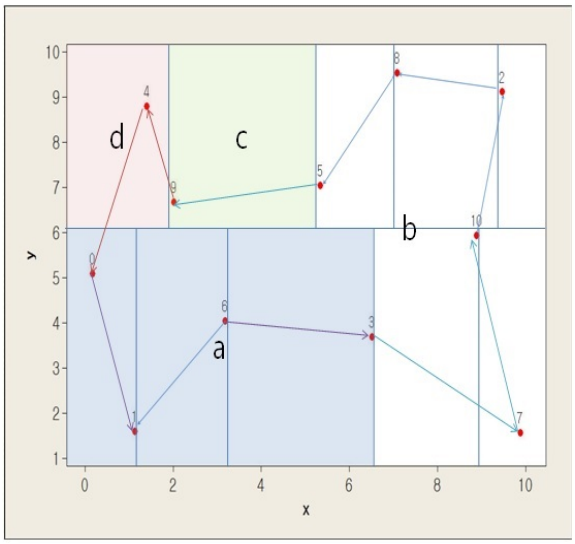

Fig. 3 Delivery route construction

3.2 Multi-Vehicle and Sweep Algorithm

It is assumed that there are two delivery vehicles and one depot. In this case each vehicle is assigned to each delivery area. Delivery area assignment can be made by many different ways. Two algorithms among them would be good. One is K-means algorithm and the other is sweep algorithm. It might be true to get good area division using K-means. However, K-means could be good for N depot problem, but not for one depot problem. More experiments will be done for this issue. In this research, the sweep algorithm is applied for area assignment with some modifications of using common area and reassignment procedure.

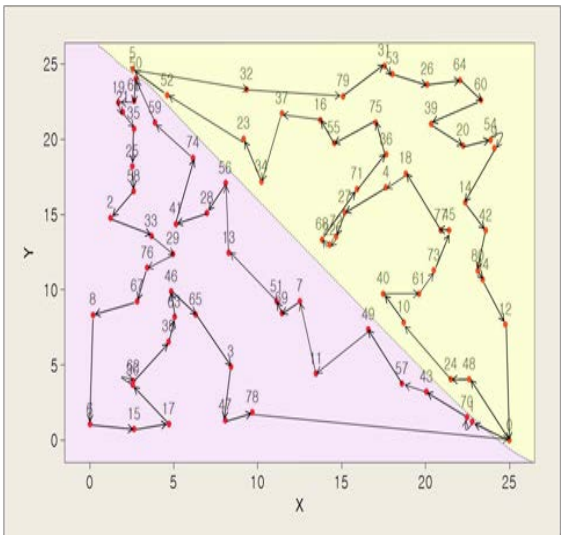

Fig. 4 Half & Half division result

The Fig. 4 is a sample result of simple sweep algorithm for two vehicle case. Bottom and upper area are separated to include equal number of delivery points. In this case the chance of having differences on completion times is bigger due to various vehicle moving speeds. Also there is no chance to adjust the difference one more time for improved results.

3.3 Sweep Algorithm and Common Area

Common area is the narrow area positioned between two wide areas in Fig. 5. The delivery points in common area are to adjust completion times of other two area by assigning more delivery point to the area finished delivery earlier than the other.

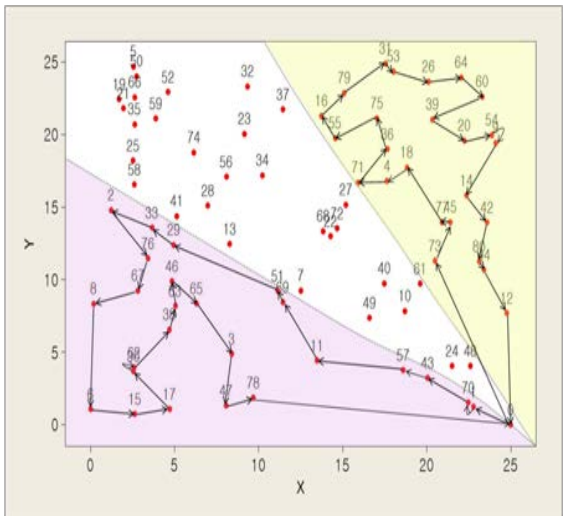

Fig. 5 Division with common zone

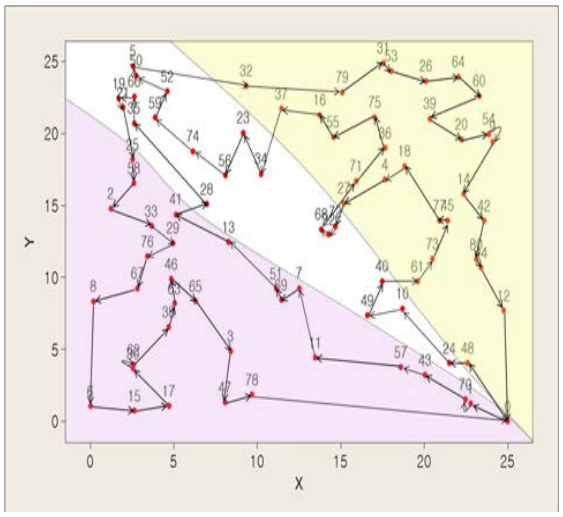

Fig. 6 Final route construction after reassignment of common area

Fig. 6 is a possible result of sharing the delivery points in common area by reassignment to other area between two for balancing delivery completion times. The vehicle took longer time on delivery with temporary assigned loads such as bottom-left one gets less additional numbers of 4 while top-right one gets 16 more from common area in reassignment stages as shown in Fig. 6.

3.4 Procedures for Route Construction

Two delivery vehicles and one depot are assumed in this study. Location of depot can be either inside or outside of delivery area, but only outside locations are studied. No significant difference is found with the position of depot while it is located on the boundary of the delivery area. The delivery area is assumed as a rectangle as shown in Fig. 7. The example cases in Fig. 4 ~ 6 are corner locations for easy of experimental design. Suggested route construction procedures are same as follows:

Step 1. Whole delivery points will be divided into 3 different groups using sweep algorithm. First group for vehicle 1 and second group for reassignment usage, and rest for vehicle 2. The size of second group will be 25 % and 37.5 % respectively.

Step 2. Initial delivery route for each area will be determined by the heuristic suggested by Moon and Park [7] excluding the common area located between the two area. And then delivery completion times for both vehicles are calculated.

Step 3. Find the differences between the completion times obtained in Step 2. Assign more delivery points to the area finished delivery earlier based on the time differences. Recalculate completion time for the area assigned more delivery points.

Step 4. Divide the rest delivery points in common area based on the completion times obtained in Step 3. More delivery points assignment to early finished vehicle

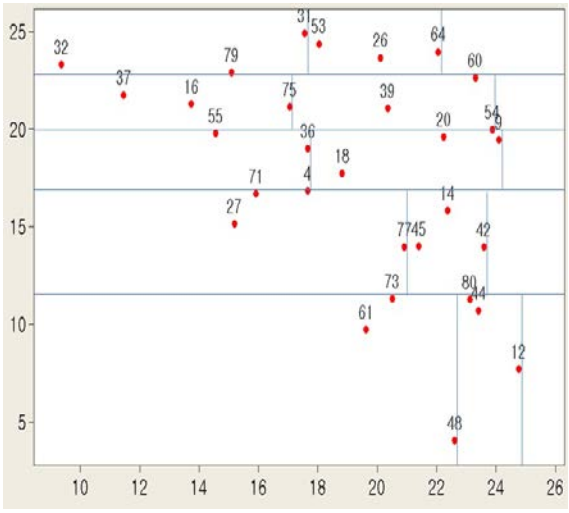

Fig. 7 Sample division with triangle shape

to balance the completion time of two vehicles.

There's no big difference in area division for one vehicle routing construction with irregular shaped area such as multi-vehicle case. Division example for triangle shape is given in Fig. 7.

4. EXPERIMENT FOR EVALUATION

Three different methods are studied to determine an efficient heuristic. One is the way assigning delivery points to each vehicle equally. Therefore, whole delivery area is divided into two by sweep algorithm as shown in Fig. 4. Results are summarized under "Half&Half" in Table 1. "Exp." stands for "Experiments number" and "Ave" for "average" in Table 1.

Other two methods are using common area, but with different sizes such as "20" out of 80 and "30" out of 80 to find better size. 20, 30, 80 are parcels. The results are presented under the name of "COM(20)" and "COM(30)" respectively.

For example, the numbers in case 1 for "COM(20)" is 237.6 for "max" and 10.62 for "diff". This means completion times for one vehicle is 237.6 and the other is 226.98. Therefore, it is possible to say that the deliver completion time for both vehicles is 237.6 as of "max" and unbalance of two vehicle completion time is 10.62 as of "diff" in Table 1. It is clear that less "diff" value method obtained less "max"

Exp	Delivery Completion Time					
	Half&Half		COM(20)		COM(30)	
	max	diff	max	diff	max	diff
1	229.65	4.02	237.60	10.62	231.80	2.44
2	295.10	48.24	271.13	6.06	283.82	5.02
3	282.03	9.43	284.82	18.74	284.82	5.97
4	278.94	2.08	285.30	16.91	285.30	4.09
5	248.60	3.08	248.60	3.08	250.81	5.59
6	228.12	48.55	208.41	6.97	214.22	12.69
7	229.98	55.37	200.08	6.09	208.58	19.25
8	402.46	188.5	387.99	126.42	365.05	75.98
9	235.50	46.30	208.41	6.97	283.34	3.72
10	284.40	25.63	287.00	13.08	278.81	4.89
11	318.50	12.46	323.42	14.28	346.54	67.32
Ave	275.75	40.33	267.52	20.83	275.73	18.81

Table 1. Comparisons of completion times

value since the delivery assignments for both vehicles are well balanced.

In comparison to "COM(20)" and "COM(30)", "COM(20)" seems better than "COM(30)" in terms of max values. That is completion time of both vehicles for delivery. "COM(30)" is good only at two cases of 1 and 8.

5. CONCLUSION

Multi-vehicle routing problems with various vehicle speeds are studied in this research. A heuristic for efficient route construction is designed and experiments for evaluations are performed. The concept of common area for reassignment and sweep algorithm is applied to balance two vehicle delivery completion times.

Three different sizes of common area are examined with 11 difference cases. First one is "no common area", and the second one is the size of 20 out of 80 total delivery points. Last one is the size of 30 out of 80. The size of 20 common area leads to good results among them. 20 out of 80 are 25 % of total delivery points. If the size of common is large, then it could be necessary to reassign many newly assigned delivery loads to each vehicle and reconstruct delivery route again. It will be a time consuming process.

Another issue is about delivery area division methods as shown in Fig. 2. Grouping delivery points by splitting straight lines does not guarantee a good result. Therefore it is necessary to group area more reasonably. The K-means algorithm is one possible candidate to apply. Even sweep algorithm is adapted here, but the K-means algorithm might be valued enough to study on the design process for VRPs.

ACKNOWLEDGEMENT

This research was supported by Basic Science Research Program through the National Research Foundation of Korea (NRF) funded by the Ministry of Education, Science and Technology (NRF-2011-0013252)

6. REFERENCES

1. Baker, B. and Ayechew, M. A genetic algorithm for the vehicle routing problem. *Com. & OR*, 2003, **30(5)**, 787-800.
2. Barreto, S., Ferreira, C., Paixao, J. and Santos, B. Using clustering analysis in a capacitated location-routing problem. *Euro. J. of OR*, 2007, **179(3)**, 968-977.
3. Cordeau, J-F., Gendreau, M., and Laporte, G. A tabu search heuristic for periodic and multi-depot vehicle routing problems. *Networks*, 1997, **30(2),** 105-119.
4. Malandraki, C. and Daskin, M. Time dependent vehicle routing problems: Formulations, properties and heuristic algorithms. *Transportation Sci*., 1992, **26(3)**, 185-200.
5. Moon, G. and Park, S. Analysis and Reconstruction of Vehicle Speeds to Design an Efficient Time Dependent VRP Heuristic. *J. of the Soc. of KISE*, 2012, **35(1)**, 140-147.
6. Moon, G. and Park, S. A Possible Heuristic for Variable Speed Vehicle

Routing Problem with 4 Time Zone. *J. of the Soc. of KISE*, **35(4)**, 2012, 171-178.
7. Park, S. and Moon, G. Optimization of Delivery Route for Multi-Vehicle under Time Various and Unsymmetrical Forward and Backward Vehicle Moving Speed. *J. of the Soc. of KISE*, **36(4)**, 2013, 138-145.
8. Moon, G. and Park, S. An Efficient Heuristic for VRP under Time Various Vehicle Speeds by Grouping Delivery Points. *Proc. Of the Sixth Ann. Int. Bus. Conf.*, **(ISSN 1947-2195)**, 2013, 111-120.

7. ADDITIONAL DATA ABOUT AUTHORS

1) Geeju Moon, Ph.D, Professor
2) Title of Manuscript: BALANCING COMPLETION TIMES FOR MULTI-VEHICLE DELIVERY WITH TIME VARIOUS VEHICLE SPEEDS
3) Full Address of all authors:
Professor , Dr.
840 Hadan-Dong, Saha-Gu,
Busan 604-714, KOREA
E-mail: gjmoon@donga.ac.kr
web.donga.ac.kr/gjmoon
Phone: +82-51-200-7695
Fax: +82-51-200-7697

1) Sungmee Park, Ph.D, Researcher
2) Title of Manuscript: BALANCING COMPLETION TIMES FOR MULTI-VEHICLE DELIVERY WITH TIME VARIOUS VEHICLE SPEEDS
3) Full Address of all authors:
Dr.
840 Hadan-Dong, Saha-Gu,
Busan 604-714, KOREA
E-mail: ninapark@nate.com
Phone: +82-51-200-6972
Fax: +82-51-200-7697

4) Corresponding Author:
Dr. Geeju Moon, Professor
840 Hadan-Dong, Saha-Gu
Busan 604-714, KOREA
E-mail: gjmoon@donga.ac.kr
web.donga.ac.kr/gjmoon
Phone: +82-51-200-7695
Fax: +82-51-200-7697

9th International DAAAM Baltic Conference
INDUSTRIAL ENGINEERING
24-26 April 2014, Tallinn, Estonia

LOAD SENSITIVITY ANALYSIS OF A LARGE DIAMETER PERMANENT MAGNET GENERATOR FOR WIND TURBINES

Pabut, O.; Lend, H. & Tiirats, T.

Abstract: *Permanent magnet (PM) and electrically-excited direct-drive generators are usually described by their high mass and production costs. Studies have proved that when increasing generator's capacity, inactive mass increases faster than the active mass. In this paper, a load component sensitivity study for the inactive mass is performed on a direct-drive PM generator via Finite Element Analysis (FEA). Taguchi method is utilized for describing the relations between design parameters and the resulting stresses and deformations. Most influential load components are determined and general countermeasures are offered.*
Key words: sensitivity analysis, permanent magnet generator, finite element analysis, Taguchi method.

1. INTRODUCTION

During past decades a high number of research papers have been presented on the electromagnetic layout of an electrical generator in a wind turbine [1-2]. Despite the numerous solutions that have been offered, the geared drive train with an induction generator, still remains the dominant technology [3]. Alongside it, various alternative drive train solutions, like the PM synchronous generator, have emerged. Although, these machines offer higher reliability and power density, they are usually described also by their high mass and production costs [4].
With machines near megawatt scale, the final cost and mass of the generator has been largely associated with the active electrical parts. However, electrical machines also contain material that fulfills a structural role and works against a number of high forces. Studies have proved that when increasing the generator capacity, inactive mass increases faster than the active mass and begins to dominate [3, 5]. This, alongside the fact that price of the active materials has steadily been dropping, indicates that when dealing with higher capacity generators, more refined methods to reduce the inactive mass are necessary. This paper aims to provide insight to the relative importance of the acting forces on the generator, in order to provide information for the initial selection of design parameter values.

2. ANALYSIS DESCRIPTION

2.1 Generator

The machine subjected to the analysis is a PM ultra large direct-drive generator with an air-gap diameter of 12 meters and rated capacity of 3 MW. The machine consists of an inner rotor with permanent magnets and an air-cooled outer stator with electrical windings. Active elements are supported by a lattice structure consisting mainly of tubular steel beams. While the rotor is supported equally from both sides, the stator has one sided unsymmetrical support, like shown in Figure 1a. This is of interest when considering the acting gravity forces, which in this case result in an air-gap deforming rolling moment.
Electromagnetic setup of the generator is similar to the one that is described in the previous work [6]. The stator coils are located in the air-gap to reduce the normal component of Maxwell stress.

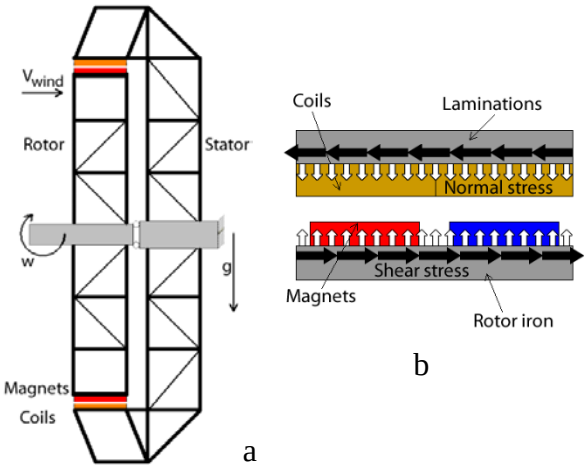

Fig. 1. Generator overall topology (a) and electromagnetic layout (b)

2.2 Acting forces

Forces present in an electrical machine are similar for most types of generators. In addition to those that can be found in regular electrical generators, effects from wind and tower top accelerations must be considered for a machine that is used in a wind turbine. As a result, in the presented analysis, following loads are considered: deadweight resulting from gravity, rotor rotational velocity, wind load on the structure, tower front-to-back acceleration and side-to-side acceleration, normal stress and generator torque.

Torque τ and rotational speed ω are proportional to the generator's electrical power output P_{el} and efficiency η (1). Therefore, they both cannot be subjected to minimization but their relation can be manipulated in a certain range if it turns out to be beneficial. The limits of this manipulation are set by maximum allowed rotational speed for the blades (tip speed limit ≈ 80 m/s). Meaning that for larger turbines and rotors, the rotational velocity is smaller.

$$P_{el} = \tau \cdot \omega \cdot \eta \qquad (1)$$

From an electromagnetic point of view, torque is a product of the tangential component of Maxwell stress, which is also designated as shear stress σ. Therefore, torque of a rotating electrical machine can also be given as

$$\tau = 2\pi\sigma R^2 l \qquad (2)$$

where R is the machine air-gap radius and l axial length of the generator [4]. Torque is the useful force in an electrical machine and does not serve to close the air-gap.

In most generator topologies Maxwell stress has also a normal component (normal stress), which is caused by the attraction of the ferromagnetic surfaces of rotor and stator. Normal component can be a magnitude greater than the shear stress and directly acts to close the air-gap. Designers have long looked for ways how to reduce the normal stress in relation to the shear stress and as a result air-cored machines have been developed [7-8]. Presented machine is a hybrid solution, as the windings are located in the air-gap, like shown in Figure 1b.

Wind turbine towers have become highly optimized and in many cases extremely soft and flexible towers are used [9]. For geared drive trains this has a low impact but direct-drives with their high mass and material distribution on the outer perimeter are vulnerable to tower top accelerations. Depending on the topology of the support structure, considerable extra stresses and deformations can occur.

From (2) it can be seen that one option to increase the generator torque and therefore the power output, is to increase the air-gap radius. Many designers have taken advantage of this, which has led to generators with ultra large diameters. As the perimeters of the machines grow, so does the force that is resulting from wind acting on the generator's structure [10]. This can be found by

$$F_{wind} = \rho/2 \cdot v_{wind}^2 \cdot A \cdot c_p \qquad (3)$$

where ρ is the air density, v_{wind} the wind speed, A surface area of the generator that is perpendicular to the wind direction and c_p the shape parameter of the surface.

Therefore, depending on the actual surface that is exposed to wind, the force F_{wind} could become a significant factor that influences the generator design.

2.3 FEA model

Framework of the generator is modeled in ANSYS Workbench environment with two-node beam elements (BEAM188) having six degrees of freedom at each node. For the beam-to-beam connections it is assumed that they have the same carrying capacity as the profiles. Therefore, different beams are connected by shared nodes and automatically transmit all moments and forces.

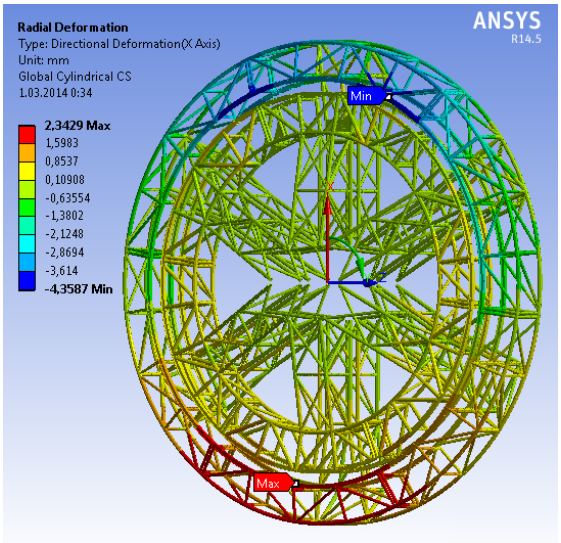

Fig. 2. FEA model of the generator

Only the framework of the generator is directly modeled while rest of the elements like magnets and coils are approximated by point masses. It is assumed that they do not add significantly to the structural stiffness of the machine. In addition, rotor shaft and stator king-pin are not modeled, as for direct-drive turbines they are mostly subjected to forces and moments from the rotor blades [7]. Therefore, their cost and end mass is not greatly influenced by the generator design parameters.

The setup and in particular the stiffness of the FEA model have been validated with an experimental study on the full scale generator structure. The dimensions of rotor and stator rings were measured with and without magnetic forces and calculated deformations were found to be in good correlation with the FEA results.

3. SENSITIVITY STUDY

3.1 Initial parameter selection

In the first part of the analysis all the seven acting load components are applied to the structure one-by-one while resulting stresses and deformations are extracted. Results are compared with values from the nominal working situation where all the components are acting with the same values simultaneously. Overall stress and deformation values in the nominal working situation are within allowed limits to obtain reasonable results.

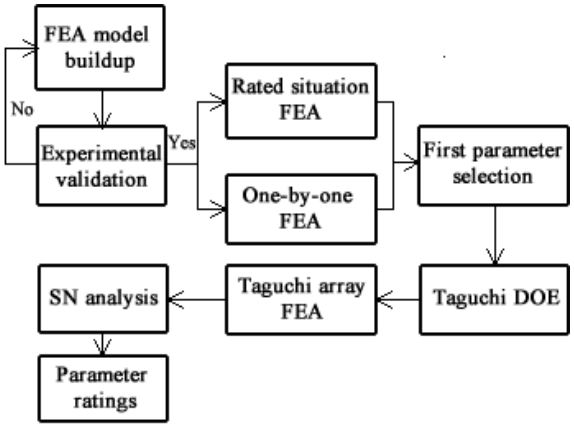

Fig. 3. Principles of the study

A cylindrical coordinate system is used to record the results and only rotor positive and stator negative radial deformations are investigated, as they serve to close the air-gap. The results of the FEA analysis are presented in Table 1, where the contribution of each component to the overall stress level is presented.

The initial study is performed to determine the most influential load components for further analysis. This enables to reduce the required number of experiments when investigating parameter interactions. From the comparison between the sum of components and actual results it is clear, that further analysis is required, as deformations differ about 20% and stresses 50%.

Only the parameters that contribute more than 5% to at least one of the outputs are selected for further investigation. These include: deadweight, front-to-back acceleration, normal stress and torque (marked green in Table 1).

Load	Rotor def	Stator def	Rotor stress	Stator stress
Deadweight	38%	64%	18%	42%
Rot speed	5%	0%	4%	0%
Side accel	4%	5%	2%	4%
Front accel	3%	2%	7%	5%
Norm stress	44%	23%	27%	21%
Torque	5%	4%	39%	26%
Wind	1%	1%	3%	2%
Sum	**1,3**	**4,8**	**109**	**185**
Actual total	**1,1**	**4,1**	**74**	**128**

Table 1. Load component contribution to overall stress level.

3.2 Taguchi analysis

Taguchi method for design of experiments is utilized to compose the mathematical model describing the relations between design parameters and the resulting stresses and deformations. Taguchi is chosen as it enables to reduce the number of required experiments even further. Five value levels are chosen for each input parameter: 100%, 60%, 80%, 120% and 140% of their rated value. The levels are chosen based on an assumption that for a defined output power the design characteristics would vary not more than ± 40%. This is important since conclusions drawn from small scale experiments are valid only over the particular experimental region [11].

Variation is applied to the rated value of the parameter, without considering the safety factor that needs to be applied to the loads [10]. The value of the parameter is changed according to the required percentage and only then multiplied with the safety factor. In case of the deadweight, only the mass of active material together with needed fixtures is varied, as only this can directly be influenced by designer's initial decisions.

Since there are four parameters and five levels, L25 orthogonal array is used. For each experiment, the stresses and deformations of rotor and stator are extracted as performance characteristics. The obtained FEM results are transformed into signal-to-noise (SN) ratios. The SN ratios are used as a measure of deviation from or nearness to the desired value. Goal of the analysis is minimization of performance characteristics. The needed SN ration are found with

$$SN_i = -10log\left(\sum_{u=1}^{N_i} \frac{y_u^2}{N_i}\right) \qquad (4)$$

where u is the trial number, N_i the number of trials for experiment i and y_u is the value of the performance characteristic for a given experiment [11]. After calculating the SN ratio for each experiment, the average SN value is calculated for each factor and level. In order to determine the effect of the variable on the process, Δ value (high SN – low SN) is found for each parameter.

Response of the SN ratios for the rotor deformation can be found in Table 2. The rakings of all four parameters with their corresponding Δ values for all performance characteristics are presented in Table 3.

Level	Dead-weight	Front accel	Norm stress	Torque
100%	0,00	0,12	-0,08	-0,11
60%	1,19	0,13	1,82	0,09
80%	0,50	-0,04	0,81	0,15
120%	-0,59	-0,14	-0,89	0,03
140%	-1,11	-0,07	-1,66	-0,17
Δ	**2,30**	**0,28**	**3,48**	**0,32**
Rank	**II**	**IV**	**I**	**III**

Table 2. Response table for SN ratios for rotor deformation.

		Dead-weight	Front accel	Norm stress	Torque
Rotor def	Δ	2,30	0,28	3,48	0,32
	rank	II	IV	**I**	III
Stator def	Δ	3,65	0,19	1,72	0,19
	rank	**I**	III	II	IV
Rotor stress	Δ	0,98	0,39	0,82	4,19
	rank	II	IV	III	**I**
Stator stress	Δ	2,49	0,06	0,62	2,59
	rank	II	IV	III	**I**

Table 3. Rankings of all parameters for all performance characteristics.

4. DISCUSSION

According to results presented in Table 3, deadweight and normal stress are the most influential factors for the air-gap deformations. For rotor, normal stress prevails but for stator, deadweight has by far the biggest influence. This can be explained by cantilever nature of the stator structure (Figure 1a). It could be compensated by adding a frontal support structure. However, it would also make the mechanical construction and specially the assembly process more complex. For the stator the deadweight is not an alternating force. Therefore, the resulting deformations could be already factored into the shape of the structure prior to the assembly and later the machine would deform itself into right dimensions. Alternatively, after the stator assembly the windings could be adjusted in order to compensate for the static deformations after stator has been lifted into the vertical position. Another option could be also utilization of materials with better stiffness to weight ratio i.e. performing structural optimization [12-15].

Frontal acceleration has a minor significance for all of the performance characteristics. This can be explained by the mechanical setup of the frame structure. As it requires space to use material effectively, it also contributes to the axial stiffness of the machine and therefore reduces the acceleration influence. But it must be noted that for disc like sheet metal structures with their material located mostly on the outer rim, this most likely does not apply.

From Table 1 and 3 it can be summarized that for this type of generator, the key influential factor determining the levels of stress and deformation, is the mass of the material located at the air-gap radius.

When taking actions to reduce the mass on the air-gap radius, care has to be taken that these actions do not increase the normal stress, as any benefits would be then cancelled out. For example one of the possible solutions could be using higher grade PM's with better mass to field strength ratio. At the same time the air-gap could be extended to keep normal stress at acceptable level. The reduced mass would also be beneficial for the other turbine parts, as it would mean for example lower loads for the yaw system.

This conclusion indicates that solutions offered in literature to use heavy but cheap magnetic materials like ferrites [16] are most likely cost wise not beneficial. The savings on magnet material costs would be lost in the extra investment that is required for the structure reinforcement.

On the stress side, the designer's aim, in addition to reducing mass of the active material, should be also limitation of the torque value. Due to the torque's direct dependency on the output power (1) and constraints laid on the rotational speed, there is usually not much room left to play. However, as a rule of thumb, the blades should be always utilized at their maximum allowed rotational speed.

Finally, electromagnetic setups that offer either considerably lower mass or normal stresses could be considered. For example solution of an ironless design presented by Gordon and Spooner [8] would fulfill these criteria.

5. CONCLUSION

Experimentally validated FEA model of a large diameter PM generator for a wind turbine has been built in ANSYS environment. The main loads acting on the generator structure have been described. Their individual contribution to the overall stress and deformation levels has been determined. Taguchi method of design of experiments has been used to study interactions of the individual load components and their relation to structural stresses and air-gap deformations. The mass of material located on the air-gap radius appears to be the most influential component when looking at both stresses

and deformations. When regarding only the deformations, normal stress has to be strongly considered and when focusing on stresses, the generator torque is the dominant parameter.
The obtained results imply that all efforts must be focused on the reduction of mass at the air-gap radius as it would bring about further reduction of structural mass.

Acknowledgements
This study has been supported by Estonian Science Foundation Grant ETF9441.
The research has been performed on Goliath Cyclos 16/3 generator.

6. REFERENCES

1. Bang, D., Polinder, H., Shrestha, G., Ferreira, J. A. Promising Direct-Drive Generator Systems for Large Wind Turbine. *Wind Power to the Grid – EPE Wind Energy Chapter 1st Seminar,* 2008, 1-10.
2. Henriksen, M., Jensen, B. Induction Generators for Direct-Drive Wind Turbines. *Electric Machines Drives Conference,* 2011, 1125-1130.
3. Zhang, Z., Chen, A., Matveev, A., Nilssen, R., Nysveen, A. High-Power Generators for Offshore Wind Turbines. *Energy Proc.,* 2013, **35(2013),** 52-61.
4. McDonald, A. S., Mueller, M. A., Polinder, H. Structural Mass in Direct-Drive Permanent Magnet Electrical Generators. *IET Renewable Power Generator,* 2007, **2(1)**, 3-15.
5. Shrestha, G., Poliner, H., Ferreira, J. A. Scaling Laws for Direct-Drive Generators in Wind Turbines. *Proc. IEMDC,* 2009, 797-803.
6. Kallaste, A., Vaimann, T., Pabut, O. Slow-Speed Ring-Shaped Permanent Magnet Generator for Wind Applications. *11th Int. Symp."Typ. Problems in the Field of Electrical and Power Engineering,* 2012, 66-69.
7. Mueller, M. S., McDonald, A. S. A Lightweight Low Speed Permanent Magnet Electrical Generator for Direct-Drive Wind Turbines. *Wind Energy,* 2009, **12(8)**, 768-780.
8. Spooner, E., Gordon, P., Bumby, J. R., French, C.D., Lightweight Ironless-Stator PM Generators for Direct-Drive Wind Turbines. *Proc. Inst. Elec. Eng. Elec. Pow. Appl.,* 2005, **152(1)**, 17-26.
9. Erich, H. Wind Turbines: Fundamentals, Technologies, Application, Economics. *Springer,* 2006.
10. Guideline for the Certification of Wind Turbines. *Germanischer Lloyd,* 2010.
11. Phadke, S. M. Quality Engineering Using Robust Design. *Englewood Cliffs, N.J., Prentice Hall,* 1989.
12. Pohlak, M., Küttner, R., Majak, J. Modeling and Optimal Design of Sheet Metal RP&M Processes. *Rapid Protot. Journal,* 2005, **11(5),** 304-311.
13. Kers, J., Majak, J. Modeling a New Composite From a Recycled GFRP. *Mechanics of Composite Materials,* 2008, **44(4)**, 623-632.
14. Majak, J., Pohlak, M. De-Composition Method for Solving Optimal Material Orientation Problems, *Composite Structures*, 2010, **92(8)**, 1839-1845.
15. Majak, J., Pohlak, M., Eerme, M., Velsker, T. Design of Car Frontal Protection System Using Neural Networks and Genetic Algorithm. Mechanika, 2012, **18 (4)**, 453-460.
16. Kallaste, A. Low Speed Premanent Magnet Slotless Generator Development and Implementation for Windmills. *Ph.D. Dissertation, TUT, Tallinn,* 2013.

7. ADDITIONAL DATA ABOUT AUTHORS

MSc. Ott Pabut
TUT, Department of Machinery
Ehitajate tee 5, 19086 Tallinn, Estonia
Phone: +372 51 644 57,
E-mail: ottpabut@hotmail.com
http://www.ttu.ee

9th International DAAAM Baltic Conference
"INDUSTRIAL ENGINEERING -
24-26 April 2014, Tallinn, Estonia

NUMERICAL METHOD FOR STABILITY ANALYSIS OF FUNCTIONALLY GRADED COLUMNS

Shvartsman, B.S., Majak, J. & Kirs, M.

Abstract: *This paper considers the issue of stability of non-uniform and functionally graded (FG) Euler-Bernoulli columns with elastically restrained ends. The boundary conditions are considered in general form covering different classical supporting conditions of the column and converted into convenient form in order to avoid handling infinity values of the stiffness coefficients. The method of initial parameters in differential form is used for the numerical solution of the problem. Several numerical examples are presented to illustrate robustness, convergence, and the numerical performance of the method considered.*

Key words: *Stability of functionally graded columns; Method of initial parameters.*

1. INTRODUCTION

The buckling problems of nonuniform and functionally graded (FG) beams/columns have been overviewed in monographs [1-4]. The analytical solutions exist for certain particular cases only [3, 4]. In more general cases of the distributions of flexural rigidity the numerical methods are employed [5-9]. In the well-known paper of Eisenberger [5] a number of examples are given for buckling of columns with different distributions of rigidity and loadings. The highly accurate results obtained in [5] are used commonly for comparison and evaluation of different numerical methods [3, 6-9].

The buckling problems of FG columns with concentrated loads are considered in recent publications [6-9].

In the current study the numerical method for analysis of buckling of FG columns is proposed. The boundary conditions are considered in general form covering different classical supporting conditions.

Current approach can be regarded as method of initial parameters in differential form. The proposed approach allows satisfying automatically boundary conditions on the lower end of the column (initial parameters). The solution of the posed boundary value problem is reduced to the solution of the two initial value problems and linear homogeneous algebraic system of order two in each iteration step. In general approach proposed the fourth-order Runge-Kutta method is employed. The refined solutions have been obtained by applying Richardson extrapolation method [10-11].

2. FORMULATION OF THE ROBLEM

Consider a functionally graded (FG) initially rectilinear column of length L under compressive force P. Using the Euler-Bernoulli law of bending states, the governing equation for the buckling of the FG column can be is given by [1 - 4]:

$$(D(x)y'')'' + Py'' = 0 \qquad (1)$$

Where x is axial coordinate, y is the transverse deflection, $D(x) = E(x)I(x)$ is

flexural rigidity. The general boundary conditions are given by

$$D(0)y''(0) = C_1 y'(0),\ y(0) = 0,$$
$$D(L)y''(L) = -C_2 y'(L),$$
$$(D(L)y''(L))' + Py'(L) = C_3 y(L) \quad (2)$$

Here C_1 is rotational spring constant at the root of the column $(x = 0)$, and C_2, C_3 are rotational and translational spring constants at the tip of the column $(x = L)$, as shown in Fig. 1. The different classical boundary conditions can be obtained for values of spring constants $C_i = 0$ or $C_i = \infty, i = 1,2,3$. For example, we have $C_1 = \infty, C_2 = 0, C_3 = \infty$ for clamped-pinned boundary conditions**.**

Instead of spring constants C_i introduce new parameters of stiffness $c_i = C_i/(C_i + 1), = 0, i = 1,2,3$. Thus, when C_i takes values from $0\ to\ \infty$, c_i varies from $0\ to\ 1$. As a result, using an inverse equations $C_i = c_i/(1 - c_i), i = 1,2,3$ the boundary conditions (2) written as

$$y(0) = 0,\ c_1 y'(0) - (1-c_1)(D(0)y''(0)) = 0,$$
$$c_2 y'(L) + (1-c_2)(D(L)y''(L)) = 0,$$
$$c_3 y(L) + (c_3 - 1)((D(L)y''(L))' + p\, y'(L)) = 0 \quad (3)$$

The values of coefficients $c_i, i = 1,2,3$ for some boundary conditions are shown in Table 1. These equations for boundary conditions are more convenient to use because different classical supporting

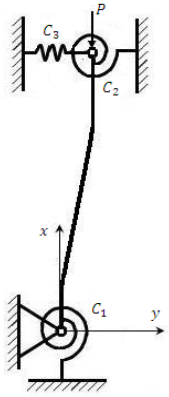

Fig. 1. The column with general elastically end constraints

	C-C	C-P	C-G	C-F	P-C	P-P
c_1	1	1	1	1	0	0
c_2	1	0	1	0	1	0
c_3	1	1	0	0	1	1

Table 1. Realization of the some boundary conditions of the column (F – free, P – pinned, C – clamped, G – guided).

conditions of the beam can be obtained for finite values of $c_i = 0\ or\ c_i = 1, i = 1,2,3$.

3. NUMERICAL METHOD OF SOLUTION

Let us introduce the following notation in order to solve the linear boundary value problem (1), (3):

$$y_1 = y,\ \ y_2 = y',$$
$$y_3 = D(x)y'',\ \ y_4 = (D(x)y'')' \quad (4)$$

As a result, the Eqs. (1), (3) is reduced to the normal system of linear differential equations

$$y_1' = y_2,\quad y_2' = y_3 / D(x),$$
$$y_3' = y_4,\ \ y_4' = -P\ y_3 / D(x) \quad (5)$$

with boundary conditions:

$$c_1 y_2(0) - (1-c_1) y_3(0) = 0,\quad y_1(0) = 0, \quad (6)$$
$$c_2 y_2(L) + (1-c_2) y_3(L) = 0,$$
$$c_3 y_1(L) + (c_3 - 1)\,(y_4(L) + P\, y_2(L)) = 0 \quad (7)$$

For solution of boundary value problem (5)-(7) consider two families of linearly independent particular solutions

$$Y_1(x,P) = \{y_{11}, y_{12}, y_{13}, y_{14}\}^T,$$
$$Y_2(x,P) = \{\ y_{21}, y_{22}, y_{23}, y_{24}\}^T \quad (8)$$

which satisfy Eqs.(5) and the boundary conditions on lower end of the column:

$$Y_1(0,P)=\{0,1-c_1,c_1,0\}^T,\qquad Y_2(0,P)=\{0,\,0,\,0,\,1\}^T \tag{9}$$

The expressions (9) follow directly from the boundary conditions (6). The particular solutions (8) can be found by numerical integration of the two initial value problems (5),(9) for fixed value of the parameter P using standard Runge-Kutta method [10]. As a result, the general solution of the system of Eqs.(5) automatically satisfying the boundary conditions (6) on the lower end of the beam can be composed as follows:

$$Y(x,P)=A_1\,Y_1(x,P)+A_2\,Y_2(x,P) \tag{10}$$

Here the integration constants A_1, A_2 should be evaluated by imposing the boundary conditions on the upper end of the column Eqs.(7). Substitution on Eq.(10) into Eqs.(7) gives two linear homogeneous algebraic equations for integration constants A_1, A_2 :

$$\begin{cases} a_{11}\,A_1+a_{12}\,A_2=0 \\ a_{21}\,A_1+a_{22}\,A_2=0 \end{cases} \tag{11}$$

where the coefficients $a_{ij}, i=1,2$ are

$$\begin{aligned} a_{11}&=c_2y_{12}(L,P)+(1-c_2)y_{13}(L,P),\\ a_{12}&=c_2y_{22}(L,P)+(1-c_2)y_{23}(L,P),\\ a_{21}&=c_3y_{11}(L,P)+(c_3-1)(y_{14}(L,P)+P\,y_{12}(L,P)),\\ a_{22}&=c_3y_{21}(L,P)+(c_3-1)(y_{24}(L,P)+P\,y_{22}(L,P)). \end{aligned} \tag{12}$$

For a nontrivial solution to the constants A_1, A_2 the determinant of the resulting coefficient matrix of the second order is set equal to zero:

$$\det\begin{pmatrix} a_{11} & a_{12} \\ a_{21} & a_{22} \end{pmatrix}=a_{11}\,a_{22}-a_{12}\,a_{21}=0 \tag{13}$$

Thus, the characteristic equation (13) for the determination of buckling load $P=P_*$ is obtained. Secant method can be used for solution of this nonlinear equation [10]. In each iteration the two initial value problems (5), (9) are solving for obtained particular solutions (8) and values functions of the left-hand side of the characteristic equation (13) are calculate by the formulas (12). Since eigenfunctions are defined up to a constant, the corresponding buckling mode can be obtained from Eq.(9) by the formula:

$$Y(x,P_*)=Y_1(x,P_*)+(A_2/A_1)\,Y_2(x,P_*) \tag{14}$$

Here constant $A_2/A_1=-a_{11}/a_{12}$ is obtained from first Eq.(11) for $P=P_*$. From Eq.(9) and Eq.(14) follows that the values of buckling shape $Y(x,P_*)$ at the points $x\in[0,L]$ may be calculated by numerical integrating the Eq.(7) under obtained value $P=P_*$ and following initial conditions:

$$Y(0,P_*)=\{0,\,1-c_1,\,c_1,\,A_2/A_1\}^T \tag{15}$$

It is should be note, in the case of uniform homogeneous beams, the Eqs.(5) have constant coefficients. Then the particular solutions (8), resulting characteristic Eq. (13) and buckling shapes Eq.(14) have exact closed-form expressions using known transcendental functions [1-4]. Such approach to obtain analytical solutions is called the method of initial parameters [2]. Method under consideration, where particular solutions (8) are obtained numerically naturally called by method of the initial parameters in differential form.

4. EXTRAPOLATION OF RESULTS

The Richardson extrapolation is a powerful technique for increasing the accuracy of difference solutions of different problems of mathematical physics [10,11]. To be able to apply the Richardson extrapolation it is necessary to know the asymptotic error expansion in powers of the step size h:

$$F(h)-F(0)=\alpha h^k+O(h^l),\quad 0<k<l \tag{16}$$

Here $F(h)$ denote the value obtained by any numerical method with step size h, $F(0)$ is an unknown exact value, α is unknown does not depend on h constant and k is theoretical order of accuracy of the numerical method. Such expansions were grounded for a wide range of difference and finite-element solutions [11].

Denote two numerical solutions found on grids $h_{i-1}, h_i = h_{i-1}/2$ as follows $F_{i-1} = F(h_{i-1}), F_i = F(h_i)$. Then using the Eq.(16) for these solutions can be obtained another approximation of the value $F(0)$ denoted by

$$R_i = F_i + \frac{F_i - F_{i-1}}{2^k - 1} = F(0) + O(h_i^l) \qquad (17)$$

Thus approximate solutions R_i have error with higher order in relation to h than F_i. This formula is simple Richardson extrapolation formula [10,11]. Therefore, if numerical solutions of the problem for two grids and the theoretical order of accuracy of the numerical method k are known, a simple linear extrapolation formula (17) eliminates the leading term from error expansion Eq.(16) and leads to reasonably accurate results [10,11].

If theoretical order of accuracy of the numerical method is not known, the ratio

$$\frac{F_{i-2} - F_{i-1}}{F_{i-1} - F_i} = 2^k + O(h_i^{l-k}) \qquad (18)$$

can be obtained, using Eq.(16) and three solutions on a sequence of nested grid $F_{i-2}, F_{i-1}, F_i, h_{i-2}/h_{i-1} = h_{i-1}/h_i = 2$

From Eq.(19) we can easily estimate the theoretical order of accuracy [10]:

$$k \approx k_i = \log\left(\frac{F_{i-2} - F_{i-1}}{F_{i-1} - F_i}\right) / \log(2) \qquad (19)$$

Here k_i is value of observed order of accuracy and Eq.(19) gives experimental method for determining or verifying the value of theoretical order of accuracy k of the method. The proximity of obtained value of observed order of accuracy k_i to theoretical value k is a confirmation of expansion (16) with leading term αh^k and it substantiates the possibility of using extrapolation formula (17) to improve the accuracy of the numerical solutions.

As it was suggested in the previous section, method of initial parameters in differential form uses the classical fourth-order Runge-Kutta method for integration. Therefore, it can be assumed that the theoretical order of accuracy of resulting numerical solutions is $k = 4$**.** In the next section, the following algorithm will be used to estimate the order of accuracy of the numerical method and acceleration of convergence of the numerical solutions.

First of all, it is necessary to find numerical solutions (values of critical load) on a sequence of nested grids $F_i, i = 1,2,3, \ldots$. Then to calculate the values of observed order of accuracy k_i from Eq.(19) for every three successive values F_{i-2}, F_{i-1}, F_i. It should converges to theoretical value $k = 4$. Then for every two successive values F_{i-1}, F_i Richardson extrapolation formula (17) can be used as follows

$$\boldsymbol{R_i = F_i + \frac{F_i - F_{i-1}}{15}} \qquad (20)$$

Moreover, to estimate the rate of convergence of the improved values R_i can be used a formula

$$l \approx l_i = \log\left(\frac{R_{i-2} - R_{i-1}}{R_{i-1} - R_i}\right) / \log(2) \qquad (21)$$

which follows from the Eq.(17) and can be obtained similar to Eq.(19).

5. NUMERICAL RESULTS

In the following the critical loads are converted into non-dimensional form as $p = PL^2/D_0$ in order to examine the effectiveness of the suggested numerical method. Here D_0 is flexural rigidity on

lower end of the column $(x = 0)$. First let us consider the clamped-clamped FG column with flexural rigidity $D(x) = D_0\,(1+x)^2$.

Latter formula covers two subcases:

a) $E - constant, I(x) = (1+x)^2$

b) $E(x) = (1+x),\ I(x) = (1+x)$

The numerical results for first critical load of the column are shown in Table 2. Here $N_i = L/h_i$ is number of divisions of the grid. As it could be expected, the observed order of accuracy k_i convergence to 4. The values of R_4 for $N_4 = 80$ and R_5 for $N_5 = 160$ in the table practically coincide. Thus, it can be concluded that all the signs in the obtained numerical value R_5 in this table are correct. To estimate the order of accuracy of refined values R_i, the values of l_i are proposed in the last column of the tables. As it can be seen from the last column of the table, l_i tends to $l = 6$. Thus, the improved values of R_i have sixth order of convergence.

The critical loads corresponding to the first five buckling modes of the column are given in Table 3. In the same table the results obtained by applying finite element method (FEM) and finite difference method (FDM) are given for $N = 100$. The results obtained in the current study (column F_3) and results of FEM and FDM are compared with R_5 , considering R_5 as exact result. It can be seen from Table 3 that current results (column F_3) are much more close to exact result, despite to lower computational complexity of the current method $(N_3 = 40)$ The eigenvalue problem needed to solve has orders 200 and 100 in the case of FEM and FDM, respectively. Lower accuracy of the FDM can be explained by second order of convergence. The order of convergence of the FEM is four, but this holds good for homogeneous uniform columns only.

i	N_i	F_i	k_i	R_i	l_i
1	10	81.19791	-	-	-
2	20	81.94311	-	81.92612	-
3	40	81.92464	3.787	81.92341	-
4	80	81.92344	3.946	81.92336	5.855
5	160	81.92337	3.986	81.92336	5.961
6	320	81.92336	3.997	81.92336	5.990

Table 2. Critical load for clamped-clamped FG column $(D(x) = D_0\,(1+x)^2)$.

	FEM [6]	FDM [6]	F_3	R_5
p_1	82.5189	81.8908	81.9246	81.9234
p_2	169.3995	168.0204	168.1922	168.1811
p_3	330.8138	327.9361	328.5068	328.4314
p_4	500.5459	495.7357	497.2012	496.9441
p_5	744.6392	736.7941	740.07601	739.2773

Table 3. Comparison of the critical loads corresponding to the first five buckling modes of the clamped-clamped FG column $(D(x) = D_0\,(1+x)^2)$.

In the case of FG columns the accuracy will be reduced, due to piecewise constant flexural rigidity used for elements in [6]. The convergence rate of the current method for FG column is four (see column k_i in Table 2). The refined solution R_i has the rate of convergence six (see column l_i in Table 2). Moreover, the results obtained for first critical load R_5 are compared with the results of exact solution given in [5]. Perfect agreement was observed in the case of different classical boundary conditions.

Next, the critical loads of the FG column with flexural rigidity $D(x) = D_0\,e^{\mu x}$ is considered. In the Table 4 the numerical results for clamped-pinned FG column is presented $(\mu = 1)$. Similarly to previous case, the values of R_4 and R_5 practically coincide. Thus, it can be concluded that all the signs in the obtained numerical value R_5 in Table 4 are correct. As it can be seen from the last column of the Table 4, l_i tends to $l = 6$. Thus, the improved values of R_i have sixth order of convergence. The similar results have been obtained for critical loads FG columns with classical boundary conditions for different values of μ. The obtained values of R_5 for FG columns with different boundary conditions presented in the Table 5.

i	N_i	F_i	k_i	R_i	l_i

1	**10**	**32.582592**	**-**	**-**	**-**
2	**20**	**32.556755**	**-**	**32.555033**	**-**
3	**40**	**32.555032**	**3.906**	**32.554917**	**-**
4	**80**	**32.554923**	**3.976**	**32.554915**	**5.934**
5	**160**	**32.554916**	**3.994**	**32.554915**	**5.982**

Table 4. Critical load for clamped-pinned FG column ($D(x) = D_0\, e^{\mu x}$).

BC	$\mu = -1$	$\mu = 0.5$	$\mu = 1$
C-F	**1.782102**	**2.844778**	**3.241181**
P-P	**5.826546**	**12.587151**	**15.838195**
C-G	**5.972525**	**12.666644**	**16.235007**
C-P	**11.988386**	**25.782548**	**32.554915**
P-C	**11.976284**	**25.785855**	**32.587811**
C-C	**23.490038**	**50.448156**	**63.852545**

Table 5. Critical loads for FG columns ($D(x) = D_0\, e^{\mu x}$).

The results given in the Table 5 coincide completely with numerical results given in [9]. However, in [9] the matrix of the eigenvalue problems has dimensions 121*121, but in the current study, only 2*2 matrix is used (standard Runge-Kutta method is employed for forming the matrix).

6. CONCLUSION

The numerical method for analysis of buckling of FG columns is proposed. The results are compared with the results of FEM, FDM and other numerical methods [5,6,9]. High accuracy of the proposed method has been observed. In future study the results of the proposed method are planned to compare with the results of Haar wavelet based methods [12,13].

7. REFERENCES

1. Timoshenko, S.P. and Gere, J.M. *Theory of elastic stability*. McGraw-Hill, New York, 1961.
2. Alfutov, N.A. *Stability of Elastic Structures*. Springer, Berlin, 2000.
3. Elishakoff, I. *Eigenvalues Of Inhomogenous Structures: Unusual Closed-Form Solutions*, CRC Press, Boca Raton, 2005.
4. Wang, C.M., Wang, C.Y. and Reddy, J.N. *Exact Solutions for Buckling of Structural Members*, CRC Press, Boca Raton, 2005.
5. Eisenberger, M. Buckling loads for variable cross-section members with variable axial forces. *Int. J. Solids Struct.*, 1991, **27**, 135–143.
6. Singh, K.V. and Li, G. Buckling of functionally graded and elastically restrained non-uniform columns. *Composites: Part B*, 2009, **40**, 393–403.
7. Huang, Y., and Li, X.-F. Buckling analysis of nonuniform and axially graded columns with varying flexural rigidity. *J. of Eng. Mechanics*, 2010, **137**, 73-81.
8. Shahba, A. and Rajasekaran, S. Free vibration and stability of tapered Euler–Bernoulli beams made of axially functionally graded materials. *Appl. Math. Modelling*, 2012, **36**, 3094–3111.
9. Yilmaz, Y., Girgin, Z. and Evran, S. Buckling analyses of axially functionally graded nonuniform columns with elastic restraint using a localized differential quadrature method. *Math. Problems in Engineering*, 2013, **2013**, 1–12.
10. Atkinson, K.E. *An Introduction to Numerical Analysis*. Wiley, NY, 1978
11. Marchuk, G.I. and Shaidurov, V.V. *Difference Methods and Their Extrapolations*. Springer, Berlin, 1983.
12. Majak, J., Pohlak, M., Eerme, M. Application of the Haar Wavelet based discretization technique to ortho-tropic plate and shell problems. *Mech. of Composite Mater.*, 2009,**45**(6), 631 - 642.
13. Majak, J., Pohlak, M., Eerme, M., Lepikult, T. Weak formulation based haar wavelet method for solving differential equations. *Applied Math. and Comp.*, 2009, **211**(2), 488 - 494.

ACKNOWLEDGEMENTS

The study has been supported by Estonian Science Foundation Grant ETF9441, target financing project SF0140035s12.

9th International DAAAM Baltic Conference
"INDUSTRIAL ENGINEERING
24-26 April 2014, Tallinn, Estonia

FINITE ELEMENT METHOD AND ITS USABLE APPLICATIONS IN WEAR MODELS DESIGN

Sivitski, A; Põdra, P.

Abstract: *FEM models allow to perform more accurate calculations of contact strength and to predict the wear characters of materials. The prognosis of material behavior under load makes it possible to save resources and to abandon a trial-and-error method. The development of a FEM model as well as operating with FEM programs is a complicated and time-consuming process. The skills of model simplification become more and more important. The shape and the number of elements, moduli of elasticity of materials and contact stiffness parameters should be also considered. At this moment there is no usable application for FEM models creation available for wear calculations. In this paper usable application for contact stress FEM calculations of coated bodies is offered, that can be used by engineers of different areas.*
Key words: Wear of materials; Coatings; FEM Hertz contact and Wear models

1. INTRODUCTION

Sliding wear is one of the most common wear types that takes place in different mechanical contacts. It has been suggested that the dominant parameters that influence the sliding wear rate are loading and sliding parameters of contact [1,2]. The sliding law of contact is easily determined by mechanism kinematics. The calculation of contact stress in the sliding contact area, defined by loading and the shapes of contact bodies, is more complicated process. According to the linear wear models, the volume wear directly depends on normal pressure in the contact. Archard's wear law, first published by Holm [3] and used for dimensionless wear coefficient K calculation, was based on the experimental observations and was initially written in form:

$$\frac{V}{s} = K\frac{F_N}{H}, \quad (1)$$

where V is the volume wear (m^3), s is the sliding distance (m), F_N is the normal load (N) and H is the hardness (Pa).
The more important wear parameter, wear depth h, is calculated by dividing both sides of equation (1) by the apparent contact area:

$$h = kps, \quad (2)$$

where p is the normal contact pressure (Pa) over that particular discrete region, s is sliding distance (m), $k = K/H$ is the dimensional wear coefficient (Pa^{-1}).
The Hertz elastic contact theory [4] has widely been used for contact stress distribution calculations. However, Hertz contact model has assumptions, such as all bodies are considered elastic, the contact between them is ellipse-shaped, frictionless and non-conforming.
For sphere on plane surface contact (see Fig.1) the contact radius r (m) can be given as:

$$r = \sqrt[3]{\frac{3F_N R_1}{4E^*}}, \quad (3)$$

where R_1 is the radius of sphere (m) and E^* is the normalized elasticity modulus (Pa) defined by equation:

$$E^* = \frac{1}{\frac{(1-\mu_1^2)}{E_1} + \frac{(1-\mu_2^2)}{E_2}}, \quad (4)$$

where E_1, E_2 and μ_1, μ_2 are the moduli of elasticity (Pa) and Poisson's ratios of two contact bodies' materials.

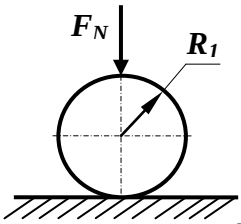

Fig.1. Sphere on plane surface contact.

The normal contact pressure p distribution is dependent on the contact radius r with the maximum value p_{max} (Pa) in the center of the contact area:

$$p_{max} = \frac{3F_N}{2\pi r^2} \quad (5)$$

The numerical method - finite element method (FEM) can be used as an alternative method for contact pressure determination. This method is useful for complex systems, when analytical solutions are not available. FEM is based on considering the bodies as sets of discrete elements and on finding approximate solutions to boundary value problems what is solutions to differential equations that satisfy these boundary conditions, of the elements. The use of FEM together with appropriate wear models is probably the only possible method to be used for coated system wear characteristics calculation.

2. FEM application for sphere-on-plane contact model

2.1 Hertz contact model of uncoated contact

Before making FEM simulations with complicated coated system, Hertz contact model with the simple uncoated bodies must be used in order to verify the FEM model.

FEM program ANSYS Workbench 14.5 was used for Hertz contact model calculations. The axisymmetric 2-D model was created to save the calculation time. The isotropic sphere had an axial modulus of elasticity (E_1) of 200 GPa (steel) and a Poisson's ratio (μ_1) of 0.3. The sphere was pressed vertically to the contact interface with a rigid counterbody – rigid plane (plane surface). The modulus of elasticity of rigid plane (E_2) was assumed to be $+\infty$ and Poisson's ratio (μ_2) equals 0.

After model geometry designed the mesh was configured (see Fig 2). The edge sizing function was used in the contact area to refine the mesh. The greater is the number of elements near contact the better the results will converge within appropriate bounds. Contact element size of $5 \cdot 10^{-6}$ m was selected and number of elements was equal to 20787. This contact element size gives the most optimum normal contact pressure results accuracy along with acceptable duration of numerical simulation and analysis.

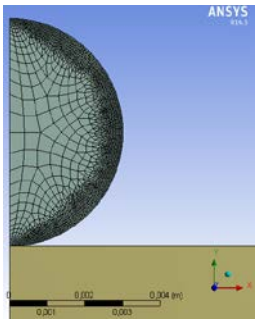

Fig. 2. Mesh of the Hertz contact model.

To prevent the two surfaces from passing through each other, Augmented Lagrange contact formulation method was used. According to Augmented Lagrange method the higher is contact stiffness the lower is penetration [5]:

$$F_N = k_N x_p + \lambda, \quad (6)$$

where k_N is contact normal stiffness (N/m), x_p is surface penetration (m), λ is an extra term (N) that makes this method less sensitive to the magnitude of the contact stiffness in comparison to Pure Penalty method [5]. For general bulk

deformation–dominated problems it is recommended by ANSYS [5] to use the normal contact stiffness factor (FKN). FKN specifies a scaling factor for contact stiffness that is automatically calculated by ANSYS. The scaling factors are usually in the range of FKN = (1...100) between sphere edge and rigid plane surface. The higher is the value of contact normal stiffness, the more accurate is the result of FEM simulation. However, too high FKN values cause difficulties with convergence. Frictionless contact was selected for Hertz contact model as frictionless behaviour allows the bodies to slide relative to one another without any resistance [5]. Sphere was defined to be the contact body. Plane was defined as rigid target body. Finally the asymmetric behaviour of contact was specified. The asymmetric behaviour of contact means that only the contact surfaces are constrained from penetrating the target surfaces. The normal force of F_N = 1 N and sphere radius R_1 = 0.003 m were used in FEM simulation. In tables 1 and 2 the results of analytical and numerical contact radius and maximum normal contact pressure are presented.

	Analytical	**Numerical**	**Relative error (%)**
Contact radius r, (mm)	**0.0217**	0.022	4.4

Table 1. Analytical and numerical results of contact radius r, (mm), FKN = 10.

	Analytical	**Numerical**	**Relative error (%)**
Normal contact pressure p_{max}, (MPa)	**1013**	987 (acc. to r value) 1002	2.6

Table 2. Analytical and numerical results of maximum normal contact pressure p_{max}, (MPa), FKN = 10.

According to the ANSYS solution results, the relative error of the normal contact pressure numerical calculation is 2.6 %. The optimal value of FKN = 10 was selected previously from a number of Hertz contact simulation results with different FKN values (see Table 3).

	FKN =1	**FKN =10**	**FKN =100**
Numerical normal contact pressure p_{max}, (MPa)	899	**1002**	1020

Table 3. Numerical results of maximum normal contact pressure p_{max}, (MPa) for different FKN values.

Figure 3 demonstrates the FEM distribution of normal contact pressure in the contact area if FKN = 10.

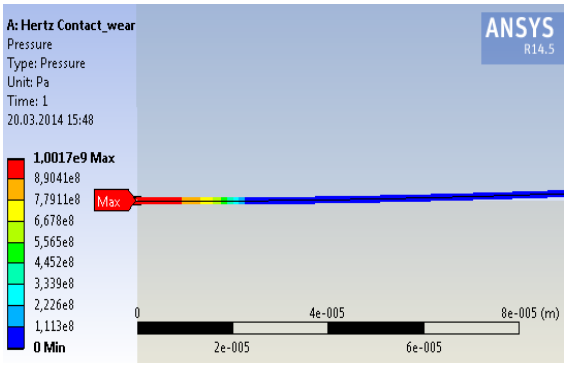

Fig. 3. Normal contact pressure distribution in Hertz contact (FKN = 10).

Result of the numerical simulation of uncoated Hertz contact revealed that optimal number of elements, element size and contact normal stiffness values are critical for normal contact pressure numerical calculations.

2.2 Sphere–on–plane contact model for coated contact

Hertz elastic contact theory formulae can be applied only in case of uncoated systems. Experimental research is therefore mostly used for coated systems wear characteristics analysis. Using FEM numerical method for coated bodies wear simulation is therefore highly interesting. Although sliding wear is affected by many aspects, such as substrate and coating materials physical and chemical properties, sliding velocity, wear test duration, temperature and humidity etc., the normal contact pressure associated with normal loading and contact bodies shapes is one of the most important parameters that should be determined. The use of FEM numerical

simulations for coated systems contact pressure prognosis helps to define the most suitable coatings for different substrate materials.

In this work coated sphere on rigid uncoated plane contact model was done with the coated sphere radius R_1 = 0.003 m and the normal force F_N = 1 N as before.

Substrate type	Substrate material designation	Hardness H_1 (HV)	Modulus of elasticity E_1 (GPa)
SF CWTS	Weartec™	843 HV0.01	199
PM CWTS	Vanadis 6	843 HV0.01	210
NS	38CrMoAl8	850 HV0.01	300
HM	H15 (WC-15Co)	1555 HV0.3	590

Table 4. Mechanical properties of substrate materials.

Mechanical properties of investigated substrate materials are presented in Table 4. Modulus of elasticity of sphere material varied from 200 GPa for cold work tool steels (CWTS), 300 GPa for nitrided steel (NS) up to 590 GPa for hardmetal (HM) and Poisson's ratio was set as 0.3 for all materials. Two types of coatings from our previous experimental research [6] were selected for simulations (see Table 5).

Coating	Type	Nano-hardness H (GPa)	Modulus of elasticity E (GPa)	E/H ratio
TiCN	Gradient	26.6±1.4	500±9.0	18.8
AlTiN	Gradient	23.8±1.0	336±13	14.1

Table 5. Mechanical properties of coatings.

These coatings' types represent the highest and the lowest modulus of elasticity of coatings used for CWTS, NS and HM. For sliding and indentation fatigue wear both elastic modulus and hardness should be taken into account. Also the E/H ratio as the limit of elastic behavior in a surface contact should be considered in this research. Studies [7,8] have proven the importance of high hardness in sliding wear. The influence of modulus of elasticity on wear resistance is still not properly explored. However some researchers [9,10,11] have found that wear resistance increases with modulus of elasticity increase. Materials with a higher modulus of elasticity usually have higher hardness.

Previous experimental research [6] revealed that coatings with lower modulus of elasticity and E/H ratio like AlTiN have lower dimensional coefficient of wear (CoW) k (mm^3/Nm) on substrates with higher modulus of elasticity (HM) (see Table 6).

	TiCN/ CWTS	TiCN/ HM	AlTiN/ CWTS	AlTiN/ HM
1. CoW k (mm^3/Nm);	$2{,}2\cdot10^{-5}$	-	$7{,}6\cdot10^{-5}$	-
2. CoW k (mm^3/Nm);	-	$1\cdot10^{-5}$	-	$6{,}9\cdot10^{-5}$

Table 6. Coefficient of wear (CoW) k of different substrate and coating combinations of 1. pin–on–disk (PoD) and 2. ball–on–disk (BoD) test with normal contact pressure comparable to current simulation results [6].

According to indentation testing (INSTRON 8800, 500 N for CWTS and 100 N for NS, stress ratio R = 0.1) and adhesion testing (Rockwell C, conical geometry angle 120°, tip radius of 200 µm) [6] results the adhesion of gradient coatings on CWTS increases with E/H ratio value increment (Fig. 4 *a*) and Fig. 5 *a*)). Conversely, higher values of coatings E/H on NS cause delamination of the coating (Fig. 4 c)).

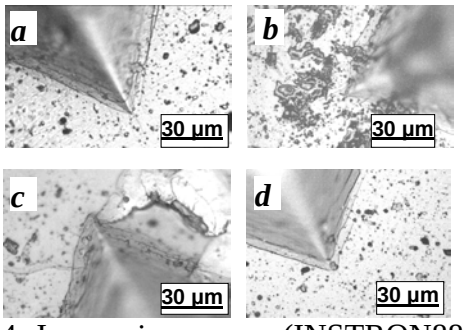

Fig 4. Impression corner (INSTRON8800) of coating (1 cycle) and crack evaluation

criteria. a) TiCN/CWTS – 0 criteria; b) AlTiN/CWTS – II criteria; c) TiCN/NS – VI criteria; d) AlTiN/NS – I criteria.

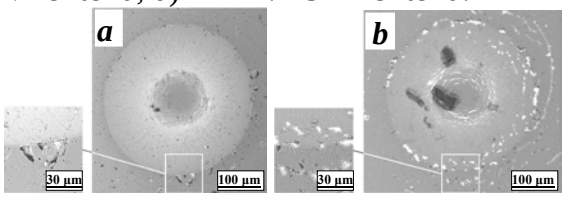

Fig. 5. SEM micrographs of the adhesion test of coatings a) TiCN/CWTS – failiure class 1; b) AlTiN/CWTS – class 2 [6].

For simulation of coated system contact pressure coating thickness of 10 µm was used. Minimum mesh element size was selected as $3 \cdot 10^{-6}$ m (see Fig. 6). Number of elements was defined as 10939. After meshing, optimal contact normal stiffness of bonded contact between coating and substrate was defined. Both substrate and coating modulus of elasticity was set to 200 GPa. FKN values from 0.01 to 1 were analyzed to find the optimal p_{max} value which correlates to analytical p_{max} = 1013 MPa.

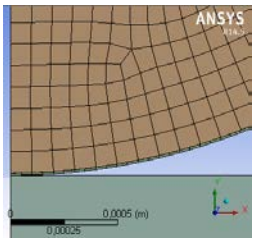

Fig. 6. Coated systems contact model mesh.

The optimal value of contact normal stiffness factor of coating and substrate contact was defined FKN = 0.2 (Fig. 7). The maximum numerical normal contact pressure was calculated p_{max} = 1070 MPa.

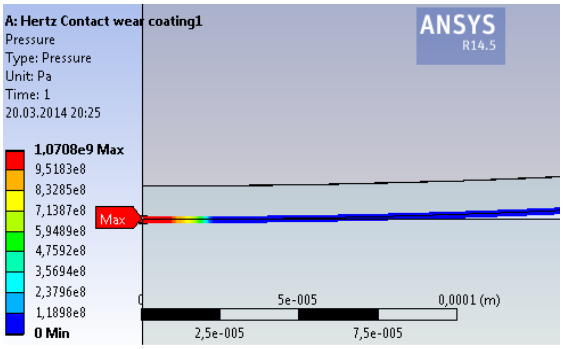

Fig. 7. Coated system contact model normal contact pressure distribution.

The maximum normal contact pressure of sphere materials and substrate/coating combinations is presented in Fig. 8. For comparison the analytical maximum values of normal contact pressure of uncoated spheres were calculated p_{max} = 1013 MPa, p_{max} = 1320 MPa and p_{max} = 2080 MPa for CWTS, NS and HM respectively (Fig.8).

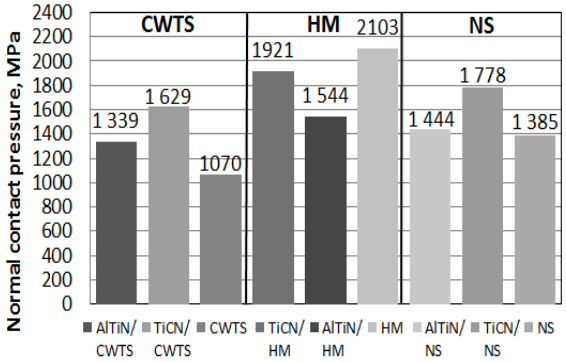

Fig. 8. Maximum normal contact pressure of different substrate/coating combinations.

Soft AlTiN coating decreased significantly the numerical value of HM's maximum normal contact pressure from p_{max} = 2103 MPa to p_{max} = 1544 MPa. On the contrary TiCN coating with highest hardness and *E/H* ratio showed practically the same value of normal contact pressure as AlTiN coating on CWTS. Having a higher hardness value, TiCN performs better on CWTS. Similarly to research [6,12] hard coating (with high *E/H* ratio) significantly deforms on soft substrate as stress is easily dispersed underneath. In spite of normal load increase, the deformation of the interface between the coating and substrate is smaller than in case of a soft coating on a hard substrate. Due to the last fact, delamination of coating can not easily arise (Fig. 4 *a*) and 5 *a*)). The soft coating (with low *E/H* ratio) on a hard substrate experiences significant deformation. If normal force does not exceed some critical value, the soft coating will perform well (Fig. 4 d)). Increase of the normal load leads to straining of adhesive interface between the coating and substrate that leads to cracking and delamination.

The results of simulations of sphere–on–plane contact model show that hard coating performs better on soft substrates and soft coatings on hard substrates. The results of FEM simulation correlate with experimental sliding wear results with comparable numerical values of normal contact pressure.

3. CONCLUSION

FEM numerical calculations can be successfully used for normal contact pressure prediction of coated bodies system. In this work the normal contact pressure of sphere and rigid plane surface contact was investigated. The results showed that the accuracy of the numerical calculations depends on the number and size of contact elements and also on the contact normal stiffness. The numerical method application for coated system normal contact stress prediction makes it possible to save resources and decrease the number of experiments in wear analysis. The created FEM contact model can be applied for normal contact pressure calculation of different coating and substrates combinations. This contact model demonstrates the influence of substrate/coating physical properties and geometrical parameters on the normal contact pressure distribution in sliding contact.

REFERENCES

1. Põdra, P. Andersson, S. Simulating sliding wear with finite element method. *Tribol. Int*., 1999, **32**, 71–81.

2. Põdra, P. Andersson, S. Finite element analysis wear simulation of a conical spinning contact considering surface topography. *Wear*, 1999, **224**, 13–21.

3. Holm, R. *Electric contacts*. Almqvist & Wiksells Boktyckeri AB, Uppsala, 1946.

4. Halling, J. *Principles of Tribology*. Macmillan, London, 1975.

5. Mechanical ANSYS Structural Nonlinearities. Introduction to Contact. Release 13.0. December 2010. http://inside.mines.edu/~apetrell/ENME442/Labs/1301_ENME442_lab6_lecture.pdf (14.03.14)

6. Sivitski, A. *Sliding Wear of PVD Hard Coatings: Fatigue and Measurement Aspects*. Ph. D thesis. TUT Press, Tallinn, 2010.

7. Bouzakis, K.-D. Hadjiyiannis, S. Skordaris, G. Mirisidis, I. Michailidis, N. Efstathiou, K. Pavlidou, E. Erkens, G. Cremer, R. Rambadt, S. Wirth, I. The effect of coating thickness, mechanical strength and hardness properties on the milling performance of PVD coated cemented carbides inserts. *Surf. Coating Tech.*, 2004, **177**–**178**, 657– 664.

8. Richardson, R. C. D. The wear of metals by relatively soft abrasives. *Wear*, 1968, **11**, 245.

9. Lancaster, J. K. The relationship between the wear of carbon brush materials and their elastic moduli. *Br. J. Appl. Phys*., 1964, **14**, 497.

10. Spurr, R. T. Newcombe, T. P. The friction and wear of various materials sliding against unlubricated surfaces of different types and degrees of roughness, in: *Proceedings of the Conf. on Lubrication and Wear Inst. of Mech. Eng. s*, London, 1957, Inst. Mech. Eng. 269.

11. Leyland, A. Matthews, A. On the significance of the H/E ratio in wear control: a nanocomposite coating approach to optimised tribological behaviour. *Wear*, 2000, **246**, **1–2**, 1–11.

12. Jiang, H. *Experimental and numerical study of polymer scratch behavior*. Ph.D thesis. Texas A&M University, 2009.

AUTHORS

Alina Sivitski
Ph. D in eng. sciences Material Science, 2010. Department of Mechatronics, Tallinn University of Technology (TUT), Estonia. E-mail: alina.sivitski@ttu.ee

Priit Põdra
Ph. D in eng. sciences, Machine elements, 1997, Kungliga Tekniska Högskolan, Stockholm, Sweden. Department of Mechatronics, TUT, Estonia. E-mail: priit.podra@ttu.ee

II PRODUCTION ENGINEERING & MANAGEMENT

9th International DAAAM Baltic Conference
"INDUSTRIAL ENGINEERING"
24-26 April 2014, Tallinn, Estonia

GREEN FRAMEWORK DEVELOPMENT FOR USED INDUSTRIAL EQUIPMENT

Bashkite, V. & Karaulova, T.

Abstract: *Current research is focused on the decision-making framework development with Lean and Green Manufacturing tools and End-of-Life scenario consideration. A specific mechanism was developed for used industrial equipment life cycle extension in order to save money, nature, and society. The proposed framework makes business more profitable by including an innovative approach of using complex TRIZ to make it more universal and easy to use for the largest variation of used industrial products. Development of an approach for used industrial product assessment improves company inventory controllability and utilization that in turn minimizes environmental impact and resource consumption during the entire product cycle.*

Key words: Green Manufacturing (GM), Used equipment, Life Cycle Analysis (LCA), End-of-Life (EOL) strategy, Theory of Inventive Problem Solving (TRIZ)

1. INTRODUCTION

Modern trends in the manufacturing world are seeking innovative solutions and non-standard approaches to achieve also environmental benefits. Conventional and commonly used manufacturing tools cannot take control over environmental impact.

"Green Manufacturing paradigm covers the whole life cycle of product, from requirements specification, design, manufacturing, and maintenance to final discarding" [1].

Elaboration of green methodologies is a very important step toward sustainable manufacturing development, which must be socially equitable, economically viable, and environmentally sound. This research is focused on the development of the GM framework for the evaluation of the actual state of used products, such as industrial equipment and the probability of different EOL (End-of-Life) scenarios. The specific mechanism is evolved for their life cycle extension in order to save money, nature, and society. The improvement of GM process quality and simultaneous reduction of cost, pollution and the environmental footprint seeks the implementation of non-standard solutions.

There are certain rules and principles how companies can become "greener", for example, 10 Golden Rules by Dr. Conrad Luttropp [2], 12 Green Engineering principles by Zimmerman [3]. In the current research they are used for the Green Matrix elaboration of an innovation-oriented approach.

This research is aimed to develop an approach towards a maximum utilization of existing industrial equipment resources at production facility within different manufacturing enterprises. The objective is green framework development for the assessment and extension of industrial equipment life cycle. The proposed framework makes SME business more profitable by using an innovation-oriented complex TRIZ to make it more universal and easy to use for the largest variation of used industrial products.

By developing the green framework, it is very important to decide at some point if it is worth it to remanufacture the current

equipment and give it the next life? GM principles are based on three main ideas – the decision must satisfy the manufacturer from economic, ecological, and social points of view [4].

2. EOL STRATEGIES FOR INDUSTRIAL EQUIPMENT

The aim of all the EOL strategies described above is to reduce the ecological impact of the discarded products, to reduce the use of virgin materials and to decrease the total amount of waste. These strategies can be classified according a specific hierarchy. According to Lansink et al., the ecological hierarchy of EOL strategies is as follows from Fig.1 [5].

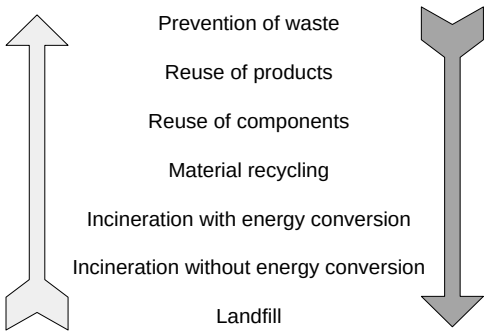

Fig.1. Ecological hierarchy of EOL options

The development strategy of eco-industrial as a basis of circular economy is moving towards closing processing and manufacturing loops in industrial systems. In order to meet the same targets for used industrial equipment, the closed loops can be achieved by implementing two ways. One approach is the realization of different EOL strategies in individual case studies what can show benefit specifically for that unit.

Very important research was conducted by Brazilian researchers Saavedra, Y. M. B., Barquet, A. P. B., Rozenfeld, H., Forcellini, F. a., & Ometto, A. R. and the exact definitions of EOL scenarios with references to the experts in this area are presented in Table 1 [6].

EOL	Main characteristics
Reuse	Products are used more than once. There is no preventative repair done and possible problems after its first life can be obtained. Reuse has no influence on product's quality, anyway it is not new.
Repair	Products' out-of-order parts are replaced and the functionality is recovered. The quality level of the new components is high, the whole item has extended the life cycle.
Refurbishment Recondition	Product major components are rebuilt to a working state. The quality level is intermediate and the life extension level is high. During this procedure there is no item upgrade to the latest functionality or technology.
Recycle	Recycle is the friendlier option from environmental impact point of view. However, the high energy, time and material consuming procedure among other options.
Cannibalization	"Recovering the used parts of products and quality depends on the EOL strategies that will be used".
Remanufacture	Remanufactured item has the same performance and quality level what is returned during this procedure with an accordance with the OEM's specification of the same new product.

Table 1. End of Life strategies

Another is the reverse logistics concept combined with EOL strategies that can be seen in the industry [7]. According to the most recent findings reviewed in these papers, the best EOL strategy for industrial equipment to prolong its life cycle is a corporation of take-back approach with the remanufacturing concept. This method is widely used in industries all over the world. Combination of remanufacturing end-of-life strategy and take-back approach

can save up to 40-60% of the spending in comparison with absolutely new item production by putting about 20% of the effort. It has been reported by many researches [8], [9] and other. The target in this research is to develop an internal tool for EOL strategy validation without implementing a take-back approach.

3. BASIC CONCEPTS OF THE RESEARCH

The main decision-making framework of the research is shown in Fig 2. It is divided into three stages:

- Calculate - Equipment state definition,
- Analyze - Remanufacturing advisability
- Innovate - Innovative solution search.

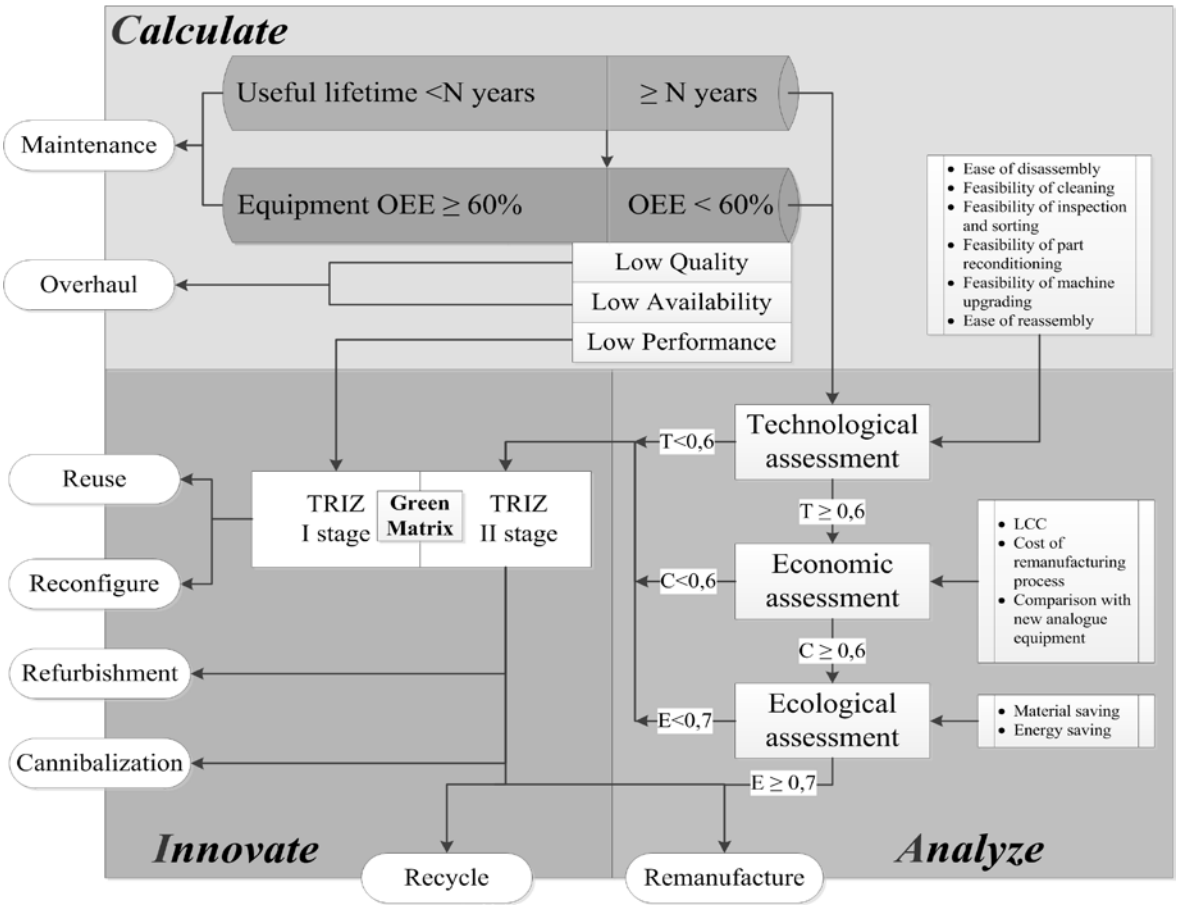

Fig.2. Decision-making framework for used industrial equipment LCA

The first part is mostly considered as a Lean tool, such as OEE, and equipment age. The age of used industrial equipment is taken into account as the primary criterion of the Calculate part. This will give the needed separation between the cases. Definitely, the first measured criterion is actually OEE All the equations of OEE calculation are presented in [10]. In the general scheme, the total OEE rate is 60% according to overall world practice in manufacturing enterprises [11].

The second part must be used if the right solution could not be found in the first part or as an alternative solution. The method for evaluating the remanufacturability of spent industrial equipment is improved and adapted from Chinese researchers: Du, Y., Cao, H., Liu, F., Li, C., & Chen, X. evaluation method for used machine tools [12]. The idea is to take into consideration three main factors: technological, economic and of course, environmental for spent industrial equipment remanufacturability benefits

assessment. The Chinese researchers added the "machine upgrading" part into technology assessment. Definitely, it is very important to consider an upgrading opportunity during the remanufacturing process. The economic issue is rated from the Life Cycle Cost (LCC) perspective, the aspect of remanufacturing cost and comparison with an analogue of new equipment. This part was adapted and improved by involving the Heinz calculation model [13] and risk analysis to obtain more precise results. The environmental benefits of used equipment remanufacturing are assessed in terms of energy and material saving.

In the Table 2 are introduced the criteria for technological, economic and environmental assessment of used industrial equipment [12].

Criteria	Index	μ, feasibility	ω, weight
Technological assessment	Ease of disassembly	μ_d	ω_d
	Feasibility of cleaning	μ_c	ω_c
	Feasibility of inspection and sorting	μ_i	ω_i
	Feasibility of part reconditioning	μ_r	ω_r
	Feasibility of machine upgrading	μ_u	ω_u
	Ease of reassembly	μ_a	ω_a
Economic assessment	Life Cycle Cost (LCC)	C_1	
	Cost of remanufacturing process	C_2	
	Overhead cost of machine tool remanufacturing	C_3	
	Total cost of equipment remanufacturing C_R	μ_e	
Environment	Material saving	μ_m	ω_m
	Energy saving	μ_s	ω_s
	Pollution reduction	μ_p	ω_p

Table 2 The criteria for technological, economic and environmental assessment of used industrial equipment

The technological assessment should be estimated in terms of the feasibility of the whole remanufacturing process. The standard remanufacturing process includes *disassembly, cleaning, inspection and sorting, part reconditioning, equipment upgrading, and reassembly* [12]. The criterion of technological assessment can be calculated using the following equation:

$$T = \mu_d\omega_d + \mu_c\omega_c + \mu_i\omega_i + \mu_r\omega_r + \mu_u\omega_u + \mu_a\omega_a \quad (1)$$

For weight scheme determination for the remanufacturability of used equipment is used method of AHP [14]. LCC is calculated according to [15] and [16]. During the stage of economic assessment it is essential to compare the remanufactured product with the new analogue one.

The third stage is dedicated to innovative solution finding by the introduction of various TRIZ tools. It was one of the major points to combine TRIZ Contradiction Matrix with 40 Principles [17] with Green Engineering (GE) 12 principles [3]. The aim was to find a fast and relevant way to solve contradictions that would somehow be linked to environmental issues. At least it is important to find the way to overcome the psychological inertia concerning ecological issues. One possible solution is to integrate GE 12 principles into GM philosophy through the TRIZ Contradiction Matrix. The concept itself was derived during the Lean&Green Waste Matrix development in [18]. Matrix was elaborated and presented in Fig. 3.

Using TRIZ Matrix for Green Manufacturing can be shown on the example one Estonian machinery company. Company has different types of machines, but mostly and commonly used are lathes and milling machines. Machinery useful life cycle is 15-20 years. Of course, the oldest equipment is already remanufactured many times and has almost all new components. The average age for lathes is 26 years and 33 years for the milling machines respectively. The overall tendency is seen in Table 3.

Improving / Worsening	21: Power	22: Loss of energy	23: Loss of substance	24: Loss of Information	25: Loss of time	26: Quantity of substance	27: Reliability	28: Measurement accuracy	29: Manufacturing precision	30: Object-affected harmful	31: Object-generated harmful	32: Ease of manufacture	33: Ease of operation	34: Ease of repair	35: Adaptability or versatility	36: Device complexity	37: Difficulty of detecting	38: Extent of automation	39: Productivity
21: Power	X	10, 35,38	18, 27, 28, 38	10, 19	6, 10, 20, 35	4, 19, 34	19, 24, 26, 31	2, 15, 22	2, 32	2, 19, 22, 31	2, 35, 18	10, 26, 34	10, 26, 35	2, 10, 34, 35	17, 19, 34	19, 20, 30, 34	16, 19, 35	2, 17, 28	28, 34, 35
22: Loss of energy	3, 38	X	2, 27, 35, 37	10, 19	7, 10, 18, 32	7, 18, 25	10, 11, 35	32	-	2, 21, 22, 35	2, 21, 22, 35	-	1, 32, 35	2, 19	-	7, 23	3, 15, 23, 35	2	10, 28, 29, 35
23: Loss of substance	18, 27, 28, 38	2, 27, 31, 35	X	-	10, 15, 18, 35	3, 6, 10, 24	10, 29, 35, 39	16, 28, 31, 34	10, 24, 31, 35	22, 30, 33, 40	1, 10, 29, 34	15, 33, 34	2, 24, 28, 32	2, 27, 34, 35	2, 10, 15	10, 24, 28, 35	10, 13, 18, 35	10, 18, 35	10, 23, 28, 35
24: Loss of Information	10, 19	10, 19	-	X	24, 26, 28, 32	24, 28, 35	10, 23, 28	-	-	1, 10, 22	10, 21, 22	32	22, 27	-	-	-	33, 35	35	13, 15, 23

Fig. 3. Fragment of TRIZ Matrix for Green Manufacturing

Since 2007 the downtime recurrence and time spent on repairs is just growing. In 6 years it is almost doubled for both types of machines.

Average repairing cost of a machine tool *(€)*						
	First period 2007 – 2009			Second period 2010–2012		
	2007	2008	2009	2010	2011	2012
Lather machine	2 980	3 015	3 030	3 080	3 140	3 190
Total cost during period	9 025			9 410		
Milling machine	3 350	3 400	3 410	3 460	3 530	3 580
Total cost during period	10 160			10 570		

Table 3. Repairing cost of equipment.

The biggest fault for lathes is setup. The milling machines are suffering mostly from electric faults and the second one is again setup. In the section of decision searching process, the main focus is on setup fault by solving defined technical contradiction between improving factors "ease of operation" and worsening "adaptability or versatility". The solution can help to prolong useful life span of lathes and milling machines. It will be the alternative option what can be also taken into account during decision making procedure or somehow combined with the main proposal. According to developed TRIZ Matrix for Green Manufacturing (Fig. 3) the following technical contradiction can be solved by using 4 different principles of TRIZ. Matrix is giving principles: 15, 34, 1 and 16 shown in Fig. 4.

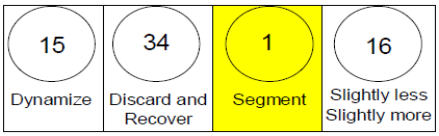

Fig. 4. Solution for "setup" fault by using TRIZ Matrix

This time all options can be used and explained. The third option "Segment" looks good due to it is not showing direction to EOL strategies, such as 3R (reduce/reuse/ recycle). For example, next possible extra options can be added to general decision, such as the manufacturing process can be divided (separated) among different machines. This will reduces the number of operations for one machine. In addition machines will be used less and the problematic spare parts will have less stress during setups. Another option is to group machines according to their specification and technical problems and tries to separate products according to that in order to keep the quality level and decrease the number of setups.

4. CONSCLUSIONS

The idea was to create a well-ordered approach for the state analysis of the used industrial equipment and possible solution finding. For that reason, the current

research was focused on the development of the decision-making framework with Lean and GM tools and EOL scenario consideration. TRIZ was used as an innovation mechanism for decision-making in the current research. The Green Matrix from the general TRIZ Contradiction Matrix was elaborated to resolve environmental conflicts by using GE principles.

The developed approach must ensure analysis of industrial equipment in the EOL stage and facilitate finding of a right decision for its utilization through the innovative solutions in order to increase the economic and ecological benefits.

5. ACKNOWLEDGEMENTS

Hereby we would like to thank the Estonian Ministry of Education and Research for Grant ETF9460 which supports the research.

6. DATA ABOUT AUTHORS

Department of Machinery TUT,
Viktoria Bashkite
E-mail: viktoria.bashkite@gmail.com
Tatjana Karaulova
E-mail: tatjana.karaulova@ttu.com

7. REFERENCES

1. Cheng Wu., Handbook of Industrial Engineering: Technology and Operation Management, *A Wiley-Interscience Publication John Wiley & Sons, Inc.*, New York, 3rd Edition, 2007
2. Luttropp, C., & Lagerstedt, J. EcoDesign and The Ten Golden Rules: generic advice for merging environmental aspects into product development, *Journal of Cleaner Production, 14*, 2006.
3. Zimmerman, J. B. (n.d.). Green Engineering. 2000
4. Manley, J. B., Anastas, P. T., & Cue, B. W. Frontiers in Green Chemistry: meeting the grand challenges for sustainability in R&D and manufacturing. *Journal of Cleaner Production*, 16(6), 2008, 743–750.
5. Lansink M., Kamer T., Vergaderjaar, 1980, 15 800, nr.21.
6. Saavedra, Y. M. B., Barquet, A. P. B., Rozenfeld, H., Forcellini, F. a., & Ometto, A. R. Remanufacturing in Brazil: case studies on the automotive sector. *Journal of Cleaner Production*, *53*, 2013, 267–276.
7. Shevtshenko, E.; Bashkite, V; Maleki, M.; Wang, Y. Sustainable Design of Material Handling Equipment: A win-win approach for manufacturers and customers. *Mechanika*, 18(5), 2012, 561 - 568.
8. Cohen, M., Replace, rebuild or remanufacture. *Equipment Management*, 1988; 16(1), 22–26.
9. Toensmeier, P. A., Remanufacture does more than just save on investment. *Modern Plastics*, 1992; 69(4), 77–79.
10. Godfrey, P. Overall equipment effectiveness, 81(3), 2002, 109–112
11. **Error! Reference source not found.**
12. Du, Y., Cao, H., Liu, F., Li, C., & Chen, X. An integrated method for evaluating the remanufacturability of used machine tool. *Journal of Cleaner Production*, *20*(1), 2012, 82–91.
13. Heinz P. Bloch, Improving Machinery Reliability, practical machinery management for process plants, Third edition 1998, Volume 1, 250-290.
14. Saaty, T.L., The Analytic Hierarchy Process: Planning, Priority Setting, Resource Allocation. 1980.
15. Bryant, J. E., Pead, E. F., & Spiller, J. V. Elements of Mechanical Equipment life-cycle cost analysis, 177–182.
16. Standard, N. (1996). Life cycle cost for systems and equipment.
17. TRIZ Contradiction Matrix, 40 Principles http://www.innovation-triz.com/TRIZ40
18. Bashkite, V.; Karaulova, T. Integration of Green thinking into Lean fundamentals by Theory of Inventive Problems-Solving tools. *Proceedings of DAAAM International*, Vienna, Austria, EU, Ed. B. Katalinic, 2012, 345 - 350.

9th International DAAAM Baltic Conference
"INDUSTRIAL ENGINEERING"
24-26 April 2014, Tallinn, Estonia

DEVELOPMENT AND APPLICATION OF A HOLISTIC PRODUCTION MONITORING SYSTEM

Eiskop, T.; Snatkin, A. & Kõrgesaar, K., Søren, J.

Abstract: *The main purpose of the current work is to analyse automatic production monitoring systems (PMS) and to propose a holistic framework of a scalable, highly adjustable and affordable, automatic PMS for increasing the competitiveness of small and medium sized enterprises (SME). PMS is a system designed for automatically acquiring relevant data from production processes with an improved efficiency and consistency compared to manual data collection.*
Practical part of the work concentrates on the development and application of this system in a wood processing company.
Keywords: Production monitoring system, real-time information, machine condition monitoring, manufacturing intelligence

1. INTRODUCTION

Importance of flexible reaction on changes in production environment, inputs/outputs and processes with minimal time has been crucial for manufacturing enterprise survival. Furthermore today's demand-driven market rises even more challenges to reduce costs, face higher product complexity and shorter product lifecycle, changing customer demands and increased regulatory compliance [1].
Meeting these demands requires timely and accurate information in regard to the state of production processes.
Gathering such data manually often undermines the reliability and quality of the data and before processing it needs to be entered to a spreadsheet, database or in an ERP system, analysed and visualised for decision making, resulting in a lack of overview in production processes.
Consequences of excessive costs inflicted by production disturbances can be avoided through implementing automatic production monitoring systems (PMS) ensuring stable quality of timely and relevant information for operative reaction on disturbances, reduced labour costs, traceability and motivation for employees.
PMS is commonly known as part of larger Manufacturing Execution Systems (MES) [2].
To avoid paying for extensive functionality, enterprises are forced to develop their own solutions ensuring that all demands of the company are met.
This study proposes a modular, highly configurable, scalable and affordable PMS, based on open-source technologies, allowing manufacturing companies to get near-real-time information about their production processes and environment.

2. AUTOMATIC PRODUCTION MONITORING SYSTEM

Monitoring machine states and production processes is a part of the many functions of MES which acts as an intermediate level between ERP and shop floor.

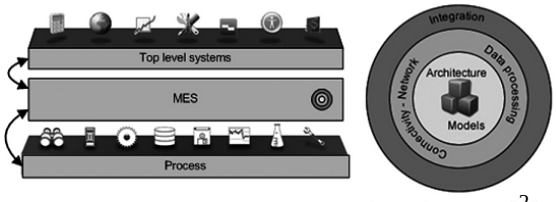

Fig 1. MES environment and its layers [2].

PMS concentrates on some of the aspects of the MES like Data Collection/Acquisition, Performance Analysis, and Process Status monitoring [2].
Although most of the bigger machine producers have fitted their machinery with monitoring hardware and have their own solution for gathering and analysing machine data, a manufacturing site rarely has the equipment of only one producer thus having to deal with several systems and spending time to consolidate the data. Solutions for data consolidation are available, but require expert knowledge for installation and are expensive.

3. GENERAL CONCEPT

A basic production monitoring system should enable at least data collection, storage and presentation [3, 4].
Based on the needs of a specific manufacturing enterprise advanced systems can additionally be set-up to include data analysis, prognostic and data exchange functions.

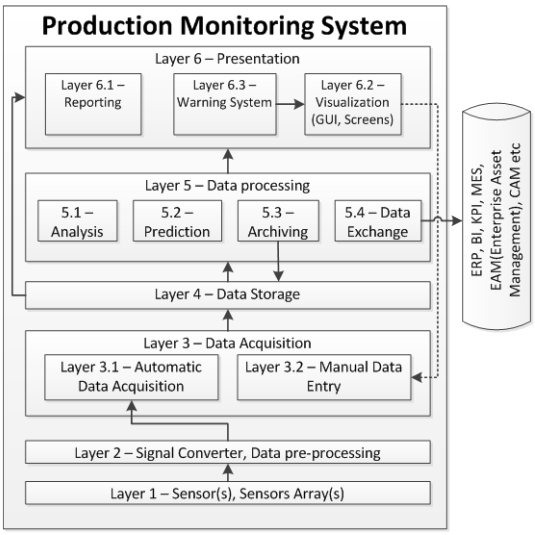

Fig. 2. Basic conception of PMS modules.

The Fig. 2 represents different levels of PMS concept: Sensor, Sensors Array; Signal converter; Data pre-processing; Data Acquisition; Data Storage; Data Processing and Presentation.

These layers are the main framework of the PMS. Sub-layers are optional functionality that can be selected but are not crucial for the system operation.
Layer 1 - Sensors and/or sensor arrays. Physical sensors for measuring specified parameters. The use of wireless sensors is recommended for quicker installation.
Layer 2 - Signal converters, Data pre-processing. Signal converters receive the raw data from Level 1 and convert it for sending to the next level. Signal converters can be PLC, Field-Programmable gate arrays or open-source electronics prototyping platforms like Arduino or Raspberry Pi.
Layer 3 - Data Acquisition. Data from Level 2 is communicated to level 4 via communications protocols like TCP/IP, ZigBee etc. The possibility for manual data entry should not be excluded since feedback from the personnel can be of great value for later analysis in correlation with the automatic data.
Level 4 - Data storage. Data from the sensors is stored in a database. In this study MySQL was used.
Level 5 - Data processing deals with different types of data manipulation - Data Analysis, Prediction, Archiving and Exchange.
Data analysis module uses statistical methods for finding patterns and trends in gathered data enabling better decision making. Prediction module analyses data with artificial intelligence and neural networks to elaborate a prediction model [12]. Archiving module stores unused or expired data based on the defined rules for increasing performance of the "live" database. Data exchange module enables the configuration of customized reports for exporting data to higher and lower level systems.
Level 6 - Presentation. This level represents the system interface for the users. Reporting module displays the data based on the selections of the user. Warning module receives alert messages from the Analysis module, displays and

records (once the user has acknowledged the alarm) them in the database. Visualisation module is responsible for displaying highly customizable and interactive web-based graphical user interfaces that are compatible with most of the modern internet browsers.

4. APPLICATION ON SHOP FLOOR

Monitoring the production processes and machine condition is not the only part of the holistic PMS. It includes other aspects that can influence the effectiveness of the production. Therefore Environment and Personnel/Asset monitoring options were added to the system (see Fig. 3).

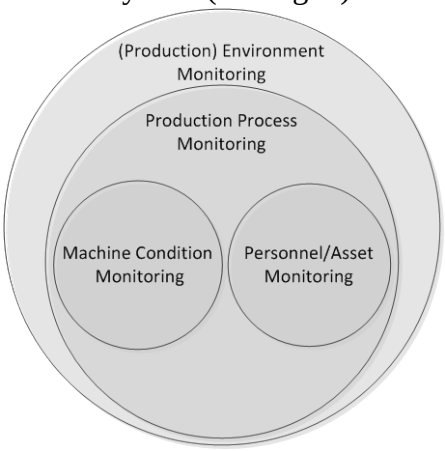

Fig. 3. PMS measurement modules.

Production Environment monitoring allows the manufacturer to monitor the environmental parameters for processes where this aspect is influencing the outcome of the production process. This includes the measurements of humidity, temperature, atmospheric pressure, speed of airflow, Volatile Organic Compound (VOC), gas content in the air (methane, butane, alcohol) etc.

Production process monitoring can be divided into 3 main groups - Product tracking, Process parameters, Process efficiency.

Product tracking involves the identification of a product on the production line, thus revealing the completion stage of the product. This is in most cases done by attaching either a barcode or RFID tag to the product and is more common in custom and mass-customization manufacturing.

Process parameter monitoring involves the monitoring of process characteristics like speed, temperature and the characteristics of the input and output material – dimensions, quality, temperature, moisture, evaporating gases, etc.

Process efficiency monitoring is evaluating the data that has been gathered and comparing it to set targets. Most common methods are OEE and statistical process control (SPC).

For accurate measurement and increased focus OEE can be broken down to 3 factors - Availability, Productivity and Quality - data for all three should be captured [9]. Machine availability can be easily found by measuring electric current rate of the machine. The workload of the machine can be compared against the readings to the reference limits defined forehand [3, 4]. Another option is to measure the output (pcs/length/volume) cycle time of the production process giving the base data for Performance calculation that is compared usually against machine Nameplate Capacity. Third factor, the Quality, poses challenges for being assessed since quality is (depending on the product) defined by many characteristics – dimension tolerances, surface quality, density, moisture, chemical content. Evaluating the surface quality and the dimensions of the product can be done automatically with smart-cameras that compare the product to a reference picture. Despite the high cost of such solutions the benefits can outweigh the costs since mistakes can be found automatically thus reducing reworking costs and capacity loss, increase production speed and yield [10]. As an alternative the quality can be assessed by production personnel and results of the inspection entered to the system via GUI. The drawback here is the subjective nature of the quality assessment

related to the (e.g. emotionality, tiredness) state of the personnel.

Single minute exchange of Dies is a tool concentrating on changeover optimisation via video analysis allowing significant reduction in changeover times [7]. A camera could be added to the system and set up for recording on request or triggered by an event like a movement or a machine stoppage, allowing quicker analysis of the root causes for availability losses.

Since the idea of the PMS is to support the production and office personnel with sufficient data for decision making and continuous improvement, other methods can be defined based on the enterprise's needs.

Machine Condition Monitoring includes the assessment of machine condition by measuring the current, temperature, vibration and noise level of the machine [8]. Based on these indicators and the Probability of Failure Curve, personnel can assess the need for maintenance and therefore reducing machine downtime and maintenance costs.

Personnel and Asset (Activity/Location) monitoring in production processes is not widely used. The main application was found to be in medical facilities and military. Personnel tracking in manufacturing enterprises could be used for identifying work time, analysing strenuous movements or creating automatic diagrams of machine and production line operator's movements to optimise the work area and reduce the time waste.

Asset location tracking could be useful for tracking forklifts to measure the exact workload and optimize the amount of forklifts used. [14]

There are several possibilities to monitor personnel and assets – RFID, Bluetooth, Infrared, Audible sound, Ultrasound, Wifi triangulation, ZigBee sensor array 2D and 3D trilateration, Kinect movement tracking [11, 12, 13].

Choosing the method for personnel/asset monitoring depends on the environment and the area that needs to be covered. For example Kinect requires direct sight whereas other proposed methods can be extended over vast areas [11, 12, 13]. Combinations of different methods can be used to compensate on the disadvantages of the described methods.

5. CASE STUDY

As a basis for this study an existing self-developed system was used. Presented system is used in day-to-day operations and has proved to be effective. During a 2-month-period, the productivity of production line was increased ~35% (See Fig 3.) compared to the average of 2013.

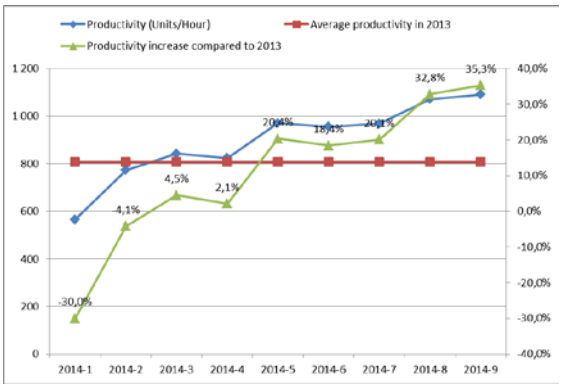

Fig. 4. Productivity (units/hour) on bottleneck production line.

The system is based on the client-server mode where the client can be any device that runs a web browser.

A personal computer was set up to be used as a server. For easy installation and development PHP (Hypertext Pre-processor) development framework XAMPP version 1.6.6a was installed. The framework includes MySQL database version 5.0.27, phpMyAdmin MySQL administration tool version 2.11.7.1, PHP 5.2.0, Apache server version 2.2.3 and FileZilla FTP server 0.9.20. beta.

As described on Fig. 5 the developed PMS uses 2 sensors and additionally data is entered to the system by the production personnel with barcode scanner and via Tablet PC screen. The sensor data is acquired by a PLC which forwards the data

to the server. The data entered manually is saved directly to the database.
Data from the database is processed and presented to the users upon request or updated on the GUIs automatically.

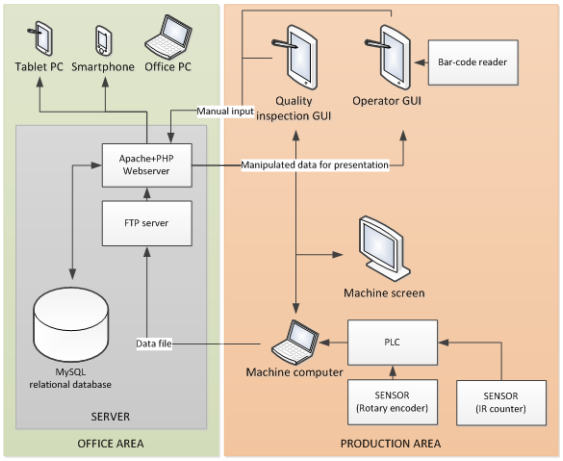

Fig. 5. PMS Information flow

The use of web-based technologies makes the system compatible with a wide range of devices that support the use of graphical interfaces and do not require vast amounts of computing power from the client devices since most of the computing is done by the server, leaving the displaying of the results as the main task for the clients (see Fig. 6).

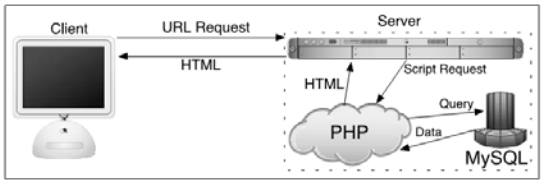

Fig 6. How most dynamic web-pages work [5]

To further reduce the load on the server and the clients, AJAX (Asynchronous JavaScript and XML) technology was used allowing updating specific objects in the GUI based on the specified interval. This enables the use of inexpensive hardware like Raspberry Pi or cheaper Android Tablet PC's as input and displaying devices and increasing the number of clients/machines connected to one server.

5.1 GRAPHICAL USER INTERFACES (GUI)

Several GUIs where programmed to allow the users interaction with the system.
The most important GUI in the system is the **Operator GUI** since only the Operator can quickly react on the system feedback and minimize the cost of interferences in the production process (see Fig. 7). Displayed on a Tablet PC the Operator can get a quick overview of the processes performance in a glimpse and give feedback to the system. The screen is divided into 3 sections (left to right) – Stoppage timeline, Stoppage overview and Shift overview.
Stoppage timeline shows the list of occurred stoppages in chronologic order and allows the operator to specify the reason for the stoppage for latter analysis.
Stoppage overview displays the summary of the timeline events summarising them by type allowing the operator to focus on the biggest losses.
Shift overview presents the following:

- General information about the production process,
- Quality inspection summary,
- Input material registration data.

General shift information includes produced quantities from the start of production and the last cutting tool change, shift duration and machine availability.
Quality inspection summary presents the information about quality assessment of the end product. Displayed in 2 sections – last 10 min (left) and whole shift (right) – gives the operator a general overview as well as the recently made inspection results since the changes might not be noticeable in the scheme of the whole shift enabling the operator to quickly react in the emergence of new issues.
Material registration module enables the operator to register material usage by registering barcodes from the material pallet label. Material characteristics information can later be used for analysing correlations between input material and

output quality and production process parameters.

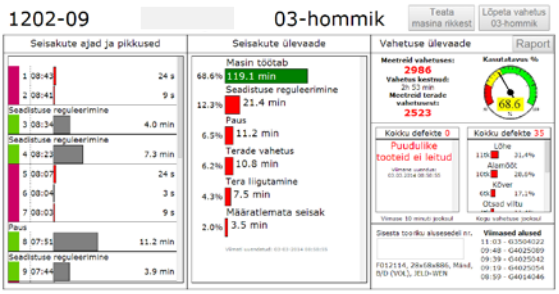

Fig. 7. Operator GUI

Quality GUIs (see Fig. 8) main purpose is the effective gathering of quality data reducing the time needed for processing and presenting real-time feedback to the operator for decision making.
The GUI features are current product description (top), defect description registration (left) and defect summary (right). The buttons on the bottom of the screen are displaying last 10 registrations for double checking and deleting, current/previous shift overview for data correction and the end product change for defining the final product.

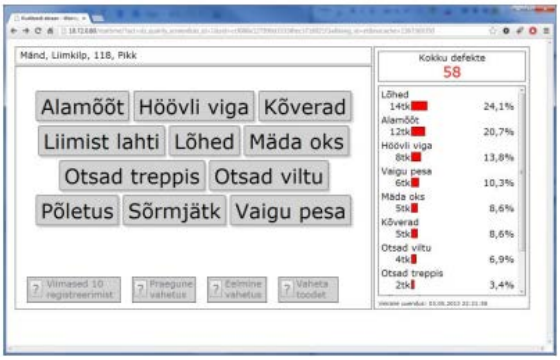

Fig. 8. Quality inspector GUI

The product information can be valuable for assessing the usage of raw material against the final product assuring the optimisation of material yield.
Machine screen is giving a general overview of the process status.
OEE is presented with gauges as 3 factors - Availability, Productivity, Quality (see Fig. 9.) for enabling to concentrate on a specific factor when engaging in root cause analysis, shortening the time for eliminating the root cause [9].

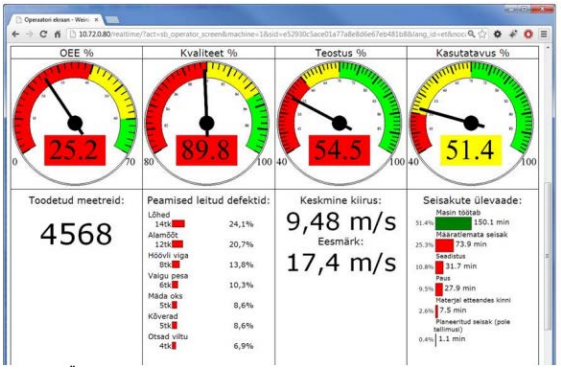

Fig. 9. Machine screen

The multiplication of these 3 factors equals the OEE of the production line [9]. Each factor has additional summary beneath them for a complete overview.

6. FURTHER RESEARCH

To further reduce the costs and facilitate rapid installation of an automatic PMS, the application of open source electronic platforms, cloud-based solutions for data storage and other alternatives should be investigated and tested in manufacturing environment.
Application of modern prognostic methods should be researched for analysing and prognostics purposes. To increase even more the savings generated by the implementation of a PMS, the proposed concept should be tested and optimized for production lines, groups of machines and factories.

7. CONCLUSION

A conceptual model for a holistic Production Monitoring System was presented and the start of practical implementation and development of the system in a manufacturing enterprise was described in a case study.
Implementing a basic PMS has made it possible for the company to increase productivity on a bottleneck line by ~35%

8. ACKNOWLEDGEMENT

This research was supported by Innovative Manufacturing Engineering Systems Competence Centre IMECC (supported by Enterprise Estonia and co-financed by the European Union Regional Development Fund, project EU30006).

9. REFERENCES

1. Corrêa, H., L. Agile manufacturing as 21st Century strategy for improving manufacturing competitiveness. *Agile Manufacturing: The 21st Century Competitive Strategy*, 2001, 2-13.
2. Saenz de Ugarte, B., Ariba, A. and Pellerin, R. Manufacturing execution system – a literature review. *Prod. Plan. Control*, 2009, **20**, 525–539.
3. Snatkin, A., Karjust, K., Majak, J., Aruväli, T. and Eiskop, T. Real time production monitoring system in SME. *Est. J. of Eng.* 2013, **19**, 62-75.
4. Snatkin, A., Karjust, K. and Eiskop, T. (2012). Real time production monitoring system in SME. In:*Proceedings of the 8th*.
5. Ulman, L., *PHP and MySQL for Dynamic Web Sites, 4th edition*. Peachpit Press 2013, 14.
6. Leachman, R., C. Closed-loop measurement of equipment efficiency and equipment capacity. *Advanced Semiconductor Manufacturing Conference and Workshop*, 1995, 115-126.
7. Yash, D., Nagendra, S. Single Minute Exchange of Dies: Literature Review. *International Journal of Lean Thinking*, 2012, **3**, 27-37.
8. Aruväli, T., Otto, T. and Preden, Jürgo. (2012). Modern Monitoring Opportunities in Shopfloor. In:*Annals of DAAAM for 2010 & Proceedings of the 21st International DAAAM Symposium.* Vienna, 2010, 573–578, ISSN 1726-9679.9.
9. Iannone, R., Nenni, E., M. Managing OEE to Optimize Factory Performance. *Operations Management*. 2013, Schiraldi, M. (Ed.), ISBN: 978-953-51-1013-2, InTech.
10. Patel, B., K., Zalte, B., M., Panchal, R., S. Review: Machine vision and its Applications. *IOSR Journal of Electronics and Communication Enginering,* 2013, **7**, 72-77
11. Gu, Y., Lo, A., Niemegeers, I. A Survey of Indoor Positioning Systems for Wireless Personal Networks. *IEEE Communications Surveys & Tutorials, 2009.* **11**, 13-32
12. Noguchi, H., Fukada, H., Mori, T. Object and Human Localization with ZigBee-Based Sensor Devices in a Living Environment. RFID from System to Applications, 2013, Reaz, M, (Ed), ISBN 978-953-51-1143-6, InTech.
12. Stamatis, G., A. Engine Condition Monitoring and Diagnostics. *Progress in Gas Turbine Performance*. 2013, Benini, E. (Ed.), ISBN: 978-953-51-1166-5, InTech,
13. Mautz, R., Tilch, S. Survey of Optical Indoor Positioning Systems. *Indoor Positioning and Indoor Navigation International Conference,* 2011, 1-7, ISBN: 978-1-4577-1805-2.
14. Gosh, S. Anurag, D., Bandyopadhyay S. Mobile Asset Utilization Improvement using Wireless Mesh Network based Real Time Locating System in Manufacturing Industries.*Procedia Computer Science,* 2011, **5** 66-73.

10. CORRESPONDING AUTHORS

MSc. Tanel Eiskop[1]; MSc. Aleksei Snatkin[1]; MSc Kristjan Kõrgesaar[1]; Søren Jorgensen[2];
[1]Department of Machinery, Tallinn University of Technology, Ehitajate tee 5, Tallinn, 19086, Estonia,
[2]Maintenance manager JELD-WEN Baltics and Finland. Diploma in Technical Maintenance management, from Fredericia Marine Engineering College and VIA-University.
E-mail: aleksei.snatkin@gmail.com;
taneleiskop1@gmail.com;
kristjan.korgesaar@gmail.com;
sjr@jeld-wen.biz

9th International DAAAM Baltic Conference
"INDUSTRIAL ENGINEERING"
24-26 April 2014, Tallinn, Estonia

DESIGN PRINCIPLES OF FLEXIBLE MANUFACTURING SYSTEMS

Hermaste, A.; Riives, J.; Sonk, K., Sarkans, M.

Abstract: *Flexible Manufacturing Systems (FMS) has been used already for a long time. Due to increasing competition among companies, use of different kind of flexible production systems is also increasing. The main objectives to implement the FMS in the company are to produce different parts or part families more efficiently. Efficiency in FMS means minimizing system unbalance and maximizing system throughput, while satisfying the technological constraint. Selection of rational FMS layout and system components in preliminary design stage is one the most difficult problem. This paper gives an overview of basic principles and criteria of selecting rational FMS layout and structure.*
Key words: Flexible Manufacturing System, design principles of FMS.

1. INTRODUCTION

Production system is a structural integrated complex of manufacturing equipment, special fixtures and tools; processes and products with the objective to fulfil a production tasks. Production tasks are directly related to the nomenclature of the products. Production system capacity is directly related to the technological possibilities of the equipment and competence of the workers [1].
Customer oriented flexible production management has led to the extensive use of various types of flexible manufacturing systems. Systems development is based on systems engineering [2]. Systems engineering is an interdisciplinary process ensures that the customers' needs are satisfied throughout a systems entire life cycle.
Flexible manufacturing system (FMS) is an automated manufacturing system consisting of multiple CNC machining centres and workstations, automated material handling and storage system and distributed computer system that is interfaced with all components in the system [3].
The FMS automatically transfers pallets between workstations, storage system and loading/unloading system. The core of FMS system is sophisticated control software that can schedule production, manage and transfer programs, and run unmanned production [4]. Installation of an FMS is usually a significant capital investment for the company but there are also many benefits: increased machine utilization, reduced factory floor space, lower manufacturing lead times and high labour productivity [5]. Managing and planning the production in the FMS is very complicated task because each machine can perform many different operations and several part types simultaneously, and each part may have alternative routes [6].
Every single flexible manufacturing system is basically unique and specially made for specific company. During the design process of flexible manufacturing system, the most complicated task is to find most rational structure for FMS and effective way to produce different parts according to the company's production needs and product types [7]. The main criteria to consider are cost of the FMS, payback

period, throughput time, utilization rate, quality of results, etc. Example of typical in-line layout FMS is shown in "Fig. 1".

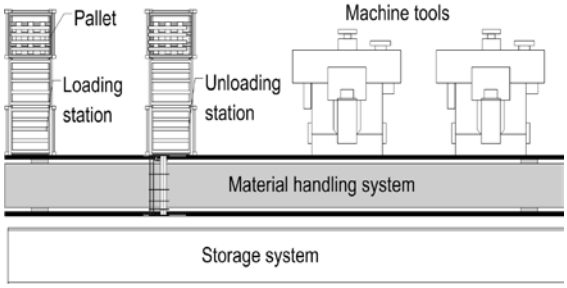

Fig. 1. In-line layout FMS with 2 machine stations.

Most of the published works in this research area focuses on determination of the position of facilities or efficient layout arrangement of FMS cells or machine tools [8, 9]. This research focuses on selection principles of rational FMS structure, by defining the criteria for system design, including data about machines (quantity, main specification), material handling system (type and layout) and storage system (type and size).

2. REPRESENTATION OF PRODUCTION SYSTEM

A production system configuration can be understood as a design task which system components are selected and arranged to form a system. The production system carries out a transformation process for changing the input into determined (task correspondent) output. However, whatever the nature of the business is, the main objective is looking for new ways of adding value either by providing benefits and products that customers are willing to pay more or by combining resources more efficiently to reduce costs. The basic for this task is the manufacturing system engineering (MSE) ontology, what was presented in [10].

For fulfilling a production task, there is necessary to have a production system which formal description is as following [11]:

$$\mathbf{T = \{N, A, S, F, P\}, (1)}$$

Where,

T – production system;

N – components of the system (e.g. 5-axes machining centre, 7-axes machining centre, washing machine, measuring machine);

A – a set of parameters, describing the system and determining the technological capabilities of the system [1]);

S – structure of the system (location of equipment's of the system and the connections between machine tools and storage, see Fig. 2);

F – number of functional connections between the elements of the system (depends of the ontology of manufacturing and defines the essence of single events, see Fig. 3). The number and essence of events depends on used technology, rate of automation and organization of production.

P – number of machining operations, taking place in the system, p1, p2,..., pn (e.g. p1 – milling, p2 - turning, p3 – boring, etc.), depends of technological possibilities of the system.

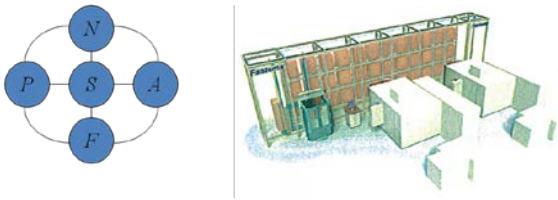

Fig. 2. From abstract description of FMS to its realization.

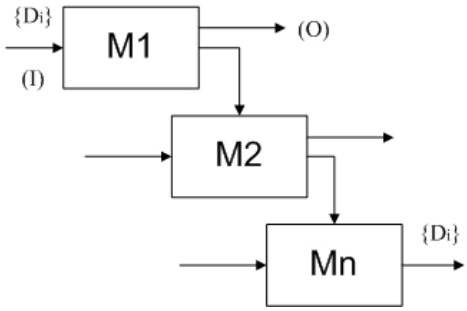

Fig. 3. Manufacturing alternatives

Structure of a FMS or other production systems with its attributes {N, A, P, F} determines technological possibilities of FMS and also preconditions for fulfilling

certain type of orders (the volume of order, delivery time, special type of manufactured products, features, etc.). Technological possibilities determine the diversity and complexity of the products the system can produce, and also determines the cost of the system.

In the process of manufacturing system engineering, the two key questions at the first stage are existing:

- manufacturing alternatives:
  - one-level manufacturing;
  - multi-level manufacturing.
- loading-unloading organisation:
  - automated loading,
  - duo-block automated loading,
  - robot-based loading.

On the basis of Fig. 2 and Fig. 3, it is possible to determine the functionality and technological possibilities of FMS.

3. PROBLEM STATEMENT

Increasing competition is forcing production companies to implement new flexible technologies and increase their automation level. The main problem in automation process is to find most rational and suitable type and structure of flexible manufacturing system for specific company, as every company has different production requirements, production equipment and products.

The design of flexible manufacturing system consists of selecting the best set of resources to satisfy the production requirements during the whole system lifecycle with the maximum expected profit [12].

Design of FMS is complicated and time consuming process, consisting of several stages. The basic problem in the preliminary design stage is to understand, what kind of FMS structure suits the best to manufacture the set of parts or products {Di}, described by the basic characteristics:

- Dimensions,
- Accuracy,
- Production volume,
- Production cycle time,
- Nomenclature (i = 1, 2,...,n).

The goal of this research is to analyse relation principles between products criteria and FMS structure.

4. DESIGN PRINCIPLES OF FMS

The design of FMS focuses on making decisions about system specification for automation of production [13].

The necessary input information for design process of flexible manufacturing system is [14]:

- Technological characteristics of the product family – material, volume, tolerances, type (prismatic, rotational), dimensions, and weight.
- Machining information of the product family – operation type, machining times, required power, required spindle speed, tool life, tool type, tool number.
- Clamping information of the product family – fixture type, fixture size, number of faces on the fixture, number of parts on the fixture.

The main output information of the design process according to the input is:

- Machine type - work cube dimension, loading weight, positioning accuracy, spindle power and speed, tool magazine capacity and type, number of controlled axes, pallet changing system.
- Machine number - number of machines for each machine type in the system.
- Material handling system - rail-guided vehicles, automated guided vehicles (AGV), industrial robots.
- Storage system – dimensions, number of sides, number of levels, number of pallet places, maximum size of pallet place, and number of material pallet places.

- Loading and unloading stations – type of the stations, number of the loading/unloading stations
- System type and layout – layout type, system type

During the design process, different decisions about system configuration has to me made according to the information available as the input.
Generally, design of the flexible manufacturing system consists of the following steps:

- Selection of machine type
- Selection of machine number
- Selection of material handling system
- Selection of storage system
- Selection of type and layout of FMS

To make these selections, some kind of decision making model is needed. Many different FMS decision support system for design process can be found in literature [15], but the output of these systems are not specific type or structure of FMS.
In this research generally, database will be created for the decision making. By analysing a variety of existing flexible manufacturing systems (built by FASTEMS) and products they produce, we can generate a database that will help to make above mentioned selections.
This database contains information about different system configurations and product specifications. Therefore, it is possible to make relations between products and systems.
In configuration design task, the alternative design solutions are concentrated into the special database and the selection criteria lead us to the possible, most suitable and rational solutions.

5. RELATION PRINCIPLES

Relation principles between system and product parameters are as following:

- Machine working cube dimensions depends on part dimensions and fixture dimensions.
- Machine loading weight depends on part weight, fixture weight and pallet weight.
- Machine positioning accuracy depends on dimensional tolerances of part.
- Machine spindle power and speed depends on cutting parameters.
- Tool type depends on part and operation type.
- Tool magazine capacity and type depends on part material, tool life and operation type.
- Number of controlled axes depends on operation type, part type and fixture type.
- Machine pallet changing system depends on material handling system type.
- Number of the machines in the system largely depends on the number of the parts that will be produced per time unit.
- Material handling system depends on part type, dimensions and weight, fixture type, pallet changing system and storage system.
- Storage system depends on type of the material handling system, number of part types, dimensions of the parts, number of machine types; size of the storage system must ensure the unmanned production of a given period.
- The layout and type of flexible manufacturing system depends on number of machines, type of material handling system, type of storage system.

These relation principles are used in the framework of the database to analyse how the product parameters affect the system structure. This information is used for

selection process of most suitable and rational structure of FMS.

6. CONCLUSION

Design principles and relation principles of flexible manufacturing system was described to find most rational FMS structure according to given product family specification.
Further research work is related to the creation of a database and analysis of relation principles to develop a decision model for design of flexible manufacturing system.

7. ACKNOWLEDGEMENTS

This research was supported by Innovative Manufacturing Engineering Systems Competence Centre IMECC, co-financed by European Union Regional Development Fund (project EU30006).

7. REFERENCES

1. Riives, J., Otto, T., Papstel, J. Monitoring of technological resources for extended usage. *Proceedings of the 4th International DAAAM Conference*, Tallinn, 2004
2. Systems Engineering Fundamentals. Defence Acquisition University Press, 2001.
3. Groover, M. P. *Automation, production systems, and computer-integrated manufacturing*, Prentice Hall, 2008.
4. Place for precision. MWP Advanced Manufacturing, May 1, 2012.
5. Shivanand, H. K. *Flexible manufacturing systems*, New Age International, 2006.
6. Mahmudy, W. F., Marian, R. M., Luong, L. H. S. Solving Part Type Selection and Loading Problem in Flexible Manufacturing System Using Real Coded Genetic Algorithms – Part I: Modeling. *World Academy of Science, Engineering and Technology*, 2012, **69**, 773 - 784.
7. Matta, A. *Design of Advanced Manufacturing Systems*. Springer, 2005.
8. Drira, A., Pierreval, H., Hajri-Gabouj, S. Facility layout problems: A survey, *Annual Reviews in Control*, 2007, **31**, 255 - 267.
9. Taho, Y., Brett, A. P., Mingan, T. Layout design for flexible manufacturing systems considering single-loop directional flow patterns, *European Journal of Operational Research*, 2005, **164**, 440 – 455.
10. Lõun, K., Riives, J., Otto, T. Evaluation of the Operation Expedience of Technological Resources in a Manufacturing Network. *Estonian Journal of Engineering*, 2011, 17, pp. 51-65.
11. Lõun, K. Formation of e-Workplace Performance Proceeding from Company's Strategy in the Engineering Industry. Doctoral Thesis, 2013.
12. Terkaj, W., Tolio, T., Valente, A. Design of Focused Flexibility Manufacturing Systems (FFMSs). Design of Flexible Production Systems, 2009, 137-190.
13. Jabal-Ameli, M. S., Moshref-Javadi, M. Concurrent cell formation and layout design using scatter search, *International Journal of Advanced Manufacturing Technology*, 2014, **71**, 1-22.
14. Tolio, T. *Design of Flexible Production Systems. Methodologies and Tools*. Springer-Verlag, Berlin, Heidelberg, 2009.
15. Stam, A., Kuula, M. Selecting a flexible manufacturing system using multiple ctiteria analysis, *International Journal of Production Research*, 1991, **29**, 803-820.

8. CORRESPHONDING AUTHOR

1) MSc. Aigar Hermaste
TUT, Department of Machinery
Ehitajate tee 5, 19086 Tallinn, Estonia
Phone: 372+620 3269,
E-mail: aigar.hermaste@ttu.ee

9th International DAAAM Baltic Conference
"INDUSTRIAL ENGINEERING
24-26 April 2014, Tallinn, Estonia

SELECTING KEY PERFORMANCE INDICATORS WITH SUPPORT OF ENTERPRISE ANALYZE MODEL

Kaganski, S.; Paavel, M. & Lavin, J.

Abstract: *Key performance indicators (KPI) are instruments, which can help companies to get necessary information about enterprise's conditions at current moment and also provide management with further plan of action. In addition, continuous study of metrics supports enterprises with regular development and innovation aspects. However, the main problem that acquires by dealing with metrics is their amount. Number of different indicators is so large, that the possibility of putting them together in one package, which would be used for specific company, is low. The main objective of this study is to analyze the influence of KPIs for product life management (PLM) and production monitoring systems (PMS) on production efficiency and on profit of small and medium enterprises (SME)[1]. One of the subtasks is to create an analyze model for enterprises that will help to understand, what types of KPIs should be studied and focused by management.*
Key words: Key performance indicators (KPI), weight factor analyze, PLM, PMS, SME

1. INTRODUCTION

The objective of this paper is to give an overview of enterprise analyze model (EAM) and its' main concepts and thoughts. The general idea of development the EAM is to simplify the choice of key performance indicators (KPIs) for different and specific small and medium size enterprises (SMEs). The model would help managers to make clear, what data should be collected for further studying and what improvements should be done in the future. During the enormous amount of KPIs (for example, there are databases/libraries, which include 17000 different metrics [2]), it's very difficult to choose, what kind of indicators should be implemented for different enterprises. Despite the fact, that data collection and analyze is one of the main activities of management, the meaning of what to measure, should be the main priority. Managers should know not only what common problems, questions and situations are appearing in SME processes in different fields (not only production, but also logistic, quality etc.), but exactly the main problems in THEIR enterprises.

Through the main KPI's for the certain company the manager can monitor the production line or unit [3], analyze different processes and techniques [4,5] depending on the availability and weight of the specified KPI's.

2. KEY PERFORMANCE INDICATORS

2.1 Definition and meaning

Measurements are important; they are showing for managers the problematic points and are helping to solve different issues for getting benefits. It is essential for companies to determine the pertinent indicators, how they relate to the formulated goals and how they depend on the performed activities [6]. Additionally, indicators can provide managers with action plan and exactly declare, what should be done in the first place.

Company can be compared with living form/organism. When we are talking about health monitoring, then the pressure is measured, also all the results from blood test and other, that can show to the doctors exactly, in what stage the patient is, are analyzed. The same should be done in every commercial organization. Considering the thoughts written above, KPIs are measurements that show the health of company and of its business development system. They combine companies' goals and strategies to its incomes, outcomes and provide management with information of common condition: past, current, future [7].

2.2 The distribution of KPIs by types

To better understand, to simplifier searching and to make right solutions, KPIs need to be categorized or divided into groups or types.

According to Corbin (2009) the type of key performance indicator affects how the measure is used. Additionally, the type of performance measure determines its impact on other performance measures [8].

From the chronological aspect, KPIs can be divided into two types: **leading indicators and lagging indicators** [7].

Leading indicators are activity or task-based metrics that are measured early and can be influenced to affect future outcomes. They are measured today to determine if goals will be met tomorrow, and they are measured early and often enough to allow for changes that can impact the predicted outcomes.

Lagging KPIs are historical measurements that look back to determine if success was achieved. Additionally they are affected by another indicator. Financial measures are lagging: they prove how well the firm has performed. Agency Gross Income (AGI) from new clients is a lagging indicator of business development success [7,8].

Vukomanović, Radujković, Nahod (2010) [9] have named the set of KPIs as Key Performance Results (KPR) and have made own classification:

- KPI-leading performance measures;
- KPO-lagging performance measures;
- PerM-perceptive performance measures.

PerMs are measures that report stakeholders' perception in projects and can be lagging or leading. Usually they are generated through interviews and questionnaires.

Furthermore they have found, that many authors, who are trying to classify indicators, are confused KPIs for KPOs and only few of them, have acknowledged, that there should be additional group PerM (Vukomanovic, 2007) [10].

There is another opportunity for classification KPIs. They can be divided into types/groups depending upon how they should be used and what exactly should they show [11]:

- Strategic/Operational;
  Longer term facilities (strategic) versus shorter term activity (operational)
- Result/driver;
  Depending of the enterprise's implemented changes and activities, metrics can show the result of those actions. The influence on understanding performance is crucial.
- Leading/Lagging (see above);
- Qualitative/quantitative;
  The satisfaction questionnaires of customers or employees can be an example of qualitative metrics. During different surveys, the data would be stored and analyzed. Calculated values will show and describe to managers exactly, what situation is at this moment. In other words, qualitative/quantitative indicators are the real-time measurements, which help to value the situation at the certain period of time. Quantitative KPIs can be used for process optimization. Additional examples of quantitative metrics are: "Employee turnover",

"Units per man-hour" or Maintenance backlog [12].

Effectiveness/efficiency;

In order to measure how much of your targets were reached effectiveness indicators can/should be used. They compare actual to expected values e.g. actual to expected sales, saving on budget etc. Efficiency indicators can measure how "well" your resources (people, machines, money) were performed. [13].

The distribution should simplify the choice of indicators. However, the groups, by which indicators are divided, are wide spreaded and include enormous amount of different KPIs. The question: „Why this or that metrics should be selected? " is still open.

3. ENTERPRISE ANALYSE MODEL (EAM)

The enterprise analyze module is a preparatory phase in KPI selection. It should help to create necessary points for further studying and should show to managers and owners the weakest spots of an enterprise. Concluding from the above written thoughts, the main goals of EAM are:

1) getting common information about enterprise;
2) making clear weak spots;
3) letting know what data should be collected and for what purpose (taking into account weak points).

EAM is module that consists of enterprise mapping and of questionnaire. When we talk about enterprise map (EM) approach, then it was created in 1998 by John Wu and has been used to support different US government agencies and private industries. EM can be compared to geographical map and gives information about location, size, field of actions, missions, visions and etc. of company [14, 15]. Received from mapping, data could be used in getting know what fields are important for company. In addition, with this we can get general information of firm and also make conclusions about necessary actions and points, which should be analyzed during the process. In figure 1 is presented map, which would be used during research for getting data for analyzing. It's a template and during research can be adapted to various SMEs and additional fields can be added.

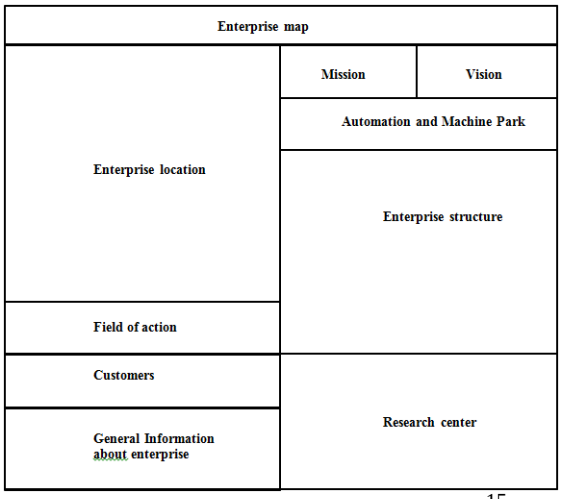

Fig 1. Enterprise map (adapted from [15])

Questionnaire is one of the oldest and mostly spread tools for data collection. The advantages of this research instrument are availability (cheap), quality and standardized answers what makes it really comfortable to use and do not need much effort. Opportunity to choice is guarantying to receive necessary data for further research.

In this study, questions are constructed in this way, that by responding on them, the potential critical fields would be brought out. In addition, to the each query would be added weights to determine significance of the issue. Every answer would have own scale to judge the impact on selecting KPIs. This would provide management with information about state of company on concrete moment and simplify the choice of metrics.

Figure 2 shows the example of questions, which would be used. The questions are form HR block and KPI „turnover rate" is linked to them.

The high turnover rate is not only problem, that companies in Europe and in other countries should face. The Boston Consulting Group in their research is mentioning that in the nearest future, companies will face five critical HR challenges: managing talent, managing demographics, becoming a learning organization, managing work-life balance and managing change and cultural transformation [16].

How many employees (white-collar workers) have left your company during last year?	
a) 0-10	(1)
b) 10-50	(2)
c) 50-100	(3)
d) >100	(4)

What is the average training time for new employee (white-collar workers)?	
a) <1 week	(1)
b) 1-2 weeks	(2)
c) <1 month	(3)
d) >1 month	(4)

	1	**2**	**3**	**4**
1	1	2	3	4
2	2	4	6	8
3	3	6	9	12
4	4	8	12	16

Fig 2. Example of questions and matrix

According weights in right column the matrix can be constructed. This way the impact on indicator „turnover rate“ can be evaluated. Furthermore, the classification of KPIs, which were suggested in previous study [1], would be used for questions' formation.

4. CASE STUDY

The EAM would be tested on real enterprise and data would be collected for further studying. On Figure 3 is illustrated all process/model of selecting KPIs for company. EAM is first phase and during it, the KPI, according collected information, should be selected.

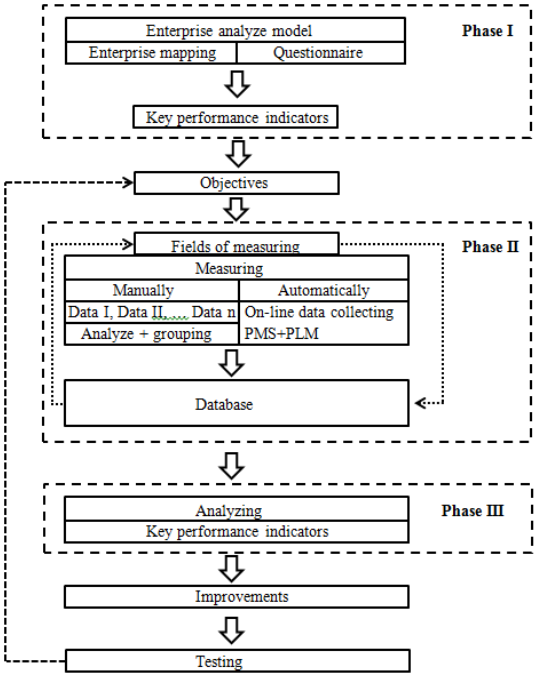

Fig 3. KPI selecting model

The second phase is measurement. First of all the fields of measuring should be selected. Knowledge of critical points from the first phase will reduce the searching sphere and configured metrics will focus attention of management on themselves.

There are two ways of collecting information: the manually and automatically.

However, there are 3 general issues that appear during data collection: untimeliness, inaccuracy and bias. Taking into account that this raw information forms the basis for production reports - and according to them, decisions are made - any problems with the primary data collection can start a chain reaction, which will have crucial impact on enterprise [17]. Taking into account disadvantages of manually information gathering, the automation should be first priority. During manual collection, different questionnaires, surveys will be filled: for example employees before leaving could evaluate employer and fill forms about pluses and minuses of work place. After that data should be sorted and transferred to main database. If forms were on paper, then step by step all should be migrated into electronic format.

In automatic data collection, support of PMS and PLM would be used. During the monitoring process, data in real time from different machines would be received. Wireless sensors will be preferred. PMS, based on wireless sensor nodes, are relatively inexpensive and it can be installed on old and modern manufacturing equipment [18]. Those sensors can eliminate the cost of cables and simplify the installation. Wireless monitoring is used rarely in the shop floors [19].
During PLM the data about products, pre-production processes will be collected. It's a huge complex of IT tools and applications, which support digital design and manufacturing practices in several ways [20].
In addition, all the information about incoming materials, outgoing goods are fixed by scanners (barcodes) and stored in enterprise resource planning (ERP) system. Modern ERP system, if it already has KPI module, can provide management with necessary data, otherwise, it could be directly connected to the database.
Third phase is analyzing. In process of it, KPI will get numerical values, which will used by management for evaluating of enterprises' condition.
Improvements and testing should be done. The process is cycle, so it should be continuing even if goals were achieved.

5. FURTHER RESEARCH

The EAM would be used for collecting data of real company. Taking into account, that the amount of various companies (different field of actions, different structures and etc.), next points/steps should be analyzed:

- optimization of EAM (mapping + questionnaire) for possibility of using by various SMEs;
- optimization and automation of data collection (e-module via Internet for surveys);
- support of PMS and PLM for additional data.

6. CONCLUSION

Considering the productivity, HR and other issues in SME, the measuring, process of collecting data and comparing them with previous (continuous improving), still remains main priority and is real challenge to the management. The EAM and selecting KPIs process in total (figure 2 and 3), were described in this paper. Further steps were defined for next research.
Described methodology and model/module, first of all, would be a good assistance for managers to simplify and automate metrics' selection and secondly, can be used for further studies in this field (process and model development).
Testing and correcting of the model in addition with data flow optimization, have been foreseen as next tasks.

7. ACKNOWLEDGEMENTS

This research was supported by ETF grants 8485 and 7852, targeted financing project SF0140035s12 and Innovative Manufacturing Engineering Systems Competence Centre IMECC (supported by Enterprise Estonia and co-financed by the European Union Regional Development Fund, project EU30006).

8. REFERENCES

1. Kaganski, S; Snatkin, A; Paavel, M; Karjust, K. Selecting the right KPIs for SMEs production with the support of PMS and PLM, *IJRSS vol. no 3 Issue no 1*, 2013.
2. Baroudi, R. *KPI mega library: 17000 key performance indicators*. Scotts Valley, California, USA 2010
3. Snatkin, A.; Karjust, K. and Eiskop, T. (2012). Real time production monitoring system in SME. *In Proceedings of the 8th Int. Conf. of DAAAM Baltic Ind. Eng.,* (Otto, T. ed.) TUT, Tallinn, 2012, 573–578.

4. Lemmik, R.; Karjust, K.; Koov, K. Service oriented and model-driven development methods of information system. In *Proceedings of the 7th int. conf. of DAAAM Baltic Ind. Eng.*, (Küttner, R. ed.) TUT, Tallinn, 2010, pp. 404- 408.
5. Karjust, K.; Küttner, R.; Pääsuke, K. Adaptive web based quotation generic module for SME's. *Proceedings of the 7th international conference of DAAAM Baltic industrial engineering*, 22-24th April, 2010, Tallinn, Estonia 375-380. Tallinn: Tallinn University of Technology
6. Popova, V; Sharpanskykh, A. Modeling organizational performance indicators. *Information Systems, vol. 35, issue 4*, 2010, 505-527.
7. Enns, B. Key performance indicators for new business development. *Critical Briefings for the Business of Persuasion*, February 2005.
8. Cobin, C. Creating effective performance measures, November 1, 2009
9. Vukomanović, Radujković, Nahod. Leading, lagging and perceptive performance measures in the construction industry. *Organization, Technology & Management in Construction: An International Journal, vol.2, No. 1*, 2010, 103-111.
10. Vukomanović, Ceric & Radujković, BSC-EFQM Based Approach for Performance Benchmarking in Construction Industry, *ARCOM 23rd Annual Conference*, 2007.
11. Barburio, F. Performance measurements. A practical guide to KPIs and Benchmarking in public broadcasters. Commonwealth Broadcasting Association, 2001.
12. On Key Performance Indicators (KPIs) [WWW] http://www.smartkpis.com/key-performance-indicator-KPI (17.02.2014)
13. Effectiveness vs efficiency [WWW] http://www.cbsolution.net/techniques/ontarget/effectiveness_vs_efficiency (17.02.2014)
14. Enterprise Architect [WWW] http://www.slideshare.net/wuchizong (18.02.2014)
15. Mapping the Enterprise [WWW] http://slideshare.net/wuchizong/enterprise-map-ee-the-unseen-enterprise (18.02.2014)
16. Jean-Michel Caye, J-N; Strack, R; M. Leicht, M & Villis, U. The future of HR in Europe, Key challenges through 2015, The Boston Consulting Group, May 31, 2007.
17. Wintriss Controls Group, Automated collection of Real-Time production data, 2013.
18. Aruväli, T; Serg, R; Preden, J; Otto, T. In-process determining of the working mode in CNC turning. *Estonian Journal of Engineering*, 2011, **17**, 1, 4-16.
19. Aruväli, T; Preden, J; Otto, T. Modern monitoring opportunities in shopfloor. *Annals of DAAAM for 2010 & Proceedings of the 21-st International DAAAM Symposium*, vol. 21, No. 1, 2010.
20. Qiu, Z.M; Wong, Y.S; Dynamic workflow change in PDM systems, *Computers in Industry 58*, 2007, 453-463.

9. ADDITIONAL DATA ABOUT AUTHORS

MSc. Sergei Kaganski; MSc. Marko Paavel; MSc. Jaak Lavin; Department of Machinery, Tallinn University of Technology, Ehitajate tee 5, Tallinn, 19086, Estonia, E-mail:
sergei.kaganski@outlook.com;
marko.paavel@ttu.ee;
jaak.lavin@imecc.ee.

9th International DAAAM Baltic Conference
"INDUSTRIAL ENGINEERING -
24-26 April 2014, Tallinn, Estonia

BIONIC ASSEMBLY SYSTEM CLOUD: FUNCTIONS, INFORMATION FLOW AND BEHAVIOR

Katalinic, B.; Kukushkin, I. & Haskovic, D.

Abstract: *This paper is focused on further implementation of cloud communication into a control structure concept of Bionic Assembly System (BAS). It presents internal structure of cloud and the information flow between the cloud and active BAS shop floor elements. Investigations are limited on normal working mode. In the comparison to the classical control structures this solution promises improvement of system performances and increase of system robustness. Developed algorithm based on the selection of the best operation for the next assembly step allows real time sequence planning considering system states.*
Key words: Bionic Assembly System; Cloud Communication; scheduling control; interface; Information Flow.

1. INTRODUCTION

Information Technology (IT) is one of the fastest developing fields of technology. IT concepts, solutions and philosophy are disseminating in all fields of science, technology and daily life [1]. The result of this dissemination is an improvement of all affected fields and the development of a new generation of products and systems. All fields of automation are benefiting from this progress. Cloud Computing is one of emerging IT Concepts [2]. This concept can be used for further improvement of internal communication within self-organizing systems.

Intelligent Manufacturing Systems group from Vienna University of Technology makes continuous research and development of a concept of self-organizing system - BAS. The description of BAS working scenarios and strategies is shown in [3], possible reconfigurations within the system in [4]. Current research of IMS group focuses an implementation of cloud communication to BAS control structure [5], [6]. This paper highlights following research results:

- BAS cloud functions
- Information exchange between a cloud and BAS elements
- Cloud Behavior in a BAS normal working scenario

2. BAS CLOUD FUNCTIONS

BAS Cloud is a part of BAS hybrid control structure, as shown in Fig. 1. It is an informational interface between subordinating and self-organizing subsystems. Cloud has the following functions:
1) Connection of self-organizing and sub-ordinating parts.
Exchange of information between a cloud and subsystems goes through communication channels. In this article flow of information from shop-floor scheduling control unit to the cloud is defined as vertical upload and in the opposite way vertical download. Flow of information from self-organizing sub-system components to the cloud is defined as horizontal upload and in the opposite way horizontal download.

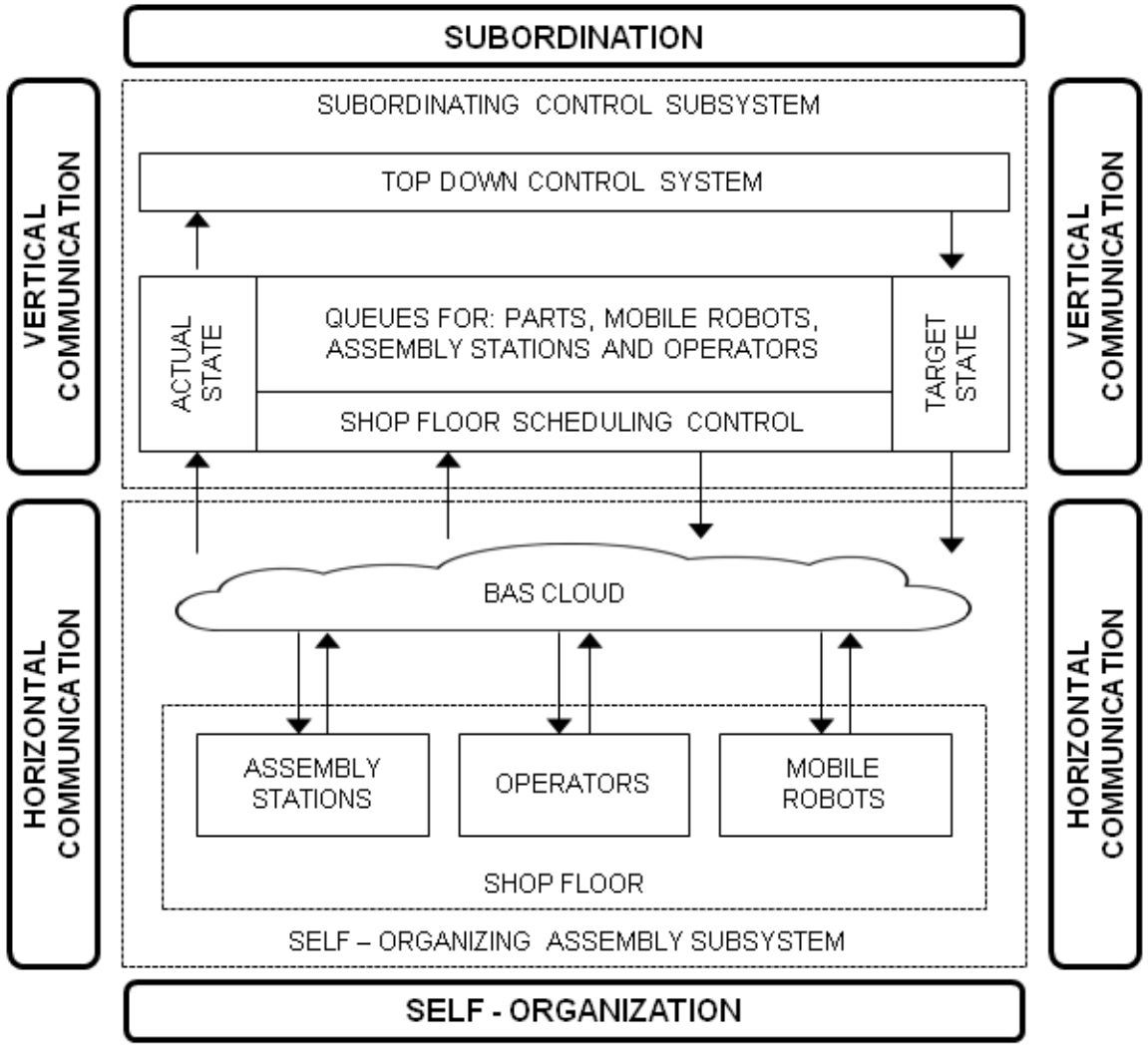

Fig. 1. Cloud-based Hybrid Control Structure of BAS

2) Internal horizontal communication organization.

Cloud has a two way communication with the shop floor elements: assembly stations, operators and mobile robots (Fig. 1.). Introduction of a cloud changes the "everyone to everyone" communication to a direct "element - cloud" interactions.

3) Memory storage.

Cloud is a passive storage element. It only stores the data, which comes from other active elements and doesn't react on system changes. It contains technological, control and system state data.

2. BAS "NORMAL" WORKING SCENARIO

This paper is limited on investigation of BAS normal working scenario. It means execution of uninterrupted sequence of assembly orders. System start-ups, shut-downs and interruptions are not considered.

A sequence of system orders is formed by sub-ordinated subsystem according to the logic of working cycles [6]. As a result of this process queues of orders for mobile robots, assembly stations, transport system and operators come to the target state module of the shop floor scheduling control unit. An order for mobile robot is

called robot assembly order (RAO). Each of these orders has a unique order ID, which consists of two parts.
The first part indicates an order number according to the logic of working cycles [6] *(l-th example of k-th Run of h-th product type with j-th priority of i-th system order)*.
The second part contains timestamp (YYMMDDHHMMSS). Shop Floor Scheduling Control vertically uploads robot assembly orders to a cloud according to the first-in-first-out principle. For each RAO data file is created, as shown in Table. 1.
This file contains RAO ID and Product Type.
According to this data, pallet type and number of assembly steps for this product are uploaded from the Product Technological Data File. After this, RAO is ready to be processed.

Robot Assembly Order Data				
Timestamp	**Data**	**Value**		
YYMMDDHHMMSS	AO ID	lkhji-YYMMDDHHMMSS		
YYMMDDHHMMSS	Product Type	Catalog number		
YYMMDDHHMMSS	Pallet Type	Catalog number		
YYMMDDHHMMSS	Number of assembly steps(NAS)	According to technological data		
YYMMDDHHMMSS	Robot ID	Catalog number		
YYMMDDHHMMSS	Pallet ID	Catalog number (Type-ID)		
YYMMDDHHMMSS	Pallet Quality State	Positive / Negative		
YYMMDDHHMMSS	Product Quality State	Positive / Negative		
Assembly sequence				
Timestamp	**Step (1...NAS)**	**Station ID**	**Operation**	**Status**
YYMMDDHHMMSS	1	AS ID	OP ID	Waiting / In Transport - Comes from a robot
YYMMDDHHMMSS	2	AS ID	OP ID	Completed / In Process / Failed / Repair - Comes from assembly station
YYMMDDHHMMSS	...	...	...	
YYMMDDHHMMSS	NAS	AS ID	OP ID	

Table. 1. Cloud-stored Robot Assembly Order Data File

Mobile robots are located in pool of robots. There are three possible robot states:

- Switched-off - robot is not participating in assembly operations before it is switched on by shop floor scheduling control unit.
- Stand-by - robot is participating in assembly operations, but has no active RAO.
- Active - robot has active RAO.

A number of stand-by robots in a system are regulated by shop floor scheduling control unit.
A robot working algorithm is shown in Fig. 3. It consists of 5 sections. These sections describe following functions of mobile robot:

1. Search of RAO
2. Reservation and preparation of RAO
3. Assembly sequence loop
4. "Best operation" search loop
5. Post-assembly actions

Section 1. All Stand-by robots check if there are any available orders on the cloud. If there is an order waiting, it proceeds to section 2. If not, it repeats the procedure.

Section 2. When an order is found, robot reserves it by horizontally uploading its own ID number into the cloud. This data comes to Robot ID field of the RAO data file (Table 1).
From this file robot downloads the required pallet type and number of assembly steps. After that it goes to the pool of pallets and gets a pallet of the specified type. Each pallet has an information tag, containing ID and quality state of Pallet. When the palette is loaded on the robot, the tag gets scanned. Robot gets Pallet ID and quality state information from this tag and uploads it to the cloud. This data comes to Pallet ID and Pallet Quality State fields of the RAO data file (Fig. 2). After this section the robot is ready to start the assembly sequence according to the AO data.

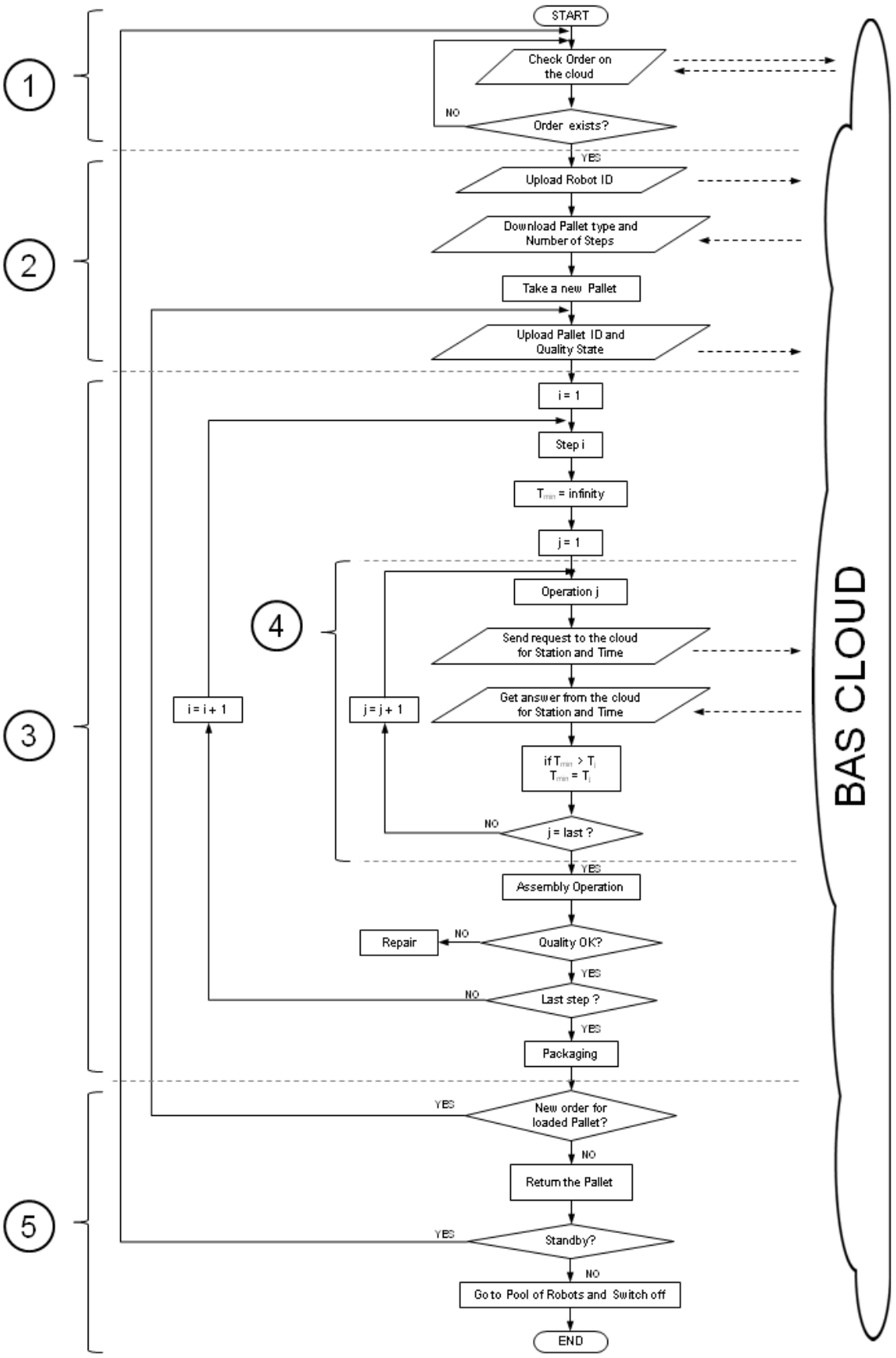

Fig. 2. Mobile robot working algorithm

Section 3. To assemble one product robot has to make a number of assembly operations. Some of these operations depend on an assembly state of the product, some could be done only in strict order. This number of assembly operations is called assembly sequence. To complete an assembly sequence, robot has to make a fixed number of assembly steps (NAS), one operation per step. NAS is stored in RAO Data File in the cloud. Efficiency of assembly system depends directly on ability to choose an assembly sequence based on the best operation for the next assembly step. A process of the search of assembly operation is described in Section 4. When assembly station for the next assembly step is chosen, robot horizontally uploads station and operation ID to the corresponding assembly step field in RAO Data File. During an assembly sequence the RAO could have six states:

1. *In Transport* - when assembly pallet is transported by robot to a chosen assembly station.
2. *Waiting* - robot waits an assembly operation in a queue in front of chosen assembly station.
3. *In Process* - Assembly pallet is on a station for an assembly operation
4. *Completed* - Assembly operation succesfully completed, quality states of product and pallet are positive
5. *Failed* - Assembly operation is not succesfully completed or quality states of product / pallet is negative. Robot has to drive this pallet to a repair station.
6. *Repair* - Pallet is on a pallet station, waiting for an operator.

The last operation of an assembly sequence is packaging. Robot drives to a packing station and leaves a product on it. When assembly sequence is completed, robot starts post-assembly actions (Section 5).

Section 4. For each assembly step robot has to find the best station from available ones.

Availability of an assembly operation depends on two factors: physical presence of the station for this operation and technological possibility to make this operation on this stage of assembly. A number of previously completed operations, required for the processing of the next one are called preconditions set. This set is available for each operation and stored in technological data file of each product.

For each of assembly operations robot checks its availability by comparing preconditions set with an own list of completed operations. If all preconditions are satisfied and this operation was not completed yet, robot requires station numbers and operation times suitable for this assembly operation. A process of the best station search is based on the smallest time resistance criteria. That means that from all suitable stations robot would choose the one with the smallest assembly time (*Tas*). This time sums from the transport time, waiting time and operation time.

Before the "Best operation" search loop *Tasmin* is set to infinity. On each iteration of a loop, if operation time of a chosen station is smaller than *Tasmin,* the current value of *Tasmin* would be replaced with *Tas*. After the loop robot gets a number of the required station.

Section 5. Robot gets an empty pallet from the packing station and checks if there is any available order for this pallet type on a cloud. If yes, robot reserves it by horizontally uploading its own ID number to the cloud. Then it horizontally uploads Pallet ID and Pallet Quality State fields of the RAO data file.

If there are no available orders for this pallet, robot brings the pallet back to the pool of pallets. After that it gets a new state from the shop floor scheduling control unit. If it stays Standby, it goes to Section 1. If it

gets Switched-off state, it drives to the pool of robots and shuts-down automatically.

CONCLUSION

Introduction of cloud communication opens new possibilities for further improvement of internal communication within self-organizing systems.
Implementation of cloud communication into the control structure of Bionic Assembly System (BAS) concept brings a number of advantages. In the comparison to the classical control structures this solution promises improvement of system performances and increase of system robustness.
Introduction of a cloud helps to organize horizontal communication on BAS Shop-Floor in a direct and simple way. It changes the “everyone to everyone” communication to a direct “element - cloud” interactions.
Developed algorithm based on the selection of the best operation for the next assembly step allows real time sequence planning considering system states.
Research is limited to a normal working mode of assembly. Future research will cover communication of other elements of self-organizing sub-system, as well as analysis of cloud behaviour in system start-ups, shut-downs and working scenarios including interruptions.

ACKNOWLEDGMENTS

This article was supported by Erasmus Mundus Multic Programme of European Union

AUTHORS’ ADDITIONAL DATA

All Authors are coming from: Vienna University of Technology, IFT-IMS Group, Karlsplatz 13/311, 1040 Wien, Austria, Europe.
Professor Dr. sc. Dr. mult. h.c. Bra nko Katalinic, President of DAAAM International, president@daaam.com, branko.katalinic@tuwien.ac.at
Dipl.-Ing. Ilya Kukushkin, PhD Student, Senior Assistant of DAAAM International, kukushkin@ift.at
Mag. ing. mech. Damir Haskovic, PhD Student, General Secretary of DAAAM International, damir.haskovic@ift.at

REFERENCES

1. Davenport, T H. Process innovation: reengineering work through information technology. Harvard Business Press, 2013
2. Blau, I., Avner C. “What type of collaboration helps? Psychological ownership, perceived learning and outcome quality of collaboration using Google Docs” In Proceedings of the Chais conference on instructional technologies research, pp. 48-55. 2009.
3. B. Katalinic, V.E. Pryanichnikov, K. Ueda, I. Kukushkin, P. Cesarec, R. Kettler, "Bionic assembly system: hybrid control structure, working scenario and scheduling," in Proceedings of 9th National Congress on Theoretical & Applied Mechanics, Brussels: 2012, pp. 111-118.
4. Kukushkin , I. K. , Katalinic , B. , Cesarec , P. and Kettler , R. (2011) Reconfiguration in self-organizing systems. Annals of DAAAM for 2011 & Proceedings of the 22nd International DAAAM Symposium "Intelligent Manufacturing & Automation: Power of Knowledge and Creativity", Editor B.ranko. Katalinic, ISSN 1726-9679, ISBN 978-3-901509-83-4, pp 641–642, Vienna, Austria, Published by DAAAM International, Vienna, 2011
5. Katalinic, B., Kukushkin, I., Pryanichnikov, V., & Haskovic, D. (2014). Cloud Communication Concept for Bionic Assembly System, Procedia Engineering, Volume 69, 2014, Pages 1562-1568, ISSN 1877-7058, doi:10.1016/j.proeng.2014.03.156
6. Katalinic, B., Pryanichnikov, V., Ueda, K., Torims, T., Kukushkin, I., Cesarec, P., Kettler, R. (2013) Control Structure and Scheduling of a Hybrid Assembly System. Estonian Journal of Engineering, 2013, Vol.19, Iss.1, pp.18-29. ISSN 1736-7522. doi:10.3176/eng.2013.1.03

9th International DAAAM Baltic Conference
"INDUSTRIAL ENGINEERING -
24-26 April 2014, Tallinn, Estonia

DESIGN OF INTERNALLY COOLED TOOLS FOR DRY CUTTING

Kromanis, A.; Pikurs, G., Muiznieks, G., Kravalis, K. & Gutakovskis, V.

Abstract: *In modern manufacturing more and more metal cutting is performed using so called dry cutting technique (no coolant). The process is used where cutting with coolant is not desired. Said dry cutting due to the non-use of coolants is also environmental friendly, which is important feature in today green manufacturing agenda. The paper gives an overview on the state-of-art internally cooled cutting tools. It also represents possible new designs of internally cooled tools for turning concentrating on today's manufacturing needs. Novel solutions and concepts are introduced. Proposed concepts will give the guidelines for further research and development to be carried on.*
Key words: internal, cooling, tool, turning.

1. INTRODUCTION

During the cutting, due to the friction and chip deformation, high cutting temperatures occur and a tool and a workpiece are subjected to increased thermal load causing significant tool wear. It causes a wear and thermal damage of the cutting tool, shortening tool life and consequently, resulting in poor surface roughness and dimensional tolerance. To reduce the cutting temperature, cutting fluid is traditionally used to remove the heat generated, decrease cutting force, and improve tool life.
Cutting fluid is also used to reduce a formation of a built-up edge and increase the removal of chips from a cutting area. However, the use of cutting fluid has its disadvantages. Depending on the workpiece, the production process, and the production location, the costs related to the use of cooling lubricants range from 7% to 17% of total costs of the manufactured workpiece [1]. Additionally, many cooling fluids contain harmful or damaging chemicals causing environment pollution and operator's health hazards, so strict environmental policies and health regulations have been introduced in connection with the increasing awareness of the environment and human health [2, 3]. To cope with said hazards it is necessary to operate in dry cutting mode, where no cutting fluid is used. Therefore components and/or products can be manufactured both ecologically and economically. Dry cutting could be solution if other obstacles would not arise. In dry cutting in result of no cutting fluid more friction and adhesion between the tool and workpiece will occur.
"Recently many research attempts has been initiated to investigate the possibility of avoiding the use of cutting fluid, such as, using new tool materials and geometries, adding a heat pipe to the cutting tool, coating with solid lubricant, and applying internal cooling, etc." [1].
The most promising solution for dry cutting seems to be the use of internal cooling. Many researchers concentrate their research in this field, but still there is no concrete solution which could be brought into industry.
This paper analyses internal cooling techniques and introduces novel solutions or concepts, on which research could be carried on.

2. PRIOR ART

In industry cooling of cutting tools as well as cutting area is provided still in a

conventional way - cutting fluid is fed into a cutting area directly. In said cutting area part of a cutting fluid evaporates and rest of cutting fluid mixes with chips. After certain time cutting fluid wears out and it cannot be used anymore.

First designs of internally cooled tools proposed the following solution: a cavity in tool holder was made; over said cavity a cutting insert was placed; cutting fluid was introduced through channel in tool holder; said cutting fluid flow to said cavity under the cutting insert; heat from cutting insert was transferred to said cutting fluid which in turn was pushed away from said cavity via outlet channel made into a holder. This is typical scheme of internally cooled tool in turning. Fig. 1 illustrates said typical scheme of internal cooling system [4].

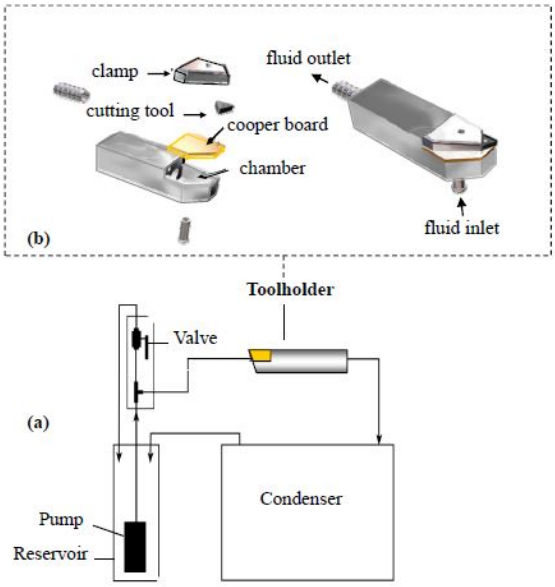

Fig. 1. Typical scheme of cooling system (a) and internally cooled tool (b) [4].

Another approach introduces s cutting tool having a cutting element such as an insert is cooled indirectly by a micro-channel heat exchanger that is mounted against the rear face of the insert (see Fig. 2). The heat exchanger is formed with an internal cavity that receives a coolant such as a cryogen [5]. Said cavity may include fins to enhance the removal of heat by the cryogen from the insert. Coolant inlet and outlet tubes are coupled to the interior of the heat exchanger to supply cryogen to the cavity. The flow rate of cryogen required to cool the insert during a given machining operation is less than 1% of the amount of standard coolant required to cool the same insert during the same machining operation [5].

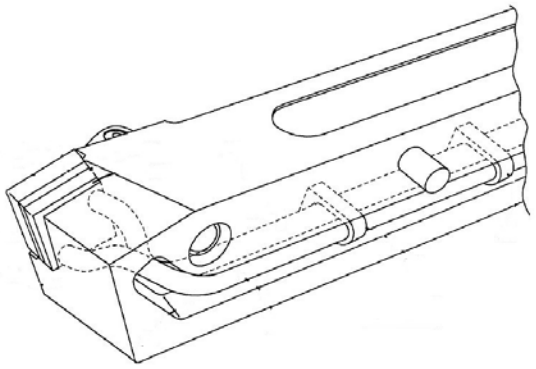

Fig. 2. Cutting tool having indirect cooling [5].

Lagerberg [6] proposes a cutting insert having a cutting edge for chip removing machining (see Fig. 3). The cutting insert comprises a supporting body comprising a porous material forming a micro-porous structure throughout the supporting body to conduct a flow of cooling medium. The supporting body having an outer periphery including an upper surface and a side face, the supporting body being enveloped by a shell substantially impermeable to cooling medium. The shell includes a wear body disposed on the upper surface of the supporting body and forming the cutting edge. The shell has at least two openings exposing the supporting body, a first of the openings disposed remotely from the cutting edge and serving as an entrance for cooling medium, and a second of the openings disposed at an upper end of the side face beneath the cutting edge and serving as an exit for cooling medium to cool the cutting edge. The outer periphery of the supporting body defining an inner volume, wherein the micro-porous structure occupying the entire inner volume [6]. Said solution partly represents a concept of internal cooling, because cutting fluid escapes through porous structure of cutting insert into environment. Said solution does not provide complete internal

cooling and cannot be considered to comply with environmental policies and health regulations. It can be considered that such tools cannot be classified as internally cooled tools.

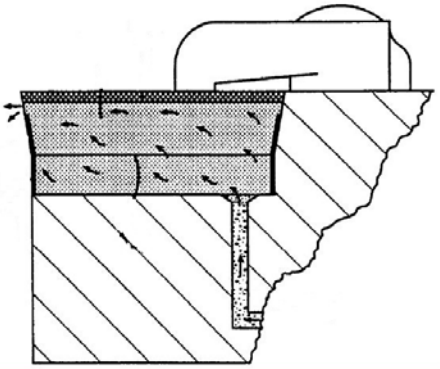

Fig. 3. Cutting holder with cutting insert having internal cooling [6].

Internally cooling tools also gives such an option as monitoring a temperature in cutting area. Bahram Keramati [7] proposes a cutting tool having on-line monitoring system measuring the heat generation rate at the cutting edge and relating this to the condition of the cutting edge. A flow of fluid coolant contacts the back surface of the cutting tool and the coolant temperature rise is measured during the machining process. The temperature difference and its rate of rise or fall is a direct indication of the heat generation rate and is related to tool conditions such as excessive and rapid wear and breakage (see Fig. 4).

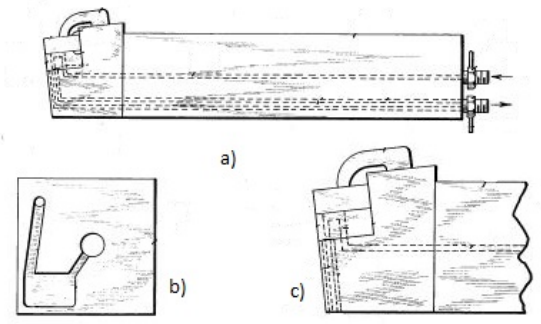

Fig. 4. a) a side view of a tool holder; b) a plan view of the coolant channel machined into the cutting tool seat; c) a partial side view of the tool holder and insert [7]

Enders [8] suggests a design of cutting tool insert that includes: a body defining a rake face, a flank face, and a cutting edge at an intersection of the rake and flank faces; and a cooling micro duct within the body (see Fig. 5). A portion of the micro duct extends along the cutting edge not more than 0.5 millimeter from the rake face, and not more than 0.5 millimeter from the flank face. The micro duct has a cross-sectional area of not more than 1.0 square millimeter. The micro duct is adapted to permit the flow of a coolant there through to transfer heat away from the cutting edge and extend the useful life of the insert. Secondary conduits having cross-sectional area no larger than 0.004 square millimeter may communicate between the micro duct and the rake and/or flank face to exhaust coolant behind the cutting edge and further enhance cooling.

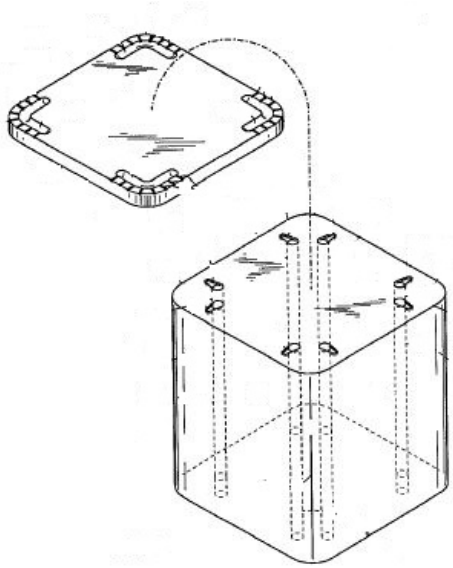

Fig. 5. Cutting tool insert having internal microduct for coolant being assembled [8].

Samir [9] describes an arrangement whereby fluid dynamics is used to provide a cooling effect to a cutting tool while in use. A cooling element comprising a long, restricted channel arranged on a support plate in a tightly spaced continuous pattern and having an inlet for any desired cooling fluid and an outlet (see Fig. 6). Cooling fluids can be contained within the system for indefinite reuse or can be cycled through (i.e. air or water). Samir [9]

suggests that preferred cooling fluids could be tap water or ambient air.

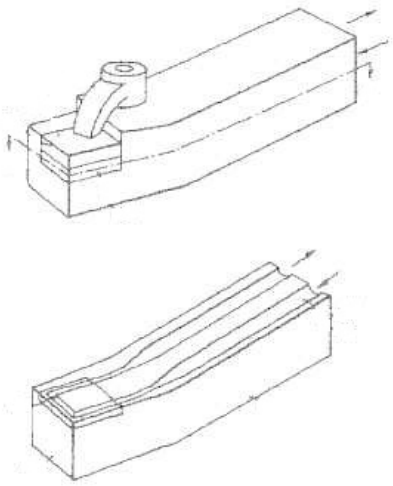

Fig. 6. Cutting tool comprising long, restricted channel [9].

Another solution proposes internally cooled cutting tool which has a "bottle-cup" insert and chamfered adaptor plate as shown in Fig. 7. "When the insert and adaptor come together, a cooling tube with triangular section will be formed for the cooling liquid to flow through. Their research concluded that under the same thermal boundary conditions, the simulated cutting tip temperatures of internally cooled tools are much lower that non-cooled cutting tool. It was also concluded that the diameter of the cooling tube has the most significant impact on the tool cooling efficiency" [1].

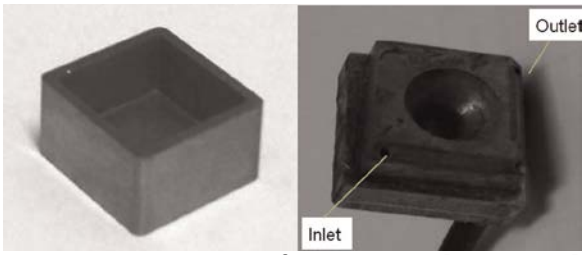

Fig. 7. Structure of insert with internal cooling [1].

In every research of internally cooled tools it was concluded that in real cutting internally cooled tools will considerably decrease the cutting temperature and thus improve the cutting process as well as tool life.

3. NEW DESIGN OF INTERNALLY COOLED TOOL

Given publications define prior art or known technical level and give a proof that tools with internal cooling can provide advantages over conventional tools, allowing to operate new tools in dry cutting without decreasing its performance.

After extensive research of known internal cooling techniques or concepts, we concluded that the field is still in conceptual level. One of the main drawbacks of internally cooled tools with closed circuit flow is its complicated manufacturing. Present designs of internally cooled tools have complicated channel systems as well as complicated insert shapes. Another reason for slow acceptance of internally cooled tools is non-existence of strict rules according to use of cutting fluids or coolants. It all can change if governments will impose stronger restrictions on use of cutting fluids. Such restrictions can come into the force if governments will tend to support green manufacturing incentives.

After research of prior art we propose our conceptual design our internally cooled tool for turning in dry cutting. In Fig. 8 is shown one of the conceptual designs of the internally cooled tool. The tool has a two part tool holder. The tool holder itself has many possibilities for improvement. Some search could be done in developing a tool holder made of different grades of material. Such a combination of materials could serve as a heat-sink. The tool holder itself can comprise different sensing devices such as thermo-couple, force sensors etc. to control the cutting process. Implementing said sensing devices into the internally cooled tool upgrades the tool to the level of smart tool. A smart tool can be used for developing adaptive control of machining process improving its productivity.

It was concluded that basically there can be indicated two possible design solutions for internal cooling of a tool. The first approach includes cooling fluid channels

that are built into the insert itself. In given solution the insert comprises multiple channels or passages forming a heat sink. The channels should be configured to provide effective transportation of heat away from cutting area. In given approach a compromise should be achieved between two important factors: structural integrity of the insert (tool) vs. cooling performance of the insert (tool).
The second solution includes cooling fluid channels that are built in a tool holder (see Fig 8 and 9). Only tool holder is modified leaving standard insert. Said tool has a good integrity but in some conditions could not be able to provide enough cooling performance, because cooling channels are further away from cutting area than cooling channels formed into the insert. The cooling performance can be improved by developing the channel of cooling fluid as well as increasing flow parameters of the cooling fluid (mainly pressure).

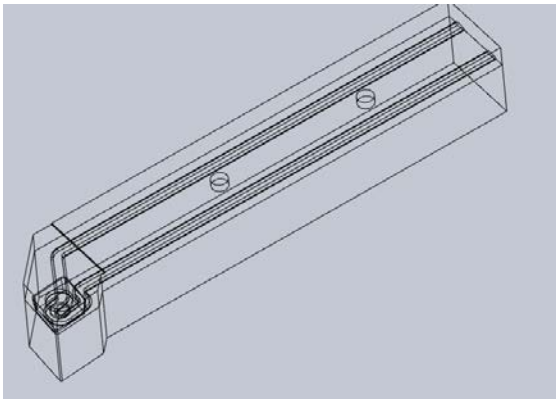

Fig. 8. Internally cooled tool with cooling channels built into the tool holder.

As mentioned above, one of the main problems for internally cooled tools are their restriction by technology or manufacturing capabilities. Usually internally cooled tools include relatively small fluid passages or channels which are complicated to manufacture, especially is standard manufacturing methods are used.
One of the solutions to ease a manufacturing of the tool is to produce a holder of the cutting tool basically in two pieces (see Fig. 9). Each piece or part comprises half of the cooling channel. When two parts are put together they form solid tool holder. The tool holder is formed as standard tool holder allowing to use it in lathes without modification or minor modification of tool holding system (see Fig. 10).

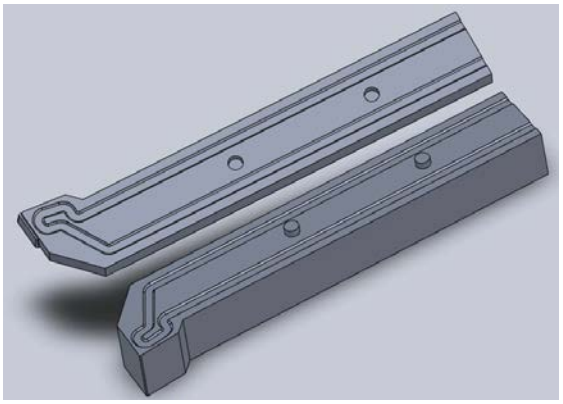

Fig. 9. Tool holder of internally cooled tool in exploded view.

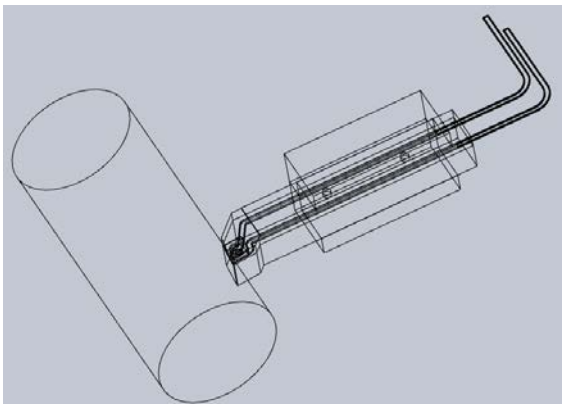

Fig. 10. Installation of internally cooled tool in a lathe.

We predict that in the future one of the most promising solution for manufacturing of internally cooled tools, especially inserts, with any possible design will be a 3D printing technology, for example a selective laser sintering (SLS). 3D printing is new and fast growing additive manufacturing technique. This technique gives a possibility to produce a tool in any possible form and configuration without any design restrictions. Tool and insert can be made in any form intended by designer. Additionally, 3D printing can be successfully used to bring newly designed tools to market in significantly faster pace. It means that further search should be done

in close cooperation with 3D printing industry.
It should be kept in mind that the new designs of cutting tool inserts and holders will need to have its own standard. The new standard will provide easier introduction of internally cooled tools in industry.

4. CONCLUSIONS AND FURTHER RESEARCH

Prior art illustrates certain trends in design of internally cooled tools. Majority of designs are still in conceptual level. Authors do not give certain reasons why internally cooled tools are not so widely used in industry. After extensive analysis we can conclude that probable reason of tools not being popular in industry is its complicated manufacturing.
Use of 3D printing techniques can significantly improve a product life cycle - from research to application in manufacturing. 3D printing could be one of the solutions to manufacture of tools in economically feasible manner.
Idea of using internally cooled tools is relatively new and said tools are not used in everyday life of manufacturing. We can predict that after implementation of tighter rules on the use of cutting fluids, researches of internally cooled tools could find its way into industry.

5. REFERENCES

1. Sun X., Bateman R., Cheng K. and Ghani S. C. Design and analysis of an internally cooled smart cutting tool for dry cutting. Proceedings of the Institution of Mechanical Engineers, Part B: Journal of Engineering Manufacture April 2012 vol. 226, no. 4, 585-591.
2. Davim, J. P., Sreejith, P. S., Gomes, R., and Peixoto, C. Experimental studies on drilling of aluminium (AA1050) under dry, minimum quantity of lubricant, and flood-lubricated conditions. Proc. IMechE, Part B: J. Engineering Manufacture, 2006, 220(10), 1605–1611.
3. Deng, J., Song, W., and Zhang, H. Design fabrication and properties of a self-lubricated tool in dry cutting. Int. J. Mach. Tools Mf, 2009, 49, 66–72.
4. Sanchez LEA, Scalon VL and Abreu GGC. Cleaner machining through a tool holder with internal cooling. In: 3rd International Workshop Advances in cleaner production. Brazil. 2011.
5. Jay Christopher Rozzi, Wibo Chen and Everett Edgar Archibald, Jr., “Indirect cooling of a cutting tool,” US Patent 8,061,241, November 22, 2011.
6. Stig Lagerberg, “Chip forming cutting insert with internal cooling,” US Patent 6,053,669, April 25, 2000.
7. Bahram Kermati, Minyoung Lee, William R. Reed, Jr., “Tool condition sensing by measuring heat generation rate at the cutting edge,” US Patent 4,757,307, July 12, 1988.
8. Enders, William, J. “Cutting tool insert having internal microduct for coolant,” International Patent Application WO2008/140999, 20 November 2008.
9. Samir B. Billatos. “Apparatus for environmentally safe cooling of cutting tools,” US Patent 5,799,553, September 1, 1998.

6. CORRESPONDING ADDRESS

Dr.sc.ing. Artis Kromanis
Riga Technical University, Department of Material Processing
Ezermalas Str. 6k-105, LV-1006 Riga, Latvia
Phone: 371 2 6779672,
E-mail: artis.kromanis@rtu.lv
http://www.rtu.lv

9th International DAAAM Baltic Conference
"INDUSTRIAL ENGINEERING"
24-26 April 2014, Tallinn, Estonia

PERFORMANCE MEASUREMENT IN NETWORK INDUSTRIES: EXAMPLE OF POWER DISTRIBUTION AND ROAD NETWORKS

Kuhi, K.; Kõrbe Kaare, K. & Koppel, O.

Abstract: *The performance of network industries has a great effect on the wellbeing of the society. Planning of such networks balances different social goals, industry trends and investment capabilities. This paper explores the possibility of developing an overall performance index to assess the performance of network industries as a whole in the example of power distribution and road networks. In this paper, performance is seen as a broader concept than the traditional quality of supply or quality of service, embracing the requirements of consumers in relation to the service provided by network authorities. The proposed overall index concept would be an additional regulatory tool to evaluate wider view of performance, to comply with consumers' requirements.*
Key words: network industries, road network, power distribution network, performance indicators, system architecture.

1. INTRODUCTION

Network industries can be defined as entities where the institution or its product consists of many interconnected nodes and where the connections among the nodes define the character of commerce in the industry [1]. A node in this context can be an institution, a unit of an institution or its product.
Examples of network industries are power supply, telecommunications and inland roads. Majority of the services provided by network industries are services of general interest. Network industries providing these services have a significant impact on competitiveness as they account for a large part of every country's gross domestic product (GDP). The products and services they offer represent a sizeable input for their economy and have an impact on economic development. [2].
Governments have stressed that evaluating network industries providing services of general interest is necessary due to the fact that these sectors are undergoing important structural reforms because of regulatory, technological, social and economic changes.
Therefore, it is necessary to evaluate and measure the performance of these sectors, to ensure that the current structural changes do not prevent those social and public policy objectives being attained [2].
There is currently considerable interest in performance measurement. The topic of performance measurement has generated much coverage over two decades in many disciplines within the private and public sectors [3].
The main objective of this research is to:

- explore the possibility of developing a general performance index (GPI) to evaluate the performance of network industries covering power distribution and road networks;
- propose high-level conceptual Information and Communication Technology (ICT) architecture reference model to allow timely data collection, prediction and analysis to support GPI calculation across network industries.

In order to limit the number of parameters affecting performance, and maintain conciseness, cognition and clarity, it is

important to find new ways to combine parameters systematically into GPI-s.
Latest developments in ICT sector, such as Big Data and analytics in conjunction with novel user interaction design patterns, pave the way to measure all important performance parameters, create radically better understanding of the problem domain, and translate that knowledge into management decisions.

2. PERFORMANCE MEASUREMENT FUNDAMENTALS

2.1. Definition

Performance measurement is the use of statistical evidence to determine progress toward specific defined social or organizational objectives (see Fig. 1).

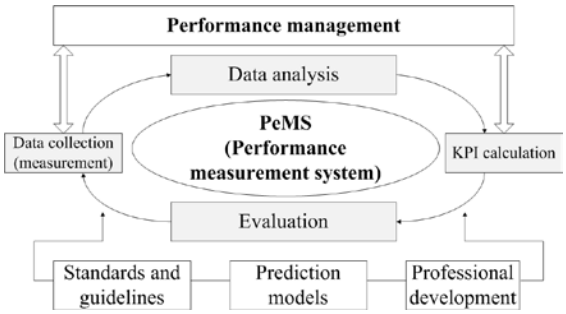

Fig. 1. Performance measurement system [4, 5]

The National Performance Review of the U.S. Federal Highway Administration provides a complimentary definition of performance measurement that is applicable in the context of network industries: “A process of assessing progress toward achieving predetermined goals, including information on the efficiency with which resources are transformed into goods and services (outputs), the quality of those outputs (how well they are delivered to clients and the extent to which clients are satisfied) and outcomes (the results of a program activity compared to its intended purpose), and the effectiveness of government operations in terms of their specific contributions to program objectives.” [6].

Every performance measurement system (PeMS) requires developing and reviewing at a number of different levels as the situation changes. The PeMS should include an effective mechanism for reviewing and revising targets and standards and should be used to challenge the strategic assumptions [7].

2.2. Performance indices

The performance index is a management tool that allows multiple sets of information to be compiled into an overall measure [8]. Chapter 2.3.contains examples of indexes used to evaluate performance of power distribution and road networks.
The “real time” data collection gives new possibilities for performance monitoring and management since the services in road or power distribution industries are "consumed" at the same time they are "produced” [2].
Performance indices provide information to stakeholders about how well that bundle of services is being provided. Performance indices should also reflect the satisfaction of the users, in addition to those concerns of the system owner or operator [6, 9].
The procedure of combining data into indices is necessary to present simultaneous information from several related areas and data sources. This process provides a statistical measure that describes the change of performance over time.

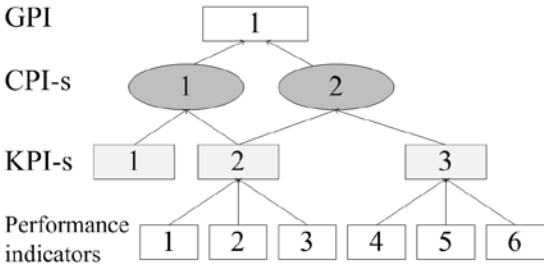

Fig. 2. Conceptual model for performance indices in network industries [4, 10, 11]

Fig. 2 proposes a generic conceptual model for performance indices. It can be exploited in network industries to evaluate performance of different network locations,

elements, and their performance trends over time.

A performance indicator (PI) defines the measurement of a piece of useful information about the performance of a program or a work expressed as a percentage, index, rate or other comparison which is monitored at regular intervals and is compared at least to one criterion. The use of PI-s goes beyond simply evaluating the degree to which goals and objectives have been achieved [4, 12].

2.3. Examples

In road industry, PI-s is defined for different types of pavements and highway categories. In the first level several single PI-s describing the characteristic of the road pavement condition are assessed [12].

The next step is the grouping of single PI-s into key performance indicators (KPI-s) and finally into representative combined performance indices (CPI-s) as:

- functional performance indices (demands made on road pavements by road users);
- structural performance indices (structural demands to be met by the road pavement);
- environmental performance indices (demands made on road pavements from an environmental perspective).

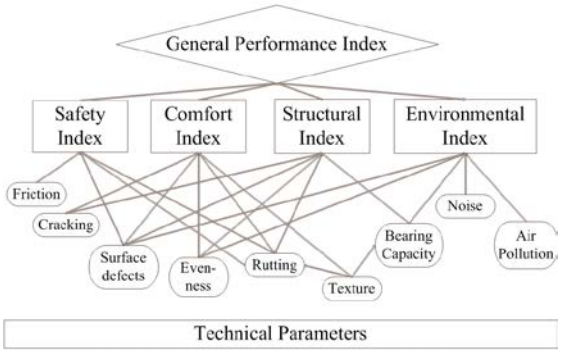

Fig. 3. Performance indices in road industry as proposed by COST354 and EVITA [4, 13, 14]

Finally, based on the CPI-s a GPI (see Fig. 2 and Fig. 3) is defined for describing the overall condition of the road pavements, which can be used for general optimization procedures [4].

Attempts had been made [15, 16, 17, 18] to create overall quality of supply and reliability indexes for power distribution network performance evaluation. However, the index systems are not yet as comprehensive as for road networks. This remains as a topic for further research.

Emerging Smart Grid developments are putting more emphasizes to understand the performance of the power network not only from power quality and grid reliability aspects, but also as a whole.

A lot of effort has been put into voltage quality research. Several indices have been taken by standardization bodies to implement [19, 20, 21]. The commercial quality, quality of service, safety of operations, socio-environmental impacts of power distribution network operations has not been investigated thoroughly.

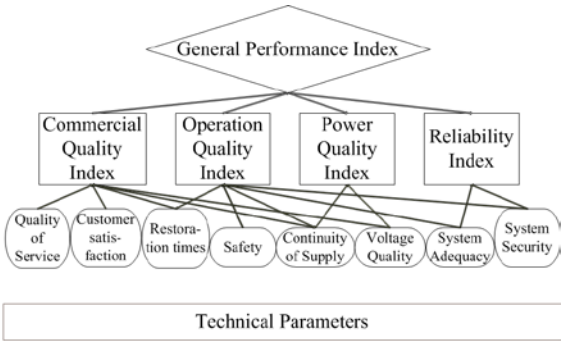

Fig. 4. Performance indices in power distribution industry [15, 18, 22]

Fig. 4 attempts to combine different sources [15, 18, 22] of information into single GPI that can be visualized and hierarchically combined for substations (areas), feeder lines, phases and metering points in distribution network.

3. SYSTEM ARCHITECTURE

3.1. Data context

The process of unlocking additional value from the existing data and combining it with new data sources (e.g. sensors, Smart Meters, Internet of Things) will have a

transformative impact on the management of network industries. More effective and therefore lower cost data communication, storage, and presentation that have better data processing mechanisms will allow the handling of the data with higher velocity, variety and volume in near future.

The proposed system architecture reference model is developed to provide high-level view of the functional components in the platform allowing processing of the technical parameters and to combine them into understandable indexes also visualizing them for the end-user.

By dividing layers of responsibilities between different functional components of the platform, we can get a clear view of the roles and responsibilities and lay the foundation for a common understanding.

The diagram on Fig. 5 shows the high-level overview of the system and specific functional layers of the platform. The reference model is based on the work done by Tallinn University of Technology [4] and TM Forum [23].

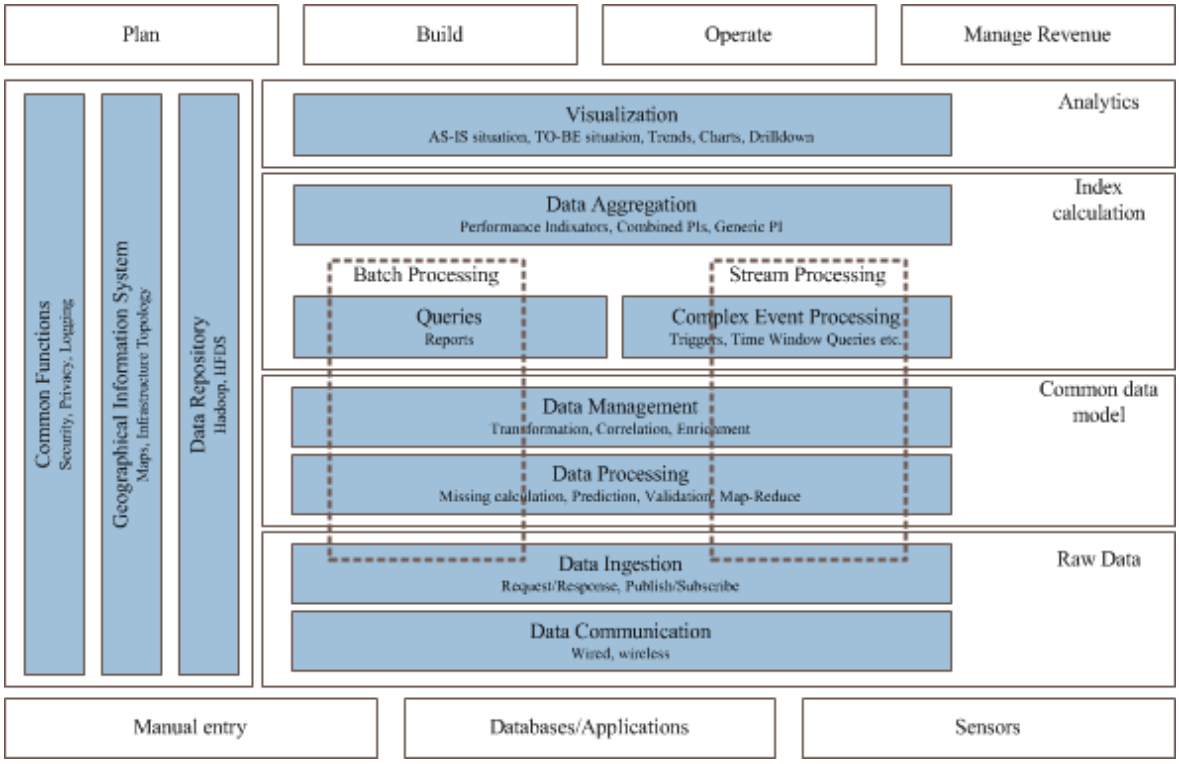

Fig. 5. Network industries Performance Evaluation System architecture reference model

3.2. Reference model layers

The purpose of the reference model is to provide high-level view of the functional components in the Performance Evaluation System.

All layers have clear responsibility borderline. Only a subset of the functionality may be needed to satisfy the requirements of a particular performance evaluation scenario.

Data communication layer is responsible for transporting the data from data sources into the processing platform. The amount and creation speed of data will play the key role in choosing the communication technology.

Data ingestion layer is responsible for integrating various data sources and importing the technical parameters into the platform. The main importance of this layer is to handle the volume, velocity and variety of the data coming into the platform. Modules of this layer must be capable of scaling out in order to accommodate the data input bandwidth and speed.

When data is missing, prediction algorithms can be applied to estimate the missing values [14]. Validation of values is also done in data processing layer. The other responsibility of this layer is to ensure data quality

Data management layer accommodates processes to perform format transformation towards uniform domain data model, correlation of events, enrichment manipulation. Batch queries over the large historical dataset using the Map-Reduce algorithm is to provide the functionality to implement scenarios that do not require real-time processing.

Complex Event Processing (CEP) layer in another hand controls the processing of streaming data, and the calculation of indices in on-going basis.

In the context of big data, both of the abovementioned layers can be implemented by massively parallel-enabled data processors.

Data aggregation layer carries the responsibility of combining the results of CEP and queries into PI-s and combined indexes.

The visualization layer is often forgotten but it is the key to make the collected data easily understandable and meaningful to the end-users.

Common functions, Geographical Information System (GIS) and data Repository are required functions to implement each of the layers.

4. CONCLUSION

Constant performance evaluation of network industries enables more effective and efficient lifecycle management. For that purpose in mind, a lot of research and standardization efforts have been made.

Road networks have comprehensive indices systems available. Power distribution systems indices focus today more on the voltage quality side and do not provide real end-to-end support for decision-makers.

Unifying and combining the different aspects of different indices into common network industries' performance index remains as further research.

However, performance of both of the industries can be analysed and visualized using the existing evaluation concepts with the ICT systems built based on the proposed performance evaluation reference architecture.

Emerging Smart Grid networks combine communication and power networks, Smart Road systems require the existence of nearby power distribution networks, real-estate development includes new roads, power and communication networks etc.

The same performance evaluation conceptual model as a system covering network industries as whole should be used to understand the performance of Smart Infrastructure.

5. REFERENCES

1. Göttinger, H. *Economies of Network Industries.* Routledge, New York, 2003.

2. *A Methodological Note for the Horizontal Evaluation of Services of General Economic Interest.* European Commission, Brussels, 2002.

3. Brignall, S., Modell, S. An institutional perspective on performance measurement and management in the 'new public sector'. *Management Accounting Research,* 2000, **11**, 281-306.

4. Kõrbe Kaare, K. *Performance Measurement of a Road Network: A Conceptual and Technological Approach for Estonia.* TUT Press, Tallinn, 2013.

5. Hagerty, J., Hofman, D. Defining a Measurement Strategy, Part III. *BI Review*, 2006, **8**.

6. *Performance Measurement Fundamentals.* U.S. Federal Highway Administration, Washington, 1998.

7. Ghalayini, A. M., Noble, J. S. The changing basis of performance measurement, *Int. J. Operations & Production Management*, 1996, **16(8)**, 63-80.

8. *How to Measure Performance. A Handbook of Techniques and Tools*. U.S. Department of Energy, Washington, 1995.
9. Sinclair, D., Zairi, M. An empirical study of key elements of total quality-based performance measurement systems: A case study approach in the service industry sector. *Total Quality Management*, 2001, **12(4)**, 535-550.
10. Kaare, K. K., Koppel, O. Performance measurement data as an input in national transportation policy. In *Proc. XXVIII Int. Baltic Road Conf.* Baltic Road Association, Vilnius, 2013.
11. Ismail, M. A., Sadiq, R., Soleymani, H. R., Tesfamariam, S. Developing a road performance index using a Bayesian belief network model. *J. Franklin Institute*, 2011, **348**, 2539-2555.
12. Litzka, J., Leben, B., La Torre, F. et al. *The way forward for pavement performance indicators across Europe. COST Action 354 Final Report.* Austrian Transportation Research Association, Vienna, 2008.
13. Lurdes Antunes, M. de. *Framework for implementation of Environment Key Performance Indicators. EVITA (Environmental Indicators for the Total Road Infrastructure Assets), Deliverable D4.1*. Institut Français des Sciences et des Technologies des Transports, de l'Aménagement et des Réseaux, and PMS-Consult, 2011.
14. Kuhi, K., Kaare, K. K., Koppel, O. Estimation of Missing or Incomplete Data in Road Performance Measurement Systems. *Int. J. Industrial Sc. and Eng.*, 2013, **7(10)**, 85-91.
15. Queiroz, L. M. O. de. *Assessing the overall performance of Brazilian electric distribution companies.* The George Washington University, Washington, 2012.
16. *Electricity Network Performance Report 2011/2012*. Ausgrid, 2011.
17. Gosbell, V. J., Perera, B. S. P., Herath, H. M. S. C. Unified Power Quality Index (UPQI) for Continuous Disturbances. In *10th Int. Conf. Harmonics and Quality of Power*, 2002, **1**, 316-321.
18. Meldorf, M., Tammoja, H., Treufeldt, Ü., Kilter, J. *Distribution Networks* (in Estonian). TUT Press, Tallinn, 2007.
19. Markiewicz, H., Klajn, A. *Standard EN 50160 - Voltage Characteristics in Public Distribution Systems.* European Copper Institute, Brussels, 2004.
20. *IEEE Guide for Electric Power Distribution Reliability Indices.* IEEE, New York, 2012.
21. *Reliability Benchmarking Application Guide for Utility/Customer PQ Indices*. Electric Power Research Institute, Palo Alto, 1999.
22. Billinton, R., Li, W. *Reliability Assessment of Electrical Power Systems Using Monte Carlo Methods.* Springer, 1994.
23. *Big Data Analytics Guidebook. Unleashing Business Value in Big Data*. TM Forum, Morristown, 2014.

6. CORRESPONDING ADDRESS

Kristjan Kuhi
TUT, Department of Logistics and Transport
Ehitajate tee 5, 19086 Tallinn, Estonia
E-mail: kristjan.kuhi@gmail.com

9th International DAAAM Baltic Conference
"INDUSTRIAL ENGINEERING"
24-26 April 2014, Tallinn, Estonia

OVERVIEW ABOUT PERSON MONITORING POSSIBILITIES IN WORKPLACE PERFORMANCE EVALUATION

Kõrgesaar, K.; Eiskop, T. & Snatkin, A.

Abstract: *Effectiveness on the shop floor level is becoming more crucial and activities carried out in the workplace have a significant affect on the company's final output- the products- and time spent on manufacturing. The main objective of this paper is to give an overview about the essence of a workplace in a manufacturing enterprise. Different systems of a workplace are introduced and performance measuring aspects appropriate for evaluating a workplace efficiency are defined.*
The contribution of a human part in a workplace effectiveness is stressed. As a result, an overview about labour performance measurement solutions is provided.
Key words: workplace, performance evaluation, labour tracking, motion tracking.

1. INTRODUCTION

Constant demand for higher quality, lower production costs, accurate on- time supply-chain - these are the tendency's manufacturing enterprises have to face on daily basis. Advanced CAD/CAE/CAM from the one side and ERP/PLM from the other side are becoming increasingly used in companies. Computer-based methods are used to support engineering decision making processes, but in spite of that they allow the integrated use of information about different aspects, like geometry and design of the product, manufacturing processes and tools, available resources, pricing, supplier data etc [1,2].

For increasing the company competitiveness and moving along with the technological progress, it is necessary for the company to establish a systems for assessing performance on most of the levels inside the organization: production and monitoring systems and workplace levels [2,3,4].
In this paper, the first part is focused on describing various workplace systems and performance measurement methods. In the second part, overview about the possibilities of labour measurement and evaluation methods, regarding operator tracking and motion tracking, is given. Proposals are made for labour tracking and motion tracking experiment framework.

2. ESSENCE OF A WORKPLACE

In terms of product complexity, production process characteristics and production batch size, three main workplace systems can be outlined (see Fig 1): human-instrument system, human-machine system (what additionally allocates into two separate subsystems) and robot-machine system.
As there are numerous ways to construct workplace allocations in order to systemize analyse models for performance measurement, given example is one of the author's subjective opinion about workplace systems.

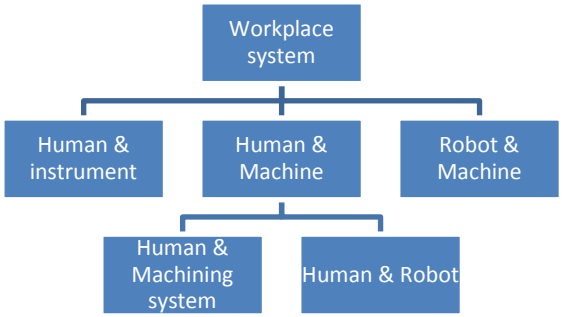

Fig. 1. Workplace systems.

2.1 Workplace systems

The human-instrument system is the closest to crafts production and the importance of human skills and knowledge's outweigh the instruments technological capability. Today human-instrument system is widespread in mass production, for example among assembly lines and in production systems, where a workplace consist of workstation and operator, who performs a specific and recurrent task. The equipment used by a human operator can vary from simple hand tools like screwdriver, hammer, to more complex instruments like soldering instruments. A workplace, where large scale construction is assembled can also be considered as man-instrument system.

When characterizing human-machine workplace system, an additional allocation to human-machining system and human-robot system has to be made. Human-machine system consist from sophisticated machine tool and an operator, or from a robot and an operator whose integration enables to produce complex and difficult shape materials [6].

Robot-machine tool system can be considered as subset of highly automated flexible manufacturing system or flexible manufacturing cell, where a system controlled by the computer, consists on different machine tools [7].

Being able to distinguish workplace systems and specifications concerning manufacturing features on the workplace, performance analyse models can be composed.

3. PERFORMANCE MEASURING ON THE WORKPLACE

Measurement of work conducted in the workplace allows to evaluate the performance of an operator, who carries out an operation or series of operations, using either simple equipment during the manufacturing process, or machine tools. The aim of operator's performance rating is used to relate the speed of accomplishment to a normal speed, which is required to finish the same type of work [8].

Performance measurement (PM) is essential to manufacturing enterprise, because without the ability to measure efficiency of an activity, it can be complicated to start controlling it and furthermore improving it [5].

In order to assess performance, critical success factors (CSF) and measurable key performance indicators (KPI) have to be defined. These indicators should reflect the criteria's, what have the utmost importance in the manufacturing processes.

In the doctoral thesis [9] author outlines a list of CSF for a workplace, that are relevant for the high performance workplace model: safety and reliability, quality, training and development, productivity, effectiveness, efficiency, flexibility. These CSF-s were brought out together with their respective KPI-s.

Since a workplace system in a manufacturing enterprise may consist of two distinguished elements- human and assisting element or just machine- it is crucial to assess a workplace in a manner, where both human and machine have been subjected to performance measurement. As the machines technological possibilities reflect its capability in a workplace, its human counterpart contribute with he's/her competencies, for instance with skills, knowledge, experiences and motivation [10,11].

Since the objective of this paper was to give an overview about workplace performance measurement from the

human's point of view, the machine performance will be uncovered.

4. HUMAN MONITORING

Workplace performs well, if a planned amount of output is generated. In a man-instrument or man-machine workplace a planned output can be disturbed by errors in instrument or machine work and by a poor performance of an operator.
American workforce management solution providing company Kronos Incorporated announced in the year 2007 a term Overall Labour Effectiveness (OLE). Resembling closely to Overall Equipment Efficiency (OEE), it was described as a partner of OEE. In essence, the diffraction between the terms is the object of measurement: OEE measures machine and OLE workforce effectiveness [12]. Since the term OLE hasn't been widely recognized by the scientific community, the author of this paper referred to the principle of the term by workforce availability, workforce performance and workforce quality.

4.1 Labour tracking

Labour tracking has been widely used in construction management, where workers have been monitored in tunnels and buildings [13], also in museums, hospitals and in large public areas to provide positioning information for the users. Although labour tracking is less used in industrial applications, the idea of tracking employees in a vast manufacturing enterprise would allow to evaluate how efficiently a worker contributes time on the workplace. In other words, workforce tracking would help to evaluate workforce availability.
Positioning systems can be categorized into global positioning systems (GPS) and local positioning systems (LPS). Limitations of Global Positioning System (GPS) have made it difficult to use it in indoor environment and, that is why LPS is implemented for indoor applications [13].

By definition, systems, aimed to work in indoor environments and localizing objects and people are known as LPS-s. LPS requires the installation of nodes to certain positions (called beacon nodes) in the facility or building, usually they are attached to ceilings or walls. Beacons sent and receive signals from the tags, attached to required object [14, 15].
Usual requirements for labour tracking are: a) accuracy b) low power consumption from the device, carried by the worker c) bi-directional communication capability for data exchange between the mobile unit and the system [16].
The term Indoor Positioning System (IPS) is closely related with LPS. IPS has been defined as a system, capable in real-time continuously determining the position of something or someone [18].
The author of [19] summarized available indoor positioning technologies as shown on figure 2. In addition, IPS-s can be classified according to different criteria: IPS need for existing wireless network infrastructure, network-based or non-network-based approach and system architecture.

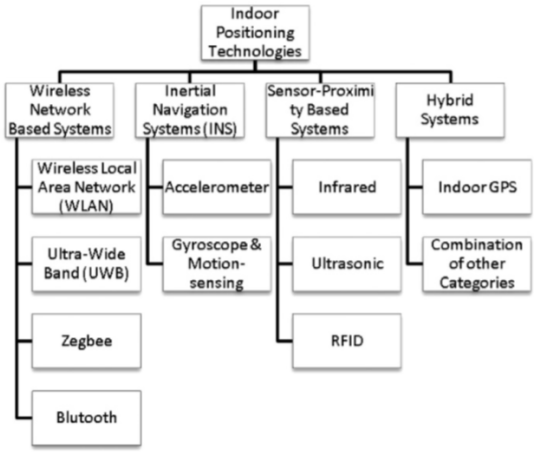

Fig. 2. Taxonomy of indoor positioning technologies [19].

A research survey [18] conducted by Yanying Gu, Anthony Lo and Ignas Niemegeers in 2009 compiled and compared IPS solutions. In the summary, different IPS-s were displayed according to the system security and privacy, cost, performance, robustness, complexity, user

preference, availability and limitations. The most relevant criteria has been considered the accuracy and precision of the system [18, 20].

The decision of selecting appropriate technology for indoor positioning is a trade-off between different aspects. Advantages and disadvantages regarding each solution mentioned in [18] should be analysed considering the environment for IPS implementation. For example in a robust manufacturing environment sensor-proximity based systems like infrared ultrasonic and radio-frequency identification (RFID) devices should be avoided, since they are more sensitive to physical interferences. What is more, IPS using Wireless Local Area (WLAN) connection requires less equipment, on the other hand consumes more electricity [16]. Nevertheless, in the global market, RFID and WiFi based solutions are major shareholders [17].

4.1.1 Framework for the case study

In a research paper [21], conducted training program involving American construction ironworkers, was described. The objective of the program was to track and monitor ironworkers in their working environment and collect necessary data in order to measure and improve safety performance and working efficiency. Since the approach of the training program is applicable for the framework of tracking labour and measuring workforce availability in a manufacturing enterprise workplace (that is the goal of authors research), the structure of the program mentioned in [21] is briefly described.

Participant's (ironworkers) were provided with Ultra-Wideband (UWB) tags, which were used for real-time information gathering, regarding velocity of the workers, equipment, and material. Added to physical equipment (cameras, receivers, reference tags) installation, a virtual works zone similar to real life, was defined. After the training program, the quantity of collected information was enough to visualize the workers path during the test (see Fig 3), he's velocity of movement and time spent in certain area. In addition, the amount of gathered information was enough to construct a virtual reality and display the training results to the participants.

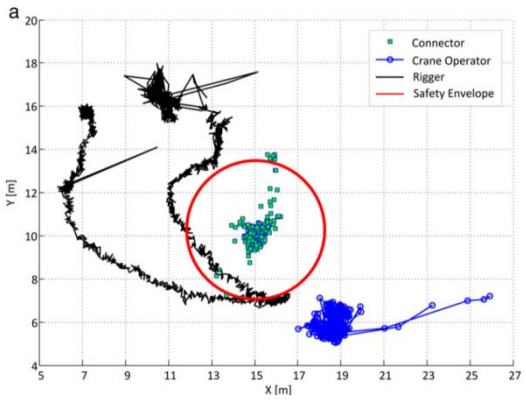

Fig. 3. Plan views of safety risk: (a) rigger on the ground passing by and entering twice a predefined safety envelope of a connector at height, and (b) crane operator on the ground temporarily entering safety envelope of a connector at height [21].

4.2 Operator motion tracking and analysis.

Human motion analysis (HMA) is a scientific approach to analyse human movement and one subset of HMA is the possibility to analyse tracked motion of the human body and body parts. Measuring and analysing body parts helps to evaluate the influence of fatigue and workplace features to human performance on the workplace. Many motion capture solutions have been used to measure human motion, regarding mechanical, magnetic, acoustic, inertial, optical and image based systems [23, 25, 27].

One technological solution for tracking operator motion is similar to the training program, described in [21]. Devices attached to different part of the operator body will allow to virtually construct 2D or 3D representation of operator posture. Motion is recorded and submitted to analysis. [24].

Xsens, as one of the leading innovator in 3D motion tracking technology, has

customized its products for measuring biomechanics in order to improve ergonomic conditions, sport performances and rehabilitation [[26]].
In addition, a motion measurement company- Polhemus- use's motion capture technology for training and simulation of welding [[22]].

5. FURTHER RESEARCH

Overview given in this paper will be the basis for selecting a suitable labour tracking and motion capture technology. After purchasing necessary devices, an experiment regarding operator movement and motion measurement will be conducted, in order to evaluate operator's performance. The goal is to construct a model to optimize human activities in the workplace.

6. CONCLUSION

In this paper, we systematically introduced different workplace systems and explained the necessity of workplace performance evaluation. The focus was on human performance on the workplace, hence labour availability and labour quality was stressed as KPI-s of workplace CSF-s. A framework for labour tracking and labour motion tracking was provided.

7. ACKNOWLEDGEMENT

This research was supported by ETF grants 8485 and 7852, targeted financing project SF0140035s12 and Innovative Manufacturing Engineering Systems Competence Centre IMECC (supported by Enterprise Estonia and co-financed by the European Union Regional Development Fund, project EU30006).

8. REFERENCES

1. Küttner, R., Karjust, K., Pohlak, M. The design and production technology of large composite plastic products. *Estonian Journal of Engineering.*2007, **13** (2), 117-128.
2. Karjust, K.; Pohlak, M.; Majak, J. (2010). Technology Route Planning of Large Composite Parts . International Journal of Material Forming, vol 3, 631 - 634. ISSN: 1960-6206 (Print) 1960-6214 (Online)
3. Karjust, K.; Küttner, R.; Pääsuke, K. Adaptive web based quotation generic module for SME's. Küttner, R. Proceedings of the 7th international conference of DAAAM Baltic industrial engineering, 22-24th April 2010, Tallinn, Estonia (375-380). Tallinn: Tallinn University of Technology.
4. Snatkin, A.; Karjust, K. and Eiskop, T. (2012). Real time production monitoring system in SME. In:*Proceedings of the 8th Int. Conf. of DAAAM Baltic Ind. Eng.*, (Otto, T. ed.) TUT, Tallinn, 2012, 573–578.
5. Hon, K.K.B. Performance and evaluation of Manufacturing Systems. *CIRP Annals-Manufacturing Technology.* 2005, **54** (2), 139-154.
6. Stephenson, D.A., Agapiou, J.S. *Metal cutting theory and practise.* CRC Taylor & Francis, Boca Raton, 2006.
7. Groover, M.P. *Fundamentals of Modern Manufacturing*. 2nd ed.Wiley, Hoboken, 2002.
8. Salvendy, G. (ed). *Handbook of industrial engineering: technology and operations management.* Wiley, New York, 2001.
9. Lõun, K. *Company's strategy based system of e-workplace performance in the engineering industry.* TTÜ kirjastus, Tallinn, 2013.
10. Riives, J., Otto, T. (ed-s). Innovative Development of Human Resources in Enterprise and Society. Tallinn, 2007. ISBN: 978-9985-59-695-1.
11. Riives, J.; Karjust, K.; Küttner, et al. Software development platform for integrated manufacturing engineering system. In *Proceedings of the 8th Int. Conf. of DAAAM Baltic Ind. Eng.*, (Otto, T. ed.) TUT, Tallinn, 2012, 555 - 560.

12. Overall Labour Effectiveness (OLE). WWW. http://www.workforceinstitute.org/wp-content/uploads/2008/01/ole-achieving-highly-effective-workforce.pdf (02.03.2014).
13. Woo, S., Jeong, S., Mok, E., Xia, L., Choi, C., Pyeon, M., Heo, J. Application of WiFi-based indoor positioning system for labour tracking at construction sites: A case study in Guangzhou MTR. *Automation in Construction.* 2011, **20** (1), 3-13.
14. Hightower, J., Borellio, G. Location systems for ubiquitous computing. *Computer.* 2001, **34** (8), 57-66.
15. Guevara, J., Jimenez, A.T., Prieto, J.C., Seco, F. Auto-localization algorithm for local positioning systems. *Ad Hoc Networks.* 2012, **10** (6), 1090-1100.
16. Hirota, T., Tanaka, S., Iwasaki, T., Hosaka, H., Sasaki, K., Enomoto, M., Ando, H. Development of local positioning system using bluetooth. *Mechatronics for Safety, Security and Dependability in a New Era.* 2006, 309-312.
17. Real-time location systems (RTLS) market by product, technology, application, industry, vertical & geography 2013-2020. WWW. http://www.prnewswire.com/news-releases/real-time-location-systems-rtls-market-by-product-technology-application-industry-vertical--geography-2013---2020-245437921.html (19.03.2014).
18. Gu, Y., Lo, A., Niemegeers, I. A survey of indoor positioning systems for wireless personal networks. *IEEE communications surveys & tutorials.* 2009, **11** (1), 13-32.
19. Razavi, S., Moselhi, O. GPS-less indoor construction locating sensing. *Automation in Construction.* 2012, **28**, 128-136.
20. Stephan, P., Heck, I., Kraus, P., Frey, G. Evaluation of Indoor Positioning Technologies under industrial application conditions in the SmartFactoryKL based on EN ISO 9283. In *Proceedings of the 13th IFAC Symposium on Information Control Problems in Manufacturing (INCOM 09)*, Moscow, 2009.
21. Teizer, J., Cheng, T., Fang, Y. Location tracking and data visualization technology to advance construction ironworkers' education and training in safety and productivity. *Automation in Construction.* 2013, **36,** 53-68.
22. Polhemus WWW. http://polhemus.com (10.03.2014).
23. Doupharate, D. I., Fethke, N. B., Nonnenmann, M. W., Rosencrance, J.C., Reynolds, S. J. Full shift arm inclinometry among dairy parlor workers: A feasibility study in a challenging work environment. *Applied ergonomics.* 2012, **43** (3), 604-616.
24. Rius, I., Gonzalez, J., Varona, J., Roca, F. X. Action-specific motion prior for efficient Bayesian 3D human body tracking. *Pattern Recognition.* 2009, **42** (11), 2907-2921.
25. Aggarwal, J.K., Cai, Q. Human motion analysis: a review. *Computer Vision and Image Understanding.* 1999, **73** (3), 428-440.
26. Xsens WWW. http://www.xsens.com (19.03.2014).
27. Welch, G,. Foxlin, E. „Motion Tracking: No Silver Bullet, but Respectable Arsenal.“ *IEEE Computer Graphics and Applications.* 2002, **22** (6), 24-38.

CORRESPONDING AUTHORS

MSc Kristjan Kõrgesaar; MSc. Tanel Eiskop; MSc. Aleksei Snatkin; Department of Machinery, Tallinn University of Technology, Ehitajate tee 5, Tallinn, 19086, Estonia, E-mail: kristjan.korgesaar@gmail.com; taneleiskop1@gmail.com; aleksei.snatkin@gmail.com.

9th International DAAAM Baltic Conference
"INDUSTRIAL ENGINEERING"
24-26 April 2014, Tallinn, Estonia

THE MODEL FOR IMPROVING THE COMPANY'S PRODUCTIVITY AND EFFICIENCY

Lavin, J., Riives, J., Kaganski S; Paavel, M.

Abstract: *The objective of this paper is to describe the improvement model of effectiveness and efficiency for manufacturing companies, which is based on enterprise's strategic objectives and on its' critical success factors. In the article, the model for small and medium production firms is described in addition with four steps for its' development: starting from the analyze of current situation and ending with creation of flexible monitoring system, which can quickly be adapted to goals of enterprise, in depending of present issues. The main idea of the model is not only to analyze the actual situation and it comparing with the company's objectives, but on investigation and detection of the critical bottlenecks, which with elimination of them would help SMEs move forward to their goals.*

1. INTRODUCTION

In order to ensure the flexibility, profitability and competitiveness of the company, management should constantly think about improvements of performance and efficiency. [1] Important is not only efficiency of individual processes but effectiveness and productivity of whole system. To achieve that, on the one hand, the proper chain of management in production is required; on the other hand, processes themselves should be cost-effective, which can be achieved with right required speed.

Business has become more and more widespread and diverse and has aimed their strategies for enhancing the long term growth, success and performance. The problem of key performance indicators optimization for product development process was considered in [2]. Today's knowledge has shown, that small and medium enterprises (SME) are balanced on the principles of scorecards [3,16], which can describe the strategic objectives of companies by dividing them into different sectors (financial, customers, internal processes, the development of human resources) [1,4]. The processes' or sub-processes' critical success factors CSF [2,17] and the identification of bottlenecks with development of suitable improvement model or method, is not feasible for SMEs [5,6,7,18]. The lack of additional resources and experience/competence in those fields are the main reasons why management is unable to analyse processes, to identify bottlenecks and to develop new methodology for their enterprises.

2. PERFORMANCE ESTIMATION AND MEASUREMENT

Company may use a variety of alternatives to reach their targets. The evaluation criteria of methods are based on the enterprises' goals [8,9]. If try to analyse the strategic objectives of SMEs, then the conclusion that manufacturing enterprises for achieving their goals are using similar methodologies, can be done. This allows to create an optimized model for all SME production firms, which can simplify not only discovering bottlenecks, analysing process but the choice of improvement activities. The sector-specific strategic objectives are used for better understanding company's goals [10]. In order to get right

understanding of company's objectives and to provide a comprehensive overview of critical success factors of the process (CSF), in other words, what should be done by management to be successful of completing the goals, the sector based objectives should be divided into process based aspects, which reflect the different facets of fundamental process.
Developing the performance management system [4] first is necessary to develop the main objective and scope. These decisions are made by the company's management in according of firm's strategy. Further, solutions should be based on existing experience of results analysing and collecting the necessary data.
In addition, the BSC functionality and descriptions of quality management procedures can be helpful.
One of the main tasks in developing of Performance Management System, are identification and grouping of KPIs. The collaboration with ERP (top-down approach) and MES (bottom-up approach) should also be analysed. [11,12].
In the top-down approach the processes are started with a definition of the higher-level issues and the top-level indicators are then broken down to increasingly more detailed indicators through a cascading process through the formal organizational hierarchy. Bottom-up processes are started from the workplaces and are based on personal responsibility and suited for designing a system that every member of the organization feels ownership for.
Measurement dimensions in developing the performance management system are also very important.

3. BOTTLENECKS ELIMINATION AND COMPANY IMPROVEMENT POTENTIAL EVALUATION MODEL

Each company has a natural tendency to perfection. In order to be successful, the overview of the company's processes for the capability should be hold by management.
The objective of the model is to identify potential bottlenecks in various business areas, to assess the danger on strategic tasks and to provide management with necessary improvement tools, taking into account the availability of resources in the company.
The structure of the model is based on the decomposition principles.
The model's approach is divided into two major parts: a qualitative and quantitative. The functionality of the model is based on company's strategic objective systems and on perfect production model. [13,18]
Typical areas of the company's strategic objectives are: leadership and employee involvement, innovation and product development, production planning and execution, process management and execution, ensuring the efficiency of the equipment, product design performance.

Having fixed the strategic objectives and critical success factors of the system [4] - the qualitative side of the model, it is necessary to get CSF's central estimates. The dividing of CSF aspects is based on corresponding studies, which were performed in years 2010-2011 by Estonian Industrial Enterprises. [5,6,7] According to those studies, the conclusion, that corresponding CSF aspects are typical for many SMEs.
Critical Success Factors (CSF) are the parameters, which are vital for the success of a process or of a business.
Consequently, the key rating of critical success factors should be accurate to current reporting of situation, objective, should reflect the current position, and also have the possibility to be analysed and predicted. The questionnaire system, which should help with achievement of performance, should be very informative.
The qualitative assessment of the model provides with the data of the company's

at current moment. (Figure 1). The qualitative rating is compared to "background" system, which takes into account real opportunities and needs. Bottlenecks and their significance are revealed during analyse. The result of qualitative analyse are the CSF of the company's strategic outlines, which are based on the on bottlenecks analyse and whose significance is assessed by management, which is based on the company's strategic objectives and development directions.
On the model development level, the relationships between CSF and KPIs are created, which can help to quantitatively evaluate the enterprise's current situation and the movement to the stated goals (elimination of bottlenecks) and which are connected to process based on measured data (factors).
After the identification and elimination of bottlenecks (improvements in process), the quantitative part of the model can be studied. The quantitative parts, which can be named "toolbox", consist of different techniques and tools, which are needed for improve of specific performance indicators.

The algorithm of quantitative aspects of the model works as follows:
1. Important relationship between the CSF and KPIs
2. KPIs measuring philosophy identify-cation due to the company's capabilities and the specific nature of the KPI.
3. Comparison of existing levels and the required level of each specific KPI.
4. The decision improvement is needed.
5. Choice of models and methods for eliminating bottlenecks.
6 Monitoring performance improvement actions.
7 The decisions for further actions.

The integration of Quantitative and qualitative aspects are almost important to achieve the effectiveness in the company. There are three important point of contact in qualitative and quantitative aspect:
- Integration between critical success factors (CSF) and key performance indicators;
- The reflected in certain specific area and operational aspects of the company's satisfaction with the extent of various centrally;
- Implementation of various methods to improve the KPIs and their impact on improvement processes as a whole, i.e. the impact of the company's strategic areas.

Hence, the value of the model lies on the continuous improvement process through iterations realization generation practice. If a qualitative side is preparing side of correcting action then the quantitative side is directly related to the performance of the various business process optimization, or growth of effectiveness.
In Qualitative aspects it is very important a precise definition.
In order to facilitate the task there is proposed two levels of decomposition:
- Structural, i.e., from the perspective of systems and processes;
- Functional, i.e., phased approach to perfection (Figure 1)

4. FOUR STEPS TO PERFECTION

Production of customer satisfied goods or products is a main activity for each manufacturing company. In the manufacturing the integration of different business processes and levels of production will take place. Each activity which will take place before the production (design a product, market demands, developed manufacturing process, used logistic system etc.) will have a significant reaction to the outcome efficiency and to the client`s satisfaction.
The workability of the model is possible to examine based on specific processes and organizational structure elements (job, department, etc.) [18]. Optimization

task is defined by a rational and efficient transformation of inputs into outputs. This transformation process requires continuous real-time management. To ensure the effectiveness of CSF-s under specified endpoints.

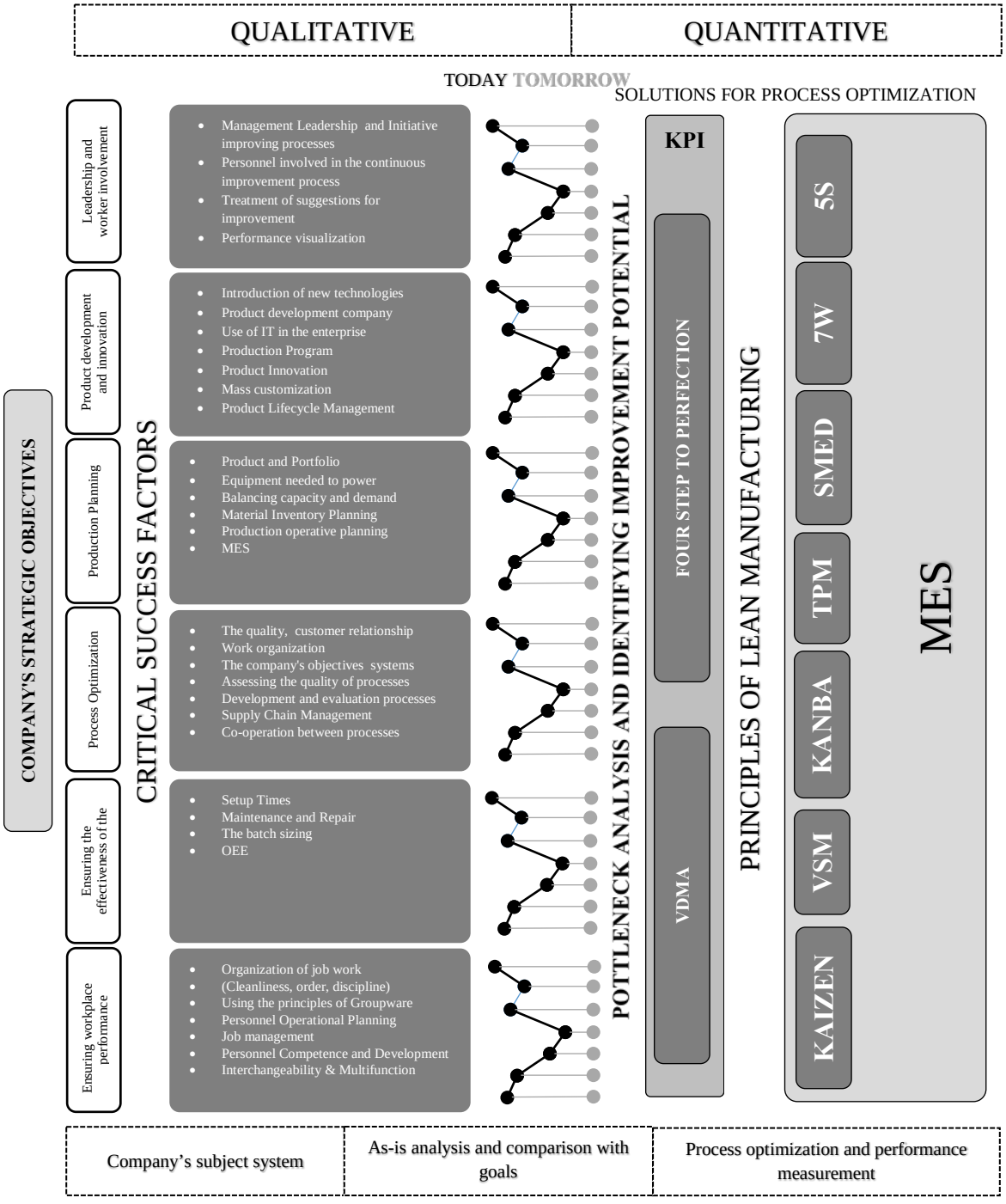

Fig. 1. The model for improving the company's productivity and efficiency

The achieved performance indicators allowing comparison with planed ones allow operatively to manage the process towards the perfection.

Perfect production model consists of four steps that lead step by step towards the goal set.

- **The first step is** the analysis of the company's current situation and

challenges, pointing out through a qualitative study, which is based on the company's strategic objectives and is structured through the critical success factors (CSF). This qualitative assessment includes an assessment of the company's processes today (process) describes the situation today compared with the company's goals are posted and highlights the bottlenecks that hinder the movement of the company posted goals.

- **Second important step is** to define and implement a process for assessing the efficiency and functioning of the Key Performance Indicators (KPIs) in order to discover untapped potential and make the future optimization of processes measurable.
  Third, an important step is the selection of models and methods, processes, speed of response and efficacy (effectiveness) Increase in wastage and elimination processes, increasing reliability while reducing the amount of stock production cycle times through a cost-saving exercise in the company. (Lean Production)
- **Fourth step** – related to manufacturing processes to ensure flexibility and profitability through. Effective (effective) planning and information flow in order to create a highly responsive control circuit.

5. CONCLUSION

The company's point of view is crucial to the success of the company's comprehensive monitoring system. The size of the activity-based decision-making model consists of qualitative and quantitative elements. The qualitative part of the analysis is directed at the company's current situation and challenges, pointing out, in quantitative terms based on the company's strategic objectives, critical success factors and key operational parameters.

Model is designed to help the company to identify bottlenecks, to evaluate the performance of their critical nature of the company's strategic objectives and, consequently, propose tools (models and methods) to address these weaknesses.

The activity-based model of decision making in today's rapidly changing business environments will help the company to maintain a flexible and respond quickly to changes in the environment. The decision-making model helps the company to make timely and accurate decisions to make new plans or make changes to existing plans. The Company shall at all times have an overview of the company's manufacturing operations in order to maintain high product quality, security of supply and production activities from profitability.

6. ACKNOWLEDGEMENTS

This research was supported by Innovative Manufacturing Engineering Systems Competence Centre IMECC, co-financed by European Union Regional Development Fund (project EU30006).

7. REFERENCES

1. Parmenter, D. Key Performance Indicators (KPI). Developing, Implementing and Using Winning KPI-s, Willey, 2010.
2. Durkutcova, M., Lavin,J., Karjust,K. KPI Optimization for Product Development Process. Annals of DAAAM 2012, Vol 23, No 1, pp 1079-1085
3. Kaplan, R. S., Norton D.P., Translating Strategy Into Action: The

Balanced Scorecard, Boston: Harvard Business School Press, 1996, 324p
4. Lavin, J.; Randmaa, M. (2012). Relationships between business objectives and the actual outcome of the business. In: Proceedings of the 8th International Conference of DAAAM Baltic Industrial Engineering 19-21st April 2012, Tallinn, Estonia: 8th International Conference of DAAAM Baltic Industrial Engineering, Tallinn, Estonia, 19-21 April 2012. (Ed.) T. Otto. Tallinn: Tallinn University of Technology, 2012, 512 - 517.
5. Varblane, U., Espenberg, K., Varblane, U., Roolaht, T. Eesti masinatööstuse hetkeseis ja arengusuunad. Tartu Ülikooli Kirjastus, 2011
6. Tootmisjuhtimise operatiivtasandi uuring, Raport, Ettevõtluse Arendamise Sihtasutuse (EAS) hanke HKL100223 tingimusi
7. Mehhatroonika valdkonna suutlikkus ja konkurentsivõime Põhja-Eesti ja Lõuna-Soome piirkonnas HeiVäl Consulting
8. Friedag H. R., Schmidt W, My Balanced Scorecard; Haufe Mediengruppe, Freiburg, Berlin, München, 2000 , 290 S
9. Wöhe, G., Einfürung in die Allgemiene Betriebswirtschaftslehre, Verlag FranzVahlen GmbH, München, 2008
10. Lavin, J, Tasakaalustatud mõõtmismudeli kujundamine Baltic Computer Systems'is, magistritöö. MBA. Tartu Ülikool, 2001
11. Lõun, K.; Riives, J.; Otto, T. (2011). Evaluation of the operation expedience of technological resources in a manufacturing network. Estonian Journal of Engineering, 17(1), 51 - 65.
12. Becker, J.,Kugelar, M.,Riesman, M., Process Management, A Guide for the Design of Business Processes. Springer 2011.
13. Kletti, J., Schumacher, J., Die perfekte Produktion: Manufacturing Excellence durch Short Interval Technology (SIT) ,Springer-Verlag Berlin, Heidelberg, 2011
14. Kletti, J. Konzeption und Einführung von MES-Systemen: Zielorientierte Einführungsstrategie mit Wirtschaftlichkeitsbetrachtungen, Fallbeispielen und Checklisten, Springer-Verlag Berlin, Heidelberg, 2011
15. Lõun, K.; Lavin, J.; Riives, J.; Otto, T. (2013). High performance workplace design model. Estonian Journal of Engineering, 19(1), 47 - 61.
16. Karjust, K.; Küttner, R.; Pääsuke, K. (2010). Adaptive web based quotation generic module for SME's. Küttner, R. (Ed.). Proceedings of the 7th international conference of DAAAM Baltic industrial engineering, 22-24th April 2010, Tallinn, Estonia (375-380). Tallinn: Tallinn University of Technology
17. Snatkin, A.; Karjust, K.; Eiskop, T. (2012). Real time production monitoring system in SME. In: Proceedings of the 8th International Conference of DAAAM Baltic Industrial Engineering 19-21st April 2012. (Ed.) Otto, T. Tallinn: Tallinna Tehnikaülikooli Kirjastus, 2012, 573 - 578. ISBN:978-9949-23-265-9
18. Riives, J.; Karjust, K.; Küttner, R.; Lemmik, R.; Koov, K.; Lavin, J. (2012). Software development platform for integrated manufacturing engineering system. In: Proceedings of the 8th International Conference of DAAAM Baltic Industrial Engineering 19-21st April 2012, Tallinn, Estonia: (Ed.) Otto, T. Tallinn: Tallinn University of Technology, 2012, 555 - 560.

7. CORRESPONDING AUTHOR

Department of Machinery
Tallinn University of Technology
Ehitajate tee 5, 19086 Tallinn, Estonia
PhD student Jaak Lavin

9th International DAAAM Baltic Conference
"INDUSTRIAL ENGINEERING -
24-26 April 2014, Tallinn, Estonia

TOOL WEAR INVESTIGATIONS BY DIRECT AND INDIRECT METHODS IN END MILLING

Leemet, T.; Allas, J. & Adoberg, E.

Abstract: *Milling is a versatile manufacturing technology. Depending on the situation, coating on the cutting tool can have significant influence to quality and cost of the process.*
In this study an attempt is made to develop methodology for relatively simple but effective means for evaluating the quality and suitability of a coating for a particular milling operation. Flank wear width is generally recognized as the key indicator for tool life criteria. In practice several other indication of worn tool are used: shape and colour of the chip, quality of the manufactured surface etc. Measurements by optical measurements are analysed. Cutting forces are measured in comparison. Three coatings were tested.
Key words: tool wear, tool life, flank wear, PVD coatings, end milling.

1. INTRODUCTION

Gradual search and evolution towards more cost effective solutions is a natural way to progress in the manufacturing industry. The question of a production cost is affected by many variables. Volumetric chip removal rate is common parameter for describing and quantifying productivity in the cutting industry [1]. Formally it stands for the product of the cutting speed with the area of engagement between tool and workpiece. Referring to metal machining operations, the cost of cutting tool exchange can be of considerable interest to the manufacturer. Variety of tools available to the machinist today is wide and expanding continuously. Often it is matter of personal preferences and previous experience that lead in the decision making process, while choosing between tools for different operations in either milling or turning. Already several production technology laboratories are offering commercial services for conducting machinability tests for machining companies. General recommendations for specific milling, turning operations for several workpiece material classes are available from handbooks and in the information from the tool manufacturers. Due to the specific nature of the cutting operation generalisations are difficult to do and extrapolation and interpolation tend not to give reliable results [2]. Meaning that different tool-operation-material combinations lead to different conditions at hand.
Current research project aims to bridge the gap between academic laboratory research and practical questions originating from machining industry. In particular an experimental method for tool life estimations in end milling operation is suggested, tested and discussed. Flank wear together with cutting forces are determined and reasoned. It is a straightforward approach designed from the perspective of simplicity and usefulness for practical machining situations.
From the previous works published on the subject following information is of a concern in the contest of the current project. Rihova et al [3] have studied the wear of turning inserts from the perspective of implementing changes in the composition of the workpiece material. While Kennedy&Hashimi [4] have proposed methods for testing coatings

under controlled conditions other than those of direct machining. Relatively similar approach as presented here was taken by Narashimha et al [5]. Where a set of turning inserts with different coatings were tested during finish turning of AISI 1018 steel under dry conditions. Their goal was to prove the positive effect of a hard coating on a tool life extent. Bouzakis et al [6] have shown that wear resistance of a coating can be related to the results of a dedicated impact test performed on a coating. Recently there have been reports on attempts for using flank wear measurements for on-line monitoring of the cutting conditions [7].

1.1. Cutting tool wear

Tool wear is an intrinsic phenomenon related to the principle of cutting operation. When referring to metal cutting, the conditions in the cutting zone are severe. Contact stresses present are those in the range of tensile strength of the workpiece material. Temperature values near the cutting wedge can rise up to around 1000 ºC. These thermo-mechanical circumstances result in the wear of the cutting tool.

Tool life definition is not an absolute term, instead users are given flexibility in setting the limits depending on the particular circumstances. Narashimha et al [5] have provided with an effective explanation stating that tool should be considered to be worn when the replacement costs are is less than the cost for not changing the tool.

Commonly recognized types of cutting tool deteriorations are wear, chipping, plastic deformation and diffusion. In principle another division can be made into two groups, where in the first wear and diffusion related types are considered to be of gradual increase in time. The second group consisting of chipping and microcracking is more abrupt and difficult to predict. Rough description of types of wear and their classification is summarized in figure 1.

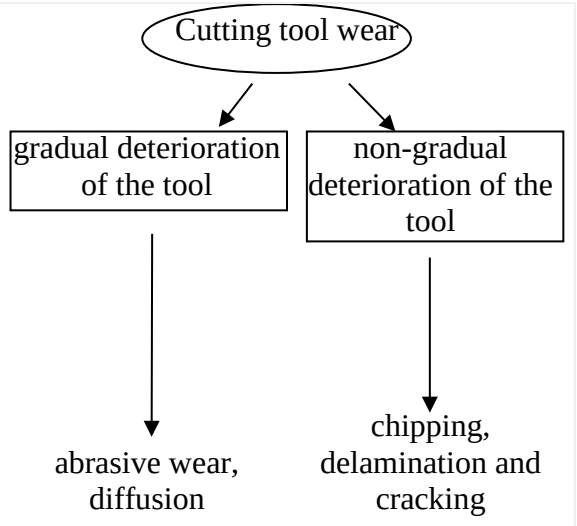

Fig. 1. Simplified overall chart of tool wear types.

When focusing on the practical side of tool life estimations, essentially two main approaches can be distinguished.

1) Establishing tool life criteria based on the value of the flank or clearance face of the cutter. This method is also used by current standards ISO 8688 Tool life testing in milling [8] and ISO 3685 Tool-life testing with single-point turning tools [9]. One of the most considerable effects due to flank wear is the decrease of the diameter of the mill. This can lead to dimensional inaccuracies and out-of shape geometrical tolerances of the workpiece.

2) Recent research results promote the wider usage of rake face wear. It has been argued that the later has pronounced influence on the fatal breakdown of the tool. Increase in the cutting force values is commonly related to the crater wear scar developments on the rake face of the cutter.

Two mentioned wear types and additionally the change of cutting edge radius could end up in the premature and unexpected fracture of the tool bit.

2. EXPERIMENTS

2.1 Tested end mills Machining operation

Milling, more specifically contouring with end mills was chosen as the machining operation to be investigated. End milling is a common material removal process. It is universal and wide spread, thus potential ways of cost reduction are of interests to manufactures and toolmakers.

Information about the end mills used in the current study is presented in Table 1. All three tested cutters were identical in geometry having a diameter of 8 mm and flute angle of 35°/38°. Commercial monolayer (Ti1-xAlx)N, nanocomposite (nc-Ti1-xAlxN)/(a-Si3N4) (nACo®) and (nc-Cr1-xAlxN)/(a-Si3N4) (nACro®) coatings were deposited in the arc plating PVD-unit PLATIT-π80. Deposition temperature was 450 °C. Coating thickness was measured using the kalotest method with a kaloMAX® tester and is shown in table 1. Hard coating and its influence to the tool life was the primary subject of study.

Coating:	Coating thickness	Adhesion
nACo	1.4 µm	HF 3
TiAlN	1.71 µm	HF 3
nACro	20.1 µm	HF 3

Table 1. Properties of coatings deposited on the tested end mills

2.2 Cutting conditions

Milling experiment was designed to ensure and retain constant cutting conditions throughout testing. HAAS SMM-HE vertical CNC machining center was used.

High-speed machining concept was adapted to current specific test run. Cutting parameters used in milling tests are given in table 2.

Tested tools were periodically checked for tool wear by flank wear measuring after cutting two layers of material. The volume of the material removed by cutting one layer was 113,5 cm^3, the tool wear was recorded periodically after cutting of 227 cm^3 of material, which corresponds to 36 m of cutting length. For the estimation of the tool wear an optical ZEISS Discovery V12 stereomicroscope with software ZEN was utilized. Every end mill was tested for 252 m of cutting length (1589 cm^3 of removed material).

Cutting speed v_C, m/min:	238
Width of cut, a_E , mm	1.6
Depth of cut, a_P , mm	4
Feed per tooth, mm/Z	0.08
Material removal rate, cm^3/min	19.2
Coolant	dry air

Table 2. Cutting parameters for testing end mills testing.

2.3 Workpiece material

HYDAX 25 was chosen as test material due to its widespread usage and relatively good machinability characteristics. Testing was conducted using material in as-received state, hot-rolled bars with rectangular cross section of 105 mm in side length, test billets were cut into pieces of 300 mm in length. The nominal chemical composition and values of mechanical properties are given in table 3

Cast analyses		Tensile test	
Element	wt. %	Measure	Value
C	0.21	Rp0.2	340 MPa
Si	0.20	Rm	552 MPa
Mn	1.04	A5	26.4 %
P	0.012	Z	56 %
S	0.106	HBW	144.7

Table 3. Workpiece material characteristics

2.4 Cutting force measurements

Difference of cutting forces for a new, unused end mill and worn end mills used in experiment was measured. Cutting force measurement system included KISTLER piezoelectric dynamometer 9257B, charge amplifier 5070 and Dynoware 2825A software. Workpiece of Hydax 25 was bolted directly onto the dynamometer, force values for three orthogonal directions

were measured. System setup is pictured in figure 2. The dynamometer was aligned and clamped onto the table of the machining centre in a way the dynamometer force measurement axes direction is parallel to the axes of the milling centre. Cutting forces were measured during the direct motion of the end mill along the X axis of the machining centre toward negative direction of the machining centre's X axis direction (from right to left as seen from machining centre's operator standpoint).
In the contexts of the study the absolute values of the cutting forces were not of primary interest. Instead, the difference of cutting forces between tested end mills was of utmost importance.

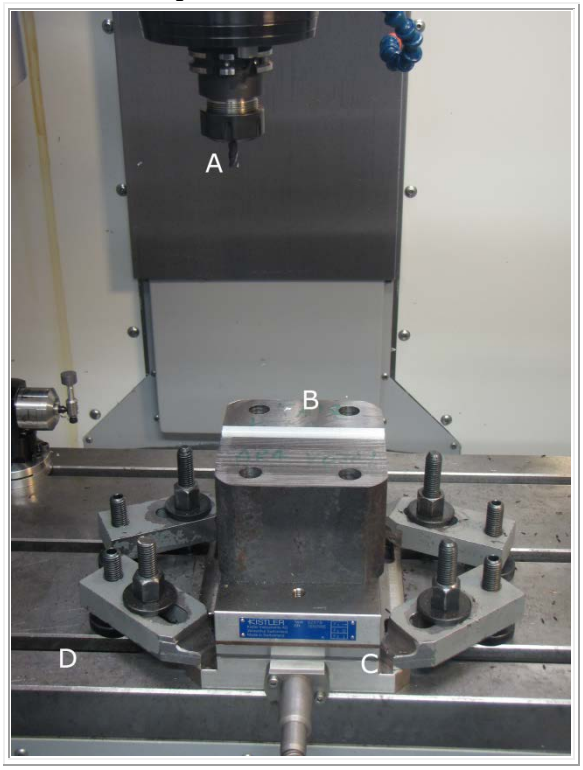

Fig 2. Setup for cutting force measurements: A) machine tool spindle with tested end mill; B) workpiece; C) dynamometer and D) table of machining centre.

3. RESULTS

From the optical and scanning electron microscopy (SEM) inspections visual proof of differences in wear resistance of compared coated end mills were found. The results of the flank wear mark size for each worn tool with different coatings is summarized in figure 3.

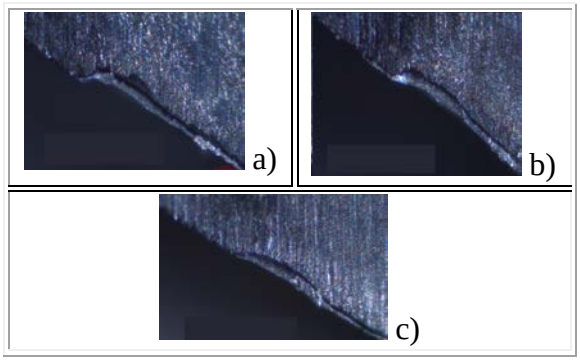

Fig. 3. Flank wear scars determined from end mills with three different coatings. a) naCo, b) TiAlN and c) nACro.

To minimize potential random errors, flank wear measurements were constantly made at the vicinity of the primary groove i.e. the theoretical line on the clearance face that is equal in height with the depth of cut. Numerical values at the end of the cutting tests i.e. after cutting 252 m are summarized in table 4.

Coating type:	Flank wear width, mm
nACo	0.120
TiAlN	0.087
nACro	0.067

Table 4. Flank wear values.

Milling as an interrupted cutting process with constantly changing theoretical chip thickness generates fluctuating cutting forces. The cutters teeth passing frequency into and out of the cut in milling depends on the rotating speed and number of teeth of the cutter, being about 633 Hz in tests carried out during this work. Nevertheless, the detailed cutting force fluctuations can still be measured by help of high sensitivity and measuring frequency piezoelectric dynamometers. An example of measured cutting forces for worn end mill with naCo coating is shown in figure 4.

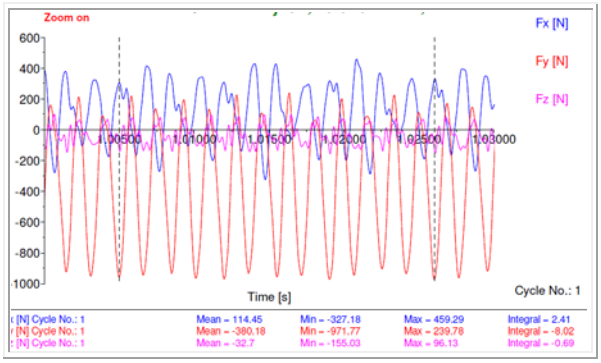

Fig.4. Cutting forces (N) for worn nACo end mill, measuring frequency 30000 Hz.

Cutting force components shown on figure 4 are directed as follows:

- F_x is directed along the feed direction of end mill (along X axis of machining centre). Positive value of F_x shows that end mill is climb milling, i.e. trying to pull the material toward itself in X axis direction.
- F_y is directed perpendicular to feed direction (along the Y axis of machining centre). Negative value of F_y means that end mill is pushing the material away of itself in Y axis direction.
- F_z is directed along the end mill rotational axis (along the Z axis of machining centre). Negative value of F_z means that end mill is pushing the material up from the table (toward itself).

Although detailed plots of milling forces can be acquired as one shown on figure 4, it is not yet sure how adequate the obtained results are. The properties of the measurement system, inertia of the workpiece etc. are likely to influence the outcome. Therefore the aim of this work was not to investigate the fluctuation of the cutting forces in detail but rather to compare the mean values of measured forces. As several tests conducted on various frequencies revealed, the mean values of cutting forces can be acquired even on low frequencies (below tooth passing frequency) without remarkable differences in calculated mean values. For comparing the mean values of cutting forces the measurements were conducted at frequency of 200 Hz. For graph plotting the results were smoothed by Dynoware computer software, the mean values of cutting forces were also calculated by Dynoware. Graphs of mean cutting forces for worn end mills after cutting the toolpath of 252 m length and for a new end mill can are presented in figure 5. Measured force values indicate that tool wear in used, specific cutting conditions leads to remarkable growth of cutting force component F_y, forcing the tool to bend away from cut surface, therefore being partly responsible in change of part dimensions. The mean values for all measured cutting force components are presented in table 5. As with the visual inspections naCo had the highest amount of wear, naCro and TiAlN coated tools were performing better in that sense with a slight advance to naCro.

	F_x	F_y	F_z
Unused tool	103.1	-138.1	-43.3
TiAlN	105.7	-277.5	-46.0
nACro	103.7	-242.1	-46.0
naCo	115.6	-365.3	-35.7

Table 5. Mean values of measured force components, N.

4. CONCLUSION

In this paper, the wear behaviour of 8 mm diameter end mills during dry machining of the HYDAX 25 construction steel was investigated. Based on the results found the following conclusions can be drawn. Two methods of tool wear estimations give consistent results. As both of them indicate the preferable coating solution at particular situation. Nevertheless it is important to stress that method discussed here should be considered as a rough reference for a specific industrial machining application. In the future work sample size needs to be raised for raising the confidence level of the results. For practical importance the tool life end condition needs to be defined by some reasoned way.

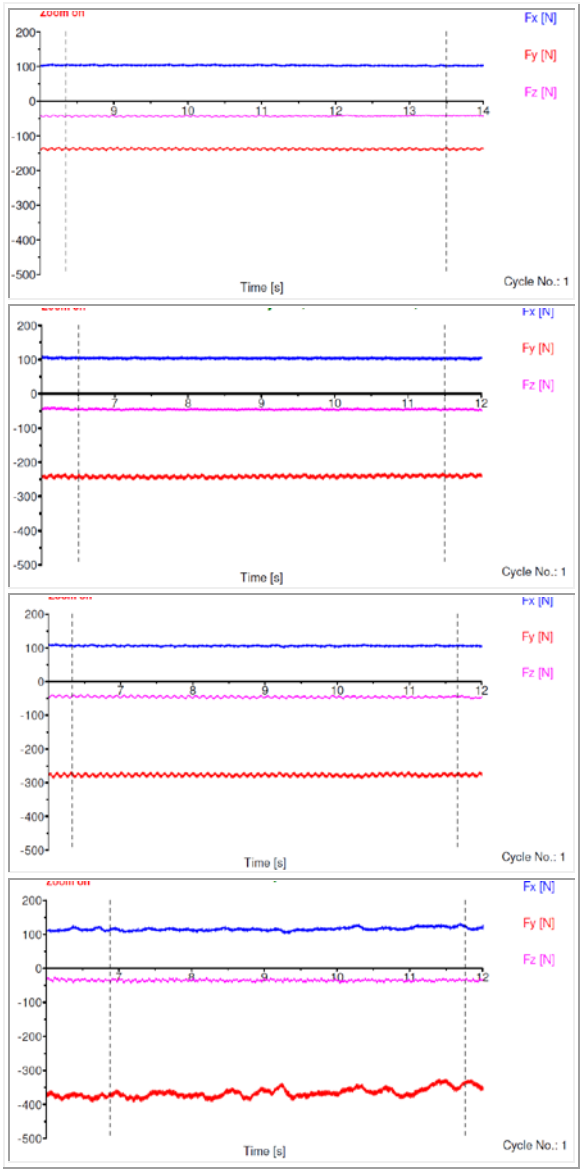

Figure 5. Smoothed graphs of measured cutting force components, from top: a) new end mill; b) worn naCro coated endmill; c) worn TiAlN coated end mill; d) worn naCo coated endmill.

5. ACKNOWLEDGEMENTS

This work has been supported by the Estonian Ministry of Education and Research within the Project No. 3.2.1101.12-0013 "Advanced Thin Hard Coatings in tooling".

6. REFERENCES

1. Kendall, L. A., Tool wear and tool life. In *ASM Handbook, Machining*, 16, ASM International, Metals Park, 1989, 37-48.
2. Ståhl, J-E. *Metal cutting – Theories and models*. Lund University, 2012.
3. Rihova, Z.; Saksl, K.; Siemers, C.; Ostroushko, D. Analyses of Wear Mechanisms Occurring During Machining of the Titanium Alloy Ti-6Al-2Sn-4Zr-6Mo. World Academy of Science, Engineering and Technology, 2012, **68**, 1515-1518
4. Kennedy, D. M; Hashimi, M.S.J. Methods of wear testing for advanced surface coatings and bulk materials. *J. Mater. Process. Technol.*, 1998, **77**, 246-253
5. Narasimha, M.; Reiji Kumar, R.; Kassie, A. Performance of Coated Carbide Tools. *The International Journal of Engineering and Science*, 2013, **2**, 47- 54
6. Bouzakis, K.-D.; Mirisidis, I.; Michailidis, N.; Lili, E.; Sampris, A.; Erkens, G.; Cremer, R. Wear of tools coated with various PVD films: correlation with impact test results by means of FEM simulations. *In Proceedings of the 7th International Conference "The Coatings in Manufacturing Engineering"*. 2008, 57-70.
7. Schmitt, R., Cai, Y., Pavim, A. Machine Vision System for Inspecting Flank Wear on Cutting Tools. ACEEE Int. J. on Control System and Instrumentation, Vol. 03, **No. 01**, Feb 2012, 27-31
8. ISO, ISO 8688 – Tool life testing in milling – Part 2: End milling. 1989
9. ISO, ISO 3685 – Tool-life testing with single-point turning tools. 1993

9th International DAAAM Baltic Conference
"INDUSTRIAL ENGINEERING"
24-26 April 2014, Tallinn, Estonia

KNOWLEDGE MANAGEMENT SYSTEMS FOR SERVICE DESK ENVIRONMENT

Lemmik, R.; Otto, T.; Küttner, R.

Abstract: *Current paper is based on Knowledge Management Systems (KMS) improvement project in cooperation between Tallinn University of Technology (TUT) and Nordic Service Desk (SD) department of a world leading IT services corporation. The project was initiated to analyze the current KMS at SD department and to propose improvement suggestions.*

Nordic SD department is using KMS in daily activities providing customer support for various international customers where SD activities are managed and coordinated by Finland head office however several 1st Level support activities are provided by subsidiaries in Estonia and Poland.

Key words: knowledge management (KM), knowledge management systems (KMS), knowledge sharing, knowledge sourcing, knowledge contribution

1. INTRODUCTION

The rapidly increasing competitiveness in market highlights the importance of design quality, maximizing productivity, multi-company collaboration, optimal price levels and predictability. The main focus of the manufacturer is to innovate, get products to the market faster, reduce errors and increase flexibility. The manufacturers have been continuing to improve their products, information systems developments and management abilities. Because of that in the past years have seen growing investments in the area of product lifecycle management (PLM), enterprise resource planning (ERP), real time monitoring and optimization [1,2,3], and integration technologies of business software and information systems [4].

On the other side in the information age, companies increasingly derive value from intellectual rather than physical assets, and employee knowledge is believed to be a company's most profitable resource. Knowledge management (KM) refers to identifying and leveraging the collective knowledge in an organization to help the organization compete [5], and knowledge management systems (KMS) are designed to allow firms to manage their knowledge resources. Initially, KM approaches focused on knowledge as objects that could be organized to support decision making, and KMS were seen as tools to manage codified knowledge, such that most KM projects were initiated top-down and driven by management. However, the rigid structure of such centrally controlled KM initiatives often exhibited poor incentives to the sharing and reuse of knowledge [6].

Over the past decade, researchers and managers have investigated methods for improving organizational performance by providing employees with better ways of accessing one another's knowledge. Such knowledge management (KM) efforts often rely on information technologies (IT), including one important class of KM initiatives that employ IT-based repositories, to capture employees' knowledge and make it available to a broad range of potential recipients. Although knowledge repositories have generated significant benefits for some organizations,

research suggests that many repositories fail to enhance knowledge transfer [7].

To succeed, a repository must contain knowledge that will prove useful for employees looking for answers to their questions and solutions to their problems. The task of ensuring the quality of knowledge in a repository often falls to subject matter experts who filter employees' contributions, rejecting those that are redundant, incorrect, ineffective, outdated, or otherwise unhelpful. Without such a validation process, a repository "soon overflows with knowledge assets of questionable value" and can, as a result, lose its credibility with employees [7].

2. PROJECT DESCRIPTION

Current project has a good opportunity to deliver Win-Win solution and to strengthen cooperation with industries and universities. Project scope is limited with analysis document as the main deliverable and no development work is provided. The main objectives are:

- Improvement of KMS
- Decrease ticket solving time
- Increase ticket solving quality

2.1. Project Phases

Describe the current KMS situation:

- Focus groups with KMS end-users
- Per focus group on-site interview
- Prepare survey to be distributed to all SD 1st Level employees

Analyze the usability of the current KMS

- Analyze the data collected during focus groups and survey
- Conclusions from business viewpoint

Improve the usability of the KMS

- Investigate the design and architecture of KMS tools
- Propose the improvement suggestions of KMS tools

2.2. Focus Group Interviews

Aspects in focus:

- Knowledge Type
- Source/Channel of Knowledge
- Knowledge Quality
- Knowledge Sharing
- Routine / Solution Reuse
- Communication Space
- Stress Level
- System Use
- IT Alignment
- Productivity
- Customer Satisfaction

Focus Groups:

- 1st Level SD employees in Estonia, 3-5 focus groups, 8 people each
- 24/7 SD employees in Finland, 2 focus groups, 4 people each
- 2nd Level SD employees in Finland, 1 focus group, 4 people

3. RESEARCH MODEL

The main focus of this paper is to describe theoretical research work which was carried out for the project to compose preliminary research model and to publish the survey.

3.1. Constructs

Constructs are based on and composed according to the research publications mainly from last 5 - 6 years on the KMS field. According to the keyword search near 100 papers were investigated and 15 of them have been directly used as references for the constructs.

Construct Name	Category	Unit of Analysis	Type of Variable	ID
Current location	Background	Individual	Control	C1-1
Current team	Background	Individual	Control	C1-2
Current position	Background	Individual	Control	C1-3
Experience in current position	Background	Individual	Control	C1-4

Experience in area of work	Background	Individual	Control	C1-5
Age	Background	Individual	Control	C1-6
Gender	Background	Individual	Control	C1-7
Work expertise [7]	Background	Individual	Control	C1-8
Training [8]	Environment	Individual	Control	C2-1
Job stress level [9]	Environment	Individual	Independent	C2-2
Time pressure [10]	Environment	Ind. / Case	Independent	C2-3
Case analyzability [11,12]	Environment	Case	Independent	C2-4
Case variability [13,14]	Environment	Case	Independent	C2-5
Satisfaction with quality of knowledge [7]	Environment	Individual	Mediator	C2-6
Sourcing from colleagues [10]	Process	Individual	Dependent	C3-1
Sourcing from local documents [10]	Process	Ind. / System	Dependent	C3-2
Knowledge contribution [15,16,17]	Process	Individual	Dependent	C3-3
Simplicity of information update functionality	Process	System	Independent	C3-4
Information update autonomy [7]	Process	System	Independent	C3-5
Frequency of accessing channel of knowledge [7]	Systems	Individual	Mediator	C4-1
Simplicity of search functionality	Systems	System	Independent	C4-2
Search results presentation	Systems	System	Independent	C4-3
Sourcing from repository [10]	Systems	Ind. / System	Dependent	C4-4
Time efficiency of retrieving knowledge [18,19]	Systems	System	Mediator	C4-5
Time efficiency of storing knowledge [18,19]	Systems	System	Mediator	C4-6
Operation efficiency [20]	Outcomes	Individual	Dependent	C5-1
Operation performance [20]	Outcomes	Individual	Dependent	C5-2
Customer satisfaction target	Outcomes	Individual	Dependent	C5-3

Table 1. Constructs for Research Model

3.2. Survey Scales

According to scale composing methods it was decided to use six point discrete scales since there is no middle point.

1	Strongly Disagree
2	Disagree
3	Inclined to Disagree
4	Inclined to Agree
5	Agree
6	Strongly Agree

Table 2.1. Consent Scale (Discrete)

1	Never
2	Very Rarely
3	Rarely
4	Occasionally
5	Frequently
6	Very Frequently

Table 2.2. Extent Scale (Discrete)

1	Estonia
2	Finland
3	Poland

Table 2.3. Location (Qualitative)

1	SD
2	SD 24/7
3	Retail
4	UAS
5	GDC SD

Table 2.4. Team Type (Qualitative)

1	UAS Specialist
2	Customer Support Specialist
3	Customer Coordinator
4	Incident Coordinator
5	Group Coordinator
6	Group Manager

Table 2.5. Job Position (Qualitative)

1	Less than 6 months
2	Range of 6 months to 1 year
3	Range of 1 to 2 years
4	Range of 2 to 5 years
5	Range of 5 to 10 years
6	More than 10 years

Table 2.6. Years Range (Qualitative)

1	21 and Under
2	22 to 34
3	35 to 44
4	45 to 54
5	55 to 64
6	65 and Over

Table 2.7. Age Range (Qualitative)

1	Female
2	Male

Table 2.8. Gender (Qualitative)

1	Less than 10%
2	Range of 10% to 30%
3	Range of 30% to 50%
4	Range of 50% to 70%
5	Range of 70% to 90%
6	Range of 90% to 100%

Table 2.9. Percentage (Qualitative)

3.3. Survey Items and Publishing

Survey items were validated by using sorting method to prove that they represent associated constructs.

Web based survey was published only in English language to 400 employees at SD 1st Level. Questionnaire was fully completed by 159 employees which result will be used for the further analysis.

Item / Question	**ID**	**Scale**	**Result**
Your current work location:	C1-1-1	Location	-
Your current team:	C1-2-1	Team Type	-
Your current position in the team:	C1-3-1	Job Position	-
How long have you been employed in the current position?	C1-4-1	Years Range	-
How long have you been working in the current area of work (including previous companies, if applies)?	C1-5-1	Years Range	-
Your age range:	C1-6-1	Age Range	-
Your gender:	C1-7-1	Gender	-
I am an expert in solving customer's technical problems.	C1-8-1	Consent	4,9
I am an expert in technical troubleshooting.	C1-8-2	Consent	4,8
To what extent are training activities available for new employees?	C2-1-1	Extent	3,9
To what extent do training programs exist?	C2-1-2	Extent	3,8
To what extent is there too much trouble at work?	C2-2-1	Extent	3,9
To what extent is there too much work to handle?	C2-2-2	Extent	4,2
To what extent is there pressure on SD employees?	C2-2-3	Extent	4,3
I have limited amount of time to complete my work.	C2-3-1	Consent	4,0
Many employees at my level are overwhelmed by time-limitations to solve cases.	C2-3-2	Consent	4,0
To what extent is there a clearly known way to solve a case?	C2-4-1	Extent	4,5
To what extent are there precise instructions that can be followed when solving cases?	C2-4-2	Extent	4,3
To what extent are there common practices to work on cases?	C2-4-3	Extent	4,3
I frequently deal with non-routine cases.	C2-5-1	Consent	4,4
The cases I work on involve answering questions that have not been asked in that way before.	C2-5-2	Consent	4,3
The content in KMS meets my needs.	C2-6-1	Consent	3,7
I am satisfied with the content in KMS.	C2-6-2	Consent	3,6
The overall quality of content in KMS is high.	C2-6-3	Consent	3,5

To what extent do you discuss problems with colleagues when you need to improve your knowledge on a topic or issue related to work?	C3-1-1	Extent	4,9
When you work on a challenging case, to what extent do you communicate with your colleagues who may have encountered similar issues?	C3-1-2	Extent	5,1
When you work on a case, to what extent do you refer to local documents stored outside the KMS?	C3-2-1	Extent	4,4
To what extent do you get useful knowledge for solving cases by reading local documents other than articles in KMS?	C3-2-2	Extent	4,2
To what extent are you contributing knowledge to KMS?	C3-3-1	Extent	3,2
Updating content into KMS is simple.	C3-4-1	Consent	3,7
When contributions are submitted to KMS, they are usually validated.	C3-5-1	Consent	3,8
Getting contributions to KMS approved and accepted is easy.	C3-5-2	Consent	3,9
In the past month, to what extent did you access KMS?	C4-1-1	Extent	3,7
Searching for content in KMS is simple.	C4-2-1	Consent	3,7
The results of search in KMS are presented in an appropriate way.	C4-3-1	Consent	3,6
To what extent do you use KMS to acquire knowledge?	C4-4-1	Extent	3,6
When you work on a challenging case, to what extent do you look in KMS to find solutions to similar cases?	C4-4-2	Extent	3,6
Retrieving content from KMS happens in a time-efficient manner.	C4-7-1	Consent	3,6
Retrieving content from KMS happens on time in order to solve case.	C4-7-2	Consent	3,7
Storing content in KMS happens in a time-efficient manner.	C4-8-1	Consent	3,7
When storing content in KMS as planned, it happens in a time-efficient manner.	C4-8-2	Consent	3,7
To what extent are you able to operate efficiently?	C5-1-1	Extent	4,8
How many cases did you solve last month?	C5-2-1	Integer	262
With respect to the cases that you solved last month, what percentage were closed during the first call?	C5-2-2	Percentage	-
What was the average customer satisfaction level you achieved last month?	C5-3-1	Decimal (Continuous)	9,2 of 10

Table 3. Survey Items and average figures

4. CONCLUSION

Survey results of the current project phase together with preliminary research model based on constructs will be input for the next project phase where the statistical analysis is done. According to the results from statistical analysis in the final project phase the research model is validated and project conclusions will be drawn.

5. ACKNOWLEDGEMENTS

This research was supported by:

- European Social Fund's Doctoral Studies and Internationalisation Programme DoRa, which is carried out by Foundation Archimedes.
- ETF grants 8485 and 7852, targeted financing project SF0140035s12
- Innovative Manufacturing Engineering Systems Competence Centre IMECC (supported by Enterprise Estonia and co-financed by the European Union Regional Development Fund, project EU30006).

6. REFERENCES

1. Lemmik, R. (2010). Model-Driven Development Method of the Virtual Data Warehouse. In: Proceedings of the 12th Biennial Baltic Electronics Conference (BEC2010): IEEE 2010 12th Biennial Baltic Electronics Conference (October 4-6, 2010, Tallinn, Estonia). (Eds.)T. Rang, P. Ellervee, M. Min. IEEE, 2010, 197 - 200.
2. Karjust, K.; Küttner, R.; Pääsuke, K. Adaptive web based quotation generic module for SME's. Küttner, R. (Toim.). Proceedings of the 7th international conference of DAAAM Baltic industrial engineering, 22-24th april

2010, Tallinn, Estonia (375-380). Tallinn: Tallinn University of Technology
3. Snatkin, A.; Karjust, K.; Eiskop, T. Real time production monitoring system in SME. In: Proceedings of the 8th International Conference of DAAAM Baltic Industrial Engineering 19-21st April 2012. (Toim.) Otto, T. Tallinn: Tallinna Tehnikaülikooli Kirjastus, 2012, 573 - 578. ISBN:978-9949-23-265-9
4. Lemmik, R.; Karjust, K.; Koov, K. Service oriented and model-driven development methods of information system. Küttner, R. (Toim.). Proceedings of the 7th international conference of DAAAM Baltic industrial engineering, 22-24th April 2010, Tallinn, Estonia (404-408). Tallinn: Tallinn University of Technology
5. Alavi, M., and Leidner, D.E. Review: Knowledge management and knowledge management systems: Conceptual foundations and research issues. MIS Quarterly, 25, 1 (2001), 107–136.
6. Corporate Wikis: The Effects of Owners' Motivation and Behavior on Group Members' Engagement; Ofer Arazy and Ian R. Gellatly; Journal of Management Information Systems / Winter 2012–13, Vol. 29, No. 3
7. How Knowledge Validation Processes Affect Knowledge Contribution; Alexandra Durcikova and Peter Gray; Journal of Management Information Systems / Spring 2009, Vol. 25, No. 4
8. Strategic human resource practices and innovation performance — The mediating role of knowledge management capacity; Chung-Jen Chen, Jing-Wen Huang; Journal of Business Research, Volume 62, Issue 1, January 2009, Pages 104–114
9. Jun Shigemi, Yoshio Mino, Tadahiro Ohtsu, Toshihide Tsuda: Effects of perceived job stress on mental health. A longitudinal survey in a Japanese electronics company, European Journal of Epidemiology, April 2000, Volume 16, Issue 4, pp 371-376
10. The Role of Knowledge Repositories in Technical Support Environments: Speed Versus Learning in User Performance; PETER H. GRAY AND ALEXANDRA DURCIKOVA; Journal of Mamigemeni Information Systems /Winter 2005-6, Vol. 22. No. 1
11. Adler, P.S. 1995. Interdepartmental Interdependence and Coordination. Organization Science 6(2) 147-167.
12. Nidumolu, S. 1995. The Effect of Coordination and Uncertainty on Software Project Performance: Residual Performance Risk as an Intervening Variable. Information Systems Research. 6(3) 191-219
13. Maarten Gelderman, Task difficulty, task variability and satisfaction with management support systems, Information & Management, Volume 39, Issue 7, July 2002, Pages 593-604, ISSN 0378-7206, 10.1016/S0378-7206(01)00124-0.
14. Determinants of the Use of Relational and Nonrelational Information Sources; J. CHRISTOPHER ZIMMER, RAYMOND M. HENRY, AND BRIAN S. BUTLER; Journal of Management Information Systems / Winter 2007–8, Vol. 24, No. 3
15. Ma and Agarwal: IT Design, Identity Verification, and Knowledge Contribution Information Systems Research 18(1), pp. 42–67
16. Wasko, M., S. Faraj. 2005. Why should I share? Examining social capital and knowledge contribution in electronic networks of practice. MIS Quarterly, 29(1)35–57.
17. Koh, J., Y.-G. Kim. 2003. Sense of virtual community: Determinants and the moderating role of the virtual community origin. Internat. J. Electronic Commerce 8(2) 75–93.
18. Bstieler, L. and Hemmert, M. (2010), Increasing Learning and Time Efficiency in Interorganizational New Product Development Teams. Journal of Product Innovation Management, 27: 485–499. doi: 10.1111/j.1540-5885.2010.00731.x
19. Cooper, R.G. and Kleinschmidt, E.J. (1994). Determinants of Timeliness in Product Development. Journal of Product Innovation Management 11(5):381–396.
20. Henderson, J.C., S. Lee. 1992. Managing I/S Design Teams: A Control Theories Perspective. Mgt. Science 38 757-777.

7. CORRESPONDING AUTHORS

PhD student Rivo Lemmik
Prof Tauno Otto
Prof emer. Rein Küttner

Department of Machinery,
Tallinn University of Technology,
Ehitajate tee 5, Tallinn, 19086, Estonia.

E-mail: rivo.lemmik@student.ttu.ee

9th International DAAAM Baltic Conference
"INDUSTRIAL ENGINEERING"
24-26 April 2014, Tallinn, Estonia

ENGINEERING CHANGE AND ORGANIZATIONAL BEHAVIOUR OF THE ENTERPRISE

Maceika, A. & Jančiauskas, B.

Abstract: *Engineering change, which requires available resources from the organization, is associated with the organizational behaviour improvement process. It must be based on the appropriate methods that allows to efficiently achieving the objectives. Organizational values, knowledge, competences, power centres, finance, culture, experimental and production facilities are the factors that are important for the engineering change in an innovative approach. Improving of the organizational behaviour includes such factors as the individual's psychological problems solution, team work performance improvement, and organization strategic development. There is no doubt that skilled designed engineering change, which is based on an appropriate practice of the enterprise's organizational behaviour, can significantly contribute to the efforts to implement the core business objectives.*

Key words: Engineering change, innovative knowledge, innovation, organizational behaviour

1. INTRODUCTION

Modern enterprises which are operating in a market economy can't exist and successfully compete on the sales market, if they are not guided by innovative engineering ideas for performance improvement.
Engineering change is based on customer needs, the desire to improve the manufacturing process, and the need to correct the mistakes that has been made. Companies have the difficulties of a clear understanding how to detect areas for changes in the engineering field, to formulate tasks and effectively implement the planned change of organizational behaviour of enterprise.
The goal of the work: to provide a research of the engineering change situation in the industrial enterprise, to make analysis of organization behavior influence on engineering change process, and to foresee the ways for enterprise activity improvement.
The subject of research: the engineering change subject and its relationship with organizational behaviour of the enterprise.

2. PROBLEM STATEMENTS

Innovative knowledge is involved in the following creative process which creates new forms of activities, methods, techniques, new services, products, their logistics and markets, and so on. As a result, the new ideas and innovations should be formulated. For this reason in our article we investigated the environment and opportunities of the enterprise engineering activities improvement in the context of engineering changes.
We are looking for purposeful engineering analysis and for the methods to managing creative effort of designing.
Obtained research results and analysis showed that from the common knowledge stream we should extract innovative knowledge and to develop new ideas and ultimately innovation on the basis of innovative knowledge.

The course of engineering change formation from the origin to content is showed up in the figure 1.
From this figure, we can see that the search for the appropriate engineering change it is purposeful to start from the general - purpose industrial engineering - technical, economic and social nature knowledge flow. This flow can be derived from the present enterprise's products analysis and their main competitors activities in the market, logistics, and industrial processes evaluation.

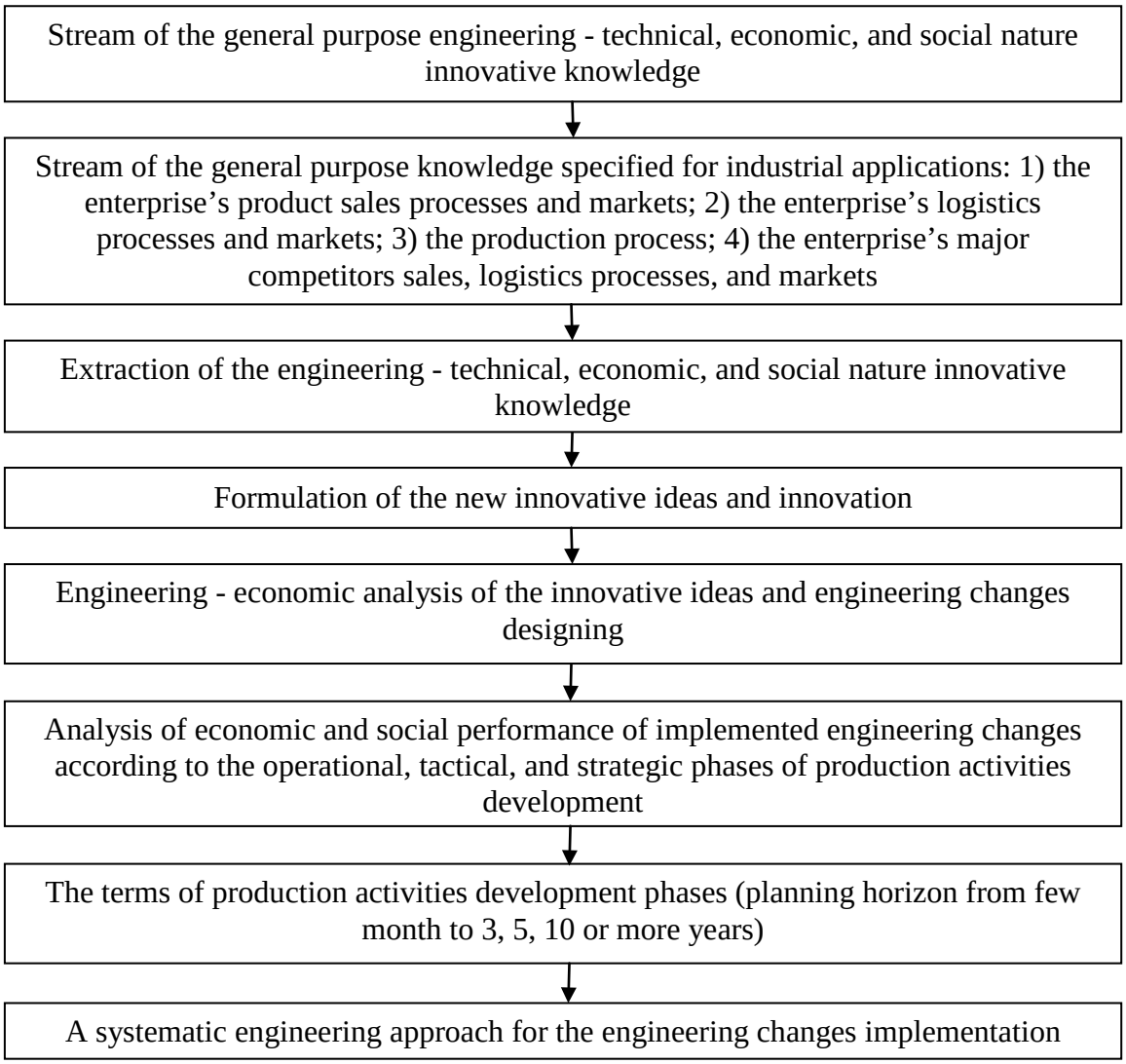

Figure 1. The scheme of engineering change search, analysis, and evaluation

This enough sufficiently stock of data and information to solve the problems in the field and the level of the problem, is helpful for engineering change by using highly innovative knowledge of sufficient quantity, relevance and usefulness. It is quite important for the process of innovative ideas generation and for the creation of innovations.

Of course, even preliminary purposeful activities, which we discussed at the beginning, not fully guarantee that we will provide an adequate performance of engineering changes. Therefore, we should not only carry out engineering - economic analysis of innovative ideas and innovation, but also to analyse the designed engineering changes.

Only at this stage, in the belief that the utility of engineering change is fully consistent with the enterprise's managers and designers economic - social expectations, the implementation to the enterprise's practice can be started, according to the layout of its operational, tactical and strategic stages of production development.

According to the G. Q. Huang et al. (2003) [1] engineering changes are the changes and/or modifications in dimensions, fits, forms, functions, materials, etc. of products or constituent components after the product design is released. An engineering change usually induces a series of downstream changes across a company where multi-disciplines work together dealing with these induced changes. Various functions across the manufacturing company have to adjust their activities in order to deal with engineering changes and their impacts.

As an engineering change is mainly related to the technical and technological, organizational and managerial progress, it is often an element of progress from academic point of view positions. This requires reorganization of the production processes or organizational behaviour development, designing of the engineering change, its implementation and the continued use through the phases of the enterprise's economic and social development.

Our previous carried out analysis shows that organizational behaviour development is appropriate to begin from its engineering and managerial staff. This staff is most closely associated with the engineering-technical, economic, and social nature data and innovative knowledge flows.

There is no doubt that engineering and managerial specialist are involved in engineering change at the implementation and practical application phases. However, in those phases it is intrusion of the already know operational specialists, that have gained considerable skills in a variety of technological operations and in practical using of the work methods. Their creative efforts and work for engineering change in form and content are related to conditions of existing and potential production situation. In this way, the preparation for the implementation of engineering change is going if not yet fully economical, but in controlled by the economic cost position situation.

We believe that properly done, on the above discussed consistent level, the management of the enterprise's engineering change implementation process can help to understand and to improve organizational behaviour. Unfortunately, investigations in the enterprises and institutions, as well as their practical experience, shows that often it happens enough consciously, in an apparent element of the verse, which creates problems of substantial misunderstanding and disproportionate desire to maximize profits.

It is clear that the proper management of activities designed through engineering change will not be made more efficient, even if its sufficient financing, unless the people do not understand and will not remove the existing contradictions in enterprise's organizational behaviour. But now, the study of published sources shows that the majority of their focus is not on engineering changes, but on changes in general, that are related to the enterprise's organizational behaviour and its improvement and that seeks to do intuitive analysis, as well as non-specific thinking to change in a systematic examination of the problem, for closer interpretation of the real causes and consequences.

In this regard, the most noteworthy S. P. Robins (2003) [2] book, that claims to explain, predict and control the human behaviour in the enterprise, or in any other organization. However, there are no claims, coupled with engineering activities, especially with the creative efforts of engineers.

Equally interesting publication on the change in manufacturing was prepared by N. Obolensky (1996) [3]. The author

examined the changes and management of business process quite creative, but did not focus on the business process most creative element usually projecting the changes in business - engineering efforts and performance management.
Valuable publication that's help to understand a body of knowledge easier, that required for problem solution, including the search for engineering change, design, and implementation, was developed by G. Probst, S. Raub and K. Romhardt (2000) [4]. In this publication many of the basics problems solution may be found. A similar idea can be found in conference publications. It is already possible to detect statements about the problems of changes management, but they are most often associated with changes in the field of human resources development, particularly looking through cultural factors influence development. However, this focus on engineering and technical progress is stopped.
For engineering change analysis, development, and use management the attention was no paid in many of technical peer-reviewed journals. For instance, in 2013 the international conference, which was dedicated for mechatronic systems and materials science [5], has only one this type abstracts from 173 deliver messages.

3. APPLICATION AREA

The main application area for the research results is industrial enterprise innovation activity. The research involved Lithuanian medical equipment manufacturing enterprise and there were questioned managerial and engineering personnel. The results of the investigation can be useful for that enterprise and worldwide in generally.

4. RESEARCH COURSE

As the first step the aim of the research was formulated. At the second step the research of the industrial enterprise personnel organizational behaviour in engineering change process situation took place. Third step involved the analysis and evaluation of the obtained from the medical equipment manufacturing enterprise data by using an average value method and after the analysis adequate conclusions were stated.

5. METHOD USED

The authors of the article carried out a number of studies, collected and analysed relevant information. Applied methods – there are survey of scientific literature and other information sources, structural system analysis, and a sociological inquiry of industrial enterprises personnel.

6. RESULTS

In our exploration of the medical equipment manufacturing enterprise showed that the engineering situation is good (specially prepared questionnaires help to inquire this company engineering and managerial staff). It was evaluated by 4.1 points of 5 possible (the responses were rated from 1 to a 5-point scale). Equipment for production tasks was rated by 4.1 points, but the task orientation and motivation was rated less – by 3.9 points in average. It follows that, in a further enterprise aging of the engineering facilities, equipment and devices, technological methods of production that combines the elements of the organizational arrangement too, the situation is not as good as they are perceived by the participants.
We believe that with no delay, it is necessary to prepare for the modernization of technical production subjects, based on engineering change and on systematic engineering method management.
These findings present actuality for the enterprise in strengthens its production engineering, information processes and logistics activities innovative

improvement, respectively, which are evaluated by 3.6 and 3.8 points.
Average values of respondent's answers and R correlation coefficient are presented in the table 1.

Evaluated parameter	Evaluation of the parameter (average points)	Correlation between the parameter and the enterprise's engineering situation (R)
Enterprise's engineering situation	4.1	1
The frequency of the engineering changes in the product	4.2	0.594
The frequency of the engineering changes in the logistic	3.6	0.576
The frequency of the engineering changes in the production process	4.6	0.494
The frequency of the engineering changes in the information process	3.8	0.396
The policy of the personnel participation in creative activities	3.4	0.785
Salary	3.7	0,301

Table 1. Average evaluation of engineering changes rated parameters

The required engineering change in the pending a medical equipment enterprise to become even more solid when, in accordance to systematic engineering approach requirements, will be completed with the innovative decisions for the appropriate logistical and engineering activities information process improvement. But ultimately, for the carefully prepared engineering change practical implementation and use it should be made improvement of the concerned conditions of internal activities and their management.
As a result, in the enterprise's organizational behaviour is appropriate to carry out the relevant innovative organizational - managerial changes. For example, performed research shows that the engineering tasks (evaluation - about 4 points out of 5) were formulated by managers and engineers engaged in the task contribution of the 3 points out of 5. We believe that this is not a bad case, but in the perception of the need for the new ideas and innovation, the ratio of engineers' engagement in the task creation required improvement.
This could be done by properly improvement of the engineering activities management, based on the vertical and horizontal management techniques improved mix ratio. This would require preparing management change in the field of organizational behaviour improvement. This is possible because the creative initiative and activity in the enterprise, according to the research results, was well tolerated. It consists of 4.2 points out of 5.
The fact that it is appropriate to prepare the changes of management activities to improve the engineering changes process was based on the survey data. Here, for example, the problem of roles structuring by allocating the tasks to engineers, was evaluated by respondents of about 3 points out of 5. These figures shows that there still exist opportunities to improve the organizational behaviour in the field of

engineering activities. According to the other study outcomes is said to be a logical component of the engineering change.

7. CONCLUSIONS

After examination of the thematic problem of this article the following conclusion are stated:

1. For the search of engineering change we recommend to use in the figure 1 presented action scheme, leading to the consistent and stable establishment of the new motivated ideas and innovations that makes up the essence of engineering change.
2. If an engineering change is created on the basis of presented scheme, it is associated with the technical and technological, organizational, and managerial progress, which is guarantee sufficient good functioning of the enterprise.
3. Our research shows that the enterprise's proper functionality guarantee can be only if the enterprise's organizational behaviour development will be with regard to the guarantor's requirements. Studies have shown that people were satisfied with the salary (3.7 points in average out of 5 possible), while the policy of the personnel participation in creative activities was assessed as moderate (3.4 points in average out of 5 possible).
4. The research shows that in a further aging of the enterprise's engineering machinery, equipment, and devices, technological methods and means of production that combines the following organizational arrangements, the situation is not as good as the perception of its participants. We believe that with out delay is appropriate to prepare situation improvement plan based on properly prepared engineering change support and on new policy of the personnel participation in creative activities.
5. It is purposeful to carry out the appropriate innovative organizational - managerial changes, namely to improve the management of engineering activities, based on the vertical and horizontal management techniques improved mix ratio.
6. In this case, it is purposeful to prepare the enterprise's engineering activities change to improve it.

8. REFERENCES

1. Huang, G. Q.; Yee, W. Y.; Mak, K. L. Current Practice of Engineering Change Management in Hong Kong Manufacturing Industries. *J. Mater. Process. Technol.*, 2003, **139,** 481-487.
2. Robbins, S. P. *Essentials of Organizational Behaviour*. Prentice Hall, Upper Saddle River, NJ, 2003.
3. Obolensky, N. *Practical Business Re-engineering.* Kogan page limited, London, 1996.
4. Probst, G.; Raub, S.; Romhardt, K. *Managing Knowledge: Building Blocks for Success.* Biddles Ltd, Great Britain, 2000.
5. Maceika, A.; Jančiauskas, B. Engineering Education Based on Engineering Change. In *the 9th International Conference "Mechatronic Systems and Materials" (MSM-2013), Vilnius, July 1-3, 2013: abstract book.* Technika, Vilnius, 2013, 154-155.

9. ADDITIONAL DATA ABOUT AUTHORS

Assoc. Prof. Dr. Augustinas Maceika
Vilnius Gediminas Technical University, Faculty of Mechanics, Department of Mechanical Engineering, J. Basanavičiaus street 28, MR-II, 1012 room, LT-03224 Vilnius, Lithuania
E-mail: augustinas.maceika@vgtu.lt

Assoc. Prof. Dr. Bronius Jančiauskas
Vilnius Gediminas Technical University, Faculty of Mechanics, Department of Mechanical Engineering, J. Basanavičiaus street 28, MR-II, 1012 room, LT-03224 Vilnius, Lithuania
E-mail: bronius.janciauskas@vgtu.lt

9th International DAAAM Baltic Conference
"INDUSTRIAL ENGINEERING"
24-26 April 2014, Tallinn, Estonia

DEVELOPMENT OF INNOVATION TEAM CREATIVE ABILITIES

Maceika, A. & Zabielavičienė, I.

Abstract: *The article contains a study of the processes occurring during the various stages of the innovation team development. Psychological problems arising from the activities through innovation team forming, differentiation, integration and maturity stages are determined. Also, the article studies the effect of divergent and convergent thinking on the creativity of the team members of various roles. Thus, distinguishing the effect of the type of thinking on the roles was found in an innovation team. Freedom, orientation towards ideas, intuition, imagination, courage, and responsibility, as the most influencing components of creativity, were established after survey data analysis. The article tries to determine the internal and external stimulus of creativity within an innovation team.*

Key words: Innovation team, creativity, creative abilities, motivation, team work, industrial enterprise

1. INTRODUCTION

In modern enterprises still more work is carried out by different teams. The improvement of team performance required a creative approach which should be based on team members' competences and creative abilities. Innovative activity creates new challenges for which it is needed to prepare team members. Innovation teams are form out of experts of many spheres and usually belonging to various departments of the company. By inputting coordinated efforts to create, spread and use of novelties it should create positive synergy.

The goal of the work: to make research of the events that taking place in the innovation team and to determine the possible components of creativity in the perception, idea generation and idea implementation stages and later determine the measures to improve the creative abilities of the team members by using the results of the study.

The subject of research: the development of creative abilities of innovation teams.

2. PROBLEM STATEMENTS

For the complex problems solution a high level of creativity of the innovation team is needed. That is when forming innovation teams it is imperative to use the results of scientific research, which provide opportunities for preliminary assessments of the team members' creativity and perspectives of its further improvement. Management of such teams becomes more complex. There is a need to create conditions for the team members' creative abilities to flourish and for their improvement. Creative persons are more sensitive to the psychological climate of the organization and for the internal motivation. The specifics of teamwork in the innovation sphere are not widely researched now. Publications on innovation theme were mostly covering only the general principles of the teamwork. That means that there is a need for focused coverage of the currently neglected theoretical factors influencing the use of the innovation team creative potential. The

research of the factors would create conditions for the methodical improvement of the innovation team formation process and for their management.

3. APPLICATION AREA

Main application area for the research results is development of the industrial enterprises personnel creativity. The research involved 70 representatives of the personnel with an engineering degree.

4. CREATIVITY MODELS AND THEIR COMPONENTS

W. Tatarkiewicz (1980) [1] stated, that creativity is a universal and unavoidable, that cognition is impossible without it, and that creativity is found in all human activities.

K. Urban's (1991) [2] model is widely used and combines six components of creativity. They are:

- Divergent thinking and acting (sensitivity, fluency, flexibility, originality, and elaboration).
- General knowledge and thinking base (openness, perception, convergent and logical thinking, analysing, synthesizing, and memorization).
- Specific knowledge base and area specific skills (creative excellence in a specific field).
- Openness and tolerance of ambiguity (not afraid to take risks, non-conformism, openness for experience, adaptation and resistance, and humour).
- Motivation and motive (thirst for knowledge, curiosity, need for novelty, playfulness, self - expression, communication, devotion / duty, need to control, and using of instruments – tools).
- Focusing and task commitment (perseverance, concentration, object – product development, devotion, and relaxation).

R. Sternberg and T. Lubert (1996) [3] also provide a componential explanation of creativity. The author presented components of creativity as:

- intellectual processes;
- knowledge;
- intellectual style;
- personal qualities;
- motivation;
- context of the environment.

Creativity is connected to the personality's need to self-actualization, originality, understanding of the mission in life, and internal motivation. M. A. Runco (2004) [4] saying, that creativity is a complex of various qualities:

- originality;
- flexibility;
- diligence;
- ability to solve problems and accept challenges;
- ability to determine changes in both technological and cultural spheres.

C. R. Rogers (1961) [5] maintains, that creativity is a universal human quality. The author claims, that the main factor for creativity to flourish is the personality's need to self-actualising, extending its potential abilities and experience, pleasure in creating. The author states these internal conditions that are needed for creativity:

- Openness for experience: extensionality.
- Internal evaluation trends.
- Ability to combine concepts or obtained elements of information in unusual ways.

The author attributes psychological freedom and psychological security to external conditions for creativity to flourish.

Now in many companies their employees' creativity is seen only as an opportunity to increase the company's revenue and profits and pays no attention to the expression of the workers intellectual prowess and independence. Company's put in no efforts to accept the value of the workers without any preconditions and requirements, that is – accepting him as he is. Only by accepting the person's personal freedom to act according to his beliefs, we can to begin

meaningfully to speak about the use of creative potential in companies and about the innovation team creation.

5. PROCESSES OF INNNOVATION TEAM FORMATION

When thinking about the creation of an innovation team, the most attention is paid to the functional roles of the members and experts are chosen according to their abilities and skills in their respective professional sphere of competence. That is why an innovation team would be best served by the nine team role list (Margerison and McCann, 1990) [6], which S. P. Robbins (2003) [7] uses to analyse the question of roles in teams. This list contains three roles which, according to the authors', should take care of generating ideas, analysing, and improving them. They would be creators - innovators, explorers – promoters, and assessors - developers. Other roles would be more oriented to implementing ideas and organizing innovative activities. Those are thrusters - organizers, concluders - producers, controllers - inspectors, upholders - maintainers, reporters - advisers, and linkers.

6. RESEARCH COURSE

The aim of the research was formulated at the first step. At the second step the research of the factors that have influence on the team member's creativity took place. For research we selected the factors that affect the team members' creativity during the creative activities stages: perception, idea generation, and idea implementation. Third step involved the analysis and valuation of the team members' creativity situation in the enterprises by using econometric methods and determination of the measures to improve the creative abilities of the team members by using study results.

7. METHOD USED

Applied methods were a survey of scientific literature and other information sources, structural system analysis, logic analysis, a sociological inquiry of people working in innovation teams, and regression analysis of quantitative survey data.

8. RESULTS

For innovation team creative activities are important stages: perception, idea generation, and idea implementation.

The creative activities stages components study is based on the questionnaire and verbal survey data of innovation teams that working in industrial companies. The determined approximating function of perception:

$$y_1 = 0.43 + 0.387x_{11} + 0.302x_{12} + 0.061x_{13} + + 0.164x_{14}; \quad (1)$$

where y_1 - perception parameter, x_{11} - freedom, x_{12} - orientation towards ideas, x_{13} - security, x_{14} - openness. The parameters were measured on a scale of 1 to 5, correlation coefficient was R = 0.783.

According to the parameters of the approximating function of perception we can state that perception in innovation teams are mostly influenced by the team members' freedom and orientation towards ideas.

The determined approximating function of idea generation:

$$y_2 = 0.54 + 0.401x_{21} + 0.304x_{22} + + 0.084x_{23} + 0.061x_{24} + 0.042x_{25}; \quad (2)$$

where y_2 - idea generation parameter, x_{21} - intuition, x_{22} - imagination, x_{23} - perception, x_{24} - resourcefulness, x_{25} - criticism. The parameters were measured on a scale of 1 to 5, correlation coefficient was R = 0.792.

The parameters of approximating function of idea generation pointed to the fact that intuition and imagination has the strongest effect on idea generation.

The determined approximating function of idea implementation:

$$y_3 = 0.52 + 0.398x_{31} + 0.192x_{32} + \\ + 0.284x_{33} + 0.022x_{34}; \quad (3)$$

where y_3 - idea implementation parameter, x_{31} - courage, x_{32} - wisdom, x_{33} - responsibility, x_{34} - perseverance. The parameters were measured on a scale of 1 to 5, correlation coefficient was R = 0,801. According to the parameters of the approximating function of idea implementation we can state that idea implementation in innovation teams are mostly influenced by courage and responsibility.

9. PREMISES OF INNOVATION TEAM CREATIVITY IMPROVEMENT

The creativity of a member of an innovation team is dependent on his divergent thinking skills. J. Almonaitienė (2011) [8] defines divergent thinking as a search for the many possible solutions for the same problem, when you return to the starting position numerous times and try to take other paths from there.

J. P. Guilford (1965) [9] believes that the most important skills in divergent thinking are:

- sensitivity to the problems (ability to notice them);
- freedom of thought (ability to generate many different ideas);
- flexibility (ability to quickly change his train of thought and topic);
- originality (rarity of ideas, novelty).

Divergent thinking is expressed by the ability to create various ways to solve problems. Convergent thinking is the opposite of divergent thinking and is characterised by the ability to select the best idea from the full list. Some tasks of the innovation team require more divergent thinking, while others – convergent thinking. Team members roles that should be responsible for idea generation, their analysis, and improvement should have divergent thinking. That would be creators - innovators, explorers - promoters, and assessors - developers. Other roles that are more involved in ideas implementation process and in organizing of innovative activities should preferably exhibit convergent thinking. Those would be thrusters - organizers, concluders - producers, controllers - inspectors, upholders - maintainers, reporters – advisers, and linkers. Generating of ideas, analysing and improving of them is the most important part of the innovation team activities and requires the highest level of creativity from the team members. That is why, when forming a team, most of the attention should be paid for the roles of the creators. This depends on the nature of the teams work.

10. CONCLUSIONS

After examination of the thematic problem of this article following conclusion are available:

1. Formation of the innovation team is a process whose management is difficult and requires experience and knowledge. When forming a team, we have to pay attention to the fact that it can be improved during all of its life cycle and the results of the innovation team will depend on its members' creativity. During each stage of the team forming process, the requirements for workers should be different. Management in different stages is also very different. That is why, when addressing problems for the teams creative work, it is necessary to know at which stage of development the team is at the given moment and use that fact to anticipate which path it will follow. After carrying out studies the psychological problems that arise when the team goes through the forming, differentiation, integration, and maturity stages were determined.

2. During the team forming stage its members searching for the recognition: they watching each other, evaluating, usually hiding their true feeling, and trying

to increase their authority. At this stage it is important to distribute roles of the team members correctly. The roles allocated to the team members who should be responsible for the creation, research, assessing, planning, organizing, motivating, communication, and implementation. When improving the creative abilities of the team members it is imperative to take into account the members' creative potential, get acquainted with their previous achievements, apply new methods of work selection (creation) and dissemination.

3. During differentiation stage team members are involved in the struggle, recognition, and consolidation activities: the members' strengths and weaknesses are revealed, misunderstandings and oppositions manifesting, the groups are forming, roles are distributed, accepted, corrected, and attempted to be re-distributed, and then the struggle for leadership can take place. During this stage it should become clear who will be the idea generator, who will help for him to generate ideas of good quality.

4. During the team integration stage its members having a struggle and searching for the recognition, consolidation, re-evaluation and starting to consolidate theirs efforts with established norms. There may appear the problem of conscious efforts reducing. Management functions are gradually distributed to the other team members taking into account the arising tasks and need for competence. The team, that having experience in successful solution of the problems and in the resource application, at this stage starting to raise the creative potential making free problem.

5. During the team maturity stage its members experiencing the period of management. They put in more efforts not for themselves, but to improve the skills of other members, needed for the compatibility of the team members in the sphere of professional competence. All of the members have leadership and membership skills. Relationships become of the non-formal type. Leadership is awarded to the team members on the basis of then needed professional competence. The team members' relations are formed and are characterised by: unity of quality orientation, emotional identification, collective decisions, and the group-thinking effect.

6. Positive psychological climate becomes easier to maintain when the members have empathy skills. This becomes easier for people that have enough experience. When team members feel that their colleague is experiencing, their relations develop differently as does their subjective reflection – the psychological climate. The empathy principle can be very successfully applied in the professional sphere. This is one of the ways to solve the most difficult problem of innovation activities' creative work – how to give up traditional thinking.

7. Socio – psychological reflection skills are also needed when communicating with other team members. By observing team members behaviour, speech, statements from a different perspective, it is possible to understand people's reactions to some actions, determine the discrepancy between the content and expression of the speech, to make conclusions whether statements are persuasive and so on. When the innovation team is made up from the experts of many spheres, having no reflection skills, much time is then must be spent to understand the entirety of the problem and to find common points of contact, by integrating the knowledge of various spheres to solve the actual tasks.

8. When carrying out the study of the innovation teams' components of creativity three main stages of creative activity were distinguished: perception, idea generation, and idea implementation. It was determined, that perception was mostly influenced by the team members' freedom, openness, orientation towards ideas and security. According to the parameters of the approximating function of perception we can posit that problem perception in

innovation teams are mostly influenced by the team members' freedom and orientation towards ideas.

9. During the idea generation stage these components of innovation teams' creativity were distinguished: intuition, imagination, perception, resourcefulness, and criticalness. According to the parameters of the approximating function of idea generation we can posit that problem comprehension in innovation teams are mostly influenced by intuition and imagination.

10. During the idea implementation stage these components of innovation teams' creativity were distinguished: courage, wisdom, responsibility, and perseverance. According to the parameters of the approximating function of idea implementation we can posit that idea implementation in innovation teams are mostly influenced by courage and responsibility.

11. When improving the creative skills of the members of the innovation teams it is necessary not only to teach for creative methods, tools, but also it is more important to free the creative potential, not overshadow it, create conditions for all members to be involved in the creative process. The team members will be then more motivated to improve themselves and to solve complex problems successfully.

12. The important components of teams creativity that were determined by studies should be taken into account and used to develop the qualities of people working in this field, this will increase the creative skills of the team and the individual members.

11. REFERENCES

1. Tatarkiewicz, W. *A History of Six Ideas: an Essay in Aesthetics.* PWN/Polish Scientific Publishers, Warszawa, 1980.

2. Urban, K. K. Recent Trends in Creativity Research and Theory in Western Europe. *European Journal for High Ability*, 1991, **1**, 99-113.

3. Sternberg, R. J.; Lubart, T. I. Investing in Creativity. *Am. Psychol.*, 1996, **57**(7), 677 – 688.

4. Runco, M. A. Creativity. *Annu. Rev. Psychol.*, 2004, **55**, 657-687.

5. Rogers, C. R. *On Becoming a Person. A Therapist's View of Psychotherapy.* Houghton Mifflin, Boston, 1961.

6. Margerison, C.; McCann, O. *Team Management: Practical New Approaches*. Mercury Books, London, 1990.

7. Robbins, S. P. *Essentials of Organizational Behaviour*. Prentice Hall, Upper Saddle River, NJ, 2003.

8. Almonaitienė, J. *Psychology of Creativity and Innovation*. Technologija, Kaunas, 2011.

9. Guilford, J. P. Potentiality for Creativity and it's Measurement. In *Readings for Introductory Psychology* (Teevan, R. C., Birney, R. C. eds.). Harcourt, Brace and World, New York. 1965, 439 – 443.

12. ADDITIONAL DATA ABOUT AUTHORS

Assoc. Prof. Dr. Augustinas Maceika
Vilnius Gediminas Technical University, Faculty of Mechanics, Department of Mechanical Engineering, J. Basanavičiaus street 28, MR-II, 1012 room, LT-03224 Vilnius, Lithuania
E-mail: augustinas.maceika@vgtu.lt

Assoc. Prof. Dr. Irena Zabielavičienė
Vilnius Gediminas Technical University, Faculty of Mechanics, Department of Mechanical Engineering, J. Basanavičiaus street 28, MR-II, 1012 room, LT-03224 Vilnius, Lithuania
E-mail: irena.zabielaviciene@vgtu.lt

9th International DAAAM Baltic Conference
"INDUSTRIAL ENGINEERING
24-26 April 2014, Tallinn, Estonia

OPTIMIZING PLM IMPLEMENTATION FROM VISION TO REAL IMPLEMENTATION IN ESTONIAN SME`s

Paavel, M.; Kaganski, S.; Lavin, J.; Sonk, K.

Abstract: *Globalization and higher requirements to stay in competition with other companies needs continuous development. There are many ways how to improve your business process. One of the opportunities is to implement PLM system to get certain benefits in cost reduction, quality improvement, time saving etc. Article gives a brief overview of PLM implementation stages from vision to real implementation. There are also described groups and staff, which should be involved in PLM implementation and brought their participation in different stages of PLM implementation. Efficient and practical groundwork what done in early stages lowers company`s implementation process and leads to better results.*
Key words: PLM, PLM implementation, PLM vision, PLM strategy, PLM implementation strategy.)

1. INTRODUCTION

Existing competitive manufacturing environment requires that companies should be more flexible, innovative and responsive to their customers' needs. Customers can choose from the wide range of products and different services. If small and medium sized enterprises (SMEs) want to get competitive advantages then they should replace their existing traditional business models to new ones [1]. The change requires also innovation in processes and methods to facilitate collaboration with suppliers and customers [2,3]. To act quickly for market changes we need to increase the speed of product development and production systems, which requires also implementation of different Enterprise Resource Planning (ERP) and Product Lifecycle Management systems (PLM).

This paper aim is to give an overview of PLM and its implementation from vision to real life implementation.

There is brought out real example how PLM system with PDM capabilities were implemented.

Currently there is no certain model for PLM implementation because all the cases and backgrounds are different. There are not a one to one defined implementation cases.

2. PLM

In 1980s engineering design entered a new era and software companies realized the potential market in form of efficient data management methodologies and began to develop the first generation commercial PDM (Product Data Management) systems. Developers were already involved in CAD (Computer Aided Design)/ CAM (Computer Aided Manufacturing) / CAE (Computer Aided Engineering) software market [4].

The Aim of Product Lifecycle Management (PLM) systems is to enable enterprises to satisfy they're needed requirements. One of the major challenges for PLM systems is the lack of integrated decision support tools to help decision-making with available information in collaborative enterprise networks [5]. PLM not just a set of technologies it is a business strategy of different complex IT tools and applications which support digital design and manufacturing practices over the whole company in several ways. It`s a holistic business concept what is developed to manage a product and its lifecycle. PLM

manages items, documents and BOM`s supports analysis results, test specifications, quality standards, engineering requirements, changing orders, environmental component information, manufacturing procedures, product performance information, component suppliers. Modern PLM system capabilities are wide. Recently the manufacturing environment became modern and competitive for mastering new design and manufacturing methods, which enables to improve the sustainability of the products [6,7]. Thanks to possibility to integrate different CAD systems, CRM systems, Microsoft Office, ERP systems to whole it forms the information backbone of a product and its extended enterprise. [8,9,10].

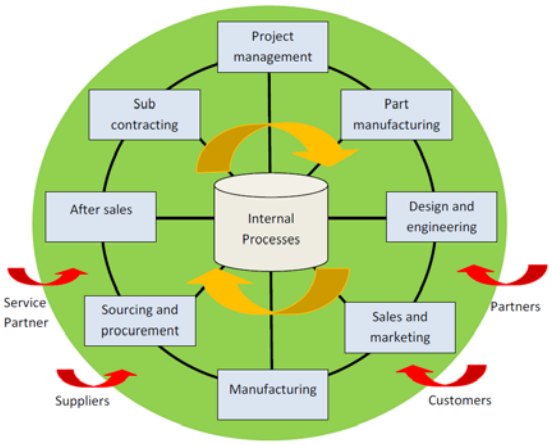

Fig. 1. PLM System [8]

Solutions what can be added to PLM such as; [11,12,13]
BOM (Bill Of Material) Management, CAD File Management, Change Management, Compliance Management, Content Management, Classification Management, Component &Supplier Management, Concept Development, Configuration Management, Design Outsourcing, Detailed Design, Document Management, Engineering Change Management, Environmental Compliance, Extended Capabilities, Fast Fashion, Formula and Recipe Management, Global Product Development, Label and Artwork management, Lean Product Development, Maintenance & Calibration, Maintenance, repair & operation Management, Manufacturing Process Management, Manufacturing Process Planning, Mechatronics, New Product Introduction, Outsourced Manufacturing, Packaging Management, Part Traceability, Portfolio Management, Product Analytics, Product Costing, Product Data Management, Product Engineering, Product Governance & Compliance, Product Life cycle Management, Program Management, Project Management, Quality Management, Quality Planning, Quality Systems, Quote Process Management, Regulatory Compliance, Reporting & Analytics, Requirements Management, Resource Management, Risk Management, Software Configuration Management, Sourcing Management, Source Code management, Specification Management, Supplier Corrective Action, Supply Chain Management, Systems Engineering, Tooling Management, Variants & Options, Visualization & Markup, Workflow Management.

3. BENEFITS FROM PLM

Companies are Implementing PLM systems to get different benefits. Benefits are coming through making you Lifecycle more understandable by using it different modules of the system. Also by better file management and information movement inside the company and also between different phases of products life. In Closed-Loop Product Lifecycle information moves from Beginning of Life (BOL) to Middle of Life (MOL) and to End of Life (EOL). Information also moves backward from EOL to MOL and BOL by closing the necessary loops in products information. [14,15]
Benefits what companies usually might get can widely divided into four bigger categories such as;

- Cost reduction
- Quality improvement
- Time saving
- Other

Expectation to reduce product cost comes through reducing the product development cost, material cost, prototyping cost, production cost and so ob by faster and controlled design and information movement. Reducing more different items and they are more standardized. Management of total production load is more simplified with the help of right product structure. By this one person can give more design for company and other engineers can deal with other projects. inventory cost is lowering because there's better overview on products and don't need to keep so big stock reserve. Service cost is reduced through better knowledge what's needed for maintenance. [8,16,17]

Potential source of quality improvement in Production Company like errors, rework, wasted efforts customer complaints, product returns, recurring product problems and conformance with customer requirements can be achieved by better and clear data and information storage. Changing documents and revisions can be electronically accepted and released why change management is faster and less faulty. Easy to find documents, protocols and standards related to product. [8,16]

Reduced project times, project overrun times, engineering change times, cycle times might come to better definition of product structures because it's easier to use already existing information and amount of overlapping work decreases. Parts and drawings history can be available with minimum effort. All this leads to reduced time to market and profit. [8,16,17]

PLM also enables to make better business decisions and results by clearer products lifecycle. Improves visibility over the supply chain, provides feedback from different phases of lifecycle and enables better management of outsourced tasks. [8,16,17]

These are only some of benefits what are expected from PLM system. The real benefits for the company depend on implemented modules and systems functionality. The comprehensive is work before PLM implementation the more effect company gets from implementation.

4. PLM IMPLEMENTATION

PLM implementation is big step to most of companies. The reasons might be very different and the expected benefits might differ depending on the company. Common in these cases is that they all need some way to achieve their goals. Figure 2 shows one possibility how to implement PLM system [8,16].

The need for Implementing PLM system should come from company`s overall vision. PLM should help to achieve this mission or help the company closer to its goals. Corporate business vision is set by company`s management and company`s activities should conform to it.

From company`s vision should come company`s business objectives. Company`s business objectives is the end result of proposed actions and says where company wants to be after a specific period of time.

From company`s business objectives should grow out input for PLM vision. A PLM vision is not an independent stand-alone unit. It has to fit with the company`s overall vision of its future, Its missions and objectives. [16]

If corporative business vision and business objectives were set by management then from PLM vision project manager is responsible for further development. Cooperating with management and steering group project manager has to describe companies PLM vision. It is high-level conceptual description of a company`s product lifecycle activities at some future time. It`s hard to look further into the future than five years from now. So the PLM vision is usually put in place for five years. It doesn't mean it's execution. [16]

PLM Vision is the best possible expectation for future situations and activities. PLM vision highlights the main features of future activities. [16]

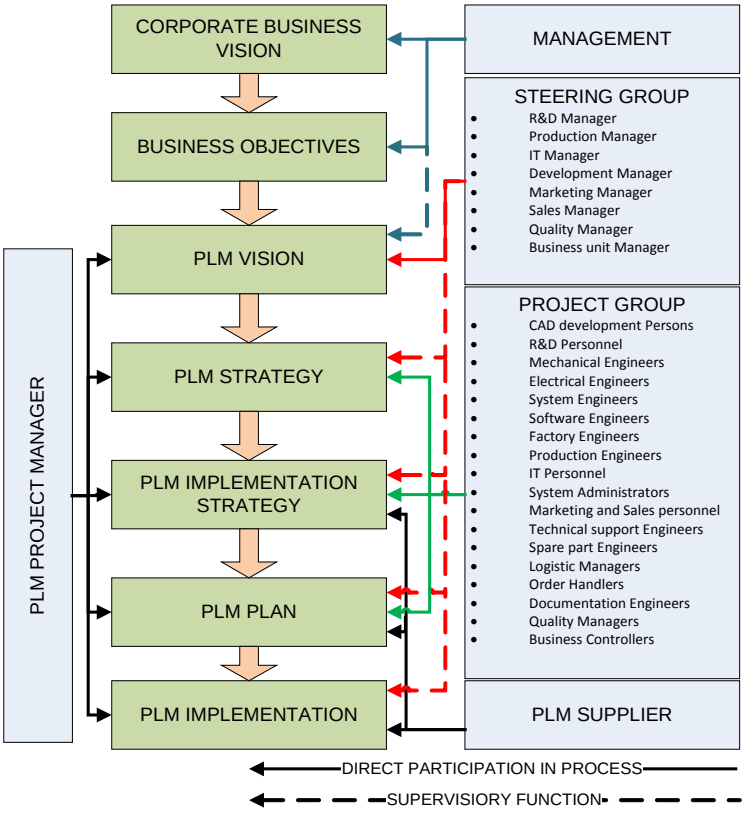

Fig. 2. PLM Implementation plan

A PLM Vision will be company-specific. It has to be clear so that everyone in company has clear agreed destination what they can fallow. Clear understanding of the objectives, scope and components of PLM.
Once the PLM vision has been agreed, a suitable PLM strategy and PLM Implementation strategy has to be developed to achieve the best results. [16]
PLM vision should be documented in a report. Executive overview should only be a few pages in length and there should be brought out things like; [18]

- The company: objectives, strategy, success factors, key issues
- The PLM Initiative
- Description of PLM Vision
- Next steps: PLM strategy, PLM implementation Strategy, PLM Roadmap, PLM Plan, schedules, resources, value, cost, ROI.

PLM strategy will be company specific. It's also possible to work at the same time with multiple different strategies and make SWOT analysis (strength, weaknesses, opportunities and threats).

PLM strategy describes how PLM resources are used at the present moment based on As is analysis. A PLM strategy for the future shows how resources will be used in future based on To-be analysis.[16]
PLM strategy is developed by Project manager and Project group, Steering group supports them with needed resources and controls that project would be in progress. In this phase project group has to work hard to achieve best result, which depends a lot in future implementation. The PLM strategy has to be documented and transmitted to everybody who`s involved.
A strategy describes how to achieve objectives; how resources will be organized and managed. Provides the best chance to achieve set goals and assures that everyone work on same target. [16]
The PLM strategy shows how PLM resources will be organized in future. The Implementation Strategy shows how resources will be organized to achieve goals what are set is Do-be analysis. The implementation strategy is sometimes

referred to as change strategy or a deployment strategy. [16]
The Implementation strategy is the starting point for developing the Implementation Plan. Developing Implementation plan for the first year and Implementation strategy at the same time helps to make sure their compatibility. [16]
Putting together implementation plan in addition to project group, what`s directly is involved, and steering group comes extra PLM supplier or implementation company. They have the knowledge to tell what program will fulfill the company`s needs. From that stage on PLM supplier or Implementation Company has to be chosen for further project development.
PLM plan deals with all of PLM such as; product data, equipment, human resources, applications and processes. Objectives, action steps, timing and financial requirements are defined. In this phase all issues and problems have to be solved and company is ready for real implementation. [16]
The main purpose of the chain from business mission and objectives through PLM Vision, PLM Strategy, PLM implementation strategy PLM plan and implementation is that the company meets it objectives. [16]

5. CASE STUDY

Bestnet AS is as Estonian Small and medium enterprise what is manufacturing and selling their own design based trailers for different purposes.
Bestnet AS business vision is "Car owners - we are your best choice for personal transportation solution. The trailers will rely on the experience of preparing a long-term, quality and environmental sustainability" [19]. Based on vision Bestnet AS made his first feasibility study in 2005 and despite the facts, that product information management grows over head, reached to conclusion that at the moment they don´t have needed recourses for implementing PLM or PDM system.
Situation changed in year 2010 when in cooperation with IMECC OÜ Bestnet AS take in their plans to implement Teamcenter Rapid Start what is with PDM capabilities.
A central issues in Implementation are coming from vision. From Bestnet AS business strategy and business objectives came small dimensional PLM vision what company wants to achieve;
1) Current design is complicated because most of parts are used at the same time in different products and making changes to them is complicated.
2) Data entry from CAD to ERP system is manual. Company wanted to get automatic data transmitting from CAD to ERP with XML file that engineering Bill of Material (eBOM) and manufacturing (mBOM) are the same.
3) Direct communication with dealers for better to ensure better service.
Based on these objectives company`s Project team and PLM supplier started to put together PLM strategy and PLM implementation strategy. What was mainly done with different managers and engineers by mapping their expectations for the system. Interviews were carried out with engineers from different department.
At the current time PLM implementation still continues. Set objectives are solved with Teamcenter Rapid Start with functionalities such as;
Secure vault, standard user roles and access security, check-in/check-out, search were - used tools, revision/version control, view & markup, Solid Edge integration, BOM management, ERP integration, manufacturing data and process management.
In the near future company should successfully complete PLM Implementation and reach its set goals.

6. CONCLUSION

PLM plays an important role in the modern production landscape. In first part of article is brought out information about PLM, its

components and benefits. How PLM is company`s specific and one possibility how implementation could be carried out. Also is brought out AS Bestnet PLM implementation progress activities.

7. ACNOWLEDGEMENTS

This research was supported by ETF grants 8485 and 7852, targeted financing project SF0140035s12 and innovative Manufacturing Engineering Systems Competence Centre IMECC (supported by Enterprise Estonia and co-financed by the European Union Regional Development Fund, project EU30006).

8. REFERENCES

1. Karjust, K.; Küttner, R.; Pääsuke, K. Adaptive web based quotation generic module for SME's. Küttner, R. (Toim.). Proceedings of the 7th international conference of DAAAM Baltic industrial engineering, 22-24th april 2010, Tallinn, Estonia (375-380). Tallinn: TUT
2. Snatkin, A.; Karjust, K. and Eiskop, T. (2012). Real time production monitoring system in SME. In:*Proceedings of the 8th Int. Conf. of DAAAM Baltic Ind. Eng.*, (Otto, T. ed.) TUT, Tallinn, 2012, 573–578
3. Karjust, K.; Pohlak, M.; Majak, J. (2010). Technology Route Planning of Large Composite Parts . International Journal of Material Forming, vol 3, 631 - 634. ISSN: 1960-6206 (Print) 1960-6214 (Online)
4. Tony Liu D., William Xu X. A review of web-based product data management systems. Computers in Industry 44 (2001) 251-262.
5. Shevtshenko, E.; Yan, W. (2009) Decision support under uncertainties based on robust Bayesian networks in reverse logistics management, International Journal of Computer Applications in Technology 36(3-4): 247-258.
6. Karaulova, T., Kostina, M., Sahno J., (2012) Framework of reliability estimation for manufacturing processes. Mechanika 18 (6): 713-720.
7. Shevtshenko, E., Bashkite, V., Maleki, M., & Wang, Y. (2012). Sustainable design of material handling equipment: a win-win approach for manufacturers and customers. Mechanika, 18(5), 561-568.
8. Saaksvuori, A., and Immonen, A. 2008. Product Lifecycle Management. 3rd Edition. Springer-Verlag, Berlin, Heidelberg.
9. Z.M. Qiu, Y.S. Wong, Dynamic workflow change in PDM systems, Computers in Industry 58 (2007) 453-463.
10. A CIMdata White Paper. PLM Market Growth in 2007 A First Look in 2008—Exceeding Expectations. March, 2008
11. http://www.product-lifecycle-management.info/plm-elements/plm-solutions.html (03.03.2014)
12. http://plmtechnologyguide.com/site/?page_id=604 (03.03.2014)
13. http://plmtechnologyguide.com/site/_wp-content/uploads/2014/02/plm_requirements_chart.png (03.03.2014)
14. Kiritsis D., Bufardi A., Xirouchakis P. Research issues on product lifecycle management and information tracking using smart embedded systems. Advanced Engineering Informatics 17 (2003) 189-202.
15. Jun H.-B., Kiritsis D., Xirouchakis P. Research issues on closed-loop PLM. Computers in Industry 58 (2007) 855-868.
16. Stark, J., Product Lifecycle Management 21st Century Paradigm for Product Realisation. Springer-Verlag, London, 2011.
17. Lee, Y-C., Sheu L-C., Tsou Y-G. Quality function deployment implementation based on Fuzzy Kano model: An application in PLM system, Computers & Industrial Engineering 55 (2008) 48-63
18. Stark, J. Global Product: Strategy, Product Lifecycle Management and the Billion Customer Question. Springer-Verlag, London, 2007.
19. http://www.tikitreiler.ee/missioon

DATA ABOUT AUTHORS

MSc. Marko Paavel
E-mail: Marko.Paavel@ttu.ee
MSc. Sergei Kaganski
E-mail: Sergei.Kaganski@mail.ee
MSc. Jaak Lavin
E-mail: Jaak.Lavin@imecc.ee
MSc. Kaimo Sonk
E-mail: Kaimo.Sonk@ttu.ee

9th International DAAAM Baltic Conference
"INDUSTRIAL ENGINEERING -
24-26 April 2014, Tallinn, Estonia

PARTNER SELECTION CRITERIA FOR VIRTUAL ORGANIZATION FORMING

Polyantchikov, I.; Shevtshenko, E.

Abstract: *This article indicates criteria which a partner should evaluate during the forming of virtual organisation (VO). This paper bases on analyses existing criteria and investigate research works which were done by different researches. The represented criteria will be used to select partner for a new project in the frame of Partner Network (PN).*

Key words: Partner Network (PN), Virtual organisation (VO), SME, Partner Selection, Key performance indicators KPI

1. INTRODUCTION

The different association of independent organizations become a popular tool to restrain the competition in the current economic situation on the global business market. "Interorganizational networks include supplier and marketing or distribution networks, technological-innovation and product-development networks, and different competitive coalitions used, for example, for establishing industry standards and for competing against other networks or a specific dominant player such as Microsoft".[1] There are many different forms of such associations exist, including, Collaboration Network (CN), Strategic Alliances (SA), Partner Network (PN), Industrial Clusters (IC), etc. These unions are mostly designed for Small and Medium Enterprises (SME) [2]. The SME have some common restrictions (budget limitation, small amount of services or products, etc.), which stimulate small companies to join together to survey on the market with tight competition [3],[4].
Each company has own preferences for partner selection during partnership formation [5]. In this work was analysed the existing preferences and finds most critical of them for companies.
The next step will be development an evaluation mechanism for partner selection from association of independent organizations. The support of selection process for PN is an essentially issue during formation of temporary alliances of VO [6]. One of the aims of the PN is a collate data about member enterprises, their capabilities and KPIs of each member [7]. These parameters and data are used in partner selection mechanism when the VO initiators (hereinafter focal player or broker) make an own decision and this part is also considered in current research work.

2. PARTNER NETWORK DISCIPLINE

a. Partner Network Notion

Partner Network (PN) origin is close with Collaborative Network (CN) and definition of PN can be applied the same, but the main difference between PN and CN is the operating environment, which is constrained with legal aspects. When companies, entering into the PN, they should sign the frame agreement with collective juridical body, representing the PN. Based on that agreement the companies, which are working on financial proposal to the customer, can quickly form

the Virtual Organization, in order to be ready for the legally respond to the market demand. [8]

PN managerial legal entity is called Partner Network Managerial Office (PNO). The main obligations of PNO are:

- represent the PN members to the customers
- measure the PN members Key Performance Indicators (KPI)
- ensure the information channel for PN members for the exchange of agreed information
- organizing the process of PN members drop off and to support the joining of new members. [8]

b. Virtual organisation

Virtual Organization (VO) a temporary alliance of independent organizations (e.g. companies, institutions, people and commercial and non-commercial organizations) that come together to share resources and skills to achieve its mission/goal, and whose cooperation is supported by computer networks [9]. VO forms from entities which constituted a PN. Normally, the process of forming VO takes a time, due to legal, technical and social aspects. The fig.1 shows the principle scheme of the VO. There are depicted important VO features on the picture, which define every VO. It is a Focal Player (FP) [8] or broker, a subset of the PN enterprises may be chosen to form a VO for some specific business opportunity [9]. It is a common goal/mission to achieve a business opportunity. It is a set of partners who has competences "required to achieve a given task or acquired by an actor in the context of achieving this task" [10]. The focal player (broker) has to select appropriate partners to achieve the project goal successfully from universe of enterprises or PN. There are introduced the competences, KPIs capacity and capability to simplify the selection process. In most cases, the process will be complicated, since a FP has to choose between many parameters and each of the parameters has own weight. The partner selection is

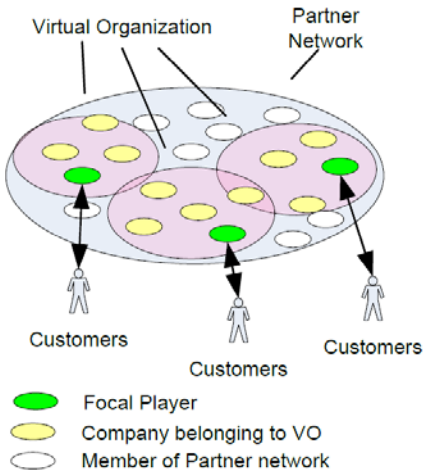

Fig. 1 Virtual Organization [8]

getting time consuming and complex procedure. Our proposal is make the process more attractive and easier for FP by using mathematics and computing methods.

c. Partner Information Artefacts

All organizations have to be introduced in the PN before join to PN. The process of joining new member comes through negations, interviews and questioners. During the joining process the Partner Network Managerial Office (PNO) collects the information in the central database. This information is called Partner Information Key Artefacts and contains required information about partner [8]. The Fig.2 shows determined "most critical artefacts that companies need to exchange in IC"[8].

The most critical artefacts has been determined on base survive of 20 SMEs from different domains. Artefacts may be exemplified as follow:

- "roles, skills, organizational structure, location
- communication
- data clusters, data elements
- machinery/benches [12];
- software application systems, ICT technology [13];

- servers, network nodes, operating systems
- critical factors, business objectives, key performance indicators (KPI)
- risks, issues, action plans
- projects“ [13]

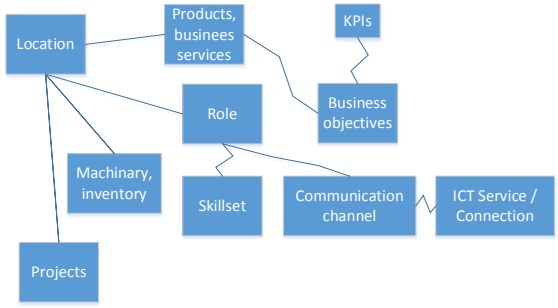

Fig. 2 Enterprise Key Artefacts

This is basic and necessary information that PN has to collect from new company, which has willingness to join the network. The information will be also used during the formation of the VO [14]. In next chapter it will be define the criteria base on the key artefacts.

3. PARTNER SELETION CRITERIA

a. Criteria in literatures

During the formation of VO organization the FP faces with a challenge of selection “proper” and “right” partner. ”However despite the growing numbers and increasing significance of strategic alliances, many fail … such failures may be for many interrelated reasons - and may be defined in various ways - two common causes are poor *partner selection* and poor *alliance management*”[15] [16] [17].
“Any collaboration begins with analyzing potential partners … Realizing potential alliance benefits depends on selecting appropriate partners”[16]. This section provides an illustration of criteria which FP takes as preferences in time the partner selection. There are many research are dedicated on partner selection topic on base on particular parameters and collaborative utilities. Feng et al. suggests a method for partner selection of codevelopment alliances using individual and collaborative utilities [18]. Wann et al. propose in the research work “how firms should select alliance partners for entering competition advantage” [19]. Author proposes the criteria and sub-criteria for partner selection. “After some interview with some experts and practitioners in high-tech industry, the study develops five big criteria to determine how to select the best partners.

- Characteristics of the partner
- Marketing knowledge capability
- Intangible assets
- Complimentary capabilities
- Degree of fitness” [19].

Geringer, 1990, has distinguished the criteria on task and partner-related dimensions of selection partner [20].
Kannan and Tan, 2002, have defined the criteria [21] as “quantifiable or “hard” criteria such as price, delivery, quality, and service are routinely used for selection and assessment [22] and “soft”, difficult-to-quantity factors such as management compatibility and strategic direction of the partner have also been shown to be important, particularly in the context of strategic buyer-supplier partnership [21], [23]”. In survey has been observed 411 US companies from different domains. Assessment criteria have been ranked partner performance by participants. This research work demonstrates FP expectation in front of partners for VO.

b. Partner selection criteria for formation VO

It was defined Enterprise Key Artefacts in the previous section. Each of the artefacts has criteria, attributes and dimension. In the selection it is presented criteria that our group found during the investigation in the research works.
In case “roles, skills, organizational structure, location” artifact can be applied criteria *Technology* [21], [22], [23],[26] which has following attributes: Technological compatibility (TCOMP), Assessment of

future manufacturing capabilities (FMC), Supplier's speed in development (SSD), Supplier's design capability (SDC), Technical capability (TCAP), Current manufacturing facilities/ capabilities (CFC).

"Communication channel" artifact defines as *Relationship* [25],[26] criteria. It criteria have attributes: Long-term relationship (LTR), Relationship closeness (RC), Communication openness (CO), Reputation for integrity (RFI).

Criteria *resources* can be applied for "Machinery/benches" artefact. In this case the attributes can be interpreted as: Competency, Quality, Time, Volume, Costs, Flexibility, Environment.

"ICT technology" has criteria as "*Information/knowledge*". The criteria have attributes: Quality, Integrity, Availability, Exchangeability, Confidentiality, Updatability.

"Key performance indicators (KPI)" are criteria itself that can be split on the attributes, which has been figured out during the interviews with mangers of production companies: volume of output during the period, kg/period, labor usage for the period of time, h/period, productivity, h/ton,,project's profitability, %, space performance, kg/m2, consumption of welding gases, bottles/period, individual performance, the number of kilograms of finished product per 1 worker per month, kg/person, number of delays of product output, outturn, %

"Projects" artifact can be applied "*Past performance - past experiences in VO*". *Namely,* " Successes and failure in past collaborative activities are evaluated as significant indicators of readiness for future collaboration" [27].

4. COOPERATION WITH OTHER RESEARCHES

The artifacts were used in this paper is a result of collaboration research with colleagues from Tallinn University of Technology.

This paper is a sequel of the research work introduced in paper "Business and it alignment in enterprise considering the partner network's constraints". The paper gives details of the enterprise artifacts which are necessary for join the new member to the PN. Also it indicates that an enterprise IT has to be aligned with its Business Model. The IT alignment is a significant activity for the company to start the cooperation on Virtual level of cooperation such as VO.

The research presented in this paper has to be verified and validated by any method. This is task of the following collaboration research with another colleague. Paper "Quality improvement methodologies for continuous improvement of production processes and product quality and their evaluation" indicates the improving methods. It also introduces the ways how to improve the management processes in VO.

The general scheme of papers interconnection is depicted on Fig.3.

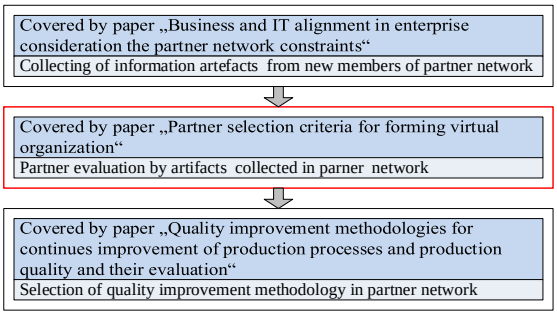

Fig. 3 General scheme of the Research

5. CONCLUSION

As the result of the research can be concluded that partner selection is a multi-decisional process and a FP should define the most significant preferences and on its base make a final decision respecting to partner. A result of the whole project can fail, if FP does not consider of the possible threats related with the selection partners.

In this paper indicates the criteria that should be considered and the criteria amount is quote many. Next research will focus on the methods and tools, which can

be applied for evaluate introduced criteria and weight the criteria to assist a partner selection process.

6. ACKNOWLEDGEMENTS

Hereby we would like to thank the Estonian Ministry of Education and Research for Grant ETF9460 which supports the research.

7. REFERENCES

1. Foss J., Networks, capabilities, and competitive advantage, *Scandinavian Journal of Management*, Volume 15, Issue 1, March 1999, Pages 1-15, ISSN 0956-5221

2. Kangilaski, T., CHALLENGES FOR SMEs ENTERING INTO THE VIRTUAL ORGANIZATION PARTNER NETWORK, By: Edited by: Kyttner, R Conference: 7th International Conference of DAAAM Baltic Industrial Engineering Location: Tallinn, ESTONIA Date: APR 22-24, 2010, Vol.2 Pages: 352-357

3. Kangilaski T., Asset Management Software Implementation Challenges for Electricity Companies, Book Group Author(s): IEEE Conference: 35th Annual Conference of the IEEE-Industrial-Electronics-Society (IECON 2009) Location: Porto, PORTUGAL Date: NOV 03-05, 2009 V. 1-6 pages: 3399-3404

4. Pribytkova, M., Karaulova, T. RELIABILITY FACTORS OF PRODUCTION PROCESS, Edited by: Katalinic, B Conference: 20th International Danube-Adria-Association-for- utomation-and-Manufacturing Symposium Location: Vienna, AUSTRIA Date: NOV 25-28, 2009, Volume: 20 Pages: 947-948

5. Kramarenko, S.; Karaulova, T., Case study of project management process improvement Edited by: Katalinic, B Conference: 17th International Symposium of the Danube-Adria-Association-for-Automation-and-Manufacturing Location: Vienna, AUSTRIA Date: NOV 08-11, 2006, Pages: 209-210

6. Kangilaski T., Communication as a Crucial Element for Enterprise Architecture Management in Virtual Organization, Edited by: Bernus, P; Doumeingts, G; Fox, M, Conference: 21st IFIP World Computer Congress (WCC) Location: Australian Comp Soc (ACS), Brisbane, AUSTRALIA Date: SEP 20-23, 2010 Volume: 326 Pages: 66-77

7. Kangilaski T., Case study: Utilities and asset management - Time for a change Book Group Author(s): IEEE, 5th IEEE International Conference on Industrial Informatics, Vienna, AUSTRIA, JUN 23-27, 2007 Pages: 579-584

8. Kangilaski T., Maturity Models as Tools for or Focal Player Forming Virtual Organizations, International Conference on Management, Manufacturing and Materials Engineering (ICMMM 2011), Zhengzhou, PEOPLES R CHINA, DEC 08-10, 2011, Advanced Materials Research Volume: 452-453 Pages: 829-832

9. Camarinha-Matos L., Afsarmanesh M., Collaborative networks: a new scientific discipline. *Journal of Intelligent Manufacturing*, 16, 439–452, 2005, Springer Science+Business Media, Inc. Manufactured in The Netherlands.

10. Kangilaski, T. (2010). Challenges for SMEs Entering into the Virtual Organization Partner Network. In: *Proceedings of 7th International Conference of DAAAM Baltic Industrial Engineering: 7th International Conference of DAAAM Baltic Industrial Engineering*, Tallinn, 22-24 April 2010. (Toim.) R. Küttner. Tallinn: Tallinn University of Technology, 2010, 352 - 357.

11. Camarinha-Matos L., Afsarmanesh M., Ollus M. Methods and tools for collaborative networked organizations. New York, 2008, Springer Science+Business Media, LLC

12. Bjorklund, S. Pribytkova, M. Karaulova, T., DEVELOPMENT THE MAINTENANCE PLAN: MAINTENANCE ACTIVITIES ON OPERATIONAL LEVEL, Edited by: Kyttner, R, 7th International Conference of

DAAAM Baltic Industrial Engineering Location: Tallinn, ESTONIA, APR 22-24, 2010, VOLS 1 AND 2, 286-291
13. Kangilaski T., ICT and Business Alignment in Virtual Organization Book, 6th IEEE International Conference on Industrial Informatics Location: Daejeon, SOUTH KOREA Date: JUL 13-16, 2008, VOLS 1-3 Book Series: IEEE International Conference on Industrial Informatics (INDIN), 1184-1189
14. Kangilaski T., Case study: Utilities and asset management - Time for a change , 5th IEEE International Conference on Industrial Informatics, Vienna, AUSTRIA, JUN 23-27, 2007, VOLS 1-3, IEEE International Conference on Industrial Informatics (INDIN), 579-584
15. Cheikhrouhou N., Abdel-Rahman H. Tawil & Choudhary A. (2013) Modelling competence-based virtual organisations using the unified enterprise competence modelling language. *International Journal of Production Research*, 51:7, 2138-2159
16. Stevan R. Holmberg and Jeffrey L. Cummings, Building Successful Strategic Alliances, Long Range Planning, vol. 42 (2009) 164-193
17. Karaulova, T.; Kostina, M.; Sahno, J., Framework of reliability estimation for manufacturing processes MECHANIKA Issue: 6 Pages: 713-720 Published: 2012
18. Feng B., Fan Z., Ma J., A method for partner selection of codevelopment alliances using individual and collaborative utilities, *International Journal of Production Economics*, Volume 124, Issue 1, March 2010, Pages 159-170, ISSN 0925-5273
19. Wann W., Shih H., Chan H., The analytic network process for partner selection criteria in strategic alliances, *Expert Systems with Applications*, Volume 36, Issue 3, Part 1, April 2009, Pages 4646-4653, ISSN 0957-4174
20. Geringer M. J., Strategic Determinants of Partner Selection Criteria in International Joint Ventures, *Journal of International Business Studies*, Vol. 22, No. 1 (1st Qtr., 1991), pp. 41-62
21. Kannan, V. R. and Tan, K. C., Supplier Selection and Assessment: Their Impact on Business Performance. *Journal of Supply Chain Management*, 2002, 38: 11–21
22. Ellram, L.M., The Supplier Selection Decision in Strategic Partnerships, *Journal of Purchasing and* Materials *Management*, (20:4), 1990, pp. 8-14.
23. Hahn, C.K., C.A. Watts, and K.Y. Kim. "The Supplier Development Program: A Conceptual Model," Journal of Purchasing and Materials Management, (26:2), 1990, pp. 1-7.
24. Barbarosoglu, G. and T. Yazgac An Application of the Analytic Hierarchy Process to the Supplier Selection Problem, *Production and Inventory Management Journal*, (38:1), 1997, pp. 14-21.
25. Sarkis, J. and Talluri, S. (2002), A Model for Strategic Supplier Selection *Journal of Supply Chain Management*, 38: 18–28
26. Choi, T.Y. and J.L. Hartley An Exploration of Supplier Selection Practices across the Supply Chain, *Journal of Operations Management*, (14:4), 1996, pp. 333-343.
27. Romero D., Galeano N., Molina A. Mechanisms for assessing and enhancing organisations' readiness for collaboration in collaborative networks, *International Journal of Production Research*, (2009), 47:17, 4691-4710

7. ADDITIONAL DATA ABOUT AUTHORS

Igor Polyantchikov
Tallinn University of Technology, Department of Mechanical Engineering
Ehitajate tee 5, 19086, Tallinn, Estonia
Email: poljantsikov.igor@gmail.com
Eduard Shevtshenko
Tallinn University of Technology, Department of Mechanical Engineering
Ehitajate tee 5, 19086, Tallinn, Estonia
Email:eduard.sevtsenko@ttu.ee

9th International DAAAM Baltic Conference
"INDUSTRIAL ENGINEERING -
24-26 April 2014, Tallinn, Estonia

VALUE-CENTERIC BUSINESS: AN IN-DEPTH ANALYSIS OF ONE CASE COMPANY

Randmaa, M. & Otto, T.

Abstract: *Many different interpretations of value co-exist. Sometimes it is the (re)-interpretation of value that reveal new value [1]. Companies, who discover changes and possibilities within the value system first and make use of these are considered to be Prime Movers and often are more successful than the late adapters [2].*
We have conducted an in-depth analysis of one successful construction company, made case analysis on literature bases and have formulated a practical methodology for analysing and developing value-centric products, services and business-models. This paper is describing data collection and analysis processes of prescriptive phase of the research.
Key words: value-centric design, business development, qualitative research, case study.

1. INTRODUCTION

In the early years of the twenty-first century, we confront unprecedented challenges in our human endeavours. We have a burgeoning and aging population; we face pressures on all types of resources from food to energy and materials; our activities have damaging impacts on many aspects of our natural environment; and we live in an intensely competitive world where economic prosperity depends on translating ingenuity into products, services, and systems for sale in world markets [3].
Traditionally manufacturing companies employ a structured approach to the development of their programme of physical products in order to secure quality levels and requirement fulfilment [4].
Regarding the services, the research domain of service marketing is focusing on establishment of a consistent delivery quality and the exploration of the detailed process in the interaction between customer and supplier [4]. New Service Development models attempt the adaption of structured development process models to the requirements of having a service process as an object of design [4].
We see that the development focus should be on value instead of product or service, as value is the core concept of integrated product, service and business development and thus propose that a value-centric model of these processes will be beneficial and is much needed [5].
It is our ambition to contribute to the shift towards value-based thinking by opening up some new perspectives for understanding the value system and noticing new product, service and business model design potentials for better competitively and efficiency of a company [5].
In this paper we first describe the need for new value-centric development models. Then we bring out major aspects in choosing data collecting and analysing methodologies for our case company.
Next we give an overview on qualitative research within Company A and bring out major success-factors with brief reasoning.
Finally we raise our next cornerstones and goals for further research.

2. NEED FOR NEW VALUE-CENTRIC DEVELOPMENT TOOLS

Globalization and information technologies have made the economic landscape more transparent, customers smarter, more demanding and networked. However, not only the changes in the landscape of economics have influenced the customer behaviour. Michael Edgar has brought out eight major changes in social sphere [6, 7]. Vargo, Lusch and Morgan also state that individuals become increasingly micro specialized- there is an increasing need for specialized services [6, 8]. It is due to these dynamic changes that new retailing formats develop and consumers want to change their mix of value providers- social and psychological cost of time changes. How consumers value different activities, products and services changes dynamically depending on customers` context and life-style.

Also the wishes of industrial customers have changed- industrial customers value how well value propositions harmonize with their existing components, processes and strategies [6, 5]. In the field of manufacturing there are also some early signs of shift from production- centred manufacturing to production-service centred manufacturing. As quality and low price of a product have become prerequisites, the market is now becoming to demand extra services from manufacturers. Distribution, product lifecycle management, database services, prototyping, testing, financial services, repair and maintenance and consulting are just few of the services customer can have benefit from. One can assume that the demands to a manufacturing company will increase in time. In order to be ready for the shift, enterprises will need to make changes in their strategy, structure, management, and start looking for partner-enterprises to unite the strengths and face the challenges of the futures high-demanding business environment [5]. Process-centric view of business changes for human-centric view of business, which means that people are seen as the active agents of business rather than processes. Verna Allee [6, 9] is developing a new promising theory and methodology for understanding the value network within and outside a business.

There may be some major opportunities to apply co-creation models between different parties of economy (customers, suppliers, retailers, producers etc.), that would change how value is created, delivered and perceived- and thereby increase efficiency and competitiveness of value systems [6, 7].

The car would have no value if no one knew how to drive, had access to fuel and maintenance, and functioned in social networks, for which particular automobiles have particular meanings, etc. The car only has value when the customer makes use of the it- in the context of his or her own life. In this case customers, manufacturers and social services co-create value [10].

3. METHODS USED FOR DESCRIBING CASE COMPANY

Design and the creativity and innovation involved in it are “living things moving in a field.” By limiting their movements, they may be described with greater accuracy, but their natural movements then slip away from the scope of such delineation [11]. It is a challenge to give valuable suggestions to an organic system.

As roots of the entrepreneurship paradigm are also in psychology and sociology, it makes sense to use qualitative methods while digging deeper into our research [12]. Qualitative approaches are used when wishing to go beyond mere description at a generalizable level in empirical investigations [12].

During the first stage of the research we gathered information, experience and feelings from within a construction company. We were included in decision-making, managing, marketing, bidding, accounting, construction, processes during

3 years, that was a sufficient time for gaining a feel of how the company worked within its economic landscape and help it develop its value propositions and business-model.

During and after active research-period we conducted various qualitative data collecting strategies, such as interviews, conversations, observations, documentary studies and self-reports.

Although the economic landscape is constantly moving and the business is constantly developing, we try to perpetuate the moments by comparing the numbers and indicators before, during and after the research. This is how we gathered quantitative data for the research.

4. RESEARCH WITHIN CASE COMPANY

4.1 General Description of Company A

Company A is a successful micro-sized company founded in 2006 and offers turn-key solutions in the area of industrial construction, using developed modular solutions. Regular clients are industrial companies and farms that need fast and effective construction service.

Company A is outsourcing all the services it needs (accountancy, construction drawings, material transport, montage etc.) and is mostly seasonal (projects are executed from late spring till early winter, when the dirt is soft). Small size gives it some advantages: low fixed costs, dynamics, independence, and efficiency, easy and transparent management.

Table 1 shows Company A`s economic indicators and descriptions of the economic environment within construction field at the time. Although the number of contracts annually has varied in time, the average contract volume has constantly been raising, even though the competition has grown and EU subsidies have been reduced. This proves that Company A`s business model is strong and working well in its niche market.

	2006	2007	2008	2009	2010	2011	2012	2013
Number of contracts	3	6	10	12	12	14	8	4
Average contract volume	33 300	33 300	36 000	38 400	33 700	53 800	163 100	237 300
Biggest changes in business environment	Economy develops fast and caotically. Many companies experience growth.	Continual re-organizatio n of economy. Determinat ion of state inspection system and standards	Economic crisis. Russia's economic stagnation, which was manifested in the re-profiling the industry in Estonia.	Export growth to EU countries.	Organizati on of the market, the outflow of constructio n workers in Finland.	The rapid developme nt of economy.	Economic crisis. Arrears.	The EU subsidy reduction. Organizatio n of the market.
Biggest changes in business model	Rapid growth of orders due to low competitio n.	Gaining experience in the business, developme nt of business standards	Previous orders are good references for new clients	Several orders to Finland and Aland	Previously built buildings work as advertisem ent	Hiring managing director	Contracts become bigger	Reduction of orders and EU subsidy. Competitio n grows
No of quotes made	36	70	120	320	380	460	460	500
Quotes to contracts, %	8,3%	8,6%	8,3%	3,8%	3,2%	3,0%	1,7%	0,8%
Turnover	100 000	200 000	360 000	460 700	404 700	753 800	1305 000	949 358
Profit	2 000	4 000	6 800	15 000	7 800	20 000	25 000	19 800

Table 1. Company A`s economic indicators with short background information

Field	Common practice in the industry	Changed practice in company A	Outcome of the changes
Contract	• Cost for a shed, guards, toilets etc. are included in price.	• If the client has a secure shed close to the building site and allows to store engineering tools there, then the price is excluded. The same goes with toilets etc.	• It is clear to every party that in the end, the client is paying for everything, so the client can customize its construction contract and service.
	• Cost for al the machineries needed is included in price.	• If the client has some sort of machinery that can be used in construction process (lift, tractor, bucket etc.), then the price is excluded.	• It is easier for Company A to organize machinery to the building site. Contract price is reduced.
	• Contract and payment schedule is fixed.	• Contract and payment schedule are beneficial for both parties (a balanced compromise is worked out).	• The contract is customizable for both parties. Contract followes good business ethics and is targeted for win-win solutions.
	• Contract is long, percise and contains juridical text, that is difficult to understand.	• Contract is short and is based on good business ethics. Main principles are agreed, and both contract partners are working to fulfill their responsibilities.	• Partners are equal and are willingly trying to fufill the contract. Often evolving in good cooperation.
Construction	• Usually site managers are not discussing with construction workers or asking for their opinion.	• Site manager is communicating closely with construction workers, to get their feedback on construction design, schedule etc.	• Quite often construction workers give good suggestions on how to raise efficiency and develop construction design. This practical knowledge can be used in coming projects.
	• Construction companies employ workers and have to pay for accomodation, duty assignment and transportation.	• Company A hires local construction workers, close to building site.	• Price for construction works reduces, local workers get some work and can suggest their local friends and companies when needed (cranes, splinters etc.).
Production	• Usually companies give drawings to production and expect exactly what has been drawed	• When giving drawings to production, Company A asks for alternative suggestions for a better price and better manufacturability. Often production company has long discussions with project designer to make compromises where practical	• Practical, cost effective design (also in the future, because project designer has been involved and educated).
Design	• Usually designing departments have no practical experience and have had no practical discussions on manufacturability of their design.	• Company A brings designers together with manufacturers to discuss about optimizing the design and reducing price.	• Price for a client reduces, the system becomes more effective.
	• Usually designers make over dimensioned drawings (because they do not need to calculate so percisely then, and then they feel less responsibility)	• Company A requires their designers to not over dimension designs, where it is not needed.	• This often makes designs ligher and reduces price.
Location	• Companies usually have representative offices. This raises fixed costs and flexibility of company	• Company A has no representatve office. It holds meetings in various cafe`s and rather visits clients at building sites	• Client does not need to pay for office or secretary to make coffe.
	• Usually construction companies hire designers, accountant etc. and makes them to work in the office.	• Company A buys designing, accountance and other services from specialists all over the country. Information is shared by e-mail or phone calls.	• Prices are usually lower than in big cities and people are better in cooperation. This also gives better flexibility compared to employed worers.
Emotions	• Usually contracts and construction works are as emotion free as possible.	• Company A enables its clients to customize its service and include them in construction process.	• This creates emotional link between the client and its new building, that is usually much appreciated. It also helps to raise efficiency within the value system.

Table 2. Common practice within the industry and tactical changes of Company

4.2 Perceptions from within Company A

Company A is customer-centric, trying to understand the context and needs of every client. It is open and honest, telling potential customers that „in the end, you are paying for everything", therefore the client is motivated to choose what he wants to pay for and what not (whether it wants to pay for additional security and storage room or let construction workers keep their machinery in customer`s existing facilities).

4.3 Tactical changes and their impact

Table 2 shows some major tactical changes of Company A and their impact, compared with common practice in the industry.

It appears that Company A is approaching its clients personally and is willing to customize offers that enable saving and economic efficiency. Company A attempts to sense the value system and use its customer`s resources, therefore engaging customers to construction process, if they feel interested. This creates emotional attachment to the new building (usually a life-dream of a man) and helps them to reduce building costs. Company A is keeping its dynamics by employing as little workers as possible, buying services from all over Estonia, to make use of the Internet era and keep the costs low. Company A brings together construction workers, designers, manufacturers and logistic companies to discuss about product manufacturability, assembly, cost etc. issues. Company A is always developing its design and services to raise efficiency and lower costs.

4.4 What Can Be Learned from Company A?

Company A is using successfully a different business model than other construction companies in Estonia.

1. Company A is aiming for system efficiency and cost reduction:
   a. Is trying to view the whole value system
   b. Is enabling its customers to contribute to construction process
   c. Is outsourcing most of the services it needs. This also keeps the company dynamic
   d. Is gathering information from construction workers, designers, production companies etc. for better ideas and development
   e. Is ordering from smaller companies from all over Estonia

2. Company A is flexible in order to achieve win-win-win solutions
   a. Contracts are simple and developed for mutual win, if possible
   b. Company A is listening to suggestions from its construction workers, manufacturers etc.

5. SUBSEQUENT RESEARCH

After analysing and understanding research data from Company A in depth, we did a literature review and case analysis on literature basis. We developed a new value-centric methodology for developing products, services and business-models. Results are presented in articles [6] and [5]. Further research will be done on other existing companies, where developed methodology will be tested.

6. CONCLUSION

Many different interpretations of value co-exist. Sometimes it is the (re)-interpretations of value that reveal new value [5]. Companies, who discover changes and possibilities within the value system first and make use of these are considered to be Prime Movers and often are more successful than the late adapters [2].

We have made the first steps to develop a practical methodology for analysing and developing value-centric products, services and business-models.

7. REFERENCES

[1] Normann, R. *Reframing business: When the Map Changes the Landscape.* Chichester: John Wiley &Sons, Ltd, 2001

[2] Kim, W. C. & Maugborne, R. *The Blue Ocean Strategy*. Harvard Business School Press, 2005.

[3] McMahon, C. *Creativity and innovation: the essence of design?* Perspectives on design creativity and innovation research. Volume 1, Issue 1, 2013.

[4] Matzen, D. *PhD thesis: A systematic approach to service oriented product development.* DTU Management Engineering, 2009.

[5] Randmaa, M; Mougaard, K; Howard, T.J & McAloone, T. *Rethinking value: a value-centric model for product, service and business development.* Proceedings of the International Conference on Engineering Design, 2011.

[6] Randmaa, M.; Howard, T.J. & Otto, T. *From product centred design to value centred design: understanding the value system.* 8th International DAAAM Baltic Conference „INDUSTRIAL ENGINEERING", Tallinn, 2012.

[7] Etgar, M. *Co-production of services*. In The Service-Dominant Logic of Marketing, (Lusch, R; Vargo, S. L. & eds). M.E.Sharpe, New York, 2006, 128-138.

[8] Lusch, R., Vargo, S., & Morgan, F. *Historical perspectives on Service Dominant logic.* In The Service Dominant Logic of Marketing (Lusch, R. and Vargo, S., eds.). M.E. Sharpe, New York, 2006, 29-42.

[9] Allee, V & Schwabe, O. *Value Networks and the True Nature of Collaboration.* Live digital edition (06.03.2012), 2011.

[10] Vargo, S., Maglio, P. & Archpru, M. *On value and value co-creation: service systems and service logic perspective.* European Management Journal (2008) 26, 145– 152.

[11] Editorial board of IJDCI. *Perspectives on design creativity and innovation research. Introduction*. Perspectives on design creativity and innovation research. Volume 1, Issue 1, 2013.

[12] Neergaard, H. & Ulhųi, J. *Handbook of Qualitative Research Methods in Entrepreneurship*, Edward Elgar, 2007.

8. ADDITIONAL DATA ABOUT AUTHORS

1) Randmaa, Merili, PhD candidate & Otto, Tauno, Professor
2) Value-centric business: an in-depth analysis of one case company.
3) MSc. Merili Randmaa
   TUT, Department of Machinery
   Ehitajate tee 5, 19086 Tallinn, Estonia
   Phone: 372+58163924,
   E-mail: merili.randmaa@ttu.ee
   www.ttu.ee
4) Dr. Tauno Otto
   TUT, Department of Machinery
   Ehitajate tee 5, 19086 Tallinn, Estonia
   Phone: 372+58163924,
   E-mail: tauno.otto@ttu.ee
   www.ttu.ee
5) Corresponding Author: Merili Randmaa

9th International DAAAM Baltic Conference
"INDUSTRIAL ENGINEERING"
24-26 April 2014, Tallinn, Estonia

DEVELOPMENT OF THE INTELLIGENT FORECASTING MODEL FOR MANUFACTURING COST ESTIMATION IN POLYJET PROCESS

Rimašauskas, M.; Rimašauskienė, R.; Balevičius, G.

Abstract: *In global manufacturing environment, high product quality, manufacturing flexibility and low production cost are the main keys to competitiveness. Additive layer manufacturing (ALM) technologies have very high level of flexibility and could be used for production of precise parts. In other hand these technologies are still very expensive. This paper presents the model of manufacturing cost estimation according to the part geometrical parameters. The manufacturing cost estimation method is based on Artificial Neural Networks (ANN). ANN is helpful in the situations when conventional linear regression does not work. The obtained results have been considered, discussed and appropriate conclusions have been drawn.*
Key words: additive layer manufacturing, cost forecasting

1. INTRODUCTION

In the rapidly changing manufacturing environment of today, it is crucial to quickly and accurately react to the ever changing demands of the environment. Such customer demands as low product price, high quality or short delivery time have become an inseparable part of manufacturing. On the other hand challenges such as these force engineers and scientists to create new technologies and seek optimal solutions. Recently a great deal of work has been done in the area of additive layer manufacturing [1]. It is necessary to admit that earlier ALM technologies were created with rapid prototyping and custom production in mind however challenges from the environment make these technologies change as well. Currently, the factor of new materials and flexibility is gaining importance. Hence with the constant improvement of technology and especially the increasing emergence of new materials, it becomes a perfect tool not only for prototyping but for serial production too. Moreover ALM technologies in specific areas such as biomedicine could be used [2, 3]. Such trends give rise to expectations that in the future these technologies will become of increasing importance in the field of manufacturing [4]. A contributing factor to such speculations is the constant expansion of open source machine supply and demand. On the other hand adoption of these technologies gives rise to a great deal of technical problems. The accuracy of equipment and produced parts as well as repeatability, recycling of materials, definition of optimal work modes, determining of manufacturing cost, these are the areas that currently require more clarity [5]. Hence the customer is interested not only in the properties of the products, but also delivery periods and product price. These qualities are inseparable from production expenditure and production time evaluation. On the other hand it is worth mentioning that ALM technologies are still fairly expensive, therefore cost forecasting in the early stages of product design becomes very important.

Manufacturing cost forecasting can be conducted using such widely known methods as:

- Parametric cost forecasting;
- Forecasting by applying artificial intelligence;

- Forecasting based on experts' experience;
- Forecasting by means of knowledge-bases;
- Forecasting by means of classifiers [6].

Parametric models work great, when a linear dependence can be established between manufacturing cost and the factors that define them. In the meantime models based on artificial intelligence are great for processing non – linear dependencies and can be used to solve manufacturing cost and quality forecasting problems [6-9]. On the other hand, forecasting by means of applying expert knowledge or experience is also suitable. However, lack of information remains a major flaw. Even though all ALM technologies share the same principle – layer by layer manufacturing, there still exist differences that influence manufacturing cost. Application of the same practical knowledge on different technologies is a very rare occurrence.

The aim of this publication is to collect and analyze information about Poly Jet technology, determine the main factors that have influence on manufacturing cost.

2. DEVELOPMENT OF COST FORECASTING MODEL STRUCTURE

A crucial step to model creation is creation of appropriate structure. It consists of selection of input variables, data collection and processing and neural network structure selection. The established network needs to be trained, its validation and testing must be performed. In this case it is not only crucial to have good knowledge of operation principles of neural networks, but also on the technologies under investigation. The publication analyzes factors of Poly Jet technology that may have influence on manufacturing cost. The technology under investigation is one of the newer industrial ALM technologies; it distinguishes itself with accuracy and good repeatability. Photopolymers with different properties are used as production materials, which allow production of products with varying mechanical and visual qualities. Other technological parameters are provided in previous publications [10, 11].

However, it is necessary to pint out main factors that influence manufacturing cost – production time, material consumptions.

$$T = T_s + T_e + T_m \quad (1)$$

where, T – total production time, T_s – setup time, T_e – post processing time, T_m – machining time, in this case – printing time.

$$M = M_s + M_m \quad (2)$$

where, M – total material consumption, M_s – support material consumption, M_m – model material consumption.

Total material consumption, as in most ALM technologies consists of model material and support material. In the meantime, manufacturing time can be divided into machining time and time meant for supplemental operations. Preparation time is intended to prepare 3D CAD model as well as to prepare the machine for operation. Preparation of 3D model varies according to the qualification of the operator, therefore it is difficult to forecast. However post processing time meant for removal of the finished part from the machine and support material from the surface is also hard to forecast as well. It depends on the experience of the operator as well as the complexity of the part. It is known that highly detailed parts, or parts with deep holes or small construction elements requires longer post processing time. In the meantime, machining time depends on model geometry, positioning, size and machine possibilities. In this case Objet 30 machine with two nozzles – one for model material, other for support material was used for experiments. Thickness of the layer being printed is constant and equal to 28 μm. Printing resolution in x and y axes is 600x600 dpi.

Maximum dimensions of a model are 294x196x150 mm. The printing speed is 8 mm per hour, as declared by vendor. Achievable printed part accuracy is 0.1 mm. However, real printing speed is highly dependent on model, therefore such forecasting method becomes very inaccurate.

In order to fully print out one layer of the part, the nozzles must perform four passes. In four passes a 65 mm wide layer is printed. Therefore the positioning of the part in the work plane is of crucial importance to the production time. A few positioning rules are known that help in lowering the production time:

- First and most important criterion is the height or the part. If possible, the part should positioned in such a way that it‘s size on the z axis is smallest in comparison to x and y axes.
- The longest dimension of the part should be parallel to x axis.
- As mentioned before, printing width is 65 mm therefore; when printing the parts with dimension with respect to y axis is larger it is necessary to perform nozzle displacement with respect to y axis. It is necessary to keep in mind that displacement in y axis direction is relatively slow.

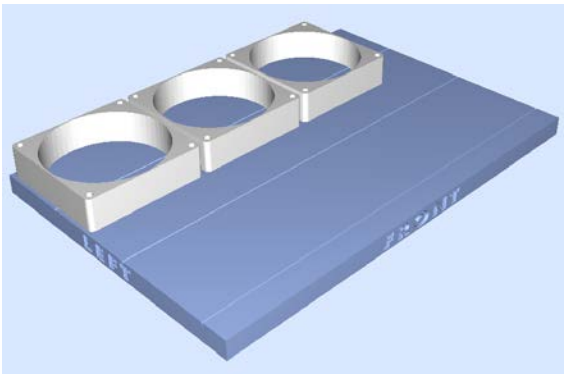

Fig. 1 Automatic placement

In the figure 1 automatic placement of three parts in in work area is displayed. Automatic placement seeks lowest manufacturing cost, i.e. production time must be smallest. However it is worth mentioning that automatic placement cannot be relied on constantly, since when aiming for the lowest production time, material consumptions are sometimes left unevaluated as well as accuracy parameters. Therefore in the first case, the manufacturing time will be 8 hours and 3 min, consumption of model material – 178 g, of support material – 88 g. After performing manual placement, according to figure 2, material consumptions doesn‘t change significantly. However production time turns out to be 10 hours 57 min.

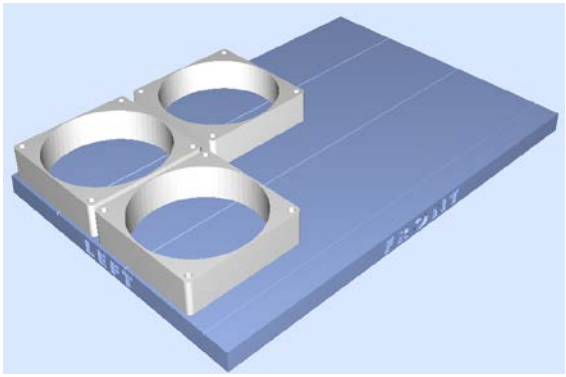

Fig. 2 Manual placement 1

Hence we see that when the dimension of part or parts in relation to y axis increases, the production time becomes longer. In the third case parts are positioned parallel to the z axis (Fig. 3).

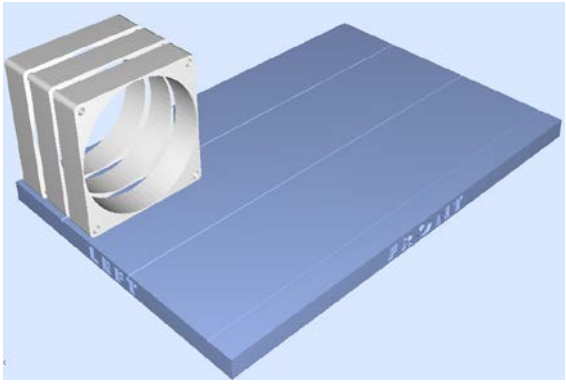

Fig. 3 Manual placement 2

Even though parts used are identical, the production time rises to 25 hours 35 min. However, the most interesting part is that the material consumption increases greatly, consumption of model material – 316 g, support material – 467 g. Increase in support material consumption can be

explained, the material is used to fill vertical cavities. However the consumption of model material can only be explained if specifics of the technology are understood. One way in which the technology differs from other ALM technologies is the mixing of support and model materials. On the other hand, model material is mixed in with intent to improve support material and its mechanical characteristics. Also the amount of material mixed in can be changed by altering parameters of the machine. Hence we see that placement of the part not only influences the duration of the production, but material consumptions as well. On the other hand part placement is very important due to before mentioned qualities in other ALM technologies as well. Separate technologies have intellectual models or decision support systems created specifically for them in order to optimize this process [12, 13].

3. EXPERIMENTAL TESTING OF MODEL STRUCTURE

Proper selection of input data is crucial for creation of a well-functioning model. It was determined in the previous chapter, that dimensions and placement of the parts are some of most crucial factors in forecasting of manufacturing cost. Hence, 100 parts of different geometries and sizes were chosen for experimental tests. All parts were produced and the dependence of production time on their dimensions was analyzed.

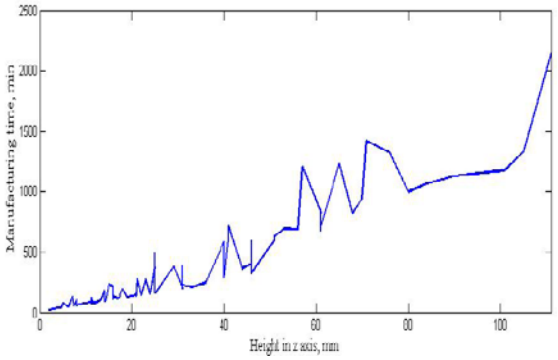

Fig. 4 Dependence between part height in z axis and manufacturing time

It is worth mentioning that the shortest production time was 26 minutes, while the longest was 35 hours and 45 minutes. Results on how manufacturing time changes according to part height with respect to z axis are provided in figure 4. This however completely disregards the width of the part with respect to y axis, as mentioned before that is a crucial factor.

A clear trend is visible in the provided figure, as the height of the part increases, so does the production time. However overall dependence cannot be considered in this case. Parts with width greater than 63 mm were excluded in the next step. This was meant to eliminate the influence the part width to the production time. As mentioned before, during one pass a 65 mm wide layer is printed.

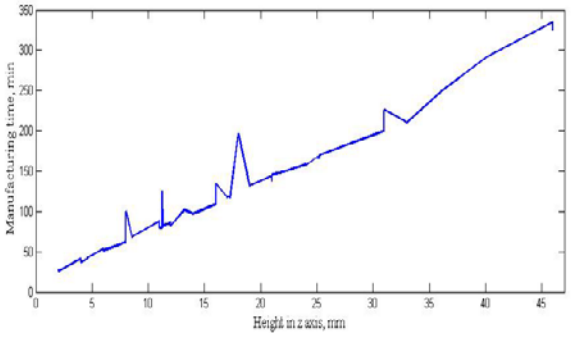

Fig. 5 Dependence between part height in z axis and manufacturing time (parts width less than 63 mm)

In figure 5, results for the performed analysis can be seen. Here it is also worth mentioning, that after discarding parts whose width is over 63 mm the analysis is performed on data from 55 parts. As it can be seen from the graph, the dependence between part height and production time is practically linear when parts with width exceeding 63 mm are excluded. On the other hand it can be seen that there are 5 parts whose manufacturing time greatly exceeds the allowed limits. However such results may be due to length of the part with respect to x axis or other geometrical parameters. Considering previous experiences it can be stated that in this case length in x axis direction has negligible or no influence on the production time. This

is perfectly illustrated by the further test. In figure 6 are two identical parts placed along x axis.

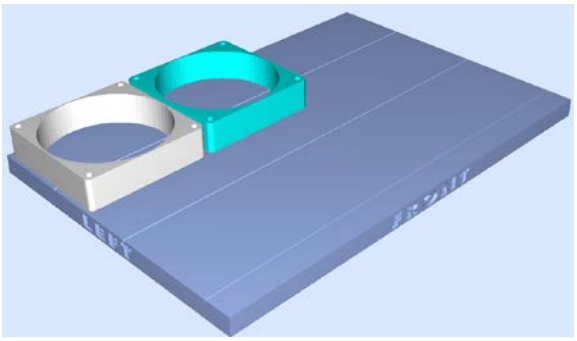

Fig. 6 Positioning of the parts along x axis

Manufacturing time for both parts is 7 hours 28 minutes, however with one part removed, production time decreases to 6 hours 50 minutes. Such difference shows that part length along x axis has negligible influence to production efficiency. On the other hand this also stands to show that material consumption is not a proper factor to production time. In this case material consumption decreases by exactly two times, however the production time decreases only by 30 minutes.

Theoretically, a neural network with one hidden layer containing sufficient neurons of that layer can approximate any continuous function. In practice, neural networks with one or two hidden layers are most frequently used [14]. This information is used when making the structure of a neural network. A network input layer is created of the following part parameters: height – part dimension in direction of z axis, width – part dimension in direction of y axis, length – part dimension in direction of x axis, material consumptions. Thus, during testing neural network with one hidden layer will be used. Transfer function will be determined experimentally. The one neuron transfer function may be expressed as follows:

$$y = f\left[\sum_{i=1}^{n} w_i \cdot x_i + b\right] \qquad (3)$$

here $x_1 - x_n$ – neuron input values, $w_1 - w_n$ – weight values, b – displacement. Mathematical model of a two layer neural network may be expressed as follows:

$$Y = f_2\left[W_2\, f_1(W_1 X)\right], \text{ or} \qquad (5)$$

$$Y = f_2\left[\sum_{i=1}^{n} w_i\, f_1\left(\sum_{j=1}^{g} w_j x_j\right)\right] \qquad (6)$$

here X – matrix of input values, W_1 – matrix of the first layer weight values, W_2 – matrix of the second layer weight values, Y – matrix of output values, w_i – weights of the second layer neurons, w_j – weights of the first layer neurons, x_j – input values, f_1 – hyperbolic tangent function, f_2 – linear transfer function.

4. FURTHER RESEARCH

Verification of the established neural network structure will be conducted in further research. Currently it is being attempted to collect a sufficient amount of verified data, to be analyzed and used to establish the intelligent model. In further steps of the investigation, application of model to forecast manufacturing cost for other machines is planned.

5. CONCLUSIONS

Performed research enables to make following conclusions:

1. During the investigation, most important factors influencing manufacturing cost were determined – dimensions of the part and placement in the work area.
2. It has been determined that height of the part in z axis direction is a critical factor to production time. While influence of part width in y axis direction, increases dramatically when part width exceeds 63 mm.
3. A neural network structure that has to be experimentally verified and applied

for practical use was proposed.

6. REFERENCES

1. Wesley, M., Cunico, M. Development of new rapid prototyping process. *Rapid Prototyping J*., 2011, **17**, 138-147.
2. Kouhi, E., Masood, S., Morsi Y. Design and fabrication of reconstructive mandibular models using fused deposition modeling. *Assembly Automation*, 2008, **28**, 246-254.
3. Tek, P., et al. Rapid prototyping for neuroscience and neural engineering. *J. of Neuroscience Methods.,* 2008, **172**, 263-269.
4. Chryssolouris, G., et al. Digital manufacturing: history, perspectives, and outlook. *Proc. of the Institution of Mech. E. Part B, J. of Engineering Manufacture*, 2009, **223**, 451-462.
5. Brajlih, T., Valentan, B., Balic, J., Drstvensek, I. Speed and accuracy evaluation of additive manufacturing machines. Rapid Prototyping J., 2011, **17**, 64-75.
6. Shehab, E. M., Abdalla, H. S. Manufacturing cost modelling for concurrent product development. *Robotics and Computer Integrated Manuf*, 2002, **17**, 341-353.
7. Wang, Q., Stockton, D. Cost model development using artificial neural networks. *Aircraft engineering and aerospace technology*, 2001, **73**, 536-541.
8. Chung, W. W. C., Wong, K.C.M., Soon, P.T.K. An Ann – based DSS system for quality assurance in production network. *Journal of Manufacturing Technology Management*, 2007, **18**, 836-857.
9. Meziane, F., Vadera, S., Kobbacy, K., Proudlove, N. Intelligent systems in manufacturing: current developments and future prospects. *Integrated Manufacturing Systems*, 2000, **11,** 218-238.
10. Bargelis A., et al. Virtual and distance labs for vocational education training of industrial employees. *Mechanika, Proc. of the 18th Int. Conf.*, 2013, 21-26.
11. Rimašauskas, M., Balevičius, G. The influence of water absorption to the properties of the photopolymer used in PolyJet process. *Mechanika, Proc. of the 18th Int. Conf.*, 2013, 212-217.
12. Phatak, A. M., Pande, S. S. Optimum part orientation in rapid prototyping using genetic algorithm. *J. of Manufacturing Systems*, 2012, **31**, 395-402.
13. Rimašauskas, M., Rimašauskienė, R. Development of decision support system for fused deposition modelling manufacturing cost estimation. *Mechanika*, 2012, **5**, 600-604.
14. Rimašauskas, M., Bargelis, A. The development of the intelligent forecasting model for productivity index in manufacturing. *Mechanika*, 2012, **3**, 354-359.

7. ADDITIONAL DATA ABOUT AUTHORS

Rimašauskas Marius, Dr. Assoc. Prof.
Kaunas University of Technology
Kęstučio 27, LT – 44312 Kaunas, Lithuania
Phone: +370 614 99258
E-mail: marius.rimasauskas@ktu.lt

Rūta Rimašauskienė, Dr. Lecturer.
Kaunas University of Technology
Kęstučio 27, LT – 44312 Kaunas, Lithuania
E-mail: ruta.rimasauskiene@ktu.lt

Gytautas Balevičius
Kaunas University of Technology
Kęstučio 27, LT – 44312 Kaunas, Lithuania
E-mail:gytautasbalevicius@gmail.com

9th International DAAAM Baltic Conference
"INDUSTRIAL ENGINEERING"
24-26 April 2014, Tallinn, Estonia

QUALITY IMPROVEMENT METHODOLOGIES FOR CONTINUOUS IMPROVEMENT OF PRODUCTION PROCESSES AND PRODUCT QUALITY AND THEIR EVOLUTION

Sahno, J. & Shevtshenko, E.

Abstract: *In order to be competitive companies try continuously improve their production processes, product quality and increase the level of customer satisfaction by implementing different quality improvement programs, methodologies and approaches. Nowadays there are different worldwide used methodologies like PDAC, 8D, Six Sigma DMAIC, 4Q which enables the companies to select and combine them for continuous improvement. In this paper will be introduced the general idea of using these methodologies, it will be followed by discussion where will be made the comparative analysis that will clarify their advantages and disadvantages and shows in what case the appropriate methodology could be selected.*

Key words: PDCA, 8D, DMAIC, 4Q

1. INTRODUCTION

Today customer satisfaction is the feeling of pleasure that occurs when a company meets a customer's expectations. Gaining high levels of customer satisfaction is very important to a business because satisfied customers are most likely to be loyal and to make repeat orders and to use a wide range of services [1, 2]. A company that succeeds on meeting and exceeding customers' expectations is guaranteed to have great Return On Investment (ROI) [3, 4]. Today the reliable and stable production processes influence on a lot of KPI that are very important for business success. In addition, metrics can provide managers with information about problematic points and show the real status of enterprise at certain time [5]. For instance the more reliable and stable production processes is the less scrap occurs, and less rework is needed, which consumes additional recourses, time and money [6]. Therefore, in order to be competitive and successful on the market place and satisfy customer, companies should continuously improve their production processes and product quality by implementing different quality improvement programs and methodologies [7]. A quality improvement effort will lead to a higher product and service quality that will lead to improved customer satisfaction [8]. In this paper will be reviewed and discussed four different quality and process improvement methodologies which are intended to solve customer complaints and problems in virtual organisation network [9, 10]. Presented findings are intended to be used as information for management decisions about what quality improvement methodology should be selected for continuous improvement in Partner Network enterprises. Figure 1 shows related research papers but in this paper will be presented the third part.

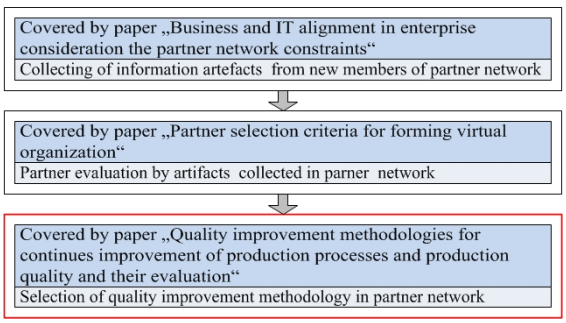

Fig. 1. Related research papers

2. LITERATURE REVIEW

2.1. Plan Do Check Act (PDCA)

In 1939 Walter Shewhart displayed the first version of the scientific method with his cycle "Shewhart Cycle": Specification, Production, Inspection [11]. In 1950, Deming modified the Shewhart cycle at a Japanese Union of Scientists and Engineers (JUSE). His straight line: Design, Produce, Sell was converted to a circle with a forth added step - Redesign through marketing research [12]. In 1950 at JUSE seminar Imai recast the Deming wheel into the Plan, Do, Check, Act (PDCA) cycle and presented the correlation between the Deming wheel and the PDCA cycle shown in Table 1 [13].

Design - Plan	Product design corresponds to the planning phase (definition of a problem and a hypothesis about possible causes and solutions)
Production - Do	Production corresponds to doing-making, or working on the product that was designed (implementing)
Sales - Check	Sales figures confirm whether the customer is satisfied (evaluating the results)
Research - Action	In case of a complaint being filed, it has to be incorporated into the planning phase and action taken for the next round of efforts (back to plan if the results are unsatisfactory)

Table 1. Correlation between the Deming wheel and the Japanese PDCA cycle [13]

PDCA cycle is targeted on the prevention of error repetition by creation standards and the ongoing modification of current standards. Using of the PDCA cycle means continuously improving process/product. It is effective in both doing a job and managing a programme. The PDCA cycle enables two types of corrective action – temporary and permanent. The temporary is aimed at results by practically tackling and fixing the problem. The permanent consists of investigation and eliminating the root causes and thus targets the sustainability of the improved process [14]. In Figure 2 shown the PDCA cycle in detail [15]. In the "*Do*" stage it is possible to involve a *mini-PDCA cycle* until the issues of implementation are resolved [16].

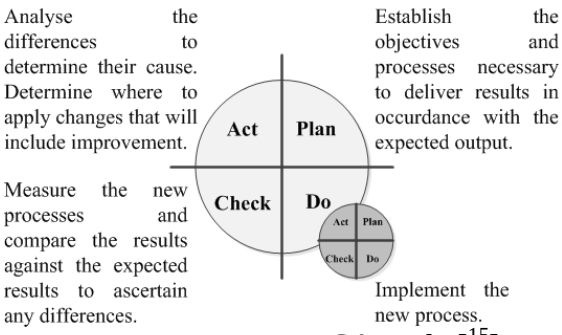

Fig. 2. Deming's PDCA cycle [15]

2.2. 8Disciplines (8D)

The 8D process was standardized during the Second World War by U.S. government, referring to it as Military Standard 1520: "Corrective action and disposition system for nonconforming material". It was later applied by the Ford Motor Company in the 1960's and 1970's. 8D has become a standard in the auto and other industries that require a structured problem solving process, which is used to identify, correct and eliminate problems. The methodology is useful in product and process improvement. It focuses on the origin of the problem by determining root cause. [17]. Further presented the detail description of every step of 8D process.

- **D0:** Planning phase: Plan for solving the problem and determine the prerequisites.
- **D1:** Use a team: Establish a team of people with product/process knowledge.
- **D2:** Define and describe the problem: Specify the problem by identifying in terms who, what, where, when, why, how and how many (5W2H).
- **D3:** Developing interim containment plan: Define and implement containment actions to catch and isolate the problem from any customer.
- **D4:** Determine, identify and verify root causes and escape points: Identify all potential causes that could explain why the problem occurred and why the problem has not been noticed at the time.
- **D5:** Choose and verify Permanent Corrective Actions (PCAs) for root cause:

Confirm that the selected corrective actions will resolve the problem for the customer.

- **D6:** Implement and validate PCAs: Define and implement the best corrective actions. Permanent corrective action.
- **D7:** Prevent recurrence: Modify the management and operation systems, practices and procedures to prevent recurrence of this and similar problems.
- **D8:** Congratulate your team: Recognize the collective efforts of the team and thank them formally.

One of the problems in the implementation of the 8D methodology is using it as a one-page problem-reporting effort. It requires the report to be written within 24 hours, but some steps can take a few hours, while others can take weeks [18].

2.3. Six Sigma DMAIC

Dating back to the mid of 1980s, applications of the Six Sigma methods enabled many organizations to sustain their competitiveness by integrating their knowledge of the process with statistics, engineering and project management [19]. Motorola was the first company who launched a Six Sigma project in the mid-1980s [20]. Initially Six Sigma was applied in manufacturing [21] but today it is accepted in healthcare [22], finance [23] and service [24]. Six Sigma is a project-driven management approach intended to improve products, services and processes by reducing defects [25]. It is a business strategy that focuses on improving customer requirements, business systems, productivity and financial performance. Utilizing analytical tools to measure quality and eliminate variances in processes allows to producing near perfect products and services that will satisfy customers [26]. Below is present Six Sigma's DMAIC description.

- **Define** step is where a problem is identified and quantified in terms of the perceived result. The product and/or process to be improved are identified, resources for the improvement project are put in place and expectations for the improvement project are set.
- **Measure** step enables to understand the present condition of its work process before it attempts to identify where they can be improved. The critical to-quality characteristics are defined and the defects in the process/product developed through graphical analysis. All potential effects on failure modes are identified.
- **Analyse** step adds statistical strength to problem analysis, identifies a problem´s root cause and determines how much of the total variation is.
- **Improve** step aims to develop, select and implement the best solutions with controlled risks. The effect of the solutions that are then measured with the KPI developed during the Measure step.
- **Control** step is intended to design and implement a change based on the results made the Improve step. This step involves monitoring the process to ensure it works according to the implemented changes, capture the estimated improvements and sustain performance [26].

2.4. 4 Quadrants (4Q)

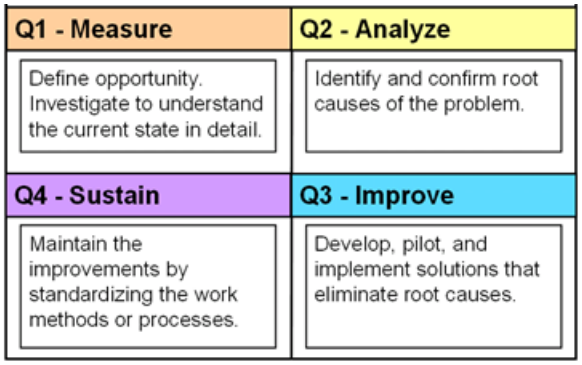

Fig. 3. 4Q process [27]

4Q is data driven problem solving process for continuous improvement also called 4Q improvement methodology that was developed and applied in ABB company in 2009 to stop "religious" fights between Lean, Six Sigma DMAIC, PDCA, 8D and other promoters arguing superiority of one approach against the other. 4Q stands for the 4 quadrants: Measure, Analyse,

Improve and Sustain. The 4Q process is a problem solving method similar to Six Sigma DMAIC. In 4Q the Define step is a part of Q1 Measure and also part of the trigger that starts a 4Q project [27]. Figure 3 shows 4Q process and Table 2 presents the basic description of 4Q steps.

Pre 4Q	Q1 Measure	Q2 Analyse	Q3 Improve	Q4 Sustain
• Develop draft problem statement • Take immediate action • Identify initial project scope • Create business case • Determine objectives • Create project charter • Create and enter project white sheet into SMT • Project sponsor approval to proceed	• Form the project team • SIPOC process map • Capture VOC & translate to CTQ • Stakeholder map • Communication & project plan • Develop 'As-Is' process map • Validate measurement system • Develop data collection plan • Collect data • Calculate baseline process performance • Revisit problem statement • Project sponsor approval to proceed	• Analyse variation • Analyse waste • Team brainstorm to identify root causes • Document root causes on Cause & Effect diagram • Select top 3-5 root causes • Validate selected root causes as actual root causes • Project sponsor approval to proceed	• Team creative brainstorm solutions • Select optimum solutions • Conduct pilot study (or Risk Analysis) • Verify & validate improvements • Develop 'To-Be' process map • Review stakeholder map & common plan • Implementation business case (cost & benefits) & solution plan • Project sponsor, process owner and budget holder approval to proceed • Implement actions on solution plan	• Select control techniques (SPC) • Standardize via documentation • Develop control metrics (KPI's) • Disengage old process • Monitor progress • Validate improvements in process performance • Share lessons learnt (organization memory, newsletters etc) • Thank the team • Celebrate success • Plan future activities • Close project

Table 2. 4Q process basic description [28, 29]

3. DISCUSSION

There are not so many differences between above observed methodologies as they follow a scientific and methodical way to solve the problems. Table 3 shows methodologies evolution (from left to right), correlation and summary.

- PDCA cycle is the classic problem solving approach used in a Lean environment and mostly in automobile industry. It is a fundamental concept of continuous improvement processes embedded in the organization's culture. The most important aspect of PDCA lies in the *"act"* stage after the completion of a project when the cycle starts again for the further improvement. PDCA is used for medium sized problems [14].
- 8D is an effective approach at finding a root cause, developing proper actions to eliminate root causes and implement the corrective actions. The goal of 8D focused on fast reaction to customer complaints. Typically the first three steps should be accomplished and reported to the customer in three days.
- Six Sigma DMAIC is systematic and fact based approach that provides a rigorous framework for project management, also used to create a *"gated process"* for project control. Six Sigma DMAIC is mostly applied to solve big problems where a lot of data available and where statistical tools should be applied. The DMAIC project may last more than three month, it depends on how complex the problem and process to be improved.
- 4Q process is a problem solving method that is similar to the above mentioned methodologies that is intended for continuous improvement of processes. It

was developed by ABB company to help to solve 90% of all issues [30].

Steps	PDCA	8D	Six Sigma DMAIC	4Q
	Plan	D0: Plan	Define	Pre 4Q
		D1: Identify team		
		D2: Define problem		
		D3: Contain symptom	Measure	Measure
		D4: Identify root causes	Analyse	Analyse
	Do	D5: Choose corrective action	Improve	Improve
		D6: Implement corrective action		
	Check	D7: Make change permanent	Control	Sustain
	Act	D8: Recognise the team		
Comparison of methodologies for continues improvement application				
Year	1939	1940´s	1980	2009
Industry	Automobile	Automotive	Manufacturing of all type, healthcare, finance, service	Automotive, electrical,
Project / problem size	Medium sized, till 3 months	Small, some weeks	Big, till 12 months and even more	Small and medium, 1 week till 2 months
Used / Applied	For continuous improvement of small problems	For automotive industry and focused on fast reaction to customer complaints	For large problems where huge amount of data and statistics used	For continuous improvement of various problem (allowed to solve 90% of all issues in ABB company)

Table 3. The evolution, correlation and summary of presented methodologies

4. CONSCLUSION

In this paper were observed different continuous improvement methodologies, their capabilities, similarity and application to different situations. Every company can select and use a proper methodology and even combine some of them in continuous improvement of their processes. It is very important that the right methodology is correctly selected according to the needs and demands of the company and further applied to the appropriate process.

5. ACKNOWLEDGEMENTS

Hereby we would like to thank the Estonian Ministry of Education and Research for Grant ETF9460 which supports the research.

6. REFERENCES

1. Anderson, E. W. and Mary W. S. *The antecedents and consequences of customer satisfaction for firms.* Marketing science, 1993, 125-143.

2. Karaulova, T., Kramarenko, S. and Shevtshenko, E. *Risk Factors in Project Management Life Cycle.* 6th International Conference of DAAAM Baltic Industrial Engineering, Tallinn, Estonia, 24-26, 2008.

3. Jones, T. O. and Sasser, W. E. *Why satisfied customers defect.* Harvard business review, 1995, 88.

4. Karaulova, T. and Shevtshenko, E. *Reorganisation of Production System on SME Enterprises.* Annals of DAAAM & Proceedings, 2009.

5. Kaganski, T., Snatkin, A., Paavel, M. and Karjust, K. *Selecting the right KPIs for SMEs production with the support of PMS and PLM.* International Journal of Research in Social Sciences, 2013, 69 - 76.

6. Karaulova, T., Kostina, M. and Sahno, J. *Framework of reliability estimation for manufacturing processes.* Mechanika 2012, 18.6.

7. Kangilaski, T. *Challenges for SMEs entering into the virtual organization*

partner network. Proceedings of the 7th International Conference of DAAAM Baltic Industrial Engineering, 2010.
8. Torbica, Z. M. and Robert C. S. *Customer satisfaction in home building.* Journal of Construction Engineering and Management, 2001, 82-86.
9. Polyantchikov, I. and Shevtshenko, E. *Collaborative framework for Virtual organization.* Proceedings of 7th International DAAAM Baltic Conference" Industrial Engineering", Tallinn, 2010.
10. Kangilaski, T. *Interoperability issues in virtual organization - how to proceed?* Emerging Technologies and Factory Automation, ETFA, IEEE Conference, 2007, 1293-1299.
11. Walter, A. S. *Statistical Method from the Viewpoint of Quality Control.* 1939.
12. Deming, W. E. *Elementary Principles of the Statistical Control of Quality.* JUSE, 1950.
13. Masaaki, I. *Kaizen: The key to Japan's competitive success.* New York, itd, McGraw-Hill, 1986.
14. Sokovic, M., Pavletic, D. and Pipan, K. K. *Quality improvement methodologies – PDCA cycle, RADAR matrix, DMAIC and DFSS.* Journal of Achievements in Materials and Manufacturing Engineering 43.1, 2010, 476-483.
15. Seaver, M. *Gower handbook of quality management.* Gower Publishing, Ltd., 2003.
16. Kondo, Y. *Companywide Quality Control: Its Background and Development. – 3A Corporation*, 1995.
17. http://www.phredsolutions.com/whatis8d.html (03.2014).
18. Rambaud, L. *8D structured problem solving: A guide to creating high quality 8D reports.* PHRED Solutions, 2006.
19. Kwak, Y. H. and Anbari. F. T. *Benefits, obstacles, and future of six sigma approach.* Technovation 26.5, 2006, 708-715.
20. Rancour, T. and McCracken, M. *Applying six sigma methods for breakthrough safety performance.* American Society of Safety Engineers, 2000.
21. Nonthaleerak, P. and Hendry. L. *Exploring the Six Sigma phenomenon using multiple case study evidence*. International Journal of Operations & Production Management 28.3, 2008, 279-303.
22. Koning, H., Verver, J. P., Heuvel, J., Bisgaard, S., and Does, R. J. *Lean six sigma in healthcare.* Journal for Healthcare Quality, 28(2), 2006, 4-11.
23. De Koning, H., Does, R J. and Bisgaard, S. *Lean Six Sigma in financial services.* International Journal of Six Sigma and Competitive Advantage 4.1, 2008, 1-17.
24. George, M. L. and George, M. *Lean six sigma for service.* New York: McGraw-Hill, 2003.
25. United States Patent, Patent Number: 5731572; Date of Patent: 24.03.1998.
26. Gregory, H. W. *Six Sigma for Business Leaders.* 1st edn. Business Systems Solutions. Inc., USA, 2004.
27. ABB Switzerland Ltd, LC Business Processes & Personal Development, www.abb.ch/abbuniversity (03.2014)
28. http://www02.abb.com/global/usabb/usabb046.nsf/0/26eade41a99458918525780100545129/$file/opx+concepts+-+4q+&+problem+solving.pdf (03.2014).
29. http://66.147.244.90/~stratey0/portfolio-view/framework-of-the-week-62-4q-methodology-measure-analyze-improve-control/ (03.2014).
30. http://www.kaizen-factory.com/2013/09/11/pdca-a3-dmaic-8dpsp-what-are-the-differences/ (03.2014).

7. DATA ABOUT AUTHORS

Department of Machinery TUT,
Jevgeni Sahno
E-mail: jevgeni.sahno@gmail.com
Eduard Shevtshenko
E-mail: eduard.sevtsenko@ttu.com

9th International DAAAM Baltic Conference
"INDUSTRIAL ENGINEERING"
24-26 April 2014, Tallinn, Estonia

ENERGY EFFICIENCY MONITORING SYSTEM FOR TECHNOLOGY MAPPING DRIVEN BY FoF CONCEPT

Sarkans, M.; Pikner, H.; Sell, R.; Sonk, K.

Abstract: *To stay competitive in the global market the enterprises must find possibilities to make production more efficient. Taking into consideration the production process what is energy consuming it is also essential to look at the energy consumption in enterprise. European Union has started an initiative FoF (Factories of The Future), where main purpose is to increase the competitiveness of the SME-s through more efficient use of the resources. One of the goals of this initiative is the energy saving in production and in factories in general. In this study under the investigation is production facility where mini-loaders and their tools are produced. The modular energy monitoring system platform is designed and tested in real production environment to prove its suitability.*
Key words: monitoring, prototype, energy consumption, welding technology

1. INTRODUCTION

To stay competitive in the global market the enterprises must find possibilities to make their production more efficient. Taking into consideration the production process that is mainly high energy consuming it is also essential to look at the energy consumption in enterprise. In European Union it is started an initiative FoF (Factories of The Future), which main purpose is to increase the competitiveness of the SME-s through more efficient use of the resources [1]. One of the goals of this initiative is the energy saving in production and in factories in general.
Several studies are made in different detail levels considering energy usage in factories and in production. Considering energy management and factory planning [2], an online monitoring approach for energy efficiency monitoring [3] and a comprehensive analysis of energy consumption of production process [4] gives a brief presentation of the issues of the energy monitoring challenges.

2. PROBLEM STATEMENT

In this study under the investigation is production facility where mini-loaders and their tools are produced. As there are many production processes in the factory in first step the welding process is studied because it is somewhat less investigated than others considering energy efficiency.
Therefore device for monitoring of welding equipment is needed for charting of the welding technology in the partner company. The solution should enable to gather welding data during the implementation of different products and to evaluate the efficiency of the current welding technology. The analysis of the gathered data enables to make improvement propositions of the welding process to the partner company.
In the long term if the solution is implemented to all welding devices in the company, it enables to gather workplace based and enterprise wide data about the welding process. This kind of solution should decrease the workload of the welding specialist, who is otherwise must gather this data manually. Based on the previous experiences the charting time can be from several hours to several weeks, depending of the product. Using the monitoring device only the gathered data

must be analysed based on suitable algorithm and the results can be presented to the enterprise.
During the welding process there are several parameters what must be supervised during the charting of the welding process and also during the welding process. Parameters that must be monitored are: welding voltage, welding current, arc time.

3. SYSTEM OVERVIEW

The energy monitorin[illegible] to be a modular and open for different kinds of factory setups. The system is a combination of different hardware and software modules.
The communication between system nodes is combination of wired and wireless data exchange. Short distance communication between measurement node and subserver is wireless and long distance communication between servers and end user is wired, primarily over the Ethernet.
End user has web based user interface that enables to access to collected data, video stream and history. Administrator user has additional features like: system parameter modification, adding new nodes and workplaces, exporting data, etc. Fig. 1 presents a system overview.
In the Fig. 1 four different levels can be distinguished. Starting from down to up, these are:

- Sensor level (marked as S1 to S4)
- Wmonitor level
- Subserver level
- Server level

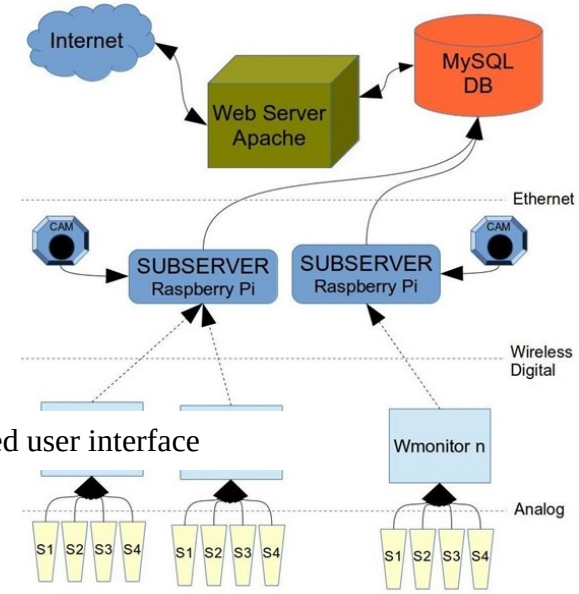

Fig. 1. Energy efficiency wireless measurement system architecture

Sensors are connected directly to the Wmonitor module and provide real-time current measurement over the analogue channel. Wmonitor passes collected data to the subserver over the air by using XRF radio modules. This enables to spread system easily in the factory floor without requiring additional wires installation. Subservers are usually used one per factory room and they communicate with the database over the conventional Ethernet connection. This can be either wired or wireless, depending on the system setup. The overview and snapshots of the workplace are taken by the cameras connected to the subserver and images are stored into database or main server file system. The main server provides web interface for end user and enables to

Fig. 2. Web based user interface

visualize data. It also combines the video stream into user interface and enables administrator to manage system parameters and perform data analysis.
The software concept is following the framework of early design and simulation toolkit developed by Sell and Petritsenko [5], in conjunction with dimensionless analysis developed by Coatanéa [6]. This framework provides tools and methodology to efficiently develop system concepts in early design stage. The framework is successfully applied for mobile robot development [7,8,9] as a mechatronic system, but is now expanded to the distributed mechatronic system like energy efficiency monitoring system, presented in this paper.
The software implementation has a three level architecture where the lowest level is controller software and the highest level is web interface and database connection. In the Fig. 2 an end user interface is presented.

3.1 Wireless network

The monitoring system is designed primarily for the use in the existing plants and factories and therefore installation of additional cables can be problematic. As the sensors must be connected directly to the energy consumer mains wire, the location of the Wmonitor module and sensors cannot be chosen very flexibly.
Based on this limitation the data between Wmonitor and subserver is transferred over the radio link. During the development, different wireless solutions like XBee, Bluetooth and XRF were tested. XRF was selected according to its better propagation characteristics in the industrial environment. Wireless connection between the subserver and all the Wmonitor modules share the same channel. All transferred packets are visible to all modules in the same channel. Package sorting is done by software, where one subserver can handle over 20 Wmonitor modules. If two or more subservers are near to each other they must be set on different channels to avoid data collisions. Fig. 3 describes the wireless communication hardware setup.

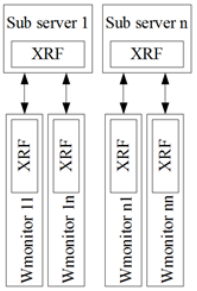

Fig. 3. Wireless network between Wmonitor modules and subservers

LLAP protocol (Lightweight Local Automation Protocol) is used to communicate between the XRF module and subserver. The protocol is human readable and composed of ASCII characters. The message is 12 characters long in 3 distinct sections [10]. Packet format is aXXDDDDDDDDD where:
1. "a" is lower case and shows the start of the message
2. XX is the device identifier (address A-Z & A-Z)
3. DDDDDDDDDD is the data being exchanged.
Example of data package: aDB15100-----

3.2 Software solution

The main server is connected to the Internet, and therefore can be located anywhere in the world. The server is connected to the MySQL database that holds all sensor readings as well as system setup and other relevant data. Sensor data entry is written by subservers that get the real-time data from sensors through the Wmonitor modules. The configuration information is needed to store the system configuration like: number of modules, types of sensors, as well as workplace information and equipment specifics. A web based user interface interacts with the database where the configuration interface enables administrator to modify all the

system settings. The main server's internal structure is shown in Fig. 4.

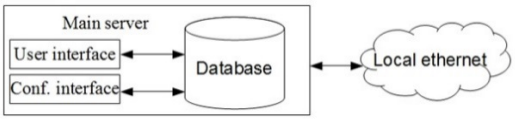

Fig. 4. Main server subsystem software

The subserver is mediating the sensor data from Wmonitor modules to the database. Number of channels, names and other parameters are obtained from the database. It also has an USB co
camera to include the real time video or
snapshot images in addition to sensor readings. The internal structure of the sub-server is shown in Fig. 5.

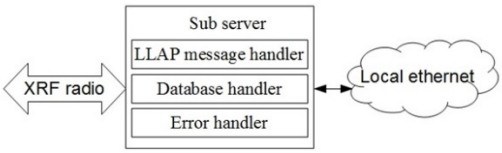

Fig. 5. Subserver internal structure and software

Wmonitor software interprets received LLAP protocol messages. In response it sends the reading of the desired channel. The internal structure of the Wmonitor module is shown in Fig. 6.

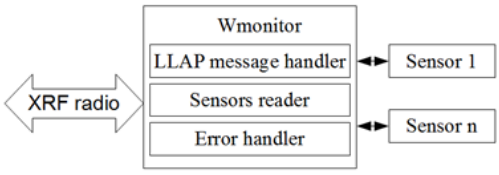

Fig. 6. Wmonitor module internal structure and software

4. ENERGY EFFICIENCY EVALUATION OF PRODUCTION

To give an overview of the factory energy consumption the overall energy profile is presented on Fig. 7 that is obtained from the web service of the Energy Company. It represents the usual energy consumption of the production facility where mini-loaders are produced. The work in the company is organised in two shifts. First shift starts at 30, where the most energy-consuming (incl. welding, mechanical treatment, plasma cutting) production activities are done. Second shift starts at 14:00 and ends 22:30, where the less energy-consuming (assembly, painting) activities are done.

Fig. 7. Factory energy consumption profile

As the graph shows, the energy consumption during night time is at level 25 kWh, what is used mainly for background processes (incl. heating, ventilation, security, appliances idle power). To give an overview of the production equipment the main consumers and their weight from overall energy consumption are given in Table 1. The energy consumption is given as an average, as the production takes place in cycles. Additionally are shown the appliances that are needed for service of the machinery like air compressors and the lighting of the working area.

The total energy consumption is higher than the peaks in the Fig. 7 but the cyclic work of the machines (welding, CNC machines) must be taken into account.

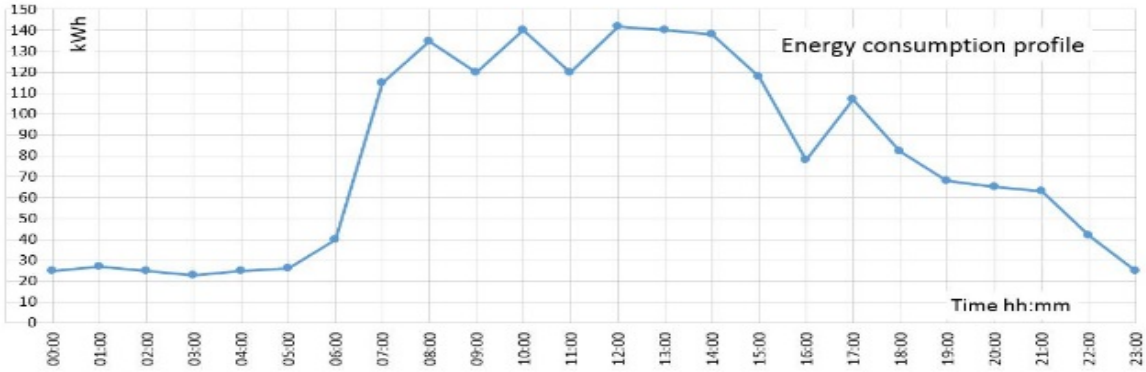

	Description	Consump-tion (kWh)	Remarks
1	Background processes	25	Heating, ventilation
2	Welding equipment	20	10 pcs, avg 2 kWh
3	Welding robot cell	5	1 pc, avg 5 kWh
4	Plasma cutting	9	1 pc, avg 9 kWh
5	Drilling	4	4 pcs, avg 1 kWh
6	CNC lathes and mills	12	4 pcs, avg 3 kWh
7	Bending	3	1 pc, avg 3 kWh
8	Sawing	4	2 pcs, avg 2 kWh
9	Air compressors	50	2 pcs, avg 25 kWh
10	Lighting	20	40 pcs, avg 0,5 kWh
11	Others	10	Other equipment
	Overall	**162**	

Table 1. Factory energy balance

4.1 Case product ”Sammet damper”

The energy profile of the product “Sammet damper” during the assembly and welding is given in Fig. 8. This product needs to be assembled, tack welded and arc welded. The tack welding action is represented in Fig. 8 by readings between 14:25 to 14:30 with values up to 2 A. After the assembly and tacking the arc welding is done shown in Fig. 8 by readings at starting times 14:38, 14:42 and 15:15. The top values during the welding are at 10 A.

4.2 Case product “mini-loader base”

The energy profile of the product “a60 mini-loader base” during the assembly and welding is given in Fig. 9. This product must be assembled, tack welded and arc welded. The time between 7:37 to 7:48 and between 8:19 to 9:33 shows the arc welding

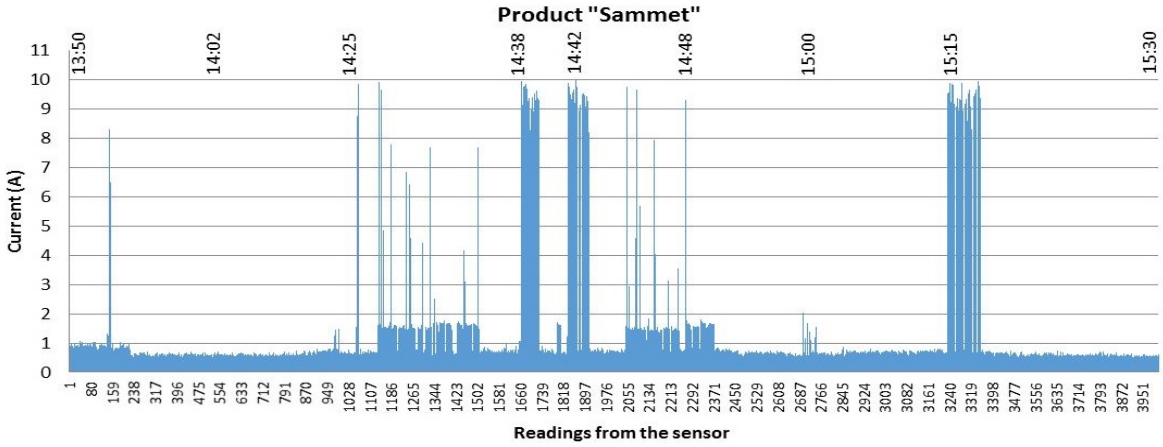

Fig. 8. Welding energy profile of product „Sammet damper“

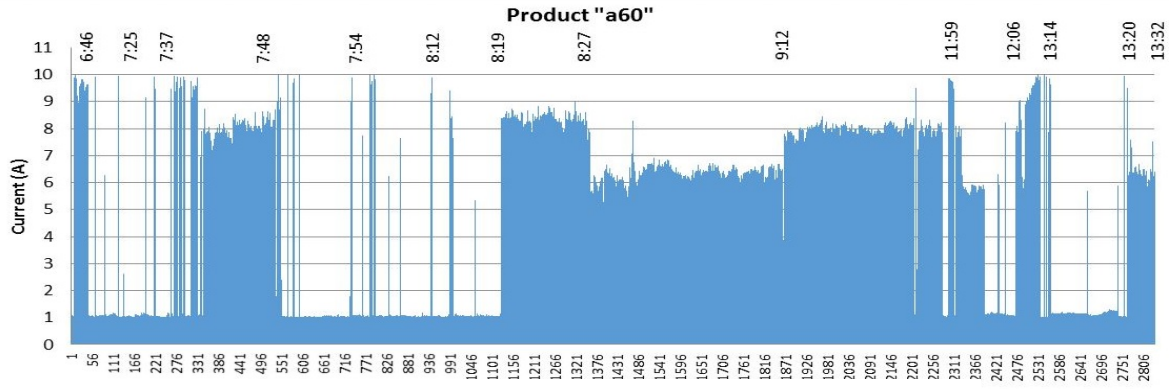

Fig. 9. Welding energy profile of product „a60“ mini-loaders base

action where the readings are near to 8 A. The product consists mainly from long welds (500 mm to 1000 mm) and materials with thicknesses from 8 mm to 12 mm are welded.
As the graphs (Fig. 8 and Fig. 9) show, each product does have it's distinguish energy profile like fingerprint. Based on the data gathered from products the energy consumption can be calculated, but additional research is needed.

5. CONCLUSIONS

Since the welding manufacturing process is not been analysed from the detailed energy consumption point of view, this study aims to fill this area.
The paper is presenting an overview of the technical solution, which proved to be suitable for monitoring and data gathering. Additional development is still needed to increase stability.
The gathered data about the welding process shows to be promising. Also the data analysis tools must be developed to show product based or time based results for the end-user.
The development will continue in the area with connection of the database engine with the production facility production planning systems.

ACKNOWLEDGEMENT

This research on the system architecture was supported by the Innovative Manufacturing Engineering Systems Competence Centre IMECC co-financed by EAS and European Union Regional Development Fund (project EU30006), Estonian Research Council (grant ETF8652). The system development and testing is supported by ITT Group OÜ.

REFERENCES

1. Factories of the Future PPP: towards competitive EU manufacturing [WWW], http://ec.europa.eu/research/press/2013/pdf/ppp/fof_factsheet.pdf, (10.03.2014).
2. Müller, E., Poller, R., Hopf, H., Krones, M., Enabling Energy Management for Planning Energy-Efficient Factories, In *Procedia CIRP*, 2013, **7**, 622-627.
3. Hu, S., Liu, F., He, Y., Hu, T., An on-line approach for energy efficiency monitoring of machine tools, In *Journal of Cleaner Production*, 2012, **27**, 133-140.
4. Ingarao, G., Vanhove, H., Kellens, K., Duflou, J., R., A comprehensive analysis of electric energy consumption of single point incremental forming processes, In *Journal of Cleaner Production*, 2014, **67**, 173-186.
5. Sell, R., Petritsenko, A., Early Design and Simulation Toolkit for Mobile Robot Platforms, In *International Journal of Product Development*, 2013, **18 (2)**, 168-192.
6. Medyna, G., Nonsiri, S., Coatanéa, E., Bernard, A., Modelling, Evaluation and Simulation During the Early Design Stages: Toward the Development of an Approach Limiting the Need for Specific Knowledge, In *Transactions of the SDPS: Journal of Integrated Design and Process Science*, 2012, **16 (3)**, 111-131.
7. Väljaots, E., Sell, R., Unmanned Ground Vehicle SysML Navigation Model Conducted by Energy Efficiency, In *Advanced Materials Research*, 2014, **905**, 443-447.
8. Sell, R., Leomar, P., Universal Navigation Algorithm Planning Platform for Unmanned Systems, In *Mechatronic Systems and Materials: Mechatronic Systems and Robotics*, 2010, **164**, 405-410.
9. Sell, R., Model Based Mechatronic Systems Modelling Methodology in Conceptual Design Stage, *doctoral thesis*, TUT Press, 2007**.**
10. LLAP - a way to talk to objects [WWW], http://www.openmicros.org/index.php/articles/85-llap-lightweight-local-automation-protocol/112-llap, (10.04.2014).

9th International DAAAM Baltic Conference
"INDUSTRIAL ENGINEERING -
24-26 April 2014, Tallinn, Estonia

POWER CONSUMPTION BASED ONLINE CONDITION MONITORING IN MILLING MACHINE

Serg, R.; Aruväli, T.; Otto, T.

Abstract: *Nowadays situation monitoring of production machinery is key factor in achieving production efficiency. Recent production equipment has often several sensors and monitoring facilities built-in but mostly for condition monitoring of a single unit. Mostly gathered data is only available to machine manufacturer. System for online machine monitoring using heterogeneous WSN has been proposed previously. Several methods of lathe condition monitoring have been researched.*

Currently easily deployable online condition monitoring system based on measurements of power consumption of milling machine is proposed and its efficiency researched.

Key words: manufacturing, condition monitoring, e-diagnostics, wsn

1. INTRODUCTION

High utilization of production machinery is one of the key performance factors for achieving high production efficiency. Possible unintentional mistakes in production planning or operating the production machine could lead to inefficient use of assets, poor quality of the products, interruptions in production process and even costly unplanned repairs. Older production equipment has usually very little or no monitoring systems installed. Machines itself are usually massive and in relatively good condition and can be used in production for some at least some years to come. Adding condition monitoring system to existing machinery adds additional value to the equipment and helps the users to increase efficiency.

Common challenge during extending existing equipment is the cost of the monitoring equipment and the complexity of the installation. Usage of WSN (Wireless Sensor Network) nodes allows keeping additional cabling minimal and cost for equipment at reasonable level.

WSN nodes can be powered by batteries or mains electric net as manufacturing equipment is usually situated close to power connections. In case of extreme radio interference some nodes can be configured as routers to amplify transmission.

Monitoring of single manufacturing unit is advantageous indeed, but same concept can be extended to whole shop floor or even larger entity. Proposed data acquisition concept can be used in wider heterogeneous sensor network. Further usage of the recorder data for planning or interfacing it to ERP (Enterprise Resource Planning) systems is out of the scope of current paper. This paper will describe easily deployable online condition

monitoring system for milling machine based on its power consumption.

2. CURRENT STATUS

Most of new production machines are equipped with various sensors and systems to monitor their status. Unfortunately the monitoring systems serve usually mostly the interests of equipment manufacturers to assist them to identify faults in normal operation. User access to gathered monitoring data is usually very limited. On another side there is great interest in the users of the equipment to optimize the usage of the machinery and minimize downtime. Also, lot of manufacturing equipment is already in use and has still working resource available, but is lacking any monitoring equipment. Various solutions for improving the situation have been proposed. One could tell the operator to manually record the status of the machine writing it down to either paper or electronic ledger. Simple traffic light like system could be installed on machinery. The disadvantage of both described examples is human factor involved in the process and local availability of the gathered data.

3. PROBLEM DESCRIPTION

Situation awareness is often modeled in layers. Widely accepted situation awareness model for humans consists of 3 layers: perception, comprehension and projection. We will extend the same model to artificial systems. On perception layer some detectable physical phenomena is measured by suitable sensor and low-level understanding of the situation is established. Based on perception higher level of situation information is built – comprehension. “Better” understanding of the situation that usually takes into account wider information (for example from other sensors or sources). Highest level of situation awareness (in current model) is projection that describes possible future situation of the entity. In current paper perception and partly comprehension levels of situation awareness are discussed. Extending the same situation awareness model to machine industry one could say that single machine condition monitoring and situation detection can be seen as perception.

4. PRIOR WORK

Sensors are often used in machine tools to detect physical parameters and to evaluate moving components condition based on gathered data [1]. WSN (Wireless Sensor Network) [2] based measurement system has been developed and described previously [3]. Several tests involving temperature [4] and vibration [5] measurements and result analysis have been made on lathe to detect working modes. Measured physical parameters can be also used for machine tool utilization monitoring [6]. Furthermore, digital object memory integrated surface roughness detection and storage methodology is introduced to use the monitoring data all over product life cycle [7].

Current monitoring in machine tools is researched mainly in condition monitoring purposes. It is used mainly to evaluate motor condition [8], but also for bearing damage detection [9].

5. DESCRIPTION OF APPLICATION

Milling machine Dyna Mechtronics EM3116 installed in TUT mechanic lab

was used for testing. Power consumption of the machine was measured with specially developed current sensor. Current sensor is designed so, that it can be easily connected by receptacle and plug just on the line of main power input of the milling machine. No additional cabling is needed as data connection is performed by NI (National Instruments) WSN solution. WSN3202 node with stock firmware, 9220 WSN gateway and specially designed software running in LabVIEW environment on a dedicated PC were used for data acquisition. Special RDBMS (Relational Database Management System) PostgreSQL 9.1 has been set up for storing data. Data communication between data producer and storage is done over TCP/IP protocol, so database server installation site is limited only by availability of internet connection. Usage on another layer in data storage (database server) enables the use of heterogeneous sensor network – sensors can be of different type. If the sensor can communicate and write data to database, then it is suitable to be used with the system. Also, getting all data from different sensors together into one database makes it easier to deduct conclusions based on several different sensors measurement results. On the same time RDBMS handles the concurrent data access and provides options for data validation, manipulation, compacting and time stamping.

6. CONDUCTED TESTS

Milling machine Dyna Mechtronics EM3116 was used for tests. Two different current measurement sensors, sensor 1 with measurement range of 32 A and sensor 2 with measurement range 16 A, both with WSN based data communication were connected to the power line of the milling machine. Data from both sensors were gathered by special application, developed in NI LabVIEW environment, and saved to cloud server database with time stamps into two separate data tables (Fig. 1).

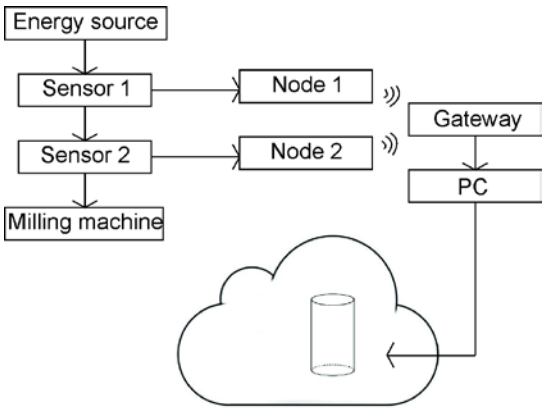

Fig. 1. Data collection scheme.

Two types of materials were used in tests: steel S355J2 and aluminum alloy 6082T6. Table 1 describes the setup for conducted tests.

Test No.	Material used	Description
1	None	Reference measurements: machine and spindle on/off
2	S355J2	Milling of steel at low feed rate
3	S355J2	Milling of steel at higher feed rate
4	S355J2	Forming the material
5	6082T6	Milling of aluminium at low feed rate
6	6082T6	Milling of aluminium at higher feed rate
7	6082T6	Forming the material

Table 1. Test parameters

Following milling program was composed:

N010 G21 G91; (set units mm, incremental movement)
N020 M03; (start spindle)
N030 F60; (set feed 60mm/min)
N040 M73 N3; (start program loop, execute 3 times)
N050 G01 Z-1,5; (move to cut depth)
N060 G01 X-95; (cut towards -X)
N070 G01 Z1; (rise tool from cut plane)
N080 G01 X96; (return to cutting start X)
N090 G01 Z-1; (lower tool to cut plane)
N100 M74; (program loop end)
N110 Z4,5; (take tool to initial Z plane)
N120 M02; (program end)

During tests 3, 4, 6 and 7 feed rate was increased to 90 mm/min and program row N030 was altered correspondingly.

7. RESULTS

The aim purpose of test 1 was to identify events of switching on/off the machine and spindle.
Current consumption is presented in fig. 2.

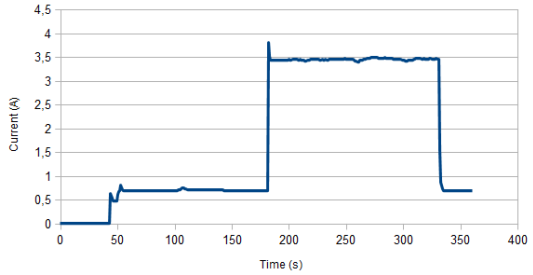

Fig. 2. Current consumption in different milling machine status: switched off, stand still and spindle turning.

Event of switching on the machine can be seen at about 50 sec from start of test and switching on the spindle at about 180 sec from the start of the test.

Tests 2, 3, 4 and 5 showed similar pattern in current consumption. Most visible result can be seen in test 3 (Fig. 3). Least visible result was found during test 5 (Fig. 4).

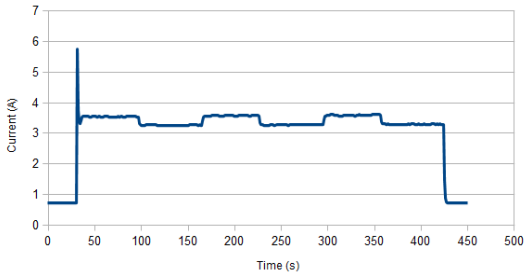

Fig. 3. Current consumption in test 3.

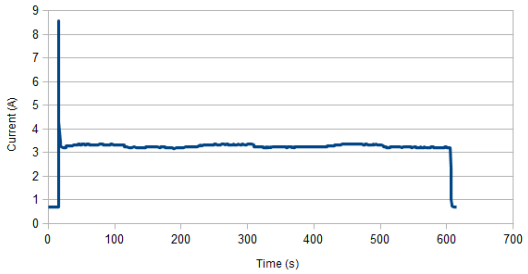

Fig. 4. Current consumption in test 5.

Measured currents for corresponding conditions are summarized in table 2.

Condition	Current (A)
Milling machine off	0
Milling machine on	0.7
Spindle on	3.2
Actual milling in test 2	3.4
Actual milling in test 3	3.5
Actual milling in test 5	3.3
Actual milling in test 6	3.4

Table 2. Current consumption in different

cutting conditions.

Measurements show that it is possible to detect milling machine on and spindle on conditions. Setting detection levels to 0.5 A and 3 A correspondingly the conditions of the machine can be deducted by the current consumption reliably. Equipment with higher accuracy is needed to detect actual milling process duration reliably.
Analysis shows that whole milling program for test 3 consumed 0.26 kWh of electricity. Total power consumption can be reduced by at least 30% with increasing return movement speed of the tool or turning off the spindle during return movements.

8. CONCLUSIONS

Test results show that proposed solution is able to monitor milling machine utilization by measuring it is current consumption. In addition, switching on the machine and spindle can be detected reliably. Actual milling operation detection is highly dependable on the milling operation specifics and requires higher accuracy equipment for reliable condition detection.

9. REFERENCES

1. Tiwaria, A. and Lewis, F. L. Wireless sensor network for machine condition based maintenance. *Proc. 8th Int. Conf. Control, Automation, Robotics and Vision*, 2004, **1**, 461-467.
2. Wright, P.; Dornfeld, D. and Ota, N. Condition monitoring in end-milling using wireless sensor networks (WSNs). *Trans. NAMRI/SME*, 2008, **36**, 177-183.
3. Aruväli, T., Serg, R., Preden, J. & Otto, T. In-process determining of the working mode in CNC turning. *Est. J. of Eng.*, 2011, **17**, 4-16.
4. Aruväli, T., Serg, R., Kaare, K. & Otto, T. Monitoring system framework and architecture over supply chain. *Annals of DAAAM for 2012 & Proc., 21st Int. DAAAM Symp.*, 2012, 661-667.
5. Aruväli, T., Reinson, T. & Serg, R. Real-time machinery monitoring applications in shop floor. *World Cong. on Eng. and Comp. Sci. 2011 Proc.: Int. Conf. on Int. Autom. and Robotics*, 2011, 337-342.
6. Aruväli, T., Serg, R. & Otto, T. Machinery utilization monitoring and pause identification prototype model design. *8th Int. DAAAM Baltic Conf. "Ind.Eng."*, 2012, 256-261.
7. Aruväli, T., Maass, W. & Otto, T. Digital object memory based monitoring solutions in manufacturing processes. *J. of Procedia Eng.*, in press.
8. Acosta, G. G., Verucchi, C. J. & Gelso, E. R. A current monitoring system for diagnosing electrical failures in induction motors, Mechanical systems and signal processing, 2006, 20(4), 953-965.
9. Blodt, M., Granjon, P., Raison, B., Rostaing, G. Models for bearing damage detection in induction motors using stator current monitoring. *Ind. Electronics, IEEE Trans. on*, 2008, 55(4), 1813-1822.

7. ADDITIONAL DATA ABOUT AUTHORS

Risto Serg, Research Laboratory for Proactive Technologies, Dep of Computer Control, risto.serg@ttu.ee
Tanel Aruväli, Dep. of Machinery, tanel.aruvali@student.ttu.ee
Tauno Otto, Dep. of Machinery, tauno.otto@ttu.ee
All authors are with Tallinn University of Technology, Ehitajate tee 5, 19086 Tallinn, Estonia.

9th International DAAAM Baltic Conference
"INDUSTRIAL ENGINEERING"
24-26 April 2014, Tallinn, Estonia

PRODUCTION MONITORING SYSTEM CONCEPT DEVELOPMENT

Snatkin, A.; Eiskop, T. & Kõrgesaar, K.

Abstract: *The main goal of this paper is to offer the concept of the production monitoring system that will help to provide an accurate overview of the shop floor activities, improve asset management, machinery utilisation and production process stability. It will provide diverse information appearance by support of data collection, analysis and storage modules.*
Key words: production monitoring system, remote monitoring, manufacturing execution system, shop floor visibility.

1. INTRODUCTION

The main aim is to offer a design concept of easy-to-use, configurable and cost effective production monitoring system (PMS) for small and medium sized enterprises (SMEs).
One of the problems facing a wide range of manufacturers is how to effectively monitor production lines and machinery to avoid malfunction and unplanned downtime and improve machine and manpower utilization [1]. Resource planning systems should calculate utilization on planning stage and PMS is an instrument that supports keeping this plan in place by supervising the resource state on production stage, together with advanced prognostics tools [2].
Production line and machinery monitoring is the necessary component of the information systems that are used in the production industry to improve efficiency and reduce losses [1].
Despite the fact that a huge number of different production monitoring solutions are offered on the market, there is always place for improvements and simplifications.
Large enterprises are used to a huge number of data to be processed. They have full time staff with expertise to manage specific applications related to production monitoring, data analysis and optimization.
At the same time, SMEs also have to deal with the growing number of data to be processed, but normally they cannot afford fully dedicated data experts. Solution to that can be to outsource some of these tasks to a third part or apply simple, affordable and easily configurable monitoring system.
It is clear that successful implementation requires a firm knowledge of the operating principles of PMS. That is why each module of proposed concept will be described first in order to explain how the system should work.

2. PRODUCTION MONITORING SYSTEM

The main task of PMS is to analyse and distribute data collected from the workshop and production line. The data should help the management and operators to get an overview of the machinery and production state.
Additionally to production plan management, there is growing interest in SMEs for asset health and utilisation monitoring, as operating costs of the machinery are considerable part of the total costs. Here special attention is paid to minimize the maintenance cost and time.
Machine state and production monitoring is one of the Manufacturing Execution

System (MES) functions [3]. The main idea of the MES is to integrate separate functions and provide linkage between business and plant floor control systems (see Fig.1).

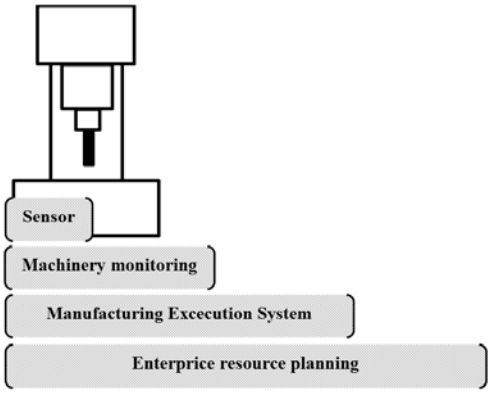

Fig. 1. Position of a MES and machinery monitoring in plant automation.

But if we look through the MES solutions of the leading providers of industrial automation systems and software (like Emerson, Honeywell, Rockwell, Invensys, Schneider Electric, Siemens, etc.), we can see that the core functions of MES are: material and inventory management, scheduling and collection of production data with limited information about equipment state. Support functions are: performance analysis and maintenance management. Most of the solutions are focused on midsize and large companies in chemical, oil and gas, food and beverage, and automotive industries. The process industries have all traditionally been heavy users of MES software, where it ensured that different variables don't exceed set parameters. But the complexity of production processes and machinery are increasing in all industries and more companies may require improved factory shop floor visibility.

3. CONCEPT

Proposed production monitoring system should be comprised of at least five main functions [4,5]: data collection, visualisation, analysis, prognostics and storage (see Fig. 2). Functionality and complexity of each component depends on customers' system specific requirements. Only the base functions and relations are described and additional modules may be added or even removed if required. The concept described below gives the idea of the system functionality.

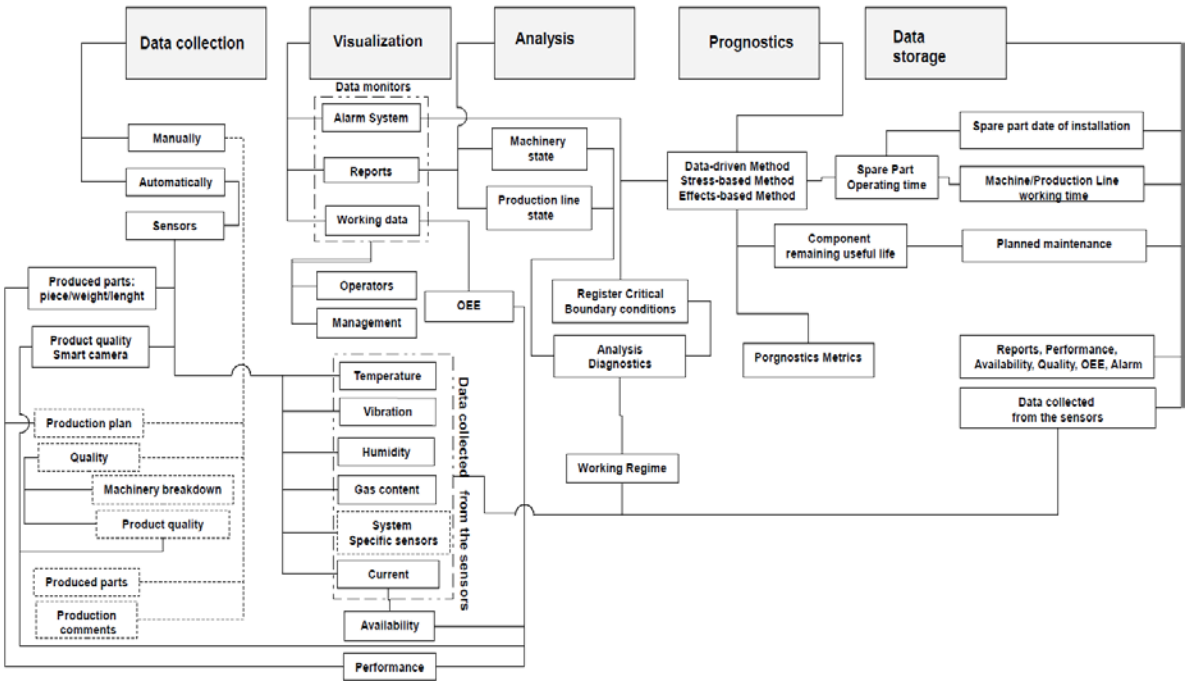

Fig. 2. Concept of a production monitoring system.

3.1 Data collection

Reduced personnel on the shop floors make it necessary to install automated data collection systems.

The most critical part is to identify what to measure, as collected data should help to acquire knowledge. Questionnaires and analysis methods may be used to specify what information is needed. Data not used for decision making could be discarded.

Different factors and criteria should be taken into account when choosing a measurement method and sensor type, like: cost; working range; ease of installation robustness; uncertainty; signal type, sample rate and availability.

Preference should be given to wireless sensors. With the use of energy harvesting it will even more enable sensor remote placement and lower installation costs [6].

The second approach is to maximally apply direct measurements methods, like machine vision systems instead of indirect methods, where collected signal is compared to the optimized signal. But when direct method is used, signal is measured and analysed directly using suitable algorithms. As an example, a smart camera used in machine vision is able to measure tool wear directly. Therefore, direct methods are more preferred than indirect methods [7].

Monitored parameter may be wrongly interpreted if there is no wide feature separation between failure and normal mode.

3.2Visualisation

Data can be presented trough LCD displays, andon boards, mobile device apps or web-based interfaces.

First data should be presented to operators, who will use this information in routine way to get indication of their job and machine state. Data could be customized to be shown in the simplest way (e.g. quantitative measurements replaced by qualitative and KPIs). Contrary, supervisors and service personnel should see more precise reports (historical data of operations performed, measured parameters etc.) for evaluation and finding the areas that may need improvements.

Each company should choose its own key performance indicators (KPIs) and the calculation methods. Most commonly KPIs are related to production output, quality and availability.

Additionally to availability (idle; production; stoppage) rate system must record the reasons of downtime. Operators can input it using touch sensitive screens, keyboard, voice recognition, etc. Multilevel tree structure may be formed to provide more detailed reason description. The figure below represents a three level downtime reason menu for a milling machine (see Fig. 3).

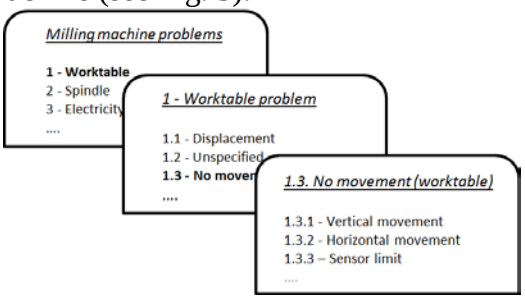

Fig. 3. Multilevel stoppage description.

After each stoppage operator selects the reason from the list, which may be updated by adding new reasons or removing obsolete ones based on the usage statistics. For undescribed reasons the choice “unspecified” can be in the list. When number of such “unspecified” downtime reasons increase to the number of interest, the list of reasons may be revised.

To make downtime cause analysis a PMS should have statistical module to track the downtime changes over the time. Additional module may be developed to measure the maintenance time effectiveness that is related to average time needed to eliminate the reason of stoppage - mean time to repair (MTTR).

3.3. Data analysis

Use of statistics is the most common approach for data analysis to extract useful information from the datasets. Different

data mining techniques in analysis are used with its own application area (Table 1.).

Method	Possible application area
Decision tree	Data pre-processing and classification.
Neural network	Pattern detection and predictive models.
Genetic algorithm	Data optimization.
Rule induction	Define relations between different data streams.

Table 1. Example of data mining methods.

Diagnostics, data analysis and prognostics help with the questions that arise during the operation:

- May system continue to operate or should be shut down for maintenance?
- How change of regime will affect the lifetime of the system and KPIs?
- What are the performance, efficiency and quality rate in real time?

3.4. Prognostics

Only if the remaining useful lifetime (RUL) and real state of equipment is known, preventive maintenance may be replaced by condition based maintenance. By use of prognostic methods preparation to maintenance can be done in advance when the system is still running and the failure is known early enough [8]. Resources could be focused on parameters of high value systems to determine the most likely scenarios with maximally eliminated inaccuracy and uncertainty.

Knowledge about the physical process determines the regression type to apply (linear, polynomial, exponential, etc.). Prognostic methods are normally divided into the three main groups: Data-driven Method, Stress-based method and Effects based method. These methods can be summarized as follows (see Fig. 4.):

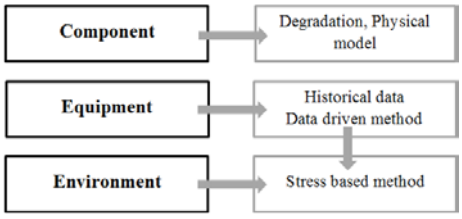

Fig. 4. Prognostic methods description.

3.4 Data storage:

Collected data should be transmitted to a database server. Different database technologies may be used like SQL (e.g. MySQL, Postgres, Oracle Database) or even NoSQL databases (e.g. MongoDB, Cassandra, HBase, Neo4j.). SQL based database systems are more widely used at the moment, as they can be easily accessed via standard Structured Query Language (SQL) statements and effectively solve data storage and replication challenges.

The amount of data saved in the database should be sufficient for data mining. Deciding what to store in the database could improve or reduce performance and thereby influence the time of analysis. It is not reasonable to store every single measurement or even analysed data set in the database when the data is not relevant in the decision making process. If we take measurements with high sample rate it may be better to transfer already selected data (e.g. in WSN node) to database [4].

At the same time, cloud based database platforms could be used for more effective resource allocation.

The main challenge here is connectivity and fusion of data form different systems [9,10,11] like ERP - enterprise resource planning CMMS - Computerized maintenance management system, etc. One of the solutions can be data integration using XML (Extensible Mark-up Language) platform [12].

5. CASE STUDY

The proposed monitoring system was applied and tested on the milling machine DYNA MECH. EM3116 in Tallinn University of Technology (TUT) laboratory. Data acquisition was performed using National Instruments (NI) equipment: Gateway WSN 9791 with NI WSN 3212 thermocouple input node for temperature measure and NI WSN 3202 Analogue input node for Voltage measure. Nodes were secured by magnet brackets to simplify installation. Data visualization

was performed through LCD monitor secured to the housing of the machine (see Fig. 5.).

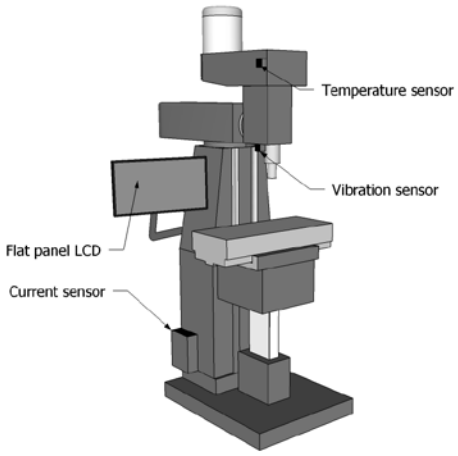

Fig. 5. Milling machine monitoring system.

The choice of NI instead of other solutions was made due to flexibility and optimality of the hardware and software in the concrete case study and using NI LabVIEW software with a graphical programming tool, helped to reduce time for programming.
High sample rate of acceleration measurements didn't allow using analogue NI WSN due to ZigBee (802.15.4) wireless standard and hardware limitations: WSN 3202 sample rate 1sample/second and ZigBee RF data rate 250kbit/s.
As an alternative for the future research open source hardware platforms like Arduino or Raspberry Pi may be used due to more acceptable price level for SMEs.
Data was saved remotely to PostgreSQL database and to local host as a separate file (see Fig. 6.).

Date: 09.01.2014 Test start time: 14:45:00

Timestap (1s)	Temperature Celsius	Timestap (1s)	Current Ampere
303	20,864441	303	0,405514
304	20,864441	304	0,359547
305	20,866158	305	0,342834
306	20,866158	306	0,223744
307	20,866158	307	3,182226
308	20,866158	308	3,192675
309	20,866158	309	2,994192

Fig. 6. Example of collected data set.
During the test were determined the set points for idle, production and heavy load operation for different cutting regimes of S235JRG2 steel (Fig. 7.).

Cutting depth	RPM	Workable movement	Current Ampere
0.5	300	150	3.0
1	300	150	3.2
1.5	300	150	3.4
2	300	150	3.7
0.5	450	300	3.2
1	450	300	3.5
1.5	450	300	4
1.75	450	300	4.3

Fig. 7 Current for different regimes.

Obtaining sample data of the failure progressions to define alarm set points for measured parameters posed to be a real challenge, as systems are normally not allowed to run until failure and the vital parts are always tried to be replaced before they fail. Therefore, as an alternative, statistical process control (SPC) was proposed for continuous automatic calculation and update of warning limits (upper/lover limit control).
After the survey (interview of operator) were determined the most common breakdown and quality problems for such type of milling machine that helped to make the list of problems for visual model.
Main window of visual module was developed using PHP language, jQuery, jqPlot allowing seamless object-oriented data updating without refreshing the whole page (see Fig. 8.).

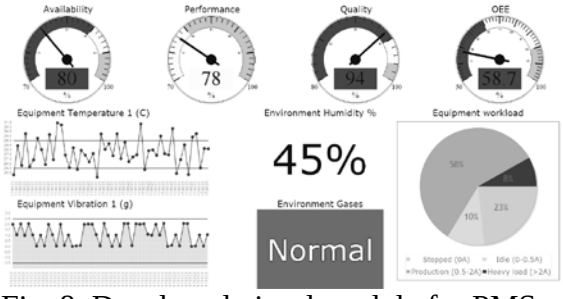

Fig. 8. Developed visual module for PMS.

6. FURTHER RESEARCH

Standardized metrics of production monitoring system will help to compare different solutions on the market and evaluate effectiveness of the existing ones. Methodology should be described how to determine what critical data to monitor and visualise. Also solutions for integration and data fusion with higher level systems (e.g.

ERP) should be developed. Proposed concept should be optimised for production lines and group of machines, where you can compare the status of all equipment to provide the total production area overview.

9. CONCLUSION

PMS concept was offered and applied for the milling machine. It provides transparency on the shop floor and improves manufacturing competitiveness. System offers predictive functionality and helps to prevent the critical components breaks.

12. ACKNOWLEDGEMENT

This research was supported by ETF grants 8485 and 7852, targeted financing project SF0140035s12 and Innovative Manufacturing Engineering Systems Competence Centre IMECC (supported by Enterprise Estonia and co-financed by the European Union Regional Development Fund, project EU30006).

11. REFERENCES

1. Jardine, A.; Lin, D.; Banjevic, D. A review on machinery diagnostics and prognostics implementing condition-based maintenance. *Mech. Syst. and Signal Processing*. 2006, **20** (7), 1483-1510.
2. Lee, J.; Lapira, Ed. et al. Recent advances and trends in predictive manufacturing systems in big data environment. *Manufacturing Letters I.* 2013, **1**, 38-41.
3. Saenz de Ugarte, B.; Ariba, A. and Pellerin, R. Manufacturing execution system – a literature review. *Prod. Plan. Control*, 2009, **20**, 525–539.
4. Snatkin, A.; Karjust, K.; Majak, J.; Aruväli, T. and Eiskop, T. Real time production monitoring system in SME. *Est. J. of Eng.* 2013, **19**, 62-75.
5. Snatkin, A.; Karjust, K. and Eiskop, T. (2012). Real time production monitoring system in SME. In: *Proc. of the 8th Int. Conf. of DAAAM Baltic Ind. Eng.*, (Otto, T. ed.) TUT, Tallinn, 2012, 573–578
6. Hadas, Z.; Singule, V. Energy harvesting-opportunity for future remote applications. In *17th Int. Conf. on Engineering Mechanics*, (Fuis, V. ed.) Brno, Svratka, 2011, 169-171
7. Shahabi, H.; Ratnam, M.; In-cycle monitoring of tool nose wear and surface roughness of turned parts using machine vision. *Int. J. Adv. Manuf. Tech.*, 2009, **40**, 1148–1157.
8. Varde, P.V. and Pecht M.G. Role of Prognostics in Support of Integrated Risk-based Engineering in Nuclear Power Plant Safety- *Int. J. of Prognostics and Health Management*, **3**, 2012
9. Riives, J.; Karjust, K.; Küttner, et al. Software development platform for integrated manufacturing engineering system. In *Proc. of the 8th Int. Conf. of DAAAM Baltic Ind. Eng.*, (Otto, T. ed.) TUT, Tallinn, 2012, 555 - 560.
10. Karjust, K.; Küttner, R.; Pääsuke, K. Adaptive web based quotation genetic module for SME's. In *Proc. of the 7th int. conf. of DAAAM Baltic Ind. Eng.*, (Küttner, R. ed.) TUT, Tallinn, 2010, pp. 373- 4380.
11. Tähemaa, T.; Karjust, K.; Pohlak, M. ERP and PLM resources in Estonian SME's. In *Proc. of the 7th Int. Conf. of DAAAM Baltic Ind. Eng.*, (Küttner, R. ed.) TUT, Tallinn, 2010, pp. 386-391.
12. Gallar, D.; Kumar, U. et al. Fusion of maintenance and control data: A need for the process. In *Proc. of 18th World Conf. on Nondestructive Testing* (Johannes, M. ed.), SAINT, Durban, 2012.

12. CORRESPONDING AUTHORS

MSc. Aleksei Snatkin; MSc. Tanel Eiskop; MSc Kristjan Kõrgesaar; Department of Machinery, TUT, Ehitajate tee 5, Tallinn, 19086, Estonia, E-mail: aleksei.snatkin@gmail.com; taneleiskop1@gmail.com; kristjan.korgesaar@gmail.com

9th International DAAAM Baltic Conference
"INDUSTRIAL ENGINEERING "
24-26 April 2014, Tallinn, Estonia

OPTIMIZING PRODUCTION TECHNOLOGY SELECTION PROCESS WITH FUNCTIONAL REQUIREMENTS

Sonk, K.; Sarkans, M.; Hermaste, A. & Paavel, M.

Abstract: *Choosing a technology to manufacture any product has never been an easy challenge. Mostly because it requires a compromise between very different and conflicting parameters i.e. product must be cheap yet with high quality. An approach using products' functional requirements along with other parameters to help with that decision process has been proposed in this paper.*
Functional requirements define what a product is meant for and what it must achieve but not how it must be achieved. This means that by describing the product with functional requirements we are open to all the different production possibilities and this helps us to change and choose an optimal manufacturing technology.
An example using three different rapid prototyping technologies (inkjet printing, selective laser sintering and fused deposition modelling) is presented. Rapid prototyping has been chosen because it allows a very diverse range of products to be manufactured.

Key words: rapid prototyping, functional requirements, technology selection, optimization.

1. PRODUCTION TECHNOLOGY SELECTION PROCESS

Selecting an optimal production technology for a product is a very complicated decision process and it is very hard to automate (or semi-automate) even sections of it. There have been some attempts to give some rules or suggestions for the process, some of which are described by Karjust [1] but all of them are specific to a certain industry
Most of the current theories, software solutions and applications are meant for companies with a defined set of production capabilities. This means that a company has similar machines for a certain operation. Acquiring a new machine just to have a different kind of technology for the same results is pointless from all viewpoints. But companies that are re-organizing their production, setting up new factories, international corporations with diverse manufacturing capabilities or a set of small companies working together on the same product order have the opportunity to use different machines for the same results. Functional requirements are meant to speed up and give objective suggestions which production technology would be most suitable for those manufacturers.

2. USING FUNCTIONAL REQUIREMENTS IN PRODUCTION SELECTION PROCESS

Most products are described as a set of physical properties (weight, measurements, materials, colour etc.) but they can be described as a set on functions as well. Even a company can be represented in that way [2]. Using functions or functional requirements is a more ambiguous way to describe something (compared to the physical parameters) but at the same time it allows us to re-evaluate a lot of different aspects about a product, in this case we are focusing on the production technology selection.

For example when describing as functional requirements we get that the bottle must hold and store drinkable liquid for a certain amount of time and it must stay intact during transportation. There are more functions the bottle must achieve but none of them define how the bottle must be manufactured leaving it open for change, discussion and different ideas. Similar approach has been described by Haas [3].

This means that by using functional requirements we can expand the technology selection beyond just physical parameters. We take into account how and where the product is going to be used and this changes the technology we choose to manufacture that product. This helps us better to choose the optimal production technology and speeds up the process.

One of the problems with international companies and huge orders is the time and cost that company must invest in evaluating manufacturing and possibilities for producing a product. This means two things: whether the company is able to produce the product and if it is, what would be the cost in time and money. We have to take into account that the machines and workers can be pre-occupied for long periods of time. This problem is magnified if the companies are in different countries or even in different parts of the same country.

Speeding up the technology selection process with functional requirements is done by a software program. The program gives different scenarios how the product could be manufactured. Functional requirements determine which machines are able to produce the product and physical parameters determine the cost and time. Similar approach, but done manually, has been described by Klooster [4] in packaging development chain.

3. CASE-STUDY: FUNCTIONAL REQUIREMENTS IN RAPID PROTOTYPING TECHNOLOGY SELECTION PROCESS

The case study is based on rapid prototyping technology. It includes the technological possibilities of three machines: selective laser sintering rapid prototyping machine (RPM), inkjet technology RPM and fused deposition modelling RPM. We have compiled a program that takes into account the specifications of the building materials used in each machine, machines' capabilities in shapes and geometry of the product, its mechanical properties (also machining possibilities) and finally size of the working area.

The machines' physical parameters are described and compared in the following categories: production time, production cost, materials yield strength, materials elasticity, materials colour, surface roughness, products usability (decorative or practical).

One of the aims of this case study is to prove that functional requirements are not only useable for determining if a product is manufacturable but also using them speeds up the process and gives an objective suggestion what kind of technology would be the most efficient one. The second aim is to develop a software program that allows technology selection to be done automatically.

The case study is based on existing information. We have a database of already completed orders from over the last year and so we know which machine was used and what was the cost producing each product (in monetary value and time).

A program was compiled where the input information is in three steps. Step 1: simple yes/no questions for determining the function of the product. Step 2: prioritizing cost, time, and quality. Step 3: products' maximum measurements.

The questions help to define functions of the product. It is in question form because

describing the functions in free-form is not understandable by the program. If all the information is entered correctly the program would give at least three different answers based on each machine.
First phase of the study is to go over the previous orders, insert the data to the program and see if the program suggests the same machine that was actually used and if the cost calculated by the program is similar to the actual cost. If the programs suggestion is different than the machine used/actual cost we analyze if the optimal technology was used.
Second phase is to insert information about new orders and see if the optimal machine is suggested. The answer still needs to be analyzed because it's un-tested software and needs reviewing by and engineer with experience and knowhow.
Third stage is making a web interface to the program and allowing potential customers to get price/time estimation online. They would answer the questions that are at the moment in development and insert the measurements of the product and be given the option to choose the priorities between cost, time and quality. Additional feature would be the option to upload a CAD model and thus allowing more accurate price calculation. This stage is also an opportunity to see the changes in customer's values [5].

4. CONCLUSION AND FURTHER RESEARCH

The case study shows that functional requirements can be used to optimize the production selection process. It is still a work in progress but we hope to start with the second and third phase very soon. The questions about the functions of the product are still the biggest weak point and need further research.
One of the goals is to make the program use real-time data directly from the RP machines. A plan is to use a similar approach as described by Aruväli [6] and because the RP machines are already accessible to computers, the real-time database should be very feasible.
We are finishing first phase in the case study at the moment and polishing the input method and especially the questions related to the functional requirements.

5. REFERENCES

1. Karjust, K.; Pohlak, M; Majak, J. (2012) Adhesion process optimization in reinforced composites. *In: Proceedings of the 8th International Conference of DAAAM Baltic Industrial Engineering.* Tallinn, Estonia: 2012, 633 - 638.
2. Sonk, K. Hermaste, A. Sarkans, M (2012). Functional requirements as a company and process modeling tool. *In: Proceedings of the 8th International Conference of DAAAM Baltic Industrial Engineering 19-21st April 2012, ,* Tallinn, Estonia: 2012, 98 - 103.
3. Haas. C & Hsieh. T-Y (1994) Determining functional requirements for large scale manipulators, http://www.sciencedirect.com/science/article/pii/0926580594900329 (2014-02-22)
4. Ten Klooster. R & Lutters. D (2008) Functional requirement specification in the packaging development chain http://www.sciencedirect.com/science/article/pii/S0007850608000668 (2014-02-12)
5. Maleki, M; Shevtshenko, E; Cruz-Machado, V. Comparative Analysis of Customer Value Dimensions. Inzinerine Ekonomika - Engineering Economics Volume: 24 Issue: 1 Pages: 488-495 Published: 2013
6. Aruväli, T.; Serg, R.; Otto, T. (2012). Machinery utilization monitoring and pause identification prototype model design. *In: Proceedings of the 8th International Conference of DAAAM Baltic Industrial Engineering.* Tallinn, Estonia: 2012, 256 - 261.

6. ACKNOWLEDGEMENTS

The study has been supported by Estonian Science Foundation Grant ETF9441.

9th International DAAAM Baltic Conference
"INDUSTRIAL ENGINEERING
24-26 April 2014, Tallinn, Estonia

CUSTOMISATION OF EXCELLENCE MODELS AND ASSESSMENT SCHEMES, CONSIDERING SECTORAL SPECIFICS

Tammaru, T. & Kiitam, A.

Abstract: *In this paper some issues of adaptation of Excellence models (EM) and customisation of assessment schemes are outlined. Some results and conclusions of application of adapted sectoral models, assessment and recognition schemes, incl quality awards in Estonia during past decade are presented.*
Key words: Excellence models, EFQM, adaptation, sectoral models, assessment schemes

1. INTRODUCTION

One of the most widespread quality related approaches throughout the world in the past decades besides implementation of standards based management systems has been the usage of excellence models for self-assessment as well as external evaluation and recognition. Companies worldwide are using the criteria of the Malcolm Baldrige National Quality Award, the European Quality Award, the Deming Prize and many other national quality awards, which are mainly based on the above-mentioned models or their adaptations. There are around 100 different EMs and recognition schemes available, e.g. 94 business excellence models and frameworks used in 77 different countries were recently identified by Talwar [1]. Besides differences in the models there are also variations in the schemes and recognition processes [3]. Although all the excellence models are based on a basic set of core values or principles, which differ in wording, but are expressions of the same excellence paradigm with the roots in total quality management (TQM).

Business excellence (the quality of management) has been defined as the ability of an organization to create desirable effect in order to increase the satisfaction of its stakeholders through efficient management activity, so increasing the probability of long term success as an organization [2].

The application of excellence models started in the private sector, mostly in large manufacturing companies, more and more service providers, SMEs as well as public sector and non-profit organizations are using BE models. The CAF-model (Common Assessment Framework), an adaptation of EFQM Model for self-assessment has been widely promoted in the past decade to introduce TQM to the public sector.

Regardless of sector, size, structure or maturity level organisations need to establish an appropriate management framework in order to be sustainable. Considerations for choosing a suitable customized approach are presented, taking into account multiple factors, such as sectoral and organizational specifics, size and maturity level of organizations are presented. Optimal complexity of assessment process is considered while keeping the common key concepts, values and principles underlying the Excellence models.

The experience of developing different schemes of implementing excellence models in Estonia during last ten years has been taken into account [3]. The research is based on the study of different schemes, general as well as sectoral (public sector, educational institutions, tourism).

2. NEED FOR CUSTOMISATION

In order to increase positive impact of use of Excellence models on performance, productivity, sustainability and competitiveness of organizations as well as society as a whole, it is necessary to use adaptation of models for different economic and societal sectors and clusters. This supports better usability and wider reception of models and promotes their substantiality, at the same time keeping assessment schemes economical and unified on basis of same reference model (the EFQM Excellence Model).

Based on statistical and qualitative data acquired from previous research (quality policy, awareness studies), the projects, including feedback received from different stakeholders of recognition schemes in Estonia (participating organizations, assessors, validators, jury members), there is vital need to adapt the general BEM models (basically the EFQM Model) to the specifics of sector, especially the vocabulary. The model and assessment process itself have been perceived as difficult to understand and/or too complex and time-consuming, mostly due to the low maturity level of BE and/or small size of organizations.

3. OPPORTUNITIES FOR CUSTOMISATION

In general, as mentioned in Conti [4], customisation of the model is essential for improvement and the plurality of models available today is a great opportunity. In terms of assessment and organisational analysis, the two mainlines of goals for use of EM are the following:

1 Scoring: use of EM for assessment of excellence level of organisation, in order to provide a measure to make
a) comparisons with other organisations, with the goal to identify the current position/level of the organisation in terms of benchmarking against other organisations of the same industry sector or, in case of cross-sectoral contest (e.g. national excellence award competition), against organisations of other sectors
b) comparisons with the past level of the same organisation, with the goal to assess the overall progress in the timeframe of comparison, e.g. the change of excellence score as compared with the same organisation one year ago or three years ago.

2 Identification of improvement possibilities (IIP), in order to propose recommendations for further activities for organisation with the goal to improve its performance indicators achieved in different categories and subcategories of the EM used. These recommendations for improvement possibilities are usually presented in the feedback report provided by the assessment team (often called as Areas for Improvement, AFIs), and are for the organisation typically /quite often the most important outcome of the assessment process.

Thus, when considering the optimisation of complexity level of the adapted sectoral model, both these aspects (scoring and IIP) should be taken into account. A problem here might be that sometimes these aspects call into somewhat different directions in terms of complexity of model. E.g., for scoring purposes the main goal of optimisation of complexity might be minimisation of workload of assessment process, while keeping the assessment precision on acceptable level. This directs search of optimum into direction of

simplicity, and may lead to reduction of number of categories or subcategories. On the opposite, the IIP-related considerations may call towards more detailed analysis of organisation's activities, in order to find more detailed proposals concerning recommendations for improvements. Therefore, finding the optimal complexity level of the model may be the finding of best compromise between these considerations concerning scoring vs IIP.

Additionally, optimal complexity level for a sectoral model depends also on the average excellence (maturity) level of organisations using this model, as with the growth of excellence level a more complex model is needed, especially as further growth of maturity requires more detailed analysis of IIP. Thus according to the growth of excellence level, the need of models, which enable advanced level of detail of organisational analysis may appear.

Therefore, provided that from the viewpoint of rising national competitiveness via use of EMs, in time scale the promoted growth of excellence level may lead to starting with simpler versions of sectoral models and then perhaps adding as additional more complex models for segment of organisations which have reached a higher maturity level (in terms of excellence level). An overview of different factors and aspects of customisation is given in Table 1.

4. CUSTOMISATION OF MODELS RECOGNITION SCHEMES IN ESTONIA

Several adaptations have been made to the EFQM Excellence Model and recognition schemes in Estonia. The most successful and long-term implementation of excellence principles in Estonia have been in educational and tourism sectors. The purpose of recognition schemes is to motivate organizations to use modern methods for developing management quality and raise overall quality awareness. Another aim of external assessments is to recognise well-performing organizations, at the same time identifying and sharing best practices, enable benchmarking and encourage benchlearning activities. Recognition also increases the reliability and image of organisations.

Estonian Quality Award model was proposed in 1999 [5] as a first attempt to customise EFQM Excellence model considering the current needs of Estonian organisations. Taking into account the quality maturity level a and size (mostly SMEs) of majority, slight simplification of the structure on subcriteria level was made. Since 2006 the scheme was fully aligned with EFQM in order to give more international weight to the recognition and assure comparability with other recognition schemes in Europe, with no customised approaches. A multi-level national recognition scheme was introduced aligned with the EFQM Levels of Excellence (LOE).

The feedback of participating organizations was mainly positive – good learning experience, valuable feedback from external assessors, input for development initiatives and business strategy – but the relatively small number of participants has been an issue throughout the whole process (6-15 participating organizations per year). The main reasons for not participating were low awareness, but also the perception that the whole exercise is too complicated and time-consuming compared to the gained benefits. An added value to the impact of the scheme is the involvement of assessors who got invaluable learning experience that they could use in their own organizations. Besides competition there was a number of organisations who participated in the self-assessment trainings but not applying for the recognition.

Factor	Aspects/ measures to be optimised/ compromised	Limitations	Considerations	Background/ comments
Model structure/ complexity	1 Number and list of EM categories and subcategories 2 Goal: minimum complexity, keeping needed comprehensive-ness level of related TQM thinking	1 Grounding on universality of TQM-related know-how and keeping needed uniformity for TQM-comprehensive-ness 2 Usability for sectoral organisations	1 Sector-specific aspects of model structure and criteria 2 Probable complexity limits: From full EFQM EM to Excellence Index	1 EFQM EM as base model 2 Inter-sectoral synergy (national level) 3 International sectoral compatibility of the model 4 An example: 2014 version of C2E
Complexity of assessment schemes/ procedures	1 Requirements concerning qualification and experience of assessors 2 Volume and content of calibration training 3 Cost of assessment	1 Keeping necessary comprehensivenes s TQM-related know-how 2 Cost limitations 3 Size of population of qualified assessors, able to participate in different external assessment schemes with adequate level of accuracy	1 Segmentation of assessment results 2 Recognition schemes	1 Inter-sectoral synergy (national level) 2 International sectoral compatibility
Assessment precision/ uncertainty	1 Size of assessment teams 2 Segmentation of results 3 Goal: minimisation of workload for sectoral models while keeping necessary assessment accuracy/precisio n	1 Assessment procedures 2 Experience of assessors	Resource requirements/limit s	
Vocabulary adaptation	Compromise between sector-specific vocabulary vs universal TQM vocabulary used	Acceptability/ compatibility for sectoral organisations/ mind-set	Promoting necessary TQM-related compre-hensiveness of vocabulary used by sector	

Table 1. Adaptation/customisation factors for sectoral/functional models

	Estonian Quality Award	Inspirational LOE (C2E)	Tallinn Educ. Inst. QA	VET Quality Award	HEI QA	Tourism Quality Program
Period	2000-2003	2006-2010	2002-	2003-2011	2009-2012	2004-2011
Model used	Adapted EFQM	EFQM	Adapted EFQM	Adapted EFQM	Adapted EFQM	Simplified EFQMbased
No of cat./ subcateg.	9 /22	9 / 0	9 / 23	9 / 22	9 / 20	5 / 15
Adapted vocabulary	No	No	Yes	Yes	Yes	Yes
Evaluat. method	Scores, RADAR	Validation, no scoring, yes/no	Scores, simplified RADAR	Scores, adapted RADAR	Scores, adapted RADAR	Validation, no scoring, yes/no
Number of evaluators	4-7	1-2	3-5	4-5	4-5	2(-3)

Table 2. Comparison of adapted models and frameworks in Estonia

During 2000-2011 several organisational excellence projects were carried out in Estonia, specifically in educational and tourism sectors. In 2003 there was a pilot project in the public sector (using CAF). Part of all these development projects was customisation of the BEM and its adaptation to sector-specific needs. An overview of the results of these customisations is given in Table 2. All the projects had also external assessments with special choice procedure and training of evaluators (assessors or validators). Although the models had been customised, mainly by rewording or simplifying the structure of assessment models through decreasing the number of subcategories, common theme in the feedback of all projects was related to the unfamiliar vocabulary of TQM, complexity of understanding and time-consuming assessment process (both internal and external). All referred models kept the basic 9-criteria structure of the EFQM Model, with the exception of tourism quality model (see Fig. 1). The tourism quality model was reduced to 5 categories. Adapted self-assessment methodology as well as external assessment (combined validation and mystery shopping) were developed. Even so, very often the feedback from participating organizations was that the whole scheme was too complex and difficult to understand. The specifics of tourism sector is large number small and even micro organisations with low maturity level, where any kind of structured management model is difficult to apply.

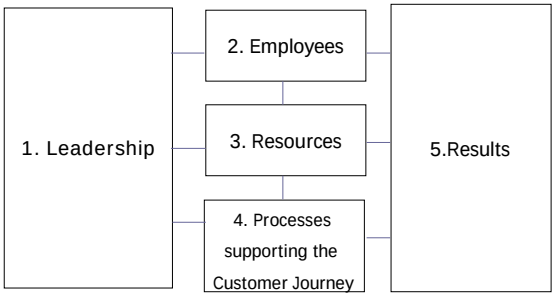

Fig. 1. Example of a customized BEM, Estonian Tourism Quality model

According to a study identifying the levels and differences regarding quality and excellence awareness practices in Estonian organizations from different sectors and of different sizes [6], two clusters of organizations could be identified: one represented organisations with higher awareness and maturity levels, mostly large and some medium-sized organizations (estimated EFQM score 171-400 p.); the other represented organisations with lower awareness and

maturity levels, as well as lower interest in quality and management tools, most of the micro and many of the small organisations (estimated EFQM score less than 170 p.). No major differences between different sectors (production and services, public and private) were identified, but there were significant differences in most factors depending on the size of organization.

Another important aspect in the use BEMs is the question of internal versus external assessment. These two assessments have different purposes and it is problematic to perform them together, using the same approaches. This has been pointed out by Tito Conti, one of the originators of the EFQM Model, already in 1991 [7]. Self- assessment is a diagnostic tool with focus on improvement opportunities, while external assessment is more focused on conformity to recognition requirements. Although all excellence projects provide participants also with qualitative feedback about strengths and AFIs, sometimes also quantitative scores, it has been argued that the value is not the same as by in-depth internal analysis. This an area of further discussion and research.

5. CONCLUSION

There is an identified need for further customisation of business excellence models and development of specific recognition schemes. Benchmarking and benchlearning is required to identify and disseminate best practices. There is also a need for more comprehensive and interdisciplinary quality and excellence related research (e.g. economic aspects of quality and excellence, links between different models and methods of organizational performance results, development of suitable models for specific target groups).

6. REFERENCES

1. Talwar, B. Comparative study of core values of excellence models vis-a-vis human values. Measuring Business Excellence, 2009, **13**, 34-46.
2. Grigg, N., Mann, R. Rewarding Excellence: An International Study into Business Excellence Award Processes. ASQ Quality Management Journal, 2008, **15**, 26-40.
3. Tammaru, T. Excellence Models and National Quality Promotion in Estonia. 2010, In: Proc. of the 7th Int. Conf. of DAAAM Baltic Industrial Engineering. 22-24th April 2010, Tallinn, Estonia, 409 - 414.
4. Conti, T. Opportunities and risks of using excellence models. JoQ paper, **5**, 2003
5. Tammaru, T. *Performance Measurement in Quality Systems, Master Thesis*. Tallinn Technical University, 1999.
6. Tammaru, T. *Eeluuring kvaliteedi-teadlikkuse programmi sihtrühmade relevantsete vajaduste leidmiseks. Projekti aruanne. Versioon 2.1.*, 2005,Tallinn, TTÜ
7. Conti, T. Company quality assessments. Total Quality Management, 1991, **2,** 167-172.

7. ADDITIONAL DATA ABOUT AUTHORS

Tiia Tammaru, MSc (Eng.), Research Scientist, Dep. of Mechatronics, TUT, tiia.tammaru@ttu.ee /Ph +372 56 636 67
Andres Kiitam, PhD / Research Scientist Dep. of Mechatronics, TUT andres.kiitam@ttu.ee / Ph +372 6203 204
Ehitajate tee 5, Tallinn, 19086, Estonia /

http://www.ttu.ee/mehaanikateaduskond/mehhatroonikainstituut/ (Corresponding Author)

9th International DAAAM Baltic Conference
"INDUSTRIAL ENGINEERING -
24-26 April 2014, Tallinn, Estonia

BUSINESS AND IT ALIGNMENT IN ENTERPRISE CONSIDERING THE PARTNER NETWORK'S CONSTRAINTS

Vaezipour, A.; Kangilaski, T

Abstract: *Cooperation between independent Small and Medium Enterprises (SMEs) is crucial to be competitive in growing global business environment. Thus, it is vital for enterprise success to consider both IT and business aspects during the development of enterprise as well as considering cooperation with the Partner Network members. Collaboration enables companies to gain new competitive advantages and to excel the individual capabilities by focusing on their core-competencies. Hence the purpose of this study is to better address the research issues in alignment area and bring insight and deep understanding into the relation of EM to improve BITA in organizations.*
Key words: Enterprise Modeling, Business and IT Alignment, Partner Network

1. INTRODUCTION

The effective use of information technology align with objective of business enterprise have discussed in many academics researches aiming at adding value to businesses and improve their financial outcomes. IT alignment has been a significant issue for IT related experts and enterprise managers for two eras [1,2]. According to [3] Business/IT alignment revolution began from early 1980s and developed by conducting many empirical case studies along the way e.g. [4,5] Studies reveled that organizations that manage to effectively align their business strategy with IT strategy have better outcomes than others. In other words, alignment supports organizations to increase their performance by using IT strategically [5,7]. Therefore, in today's competitive and ever growing global business environment, it is vital to consider both IT and business aspects during the development of enterprise, moreover it is more beneficial to get support from partner network and share competence and resources. Thus, in order to have effective cooperation in SMEs, there is a need for enterprises to follow dynamic structure and identify important factors for understanding dynamic business [8].

The paper organized as follows. Section 2, gives and overview of the related research on partner network, and business/IT alignment in enterprises, Section 3 describes important artefacts in dynamic business, Section 5 further presents parallel research activities.

2. RELATED RESEARCH

2.1 PARTNER NETWORK

Like most industries nowadays, manufacturers are under great pressure to deliver products in an ever growing competitive business environment. This means that companies in better financial and market position (called Focal Players (FP) are forming new networks in order to be more competitive and flexible. Building ecosystems means that the necessary companies are initially recruited among the partners and are employed as subcontractors for the necessary tasks by the FP. In case the needed competencies are not represented in the network or they are not of a sufficiently high quality, the

external companies will be asked to participate [9].

Partner Network (PN) can be defined as a group of networks that work together to enhance the capabilities of each other. The definition of PN is very close to Collaborative Network (CN) where the aim is to aligning activities so that more efficient results achieved [10].

Effective Business and IT alignment (BITA) support business organization to achieve business goals through information systems. In case of certain organizations, PN can be of great value to improve marketplace competitiveness and financial performance [11,12].

2.2 BUSINESS/IT ALIGNMENT (BITA)

In many situations there is a need to integrate enterprises, in our case aligning business and IT in PN. In such processes aligning should be fulfilled explicitly and this processes can only resolved through supportive information system tools. There are many IT management literatures that argued the need for aligning IT and business. e.g. [13,14] Having a clear relations among various levels including, "the enterprise level (strategies, process architecture etc.), the business process level (value chain, management etc.), and implementation level (IS/IT architecture, work practice etc.)", is a necessity in business and IT alignment [15]. Good alignment implements IT which is compatible with organization's business strategy, goals and specific requirements in a timely manner [16]. Although business/IT alignment is concerned as the top management issue in 2003 and 2004 and it is getting more important over the past two decades, many researchers discuss that alignment is not always desirable. Moreover, it is more theoretical and due to many unpredictable situations, it can't be successful in real life [3]. In alignment context, enterprise modeling, have been using for a long time to support business management [17]. Enterprise Modeling (EM) and business process management are commonly used to support enterprises for evaluating the existing situation as AS-IS and develop it to as TO-BE state [18,19]. Furthermore, in order to create alignment, there is a need to consider various dimensions of the enterprise architecture and relations among them. For example organization, strategies, business models, work practices, processes, and IS/IT structures [20, 21, 22].

3. IDENTIFYING INFORMATION ARTEFACTS

According to our research group analysis for BITA, it is vital to identify and document some specific business artefacts which cover valuable information to understand the business dynamics. In addition, having a successful and effective collaboration among partners requires identifying required information from enterprise perspective, which means detecting the key artifacts of information that supposed to exchange.

Our research group has access to the PN that covers more than 20 SME-s operating in electricity and oil production as well as in technology industries. Based on these analyzes the following artefacts, which needed for the company is identified:

- Customer describes and classifies both existing and potential customers,
- Business scenario, business process, process step, events, business rules describe business activity flow with different generalization levels,
- Data clusters, data elements data clusters will group a logical set of data (e.g. customer information needed to perform business process or which is exchanged between roles or through the communication channels; data elements are needed to identify some critical fields (e.g. customer name),
- Software application systems, ICT technology describes major ICT applications, which support business

processes; at the same time, it is important to know technologies, based on what the applications are developed (e.g. programming languages, database, protocols),

- Servers, network nodes, operating systems describe the infrastructure where ICT applications run;
- Risks, issues, action plans describe both all most important risks and known errors, and how to operate in those circumstances,

In addition, the following artefacts are important also to exchange within PN, as these cover valuable information to the PN members who planning to form further VO-s (see Fig 1):

- Products, business services describe products and services available for customers or partners,
- Roles, skills, organizational structure, location describe available or needed skills, their owners and these skills' physical location; Using this roles, the stakeholders can be modelled,
- Communication channels describe the way the information is being exchanged; it may include events like meeting, oral communication, as well as communication through electronic environment (e.g. teleconferences, e-mail, fax),
- Machinery/benches it is important to know which kind of machinery/ benches (e.g. lifter, excavator, track, plasma cutter, oppression bench, bender) is available in the organizations,
- Critical factors, business objectives, key performance indicators (KPI) describe business perspectives,
- Projects executive summary about previous, ongoing and further projects to make the organization attractive for the potential partners.

The importance of these artefacts for PN is that based on these, the FP will start to elect partners for the business opportunities that they have identified. Thus this information and its up-to-date status are crucial for smooth PN operation.

To make an architectural description, these artefacts are also interconnected via many-to-many connections. As known the effort to keep information up-to-date demands about amount of the information. Thus, the amount of interconnections should be minimized to keep the documentation as simple as possible. One option is proposed in Fig. 1, where most critical artefacts are emphasized.

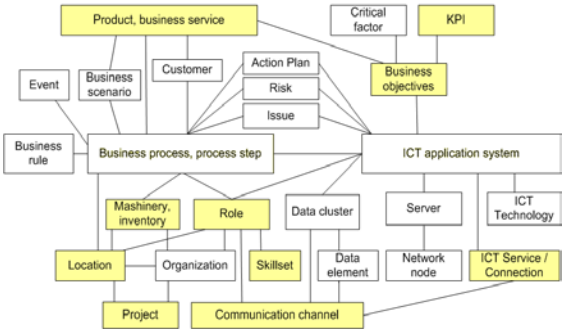

Fig.1. Identified Enterprise Key Artefacts

4. EM AS TOOLSET FOR MANAGING KEY ARTEFACTS

The effective use of information technology aligns with objective of business enterprise identified as one of the top IT management concerns since 1980. Alignment Studies reveals that alignment is a continuous process because organizations, markets, economies and technologies are constantly changing [1]. The main advantage of information technologies (IT) are supporting organization processes and organizations need but quite often IT side does not fully support business side therefore as Kaidalova et al. indicates in [23], there is a need to reduce a gap between organizational context and technology within enterprises. To achieve this, it is necessary to capture and analyze both business and IT dimensions of enterprise operation and have clear understanding about current status of business processes. There is also a need to keep track of

business changes and business redesign to stay competitive in today's dynamic business environment [24]. In this regard, EM is currently one of the most powerful and widely used facilitates alignment of business with IT [23, 24, 25].

EM is series of activities which leads to a cohesive and commonly shared model, describing different aspects of enterprise. An Enterprise Model investigate a problem domain from different viewpoints through number of related "sub-models", e.g. processes, business rules, concepts/information/data, vision/goals, and actors. Thus, understanding relations between sub-models support enterprises to discover the domain knowledge, trace components and decisions made in a coherent model [24]. One of the most common reasons to use EM is development or refinement of enterprise information system. Indeed, it is crucial for enterprise success information technology that supports business needs, processes and strategies [23]. Aversano et al. indicates in [26], in order to have a beneficial alignment it is vital to consider the following set of phases: deliberate different entities and relations among business and IT which are of great value in alignment process; Measurement of the alignment degree existing between the chosen assets for establishing if improvement actions are necessary; Evolution for improving the degree of alignment.

By the help of EM tools it is relatively easy to document these artefacts. There are several freeware tools such as Archi, Signavio, ARIS Express etc., and also a commercial tools like Troux, ARIS, QPR, Casewise etc. The valuable overview is done by Institute For Enterprise Architecture Developments [27].

5. PARALLEL RESEACH ACTIVITIES

Usually companies BITA focuses mainly for core business processes. Belonging into the PN, will extend companies need for more open communication in sense of collecting and exchanging inform concerning artefacts, which is needed to provide to PN. This is additional cost for companies participating in PN, which could be considered as part of marketing, as it promotes companies reputation inside the network. Mostly companies will be considered it as a constraint which should be taken into account when implementing new IT systems.

In addition, the most likely there are artefacts which information is not collected in a systematic way, and which are handled on the paper based approach. These artefacts management must be digitalized, which is also additional cost for companies.

The usage of these artefacts is represented with paper "Partner selection criteria for forming Virtual Organization". This paper introduces criteria which a partner should evaluate during the forming of VO selecting partners for a new project in the frame of PN.

Proposed research results are also usable for second research paper "Quality improvement methodologies for continues improvement of production processes and production quality and their evaluation".

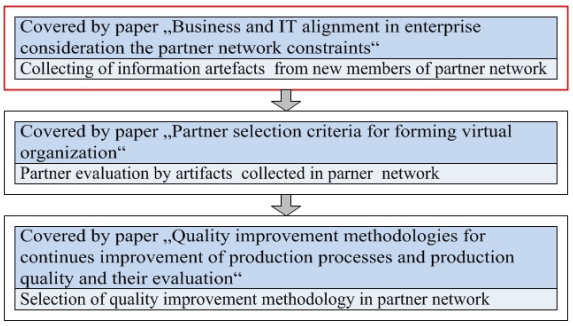

Fig.2. Related research papers

6. CONCLUSION

There are numerous small production companies in production field in Eastern Europe. Competition for market share has raised the need for closer cooperation in extending customer base and for looking for the solution to reduce the working capital within their supply chain. When

merged into the ecosystems, the velocity, visibility, scalability, innovation and cost govern are these competitive advantages, which let them compete with bigger companies. Restructuring, merging, and acquisition these are important topics in today marketplace.

The current article contributes to proposing key artefacts that should be collected by PN and explaining the concept of BITA.

As handling these artefacts is capacious, there is a need for tool which will support these artefact management.

Our team has successfully implemented Software AG tool ARIS for some of companies inside our test bench to handle EM (company in electricity production field and in company in technology industry).

ACKNOWLEDGEMENT

Hereby we would like to thank the Estonian Ministry of Education and Research by Grant ETF9460 and Estophilus which supports the research.

7. REFERENCES

1. Luftman, J., et al., Key Issues for IT Executives 2005. *MIS Quarterly Executive,*2005, **5(2)**, 81–101.

2. Polyantchikov, I. et al., Enterprise Architecture Management-Based Framework for Integration of SME into a Collaborative Network , *13th IFIP WG 5.5 Working Conference on Virtual Enterprises*, (CamarinhaMatos, eds.), Bournemouth, 2012, **380**.

3. Chan, Y. E., Reich, B. H., IT alignment: what have we learned?. *Journal of Information technology*,2007, **22(4)**, 297-315.

4. Chan, Y.E., et al., Business Strategic Orientation, Information Systems Strategic Orientation, and Strategic Alignment. *Information Systems Research,*1997, **8(2)**, 125–150.

5. De Leede, J., et al., Innovation, Improvement and Operations: An exploration of the management of alignment, *International Journal of Technology Management,2002,* **23(4)**, 353–368.

6. Chan, Y.E., et al., Antecedents and Outcomes of Strategic IS Alignment: An empirical investigation. *IEEE Transactions on Engineering Management*,2006, **51(3)**, 27–47.

7. Kramarenko, S., Shevtshenko, E., *Decision Support System for Multi-Project Cash-Flow Management, In 20th International Conference on Danube-Adria-Association-for-Automation-and-Manufacturing Symposium,* (Katalinic, B., eds.), *Annals of DAAAM and Proceedings*, Vienna, 2009, **20**.

8. Karaulova, T., et al., Re-organization of Production System on SME Enterprises, *In 20th International Danube-Adria-Association-for-Automation-and-Manufacturing*, (Katalinic, B., eds.), *Annals of DAAAM and Proceedings*, Vienna, 2009,**20**, 869-870.

9. Kangilaski, T., Challenges for SMEs entering into the virtual organization partner network. *In Proceedings of the 7th International Conference of DAAAM Baltic Industrial Engineering,*2010, 1-2.

10. Karaulova, T., et al., Knowledge management for network of enterprises, *In 17th International Symposium of the Danube-Adria-Association-for-Automation-and-Manufacturing,* (Katalinic, B., eds.), *Annals of DAAAM for 2006 & Proceedings of the 17th International DAAAM Symposium*, Austria, 2006, 197-198.

11. Maleki, M., et al., Comparative Analysis of Customer Value Dimensions. *Inzinerine Ekonomika-Engineering Economics*, **24**, 2013, 488-495.

12. Shevtshenko, E., et al. Sustainable design of material handling equipment: a win-win approach for manufacturers and customers, *Mechanika*, 2012, 561-568.

13. Lankhorst, M., Enterprise Architecture at Work Modelling, Communication, and Analysis. *Springer*, 2005.

14. Peppard J., Briding the gap between the IS organization and the rest of the business: plotting a route. *Information Systems Journal*, 2001, **11**, Issue 3, 249-270.
15. Karaulova, T., et al., Risk factors in project management life cycle, *In 6th International Conference of DAAAM Baltic Industrial Engineering*, (Kyttner, R., eds.), *Proceedings of the 6th International Conference of DAAAM Baltic Industrial Engineering*, pts 1 and 2,Tallinn 2008, 327-332.
16. Harmon, P., The Scope and Evolution of Business Process Management in vom Brocke J., Rosemann M. (Eds.). *Handbook on Business Process Management, Springer*.2010.
17. Luftman, J., Brier, T., Achieving and Sustaining Business–IT Alignment. *California Management Review*,1999, **42(1)**, 109–122.
18. Hayes J., The Theory and Practice of Change Management. *Palgrave macmillan*, 2007.
19. Karaulova, T., et al., Process Analysis and Reliability Evaluation, *In 19th International Symposium of the Danube-Adria-Association-for-Automation-and-Manufacturing*, (Katalinic, B., eds.), Annals of DAAAM and Proceedings, Slovakia, 2008, 701-702.
20. Lind M., Seigerroth U., Collaborative Process Modeling: The Intersport Case Study, in vom Brocke J., Rosemann M. (Eds.). *The International Handbook on Business Process Management, Springer*, 2010.
21. Lind M., Seigerroth U., A Multi-Layered Approach to Business and IT Alignment. *Hawaii International Conference on System Sciences* (HICSS43), Hawaii 2010, 5-8.
22. Karaulova, T., Otto, T., Development of database of business processes for SME on the base of quality system, *In 16th International Symposium of the Danube-Adria-Association-for-Automation-and-Manufacturing*,(Katalinic, B., eds.), Annals of DAAAM for 2005 & Proceedings of the 16th International DAAAM Symposium, Croatia, 2005, 179-180.
23. Kaidalova, J., et al., Practical Challenges of Enterprise Modeling in the Light of Business and IT Alignment. In The Practice of Enterprise Modeling, *Springer*,.Berlin Heidelberg, 2012, 31-45.
24. Stirna, J., Persson, A., Anti-patterns as a Means of Focusing on Critical Quality Aspects in Enterprise Modeling. In: Halpin, T., Krogstie, J., Nurcan, S., Proper, E., Schmidt, R., Soffer, P., Ukor, R. (eds.) BPMDS 2009 and EMMSAD 2009, LNBIP 29. *Springer*, Heidelberg, 407-418.
25. Seigerroth, U., Enterprise Modelling and Enterprise Architecture: the constituents of transformation and alignment of Business and IT. *International journal of IT/Business Alignment and Governance* (IJITBAG), 2011, **2,** ISSN 1947-9611.
26. Aversano, L., et al., A literature review of Business/IT Alignment Strategies. In Enterprise Information Systems, 2013, *Springer*, Berlin Heidelberg, 471-488
27. Institute For Enterprise Architecture Developments: Enterprise Architecture Tool Selection Guide v6.3, 2011, 25p.

8. ADDITIONAL DATA ABOUT AUTHORS

Taivo Kangilaski
Tallinn University of Technology, Department of Computer Control; Ehitajate tee 5, 19086, Tallinn, Estonia.
Email: taivo.kangilaski@dcc.ttu.ee

Atiyeh Vaezipour
School of Engineering, Jönköping University; P.O. Box 1026; 55111 Jönköping, Sweden.
Email: atiyeh.vaezipour@gmail.com

III MECHATRONICS AND SYSTEM ENGINEERING

9th International DAAAM Baltic Conference
"INDUSTRIAL ENGINEERING"
24-26 April 2014, Tallinn, Estonia

UNCERTAINTY EVALUATION OF ANGLE MEASUREMENTS BY USING 3D COORDINATE MEASURING MACHINE

Dhoska, K.; Kübarsepp, T. & Hermaste, A.

Abstract: *The accurate method for angle measurements of a complicated geometrical object has been elaborated by using Moving Bridge TESA MICRO-HITE 3D Coordinate Measuring Machine (CMM). This type of 3D CMM allow high accuracy measurements of complicated geometric objects with resolution 0.0001 mm. The measurements were conducted for machined mechanical parts of a three element optical photodetector where each element is aligned at incidence angle close to 45^o. The measurement method and standard uncertainty estimation of measured angles for the photodetector are briefly described in this paper.*
Key words: Coordinate Measuring Machine, metrology, angle measurement, standard uncertainty.

1. INTRODUCTION

In industrial manufacturing, inspection process is usually carried out for assuring and controlling quality of a product. Before manufacturing in serial line the product is subjected to verification of the geometric features, dimensions and tolerance specifications with respect to the product design specifications. For that purpose reliable measurement methods including justified uncertainty estimates are used or developed. Our research group has elaborated accurate method for angle measurements of a complicated geometrical object by using Moving Bridge TESA MICRO-HITE 3D CMM. This type of 3D CMM allow high accuracy measurements of complicated geometric objects with higher resolution. The measurements were conducted for machined mechanical parts of a three element optical photodetector where each element is aligned at incidence angle close to 45º as shown in Fig. 1.

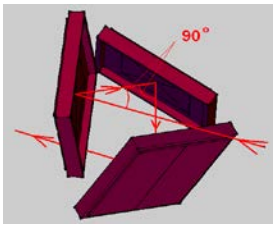

Fig. 1. Scheme of three photodiodes aligned in the photodetector. The beam indicating optical path between the centres of photodiodes is shown as arrowed line.

The measurement method and standard uncertainty estimation of measured angles for the photodetector are briefly described in this paper.

2. THEORETICAL BACKGROUND

The reliability of angle measurements realized in 3D CMM can be performed by establishing the traceability to the international standards as shown in Fig. 2.

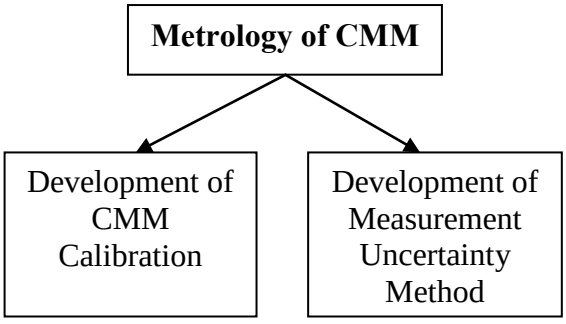

Fig. 2. Traceability arrangement for angle measurements by 3D CMM

The series standard ISO 10360 gives the guide and instruction for technical requirements for the calibration of CMM [1]. Based on the standards ISO 10360-2 (measuring errors for linear dimensions) and ISO 10360-5 (contact probing error) we have adopted the simplified case of these standards [2, 3]. The reason is that we have not considered all the volume of machine but only the volume where the measurements were carried out. The linear statistical behaviour model of 3D CMM could be used for estimation of the measurement uncertainty and in investigating the errors of this machine accompanied with orientation and length in working volume. Referring to this model and in order to take into account various influencing sources we have employed the evaluation of uncertainty of the distance between two points [4]:

$$L = \sqrt{(x_2 - x_1)^2 + (y_2 - y_1)^2 + (z_2 - z_1)^2}\ . \quad (1)$$

The angle between two points is estimated as:

$$\cos\alpha = \frac{x_2 - x_1}{\sqrt{(x_2 - x_1)^2 + (y_2 - y_1)^2 + (z_2 - z_1)^2}}$$

$$\cos\beta = \frac{y_2 - y_1}{\sqrt{(x_2 - x_1)^2 + (y_2 - y_1)^2 + (z_2 - z_1)^2}} \quad (2)$$

$$\cos\gamma = \frac{z_2 - z_1}{\sqrt{(x_2 - x_1)^2 + (y_2 - y_1)^2 + (z_2 - z_1)^2}}$$

Furthermore, uncertainty of the distance is expressed in Equation (3):

$$u^2(L) = L^2 \frac{E_k^2}{3} + \frac{E_G^2}{3} + \frac{R^2}{3}, \quad (3)$$

where E_k and E_G are the parameters based on the specifications of the 3D CMM. The first parameter is related to the maximum permissible measuring error of the linear spatial diagonal of the measuring volume and the second parameter is related to the maximum permissible probing error. R is the resolution of the machine.

In the section four we have evaluated the other possible sources of uncertainties that can influence in angle measurements results, also. Based in our simplified case the other sources of uncertainties are calibration of the 3D CMM, probing error, reading of indication and repeatability of the measurements results.

3. MEASUREMENT METHOD

The Moving Bridge TESA MICRO-HITE 3D CMM is located to the laboratory of the Faculty of Mechanical Engineering at Tallinn University of Technology. This is high accuracy 3D CMM as shown in Fig. 3.

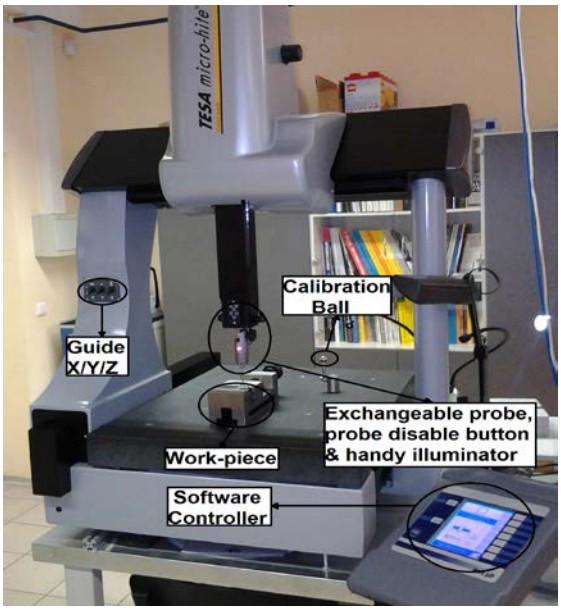

Fig. 3. Schematic view of Moving Bridge TESA MICRO-HITE 3D CMM.

The measuring range (X/Y/Z) of the machine is equal to 460 mm x 510 mm x 420 mm with resolution 0.0001 mm where the controlled temperature of the environment during measurements was 20 ± 1.1 ^{o}C as can be referred to the specifications of the machine. A function of 3D CMM consist in a probing system that can measure the coordinates by contacting the surface of the work piece and a guide to linearity transfer the probing system along the X, Y and Z axes that can run at determined angles to each other. The offset triangular bridge design provides a low center of gravity and optimum stiffness-to-mass ratio. Air bearings ensure frictionless motion in all three axes [5]. The 3D CMM is connected with software to

control the coordinate transformation and the measuring machine. Interactive TESA REFLEX™ software allows performing complex inspection routines quickly and efficiently.
Measurement method for determination the angle of three-element photo-detector is complicated as shown in Fig. 4.

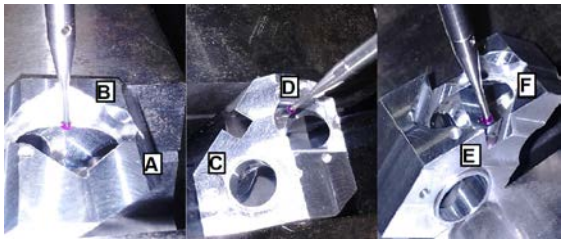

Fig. 4. Illustration of the measurement method for determination of the angle of three-element photo-detector realized by TESA MICRO-HITE 3D CMM

Before starting angle measurements of the planes we have placed three element photodetector in work-piece and calibrated touching probe at calibration ball of the machine. As can be seen in Fig. 3, the touching probe was mounted in vertical positions under 0^o angle and the calibration was realized on the distributed points around the calibration ball. Based on manual of the machine for having accurate positions of the touching probe we have used the criteria of the distributed points which should be not less than six points. Afterward the successful calibration position would be shown in the display of the software controller and being ready for starting measurements.
In the measurements, angles were determined between pairs of planes AB, CD an EF. The planes denoted as A, C and E were used as reference planes. The planes B, D, and F were assumed to be parallel with the planes of photodiode active surfaces (Fig. 1), i.e. close to 45^o in respect to reference planes. First, the reference plane A, C or E was fixed and the angle between reference plane and indicated plane was measured by using touching probe system with diameter 2 mm. The measurements were conducted on distributed points across the indicated planes to cover as uniformly as possible each entire plane. The number of the readings taken during measurements for each angle plane was ten.
By using our method angle measurements of geometrical objects with complicated shape can be performed at high accuracy, as demonstrated on three element photodetector body part with approximate size of 40 mm x 32 mm x 32 mm.

4. UNCERTAINTY OF ANGLE MEASUREMENT

The versatility that allows 3D CMM to inspect a wide range of features and part types makes evaluating the measurement uncertainty a multifaceted problem [6]. For this reason we have used simplified case of these standards where a Guide to the Expression of Uncertainty in Measurement (GUM) establishes general rules for identifying measurement variability (sources of uncertainty) and evaluating measurement uncertainty [7]. Before starting an evaluation of uncertainty, we have defined angle measurement model by taking into account influence sources which can be expressed as:

$$y = x + K_{CAL} + K_{PROB} + K_{READ} + \\ + K_{REP} + K_L \qquad (4)$$

where x is the measurement value of the angle, K_{CAL} is the correction from calibration of 3D CMM, K_{PROB} is correction that arise from probing error, K_{READ} is the correction from reading of indication, K_{REP} is correction that arise from repeatability and K_L is the correction from distance between two points.
Based on the law propagation of uncertainty and uncertainty of input quantities we can evaluate combined uncertainty as expressed below:

$$u_c^{\,2}(y) = \sum_{i=1}^{n} \left(\frac{df}{dx}\right)^2 \cdot u^2(x_i), \qquad (5)$$

where $u(x_i)$ is standard uncertainty of the input quantities and $c_i = df/dx$ is sensitivity coefficient.

The combined uncertainty could be expressed as:

$$u_c^{\,2}(y) = c_1^2 \cdot u_{CAL}^2 + c_2^2 \cdot u_{PROB}^2 + c_3^2 \cdot u_{READ}^2 + \\ + c_4^2 \cdot u_{REP}^2 + c_5^2 \cdot u_L^2 \quad (6)$$

where u_{CAL} is calibration uncertainty of the machine, u_{PROB} is probing error uncertainty, u_{READ} is standard uncertainty of the readings, u_{REP} is repeatability of the two series of standard uncertainty, u_L is uncertainty of the distance which is expressed in equation (3).

As the calibration uncertainty contribution, the specifications of the 3D CMM as is used

$$u_{CAL} = \frac{U_{CAL}}{k}, \quad (7)$$

where U_{CAL} is expanded calibration uncertainty of the machine with coverage factor $k = 2$.

Uncertainty due to probing error is expressed as

$$u^2{}_{PROB} = u^2{}_F, \quad (8)$$

where u_F is standard uncertainty of the form error which is calculated directly from 3D CMM.

The standard uncertainty due to the reading of indications of the angle measurements is calculated as standard deviation (S_x) of the readings, expressed as

$$u_{READ}^2 = S_x^2. \quad (9)$$

The standard uncertainty due to repeatability is calculated from two series of the standard uncertainty of readings as shown in equation (10)

$$u^2{}_{REP} = \frac{u^2{}_{READ1} + u^2{}_{READ2}}{2}. \quad (10)$$

The sensitivity coefficient was calculated from equation (2). The maximum partial derivate was chosen from:

$\frac{d(\cos\alpha)}{dx}$; $\frac{d(\cos\alpha)}{dy}$ and $\frac{d(\cos\alpha)}{dz}$ as sensitivity coefficient used in Table 1.

In the end we can evaluate combined standard uncertainties $u_C(y)$ in accordance with simplified equations (6) and expanded uncertainty U is obtained through multiplication by a coverage factor, $k = 2$, as expressed in below equation

$$U = k \cdot u_C(y). \quad (11)$$

Furthermore by using above equations we can summarize in table 1 all the sources of uncertainties associated with their values and in table 2 estimated values with expanded uncertainty for each angle of the optical three element photodetector.

As can be seen, the larger uncertainty components arise from the reading of indication and repeatability between two series. The non-uniform plane can be influenced strongly in repeatability of the angle measurements.

Source of Uncertainty	Standard Uncertainty	Probability Distribution	Sensitivity Coefficient	Uncertainty [°]
Calibration	$7.9 \cdot 10^{-2}$ [mm]	normal	$1.7 \cdot 10^{-2}$ [°/mm]	$1.4 \cdot 10^{-3}$
Probing error	$2 \cdot 10^{-3}$ [mm]	normal	$1.7 \cdot 10^{-2}$ [°/mm]	$3.4 \cdot 10^{-5}$
Readings	$3.5 \cdot 10^{-2}$ [°]	normal	1.0	$3.5 \cdot 10^{-2}$
Repeatability	$4.8 \cdot 10^{-2}$ [°]	normal	1.0	$4.8 \cdot 10^{-2}$
Distance	$7.8 \cdot 10^{-2}$ [mm]	rectangular	$1.7 \cdot 10^{-2}$ [°/mm]	$1.3 \cdot 10^{-3}$
Combined uncertainty, *k=1*				$5.9 \cdot 10^{-2}$
Expanded uncertainty, *k=2*				$1.2 \cdot 10^{-1}$

Table 1. Sources of uncertainties associated with their values.

Angle	Estimated Value [^{o}]	Expanded uncertainty [^{o}]
∠AB	45.11	0.12
∠CD	44.96	0.12
∠EF	45.08	0.12

Table 2. Estimations of angle measurements associated with expanded uncertainty.

The estimated results in above tables of the angle measurements have shown that expanded uncertainty of 45^o (approximate value) angle measurements was 0.12^o.

5. CONCLUSIONS

The accurate method and uncertainty estimation of the angle measurement have been realized by using Moving Bridge TESA MICRO-HITE 3D CMM. The accuracy of the angle measurement result can be extracted through evaluation of the measurement uncertainty. The linear statistical model and GUM have been used for evaluation of the measurement uncertainty in accordance with the series standards ISO 10360 [1-3].

The novelty of this research work is that our angle measurement method associated with their uncertainty can be used for complicated geometrical object measured by 3D CMM at high accuracy.

The method was tested with three element photodetector manufactured body part with size approximately 40 mm x 32 mm x 32 mm. The expanded uncertainty of 45^o angle measurements was 0.12^o. The further studies would reveal whether this method can be applied for any angle measurement with lower uncertainty.

The thorough uncertainty analyses show that the larger uncertainty components arise from reading of indication and repeatability of the measurements results.

6. REFERENCES

1. *ISO 10360.* Geometrical Product Specifications (GPS)—acceptance and re-verification tests for coordinate measuring machines (CMM). Switzerland; 2001

2. *ISO 10360-2:2009.* Geometrical product specifications (GPS) -- Acceptance and reverification tests for coordinate measuring machines (CMM) -- Part 2: CMMs used for measuring linear dimensions.

3. *ISO 10360-5:2010.* Geometrical product specifications (GPS) -- Acceptance and reverification tests for coordinate measuring machines (CMM) -- Part 5: CMMs using single and multiple stylus contacting probing systems.

4. R. D'Amato, J. Caja, P. Maresca, E. Gómez, Use of coordinate measuring machine to measure angles by geometric characterization of perpendicular planes-Estimating uncertainty, *Measurement*, 2014, **47**, 598–606.

5. TESA MICRO-HITE 3D Coordinate Measuring Machine Brochure, http://www.primetechsales.com/uploads/Brochure_MicroHite_3D.pdf

6. S.D Phillips, B. Borchardt, W.T Estler, John Buttress, The estimation of measurement uncertainty of small circular features measured by coordinate measuring machines, *Precision Engineering*, 1998, **22**, 87-97.

7. *ISO/IEC Guide 98:1995.* Guide to the expression of uncertainty in measurement (GUM). International Organization for Standardization: Geneva.

7. ADDITIONAL DATA ABOUT AUTHORS

Klodian Dhoska, doctoral student,
Department of Mechatronics, Tallinn University of Technology, Ehitajate tee 5, 19086, Estonia.
Email: klodian.dhoska@ttu.ee.
Tel: +372 620 3211.

9th International DAAAM Baltic Conference
"INDUSTRIAL ENGINEERING -
24-26 April 2014, Tallinn, Estonia

DEVICE FOR MUSCLE COORDINATION IMPROVEMENT

Gorordo, I.; Mäntylä, J.; Popkov, A.; Saastamoinen, J.; Sepponen, R.; Kiviluoma, P. & Kuosmanen, P.

Abstract: *Currently devices for improving muscle coordination are mainly installed in hospitals and used for rehabilitation after an injury. These devices are relatively expensive and are not publicly available for a wide range of users. A simpler and cheaper device would enable more common use of neuromuscular training. Especially senior adults would benefit from this kind of exercise. The device presented in this study is designed for training of the biceps and shoulder muscles. The coordination improvement is obtained by applying controlled resistance which can be adjusted according to the needs of an individual user.*
Key words: Muscle coordination, neuromuscular control loop, free motion.

1. INTRODUCTION

The lack of regular exercise or physical inactivity has been proved to have a relevant effect on the progression of many chronic diseases but even more important in the case of elderly people [1]. Exercise is also beneficial for improving quality of life, balance, and reducing the risk of falls [2]. One of the most common recommended exercises to improve arm muscle strength and coordination is small weight lifting. The problem with this kind of training is that the safety of the user is not guaranteed. Once the exerciser cannot handle the weight, it may end falling or hurting the muscles and the joint of the user. Also, in this kind of exercise the load cannot be altered. For different weights various dumbbells will be needed.

Fig. 1. Biodex System 4 Pro [3] isokinetic dynamometer is used for training joints.

Other similar devices such as isokinetic dynamometers (Fig. 1), provide constant velocity in the exercised extremity with variable resistance throughout a joint's range of motion. In the case of the elbow joint ranges from 0° to 120° [4]. This resistance is provided using an electric or hydraulic servo-controlled mechanism at a user-defined constant velocity [5].
The term 'isokinetic' is defined as the dynamic muscular contraction when the velocity is controlled and kept constant. Because of the biomechanical properties of the musculoskeletal system, the muscular force varies at different joint angles, offering optimal loading of the muscles in dynamic conditions [6]. Furthermore, unlike gravity loaded systems, this kind of exercise does not store potential energy providing safe training to the user [6]. The problem with this kind of equipment is that they are mainly designed for hospitals and mostly used for rehabilitation after an injury. For this reason, usually they are big,

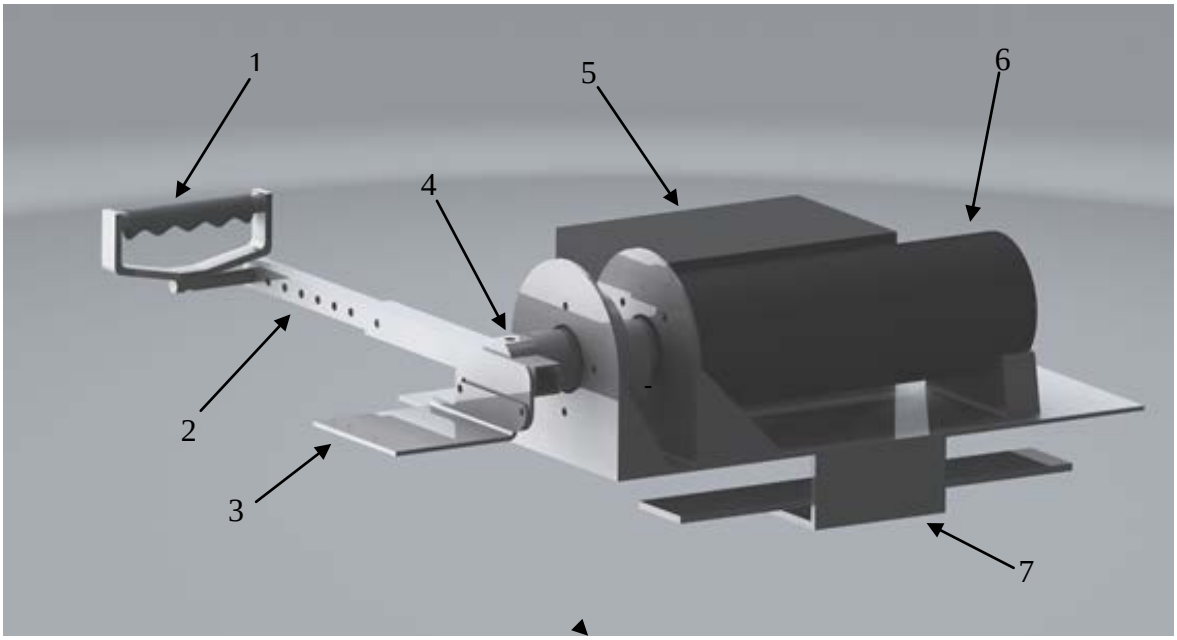

Fig. 2. Mechanical architecture of the device: 1. handle, 2. arm, 3. arm support, 4. arm and motor connector, 5. power supply, 6. DC motor, 7. clamps

expensive and not easily movable, limiting their accessibility for daily exercise. The implementation of simpler and cheaper devices would allow daily neuromuscular training for senior adults.

The presented device in this research uses either variable or static resistance to train neuromuscular system on the biceps and shoulder muscles. Using the device regularly will improve coordination while performing daily actions of elderly people, enhancing their quality of life. Overall, the reduced size of the machine and its adaptability to different users enables a wider range of users, not only for hospital or rehabilitation purposes.

2. METHODS

Device uses a geared DC motor for generating the load, which is applied to the user by a mechanical handle (Fig. 2). Motor is driven with an H-bridge circuit controlled with a Pulse Width Modulated (PWM) signal by the microcontroller. Feedback from the motion is measured with optical pulse encoder from the shaft of the motor.

The control logic for the load consists of different operating modes (Table 1). All of them prevent any rapid movements or loss of stability of the arm. The handle can be safely released anytime without leading to any dangerous movements. In the so called zero position, where the user doesn't apply any torque to arm, it stays in place. No torque is applied by the motor. When the user starts to turn the handle the torque steadily increases, until the maximum torque, depending on the settings and operating mode, is achieved. Handle will continue rotating with constant torque over this point. If the user can't hold the handle or lets it turn back, the torque is steadily reduced until the handle has rotated back for a predetermined angle. This doesn't mean the handle rotates back to the same zero position where the movement began, but the zero position follows the rotation. This way, the handle always rotates back just a little and the load stays safe. Even when the handle is completely released, it only rotates back about the same amount. This kind of operation ensures the safety of the exercise, unlike the small weight lifting where the weight drops if released.

In the simplest 'static' operating mode, the torque on the handle stays on a constant value which can be adjusted with one of the potentiometers. In the 'dynamic' operating mode the load consists of static part and the dynamic part which are summed together. The dynamic part of the load is basically a sinusoidal signal of which frequency and percentage of the total load can be adjusted with potentiometers. The third operating mode, 'external' uses an analog input where load can be applied as an analog voltage between 0 to 5 Volts. This option makes it possible to vary load for example with music. The waveform is extracted from the analog signal and it is used to generate the load for the handle. The amplitude of the load as well as the percentage of the dynamic part of the load can be adjusted with potentiometers just like in the case of the 'dynamic' operating mode.

Mode	Description	Variables
Static	Adjustable but constant load.	The value of the load
Dynamic	The load is variable according to a sinusoidal wave.	The amplitude and frequency of the wave.
External input	The variation of the load is taken from an external analog signal.	The amplitude and the frequency of the signal.

Table 1. Summary of the different modes and the adjustable variables.

The built prototype has a simple interface for adjusting the load according to the needs of the user. This interface consists of three potentiometers, a switch and a liquid crystal display (LCD). The switch is used for selecting the operating mode. The active mode and all the user adjustable parameters are shown in the LCD. One potentiometer sets the upper limit of total load and in 'static' mode this is the only parameter that is needed to adjust. Second potentiometer adjusts the percentage of the dynamic part of the total load. Finally, the third one adjusts the frequency of the sinusoidal signal in the 'dynamic' operating mode.

The use of dynamic load instead of static one, when training body has been studied several times, but literature shows [7] that there is not a clear neuromuscular improvement on dynamic load compared with static training. Yet, some of the researches showed that the use of low frequency (30-50Hz) vibration may have an acute outcome in vibration training [7]. This is the reason why it was decided to keep both options available, including a third different option which would help train also the memory of the user.

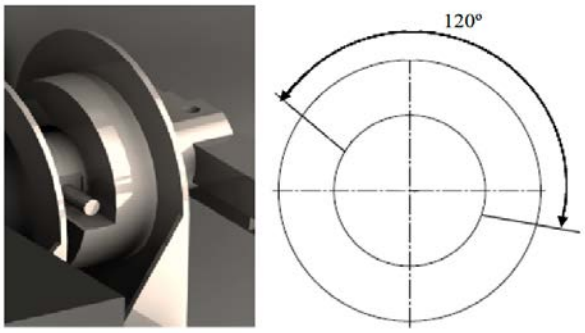

Fig. 3. Mechanical limit switch to ensure user's safety.

The control logic ensures that the applied load always stays stable and safe, but in case of failure, there are both electrical and mechanical limits for protecting the user (Fig. 3). Electrical limits force the H-bridge control signals to OFF state in case of the failure of the microcontroller. This prevents the handle to turn to unsafe angles. In addition, there are also mechanical limits that make it impossible to turn handle to angles where the user could get hurt.

The actual device is designed to be compact and easy to move. The actual mechanical structure has two separate functions. First, it has to be able to transfer torque of the DC motor to the arm of the trainer. The second task is to support and

make sure that the device does not move while exercising with the device fastened to the table.

Transferring the motion to the trainers arm is made by using extension of the shaft, extra bearing, support of the arm and the handle. The most visible of those parts is the handle. The length of the arm can be adjusted to fit the trainer's dimension. The support of the arm is made so that the angle can be modified, which ensures that the arm rests along the whole support, distributing the resistance force uniformly.

The mounting of the motor can be performed by clamps or bolts. The clamps are designed to able safe mounting to different kind of tables. The robust and heavy structure of the device ensures safe training.

One challenge of the mechanical design is to ensure that the range of the motion is wide enough. The DC motor is lifted over the base plate to make sure that the training angle is not too limited. So, the movement of the arm is limited in the other end by the table, but in the other end movement is limited by the trainer. Trainer can control the length of the rotation movement by adjusting the position compared to device. Therefore the seat height is one key parameter that is affecting to the training experience. The height of the table has to be taken into account when choosing the place for the device.

3. RESULTS

The equivalent mass resistance generated by the motor were measured with a force sensor placed between the handle and the flat surface, so that the sensor measured the force generated by the motor. Actual force needed to rotate the motor varies depending of the distance between the axle and the handle.

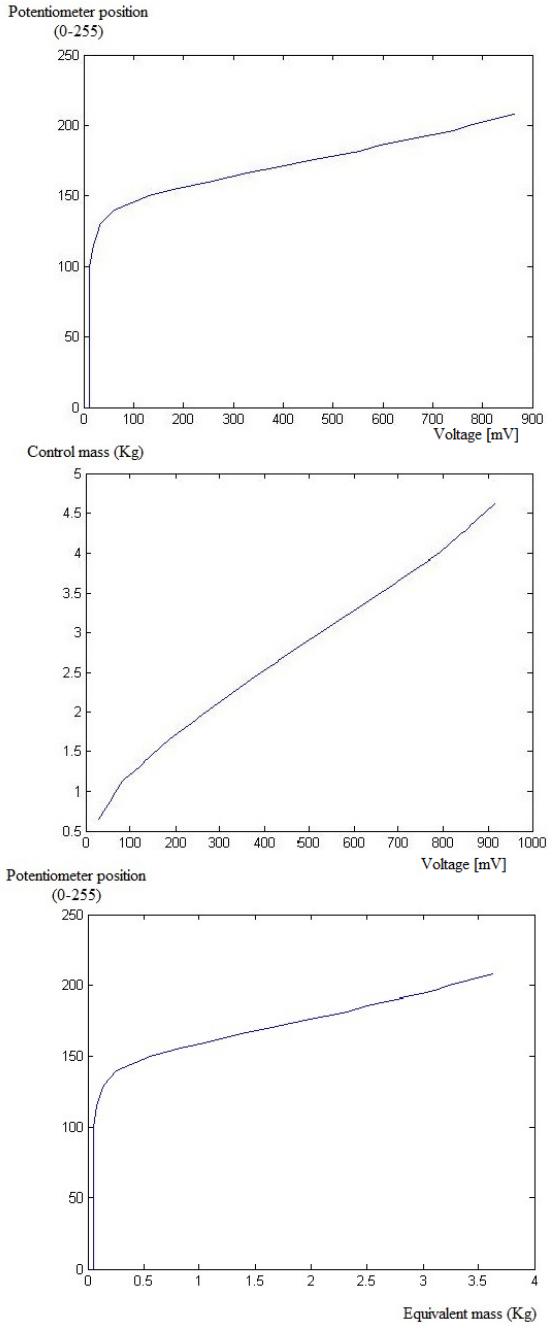

Fig. 4. Measurements for the static mode. First, the measured values by the sensor in mV, next the read values with the control masses and finally the conversion of the read values to kilograms.

The measurements were made using estimated average distance. To be able to convert the measured values into equivalent mass values, different control masses were used and measured with the force sensor as

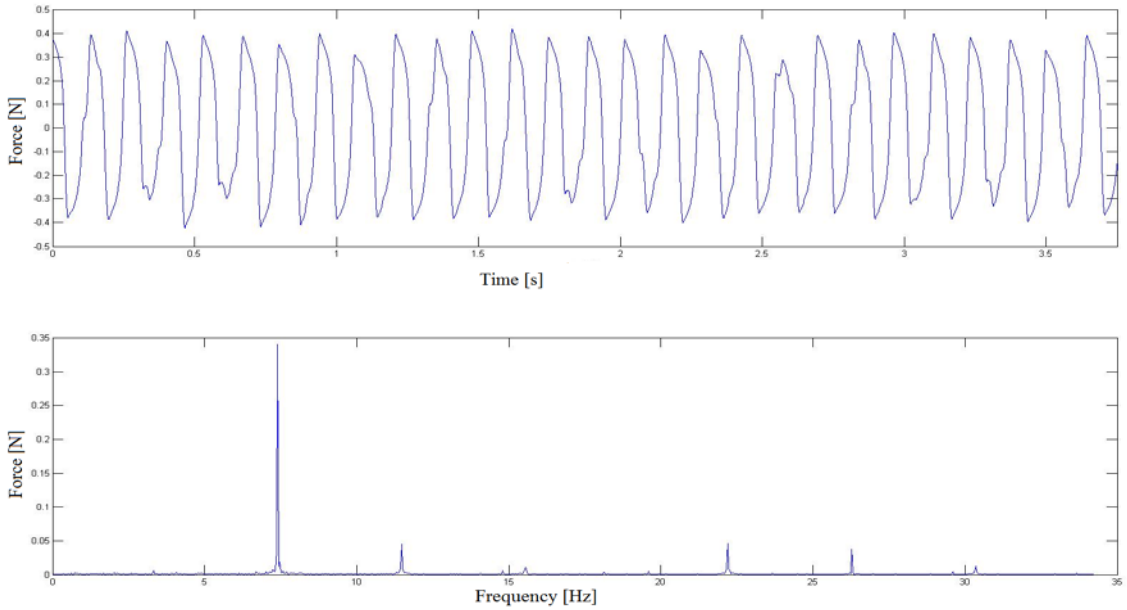

Fig. 5. Measured values in the dynamic mode with a 7 Hz frequency signal

shown in Figure 4. Also in Figure 4 the load values for the different positions of the potentiometer after the conversion are shown. Those values represent equivalence of the load to the free dumbbell (when arm is in the horizontal position). The minimum load is aprroximately 0.4 kg and the maximum about 4 kg. The maximum torque of the motor is limited by power supply. The maximum torque can be increased by changing more powerful power supply, which enables using modified construction to larger muscle groups. The minimum load is determined by the resistant torque of the gearbox, bearings etc.

In Figure 5, the upper graphic shows the measured force by the force sensor. The frequency of the dynamic signal is 7 Hz, which can be seen as a main signal on the graphic below along with other different frequency signals produced by some disturbances in the measured values.

4. DISCUSSION AND CONCLUSION

The described prototype demonstrates to be a beneficial alternative to the actual arm muscle exercise machines. The device provides both enough resistance (max. 4 kg) to work the muscles and the possibility to modify the variable load according to the user to improve the neuromuscular system.

In the measurements the accuracy of the sensor may have altered the real resistance provided by the motor. The quality of the gearbox and the alignment of the shaft may have affected the accuracy, as well.

The prototype could be redesigned to reduce the size and the actual 12 kg mass of the machine. Not only the motor and the power supply are oversized, the mechanical structure is designed to be made out of steel. Other materials such as aluminium could be used and the sizing of the elements could be optimized. Nevertheless, it is proved that smaller and cheaper devices could be developed for daily muscle exercise by elderly rather than isokinetic dynamometers or dumbbells.

Further development could be done to implement other technology to improve the experience of the user. Technologies such as connecting the movement of the arm to a visual interface, for example a game where the user should have to keep a point in the middle of a circle by trying to move the arm with a constant velocity. Other option will be to link the movement with music, that way the load will follow the music so the user will be able to predict when should apply more or less force to continue the movement steadily. These implementations will be beneficial to train not only the body but also the memory of the user.

Similar devices could be designed to exercise other parts of the body (e.g. legs or hip), helping elder people with some issues such as stability while standing or reducing the risk of falls.

5. REFERENCES

1. Roberts, CK. Barnard, RJ. Effects of exercise and diet on chronic disease. J Appl. Physiol. 2005, 98, 3–30.

2. Papaioannou, A. Adachi, JD. Winegard, K. Ferko, N. Parkinson, W. Cook, RJ. Webber, C. McCartney, N. Efficacy of home-based exercise for improving quality of life among elderly women with symptomatic osteoporosis-related vertebral fractures, Osteoporos Int. 2003,14,677–682.

3,Biodex System 4 Pro, http://www.biodex.com/physical-medicine/products/dynamometers/system-4-pro (10.3.2014)

4. Vasen, A. Lacey, S. Keith, M. Shaffer, J. Functional range of motion of the elbow. The Journal of Hand Surgery 1995, 20, 288-292.

5. Drouin, JM. Valovich-mcLeod, TC. Shultz, SJ. Gansneder, BM. Perrin, DH. Reliability and validity of the Biodex system 3 pro isokinetic dynamometer velocity, torque and position measurements. European Journal of Applied Physiology 2004, 91,22-9.

6. Baltzopoulos, V. Brodie, DA. Isokinetic Dynamometry Applications and Limitations. Sports Medicine 1989, 8 (2), 101-116.

7.Luo, J. Mcnamara, B. Moran, K. The use of vibration training to enhance muscle strength and power. Sports Medicine 2005, 35, 23-41.

6. CORRESPONDING ADDRESS

Panu Kiviluoma, D.Sc. (Tech.)
Aalto University School of Engineering, Department of Engineering Design and Production
P.O. Box 14100
00076 Aalto, Finland
Phone: +358 50 433 8661
E-mail: panu.kiviluoma@aalto.fi
http://edp.aalto.fi/en/

7. ADDITIONAL DATA ABOUT AUTHORS

Gorordo, Ibai, B.Sc
Phone: +358 414919686
E-mail: ibai.gorordo@hotmail.com

Mäntylä, Jesse, B.Sc
Phone: +358 504921123
E-mail: jesse.mantyla@aalto.fi

Popkov, Alexander, B.Sc
Phone: +358 44 7677843
E-mail: alexander.popkov@aalto.fi

Saastamoinen, Joel, B.Sc
Phone: +358 408468403
E-mail: joel.saastamoinen@aalto.fi

Sepponen, Raimo, D.Sc. (Tech.), Professor
E-mail: raimo.sepponen@aalto.fi

Kuosmanen, Petri, D.Sc. (Tech.), Professor
Phone: +358 500 448 481
E-mail: petri.kuosmanen@aalto.fi

9th International DAAAM Baltic Conference
INDUSTRIAL ENGINEERING
24-26 April 2014, Tallinn, Estonia

TRACEABILITY FOR ROUNDNESS MEASUREMENTS OF ROLLS - European Metrology Research Programme, project No. IND62

B. Hemming, T. Widmaier, I. Palosuo, V-P Esala, P. Laukkanen, L. Lillepea, K. Simson, D. Brabandt, J. Haikio

Abstract: *The roundness of rolls is critical for the operation of the paper machines and for the rolling mills in the steel industry. Therefore the rolls are periodically reground and roundness measurements are made throughout the grinding process. During the last decades several manufacturers have developed measurement systems for large rolls of diameter 500 to 2000 mm. The multi-point measurement algorithms of the systems are typically based on measurement algorithm by Ozono. The advantage of this method is that it can separate the movement and the geometry of the measured rotor, i.e., roll. From a metrological and quality perspective every serious measurement should be traceable and every measurement result reported together with an estimation of measurement uncertainty. Therefore, calibration discs are developed and traceable calibrated in laboratories of MIKES and Metrosert with a known measurement uncertainty. By measuring these standards by multi-point roundness instruments in industry new procedures to get traceability for roundness measurements of rolls, will be developed.*

Keywords: metrology, roll, roundness, calibration

1. INTRODUCTION

Roundness is an important feature for all rotating machines where smooth rotation of the rotors or even surface quality and even thickness of the end product is needed, such as paper machines, printing machines, engines and generators etc. In length measurements diameter is often measured as a two point measurement which is affected by out of roundness of the part. Therefore measurements of roundness are also useful when the specific diameter is critical or important.

In paper mills the roundness measurements are commonly carried out when the roll is located on a lathe or on a grinding machine (Fig. 1). There the heavy rolls are rotating with their own bearings or they are supported by sliding pads. With this measurement setup it is difficult to avoid a rotational error of the centreline of the roll, and thus one or two point measurement methods cannot separate the rotational error movement of the workpiece from its geometry. This is the reason for the usage of multi point measurement devices in the paper industry [1]. Most of them are based on the Ozono[2] method.

In the steel industry the roundness tolerances of the rolls are not as tight as in the paper industry, and thus the common measurement device there is a two point measurement device. [3-6].

The reliability of a measurement instrument is ensured by calibration. Ideally the calibration is performed using traceable calibrated measurement standards with a stated calibration uncertainty for the given reference values.

Fig. 1. Four point roll measuring device of a grinding machine.[1]

This gives the possibility for the end user to make traceable measurements with a known measurement uncertainty. As a part of an EMRP project "Traceable in-process dimensional measurement" calibration discs are developed and manufactured. The design of these discs is presented in this paper. The evaluation of measurement uncertainty will be presented in a future paper.

2. MATERIAL ROUNDNESS STANDARDS

Roundness material standards are needed when calibrating a roundness measuring device. There are two main categories of standards:

- standards with nearly zero roundness error
- sensitivity standards or magnification standards with intended form error

Typically the size of parts which need to be measured at high accuracy have diameters in the range 1 to 500 mm. This means that most measurement equipment are built for this range and as a result from this is that roundness standards have nominal diameters in the range 20 to 100 mm. In Fig. 2 a typical laboratory roundness measurement setup is shown. The standards used in metrology laboratories are too small to be used to calibrate large roundness instrument intended for diameters at several meters. Therefore the needs of industry are not met by existing roundness standards.

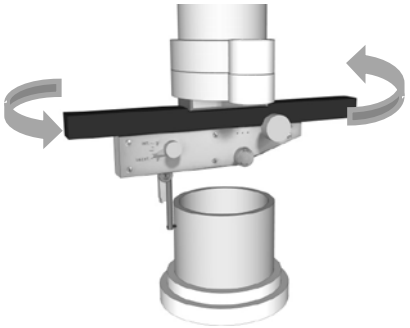
Fig. 2. Measurement of roundness.

2.1. Hemispheres

In roundness metrology glass hemispheres are manufactured to be as round as possible (Fig. 3). Typically they have roundness errors in the range of some tens of nanometres. They reveal radial errors in the rotation or axial reference for the roundness measurement.

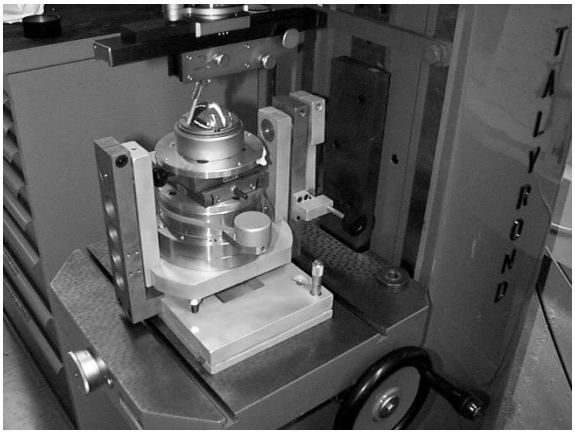

Fig. 3. A hemisphere at a roundness measurement instrument.

2.2. Flick standards

Flick standards are cylinders with a flat part (Fig. 4). The flat feature of the otherwise round cylinder makes an inward out of roundness. The magnification error or sensitivity of a roundness instrument can be calibrated by measuring the Flick standard. Flick standards can be compared to gauge blocks. Similarly to the typical use of gauge blocks, one or two standards are not

[1] RollResearch Int. Ltd.

enough and quite a large set of Flick standards is needed to check the magnification error of a roundness instrument. Although the geometry of a Flick looks simple it is non-trivial to calibrate [7].

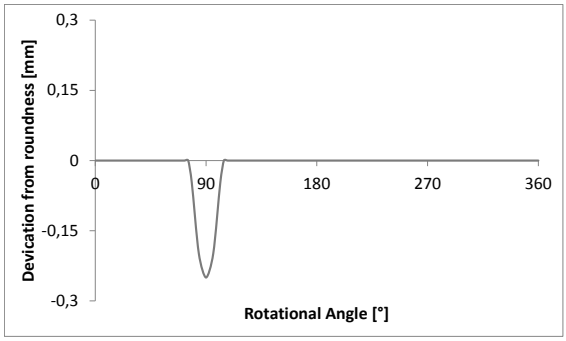

Fig. 4. Flick standard[2] above and below deviation from roundness.

All Flick standards are of plug-type intended for external measurement. In all roundness measurements the selection of filter affects the results and this is especially true for Flicks. As roundness is a measurement of form, short-wave roughness is usually filtered out. In a roundness plot the Flick area appears as a deep valley and is therefore reduced by any filtering. The frequency content of a Flick makes it not ideal for equipment relying on the Ozono method where analysis is done in frequency domain.

2.3 Ellipse standards, single wave

The ellipse standard is a cylinder with an elliptical form error. This form error linearly depends on the height (Fig. 5). At MIKES two standards are used. One with roundness error in range 5 to 30 µm and another with roundness error in range 35 to 300 µm. If the roundness instrument is able to measure at different heights automatically, a large amount of roundness results can be plotted quickly.

A drawback is the critical dependence between position (height) and magnitude of elliptical form. The uncertainty in the height produces an uncertainty in the reference value

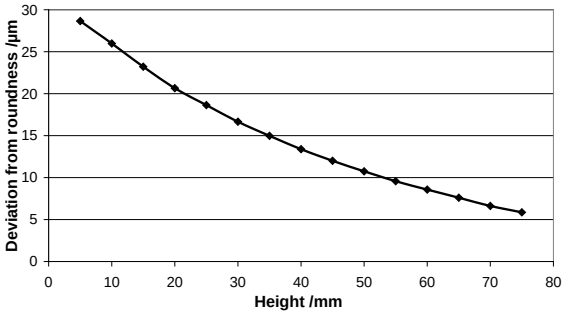

Fig. 5. Ellipse standard with internal cylinder above and below deviation from roundness.

2.4 Multi-wave standards

A recent example of multi-wave standards (MWS) are those developed by Fraunhofer Institute for Production Technology (IPT). Their profiles contain a superposition of sinusoidal waves with wave numbers 5, 15, 50, 150 and 500 UPR (undulations per revolution). The advantages of MWS compared to Flicks are better signal to noise ratio and low sensitivity to noise in measured profiles [8]. A Euramet comparison of a Flick standard and MWS showed that the spectral analysis (harmonics) of MWS leads to good agreement and stability [8].

[2] V-P Esala

2.5. Asymmetric multi-wave

The asymmetric multi-wave standards have been developed to calibrate large roundness measuring machines based on the Ozono-method. These machines are used when rolls in paper- and steel industry are grinded in the production process (Fig. 6). There the grinding process is often controlled according to the measured geometry data. The measuring range for diameter is 300 to 2000 mm.

As with MWS these discs have waves but the shape is not symmetric (Fig. 7). The shape and the waves are found suitable for the Ozone method. Because of the large size typical roundness measuring machines cannot be used for calibration. Instead either CMM or specially built setups for roundness measurement must be used.

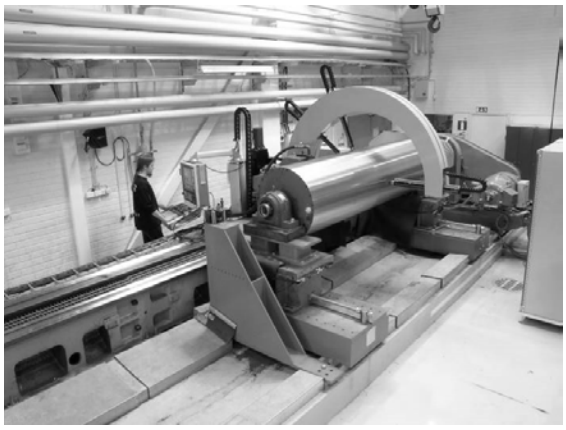

Fig. 6. Four-point measurement instrument.

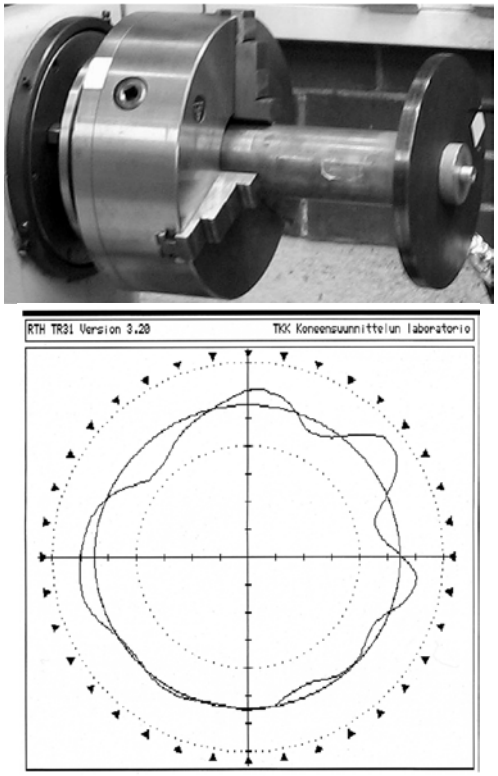

Fig. 7. Disc above and below roundness plot [4].

3. PROPOSED ROUNDNESS STANDARDS

The measurement standards are intended to quantify error sources found in large measurement systems that are based on the Ozono method. The developed measurement standards are also useful for calibration of two-point and one-point measurement systems. The error sources which are expected to be found are errors of the transducers, angular orientation error and positioning error of transducers. Thermal expansion and vibration of the measurement frame (Fig. 8) are other possible error sources.

The algorithm of the measurement systems have already been validated by simulation, but functional testing is possible and valuable to perform with the developed discs.

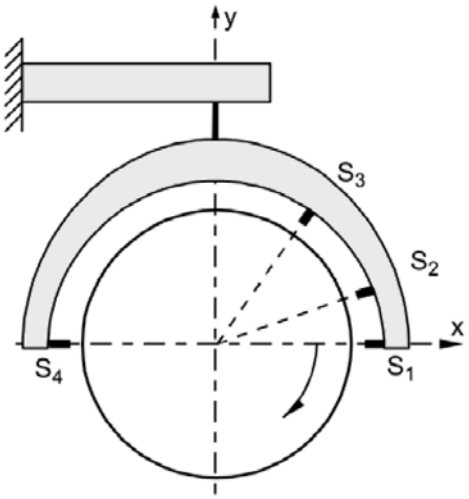

Fig. 8. Typical orientation of probes in a four-point measurement systems

All standards are discs with the diameter of 500 to 550 mm. This is the largest diameter that can be easily measured in laboratories and not too small to be measured by in process roundness measurement systems in industry. Larger discs were also considered but weight and handling would bring problems. The thickness of the discs will be 30 to 50 mm which is enough for robustness and yet not too heavy to handle. The types and requirements of the selected standards are shown in Table 1.

The type A standard is almost perfectly round. With a roundness error below 2 µm this standard helps to reveal errors like noise and thermal drift.

Name	Form	Roundness error / µm
Type A	round	0 to 2 µm
Type B	21 UPR	20 to 25 µm
Type C	asymmetric multiwave, 2 to 30 UPR	10 µm / undulation

Table 1. Requirements for the measurement standards.

Type B is selected as it has one characteristic form of a 21 UPR wave. The hypothesis is that the characterisation of a single probe of a multi-point measurement system is straightforward with a disc with single harmonic content. The type C, asymmetric multi wave, consists of several waves. Standards of this type have previously been used and they are expected to work as overall test standard.

Previously only type C discs have been used in the calibration. However it is assumed that using multiple discs different types of error sources can be evaluated.

All standards will be calibrated by roundness measuring instrument with a rotary table. Additional measurements to get other form errors like cylindricity will be done in a CMM.

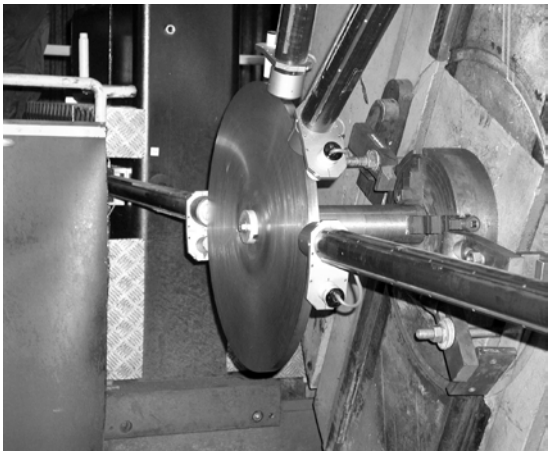

Fig. 9. Calibration of a multi-point roundness measurement device.

7. CONCLUSION

The Flick standard is the most used type of magnification standard for one-point roundness instruments, but is not ideal with multi-point instruments.

The diameters of the most roundness standards are below 500 mm and are intended for use in metrology laboratories and are not suitable to ensure traceability for measurement of large parts in industry. Some asymmetric multi-wave standards are

large and already used in paper- and steel industry. Other standards proposed in this paper will be manufactured. In future tests with these standards will be performed in the industry. Using all these standards traceability will be achieved and uncertainty for roundness will be evaluated.

ACKNOWLEDGEMENT

This work was funded through the European Metrology Research Programme (EMRP) Project IND62 TIM. The EMRP is jointly funded by the EMRP participating countries within EURAMET and the European Union.

REFERENCES

1. Kiviluoma, P. 2009. Method and device for in situ runout measurement of calender thermo rolls. Doctoral dissertation. Helsinki University of Technology, Espoo. ISBN 978-952-248-259-4.
2. Ozono, S. (1974). On A New Method Of Roundness Measurement On The Three Point Method, Proceeding of the ICPE, pp 457-462, Tokyo, Japan, 1974.
3. Juhanko, J. 2011. Dynamic Geometry of a Rotating Paper Machine Roll. Aalto University Publication Series Doctoral Dissertations 117/2011. 172 p. ISBN 978-952-60-4363-0.
4. Kotamäki, M. 1996. In-situ measurement and compensation control in external grinding of large cylinders. Helsinki: Acta Polytechnica Scandinavica, Mechanical Engineering Series No. 121. 123 p.
5. Kuosmanen, P. 2004. Predictive 3D roll grinding method for reducing paper quality variations in coating machines. Helsinki University of Technology Publications in Machine Design 2/2004, Espoo. ISBN 951-22-7014-5.
6. Widmaier, T. 2012. Optimisation of the roll geometry for production conditions. Aalto University Publication Series Doctoral Dissertations 156/2012. 184 p. ISBN 978-952-60-4878-9.
7. Thalmann, R., Spiller, J., Küng, A. and Jusko, O., 2012 *Meas. Sci. Technol.* **23**. Calibration of Flick standards.
8. Jusko, O., Bosse, H., Flack, D., Hemming, B., Pisani, M. and Thalmann, R., 2012 Meas. Sci. Technol. **23**. A comparison of sensitivity standards in form metrology—final results of the EURAMET project 649.

CORRESPONDING ADDRESS

Björn Hemming, D.Sc. (Tech.), I. Palosuo M.Sc. (Tech.), V-P Esala M.Sc. (Tech.), P. Laukkanen BEng.

Centre for Metrology and Accreditation (MIKES), P.O. Box 9, FI-02151 Espoo, Finland, bjorn.hemming at mikes.fi

ADDITIONAL DATA ABOUT AUTHORS

Thomas Widmaier, D.Sc. (Tech.) Aalto University, Department of Engineering Design and Production, P.O.Box. 14400, 00076 Aalto, Finland, thomas.widmaier at aalto.fi

L. Lillepea, M.Sc. (Tech.), K. Simson Metrosert M.Sc. (Tech.), Metrosert AS, Teaduspargi 8, Tallinn, Estonia

Daniel Brabandt, Dipl.-Ing Karlsruhe Institute of Technology, wbk Institute of Production Science, Kaiserstraße 12, 76131 Karlsruhe, Germany, daniel.brabandt at kit.edu

Janne Haikio, M.Sc. (Tech.), RollResearch International Ltd., Luoteisrinne 4D, 02270 Espoo, Finland, Janne.Haikio at rollreseach.fi

9th International DAAAM Baltic Conference
"INDUSTRIAL ENGINEERING
24-26 April 2014, Tallinn, Estonia

Technology for rapid foot support making

Karu, M.; Henno, E.; Veskimeister, V.; Tamre, M.; Juurma, M.; Hiiemaa, M.

Abstract: *Nowadays many individuals e.g. athletes, youngsters, persons with growth problem, insured persons, persons with collapsed arch, etc. need personally manufactured foot sole supports. At the moment there are three main solutions how to make foot sole supports. The first method uses sensor-mat, second method uses optical scanning method and the third method is done with foam moulding. All these solutions have certain drawbacks.*
We have decided to use optical scanning method to get digital foot sole into the computer giving opportunity to add sensor mat recordings to the model by expert and represent 3D foot sole with foot robot to avoid extra costs for mould materials for vacuum moulding.

Key words: foot sole supports, stereo-vision, medicine, robotic device

1. INTRODUCTION

In today's world many athletes need foot sole support to improve their performance and prevent injuries and also individuals who trouble with collapsed arch, which leads to back pain and tired foot. Foot supports are also necessary for injured, handicap persons or children in certain ages troubling with growth problems, so this problem affects many people in all EU.
Nowadays, there are two most common technologies of making them. First Technology utilizes a pressure sensor plate or sheet and converts the registered Pressure distribution into the foot under surface into a 3D model – this method uses pressure data. The result might not be very accurate and there is a need to apply a specific medical data processing algorithm to perform real pressure distribution reflecting all foot incorrectness caused by diseases or just foot modifications into correct foot profile that is needed for making medically prescribed or desired for a specific motion foot insert supporting foot the best way. This kind of data processing takes a lot of time because it needs usually doctor consultancy and the problem is that it is not easy to get full accurate impression from the 3D model on the computer screen to introduce needed small surface profile corrections into the model. Second method uses foam, plaster or vacuum moulding to get foot model. This method has drawbacks, as it is time and material consuming, not very accurate and there is no direct foot digital model.
We are now searching for a method, which uses optical scanning means. Using stereo-vision principle to get a three-dimensional information from foot sole surfaces and represent by a robotic device. The model can be used directly to make thermoplastic sheet foot supports. This new technology would be very essential for making medical services more flexible and human friendly.

2. OPTICAL SCANNING METHODS

There are different scanners on the market. Some 3D scanners are using Laser scanning method. [1]
The second scanning method we can use is based on optical method, where stereo vision principle is used. This method uses two cameras, where distant between these two cameras must be set and measured. [2]

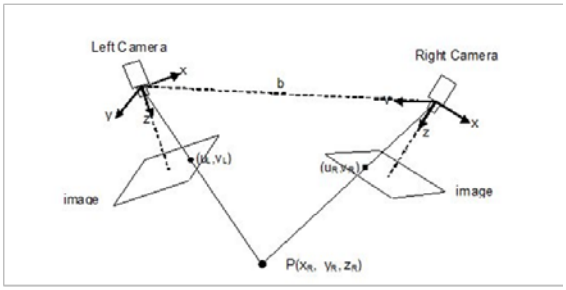

Fig 1. Stereo vision principle in real life [3]

Stereo vision principle is used also with method, where two cameras and projector are used. Projector is needed to calibrate these two cameras.

3. FIRST EXPERIMENTS

In the first experiments National Instruments Smart Cameras with Lab View were tested, as well as a system which uses only one camera and mirror system and is therefore cost efficient. The simplest solution tuned out to be one mirror system in which the camera's field of view is divided by a mirror so that the same object reflection in a mirror is from a slightly different angle.

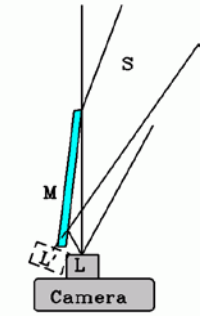

Fig 2. System with one camera [4]

With one mirror system a problem occurs because of the same image optical paths have different lengths which makes it difficult to focus with that equipment's depth of field.
In addition, there were problems with image size, displacement and angle. If an image is projected onto a sensor at an angle then it creates perspective influences and interferes with stereo-vision operating principles on making 3D image. Although there are examples of using one mirror systems in stereo-vision, it is not reliable or accurate enough, so the classical two camera stereo-vision system was used instead. Two camera system is more expensive but is free from disadvantages mentioned above.
National Instruments Lab View software used has additional library with stereo-vision operating principle examples. One of which the output is three-dimensional result with colour-mapping. Initial tests were made by modifying these examples. Having calculated the dimensions of our camera system, distances and suitable lenses, two LED luminaires to illuminate on an angle both sides of the object were set up and the system was calibrated using point matrix on a white paper sheet. Size of the points and distance between was known. Calibration was made more difficult because cameras depth of field was at an angle to the paper sheet and also Lab View calibration system was lacking accuracy and speed. After calibration it was clear that the result is not satisfactory and the uncertainty is an order of magnitude worse than needed.

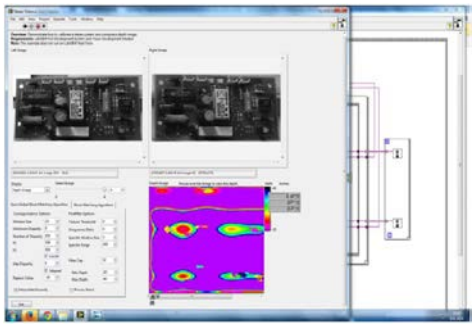
Fig 3. Experiment in Lab View

After the tests a conclusion was that 3D image using National Instruments Smart Cameras and Lab View might be sufficient for some simple solutions but such a system does not satisfy our demands because of the desired accuracy ± 0.5 mm.

4. CURRENT STATE

The next experiment was made using a professional 3D scanner (3D3 scanner) to be sure that the idea is realizable. The scanner uses two special cameras combined with projector. In addition, it has a much more powerful program than Lab View stereo vision. It allows to make several pictures from different angles, it finds the object by projector that calibrates the cameras and generates 3D image improving dimensions with every recording. Despite all that professional system the result was not satisfactory and neither was the uncertainty of the model.

Fig. 4. The result when using a professional 3D scanner

There were two main reasons of unsatisfactory result:

1. Human skin is bad for scanning because human skin is quite dark, which absorbs light and degrades our scanning and its accuracy,
2. Because many pictures are required for this scanning process then patient cannot hold his leg completely fixed and that makes the model inaccurate (see fig 4).

As the model was not precise enough, even when using a professional 3D scanner, the conclusion is that scanning method can be done using regular scanning method with fixed cameras, where extra lightning is added to avoid absorption from the skin. Also human leg has to be completely fixed, which can be achieved when person is standing on some transparent object, for example class.
In proof of that the same experiment was made, but this time it was not the patient's foot, that was scanned, but a gyps mould of his foot. When the object was not dark or moving, the result and its uncertainty was satisfactory.

Fig 5. Result when using gyps mould

5. DISCUSSION

The goal is to use stereo vision principle to get depth picture. From the depth picture we want to create foot model with robot for vacuum moulding. Before making the model also sensor mat can be used to see the different pressure points while patient is walking or standing. From all the collected data depth picture can be changed digitally before vacuum moulding to construct accurate individual sole supports.

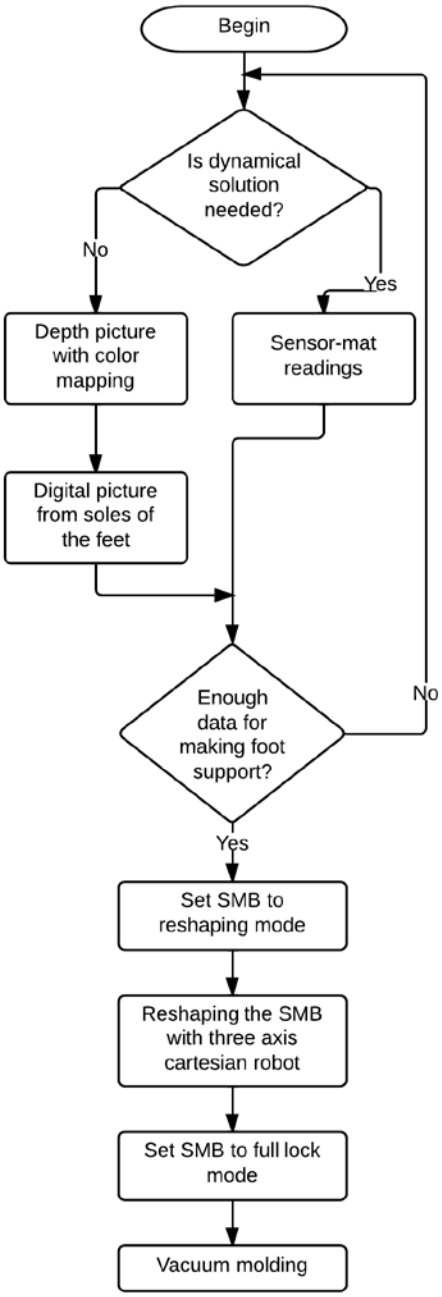

Fig 6. Algorithm

Given algorithm explains method for making foot sole supports efficiently without spending money on moulding material. Patients need foot sole supports for different reasons and therefore the scanning method of the foot soles must be flexible. Patient foot soles can be scanned with optical solution (using laser scanner or stereo vision principle) and extra information can be added using sensor mat to observe pressure points while patient is walking or standing still. Changes are done on the digital picture by expert and Shapeable Mould Box (SMB) is used to reshape the patient foot sole for vacuum moulding.

SMB uses pins as physical pixels and these pins are repositioned by dedicated robot, before reshaping the SMB it must be set to reshaping mode, where frictional forces will lock the pins. When SMB has been reshaped by robot, it will be fully locked for vacuum moulding

SMB uses the same principle as Dynamic Shape Display (DSD) that can render 3D content physically. Nowadays there few DSD's and they use matrixes made of servo motors and lines to connect motors and pins (also piezo DSD-s can be used) [5-6].

SMB uses smaller pins and these pins are placed closely to each other therefore it is more accurate than DSD. This solution is also cheaper to manufacture because SMB do not need real time reshaping and robot can repositioned the pins with sufficient accuracy.

6. CONCLUSION

Experiments with different stereo vision methods have shown that it can be used if patient steps on glass and foot sole is recorded to computer with regular scanning method where two cameras record 3D picture. Stereo vision method must be used with extra lightning to avoid absorption from foot sole skin. Foot sole supports are made for different reasons and therefore dynamical solution can add extra information before giving the mould shape with SMB. The shapeable mould box has pins that are placed close to each other and robot repositions the pins. Because real time reshaping for SMB is not needed, then one dedicated robot will be enough for reshaping. SMB has double locking system, where first lock is used for reshaping and second lock for vacuum moulding

7. ACKNOWLEDGEMENT

We would like to thank professor Mart Tamre for instructions of scientifical language and style usage. We would also like to thank researcher Henri Lend for the usage of professional 3D scanner.

8. REFERENCES

1. Laser scanning [WWW] http://www1.cs.columbia.edu/~allen/PHOTOPAPERS/pipeline.fausto.pdf (03.03.2014)
2. 3D scanning [WWW] http://iphome.hhi.de/fechteler/papers/icip2007b_FechtelerEisertRurainsky.pdf (03.03.2014)
3. Lab View 3D model [WWW] http://www.ni.com/white-paper/14103/en/ (03.03.2014)
4. Information about using mirrors for stereo vision http://www.lhup.edu/~dsimanek/3d/stereo/3dgallery16.htm (03.03.14)
5. DSD example [WWW] http://tangible.media.mit.edu/project/inform (03.03.2014)
6. DSD using piezo principle [WWW] http://www.ngk.co.jp/english/research/electronics.html (03.03.2014)

ADDITIONAL DATA ABOUT AUTHORS

Karu Mihkel, Mechatronics MSc student
Department of Mechatronics, Ehitajate Tee 5, Tallinn 19086, Estonia,
mihkel.karu@hotmail.com
+372 53659014

Henno Elvis, Mechatronics MSc student
Department of Mechatronics, Ehitajate Tee 5, Tallinn 19086, Estonia,
elvis.henno@eesti.ee
+372 53919666

Veskimeister Vello, Mechatronics MSc student
Department of Mechatronics, Ehitajate Tee 5, Tallinn 19086, Estonia,
veskimeister1@hotmail.com
+372 56626071

Tamre Mart, PhD, professor,
Department of Mechatronics, Ehitajate Tee 5, Tallinn 19086, Estonia,
mart.tamre@ttu.ee
+372 620 3202

Juurma Märt, PhD student,
Department of Mechatronics, Ehitajate Tee 5, Tallinn 19086, Estonia,
mart.Juurma@ttu.ee
+372 620 3207

Hiiemaa Maido, PhD, researcher,
Department of Mechatronics, Ehitajate Tee 5, Tallinn 19086, Estonia,
mart.tamre@ttu.ee
+372 620 3211

9th International DAAAM Baltic Conference
"INDUSTRIAL ENGINEERING -
24-26 April 2014, Tallinn, Estonia

AUTOCORRELATION INFLUENCE BY GEOMETRICAL DEVIATIONS MEASUREMENTS

Kulderknup, E.; Pandis, A.

Abstract: *Required accuracy level of the items geometrical deviations have importance for quality assurance of the products in machinery. For the real detail, geometrical deviation is realized through production process and controlled through measurements. In practice not all factors have random influence and can not be measured directly. One of the factors which can not be viewed directly and rarely taken account is the autocorrelation effect. Autocorrelation influence is handled up-to-now widely for electrical processes. In machinery special importance has autocorrelation for measurements which are carried out automatically and rapidly.*
This study work gives as novelty the model of autocorrelation estimation by the geometrical deviations measurements of the machinery products. Used are practical results of the measurements. Geometrical deviation is mainly limited in form of the straightness in this study work.

Key words: Autocorrelation, uncertainty, straightness deviation.

1. INTRODUCTION

Required accuracy level of the geometrical deviations has importance for quality assurance of products in machinery. Item geometrical deviations are determined by designer and have standardized normative values. For the real detail or part of devices geometrical deviation is realized through production process and controlled through measurements. Above both have uncertainties and those shall be taken account for estimation of process capability indices like C_p or C_{pk} or similar. Bases for the capability indices are statistical estimates which assume mainly random distribution of data. On the other hand, also the uncertainty estimation of processes and measurements needs statistical calculations or expert analyse like shown in Guide of Uncertainty of Measurement (GUM). Expert analyse shall involve all possible influence factors and have deep knowledge of the process.
In practice not all factors have random influence and can not be measured directly. One of the systematic factors which is rarely taken account is the autocorrelation effect. Autocorrelation is the cross-correlation of a signal with itself.
Special importance has autocorrelation for mechanical processes and for measurements which are carried out automatically and rapidly. There is no time to recover of the instrument sensor which is main source of an autocorrelation effect.
Handled geometrical deviation is limited in this study in form of the straightness and parallelism and surface production process is the milling. Used are practical results of the items measurements. As theoretical base were used existing mathematical autocorrelation estimation principles.
This study work gives as a novelty the model of autocorrelation estimation by the geometrical deviations measurements of the machinery products. Autocorrelation effect is estimated for distance and not at different times. This study work is further development of works which handled statistical aspects of geometrical deviations measurements.

2. INFORMATION

2.1 Autocorrelation theory

Autocorrelation theory based on general long-time correlation theory. For measurements in machinery can used also regression analyse, but in this case, autocorrelation is only one of the influence factors among others. Systematic deviations by measurements were tackled widely in general form [1] and [2] and for industrial metrology [3]. Correlation problems by measurement uncertainties are studied in modern way in [4] and [5]. Systematic effects are described and detected as an autocorrelation effect of the deviations, when it produces observable residuals.

Autocorrelation theory presents that it is the cross-correlation of an input signal with itself. The autocorrelation of a random process in statistics describes the correlation between values of the process at different times, as a function of the times. Autocorrelation influence is more understandable for the processes which have periodical wave form. There can be used suitable Fourier formulas for reference model determination. Such is a case by measurements of electrical parameters. The autocorrelation effect has feature, that it can have variation during one measurement cycle.

Autocorrelation quantity R of results, having different times t_i and t_{i+1}, can be calculated by Equation (1)

$$R(t_t, t_{i+1}) = \frac{E[(X_{ti} - u_{ti})(X_{ti+1} - u_{ti+1})]}{\sigma_{ti}\sigma_{ti+1}} \quad (1)$$

where X is value of repeatable process quantity, index i presents a point in time after the start of that process and E is the expected value of the process.

The process under investigation shall be known and have defined values for arithmetical average μ_i and variance σ_i^2 for all times i. If the process quantity correlation is firmly presented, its value lies in the range from −1 up to 1. Values −1 and 1 give complete autocorrelation between results at time point **i** and i+1.

The Equation (1) can be modified for more practical form for measurements as follows and can be calculated the autocorrelation coefficient r_a:

$$r_a = \frac{\bar{y}_i \bar{y}_{i-1} - (\bar{y}_i)^2}{\sigma_y^2} = \frac{\Sigma y_i y_{i-1} - n(\bar{y}_i)^2}{\Sigma y_i^2 - n(\bar{y}_i)^2} \quad (2)$$

where $\bar{y}_i$ and $\bar{y}_{i-1}$ are mean values of measured results during single cycle and n is quantity of involved values during one cycle.

For the real technical processes where exists continuous function $f(t)$ the autocorrelation is suitable to found by Equation (3):

$$R_f(t) = \lim_{T\to\infty} \frac{1}{2T} \int_{-T}^{T} f(t_i) f(t_{i+1})\, dt \quad (3)$$

where T is time value.

The traditional tests [6] for the autocorrelation detection are the Durbin–Watson statistic or if the variables include a lagged dependent variable, the Durbin's statistics. For detection of autocorrelation of higher orders the Breusch–Godfrey test is used. This involves an auxiliary regression analyse, where the residuals obtained from estimating the model of interest are regressed. Autocorrelation effects importance can be estimated using Anderson critical values. If autocorrelation coefficient r_a is smaller than critical value, then autocorrelation can be estimated as no having importance.

2.2 Measurement of straightness and autocorrelation effect

In machinery the normative values of the straightness deviations.are on the level from 0,1 μm up to 50 μm. Straightness deviation is a maximum distance between parallel two lines laid in optimal way trough to the measured surface minimum and maximum points. Scheme of measurement is given on Fig 1. To have more exact view of influence possibilities of the autocorrelation effect there shall be analysed whole measurement process. Table 2 gives influence factors list,

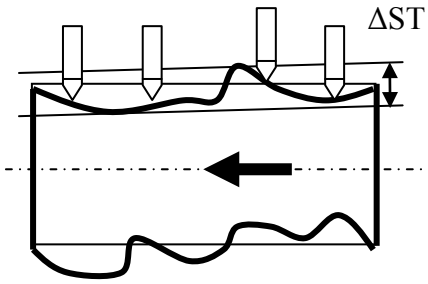

Fig. 1 Measurement scheme for the straightness deviation

which are used for measurement model of the straightness measurement process. Values of uncertainty components based on above model are given in Table 1. In Table 1 are presented only components which have importance in this accuracy level. Autocorrelation effect by straightness deviation measurement is caused mainly by the measurement instrument rigidness, where the sensor can not follow exactly the item profile of surface. In specific cases the autocorrelation is caused also by clearances, then clearness gives continually systematic deviation. Important role for the autocorrelation effect has movement velocity, distance between measurement points and measurement force.

Quantity X_i	Estimate x_i	Contribution to $u(y_i)$
Measuring instrument	U_{MI}=0,003 mm	0,001 mm
Reading	Scale value 0,001 mm	0,0005 mm
Reference line determination	Regres analyse ±0,2 μm	0,0001 mm
Object surface*	Ra = 0,3 μm	Minor
Measurement force*	5 N	0,0005 mm
Move-ment*	Velocity. Measurement points interval	From minor up to 0,0005 mm
Temperature variation	0,1 °C	Minor
Operator	Minor	Minor
Straightness deviation	Δ_{STR} = 0,011 mm	u_{STR}= 0,002 mm, k=1

* Influence of autocorrelation is possible

Table 1. Uncertainty components estimation summary results

Operator
Accurateness
Visual acuity
Attentiveness
Commitment
Competence
Experience
Measuring instrument - design
Design
Dimensions
Material
Environment and variation
Sensor
Measuring instrument - properties
Calibration
Repeatability
Reproducibility
Behaviour during test
Reading
Adjusting tool tolerances
Straightness measurement Deviation = $f(X_i)$, where X_i are factors
Environment
Humidity, RH
Temperature
Vibration
Barometric pressure
Pureness
Interference fields
Measurement object
Design
Size
Chemical quality
Tolerances
Machining accuracy
Measurement method
Reference line
Object vs. measuring instrument
Velocity and force
Distance between points

Table 2. Influence factors X_i by straightness deviation measurement

2.3 Practical measurement results

In this study work were used measurement instrument which was traceable calibrated high accurate dial gauge with scale value 1 μm and with uncertainty U=2 μm, k=2. In

this stage, measurements were simplified and task was to find main directions. Measurements were carried out with two various velocity v_i of movement of detail, v_1=(1±0,1) cm/s and v_2=(0,5±0,1) cm/s and with two various intervals h_i between measurement points, h_1=(0,6±0,1) cm and h_2=(0,3±0,1) cm. Autocorrelation coefficient r_a was estimated using Equation (2) for each combinations of h_i and v_i. Summary results of calculation are given in Table 3. Critical values of autocorrelation by Anderson [6] on a confidence level α=0,05 are r_a=0,345 (df=5, h=0,6 cm) and r_a=0,348 (df=11, h=0,3 cm). Calculated values of autocorrelation coefficient r_a assured the assumptions, that minor autocorrelation effect is by static measurement and essential by rapid measurements.

No	Velocity v_i	Interval h_i	r_a
1	1 cm/s	0,6 cm	0,45
2	1 cm/s	0,3 cm	0,78
3	0,5 cm/s	0,6 cm	0,40
4	0,5 cm/s	0,3 cm	0,84

Table 3 Summary results of autocorrelation coefficient determination

2.4 Measurement of parallelism and autocorrelation effect

Item parallelism deviation is maximum distance between lines which are set on parallel way to the reference surface. Uncertainty components are mainly the same as for the straightness. Additional components give appliance which ties two separate dial gauges and reference line determination. Autocorrelation effect is mainly the same as for straightness measurement. Influence gives appliance rigidness which cause also residual movement of the second measuring instrument.

3. CONCLUSIONS

Measurements results and uncertainty estimation give base for assumption that exists autocorrelation effect by measurement of straightness. Process characteristics values have clear influence by measurements. Further investigation shall show more exactly influence structure. Taking account the autocorrelation effect, it allows to make more accurate the measurement process in practice.

4. REFERENCES

[1] Granovskiy, V, Siraya, T. Systematic errors: Methodology of detection, elimination and evaluation. *Proc. of XX IMEKO World Congress*. IMEKO, Busan. 2012.

[2] Schmitt, R., Zheng. H., Nisch, S. Process control oriented geometric products specification and data analysis. *Proc. of XX IMEKO World Congress*. IMEKO, Busan. 2012.

[3] Dunn, Patrick F. *Measurement and Data Analysis for Engineering and Science*. McGraw–Hill, New York, 2005.

[4] Sommer, K.D., Siebert, B., Hauswaldt, A-L. Novel and established concepts for considering correlation in uncertainty evaluation. *Proc of XIX IMEKO World Congress*. IMEKO, Lisbon, 2009.

[5] Kessel, R., Kacker, R. Correlation in uncertainty of measurements - A discussion of state of the art techniques. *Proc of XIX IMEKO World Congress*. IMEKO, Lisbon, 2009.

[6] *Teoria statistiki*. Pod red. prof G.L.Gromõko INFRA-M, Moscow, 2009, (in Russian).

ADDITIONAL DATA ABOUT AUTHORS

1) PhD Edi Kulderknup, TTU, Institute of Mechatronics, associated professor, edi.kulderknup@ttu.ee

Eng Argo Pandis, Tepso Laborid Ltd. argo@tepso.ee

2) Autocorrelation influence by geometrical deviations measurements

3) Corresponding Author: Edi Kulderknup

9th International DAAAM Baltic Conference
"INDUSTRIAL ENGINEERING
24-26 April 2014, Tallinn, Estonia

DEVELOPMENT OF VIRTUAL REALITY INTERFACE FOR REMOTE ROBOT CONTROL

Lees, Ü.; Hudjakov, R.; Tamre, M.

Abstract: *This paper discusses different options to apply Virtual Reality for practical industrial applications and provides one of very practical and new example system developed by the authors.*
Key words: Virtual reality, telepresence

1. INTRODUCTION

Virtual reality technologies are one of the fastest developing technologies during last decade. Moreover, technology forecasts predict that virtual reality technologies belong among ten most significant and important technologies changing the world and how humans communicate during next five years. On recent technology trade fairs and Internet sites, all big technology companies demonstrate some new virtual or augmented reality device where some more widely known are Google Smart Glasses, different 3D screen and camera systems. Most of them are still focused for gaming application because this sector is one of the fastest and highest return potential in short term perspective. Despite of this virtual reality applications are starting to find their place for industry too. One of the first sector that attracted virtual reality technology was medical sector because the technology gives to doctors' ability to get more realistic feeling what could happen during an operation or even perform distance operations. Production sector have been careful taking into use virtual reality applications, which is in some extent connected with preconceptions dealing with something that have been used previously mainly for gaming, free time applications, and from the other hand connected with the lack of practical applications and industry suitable virtual reality devices.

Tallinn University of Technology Department of Mechatronics has long experience in developing different machine vision systems and smart algorithms. Rapid development of virtual reality hardware components in the world during some last years have provided a unique and promising base platform to develop new virtual reality applications for industrial robot control. It is well-known that for example the operator of a Explosive Ordnance Disposal (EOD) robot or operator of a precise assembly robot systems or operator of complex processing robotic machine have difficulties in getting real imagination what is happening in 3D in the robots very operating zone. 2D camera pictures or just trust of the machine programming is not enough in many cases. To control the process precisely the operator must interfere it in many cases. Even more, to provide options for remote consultancy for a specific industry processes, it is needed to enable to get real 3D imagination of the process to an engineer remotely.

According to Michael Abrash [1] all following conditions have to be satisfied in order to create sensation of presence:

- Field of view must be more than 80 degrees
- Image resolution must be at least about 1000x1000 pixels per eye
- Pixel persistence less than 3ms
- Refresh rate of about 95 Hz
- Global display - all pixels should be updated simultaneously as opposed to updating line by line
- Optics that allow control of focal length and viewing distance
- Robust angular and positional tracking
- Low latency - reaction from head motion to finishing display update should be below 25 ms

Up until now the limiting device, that has held back virtual reality revolution, has been the virtual reality goggles. The existing models had too small field of view or were too heavy or expensive for wider audience. The breakthrough in virtual reality glasses has been enabled by recent emergence of mobile technologies and advances in computer graphics. Availability of high resolution, small form factor, low power and cheap displays as well of existence of low latency embedded orientation sensors are necessities for building a modern head mounted displays. Advances in computer graphics have enabled to do away with expensive and, more importantly, heavy optics.

One device that relies on aforementioned technological advancements is Rift from Oculus. It puts a single high definition display in close proximity of wearers eyes and renders a stereo

image onto the display. The display is too close to the wearers eyes for sharp image, to alleviate the problem a single lense is installed between the screen and the eye. The lense will focus the eye to infinity, and provide 100 degrees field of vision. In addition the lense will warp the image so that there are more pixels in the center of the view area than in the edges which is in line with human physiology - the center of the eye has higher definition than peripheral vision. Unfortunately the single lense will distort the image. The distortion of the lense is compensated by distorting the projected image in opposite direction making the wearer to see orthogonal image.

Most of the cues for spatial vision come from imagery itself - perspective, lighting, etc. For added realism additional cues can be added such as stereo vision and head tracking. Each added cue will increase the realism of the scene. The Rift display is coupled with accelerometer that is used to measure head position. The system is continuously rendering an image based on wearers head position providing head tracking functionality.

For telepresence applications the virtual reality glasses have to be coupled with cameras. Applications such as EOD robot control or remote service benefit from depth perception. For generating stereo imagery a pair of cameras can be used. The pair of cameras must be mounted approximately 65 mm apart, which is about the average distance between human eyes. It would be good if the distance could be adjustable but changing the camera position would invalidate the delicate camera calibration.

Better depth perception comes from head tracking; to enable that the camera pair must be mounted on a moving platform. In order to avoid image tilting during head movement due line-by-line image scanning the cameras must have global shutter. To avoid depth distortion during head movement the cameras must be synchronized. An object that is at given distance from cameras appears shifted when the images are overlied. The shift or *disparity* between camera images must stay constant during camera movements which in turn requires synchronized image acquisition.

The target of current development project is to create a telepresence application using modern hardware.

2. THE FIRST PROTOTYPE

The emphasis of the first prototype (Fig. 1) was quick development; there was abundance of information about problems of virtual world rendering but not much was known about physical device requirements. The intention of the first prototype was to gather preliminary information about design constraints, it was made of low

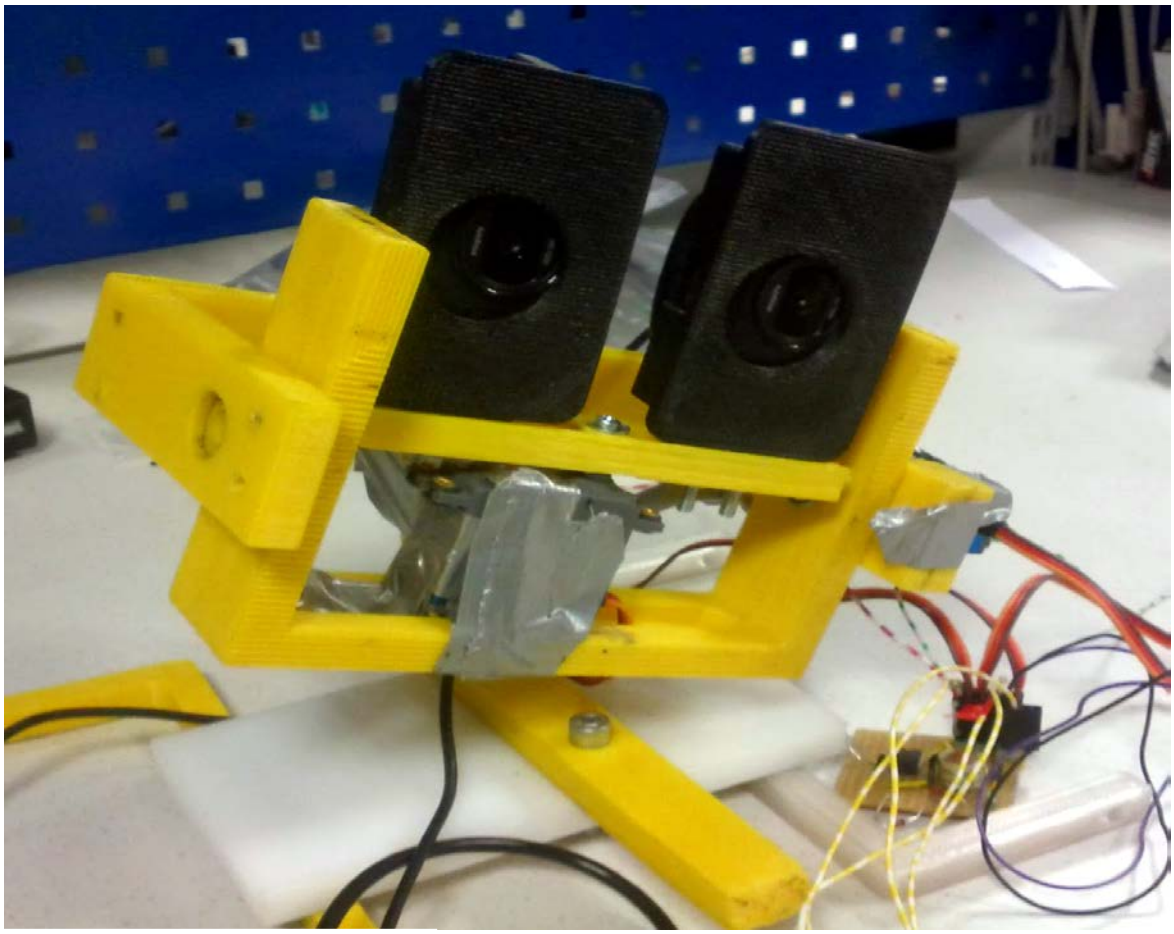

Fig. 1. The first prototype.

quality 3D printed parts, HobbyKing HK15298B servo motors and Logitech C525 web cameras.

The first problem with the web cameras was that they were not optically aligned and there was no precise mechanism to do so. The cameras were mounted on a loose 3D printed bracket that did not allow fixing them on steady position causing misalignment. Presenting the cross-eyed picture to user of the device induced motion sickness. Even when the optical axes were somewhat aligned the picture was only good for objects that were more than 2 meters away. Evidently there is a need to design an optical axis alignment tools to the second prototype and also do the camera distortion calibration/compensation in software.

The second problem with the web cameras was that they had a rolling shutter meaning that the lines were scanned line by line. While it was not a problem when camera was stationary or even when camera was rotated by hand it significant problem during head movements; turning the head sheared the whole image. Both cameras were working in live mode; image acquisition was not synchronized. This should have caused distortion of depth of objects on stereo imagery during head movements, but none of this was observed. It is possible that the depth distortion was masked by image shearing and motion blur artifacts.

Overall the first prototype failed to produce any noteworthy depth perception through stereo imagery. Significant camera calibration needs to be done for tapping stereo imagery and reducing the sickness. There was, however, definite depth perception from monocular imagery. The effects of motion parallax and occlusion combined produced a much better depth perception than what can be observed on pre-calibrated stereo imagery.

The used servos packed motor, encoder controller and a gearbox into a single unit; they were controlled using pulse-width-modulation (PWM) signal. There were three servos for rotating the cameras over three euler axes. The servos were responsible for major part of the latency in the system; The head movement could be detected within a millisecond, but issuing the PWM positioning signal to servo motor took 20

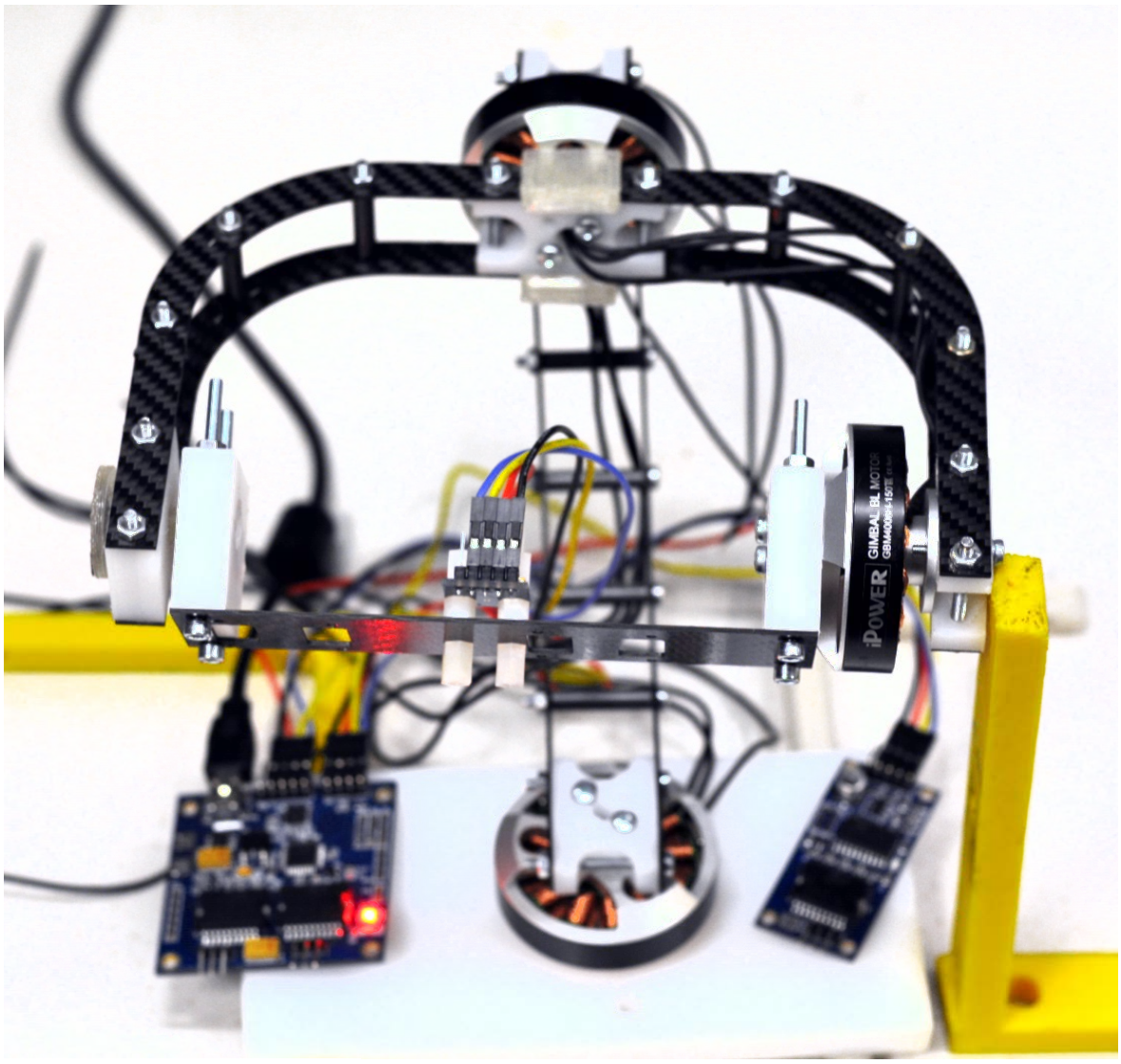

Fig. 2. The second prototype.

milliseconds. The high gearing ratio of the servo added further delays during head movements causing the picture to lag behind head movement - the gimbal system has to be able to achieve angular accelerations of over 900 rad/s² and angular velocities of over 9 rad/s for accurate head tracking [2]. Having a total system latency below 20 milliseconds is important for presence but before the servo latencies are suppressed it is difficult to evaluate the feasibility of the system in a real world scenario.

3. THE SECOND PROTOTYPE

The second prototype (Fig. 2) is in works at the time of writing and will be based on both experiences gathered from first prototype and on further research on the subject. The camera mount will be based on gimbal camera stabilizers that are used together with model helicopters, it will be made of carbon fiber to keep the weight down. The new cameras are designed for stereo imagery applications. The body of the apparatus will be made from carbon fiber in order to keep the weight down and deliver fast reaction times and lower latencies during head movements.

Using light and high torque GBM4008H-150T motors from gimbal stabilizers help to keep the apparatus compact. Instead of connecting the motors directly to encoders it was chosen to use an accelerometer sensor that is directly connected to camera bracket. The main advantage is that it helps to stabilize the camera even when the apparatus is attached to EOD robot - it considers both operator view direction and the position on the carrying EOD robot. The other advantages are the compact size, light weight, easy attachment and easier calibration procedure of such feedback. Conveniently there's a three axis brushless DC motor controller available from BaseCam Electronics that supports accelerometer for feedback. The controller has analog inputs for positioning signal allowing to eliminate most of the PWM delay.

The chosen Leopard Imaging LI-USB30-M021 cameras are of industrial origin; they are designed for monitoring high speed operations and support high resolution imagery. The cameras have global shutter, meaning they acquire all pixels at once, and deliver the frames at rate of 60Hz over USB3 to host device. There is a synchronization input for coherent imagery. Finally the cameras are of compact size helping to reduce the size and weight of the apparatus for lower latency.

4. CONCLUSION

There has been a recent breakthrough in virtual reality technology that enables a whole range of new applications. The article focuses on building a telepresence device and enlists some of the hardware challenges in design of such device together with possible solutions. The major challenges are identified as optical calibration and responsiveness of the robot. The stereo camera imagery needs to be meticulously calibrated in order to provide believable stereo imagery for depth perception and the robot has to be able to perform rapid movements in order to track fast head movements.

5. REFERENCES

1. Michael Abrash, „What VR Could, Should, and Almost Certainly Will Be within Two Years", Speech at Steam Dev Days, Feb 11, 2014
2. W. R. Bussone, „Linear and Angular Head Accelerations in Daily Life", Masters Thesis, 2005

6. ADDITIONAL DATA ABOUT AUTHORS

Corresponding author
Robert Hudjakov, robert.hudjakov@gmail.com

Co-authors
Robert Hudjakov, PhD researcher
Department of Mechatronics, Ehitajate Tee 5, Tallinn 19086, Estonia,
robert.hudjakov@gmail.com
+372 5245445

Ülari Lees, Mechatronics student
Department of Mechatronics, Ehitajate Tee 5, Tallinn 19086, Estonia,
ulari.lees@ttu.ee
+372 6203200

Mart Tamre, PhD, professor,
Department of Mechatronics, Ehitajate Tee 5, Tallinn 19086, Estonia,
mart.tamre@ttu.ee
+372 620 3202

9th International DAAAM Baltic Conference
INDUSTRIAL ENGINEERING -
24-26 April 2014, Tallinn, Estonia

AUTOMATION OF AN EXCAVATOR BOOM MOVEMENT IN 3-DIMENSIONS

Liukkonen, J.; Knuuttila, P.; Nguyen, T.; Ingale, S.; Kiviluoma, P.; Korkiala-Tanttu, L. & Kuosmanen, P.

Abstract: *Mass stabilization is the process of mixing binder into soil to improve its strength and stiffness. Stabilization is carried out using a specialized tool attached at the end of an excavator boom. The purpose of this project is to automate the boom movement of a mini excavator to better understand how automation affects the speed and accuracy of the system. The movement was automated using AT90CAN128 microcontroller connected by CAN bus to proportional valves which control the hydraulic cylinders of the boom based on the angle feedback from the resolvers. It was possible to move the bucket attached at the end of the boom reliably from point to point inside the reachable space of the excavator.*

Keywords: mass stabilization, robotic excavator, PID control, kinematics

1. INTRODUCTION

Mass stabilization is the process of hardening soft soil by mixing in a binding agent. Mass stabilization unit consists of one human operated excavator and a separate binding agent tank [1]. Typically large areas need to be stabilized and maintaining a consistent quality during this process is a difficult and time consuming task. The repetitive nature of the process suggests substantial benefits in automatizing the task.

This research focuses on automating the boom movement. The purpose is to reduce the effect of control movements of the operator to achieve more accurate and efficient result of mass stabilization. Independent movement of the excavator together with the tank is left out of this research. The research builds on the previous studies carried out by Martikainen et al. [2] and Kiviranta [3]. The goal is to extend the results of one-dimensional movement of the bucket tip by Martikainen et al. into full three-dimensional movement. Other groups such as Lee et al. [4] have also conducted research into automated boom movement for automated levelling work.

2. METHODS

The excavator used in the project (JCB Micro 800) is automated using electrohydraulic valves (Sauer-Danfoss, PVED-CC Series 4) and resolvers (Axiomatic AXRES-CO-V2-1X-H) which are connected through CAN bus to a microcontroller (AT90CAN128). The electrohydraulic valves of the excavator allow operation of the boom using a microcontroller and resolvers attached to each joint which provide accurate information of the joint angles. Since the original diesel engine of the excavator had been replaced with an electric motor, the resolvers were connected by twisted pair cables to minimize the electromagnetic interference.

A printed circuit board and the supporting electronics were built to interface the microcontroller with the electrohydraulic valves and the resolvers. Bucket tip coordinates specified in the custom made

PC software were supplied to the microcontroller via serial port. In the microcontroller, a software PID controller adjusts the flow for each valve based on the difference between the reference angle and the current angle for each joint. The control messages for the valves are sent through CAN bus and define the flow and spool drive direction. Figure 1 has a flowchart of the interaction between the system components.

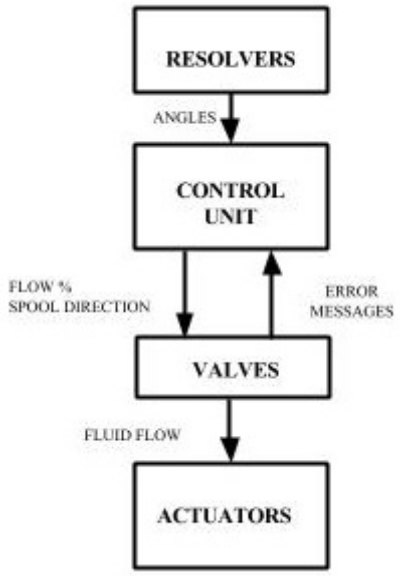

Fig 1. System schematic. The interaction between system components.

The desired path for the bucket tip is determined by an array of waypoints. Each waypoint consists of *x*, *y* and *z* coordinates of point O_3 as illustrated in Figure 2. These waypoints can be converted into joint angles by using inverse kinematics equations presented by Koivo [5]. Equation 1 describes the angle of the excavator boom slew joint

$$\theta_1 = \tan^{-1}\left(\frac{p_{oy}^D}{p_{ox}^D}\right), \qquad (1)$$

where p_{oy}^D is the *y* coordinate of point O_3 and p_{ox}^D the *x* coordinate. Equation 2 gives the angle of the link 2 around the Z_1 axis

$$\theta_2 = \tan^{-1}\left(\frac{p_{oz}^D}{d}\right) + \tan^{-1}\left(\frac{\sqrt{4a_2^2\left(\left(p_{oz}^D\right)^2 + d^2\right) - \left(\left(p_{oz}^D\right)^2 + d^2 + a_2^2 - a_3^2\right)^2}}{\left(p_{oz}^D\right)^2 + d^2 + a_2^2 - a_3^2}\right), \qquad (2)$$

where p_{oz}^D is coordinate of point O_3. Parameters a_2 and a_3 describe lengths of link 2 and 3, and d used to shorten the equation is defined as

$$d = \cos(\theta_1)p_{ox}^D + \sin(\theta_1)p_{oy}^D - a_1. \qquad (3)$$

where a_1 is the length of link 1. All the link lengths are given in Table 1.

	Link length (m)
a_1	0.180
a_2	1.340
a_3	0.945
a_4	0.460

Table 1. Link lengths of the excavator boom.

Equation 3 gives the angle of the link 3 around the Z_2 axis.

$$\theta_3 = \tan^{-1}\left(\frac{c_2 p_{oz}^D - s_2 d}{s_2 p_{oz}^D + c_2 d - a_2}\right) \qquad (4)$$

Finally, equation 4 gives the angle of coordinate frame O_4 around the Z_3 axis

$$\theta_4 = \theta_b + \theta_{dg} + (2\pi - \theta_2 - \theta_3), \qquad (5)$$

where θ_b is the angle between the bottom of the bucket and the X_4 axis. The digging angle θ_{dg} describes the angle between the bottom of the bucket and horizontal ground plane.

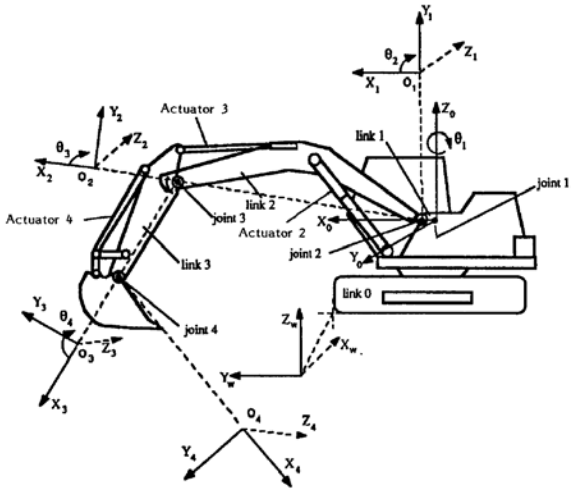

Fig. 2. The assignment of the coordinate systems [5].

For the purposes of this small scale prototype, the bucket is kept perpendicular to the ground to mimic the orientation of the power mixer. Thus, determining the final position of the bucket tip requires three joint angles, namely $\theta_1, \theta_2, \theta_3$ and the digging angle of the bucket θ_{dg}. It directly follows that the *x* and *y* coordinates of the bucket edge are the same with joint 4. The bucket length thus defines the difference in the *z* coordinate.

The waypoints are preloaded into the microcontroller memory via serial port. The reachability of each point is checked before coordinates are sent to ensure a predictable operation of the excavator. The reachable space of the excavator boom can be calculated when the link lengths and the minimum and maximum angles of each joint are known.

The reachable space can be visualized by plotting a slice of the 3D space according to Figure 3. This method is also very suitable for graphical user interface where the user can clearly see the reachable plane for a given *z* coordinate of the bucket tip.

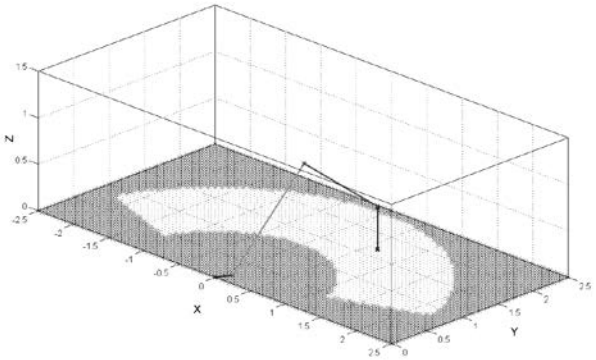

Fig 3. A slice of the reachable space of the excavator and an illustration of the orientation of all the boom links when the bucket tip is in coordinates (0.8, 1.5, 0.1).

The area to be stabilized can be divided into rectangular pieces. The mixing head is kept at roughly constant depth as it is moved through the soil. The system parameters can be optimized if the largest rectangle for a given depth (*z* coordinate) is known. The dimensions of the rectangle with the largest area can be derived as

$$x_{rect} = \frac{1}{2}\sqrt{8R^2 - 2k^2 - 2k\sqrt{8R^2 + k^2}} \quad (6)$$

and

$$y_{rect} = \frac{1}{4}\left(\sqrt{8R^2 + k^2} - 3k\right), \quad (7)$$

where *R* is the reach of the excavator and *k* is the radius of the unreachable area close to the excavator as illustrated in Figure 4.

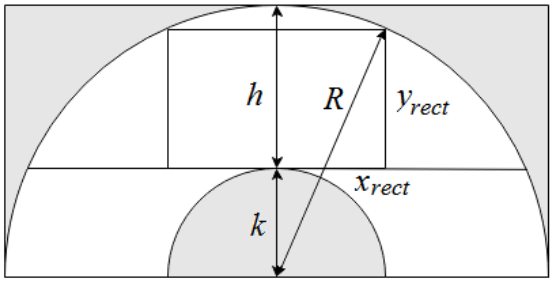

Fig 4. The rectangle inside a slice of the reachable space. The white area depicts area the excavator boom can reach for a given constant height of the bucket tip. The slew joint axis is at the origin.

3. TEST PLAN

Testing the accuracy and speed of the automatic operation is important for quantifying the possible performance gains in mass stabilization. To test the accuracy, a strategy for moving from one waypoint to the next must be devised. A waypoint strategy is characterized by the placement of the waypoints, e.g., the distance between the waypoints, and the tolerances associated with each waypoint. Each waypoint has a surrounding tolerance radius associated with it. If the resolvers indicate the bucket tip to be within the radius, the control algorithm then directs the bucket tip to move to the next waypoint. Modifying these factors will result in changes in performance measures. The goal was to find an optimal waypoint strategy within this control framework.

To determine the value of the usable tolerances, the accuracy of the system has to be measured.

Before the tolerances can be measured the resolvers must be calibrated. The system was calibrated by measuring the maximum and minimum readings for each resolver. The actual angles of the boom joints were then calculated by measuring the height of each joint from level floor and using trigonometric relationships to obtain the maximum and minimum joint angles corresponding to the resolver values.

4. RESULTS

In order to determine the reliability of the resolver data, the real position of the bucket tip was measured from five different points and the results were compared with the position indicated by the resolver data and the kinematics equations. The comparisons are shown below in figures 5 and 6. The bucket joint angle θ_4 was not included in the measurements. The bucket was always set so that the line from the bucket joint to the bucket tip was perpendicular to the ground.

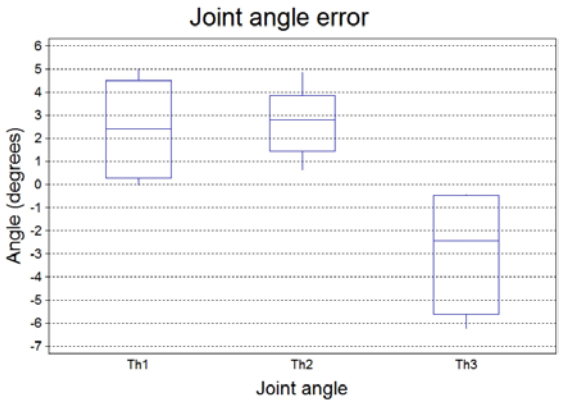

Fig 5. Box-Whisker plot for the joint angle error of the resolvers. The error in degrees of θ_1 was between [0.5, 4.98]. θ_2 had error between [0.65, 4.85] and the error of θ_3 was between [-0.44, -6.24].

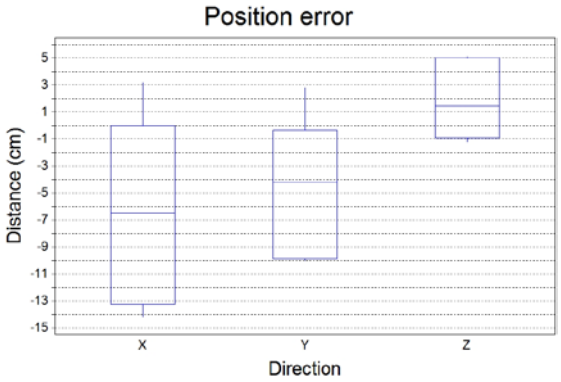

Fig 6. Box-Whisker plot for position error of the bucket tip. The error in x-direction was between [-14.2, 3.2], for y-direction the error was between [-10, 2.8], and for z-direction [-1.2, 5.1].

The joint angles had errors less than 6 degrees for all the joint angles. The absolute error in distance was on the average 11.33 cm or 6.43%. The standard deviation was 4.05 cm or 2.8%. The resolver data were concluded to be sufficiently accurate for this application based on the comparison.

The calibration step is crucial for achieving high accuracy and these results could perhaps be further improved.

5. CONCLUSIONS

The initial test results showed that the boom can be reliably moved within the reachable space of the excavator when no

external forces act on the boom. Thus the excavator is used in this research primarily as a test platform for automated boom movement. In mass stabilization the excavator joints have to tolerate large lateral loads.

Currently, an important next step would be to develop a system for monitoring the forces applied to boom and the power mixer unit to avoid damage to the tool when encountering hard obstacles, such as rocks hidden in the soil. Beyond that, the problem of autonomous movement of the excavator and binding agent tank must also be solved to achieve full automation.

6. REFERENCES

1. Lahtinen, P. and Niutanen, V., *Development of In-Situ Mass Stabilization Technique in Finland*, . Deep Mixing 2009 Okinawa Symposium, International Symposium on Deep Mixing & Admixture Stabilization Okinawa, Japan, May 19-21, 2009.

2. Martikainen, J., Pahlsten J., Söderena P. & Ubiagege C., "Automation in Mass Stabilization," 2013, 8th International DAAAM Baltic Conference (Speech).

3. Kiviranta, J., *Instrumentation of an Automated Excavator*, Master's Thesis, Helsinki University of Technology, Espoo, 2009.

4. Lee, C. S., Bae, J., and Hong, D., "Contour Control for Leveling Work with Robotic Excavator," Int. J. Precis. Eng. Man., 2013, **14**, 2055–2060.

5. Koivo, A. J., "Kinematics of Excavators (backhoes) for Transferring Surface Material," J. Aerosp. Eng., 1994, **7**, 17–32.

7. CORRESPONDING ADDRESS

Panu Kiviluoma, D.Sc. (Tech.)
Aalto University School of Engineering, Department of Engineering Design and Production
P.O. Box 14100
00076 Aalto, Finland
Phone: +358 50 433 8661
E-mail: panu.kiviluoma@aalto.fi
http://edp.aalto.fi/en/

8. ADDITIONAL DATA ABOUT AUTHORS

Liukkonen, Jere, B.Sc. (Tech)
Phone: +358 45 112 5028
E-mail: jere.liukkonen@aalto.fi

Knuuttila, Pekka, B.Sc. (Tech)
Phone: +358 40 560 9767
E-mail: pekka.knuuttila@aalto.fi

Nguyen, Tien, B.Sc. (Tech)
Phone: +358 44 096 4507
E-mail: tien.vannguyen@aalto.fi

Ingale, Saurabh, B.Sc. (Tech)
Phone: +358 41 483 3068
E-mail: saurabh.ingale@aalto.fi

Korkiala-Tanttu, Leena, D.Sc. (Tech.), Professor
Phone: +358 50 3124 775
E-mail:leena.korkiala-tanttu@aalto.fi

Kuosmanen, Petri, D.Sc. (Tech.), Professor
Phone: +358 500 448 481
E-mail:petri.kuosmanen@aalto.fi

9th International DAAAM Baltic Conference
"INDUSTRIAL ENGINEERING -
24-26 April 2014, Tallinn, Estonia

INFLUENCE OF THE HIGH-SPEED MILLING STRATEGY ON 3D SURFACE ROUGHNESS PARAMETERS

Logins, A.; Torims, T.; Gutierrez Rubert, S. C.; Rosado Castellano, P.; Torres, R.

Abstract: *High-speed machining is an effective modern machining method used in die-cast material processing, to increase the efficiency, quality and accuracy of the machined surface and to reduce costs and machining time. The aim of this research is to explore the technological strategy and influence of the processed materials on the 3D surface roughness parameters and provide recommendations for manufacturers on how to obtain the prescribed surface roughness parameters. This paper covers analysis of the following factors: feed rate, manufacturing strategy, overlap and material influences on the most characteristic 3D surface parameters. The results are based on ANOVA—analysis of variance—where differences between groups of means are analysed using a collection of statistical models. This method enables the comparison of three or more group variables for statistical significance. The present paper provides analysis and relevant conclusions on the most significant impact factors: material and the high-speed milling manufacturing strategy.*

Key words: *high-speed milling, 3D surface roughness, technological milling strategy, ANOVA, analysis of variance*

1. INTRODUCTION

Up until recently, the 2D surface roughness standard *ISO* 4287:1998 was used in manufacturing. However, this has now been replaced by the 3D surface roughness standard *ISO* 25178: 2012 (e.g. [3]). As yet, there is no reciprocal, correlative information regarding surface roughness and machining technology parameters for this standard. Given the changes in technological machining parameters and measured 3D surface roughness parameter variances, there is a need to draw conclusions and analytically describe certain relationships between the technological machining process parameters and surface roughness.

The overall aim of this research is to identify mathematically the most critical technological parameter influencing each specific 3D surface roughness parameter. At the end of this research, the authors prepared several recommendations for manufacturers on how to apply these technological parameters during the manufacturing process, in order to minimize surface roughness.

2. HIGH SPEED MACHINING

High-speed milling (HSM) is a modern technological manufacturing method, as compared to traditional machining with chip removing methods (turning, milling and grinding), which aims to increase manufacturing efficiency and improve surface quality, whilst at the same time reducing manufacturing time and costs. The high-speed milling method has many benefits compared with conventional milling. Very often, high-speed milling is considered merely as a way to improve productivity resulting from faster cutting speeds than those used conventionally. High-speed milling is widely used in

modern tool manufacturing and die-cast material machining, which has strict requirements for low surface roughness (e.g. [2]).

Based on this research in the Department of Mechanical and Materials Engineering at the Polytechnic University of Valencia, the most popular die-mould steel samples were machined using various combinations of cutting parameters (feed rate, strategy and overlap). Such cutting parameters as depth of cut and cutting speed were kept constant.

The Gentiger GT-66V-T16B high-speed milling machine was used for the experiment, which has a spindle speed of up to 16,000 min^{-1}. In addition, the machine power is sufficient to process highly durable materials operating at high-speed with a rapid feed rate. The machine spindle power can reach 26 kW, the rapid feed rate is 30 m/min and working feed rate is up to 20 m/min. The machine is equipped with a Siemens 840D NC controller and BT-40 cone-type spindle.

3. 3D SURFACE ROUGHNESS MEASUREMENTS

The actual surface of every existing object in real life is three dimensional (e.g. [1]). In order to successfully characterize the surface roughness, it is not enough to describe it with only a single parameter (e.g. Sa – the arithmetic mean height of the surface). Complex surface characterization is required, using parameter groups. Today the extensive review of surface roughness and numerical values provide us with 3D roughness measurement methods and a standard. The method is based on the measurement point determination, which is done using both random methods, through a graphical approximation and determining the number of points where the values of parameters are stabilizing. (e.g. [4])

The number of data points has to be optimal. Too few data points lead to inaccurate results and increased distribution amplitude; but too many data points substantially increase measuring time without broadening the range of fundamental information. (e.g. [4])

In this research, all machined samples were measured using the Taylor Hobson Form Talysurf Intra 50 measuring device with TalyMap Expert data software. All the measurements were taken in the Material Processing Technology Department at Riga Technical University.

4. APPROACH

Experiments were performed on 3 high-strength materials: two types of steel widely used in die mould manufacturing and titanium. The steel grades are 1.2312 (40CrMnMo58-6) and 1.1730 (C45W).

This research began in the Department of Mechanical and Materials Engineering at the Polytechnic University of Valencia and incorporates work at the Material Processing Technology Department of Riga Technical University, based on research into the impact of high-speed milling on 3D surface roughness parameters [1].

A variable combination of feed rate, strategy and overlap factors was selected. Such cutting parameters as depth of cut and cutting speed were kept constant. One of the most potentially significant factors affecting the cutting quality and manufacturing speed is the feed level. The cut feed level is determined taking into account recommendations from tool manufacturers, as specified in the cutting tool catalogue. Also, machining may be repeated in different directions by different paths or cutting strategies. The overlap influences the processing time, costs and roughness. Likewise materials with different mechanical properties have differing impacts on the machining results. Each material sample was divided into 16 subsamples, eight per side, cf. Fig.1.

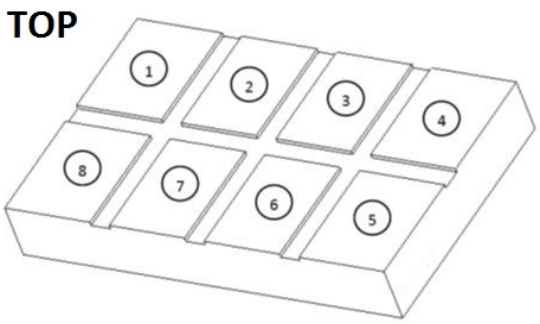

Fig. 1. One side of the work piece with the eight sample sections

After all of the samples were machined, 3D roughness measurements were taken. Several photographs were also taken of the surface using a microscope, in order to compare the images with the images provided by the Talymap Expert software for the surface roughness measurement. For each of the 3 materials, 16 surface roughness measurements were taken. The results were initially sorted by the groups they belonged to and the most significant parameters were chosen using the correlation matrix in the Rcommander software. By preparing the correlation matrix of *n* random variables and including a set of 3D roughness parameters, we obtained the most significant, distinctive parameters for each group. They are Sa – the arithmetical mean height of the surface, Sku – the kurtosis of the scale limited surface, STp – the height of the bearing area ratio curve, Str – the texture aspect ratio and Svi – the valley fluid retention index.

5. ANALYSIS

The chosen 3D roughness parameters were collated in spreadsheets, to prepare graphs illustrating the roughness parameter changes affected by feed level, overlap and strategy type. Fig. 4. and Fig. 5. show the differences between the surface roughness parameters applying the linear pattern (LP) and circular pattern (CP) in the machining process, where overlap and feed levels are kept constant. Multiway ANOVA data analysis software, such as Rcommander, with libraries of statistics provides more extensive information about the influences of technological parameters on roughness.

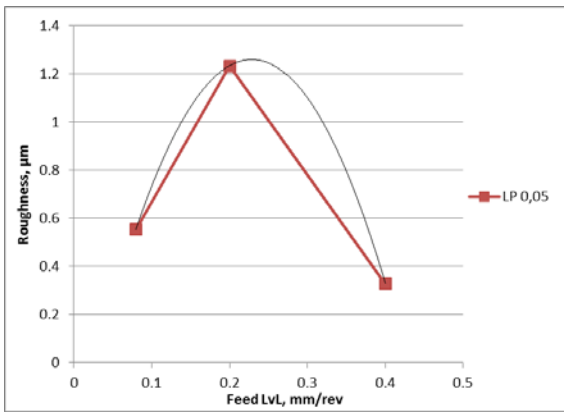

Fig.2. The linear pattern strategy type with a 0.05mm overlap influences the Sa parameter (material 1.1730)

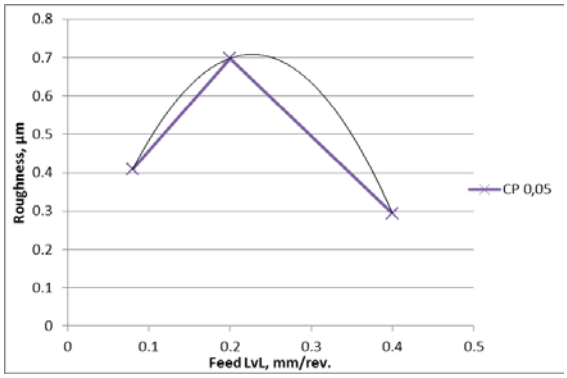

Fig.3. The circular pattern strategy type with a 0.05mm overlap influences the Sa parameter (material 1.1730)

As can be seen from the retrieved data, their value is similar to that shown by the mathematical regression, although the overall surface roughness is slightly lower using a circular milling pattern. This is also seen in the surface images (Fig.4.and Fig.5.)

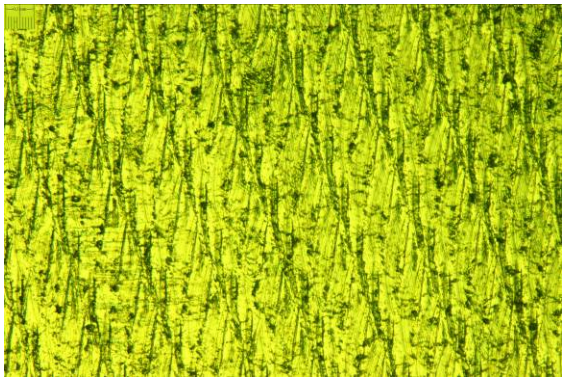

Fig.4. Sample no. 6. (LP 0.05, Feed 0.4 mm^{-1}) microscope camera image

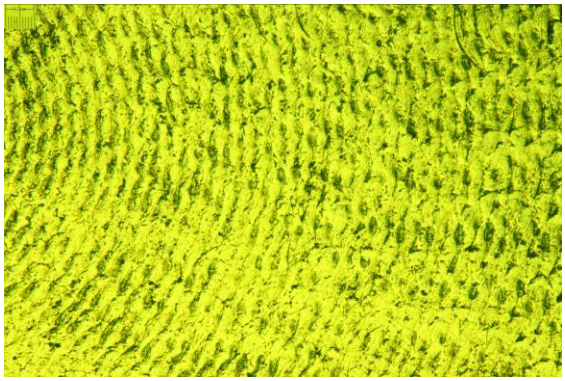

Fig.5. Sample no. 13. (1.1730, CP 0.1, Feed 0.4 mm^{-1}) microscope camera image

The polynomial regression trend line equation with argument x for the first example with a linear pattern shows that one of the technological parameters has a major influence; in this case, it is the feed level:

$$y = -31.818x^2 + 14.568x - 0.4076 \quad (5.1)$$

The same situation occurs with the second, circular pattern. However the equation ratios confirm that differences between feed levels are lower:

$$y = -13.84x^2 + 6.29x - 0.01 \quad (5.2)$$

The situation is slightly different in the case of a linear cutting pattern, where the cutter overlap is 0.1mm. This situation is described below and shown in Figures 6. and 7. Here the roughness parameter Sa increases together with the feed level. This is also shown by the difference between the equation ratios:

$$y = -8.14x^2 + 6.27x - 0.13 \quad (5.3)$$

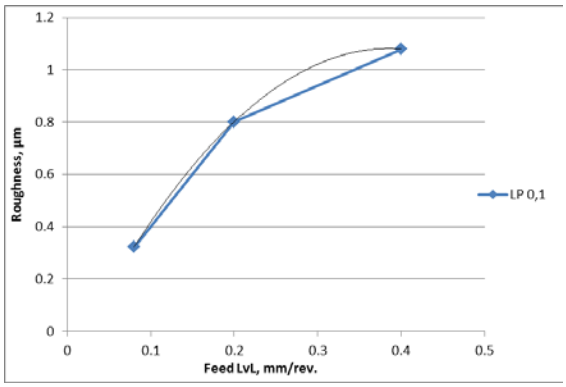

Fig.6. Influence of the linear pattern strategy type and 0.1 mm overlap on the Sa parameter (material 1.1730)

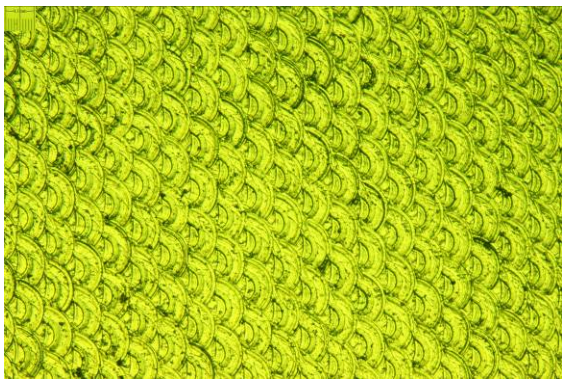

Fig.7. Sample no. 1. (1.1730, LP 0.1, Feed 0.07 mm^{-1}) microscope camera image

For material type 1.2312 (40CrMnMo58-6), the situations in terms of the graph lines are comparable. The surface roughness distribution for samples such as LP 0.05 and CP 0.05 are similar and differences between surface roughness for different feed levels are almost imperceptible. The roughness distribution of feed level for samples with LP 0.1 is different. As we can see from Fig. 8., with a low feed level (0.07) the roughness parameter Sa is lower and at a medium feed level it is highest, but at the high feed level the parameter decreases again.

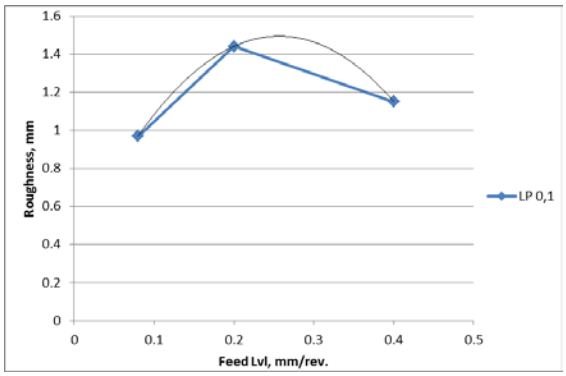

Fig.8 Influence of the linear pattern strategy type and 0.1 mm overlap on the Sa parameter (material 1.2312)

Equation with ratios for this polynomial line:

$$y = -16.795x^2 + 8.6273x + 0.3863 \quad (5.4)$$

The Rcommander mathematical analysis software was used to validate this schedule, replacing all technological parameters with factors. ANOVA analysis between pairs of technological parameters is done firstly for all material types. The pairings that cross-reference the parameters are: feed level–strategy type, feed level–cutting direction, strategy type–cutting direction, feed level–overlap and overlap–cutting direction. A similar correlation was also conducted previously for each of the chosen roughness parameters, in order to compare their influence on each of the chosen parameters.

The use of the condition of cutting direction for example is not objective for analysis where one cutting direction is advantageous for only a few samples, rather than all. It thus had to be abandoned. Finally, pairs of all of the technological parameters were correlated, resulting in only two different technological parameters, which had the most significant impact, and all 3 kinds of materials. Final analysis between these parameters and the materials was then conducted for each chosen roughness parameter, to identify the most significant parameter. For parameters Sa and Svi, the most significant factor is strategy type (the significant ratio is respectively 0.002 and 0.04). For parameters Sku and Stp, the most significant factor is material type (0.01 and 0.03). For the roughness parameter Str, the most significant factor is feed level (0.001), with the second most significant factor being material type (0.09).

6. SIMULATION

A simulation was also undertaken with the developed application, coded using software called Python, to capture the cutters' cutting edge behaviour on the material surface. It is based on actual surface pictures taken by the camera from sample no. 18 (1.2312, LP 0.1, Feed 0.2 mm^{-1}) and the technological parameters used during the sample machining process, cf. fig. 9. The simulation shows the movement of the cutting edge over the material, cutting edge velocity vectors and surface texture changes.

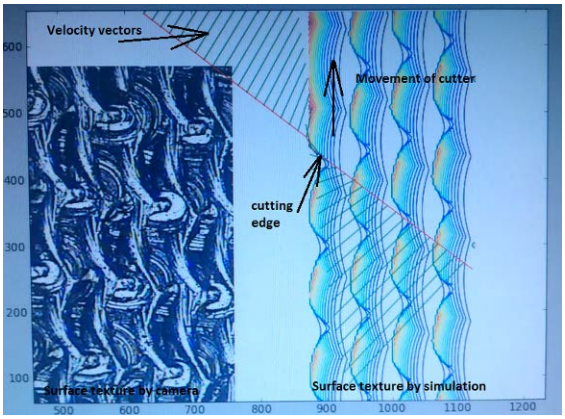

FIG.9. Simulation of sample no. 18, made using ActivePython 2.7.2.5 software

7. CONCLUSIONS

The greatest influence among the selected technological parameters is the material or the influence of the material's mechanical properties. The material influence is reflected in two parameters: Sku and STp. Materials with the highest hardness affect the distribution of "peaks" over the surface. Other mechanical properties affect the bearing ratio index. It is possible to determine whether the surface has peaks of several different heights, or whether their height is evenly distributed (Fig.10).

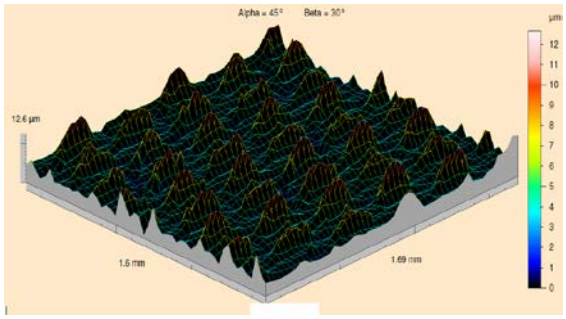

FIG.10. Sample No. 16, surface peakedness – surface peak distribution

The greatest influence when looking at one type of material is strategy type. It appears to be better to use the circular machining strategy. Samples machined in this way have lower values for the surface roughness parameters Sa and Svi. In terms of the strategy's influence, the overall surface roughness changes, so this value is easy to express with the parameter Sa (Fig. 11).

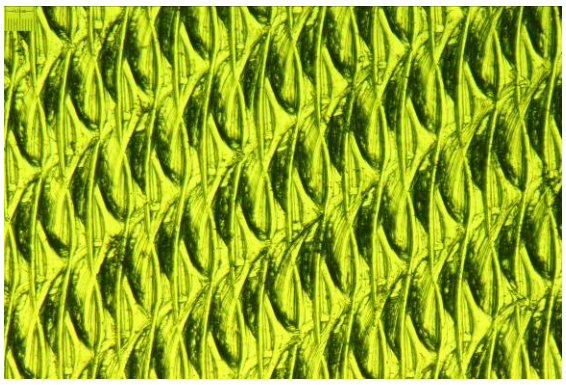

FIG.11. Sample no. 3. (1.1730, LP 0.1, Feed 0.4 mm^{-1}) surface image taken by camera

The third major influence is feed rate, which is significant only for the Str parameter. It was shown that it depends on the feed level invited vibrations, texture aspect ratio grooves or drop off.

Vertical cutter displacement is probably not the best option for such machining because, as shown in the simulation, velocity vectors in some of the cutter edge positions do not match the cutting direction.

Titanium cannot be processed with the same technological parameters as those used to process die mould materials. Titanium has a different distribution of surface roughness parameter values compared with die mould manufacturing steels.

The research will be continued and further experiments will be conducted during our future work.

1. REFERENCES

1. Brutans, V., Kumermanis M., Rosado Castellano, P., Torres, R., Gutierrez Rubert S. C., *The Impact of High-Speed Milling on 3D Surface Roughness Parameters*, 8th International DAAAM Baltic Conference "Industrial Engineering", 19-21 April 2012, Tallinn, Estonia, 4 pages;
2. Kauppinen V., *High-speed Milling – a New Manufacturing Technology*, 4th International DAAAM Conference "Industrial engineering – innovation as a competitive edge for SME", April 2004, Tallinn, pp. 131-134;
3. Vorasri, M., Jirapattarasilp, K., Kaewkuekool, S., *The Effect of High-Speed Milling on Surface Roughness of Hardened Tool Steel*, World Academy of Science, Engineering and Technology 59, 2011, pp. 469-472;
4. Griffiths, B., *Manufacturing Surface Technology*, Penton Press, London, 2001, 238 pages;
5. Kauppinen, V., *High speed machining of hard-to-machine materials.* 4th International Conference on Metal Cutting and High-Speed Machining ICMC, Darmstadt, 19-21 March, 2003;
6. Wang, M.Y., Chang, H.Y., "*Experimental Study of Surface Roughness in Slot-End Milling AL2014-T6*", International Journal of Machine Tools and Manufacture, Vol. 44, No.1 (2004), pp. 45-49 and 51-57.

9th International DAAAM Baltic Conference
"INDUSTRIAL ENGINEERING -
24-26 April 2014, Tallinn, Estonia

DEVELOPMENT OF DUAL HEAD INKJET DISPENSER FOR PHARMACEUTICALS

Lohani, V.; Sandström, V.; Shekh, A.; Teinonen, H.; Korkolainen, P.; Kiviluoma, P.; Widmaier, T.; Sandler, N. and Kuosmanen, P.

Abstract: *The need for individual dosage of medicine has been a challenging issue in health care. The suitable dosage varies especially for children and adults in the microgram scale. This demand is likely to grow by additional information about individual's medicine responses gained by gene mapping. To test possibilities of new dosing methods a commercial thermal inkjet printing head was customized for printing liquid pharmaceutical onto a substrate. The results prove that the dual inkjet printing process is faster and more flexible than one head printing. Compared to traditional processes, the tested process dispenses the drugs with faster production cycle, fewer processing steps and on-demand individualized precise doses.*

Key words: medicine dispenser, dual printer head, inkjet printing, personalized medicine, precise dose.

1. INTRODUCTION

There is a constant demand for easy-to-use and inexpensive methods of dispensing small customized doses of medicinal products [1] at hospital pharmacies. The individuals most in need of these solutions are babies and elders. It is also expected that once estimating each individuals' responses to each individual drug compound become possibly due to gene mapping, the demand for exact doses rises as part of personalized medicine. To this date very few medicinal products in solid form are available in small enough discreet steps to cater for this need.

1.1 Personalized medicine

Medicine is likely to move from reactive to a proactive discipline that can be described as the P4 medicine, personalized medicine or precision medicine. Genomic medicine and medication are part of this change, providing precise tools to effectively counter or cease disease progression. This approach is going to require cost-efficient and easy-to-use utilities to produce or dispense customized combination drugs that would vary in consistency from individual to individual. [2]

1.2 Classic method to customize dosage

To this day these custom doses are done by using the traditional mortar and pestle method, in which a number of pills are crushed and a certain percentile is approximated. This method suffers from poor accuracy, laborious process and hard-to-use product.

1.3 Thermal Inkjet - TIJ

Thermal inkjet is an inkjet design where ink nozzles contain a resistor heater that creates a local vapor bubble. This bubble then grows to push a constant volume droplet of ink out of the nozzle before collapsing to be filled with ink again. This process can be seen in Figure 1. A film resistor superheats a small fraction of the ink to create a rapidly growing gas bubble that fires a droplet out of the

nozzle. Inkjet's advantages are listed as follows by the manufacturer HP: high firing rate, small droplet size and low cost of ownership. [3]

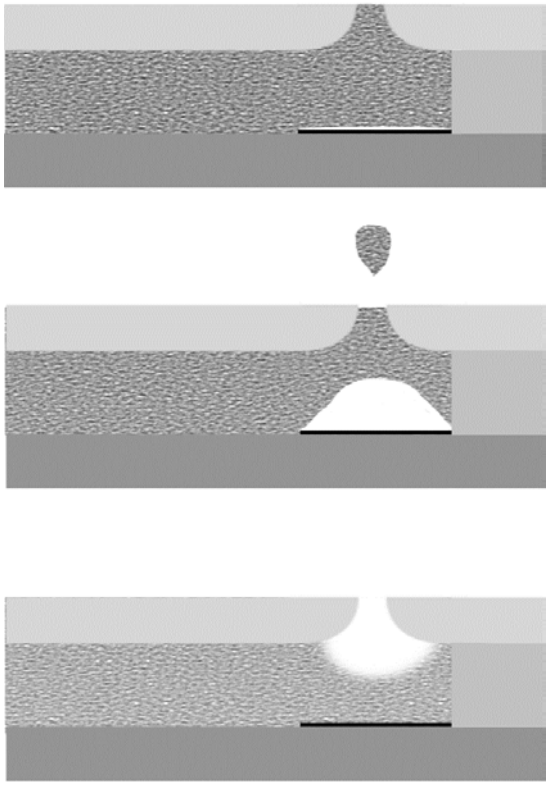

Fig. 1. TIJ nozzle's firing cycle

There have been previous efforts to design custom dose medicinal product dispensers based on TIJ. The previous efforts [4] have led to some working prototypes, although these devices have not yet been adopted to real life scenarios. Our objective was to develop an amended version of the medicinal product dispenser to support simultaneous use of two printing heads, to create easy-to-use user interfaces and to solve issues found in the previous version.

1.4 Application area

Possible users for a custom dose dispenser would be at first hospital pharmacies and then common pharmacies. However, application area can't be limited to commercial solutions, should required technology and knowledge become widely available to the general public.

2. METHODS

2.1 Hardware

This device is built on a 3D printer with two HP inkjet printer heads model 51604A installed. Two Q7453A Carriage assemblies with 10 inches flex were installed for dual printing technique. The stainless sheet was placed in a printing bed and magnet clamping system was used to fix the printing paper. A4 and A5 size were calibrated on the surface of the sheet.

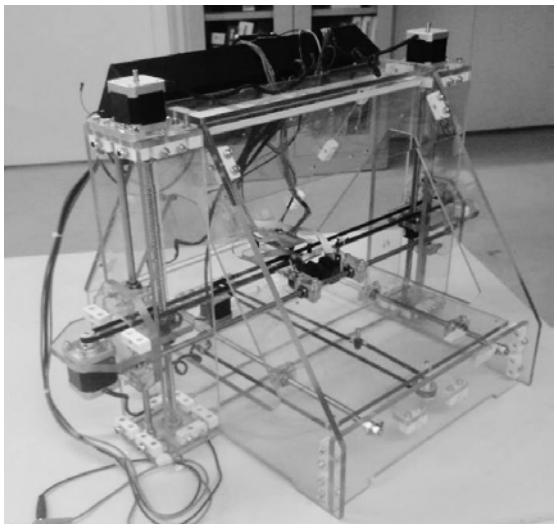

Fig. 2. A dual head Inkjet dispenser

The controlling of two printer heads was done with a mux shield stacked on the microcontroller; Arduino Mega 2560. This was then connected to darlington transistor arrays ULN2803 as depicted in Figure 3. The darlington arrays were powered by external 20V supply. Each component contains 8 darlington transistors. These transistors were used to amplify the output signal [5]. Similarly, x, y and z-axis movements were controlled via microcontroller. Proximity sensors were placed at different location to limit the axes movement in defined region.

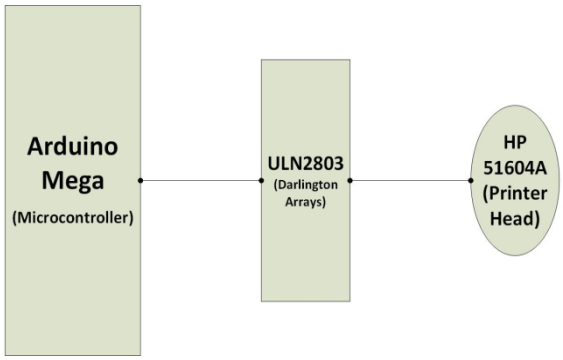

Fig. 3. Schematic of Darlington arrays, Printer head and Microcontroller

The functionality of medicinal product printing itself is possible by following the same procedure as printing with ink. [6] The technique of TIJ nozzle's firing cycle is illustrated in Figure 1. Each of the firing signals produce an almost stable-sized droplet that is then precisely placed on the substrate.

2.2 Software

The main goal behind the software was to make an easily approachable, user friendly graphical interface that still gives full control over the printing process. This was achieved by defining readymade print programs for the operator to use. In an ideal case, the operator would only need to open the desired print program from a file and press the print button in order to start the print process.

Thought was also put into the layout of the main view in order to make it as simple as possible, while still providing the crucial information about the current print program. The main view shows the substance and amount of substance of each printer head, print program description as well as a visual preview of what the program is to print.

The parameters of the different print programs are fully modifiable, and can be saved easily. For the more advanced user, there is also a list of different substances used in the print programs that can be modified as required.

2.3 Testing Method

Two different drug solutions were used to print drug solutions on the starch based substrate. Cyanocobalamin solution consists of 10 mg/ml Cyanocobalamin in glycerol and water in 10:90 ratios. Riboflavin sodium phosphate (RSP) solution constitutes 50 mg/ml RSP in glycerol and water by 10:90 percentages by volume. The substrate was placed on the printer's bed and fixed with magnet. The drug solutions were filled into printer head using syringe. Then, multiple layers of the drug solutions were printed on the substrate. The surface area of each sample was 1 cm x 1 cm.

2.4 Quality Assurance

Blending dye to the drug eases to inspect visually correct amount of printed drug. This is a simple, effective, and quick procedure to check the precise dose. However this works perfectly if only one drug is printed at a time to a specific place on substrate. Mixture of different coloured drugs makes difficult to distinguish the ratio of the drugs printed on the substrate.

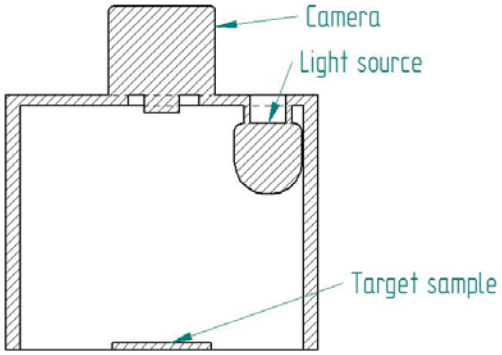

Fig. 4. Cross section of the camera setup

To mitigate online quality assurance, a machine vision system was designed. The system consists of a camera connected to a computer running machine vision software. The specifications of the camera are 1/3" CCD sensor and 3 MP, Carl Zeiss lens. The camera was installed in the same cradle as the printer head to allow easy positioning of the camera. The

camera was equipped with its own light source and shielded from ambient light to improve image quality. The setup, illustrated in Figure 4, minimizes variance between the pictures and better calibration can be achieved.
The camera is mounted at the height of 72 mm from the surface of the substrate. This set up provides the camera a resolution of 50 µm per pixel. Higher theoretical resolution could be achieved with same sensor but the mounted lens is not capable of producing better resolution. Calibration of camera system is done by comparing test results from a mass spectrometer i.e. off-side and the camera i.e. online. Same test samples are used in both measurements. A camera system has to be calibrated for each colour separately to get accurate results.

3. RESULTS

3.1 Hardware

A printed circuit board is utilized to connect darlington transistors between printer head HP 51604A and microcontroller, Arduino Mega 2560. The calibrated printer's bed is depicted in Figure 5.

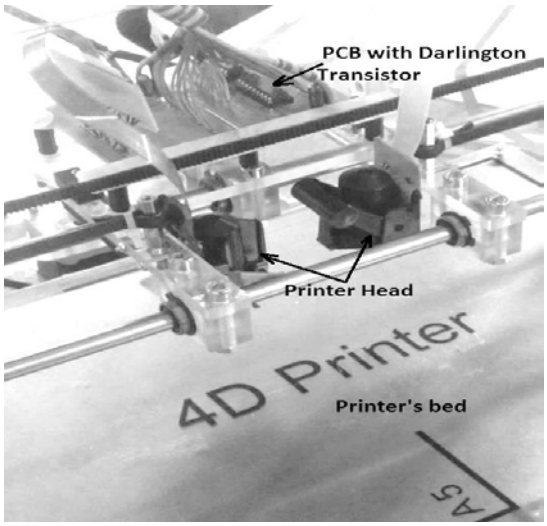

Fig. 5. Dual printer head with darlington transistors

3.2 Software

In order to ensure the ease of use of the software, a number of trials with persons, to whom the software was previously unknown, were conducted. The task was to complete three different smaller tasks, and the user-friendliness of the program was evaluated based on the feedback from these tasks.
The results of this trial conclude that the software's intuitive user interface and logic make an excellent first version of a de facto tool of tomorrow.

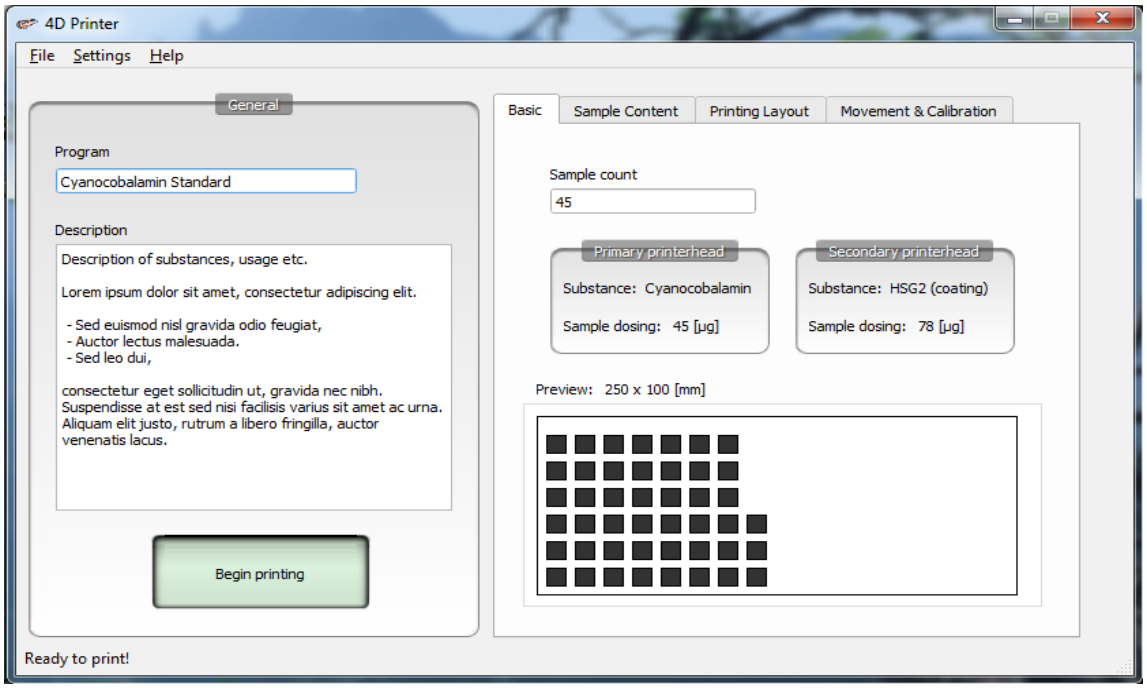

Fig. 6. Graphical user interface

3.3 Test and Quality assurance results

The dual head inkjet dispenser works as defined by requirements. Multilayer of different drug solutions was printed in an efficient ways. The results of this experiment can be seen in Figure 7. The routine proved to be a success and no notable disintegration of the substrate was noticed. The efficiency of the heating arrangement was verified, too. The initial results of online and off-side measurements are correlated.

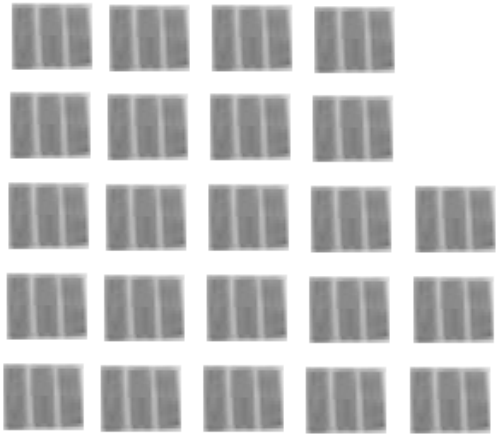

Fig. 6. Printed drugs solution on substrate

4. DISCUSSION

The research focused on the development of dual head inkjet dispenser for pharmaceuticals. A fully functional dispenser was developed. The calibrated printer's bed and clamping systems facilitates the easy to handling processes. It is also validated that dual inkjet printing process is faster and more flexible than single head printing. Similarly, the tested process dispenses the drugs with faster production cycle, fewer processing steps and on-demand individualized precise doses.

The online quality assurance is still under development. Some of the results correlate the measurement between online and off-side measurement. There are needed more in depth research in this matter.

4.1 Printed medicine isolator

With the technology at hand, it would be possible to add a separate printer head that would print an edible physical obstacle on the substrate to isolate different component from each other. Similarly it would be possible to print the substrate itself on the go as proposed by Gbureck et al. [7].

4.2 Alternative Applications

As highlighted before, a medicinal product dispenser capable of producing customized doses cost-efficiently would be an essential part of P4 revolution. The device's improved versions could be used to create individually optimized micronutrient portions for daily intake or to ensure right and proper use of prescribed medicinal product. The latter could be enforced by different verification measures.

A version for home use of the device is a possibility as the GUI proved to be easy to use even for a layperson. The home use version could be based on a system of automatic recognition of medicinal product cartridges bought from pharmacies.

5. CONCLUSION

The approach using multiple printer heads to enhance medicinal product dispensing efficiency and usability was tested and proven useful in various cases. The most important drawback of the previous versions, the quality assurance, was also addressed and it was found to satisfy initial requirements and the device can now be adopted for trial use.

The study lays foundation for further improvement of the custom dose medicinal product dispensers. The designed device poses a great advancement to availability of simple and cost-efficient devices for custom dose dispensing that are essential for personalized medicine.

6. CORRESPONDING ADDRESS

Panu Kiviluoma,
Aalto University School of Engineering
Department of Engineering Design and Production
P.O.Box 14100,
00076 Aalto, Finland
E-mail: panu.kiviluoma@aalto.fi
Phone: +358 50 433 8661

7. ADDITIONAL DATA ABOUT AUTHORS

Lohani, Vishesh
Email: vishesh.lohani@aalto.fi
Ph.: +358-40-8735405

Sandström, Valter
Email: valter.sandstrom@aalto.fi
Ph.: +358-50-4654549

Shekh, Arju
Email: arju.shekh@gmail.com
Ph.: +358-40-9666051

Teinonen, Henri
Email: henri.teinonen@aalto.fi
Ph.: +358-40-7057108

Korkolainen, Pauli
Email: pauli.korkolainen@aalto.fi

Widmaier, Thomas
E-mail: thomas.widmaier@aalto.fi

Niklas Sandler, PhD (Pharm.), Prof.
Email: niklas.sandler@abo.fi

Kuosmanen, Petri, D.Sc. (Tech.), Prof.
E-mail: petri.kuosmanen@aalto.fi

8. REFERENCES

1. Parliament, E. U. Directive 2004/27/EC of the European Parliament and of the Council of 31 March 2004 Amending Directive 2001/83. EC on the Community Code Relating to Medicinal Products for Human Use, 2004.

2. Hood, L.; Friend, S.H. Predictive, personalized, preventive, participatory (P4) cancer medicine. Nature Reviews Clinical Oncology, 2011, 8.3: 184-187.

3. Nigro, S.; Smouse, E., Hewlett-Packard Inkjet Printing Technology: the sate of the art.

4. Takala, M.; Helkiö, H.; Sundholm, J.; Kiviluoma P.; Kuosmanen, P. “Ink-jet printing of pharmaceuticals”, Proceedings of the 8th International DAAAM Baltic Conference, 19 - 21st April 2012, Tallinn, Estonia.

5. Aaltonen, O.; Ritari, A.;Vähä-Ojala, T., Kolakovic, R., Sandler, N., Kiviluoma, P. and Kuosmanen, P., “Printing pharmaceuticals with thermal inkjet printhead”, 2013, Aalto University

6. Kolakovic, R.; Viitala, T.; Ihalainen, P.; Genina, N.; Peltonen, J.; Sandler, N. (2013)., “Printing technologies in fabrication of drug delivery systems ”, Informa Healthcare, 2013, Vol.10, No. 12, pp.1711-1723(13).

7.Gbureck, U, et al. Low temperature direct 3D printed bioceramics and biocomposites as drug release matrices. Journal of Controlled Release, 2007, 122.2: 173-180.

9th International DAAAM Baltic Conference
INDUSTRIAL ENGINEERING
24-26 April 2014, Tallinn, Estonia

Gesture Controlled Human Machine Interface for Future Machines

Praks, T.; Romot, C.; Sillat, M.-L.; Soomänd, K.; Hiiemaa, M.; Tamre, M. & Juurmaa, M.

Abstract *Human-machine interfaces (HMIs) of stationary industrial machines are often stationary or require a teaching pendant. A stationary control panel limits the mobility of the operator while a remote can be dropped, broken or misplaced. Machine vision is a viable alternative for physical HMIs. To demonstrate the potential of machine vision in these circumstances, this paper describes an application in which a quadrocopter is controlled using hand gestures. In the application described in this paper, an operator manipulates the quadrocopter using predefined hand gestures to initiate predefined maneuvers. This work demonstrates the uses of discrete hand gestures and draws comparisons between the discrete control and continuous control. Similar solutions to those described in this paper can be used in a variety of systems and possible applications range from industrial robots to household electronics.*

Keywords: machine vision, hand gesture recognition, robot control, industry

1. INTRODUCTION

Machine vision is widely used in many industries in applications ranging from product quality control, to fingerprint recognition. In the last decade, vision based systems have developed rapidly and have become common in our everyday lives whether we notice it or not. Although the concept of using machine vision for controlling industrial machines or manipulators has been around for years, it has only lately become feasible due to the technological achievements in the field. Several works [1-4] have already been conducted to prove that this method is a viable option in the future for replacing the bulky and inconvenient HMIs of today.

In this work a simple vision based control system was used to control a quadrocopter to demonstrate the potential of said systems. Similar works have been done using hand tracking and gesture recognition but several problems arise when controlling such an unstable platform with continuous hand tracking. Most importantly - the precision suffers due to the lack of feedback to the user and this is unacceptable in industrial machines. This work concentrated on exploring the advantages and disadvantages of using discrete control as opposed to continuous control. For this the quadrocopter was used as a testing platform to explore the viability of discrete hand gestures and the results are compared with similar works that use continuous control. To draw more comparisons with already conducted works, both discrete and continuous actions were performed, but for every action the initiating command was always discrete. Although we were not strictly following the scientific method, comparisons could be drawn and conclusions could be made.

2. WORKING PRINCIPLE

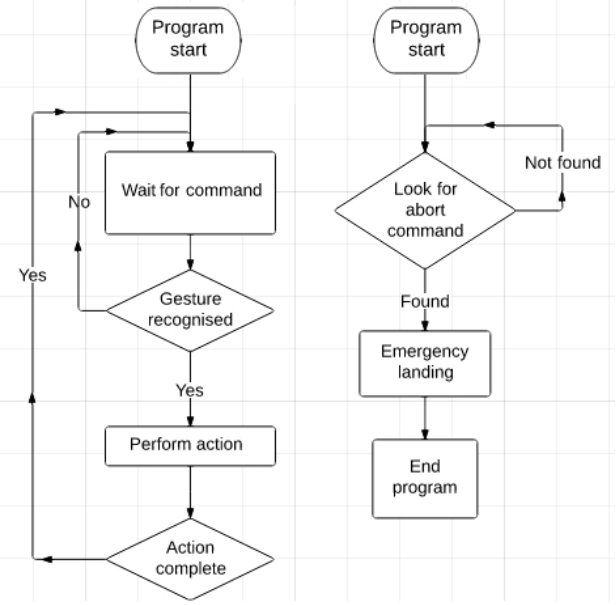

Fig 1. Algorithm

For the demonstration of the concept described in this paper several different methods were considered and the following method was chosen. System design can be separated into three main parts. The computer is the systems control device which uses information from the camera as an input. The computer processes the information using machine vision principles and sends a detected command to the Ar. Drone. For this system the command protocol from the user is read one command at a time. Meaning that during the time when one action is in progress all the other incoming commands are ignored. The other possibility would have been to buffer all the recognized commands while one action is in progress and later perform the buffered operations as a sequence. Unbuffered command protocol was chosen because sequenced control was not needed to demonstrate the purposes of this work. Working principle of the system has been shown with the flow chart (Fig. 1) and described below:

1. USB camera takes images continuously
2. The images are processed with several filters and analyzed.
3. A shape matching tool checks if a certain gesture is present
4. Results are transmitted via Wireless to the Drone

3. MACHINE VISION ALGORITHM

3.1 Image processing

Before any information can be extracted from an image, some processing is required. As the object of this work is to distinguish the hand gestures, the hand has to be separated from the background. For this, a research was conducted to explore the options for achieving the best results. A couple of methods used were the following:

1. Using an RGB camera and applying a threshold to the HLS color plane to extract a grey object.
2. Using an infrared camera and applying a threshold to extract the warm objects
3. Using either a RGB or B/W camera and well distinguishable background and applying a corresponding threshold (to extract dark objects or light objects)

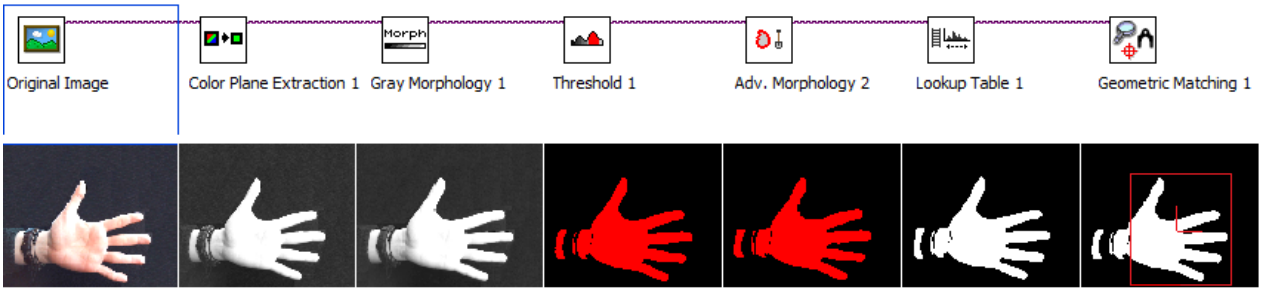

Fig. 2. Dataflow diagram (with examples)

The simplest and most convenient method for this work was the third option. This method allowed to easily set up and conduct experiments to identify the advantages and disadvantages of the two control methods under examination.

For this work a black background was chosen and a simple rig was built to mount the camera and lighting. From there the image processing algorithm could be built. Next the algorithm was optimized with National Instruments' software package Vision Assistant. In the next image the chosen processing steps and associated image (Fig. 2) is shown.

The following processing steps are seen in the image:

1. Original image
2. Color plane extraction (red)
3. Grey morphology (open)
4. Threshold (light objects)
5. Advanced morphology (remove small objects)
6. Lookup table (equalize - convert into grayscale)
7. Geometric matching (to test template matching)

The optimized processing sequence was realized in LabView where the image was analyzed.

3.2 Hand gesture recognition and detection

In order to develop human-machine interface guided by hand gestures, the machine vision mathematical algorithms development is the crucial part of the assignment. There are several methods for hand detection and tracking in real time. Gesture recognition can be used for robot control. In the Fig. 1 it can be seen, that part or the hand detection testing was also done in the Vision Assistant software because its convenient testing ground. However due to the limitations in the environment further analysis was performed in LabView.

In general, we can divide hand gesture recognition and detection into two parts: firstly removing the background, so that in the foreground we only have our hand. Secondly, recognizing the gesture. For successful body language recognition, reliable image processing is a must. In order to extract hand from the background, there are several methods (as in [2-4]):

1. background subtraction;
2. edge detection and matching;
3. blob detection and matching;
4. skeleton extraction;
5. fingertip recognition;

In this paper the method of edge detection and contour matching were used for speed and simplicity. Templates of gestures were saved on the computer and searched from every taken image. Although the used matching algorithm allowed to extract gesture position and rotation within the image, this information was not used.

3.3 HMI creation: machine vision algorithm and quadrocopter control software integration

In order to prove the concept of successful

image processing, final human-machine interface was created by connecting image processing software with AR Drone custom designed AR Drone program in LabView. Then master computer was connected with AR Drone via Wi-Fi to run the software and test the full system. After couple of tests we improved the safety of AR Drone LabView program by building different safety circuits in order to avoid collapses if errors occur.

4. COMPARING THE DISCRETE AND CONTINUOUS CONTROL

4.1 Testing

To draw comparisons between the discrete control and continuous control, several tests were conducted to evaluate the performance of the discrete method. Various tests were chosen so, that the results could be compared to other works with similar setups but with continuous control.

Some of the tests were the following:

1. Showing a single hand sign to have the robot perform a predefined sequence of actions
2. Showing a single hand sign to have the robot perform a predefined action for as long as the sign is shown

4.2 Comparison of discrete and continuous machine vision methods for robot control

Based the test described in the previous chapter and in articles [1-4] comparisons between discrete gesture control and continuous hand movement control were made and the results were the following:

Continuous tracking:

+ Intuitive control

+ Speed/movement proportional to hand movement

+ Positioning errors can be eliminated by the operator

- System works in sync with the human operator not independently. Human has to be present for the whole process

- May need specific markers for accuracy

- False readings can cause damage to the device or operator

Discrete gestures:

+ Simple, distinctive gestures that need to be shown to the camera once - to initialize execution of a certain task or movement

+ Industrial machines often do not need tracking control. Simple commands to execute a task or string of tasks are sufficient

+ For discrete control, false readings are not a problem - if no detection, then hold action or finish the current task and stand by

+ Discrete gestures provide the option to insert long command sequences to be completed by the robot

- No precise speed or position control, all commands need to be preprogrammed

- Higher learning curve - operator needs to know the specific gestures

5. FUTURE USES AND FURTHER DEVELOPMENT

As this work was conducted on a quite basic level to research the possibilities of machine vision and propose a method that could be used in many different occasions, then it can be understood that this methodology is not fully developed. Nevertheless, further work may give numerous uses for this method, one of which was described below. Discrete hand gesture control can be used with industrial robots. For example, the operator is on one side of the factory floor in the field of view of the camera but far away from the palletizing robot control station. There is a need to change operating tasks, e. g. the product has changed and leftover products must be placed in the recycle bin. Operator makes certain hand gestures towards the camera and the robot is reprogrammed to make certain movements, without the need for the operator to come to the palletizing robot.

7. CONCLUSION

Controlling a quadrocopter in real time, through the hand gestures is a novel approach. This work described the use of discrete hand gesture recognition to control the machine. Several tests were conducted to see the benefits and drawbacks of such control and a comparison to continuous gesture tracking was made. A conclusion could be drawn that discrete gesture control is more appropriate with conservative industrial robots and other machines that have to be safely halted at mechanically stable states between discrete operations. The method described in this work can be used widely in many applications, when developed further.

8. REFERENCES

1. Chaudhury, B.; Single axis manipulator control using machine vision and Virtual Reality technique; Industrial Electronics, 2008; pages: 2555 - 2560
2. Lee, D. & Park, Y.; Vision-Based Remote Control System by Motion Detection and Open Finger Counting; IEEE Transactions on Consumer Electronics Vol. 55, No. 4; 2009; pages 2308 - 2313
3. Bérci, N. & Szolgay, P.; Vision Based Human-Machine Interface via Hand Gestures; Circuit Theory and Design; 2007; pages: 496 - 499
4. Moni, M. A. & Ali, A. B. M. S.; HMM based Hand Gesture Recognition: A Review on Techniques and Approaches; Computer Science and Information Technology; 2009; pages: 433 - 437

9th International DAAAM Baltic Conference
"INDUSTRIAL ENGINEERING"
24-26 April 2014, Tallinn, Estonia

OPTIMAL USE OF SPECTRAL INFORMATION FOR WASTE PAPER DETECTION

Põlder, A.; Juurma, M.; Tamre, M.

Abstract: *Many industrial scale sorting systems use sensors working on different electromagnetic wave ranges for material detection and classification. Waste material detection and sorting based on electromagnetic spectral data is possible but due to high cost of hardware and processing power needed, it must be limited on certain wavelengths to use it in specialized industrial application. The selection of optimal wavelength is always tricky and time-consuming task on the other end it reduces the amount of data to be processed and decreases the throughput of the whole detection system. By using proper number of wavelength ranges, processing cost could be decreased significantly. Choosing the correct spectrum ranges from available spectrum is a complicated and target specific task. Waste paper sorting is one of them.*

In this paper, the selection of suitable spectrum ranges for waste paper detection system is discussed. The data are discussed on the base of real example subsets which give significant results for classification purposes and discard the ones containing irrelevant or redundant information. Important criterion for subset selection is that the feature subsets should match to commercially available equipment or consist of reasonable spectrum ranges, which could be used as a basis of machine vision system design.

Key words: hyperspectral data, feature selection, paper classification.

1. INTRODUCTION

To maintain competitive edge and to be profitable in nowadays waste material sorting industry it is necessary for the sorting companies to achieve the maximum output of their sorting systems and meanwhile keeping the system costs as low as possible.

Wood, base material of paper, is a natural resource and correct waste paper sorting significantly increases the reuse of this natural resource thus decreasing the environmental footprint and preserves natural resources.

With the increase of the environmental consciousness and demands on the waste reuse more and more precise waste sorting with high output is required. In order to achieve that, the sensor systems in waste sorting hardware need to become more flexible and faster to satisfy the demand.

The hyperspectral imaging produces high dimensionality data which have several downsides as huge volume leading to problems with data transmission and storage and presence of redundant and irrelevant information.

The hyperspectral data acquisition hardware is complicated and expensive and for online sorting systems it is often too slow due to sensor long integration times, amount of data produced and stemming from this increased processing power requirements. However, it is believed that hyperspectral data contains enough information that could be used to design faster custom made multispectral systems.

2. FEATURE SELECTION PROBLEM

To eliminate the problems caused by high dimensionality data it is necessary to

reduce the amount of data in a sensible way. Data reduction methods can be divided into two main categories: feature extraction and feature selection. Feature extraction methods (e.g. LDA, PCA) map the feature space into a lower dimensionality space resulting with an output that has usually lost the physical meaning. Feature selection methods (e.g. exhaustive search, greedy algorithms) on the other hand, selects of the subsets of dimensions preserving the physical meaning of data. To reduce the amount of data and retain the physical meaning of it the feature selection methods should be used.

High dimensionality data sets usually contain irrelevant features which do not contain any useful information and redundant features which do not give us any additional information [1].

It is proven that in order to classify unknown test sample the number of training samples per class must be at least ten times higher than the number of features [2]. If the ratio is too small the poor generalization of the data is expected which results performance differences in between classification of training and testing sets [3].

Feature extraction of high dimensionality data which contains redundant and irrelevant features results in poor estimates of matrices which are often required by dimensionality extraction methods and in poor generalization. Indicating that using all the available features and applying only the dimensionality extraction methods still performs poorly [4].

Using feature selection methods the abovementioned effects are reduced. Feature extraction methods performance increases if the feature selection is applied to the data.

One approach for feature selection is maximising relevance and minimising redundancy. One proposed method for minimising redundancy is to calculate metrics between each feature i.e. spectral band [5]. Several different metrics can be used (e.g. MSE, Euclidian distance), the correlation is best suited for similarity measurements [5]. After that it is possible to construct matrix where higher values indicate high redundancy. The redundant bands can be removed by locating those values and eliminating the bands which respond to them.

Another interesting method for spectral feature selection could be the use of entropy-based genetic algorithm discussed in [6]. Entropy in information technology is a measure of information contained in the spectral bands. It can be used as a fitness function for genetic algorithm optimization problem. Genetic algorithms have mainly been used as function optimizers but it is shown [7, 8] that GA can be used to solve many different types of problems. In the case of hyperspectral feature extraction, GA is a feasible search algorithm because the feature space is not uniform and the source of the data (a vision system) is noisy. GA as a general purpose optimizer has the property of being robust with moderately noisy problems because it accumulates fitness statistics over several generations.

3. REDUNDANT INFORMATION

In this paper we are testing the simple correlation based feature selection method to reduce the redundancy which is needed for waste paper classification. Data was acquired by the hyperspectral camera in 1040 bands with a 400 nm – 1000 nm spectral range, with 0.58 nm increments. Data cubes are normalized.

On Fig. 1. the normalized spectral frame of the data cube is shown, spatial information can be observed in horizontal axis and spectral information in vertical axis. On Fig. 2. the spatial frame of the same data cube is shown.

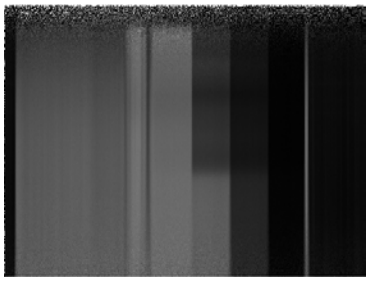

Fig. 1. Spectral frame of the data cube

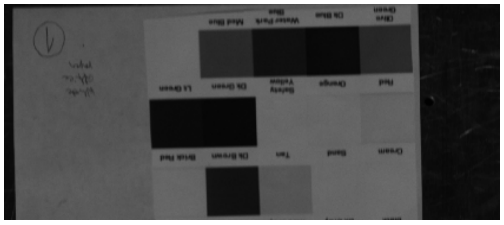

Fig. 2. Part of the spatial frame of the datacube

Different types of materials are divided into classes which are constructed based on 4 data cubes containing spectra of different materials which need to be classified (for example office paper, newspaper, magazines). The data is not sufficient for final feature selection and classification task rather it is used to test the algorithms and to learn the overall task.

Firstly the classes of different materials are defined by selecting regions of interest from data cubes spatial representations. The classes are defined as mean spectrums of 100 randomly selected pixels belonging to specific material. The mean value and standard deviation of each class spectra points is calculated. Standard deviation is used for estimating the uniformity of the class. In the future when additional feature selection method (e.g. genetic algorithm) is implemented the classes are recreated. Classes based on an averaged spectrum decreases the processing time.

On Fig. 3. and Fig. 4. the mean spectra of two classes are shown, one with small standard deviation and second with higher standard deviation around 530 to 780 nm indicating some possible problems with class construction, this class should be reconstructed. Approximately from 400 nm to 500 nm and 900 to 1000 nm all the data samples contain considerable noise and therefore those parts are not considered.

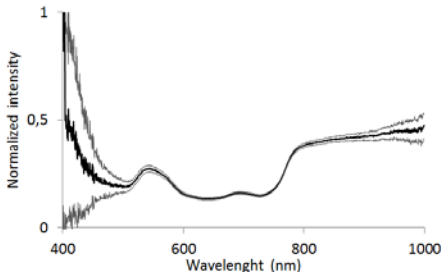

Fig. 3. acceptable class

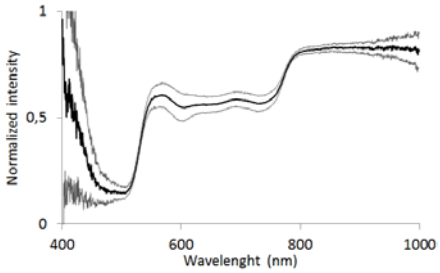

Fig. 4. problematic class

Next step is to calculate the spectral cross correlation of the classes like described in [3, 5]. Correlation coefficients in between all spectral bands are calculated and displayed. On Fig. 5. the spectral cross correlation matrix of office paper samples are visualized.

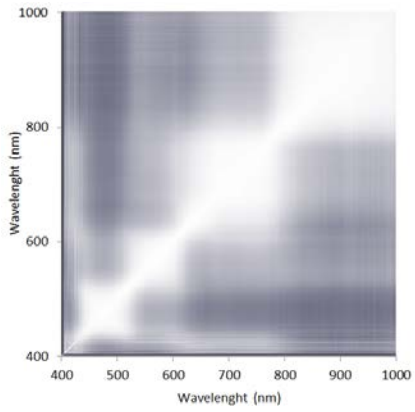

Fig. 5. Visualized spectral cross correlation matrix

Each pixel row and column indicates one specific band from spectra, bright areas indicate high correlation and darker areas indicate low correlation.

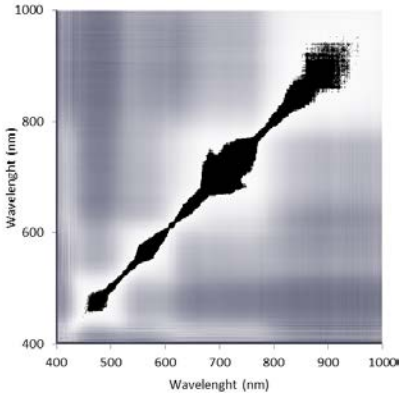

Fig. 6. 0.9 threshold applied to matrix

After applying 0.99 threshold to the image (Fig. 6.) the special pattern is highlighted (in black). The matrix is symmetrical and the diagonal axis can be ignored.
Based on visual information it is possible to roughly estimate that most of the redundant features are located in following approximate waveband regions: 460 nm – 490 nm; 550 nm – 590 nm; 660 nm – 770 nm and 810 nm – 940 nm. The regions from the beginning and in the end of acquired spectra contain considerable amount of noise and therefore should be ignored (400 nm – 500 nm; 900 nm – 1040 nm). On Fig.7. some spectra of classes are shown.

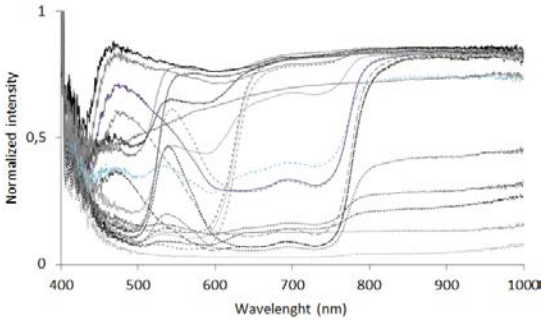

Fig. 7. Some spectrums of classes

It indicates that abovementioned rough redundant regions (Fig. 6.) are visible on the spectra of classes (Fig. 7.). On those areas all the spectra have basically constant values and do not contain any additional information.
Next step is to automatically select/remove the rows and columns which are redundant [3].

For that the highest correlation coefficient from the matrix is found (excluding elements on main diagonal). The coordinates of that value indicates the two bands. The highest value from that row and column is found and the band with the highest value is removed. Process is repeated until the desired numbers of bands are removed or the desired threshold value is reached. For example on Fig. 8. 400 redundant bands are highlighted on horizontal axis (dark vertical stripes).

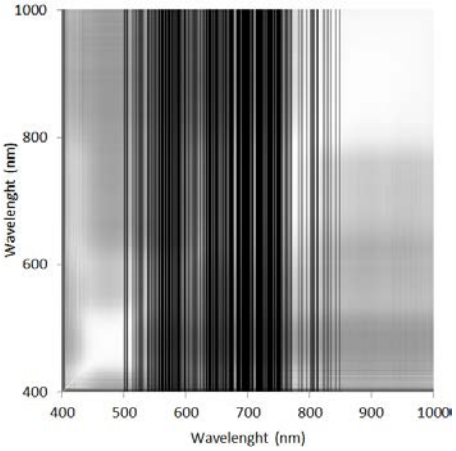

Fig. 8. Redundant bands

Tested method does not select the bands in sequence but based on highest correlation and therefore it can be more aggressive in some regions. For example on Fig. 7. And Fig. 8. the region from 850 nm to 1000 nm contains visibly redundant information but due to noise the inter-band correlation is smaller and bands from other (non-noisy) regions is selected firstly.
At the moment it is not possible to estimate the performance of tested method since the further feature selection and classification has to be implemented to measure the output of the classification system. Described method can be used for visualization of probable bands which could be ignored in further classification steps and rough removal of bands.

4. FURTHER RESEARCH

Tested method can be used for rough removal of features, after that it is

necessary to implement next step of the feature selection, for example using genetic algorithms for selecting smaller amount of features which contain information that can be used for successful training and classification of objects on spatial image.
Total costs of final inspection system can be decreased and the overall structure of the system can be simplified by selecting only important features. One way would be to build the system based on band pass filters responding to selected wavelengths.
The overall system performance can be increased by selecting minimal amount of features and design the acquisition hardware based on that information. By using custom imaging sensors or building a system using band-pass filters it is possible to increase the acquisition speed and reduce the amount of data etc. Also it is possible to use LEDs or laser diodes only at specific narrow wavelengths which further improve the system throughput by reducing system integration time [4].

5. CONCLUSION

This paper describes some feature selection methods. The spectral cross correlation method is applied to the existing data to estimate the amount of redundant features. Future research will implement additional feature selection methods based on features selected by tested method.

6. REFERENCES

1. Zhao, Z., Morstatter, F., Sharma, S., Alelyani, S., Anand, A., Liu, H., *Advancing Feature Selection Research-ASU Feature Selection Repository.* Tech. rep., Computer Science & Engineering, Arizona State University, 2010.

2. Jain, A. K., Duin, R. P. W. Statistical Pattern Recognition: A review. *IEEE Trans. PAMI*, 2000, **22**(1), 4-37.

3. Nakariyakul, S., Casasent D. Hyperspectral ratio feature selection: agricultural product inspection example. *Proc. SPIE, Nondestructive Sensing for Food Safety, Quality, and Natural Resources*, 2004, **5587**(1), 133-143.

4. Casasent, D., Chen X. W. Waveband selection for hyperspectral data: optimal feature selection. *Proc. SPIE, Optical Pattern Recognition XIV*, **5105**, 2003.

5. Ahmed, A. M., Elramly, S., Sharkawy, M.E., Hyperspectral Band Referencing Based On Correlation Structure. *Inter Conf IEEE, ICCSCE,* 2012, 5-10.

6. Shen, S. Optimal band selection and utility evaluation for spectral systems. In *Hyperspectral Data Exploitation: Theory and Applications* (Chang, C-I., ed.). John Wiley and Sons, New Jersey, 2007, 227-244.

7. Coley, D. *An introduction to genetic algorithms for scientists and engineers.* World Scientific Publishing, Singapore, 1999.

8. Mitchell, M. *An Introduction to genetic algorithms*. MIT Press, Cambridge MA, 1999.

7. DATA ABOUT THE AUTHORS

Põlder Ahti, doctoral student,
Department of Mechatronics, Ehitajate Tee 5, Tallinn 19086, Estonia,
ahti.polder@ttu.ee
+372 620 3207

Juurma Märt, doctoral student,
Department of Mechatronics, Ehitajate Tee 5, Tallinn 19086, Estonia,
mart.Juurma@ttu.ee
+372 620 3207

Tamre Mart, professor,
Department of Mechatronics, Ehitajate Tee 5, Tallinn 19086, Estonia,
mart.tamre@ttu.ee
+372 620 3202

9th International DAAAM Baltic Conference
"INDUSTRIAL ENGINEERING"
24-26 April 2014, Tallinn, Estonia

THE EFFECTS OF MINITUARISATION OF PROJECTION STEREOLITHOGRAPHY EQUIPMENT ON PRINTING QUALITY

Rayat, H.; Pulkkinen, V.; Johansson, M.; Nyfors, V.; Partanen, J.; Kiviluoma, P. & Kuosmanen, P.

Abstract: *Additive manufacturing methods are popularly used in rapid prototyping and rapid manufacturing in the industry and recently they have gained popularity also in hobbyist crowds. Miniaturization of an additive manufacturing device would make it more portable, affordable and thus more accessible for everyone, but it is also important that the manufacturing quality is not remarkably reduced. In the scope of this survey, a miniature stereolithography 3d printer was built to study the effect of low cost, system components on the printing quality.*

Key words: projection stereolithography, additive manufacturing, portable.

1. INTRODUCTION

Stereolithography (SL or SLA) is the oldest method of additive manufacturing, patented already 1986 by Charles Hull. [1] In SL, solid objects are often made by curing resin with light rays of the ultraviolet region or by a high power laser (Figure 1). If a projector is used as a source of light, the method is called projection stereolithography (PSLA). As SLA is one of the oldest additive manufacturing methods, it is also one of the most accurate ones to date. Resolutions of manufacturing axes can go as low as 50 nm [2]. The SLA is however restricted by its materials which are typically polymer based.

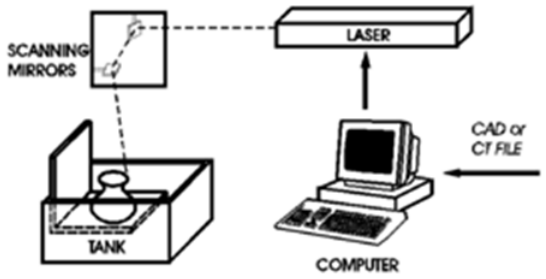

Fig.1. Setup for SLA equipment. CAD file is uploaded to a computer which controls the laser, scanning mirrors and platform in the tank filled with resin to build the desired object. [3]

The purpose of this study was to build a low-cost, small and even portable, PSLA device which could also compete with the commercial devices with its printing quality. In PSLA manufacturing, thin layers (usually < 300 µm) of the object are formed on a platform one at a time by projecting an image with resembles a single layer of the object being manufactured. This platform has one movement axis which allows these layers to be stacked on top of each other. Stacked layers form the final three-dimensional object.

2. RESEARCH METHODS

For research purposes a testing apparatus was built, that would allow the testing of benefits and downfalls of each component orientation setup used in SLA –systems. These orientation setups can be seen in Figure 2. Movement of the platform was achieved by a 1 mm screw pitch. Tests

were done with a layer thickness of 125 µm which corresponds to a 1/8 turn of the screw.

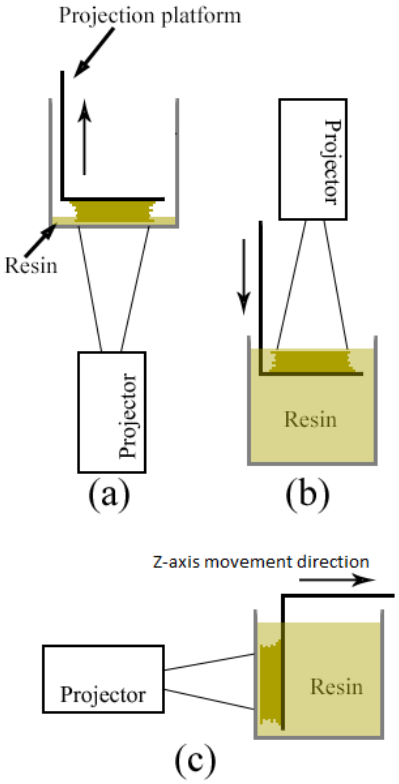

Fig.2. Different component orientation setups used in SLA-systems

First method that was tested was the top-down-orientation (Fig. 2.a). In this orientation the projector was placed under a clear plastic container and the projection platform was placed inside against the bottom of the container, only leaving one layer thickness gap in between the two. When a layer was cured the platform was raised to detach the cured layer from the bottom and to let new resin flow in between the already cured layer and the bottom of the container. After this the platform was lowered back leaving one layer thickness gap between the bottom and the lastly cured layer.

During the testing progress it was noticed that the surface tension of the resin leads to a problem that the surface isn't completely flat. This leads to serious deformations, for example air bubbles inside the object. This problem could be solved with a sweeper that flattens the surface just before curing [4], but with the size limitations that was not possible to carry out.

The third method is a less traditional horizontal setup (Fig. 2.c). In this method the projector is set to project the picture through the side of the container and the projection platform is again inside the container against the sidewall. The platform is then moved horizontally as the layers are cured.

The resins used in these tests were Photopolymer PIC 100, and and PIC 100 with added EC 500 by EnvisionTEC. The PIC 100 reacts best with wavelengths close to the ultraviolet spectrum and added EC 500 makes it more sensitive to ambient light. Tests were carried out with two different types of projectors, Digital Light Processing (DLP) –projector and laser projector, using a diffusing-wave spectrometer. The results can be seen in Figure 3. As can be seen, the DLP-projectors (line) light spectrum goes much closer to the ultraviolet area (below 400 nm) than the laser projector (cut-line). This was further confirmed with a curing test in which the laser projector was not able to cure the resin at all.

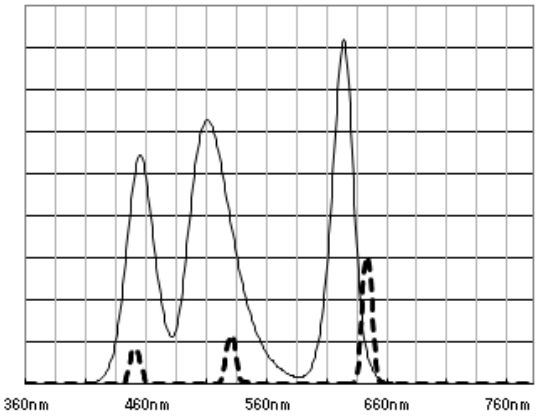

Fig.3. Diffusing-wave spectrometer test results. Result of DLP projector is shown in solid line and laser projector in cut-line.

3. RESULTS

The Z-axis resolution was tested with previously mentioned test rig. Resin was placed on a see through platform as light was projected on the resin from beneath.
In the first test, the used resin was the PIC100 with a projection distance of 19 mm.

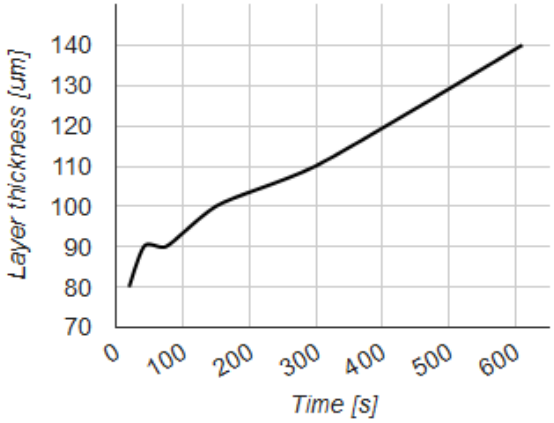

Fig.4. Curing thickness as a function of curing time.

Figure 4 show that the layer thickness is approximately linear function of curing time. The PIC 100 with added EC 500 was tested in a similar way as the PIC100, with only difference being the distance of the projector and the projected surface (120 mm). The resin was cured onto the up and down moving platform. The first five layers were cured as a whole square using a curing time of 180 s. Secondly eight "chess board" layers were cured using a 60 s curing time. For each layer the platform was moved 125 µm. This adds up to a total of 1625 µm printed, which can be seen from Figure 5.

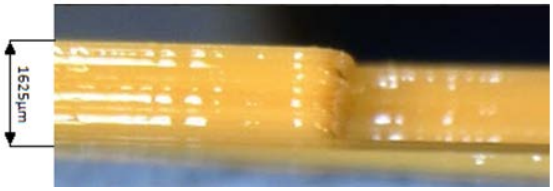

Fig.5. Side view of cured "chess board" from side

The main limitation of the resolution in the X-Y-plane is the resolution of the projector. The theoretical resolution can be calculated from the resolution of the projector and the size of the projected picture. The X-axis length of the projected picture in the test was 39 mm and the X-axis resolution for the projector is 854 pixels. With these numbers a resolution of 21.9 pixels/mm can be calculated.

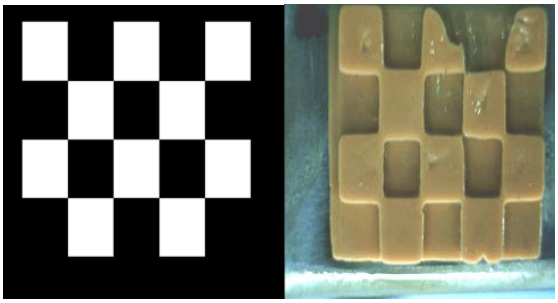

Fig.5. The projected pattern and the end result side-by-side.

In the projected checkerboard pattern, the width of one white square was 86 pixels. This would result in squares with a width of 3.9 mm. The squares printed were measured to be 4.3 mm wide by average. Figure 5 shows some geometric errors as well: the sharp corners were rounded during the curing process and some other deformations are noticeable in the second and third square of the top row. These geometrical anomalies could be solved by focusing the picture better and using more transparent glass to project through.

4. DISCUSSION

4.1 Device orientation

The major benefit of top-down method was the minimal amount of resin needed. There only needs to be minimum of one layer thickness of resin on the bottom of the container, but of course it has to be taken care of that the resin covers the whole region of the projection platform. Another benefit is that the height of the object isn't restricted by any physical dimension of the components. The only problem with this setup was that sometimes the layer would stick to the bottom of the container instead of detaching. After coating the container

with non-sticking silicone elastomer this was no longer a problem. For tall and thin objects there might be a need for some reinforcement structures to keep the part in one piece during the building process.

In the second method, the bottom-up – orientation (Fig. 2.b), the projection happens straight on to the surface of the resin and the platform is then moved downwards after the layer cures. With this method the sticking is no problem and container wouldn't need the silicone coating. First downside comparing to the first method is that this method needs a full container of resin to work. Also the height of the container physically restricts the size of the object that can be manufactured.

Horizontal orientation was tested last. The major difference compared to the top-down –orientation is that this method needs the full container of resin to work. Otherwise the benefits and downfalls are similar; the surface of the containers sidewall provides a flat area to project layers on but it still needs to be coated with the silicone elastomer. Because the density of the cured material and the resin is the same there is no need for any additional reinforcement structures for the part.

The greatest benefit that the horizontal gives is the stability of the setup. The top-down and bottom-up orientations have their centre of mass relatively high with a small area to stand on, making them unstable. The horizontal setup gives larger area to stand on with a lot lower centre of mass.

4.2 Accuracy

The z-axis resolution of the device is restricted theoretically only by the incremental movement of the platform. In this study, the lead screw was operated manually by turning the screw ⅛ revolutions at a time which corresponded to an approximate of 125 µm translation of the platform. Difference and variation in layer thicknesses this way were inevitable. To increase the resolution z-axis, a stepper motor will be used in the final assembly. With a stepper motor, a resolution of 10 µm for layer thicknesses on translation side is well achievable. However, the linear translation of a single step is not absolute. The accuracy and same time the resolution of the z-axis can be enhanced with the use of reduction gear [5].

The z-axis accuracy is also affected by the curing depth and depth focus. Curing depth is the maximum curing depth of a single layer a source of light can cure with single type of resin. Depth focus is the depth in where the projected picture is in focus. These properties can be enhanced with optics. These properties usually do not radically restrict the resolution, but sets the maximum layer thickness producible with constant accuracy. These were not in the scope of this research and a single layer thickness of 125 µm was used which was found to establish sufficient results through trial and error.

The resolution of both X and Y-axis was found to be near 0.4 mm. Theoretically it is restricted by the projector output resolution as well as the projected picture size on the inner wall of the container. X and Y-resolution seemed to mainly suffer from the blurriness and roundness of projected sharp edges. This may be due cross-talk effect, where polymers near the light might also get cured [6]. Also, the variation of light intensity in different parts of the picture is believed to derive from projector properties. This feature can later on be corrected for example by using intensity corrected background image.

There are many possibilities that can be achieved with a MiniPµSLA system. A MiniPµSLA system can easily be transported and used anywhere. The user will have the possibility to build accurate and robust parts.

5. REFERENCES

1. U.S. Patent 4575330 A, 1984, *Apparatus for production of three-dimensional objects by stereolithography,* Charles W. Hull.

2. Emons, M., Obata, K., Binhammer, T., Ovsianikov, B., Chichkov, B. and Morgner, U. *Two-photon polymerization technique with sub-50 nm resolution by sub-10 fs laser pulses.* Optical Materials Express, 2012, vol. 2, issue 7, p.

3. Aaroflex Inc. *The "magical" stereolithography process.* 1997. http://www.aaroflex.com/stereo.htm (March 13, 2014)

4. Reeves, P. *Reducing the surface deviation of Stereolithography components.* Doctor of Philosophy Thesis, University of Nottingham, 1998.

5. Lehtinen, P. *Projection microstereolithography equipment*. Master of Science Thesis, Aalto University, School of Science, Espoo, 2013.

6. Sun, C., Fang, N., Wu, D. and Zhang, X. *Projection micro-stereolithography using digital micro-mirror dynamic mask*. Sensors and Actuators A: Physical, 2005, vol. 121, issue 1, p. 113–120.

CORRESPONDING ADDRESS

Panu Kiviluoma, D.Sc. (Tech.)
Aalto University School of Engineering
Department of Engineering Design and Production
P.O.Box 14100, 00076 Aalto, Finland
Phone: +358 9 470 23558,
E-mail: panu.kiviluoma@aalto.fi
http://edp.aalto.fi/en/

ADDITIONAL DATA ABOUT AUTHORS

Rayat, Hardeep, B.Sc (Hons)
Phone: +358 40 198 8998
E-mail: hardeep.rayat@aalto.fi

Pulkkinen, Valtteri, B.Sc
Phone: +358 50 588 2127
E-mail: valtteri.pulkkinen@aalto.fi

Johansson, Max, B.Sc
Phone: +358 408414867
E-mail: max.johansson@aalto.fi

Nyfors, Veli-Matti
Phone: +358 445448125
E-mail: veli-matti.nyfors@aalto.fi

Partanen, Jouni, D.Sc. (Tech.), Professor
Phone: +358 50 5769 804
E-mail: jouni.partanen@aalto.fi

Kuosmanen, Petri, D.Sc. (Tech.), Professor
Phone:+358 9 470 23544
E-mail: petri.kuosmanen@aalto.fi

9th International DAAAM Baltic Conference
"INDUSTRIAL ENGINEERING"
24-26 April 2014, Tallinn, Estonia

AUTOMATED INSPECTION SYSTEM OF ELECTRIC MOTOR STATOR AND ROTOR SHEETS

Roosileht, I.; Lentsius, M.; Mets, O; Heering, S; Hiiemaa, M. & Tamre, M.

Abstract: *In manufacture of machine parts, an automated product inspection can save time and resources. Large scale electric motor stator and rotor sheets are manufactured by stamping. The sheet metal is usually stored outdoors and brought into the factory before processing. The difference in temperatures and other factors create the need to inspect the produced sheets to verify that they meet specifications. This is often done by hand, but this operation is time consuming and is prone to human error. The aim of this work is to explore the possibility of using a machine vision system to solve this task. Images of the sheets are analysed by the custom software, taking into account the thermal expansion of the material.*
Key words: Machine vision, measuring system,

1. INTRODUCTION

A problem has risen in the production of electric motor stator and rotor sheets on how to keep those large-scale parts inside strict precision requirements. The temperatures fluctuations, the ware of the stamping tools and different material batches create a need for strict quality control. At the moment the parts are measured manually after stamping and only the outer and inner diameters are checked. This method isn´t satisfactory for the high precision needed – possibility for measuring error is great and it can't be assured that the necessary tolerances are kept. The certainty that the tolerances are met is essential at this stage of production – it will prove very costly when a pre-assembled rotor wouldn't fit inside the stator at the later stages of production. Moreover, it takes a lot of time and effort from the machine operators to measure such large-scale parts manually. Due to large difference in part sizes and small tolerances a special coordinate-measuring machine would be otherwise needed and it is considered too expensive. Thus it was decided to look into the possibility of constructing a machine vision based measuring device for that task.

The stator and rotor sheet parts (later referred only as sheets) are manufactured from a 0.5 mm thick electrical steel. Sample technical drawings (see Fig. 1) were acquired from manufacturer and are the basis of our work so far.

Another objective stated in the assignment was the possibility to measure sheets with different diameters and shapes – the system needs to be quite versatile and reconfigurable for different part sizes – this would be done once every couple of days

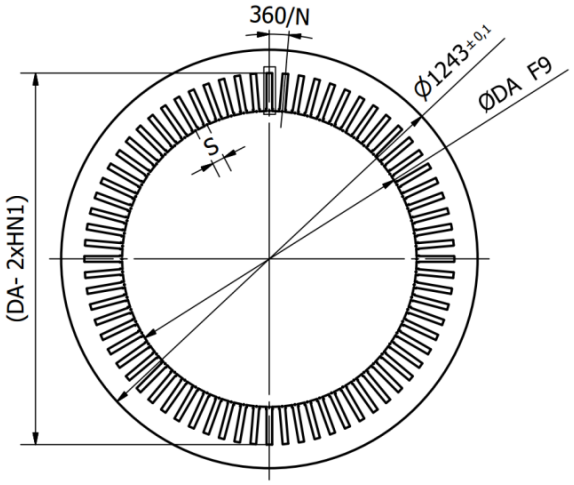

Fig. 1 Stator sheet part

Dimensions of the sheets are dependent on the temperature during and after the stamping. According to the manufacturer the temperature is one of the key issues for keeping the tolerances within limits. This was also considered when developing the measuring system.
Moreover, the logging of all the measuring data and statistical analysis of it should also be incorporated into the system.

2. INSPECTION SYSTEM

2.2 System overview

As the main goal of this work was to study the possibility of using a machine vision for making precise measurements in described situation the actual measuring device was not constructed to every last detail – it is dependent on the concrete specifications needed from the company and will be designed based on those. Despite that, the outline of the inspection system was designed, appropriate components were chosen and a software algorithm was created. For research, a smaller scaled system was designed and produced, more on that in Section 3.1.
For the full-scale system, it was decided to use following concept: two cameras are placed over the work area so that segment of the sheet from each end would be in a frame. This allows measuring the inner and outer diameter as well as the grooves of the sheet. As the image frames are not overlapping, it raises the question of distance measurement between the cameras. To overcome that, following concept was invented: the distance measurements are bound to the worktable through precisely fabricated reference sheet part. The edge of the reference sheet is caught into the frames of both cameras and is used as an origin for taking the measurements. Since the length of the reference sheet is precisely known, the full measurements can be calculated. A precise positioning of the cameras in relation to the measured sheet isn't necessary as long as the camera's distance from the measured object is fixed. That means the sheet could be positioned arbitrary on the work area and we would still get accurate measurements.
Additional task was to measure sheets with different diameter. With this concept it is easily done – reference sheet is changed and cameras moved. For added ergonomics the system can also be made automatically adjustable. The system consists of two cameras, a computer, two flash units, temperature sensors and a diffuser (Fig. 2)

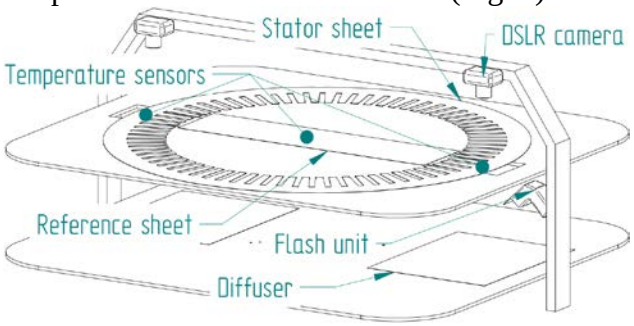

Fig. 2 Overview of the system

The object is lit from beneath by two flashes, one for each measuring area, which are directed at a diffuser to provide uniform lighting (Fig. 3.). The flashes produce a very intense light, overpowering any ambient light and giving a clear outline of the object. Tests showed that the area lit by the flashes needs to be sufficiently concealed from the rest of the room to prevent unnecessary reflections.

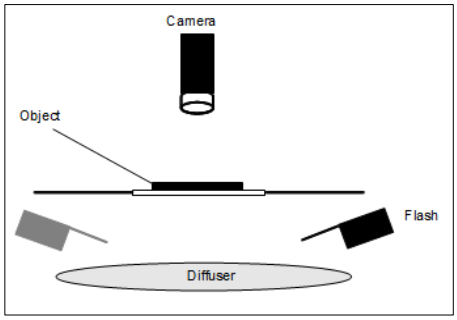

Fig. 3 Lighting setup

Another important task of the system is taking into account all the temperatures involved. To accurately verify if the sheets fit inside strict precision requirements the thermal expansion needs to be considered. Firstly, calculations show that in the case of the sheet's outer diameter being 1243

millimetres, a 10 °C temperature rise would result in 0.11 mm expansion which exceeds the required tolerances. For purposes described, sheet's and reference sheet's temperatures are measured during the inspection (see Fig. 2). Secondly, the temperature differences before, during and after stamping process lead to the part not complying with specifications and monitoring those would be really helpful. Measuring this data needs to be integrated into the system so it could be evaluated beforehand if the finished part would be precise enough to pass the inspection. It would help to decrease wasted production time and reduce scrap material. The information necessary to decide if the material temperature meets the allowable limits comes from the data logging statistics described in Section 2.4.

2.2 System components

The main components of our inspection system include cameras, lenses, flashes and temperature sensors. Next, a preliminary selection of those components is made.

For the cameras we used quite new approach to the machine vision systems – commercially available digital SLR cameras. DSLRs fit perfectly to our situation – large requirements are put on image resolution and the measuring process isn't time-critical. Furthermore, almost no effort is needed from us to integrate different parts of the system, as lenses, flashes and a computer. DSLRs offer supreme image quality to most machine vision cameras.

The camera we will use for this task is the Canon EOS 100D. It has the largest image resolution in it's class with 18 megapixel 5184 by 3456 resolution. For the camera lens we will use the Canon 50mm f/1.8 II. It offers distortion free and sharp images. For the flashes, almost any professional xenon tube flash will do, as an example the one's used while testing were Canon Speedlite 430EX and 580EX II.

Temperature of the sheet is measured with an infrared temperature sensor. To get an accurate measurement, the emissivity of the material and possible background reflections need to be taken into account.

Suitable temperature sensor for this task would be PC151MT-0 from Calex. It has configurable emissivity settings, reflected energy compensation and a built-in RS485 interface [2].

2.3 Algorithm and user interface

A custom software was designed during this project using NI's Labview and it's Vision environment. Also, a preliminary user interface was made (Fig. 4). The algorithm designed is capable of measuring the parts automatically or manually, images are calibrated accordingly (Fig. 5), large number of parameters can be modified during system setup, and all the data is logged.

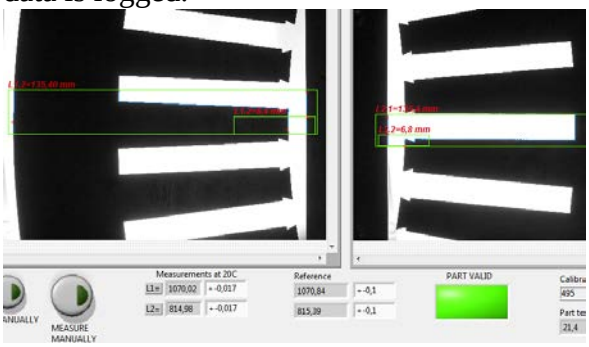

Fig. 4 User interface

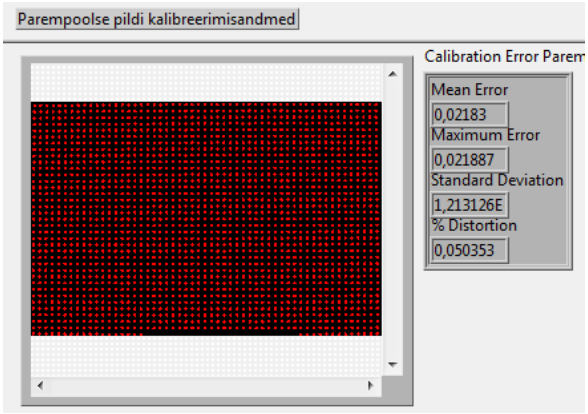

Fig. 5 Calibration matrix

2.4 Data logging

A computer based measuring system gives us one additional opportunity – it is really easy to implement the collection and statistical analysis of all the data gathered.

The measured values, calculated uncertainties, temperatures of the sheet before and during stamping and during the measurement, inspection system's reference temperature, the exact time and part numbers currently measured are logged by the algorithm. Additionally, even the material supplier and batch details, sheet's tracing code, stamping process settings and any another relevant information could be logged.
As described before, such statistics are really useful for future quality improvements. The producer could even take into account how the material from different suppliers influences the stamping process and set up the die according to the sheet properties and thus provide more uniform quality. Additionally, any issues with production quality can be precisely traced down to initial process parameters.

3. RESULTS

3.1 Test rig

To evaluate the precision capabilities of our inspection system to be developed, we need an estimate of the uncertainties involved using such technology. In order to do that, we constructed a test rig and estimated it's measuring. Then we would get an estimate of the precision our full-scale system is capable of.
Compared to the designed inspection system, our test rig uses different camera, instead of Canon 100D we used Canon 350D – an older model from Canon lineup. It has 8 megapixel sensor with image size of 3456x2304 pixels instead of 18 megapixels of 100D. Otherwise, camera lenses and flashes were exactly the same.
To assume the limiting factor of the system precision is only the camera resolution, it would mean that the full-scale system should be roughly 1.5 times more precise than our test rig. Of course in addition to the resolution many parameters have an impact on uncertainties, but those have roughly the same magnitudes on the full scale system.

3.2 Results obtained

To obtain the data necessary for calculations, four different reference objects were measured repeatedly – three of them are shown in Fig. 6.

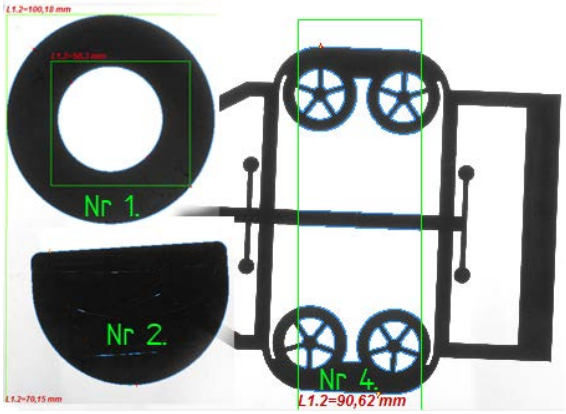

Fig. 6 Reference objects

For the purpose of uncertainty calculation, the reference objects were measured with micrometer caliper. The lowest uncertainty was achieved from reference object nr. 4 and was the basis of calculations – $X_{ref} = 90.60\ mm,\ u(X_{ref}) = 0.005\ mm.$
Ten measurements of the reference object were taken in different parts of the work area. First 5 results of the measurement series can be seen in the table, no bias correction made.

Measurement	Value [mm]
x_1	90.620564
x_2	90.629816
x_3	90.604024
x_4	90.627517
x_5	90.616431
mean value $\bar{x}$	90.616

Table 1 Object nr 4 measurements

3.2 Uncertainty calculation

A direct method for measurement uncertainty determination consists of the following steps: Investigation of precision; Investigation of trueness (bias); Correction of bias; Determination of measurement uncertainty [3].
In our work we used the procedure One-Point Protocol approach – it is applicable if it can be taken for granted that the result obtained on the reference object can be

considered as a representative point for the entire measuring range. In our case this is so – there should be no precision difference along the measuring range for the machine vision system. The procedure goes as follows: the reference object will be measured repeatedly (at least n = 6 times) under normal operation conditions. From those measurements appropriate standard deviation is obtained. This will thereafter be called "procedural standard deviation" and the symbol s_v will be used. [3]

Next we should investigate the bias of the measurements. A machine vision measurement system is in most cases prone to some bias – it is dependent on how the algorithm is detecting the edges of the parts. The bias could be minimized by either changing the edge detection algorithm or mathematical correction of it. Correction of bias is reasonable because in case of machine vision system it can be taken for granted that the bias is constant over the entire measuring range. What is special for a machine vision measurement system is the fact that presence of bias is dependent on measurement taken.

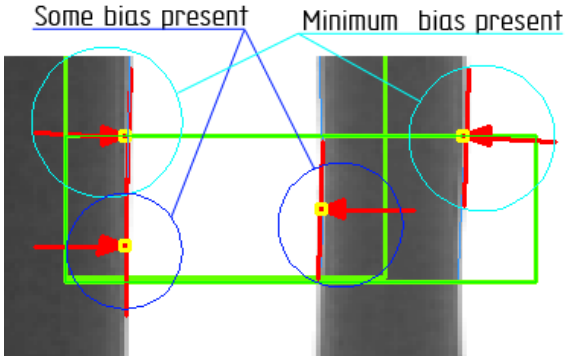

Fig. 7. Measuring bias

As seen in Fig. 7, if a measurement is taken from rising edge to another rising edge there is virtually no bias present. Currently we will consider measuring bias in uncertainty calculations as this is consistent to our test measurement conditions, but in case of normal operation, the measuring algorithm must take into account the measuring condition and automatically decide if bias correction is needed. If a constant absolute deviation can be expected, the mean deviation Δ will be subtracted from measurement result:

$$\Delta = \overline{x_{meas}} - x_{ref} \qquad y_{corr} = y_{meas} - \Delta \quad (1, 2)$$

Here $\overline{x_{meas}}$ is the mean value of the calibration measurements, x_{ref} the reference value of the measurand, y_{meas} the measurement result from the algorithm during normal operation and y_{corr} the corrected measurement result. [3]

The standard uncertainty of the corrected measurement result is calculated according to the rules of uncertainty propagation. For a correction according to (2) this gives us

$$u(y_{corr}) = \sqrt{{s_v}^2 + \frac{{s_v}^2}{n} + u(X_{ref})^2}, \quad (3)$$

where s_v is procedural standard deviation and $u(X_{ref})$ is standard uncertainty of the reference value. [2,3]. So, to determine the measurement uncertainty we followed the procedure. First we must know the s_v – reference object was measured repeatedly and standard deviation was calculated.

Two different procedures exist for the determination of that. The Type A procedure is calculated by using statistical methods and the Type B procedure is used for the estimation of uncertainties caused by individual factors, due to systematic effects. To find out the standard deviation of the reference measurement series we used Type A evaluation procedure - experimental standard deviation s of the measurement series can be used as an estimate of the standard deviation. [2,3]

$$s = \sqrt{\frac{\sum_{i=1}^{n}(x_i - \bar{x})^2}{n-1}} \qquad (4)$$

$\bar{x}$ is arithmetic mean, x_i is i-th measured value and n is number of measurements.

According to the procedure we can equate that to s_v.

The expanded uncertainty of measurement is obtained by multiplying the standard uncertainty by a coverage factor k. A value of k = 2 is recommended, which roughly corresponds to a confidence level 95%. [2]

$$U = k \cdot u \qquad (5)$$

From the data gathered (see Table 1) we can calculate the standard deviation s (4):

$$s = s_v = 0.0099\ mm$$

As discussed in Section 3.1, during testing we used a camera with lower image resolution and quality. For the full-scale system s_v would roughly be 1.5 times less. Standard uncertainty of the full-scale system's one measuring area calculates (3), $u(X_{ref}) = 0.005\ mm$. (Section 3.2) :

$$u(y_{1.1}) = \sqrt{0.0066^2 + \frac{0.0066^2}{10} + 0.005^2} = 0.0083\ mm$$

and the uncertainty of the whole measurement:

$$u(y_1) = \sqrt{u(y_{1.1})^2 + u(y_{1.2})^2 + u(y_{ref})^2}, \qquad (6)$$

where y_1 is the sheet's diameter, $y_{1.1}$ and $y_{1.2}$ measurements from the reference sheet to the part's edge and $u(y_{ref})$ is the standard uncertainty of the reference sheet. So:

$$u(y_1) = \sqrt{0.0083^2 + 0.0083^2 + 0.005^2} = 0.013\ mm$$

And for expanded uncertainty we get (5):

$$U = 2 \cdot 0.013 = 0.026\ \text{mm}$$

In the future, additional uncertainty components could be added which were not taken into account now due to their small contribution, as an example from temperature measurement errors and fluctuations. We can confidently say that the current precision is more than enough to meet our assignment.

5. CONCLUSION

Proposed system is a viable option for low-cost automatic measuring of stator and rotor sheets, moreover, the technology can be used for accurate measurement of any flat sheet-metal part. It is highly customizable and can be improved upon in almost all aspects with additional resources. In addition to accurate measurements, the statistics are gathered which are really useful for future quality improvements.

6. REFERENCES

1. CALEX PC151MT-0 – Technical Data http://www.calex.co.uk/downloads/manuals/PyroCouple%20manual_c.pdf (16.03.2014)
2. *Guide to the expression of uncertainty in measurement*. International Organization for Standardization, Geneva, 1998.
3. *Guide to the Evaluation of Measurement Uncertainty for Quantitative Test Results.* EUROLAB Technical Report, Paris, 2006

7. ADDITIONAL DATA ABOUT AUTHORS

1) Ingmar Roosileht, master´s student
Tallinn University of Technology, Department of Mechatronics, Ehitajate tee 5, Tallinn 19086, Estonia
ocvatorium@hotmail.com
+372 56 28 7331
2) Oliver Mets, master´s student
Department of Mechatronics
mets.oliver@gmail.com
+372 56 96 0810
3) Marek Lentsius, master´s student
Department of Mechatronics
lentsius@hotmail.com
+372 523 4525
4) Siim Heering, master´s student
Department of Mechatronics
siimheering@gmail.com
+372 53 455 701
5) PhD. Maido Hiiemaa
Department of Mechatronics
maido.hiiemaa@ttu.ee
6) PhD. Mart Tamre
Department of Mechatronics
Mart.Tamre@ttu.ee

9th International DAAAM Baltic Conference
"INDUSTRIAL ENGINEERING"
24-26 April 2014, Tallinn, Estonia

BULK MATERIAL VOLUME ESTIMATION METHOD AND SYSTEM FOR LOGISTIC APPLICATIONS

Dmitry Shvarts, Mart Tamre

Abstract: *This paper introduces a new method and a portable system for bulk material volume assessment on the base of machine vision technology, smart algorithms and mobile devices. The new method and algorithms are discussed on the example of the timber volume estimation system applicable for logistics companies. Practical results are demonstrated and use of algorithms for different conditions discussed and future directions for technology development outlined.*
Key words: machine vision, image processing, portable system, logistics.

1. INTRODUCTION

Organizing and controlling of unpacked piece materials and goods is usually connected with many problems, one of which is difficulty and very high uncertainty of estimation the amount of the material in different checkpoints of the logistics chain [[1]]. Even more, in many cases it is needed to assess the amount of the material on the transport stage where the stationary equipment like weighing cannot be used.
Rapid development of mobile technology and especially capabilities of the cameras integrated into mobile phones or tablet computers and efficiency of the computing power have created new opportunities to develop advanced mobile technologies to support logistics. One of these options is use of a mobile device camera with the device itself a portable smart machine vision and communication system to determine bulk materials or goods amount or volume.
Timber is one of the most widely used materials in in different applications like construction, furniture making, and joinery, etc. Organizing and managing logistics of this kind of bulk materials depends greatly on the correctness and accuracy of determining the material volume. The bulk price, quantity of the output products, transportation cost and even potential load carrying problems of trucks, ships and roads depend on the bulk materials amount allocation correctness.
There is a widespread belief that the cubic volume of timber can be calculated by measuring the high and width of the pile or truckload multiplying the result with the length of timber [[2]]. Nevertheless, the existing methodologies are time consuming and very inaccurate due to the fact that log like bulk material dimension (diameter) is not constant (Fig. 1).

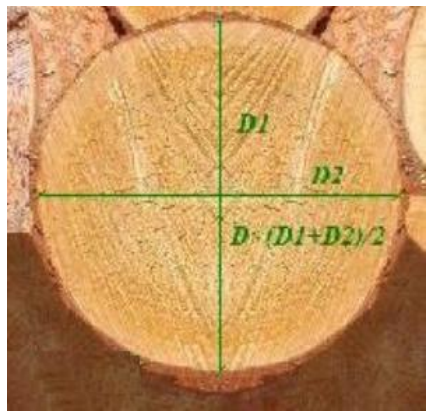

Fig. 1. Common technique, which applied for measurement of timber volume. D = (D1+D2)/2

As a result, the uncertainty of such measurements can reach up to 30 percent,

which on ones turn means either paying 30 percent more or less than the actual material amount or loosing transportation carrying capacity.

This paper introduces a new method and a portable system for bulk material volume assessment on the base of machine vision technology, smart algorithms and mobile devices. The new method and algorithms are discussed on the example of the timber volume estimation system applicable for logistics companies. Practical results are demonstrated and use of algorithms for different conditions discussed and future directions for technology development outlined.

2. PROBLEM STATEMENT

The main research objective is to develop machine vision based techniques, which identify the volume of the bulk materials. The method is discussed on the example of the timber volume estimation system. The nature of the problem and the methodology offers the further perspective benefit (the secondary objective) assessment the quality and other properties of the examined timbers, such as minimum and maximum diameter, the number of the timbers that are stacked in a pile.

The low processing speed, due to the huge amount of data, restricted main memory, short battery life prevent the implementation of computer vision algorithms in real-time mobile applications [3]. However, the modern cellphones and tablets provided with various devices such HD camera, GPS system, touch screen. The new technologies transform the phone to something more than simply phone.

The extra challenge is the development the system for portable devices. Well known that computer vision algorithms are very sensitive to small changes in lighting conditions. The users may use the system by various weather conditions and by different climate seasons. Therefore, during the development of the system the probability of existence such kind of problems has to take into account.

2.1 Methodologies

The system consists of four major components, image acquisition, image pre-processing, feature detection, volume estimation.

2.2 Image Acquisition

Today it is difficult to find a phone or tablet without a camera. The increasing popularity of digital photography reduces significantly the camera's cost. The cameras become smaller and their properties have improved. The Android API provides access to the camera’s features and allows to control the camera and take the pictures inside the application [4].

In order to take a picture it is very comfortable to make use of an already available application provided by the operating system. For instance, android's image acquisition application has extra features, such as adjusting the auto-focus, brightness, shutter speed and aperture of the camera in fully automatic mode. At the same time, the end user is still responsible for the image quality. The user has to control the process, in order to avoid the backlighting situation, to control the picture's background and distance between the camera and scene. Conflicting with these rules leads to difficulties during the image processing stage.

2.3 Image Preprocessing

In many practical situations, the objective circumstances do not allow to take a picture ready for further processing. The image preprocessing stage aims to prepare the image for feature detection. Two main tasks have to be accomplished during this step:

- setting the region of interest (ROI) in an image;
- automatically normalize the image brightness.

The first step, ROI setting, used in order to isolate the object from the rest of the scene (Fig. 2).

Fig. 2. Setting the region of interest on the image.

The elements of the image, outside the selected region considered as a background. The second step aims to improve the image quality, for instance, brightness, as presented in Figure 3. The original image is too dark for execution of the main step, object detection, and requires brightness adjustment.

a)

b)

Fig. 3. Image of the examined scene. a) original image; b) the image after brightness adjustment.

2.4 Feature detection

The feature detection is a main part of the system and based on image segmentation. The aim is to separate the objects of interest from the background. The result of this step is very critical for the final task, volume's assessment. Therefore, a key requirement for the applied algorithm is robustness.

There are several ways for achieving this goal. Very common group of methods separate the pixels based on some homogeneous characteristic of the object such as intensity or color [5].

Color is powerful key for segmentation but due to problem with color inhomogeneity, the developers face with difficulties with the implementation such kind of methods for the outdoor application. In fact, if we consider an image, which is represented in RGB color space, the observed chromaticity varies with lighting (Fig. 4).

a)

b)

Fig. 4. Images of the same scene, but created under different lighting conditions.

Solutions that are more robust could be achieved by considering the chromaticity in term of two characteristics: hue and saturation. The two commonly known are HSV and CIE LCh (CIE stands for "International Commission on Illumination", and L*c*h means L – Lightness, c – Chroma or "saturation", h-Hue) [6]. The H, S, V components presented in the Figure 5.

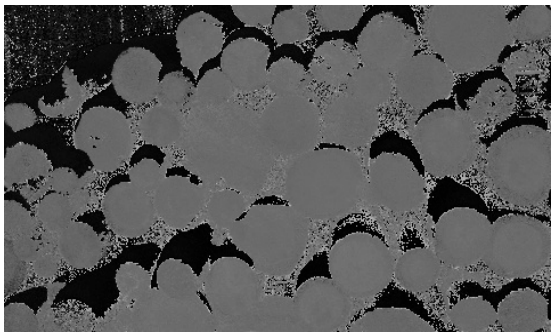

a)

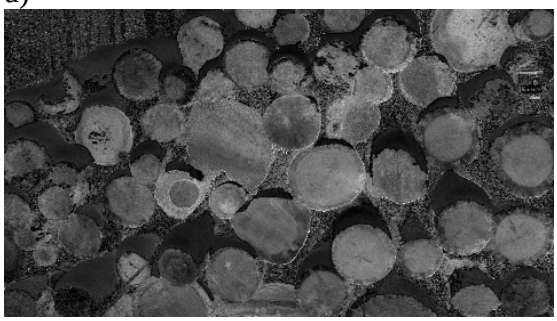

b)

c)

Fig. 5. Three components of the image in HSV color space. a) H – hue; b) S – saturation; c) V – intensity.

The graphs on the figure 6 show the range of the closest spectral color and the saturation value for timber. Using this information, we can separate object's pixels from the background pixels.

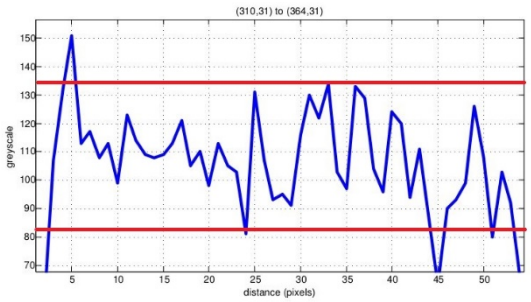

a)

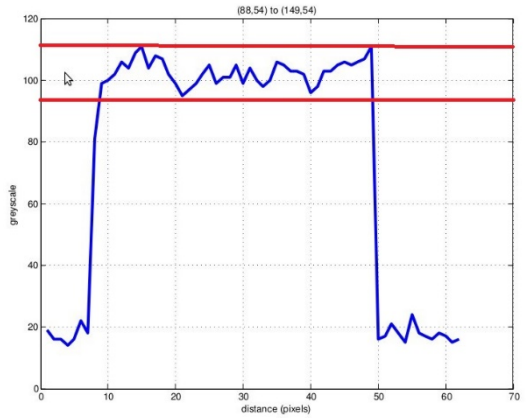

b)

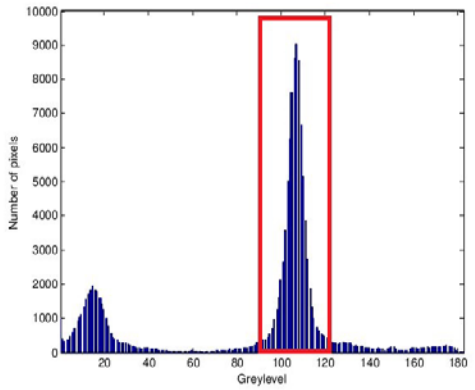

c)

Fig. 6. Range of hue (H) and saturation values (S) that correspond to the timber. a) The range of the saturation corresponding to the timber. b) The hue range corresponds to the timber; c) The histogram of the hue component of the image. The pixels inside the red box correspond to the hue distribution of the timber.

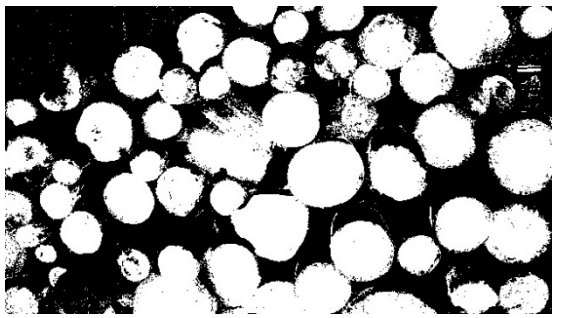

Fig. 7. Resulting image example.

From the figure 7, we can see that the resulting logical image is still far from perfect. Many pixels classified as a timber. The logs have holes due to dirt, soil or

shadows from the nearest logs. We have to improve the result by applying a morphological closing and opening operation [7]. The result is shown in the Fig. 8.

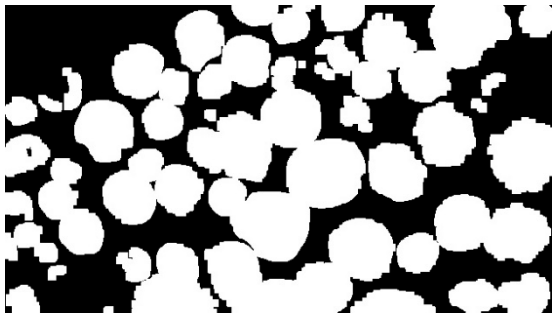

Fig. 8. The result image after morphological opening and closing operation with a small kernel.

Finally, we can calculate the image area occupied with timber. The resulting image is shown in the Fig. 9.

Fig. 9. The resulting image example. The pixels, which classified as a timber painted with random color.

3. RESULTS

The proposed algorithm was tested on the phone SONY XPERIA GO. The Table 1 presents the features and specifications for this phone.

Processor	1 GHz NovaThor™ U8500 Dual-core Cortex A9
Camera	5 megapixel camera with auto focus
	16x digital zoom, LED flash
RAM	512 MB
Display	3.5 inch scratch-resistant TFT touchscreen
	16 million colours, 480 x 320 pixels

Table 1. Specification of Phone SONY XPERIA GO

The image was taken by standard Android application and stored in SD card. The main window of the application on the phone screen is shown in the Fig. 10.

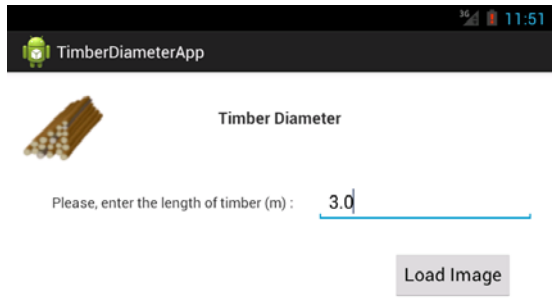

Fig. 10. Main window of Timber Diameter app.

The user prompted to set the length of the timber and load the desired image from the memory. After the image is loaded, the user sets the ROI and pushes the menu button for the image processing (Fig. 11). The system first calibrates itself. It means the system determines the relationship between the pixel and the metric units.

Fig. 11. Second screen for setting the ROI. The calibration standard is shown inside the box.

For this purpose, the small blue circle with known size is used. The system detects the circle and estimates the radius in pixels. Then the system estimates the area which is

occupied by the timber in pixels and converts it to the metric unity. The resulting image is presented in Figure 12. As shown in the image almost all the timber detected and their area is used for the volume estimation. The estimated timber volume is 21.28 cubic meters. The application was tested on several examples. The estimated by the phone results were close to the actual amount of timber.

Fig. 12. The message gives the information about estimated volume of timber.

4. CONCLUSION

A new method is proposed and presented for the bulk and piece material volume estimations. This method could be successfully used for fast estimate the volume of bulk materials in logistics and storage applications. The example of the use of the method was demonstrated for timber volume estimation. The novel approach allows to use the application on the mobile devices making it therefore very convenient for the everyday use. The analysis of the application reveals some problems and future work direction that should be focused further. The accuracy of detecting object is highly depend on the size of objects. For the current application, we determined experimentally that, the timber could be measured if its diameter is more than 10 pixels on the image taken by the mobile device. If the objects are smaller on the image only the total area of the objects pile could be estimated like show in the Figure 13. The method is in developing phase and it is our estimate that the results could be used for many everyday applications starting from the home use to real industrial logistics applications.

Fig. 13. Detecting the total area of the logs in pile.

5. REFERENCES

1. Wu, Chun-ho. Evolutionary computation in machine vision for manufacturing and logistics industry. The Hong Kong Polytechnic University. [WWW] http://hdl.handle.net/10397/5339, (13.03.2014).

2. Oester, P., Bowers, S. Measuring timber products harvested from your woodland. *The woodland workbook*, June 2003.

3. Wang, G.; Xiong, Y.; Yun, J. & Cavallaro, J. R., Accelerating computer vision algorithms using OpenCL framework on the mobile GPU - A case study., *in* 'ICASSP' , IEEE, 2013, pp. 2629-2633 .

4. API Guides, Camera [WWW] http://developer.android.com/guide/topics/media/camera.html (13.03.2014)

5. Corke, P. *Robotics, Vision & Control*. Springer, 2011.

6. X-Rite, Inc. *A Guide to Understanding Color Communication*.X-Rite, 1993.

7. Baggio,D.L, Emami,S et al. *Mastering OpenCV with Practical Computer Vision Projects.* Packt Publishing, Limited, 2012.

9th International DAAAM Baltic Conference
INDUSTRIAL ENGINEERING
24-26 April 2014, Tallinn, Estonia

TRACEABLE IN-PROCESS DIMENSIONAL MEASUREMENT – European Metrology Research Programme, project No. IND62

Simson, K.; Lillepea, L.; Hemming, B.; Widmaier, T.

Abstract: *Manufacturing of precision complex parts includes using machine tools that have an on-board metrology system for in process quality control purposes. Developments in the industry show that there is a need for higher accuracy and the measurements must be traceable. To satisfy these requirements the measurement uncertainties have to be reduced to a few micrometers within a meter cube. Objective of the project is to develop standards and procedures to verify traceability of the measurements made by in-process metrology tools. The project will serve as an input to further developments in coordinate metrology and has a direct impact on industry as well. The main beneficials are mechanical engineering and industry, process engineering and production technologies and the automotive industry.*

Key words: traceability, machine tools, calibration, thermal influences

1. INTRODUCTION

The foundation of effective manufacturing is minimization of scrapping, process time and production resources. In the industry of manufacturing high precision parts one of the tools to be effective, is to use in-process metrology. The philosophy is to make measurements alongside to milling, grinding, turning and other treatments. To do so, machines are often equipped with dimensional measurement tools like tactile probes or optical scanners. Using it will lead to reduction of production costs and increase in efficiency. The prerequisite of abovementioned aspects is to have traceable measurements at satisfying uncertainty level. Reliable dimensional measurements on metal cutting machine tools have a huge economic impact, especially at the last phase of manufacturing. The metrological methods and material standards developed for measuring instruments need to be further developed to suit in-process measurements.

2. NEEDS OF INDUSTRY

There is a strong need for fabricated parts to be inspected quickly and with high accuracy (for conformance testing to specified tolerances) on machine tools directly on the manufacturing floor, i.e., while the machined part is still clamped on the machine. To satisfy future production requirements, the measurement uncertainties have to be reduced to a few micrometers within a meter cube.[1]

3. RESEARCH AREAS

The project involves many stakeholders with different expectations. Therefore it is very important to prioritize the areas of in-process metrology. A survey has been conducted and the results have been implemented in selection of research areas [1].

Measurement errors on machine tools result from different sources and they can be influenced by various shop floor conditions. In order to detect measurement errors on machine tools, to evaluate them and then to correct them, one demands suitable written and material standards and procedures. These have to take into account environmental conditions of the manufacturing floor and need to be compliant with existing standards. As up to 75 % of the overall geometrical errors of machined workpieces can be induced by the effects of temperature [2], these material standards must be thermally and geometrically stable.

In frames of the project highly accurate multipurpose material standards will be designed and manufactured. These will be robust against environmental influences and high mechanical stress. They will be used for mapping of volumetric and task-specific measurement errors of machine tools.

For simulating in-situ varying manufacturing and machine tool environmental conditions a suitable portable shop floor environmental chamber will be designed and manufactured.

To determine geometric measurement errors after workpiece machining, under the influence of varying environmental conditions, procedures will be developed. Measurement performance and the task specific measurement uncertainty will be assessed using multipurpose material standards and workpiece replica measurement standards.

4. MEASUREMENT SETUP

As there are different manufacturing setups, there are also different measurement setups.

4.1 On board measurement tools of working machines

Some of the multi-axis turning and milling benches have additionally to the cutting tools also a measuring head that makes the cutting machine into a CMM-like measurement machine. There can be several different measurement heads but the positioning measurements are done using mostly scales or encoders. So the coordinates of measured points are calculated from readings of machine scales/encoders and information from measuring head. Scales can be influenced by temperature fluctuations, high levels of mechanical vibration and dust or particles from cutting process. The temperature related uncertainties are minimized mostly on two ways- either using a thermo-invariant material for scales or by maintaining and monitoring the environment and using the data for compensation calculations. Additional temperature-related effect is possible bending of measurement head and/or machine guideways due to temperature gradients in machine volume. For vibration control mostly air bearings are used. For protecting the scales from dust different encasings are constructed and/or the apparatus is equipped with pressurized air nozzles for cleaning the scale.[3]

4.2 Sensors

Sensors that are connected to the positioning devices can be classified either to contact or non-contact sensors.

Contact sensors have mostly single or multi stylus setups using a glass, ceramic or metallic contact surfaces with different sizes and shapes depending on measurement requirements. The sensing part can be capacitive sensor, inductive sensor, gauge with a thermoinvariant scale, linear variable differential transformer or strain gauges.

Capacitive sensors are affected by thermal expansion and change of dielectric constant. Thermal expansion is dependent

on ambient temperature and dielectric constant is dependent on air humidity.

As capacitive sensor, the inductive sensor is also affected by temperature changes. Additionally accuracy is dependent on fluctuation of supply voltage and proximity of other metal objects.

Linear variable differential transformer (LVDT) is reported to be a reliable sensor setup with only one significant uncertainty source from fluctuating supply voltage. The supply voltage fluctuations are mostly caused by temperature fluctuations.

Gauges with thermoinvariant scales are affected mostly by systematic effects. The ambient temperature and temperature fluctuations during measurement are only minor issues compared to i.e. orthogonal measuring setup.

Probes using strain gauges are working on a principle in which resistance of the gauge lattice changes as the lattice is being deformed. The resistance is measured at terminals. This kind of sensor is affected by temperature as the lattice is expanding (or shrinking) due to thermal expansion effect. There are several techniques to compensate it making the sensors invariant compared to the accuracy of the sensor carrying system. [4]

The non-contact sensors are mostly using optical measurement principles, but there are some other principles as well. Optical sensor principles are mainly laser triangulation, laser scanner, photogrammetry, fringe projection, moiré projection and laser speckle that are used in the abovementioned positioning systems.

Laser scanners are affected by temperature, atmosphere and interfering radiation. The scanners are functioning correctly only in a certain temperature range. It should be noted, that the temperature in the laser scanner can differ significantly from the surrounding environment due to self-heating. As the measurement is done by propagation of speed of light, the result is affected by the change of the speed due to atmospheric pressure change, dust particles and humidity. Laser scanners are operating in a certain frequency range and if the surrounding radiation like sunlight or lightning is significantly stronger than the measuring signal the measurement result can be affected. [5]

Structured light based measurements, like fringe projection, moiré projection and laser speckle are mostly influenced by similar environmental conditions. The result is dependent on temperature, humidity and other influences that change the speed of light in environment. [6, 7]

The material of the object, its surface roughness and finishing affect significantly the optical measurements. Also tactile sensors are affected by surface texture but the effect is small and can be estimated.

5. THERMAL INFLUENCES

Temperature is one of the most important environmental conditions in dimensional measurements and is therefore mostly to be investigated. Temperature affects directly the workpiece and also measurement equipment.

It is important to understand the background and sources of thermal influences. In general thermal influences on machine tools can be classified in six basic groups as shown in the Diagram 1.

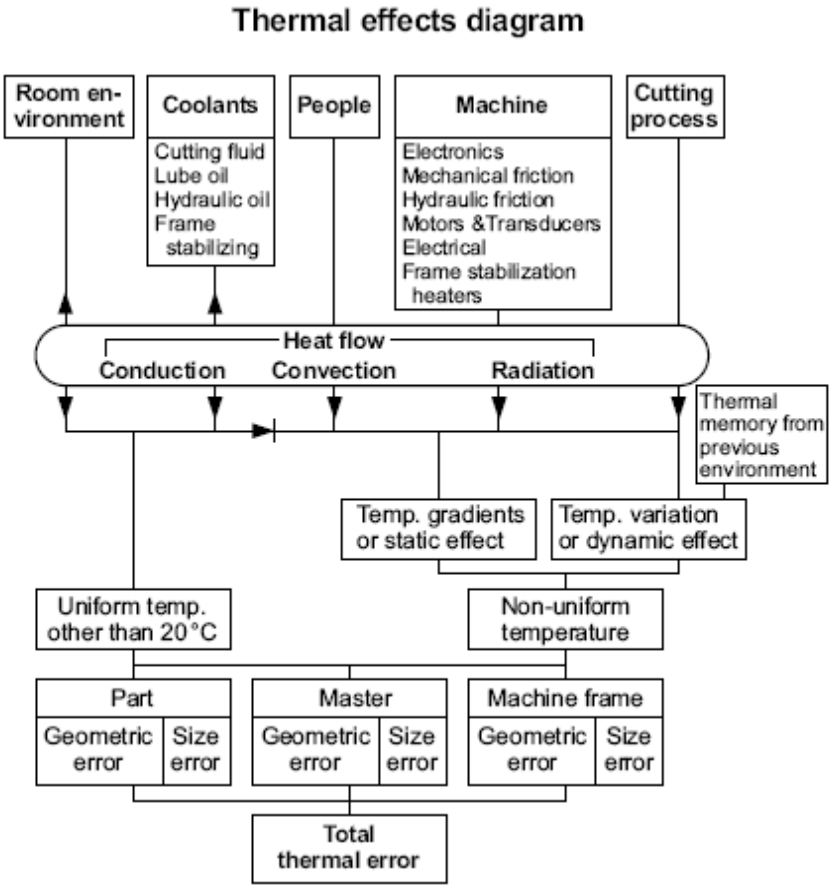

Diagram 1 Thermal effects diagram [8]

Such effects are:

- heat generated from the process,
- heat generated by the machine,
- heat exchange due to mitigating devices (cooling and heating),
- heat exchange with the environment, or
- thermal memory from any previous environment (inertia).

All these effects cause thermo-mechanical deformations and as a result inaccuracies on the machine tool and on the manufactured workpiece.

6. STATUS

The project is ongoing and the results will be available during 2015. Until now most of the work has been done in the field of researching industry and stakeholders needs. Relevant written standards regarding in-process measurements have been researched including existing standards of dimensional measurement and those under development.

The influence of temperature as well other environmental conditions have been researched for contribution to measurement errors and accuracies.

The climate chambers specification is being designed at the moment to facilitate research of different shop floor conditions influence on measurement errors and uncertainties.

The results and status of the project is available on the official project website at http://www.ptb.de/emrp/tim.html .

7. IMPACT AND BENEFICIALS

Direct beneficiaries of this project are manufacturing industries, machine tool

manufacturers, machine tool end-users and standardization bodies that will exploit new standards, procedures and good practice guides. This includes a guide for evaluating the influence of harsh environmental conditions on measurement results, handbook for all the manufactured standards, guideline specifying the measurement and calibration tasks and much more.

This project will provide traceable and reliable procedures for improvement of machine tool measurement performance. It will help to overcome the obstacles related to the need for more accurate and traceable measurements. It is important to provide much needed understanding of the influences of shop floor conditions on the quality of machined parts.

In order to ensure the adoption of the results of this project, several workshops will be held, good practice guides will be published and participants will discuss the topic in different seminars and conferences. During the project developed material standards are tested in industry and the experience from these tests will be used for the handbooks and practice guides. As many of the project partners are active in standard committees, workgroups and technical committees, the outcomes will be raised for adoption in the corresponding instance.

The outcome of this JRP will not only provide technological benefits to European industries but it will also facilitate strong economic and social development. Machine tool and manufacturing industries are strong cornerstones of the European economy. In a similar manner the ability of the industries to remain competitive is crucial for maintaining living and social standards in European member states.

8. ACKNOWLEDGEMENT

This work was funded through the European Metrology Research Programme (EMRP) Project IND62. The EMRP is jointly funded by the EMRP participating countries within EURAMET and the European Union

9. REFERENCES

1. NPL, Report on the end-user survey of the existing measurement standards for different applications in in-process metrology. IND62 TIM Deliverable WP1.1.3, 2013

2. J. Mayr, J. Jedrzejewskic, E. Uhlmannd, M. Donmeze, W. Knapp, et al, (2012): Thermal issues in machine tools, CIRP Annals – Manufacturing Technology, Vol. 61, No. 2, p. 771-791

3. A. Kawalec, M. Magdziak, I. Cena. Measurement of free-form surfaces on CNC milling machine considering tool wear and small changes of its working length and offset radius. Advances in manufacturing science and technology. Vol. 35, No. 1, 2011

4. Tudic, V, "Uncertainty evaluation of slope coefficient of high precision displacement sensor", Multimedia Signal Processing and Communications, 48th International Symposium, Page(s):231-234, June 2006

5. W. Boehler, A. Marbs. Investigating Laser Scanner Accuracy. Institute for Spatial Information and Surveying Technology, FH Mainz, University of Applied Sciences, Mainz, Germany, 2003

6. L. Chen, C. Quan, Fringe projection profilometry with nonparallel illumination: A least-squares approach, Optics Letters, 30, pp. 2101-2103, 2005

7. N. Mùnera, G.J. Lora. Evaluation of fringe projection and laser scanning for 3d reconstruction of dental pieces. Dyna 171, 2012

8. J. Bryan. International status of thermal error research. Annals of the CIRP, 39(2):645–656, 1990.

9th International DAAAM Baltic Conference
"INDUSTRIAL ENGINEERING"
24-26 April 2014, Tallinn, Estonia

DESIGN OF EXPERIMENTAL STAND FOR HUMAN GAIT IMITATION

Zhigailov, S. ;. Musalimov, V.; Aryassov, G.

Abstract: *As an experiment for the doctoral thesis the idea of creating a mechanical model for the simulation of gait with which could be to measure the movements of the various parts of a person's legs while walking could be measured is proposed. In fact the installation of sensors on the man's leg in many places cannot provide accurate measurements of displacements (accelerometer mounted on the muscle contractions because it`s contractions does not give accurate results) [1]. So, one of the most logical way to provide measurements is creation of mechanical model (stand) - a prototype imitating walking human leg. Displacements of moving parts of stand can be measured by sensors – accelerometers [2]. Certainly obtained accelerations using sensors must be made in accordance with accelerations of human leg parts.*
Key words: stand, gait simulation, accelerometer

1. INTRODUCTION

Despite the accelerating pace of development of medicine and science in general, many problems still remain relevant and unresolved. One of these problems - a complex of numerous diseases associated with man locomotion apparatus (LA). There are 75% of Europeans and 85-90% of Russians suffer from diseases of LA [3]. It is noteworthy that there is no social, gender or age group of people which could be considered out of risk of such diseases. The main causes of diseases ODA considered sedentary life or work, lack of time and energy to do physical exercises, overweight, mechanical traumas, excessive exercise, hypothermia, wearing trainings with high heels or even without them. However, despite the high prevalence of such diseases in the world there is no satisfactory ways of diagnosis, treatment and recovery of locomotion function. The disadvantages of the existing solutions are no satisfactory automatic diagnostic systems of a particular disease (visual diagnosis determines the existence of the human factor the means the increase of the possibility of making mistakes in diagnosis), and the high cost of the technological equipment, absence of guarantee of full recovery, insufficient accounting for individual characteristics of human limbs and so on. The aim of this work is to create a prototype of mechanical legs and hip, with which it will be possible to explore the human gait.

2. MAIN TASKS OF THE STAND

Before making design of the stand, you must determine what constructive tasks you put before them and what types of movements it should perform. Structurally, the geometric shape of the stand should be possible to match the shape of the human pelvis and legs. Functionally, the mechanical components of the stand must make movements similar to those that make a person's legs and pelvis while walking. Constructive part is clear – we find an average statistical length of leg and width between hips of an adult male with a coefficient 0.5 (divided on 2). The functional point of view of human gait can be divided into several movements, as shown in (Fig. 1).

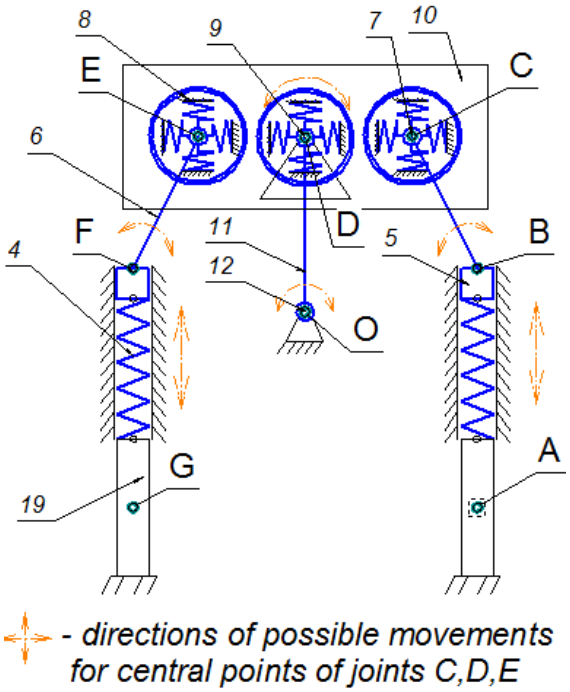

Fig. 1. Kinematic scheme of system

Mechanical components located between points A and B, F and G correspond to the feet of man. The legs can be raised and lowered vertically during simulate walking through 4 adjustable spring receiving vibrations from the wheel 19. Joints at points B and F indicate some deviations from the vertical axis of the leg movements that occur when walking. Connecting links 6 are used to adjust the central abnormalities of the upper plate 10 (pelvis) in relation to the feet. Deviations from any leg axis is going due to the plate 10 rolling around a central point D of the joint 9 (lifting - lowering the hips) and rotation of the entire plate - pelvis about a central point O of the support joint 12. Scrolling plate around the point D and movement of the plate 10 around the point O provide planar motion - wagging the hips. Elastic elements - springs 8 installed inside the round dampers and attached to the corresponding joints to transmit the movement and dampen vibrations of the entire system. Moreover, springs reduce the dependences between legs.

3. CONSTRUCTION AND PRINCIPLES OF WORK

The main technological assemblies of its mechanical design for definition of operating principle of stand are separately shown (fig. 2).

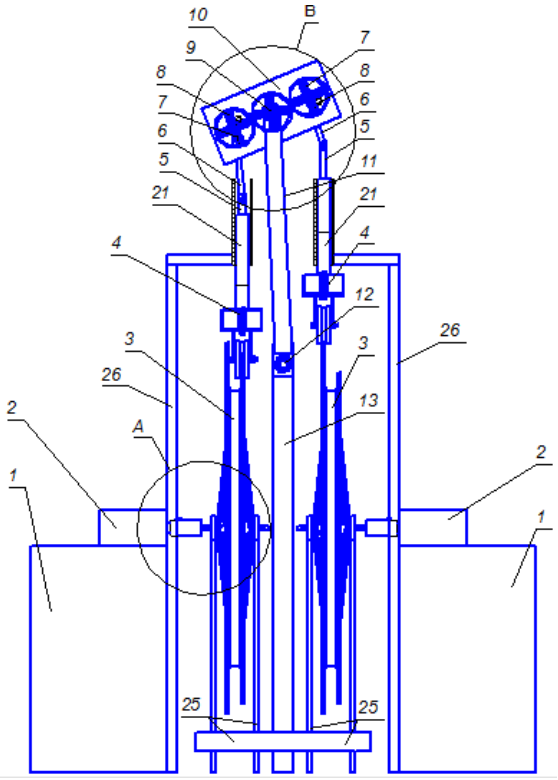

Fig. 2. The design of an experimental stand and its main technological assemblies (front view)

To begin we launch synchronized stepper motors 2 mounted on the frames 1. Using controller and adjusting the required number of motor rotations per minute (25-60 rpm), the torque is being transmitted to bicycle wheel 3 set on frame 25. The usage of frame 25 is necessary to reduce the rotation moment which has influence on the type and characteristics of motors. The plywood profiles 18 are glued on the outer edge of the rim on both sides of wheel 3. Basically, the shape of profiles 18 plays very important role because it responds not only for character of vibrations but for the causing of movements of mechanical system of stand at all. The shape of plywood profiles is calculated from

experiments with accelerometers installed on the heel and instep of walking adult men. After we found the average length of the step (1.35 seconds and 135 measurements) and having in attention the initial conditions (at least 4 profiles (90 degrees for each profile) should be glued on the one side of rim of every wheel 3), we get a good coefficient for building the shape of accelerations 0.67 degrees for 1 measurement. As example the profile of heel accelerations is shown (fig. 3).

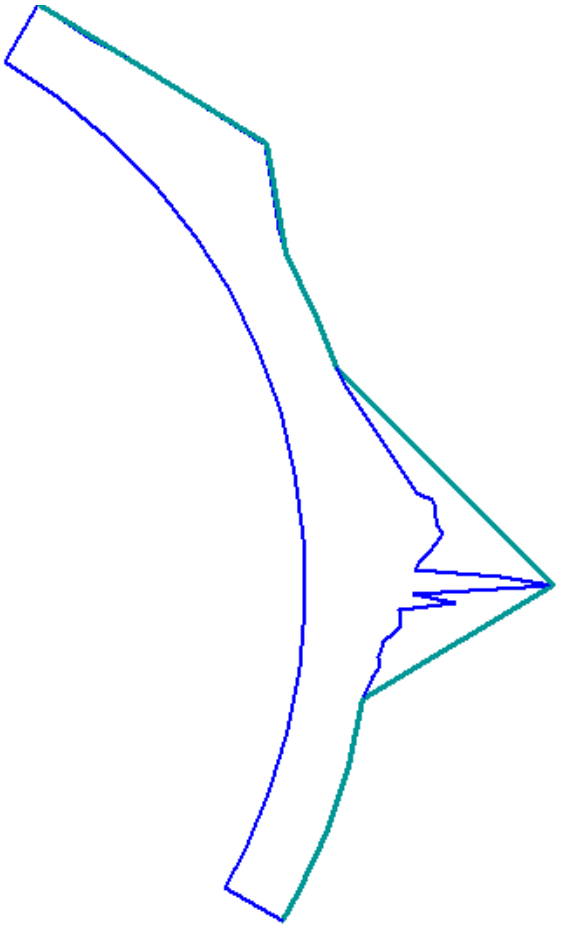

Fig. 3. The profile of heel averaged accelerations

The thin blue line shows the real shape of obtained curve, the bold green line means the borders of profile cutting. Another one initial condition is necessity to use 3 different profiles of accelerations for heel, instep and combined profile. The last one profile we get after analyzing and calculating of experimental measurements for heel and instep matching their peak accelerations. Because it is possible to use only the same acceleration profile during the experiment, 3 is the minimal number of different using wheels 3. According to calculations the maximal difference between the heights of small wheels 19 (minimal and maximal point) is 8.05 cm.

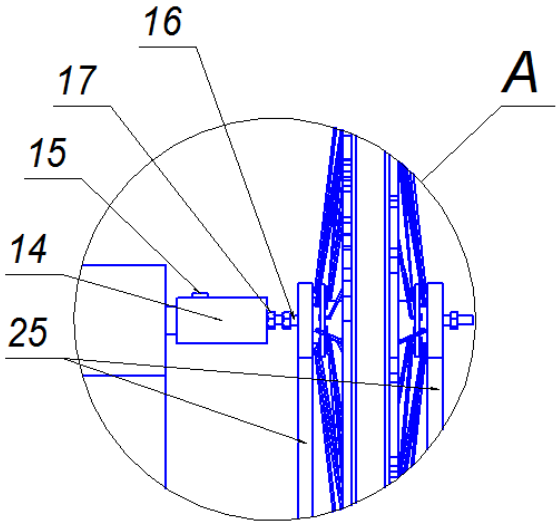

Fig. 4. Technological assembly A. Transmitting of rotation

Torque transmission is provided with using coupling 14. On one side of coupling 14, a hole corresponding to the shape of the motor shaft (with a key) and on the opposite side an inner thread are cut. In thread of coupling 14 a pin 16 is screwed up. Tightening the screw in the key 15, inserting the pin 16 into the hub of a bicycle wheel 3 and installing locknut 17 (fig. 4), we have a strong mechanical junction. Next, going by plywood profiles 18 glued to the rotating bicycle wheel 3, a carriage wheel 19 causes the mechanical system of the stand to make plane vibrations, imitating human leg lifting during the process of walking. Since the profiles 18 are situated in relation to each other at 45^0, the system with increasing angular velocity of rotation of bicycle wheels becoming more and more "swinging". Figure 1 shows the maximum phase of the system "swing" of the system. When a carriage wheel 19 is going to the peak of the plywood profile 18 (fig. 6c), the right leg lifts up.

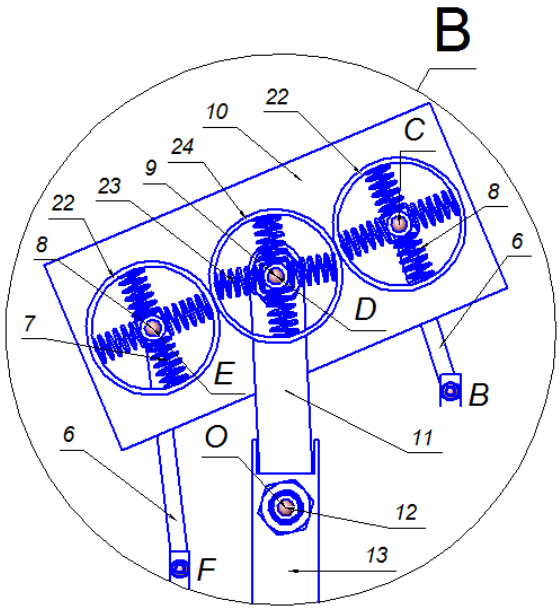

Fig. 5. Technological assembly B. Movements of pelvis

Then the spring 4 is compressed with subsequent transmission of force to the round pipe 5, moving within a wider stationary pipe 21 playing a role of a guide. The parameters on spring 4 is easy to find knowing the shape of profiles, maximal difference between the height of lengths in relation to the floor and the minimal force enough for pressure on wheel 19 to avoid jumping it. The pipe 21 is attached to bracket of wheel 19 at bottom and restricted radially with frame 26. Since the spring 4 is selected with the reserve, it is possible to install the simplest limiter 20 consisting of standard plates and threaded connections. Pipe 5 working as a piston transfers force to the intermediate joint 6, which puts pressure on the axle 8 (hip joint) (fig. 6b).

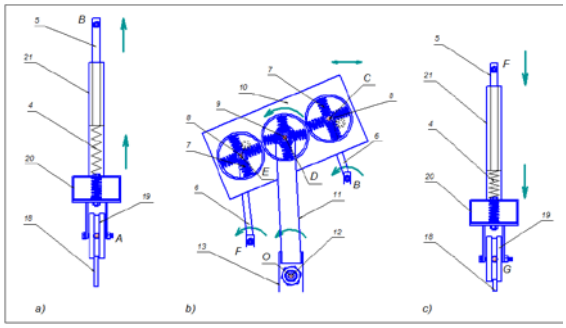
Fig. 6. Movements of stands parts

The right axle 8, in turn, causes compression of the upper and left springs 7, resulting in movement of the joining plate 10 (pelvis) compressing left axle 8 and causing its horizontal and vertical displacements on left springs 7. Joining plate 10 performs composite plane motion two: on the one hand it rotates around the central point of joint 9. On the other hand it moves to the left together with the pipe 11 (i.e., performs motion around a central point of joint 12) pressing the springs 23 and seal 24. To limit the displacement angle of pipe 11 with the plate 10, the pipe 13 (supporting all the construction) has projections on its edges, restricting the fall of elements 11 and 10. Pipes 11 and 13 are connected with axle 12 (supporting joint) which is passed through those pipes. Since plywood profiles 18 should be set oppositely (for example with in relation to each other by 45 degrees) the profile peaks do not match. This provides the possibility of movement of the components of the left "leg" in the opposite direction in comparison with the components of the right leg (fig. 6a). The left leg goes down by the similar way. Firstly, left hip joint 8 presses on the lower left spring 7 and makes the intermediate joint 6 to move pipe 5 down. Left pipe 5 moves down and compresses spring 4, pulling a carriage wheel 19 to plywood profile 18. Passage of each profile peak corresponds to one human step.

The most likely place in a stand for installation of accelerometers is pipe 5. It is planned to use accelerometer with Bluetooth module. Measuring the accelerations causing with vibrations of plywood profiles, it will be possible to find the speeds and displacements of pipe 5. By that we can practically find the upper part of leg what we couldn`t do before because of impossibility to install accelerometers directly on muscle.

4. ADVANTAGES OF DESIGNED STAND

The stand for imitation of man path was introduced in this paper. The main advantage of such mechanical system is very simple construction and big number of things to measure. For example launching stepper motors with different rotation speeds will allow us to simulate lameness.

5. CONCLUSION

Describing the stand, the good and simple mechanical model for making experiments was designed. It is possible to use that for measuring parameters we couldn`t practically measure before. After all, the analytical model for making theoretical calculations on the base of shown stand can consist from 3 basic steps:

1) Finding the degrees of freedom of moving elements of the stand
2) Finding the general equations of the kinetic (T) and potential (V) energies, applicable to the experimental stand
3) Finding the Lagrange equations of the second kind (L=V-T).

6. REFERENCES

1. Zhigailov, S., Kuznetcov, A., Musalimov, V., Aryassov, G. *Measurement and analysis of human lower limbs movement parameters during walking, The 9-th International Conference Mechatronic Systems and Materials (MSM 2013),* 1-3 July, Vilnius, Lithuania, (in press)
2. Aryassov, G., Kuznetcov, A., V. Musalimov, V., Zhigailov, S. *Lower Limb Mathematical Modeling with Inertial Motion Capture during Normal Walking*, 4th International Conference on Integrity, Reliability & Failure, Funchal, (2013), (in press)
3. *Big medical encyclopaedia* http://bigmeden.ru/article/%D0%9D%D0%BE%D0%B3%D0%B0
4. *Site describing modern problems of human locomotion apparatus* http://aupam.narod.ru/pages/fizkult/kod_dikulya/page_01

Sergei Zhigailov, Doctoral student, Tallinn University of Technology, Department of Mechatronics, Ehitajate tee 5, Tallinn, sergsil@gmail.com

Viktor Musalimov, Professor, Head of mechatronics department, ITMO, Kronverk prospekt 49, Saint-Petersburg, Russian Federation, musVM@yandex.ru

Gennady Aryassov, Ass.Professor, Tallinn University of Technology, Department of Mechatronics, Ehitajate tee 5, Tallinn, gennadi.arjassov@ttu.ee

9th International DAAAM Baltic Conference
"INDUSTRIAL ENGINEERING" -
24-26 April 2014, Tallinn, Estonia

ELECTRIFICATION OF EXCAVATOR

Vauhkonen, N.; Liljeström, J.; Maharjan, D.; Mahat, C.; Sainio, P.; Kiviluoma, P. & Kuosmanen, P.

Abstract: *When using work machines in enclosed sites a significant cost is additional ventilation. The need of additional ventilation can be partly or completely excluded by using electric driven work machines.*
For this study a JCB Micro excavator was chosen as a building platform. The 14 kW diesel powered engine with its required equipment was replaced with a 10 kW electrical motor. Four lithium titanate batteries, with a total voltage level of 96 V and a capacity of 60 Ah, powers the electric motor. The overall success of the project was evaluated with measurements, which compares the same excavator with the two power sources.
With electric drive while maintaining the same performance, the operating time was substantially reduced compared to diesel powered drive.
Key words: excavator, electrification, electric motor, electric drive

1. INTRODUCTION

When using excavators indoors there are a few things to consider. Firstly, the space of an enclosed location is limited. Usually this means smaller sized machines. Secondly, when working in enclosed spaces ventilation is usually at best weak. Additional ventilation has to be built for the exhaust gas outlet. This means that work site manager has to make plans and build the additional ventilation, which makes the use of an excavator indoors considerably more expensive than outdoors. The need of additional ventilation could in some cases be avoided if the work machines were powered with non-combustible engines.
This study aims to convert a working JCB Micro excavator to an excavator that runs entirely on electrical power. Even then the excavator has to be able to do the same tasks as prior to its conversion. This is evaluated by doing same set of measurements before and after the conversion to define the performance difference. Besides performance the operational time in both excavators are compared.
The conversion process is done with a low budget, so the outcome of the conversion is to be considered as an inexpensive prototype. The main objective is to get the excavator in working condition so that the measurements can be performed. Aspects like weatherproofing according to industry specifications are considered as additional features.
One fully electrical hydraulic mini excavator has been introduced in 2011. The manufacturer claimed this excavator was on par with their, at the time, current mini excavator in terms of performance and that its lithium-ion batteries could power the excavator for up to six hours of uninterrupted service. However, so far the excavator has not been made commercially available. [1]
Many excavator manufacturers are providing partially electric driven excavators named hybrid excavators. In these excavators the rotation of the cabin is generally powered with an electric

motor. This system often utilizes regenerative breaking to slow down the rotation. An electric motor can also be integrated into the diesel motor output to provide additional power when the diesel motor needs to rapidly accelerate. These electric motors can be powered with super capacitors. When aforementioned systems are utilized the overall fuel efficiency is improved by about 20% compared to a conventional excavator. [2]

Recent studies in excavators have mainly concentrated on improving the overall fuel efficiency of hybrid excavators with different methods, such as improved control strategy and energy recovery. [2][3][4]

This article begins with the methods of this study. In methods the conversion process and the comparing measurements are elaborated. The conversion process consists of the disassembly, part selection and manufacturing, and assembly. After this the results of the project are shown. This means showing the outcome of the conversion process and the measurements. Finally, there is the conclusion, which in turn also includes the discussion of the results.

2. METHODS

2.1 JCB Micro

The converted JCB Micro excavator is powered by a diesel engine producing 14 kW at 2200 rpms. The excavator weighs 1.1 tons and has a fuel tank of 14 liters. The excavator is however not in original condition, as it has been modified for prior projects. The excavator has been fitted with electrically controlled proportional valves and a control unit. There will be no additional modifications in the hydraulics in this conversion process. Thus, the electrical motor will operate at same range of speed than the diesel engine but the difference in torque will affect the hydraulic pressure.

2.2 Fuel consumption measuring installment

To be able to measure the diesel consumption of the excavator for the measurements a fuel measuring installment was built. The setup can be seen mounted to the excavator in Figure 1.

On the right side of Figure 1 is the lower half of the measuring tube, which shows the volume of fuel. As the refueling has been done prior to a measurement, the volume in the tube is read from the scale. After the measurement the reading is taken again. The fuel consumption can then be evaluated from the difference.

Under the measuring tube is the fuel output and return. The output line leads to the input of the fuel rail of the diesel engine. As the flow rate of the fuel in the fuel rail is constant there needs to be a return for the leftover fuel, which in this case is lead to the return of the measuring tube.

Because of the small volume of fuel that fits in the measuring glass, there are four control valves which are used to switch the fuel source between the fuel tank and

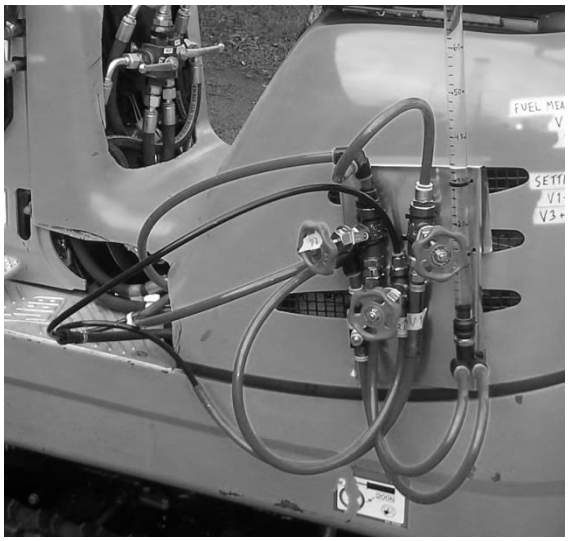

Fig. 1. Fuel consumption measurement installment.

fuel consumption measurement installment.

2.3 Measurements

To determine the outcome of the conversion a set of measurements for initial state were done. One of the main focuses when planning the measurements was to make them simple to perform. The individual measurements would thus have a smaller deviation, which in turn would make the comparison more valid. Because none of the researchers had experience in operating excavators, doing measurements involving fine series of movements would be very difficult to repeat accurately.

The test procedure consisted of a total of seven different measurements. The measurements were:

1. Driving forwards 50 meters.
2. Turning the cabin around 5 times.
3. Fully swinging the arm up and down 5 times.
4. Fully turning the boom left, right and left 3 times.
5. Offloading a sand pile.
6. Idling with full throttle.
7. Idling with no throttle.

All measurements were performed on level ground paved with asphalt, except for measurement #5, which was performed on even soil.

The different measurements were repeated 3 times, except for measurement #5 which was repeated twice, and measurements #6 and #7 were done once.

Main quantities in these measurements were time and fuel consumption. The fuel consumption measuring installment is described in chapter 2.2. The energy consumption for the electric driven excavator was read from the control unit, which has been described later in this chapter. For accurate fuel consumption the temperature of the diesel in the measuring device was measured before and after each measurement. Other parameters documented were weight of the driver, the ambient temperature, the engine temperature, and the hydraulic oil temperature.

2.4 Conversion process

All operations in JCB Micro are achieved with pressurized hydraulic fluid. These operations include turning the cabin, swinging the boom, arm and bucket, lifting and lowering the plow, running the continuous tracks, and using the extendable undercarriage.

The pressurization of the hydraulic fluid is achieved by running a hydraulic pump. The powering of the hydraulic pump is done with the combustion engine. The hydraulic pump and the combustion engine are connected using a transmission and a coupling. This is shown in Figure 2.

In this study these components, except for the hydraulic pump, were replaced with an electric drive.

Liquid cooled Golden Motor HPM-10KW was chosen for the electric motor [5]. As a brushless DC motor it is capable of producing maximum power of 10 kW at 96 V and has operational speed range of 2000-6000 rpm. With optimal driving conditions the motor can achieve 92% efficiency.

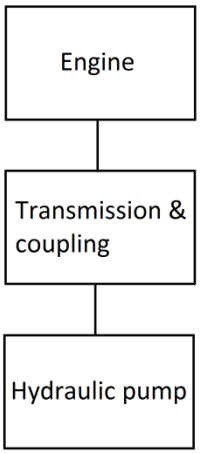

Fig. 2. Mechanical power chain of an excavator.

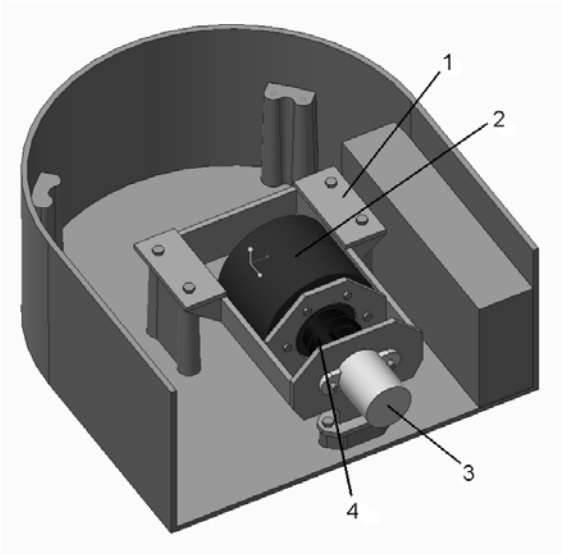

Fig. 3. Sheet metal structure (1) for the electric motor (2) and the hydraulic pump (3). Torsionally flexible coupling is also represented (4).

The coupling of the electric motor and the hydraulic pump was done using KTR ROTEX 42 GG torsionally flexible coupling [6].
The power source for the motor consists of four Altairnano lithium-titanate battery modules, each operating at 24 V and with a 60 Ah nominal capacity [7]. These batteries will be combined in series to produce the necessary 96 V to power the electric motor.
For operating the electric motor a ready-made control unit was used. The unit houses a Sevcon Gen4 controller, which was configured to work with the particular electric motor. All wiring from the electric motor and the batteries are connected to this unit. The unit also contains the on/off switch of the electric motor and an emergency stop button. The control unit is configured and values are read from the CAN-bus.
The energy consumption for the electric driven excavator was logged from an Altairnano controller, which was attached between the batteries and the control unit.
Speed regulation of the electric motor is achieved with a potentiometer, which is wired to the control unit. Besides the speed regulation there is a switch for putting the electric motor in drive mode.
For the electric motor and the hydraulic pump a welded sheet metal structure was built (Figure 3).
Additionally the mounting for the batteries and the control unit were built using store bought materials. Because the electric driven excavator is a prototype and consideration of keeping the two back mountings of the combustion engine (seen in Figure 3) intact the battery could not been placed inside the excavator and therefore had to be placed behind the driver. Because of the size of the prebuilt control unit, it had to be located outside the excavator above the batteries.

3. RESULTS

The excavators before and after the conversion were able to do comparable load intensive tasks (measurements #1-4, section 2.3) in approximately the same amount of time, which indicates that the excavators are capable of doing the same tasks. This statement is confirmed by that the electric driven excavator was able to perform in the same way as the combustion driven excavator when offloading a sand pile.
Table 1 and 2 shows the average energy consumption for each measurement,

Measure-ment #	Average fuel consumption [l/h]	Average energy consumption [kWh]
1	1.35	14.02
2	1.27	13.16
3	1.46	15.09
4	1.93	20.03
5	1.56	16.15
6	1.12	11.64
7	0.51	5.32

Table 1. Average fuel consumption for the measurements.

Measurement #	Average energy consumption [kWh]
1	2.96
2	2.55
3	3.76
4	5.59
5	3.10
6	1.35
7	0.46

Table 2. Average energy consumption for the electric driven excavator.

which are respectively for the combustion driven and electric driven excavator. Number of the measurement corresponds to the numbered list in chapter 2.3. Table 1 shows besides the calculated energy consumption the fuel consumption.

When comparing the tables there's a big difference in the average energy consumptions between the excavators. When doing load intensive tasks the energy consumption of the electric driven excavator is approximately 20% of the energy consumption for the combustion driven excavator. The power consumption is lowered to approximately 10% when the task doesn't demand much power, which is the case with the idling measurements (measurement #6 and #7).

By knowing the energy consumption, maximal energy storage and overall energy to work conversion efficiency of the excavator the operational time can be calculated. When calculating the operational time for the diesel driven excavator based on the measurement results, which is offloading of a sand pile (measurement #5), the operational time is approximately eight hours. The same calculation for the electric driven excavator gives approximately two hours operating time.

4. CONCLUSION

In this study the conversion process of a JCB Micro excavator from a diesel driven state to an electric driven state was presented. The conversion process mainly focuses around finding suitable electric motor, batteries and transmission. Also the mounting of these parts takes its time to plan and to build and especially the parameterization of the electric motor proved to be time consuming. Besides getting the electric driven excavator to function there was measurements made to compare the two excavators with different power sources.

The performance difference of the different excavators proved to be minimal. However, the operational time of the converted excavator is clearly reduced; despite of using four high-grade lithium-titanate batteries and having an advantage of the electric motor's much higher efficiency. This means the operational time is about two hours (when using the full capacity of the batteries) depending on the power usage. With the fuel combustion engine and the 14 liter tank the operation time was calculated to be around eight hours.

The comparable short operational time for the electric driven excavator could be improved by providing the excavator with a smarter power controlling system, for example an automatic shutdown of the excavator when not operated. Also, by finely tuning the electric motor and using this motor at the optimal speed by implementing an appropriate gear ratio the overall efficiency could be increased.

The study shows that electric powered excavators can potentially be used in some cases where a fuel driven excavator is more expensive to use. The limiting factor of electric powered excavator is mainly the low capacity of the batteries and the long charging times of the batteries compared with the conveniences when using fuel driven

excavators. Also the purchasing price of an electric driven excavator would be higher because of the expensive batteries.

5. REFERENCES

1. Takeuchi Manufacturing [US], Ltd. News Announcement: Takeuchi Introduces World's First Fully Electric Hydraulic Excavator [WWW] http://www.takeuchi-us.com/www/blog/viewpost/43 (8.3.2014)

2. Hakgu, K., Jaewoong, C., Kyongsu, Y. Development of supervisory control strategy for optimized fuel consumption of the compound hybrid excavator. *Journal of Automotive Engineering*, 2012, **226**, 1652-1666.

3. Wang, T., Qingfeng, W., Tianliang, L. Improvement of Boom Control Performance for Hybrid Hydraulic Excavator with Potential Energy Recovery. *Automation in Construction*, 2012, **30**, 161-169.

4. Tianliang, L., Qingfeng, W., Baozan H., Wen G. Research on the Energy Regeneration Systems for Hybrid Hydraulic Excavators. *Automation in Construction*, 2010, **19**, 1016-1026.

5. Golden Motor [WWW] http://goldenmotor.com/ (2.3.2014)

6. KTR. ROTEX [WWW] http://www.ktr.com/root/img/pool/pdf/produktkataloge/en/en_gesamt/001_rotex_en.pdf (2.3.2014)

7. Altairnano. 24 V 60 Ah Battery Module [WWW] http://www.altairnano.com/wp-content/uploads/2011/10/60Ah-DataSheet.pdf (2.3.2014)

CORRESPONDING ADDRESS

Panu Kiviluoma, D.Sc. (Tech)
Aalto University School of Engineering, Department of Engineering Design and Production
P.O. Box 14100
00076 Aalto, Finland
Phone: +358 50 433 8661
E-mail: panu.kiviluoma@aalto.fi
http://edp.aalto.fi/en/

ADDITIONAL DATA ABOUT AUTHORS

Vauhkonen, Niclas
Phone: +358 50 553 4699
E-mail: niclas.vauhkonen@aalto.fi

Liljeström, Jan
Phone: +358 50 521 7589
E-mail: jan.liljestrom@aalto.fi

Maharjan, Devendra, B.Sc. (Tech.)
Phone: +358 46 641 7644
E-mail: devendra.maharjan@aalto.fi

Mahat, Chiranjeevi, B.Sc. (Tech.)
Phone: +358 44 016 8648
E-mail: chiranjeevi.mahat@aalto.fi

Kuosmanen, Petri, D.Sc. (Tech.), Professor
Phone: +358 0500 448 481
E-mail: petri.kuosmanen@aalto.fi

Sainio, Panu, Lic.Sc. (Tech.), Chief Engineer
Phone: +358 50 567 8396
E-mail: panu.sainio@aalto.fi

9th International DAAAM Baltic Conference
INDUSTRIAL ENGINEERING
24-26 April 2014, Tallinn, Estonia

PREDICTIVE CONTROL FOR CONTROLLING AND DRIVING AUTONOMOUS VEHICLES

Vu Trieu Minh

Abstract: *This paper presents the use of model predictive control (MPC) for driving autonomous vehicles with front steering and front-wheel drive. Simulations show that the MPC controller can drive the vehicle along the reference paths and guarantee the system stability even when some initial conditions lead to violations of constraints.*
Key words: Tracking path, predictive control, trajectory generation, autonomous vehicle.

1. INTRODUCTION

This paper presents the use of model predictive control (MPC) for driving autonomous vehicles with front steering and front wheel-drive. The linearized MPC algorithm has been formulated for those vehicles which can be able to track on feasible trajectories generated online from the vehicle nonlinear dynamic equations.
To deal with the system uncertainties and the model-plant mismatches, some robust MPC schemes are being developed accounting for the modeling errors at the controller design. Schemes for robust MPC tracking setpoints can be referred to from Minh V.T and Hashim F.B (2011) [6], where the system's uncertainties are represented by a set of multiple models via a tree trajectory and its branches, and the robust MPC problem is to find the optimal control actions that, once implemented, cause all branches to converge to a robust control invariant set. Other MPC algorithms for controlling vehicle speed and engine torque are referred to from Minh V.T. *et al.* (2012) [8], where a real time transition strategy with MPC is developed for achieving quick and smooth clutch engagements for hybrid electrical vehicles.
Robust MPC schemes for input saturated and softened state constraints can be referred to from Minh V.T and Afzulpurkar N (2005) [5], where uncertain systems are designed with the use of linear matrix inequalities (LMIs) subject to input and output saturated constraints. Nonlinear MPC (NMPC) calculations are referred to in Minh V.T and Afzulpurkar N (2006) [4], where three NMPC schemes with zero terminal region, quasi-infinite horizon, and softened state constraints are presented and compared. In these NMPC schemes, all online inputs solution from the NMPC optimizer is implemented for the close-loop control by solving on-line the ODEs repeatedly.
Control of tracking vehicle with MPC can be referred to recently in several research papers. However the idea of using MPC for tracking trajectories generated online from ODEs with time variant system is still missing. An MPC scheme for autonomous ground vehicle can be read in Falcon P. *et al.* (2008) [2], where an initial frame work based on MPC is presented. However, this paper fails to mention the real-time solving of the vehicle ODEs equations and the calculation of the optimal controlled inputs for the vehicle velocity and its steering velocity. Similarly, another paper on MPC for path tracking of autonomous vehicles is presented by Lei L. *et al.* (2011) [3], where the vehicle equations of motion are approximately linearized from the vehicle coordinates and the heading angle. However the paper fails to include the steering angle into the dynamic equations.

A robust MPC for mobile vehicle trajectory control can be read in Baharonian M. *et al*. (2011) [1], this paper comes out with an assumption that there is already a virtual reference trajectory and then, the control problem becomes too simple and trivial. An adaptive trajectory tracking control of wheeled mobile is developed by Wang J. *et al.* (2011) [11], however this paper does not mention on how a feasible trajectory can be generated and how optimal control actions can be achieved for the best tracking performance. Other references on MPC are referred to in Minh V.T. *et al.* (2011) [7] and in Minh V.T. & Rashid A.A. (2012) [9].

The paper is organized as follows: section 2 describes the system modeling; section 3 develops MPC schemes; section 4 illustrates some MPC performances; and finally, a short summary is concluded in section 5.

2. SYSTEM MODELING

Consider a vehicle rolling without slipping, the vehicle dynamics can be written in a set of first-order differential equations from its configuration variables. If the vehicle has the rear-wheel driving, the vehicle kinematic model, shown in Fig.1, can be derived in equation (1):

$$\begin{bmatrix} \dot{x} \\ \dot{y} \\ \dot{\theta} \\ \dot{\varphi} \end{bmatrix} = \underbrace{\begin{bmatrix} \cos\theta \\ \sin\theta \\ \dfrac{\tan\varphi}{l} \\ 0 \end{bmatrix}}_{X_1} u_1 + \underbrace{\begin{bmatrix} 0 \\ 0 \\ 0 \\ 1 \end{bmatrix}}_{X_2} u_2 \qquad (1)$$

From (1), the four components of function X_1 are: $X_1^1 = \cos\theta$, $X_1^2 = \sin\theta$, $X_1^3 = \dfrac{\tan\varphi}{l}$, and $X_1^4 = 0$. The four components of function X_2 are: $X_2^1 = 0$, $X_2^2 = 0$, $X_2^3 = 0$, and $X_2^4 = 1$.

In Fig.1, r is the vehicle wheel radius and l is the base length; x and y are the Cartesian coordinates of the rear wheel, θ measures the orientation of the vehicle body with respect to the x axis, and φ is the steering angle.

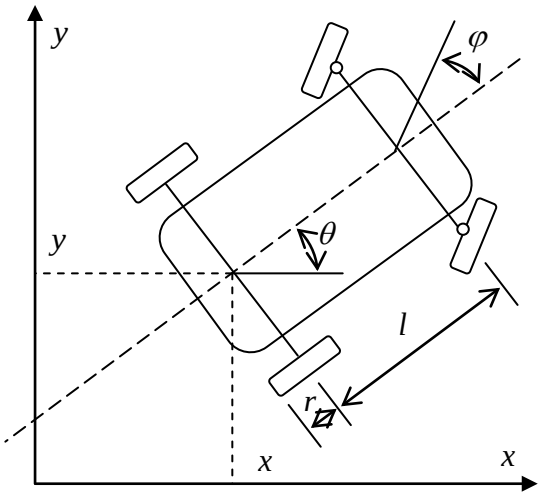

Fig. 1. A simplified vehicle model

In equation (1), the vehicle motion is controlled by two inputs, u_1 is the linear driving velocity, and, u_2 is the angular steering velocity. There are four (4) state variables, namely the position of the vehicle $x_1 = x$ and $x_2 = y$; the angle of the vehicle body orientation with respect to the x axis, $x_3 = \theta$; and the steering angle, $x_4 = \varphi$.

The system in (1) is a nonholonomic and if $\varphi \neq \dfrac{\pi}{2}$, this system is fully controllable. This means that the system in (1) can be transformed from any given state to any other state and all of its state parameters are under controlled by the two input vectors.

The vehicle model in (1) is nonlinear and has the first order derivative form:

$$\dot{X} = f(x,u) \qquad (2)$$

where the state variables are $x \in [x, y, \theta, \varphi]^{'}$, and the inputs are $u = [u_1, u_2]^{'}$. The nonlinear equation in (2) can be expanded in Taylor series around the reference setpoints (x_r, u_r) at $\dot{X}_r = f(x_r, u_r)$, that:

$$\dot{X} \approx f(x_r, u_r) + f_{x,r}(x - x_r) + f_{u,r}(u - u_r) \qquad (3)$$

where $f_{x.r}$ and $f_{r.x}$ are the Jacobean of f corresponding to x and u, evaluated around the reference setpoints (x_r, u_r).

Subtraction of (3) and $\dot{X}_r = f(x_r, u_r)$ results a linear approximation to the system at the reference setpoints in continuous time (t) form:

$$\dot{\tilde{X}}(t) = A(t)\tilde{X}(t) + B(t)\tilde{u}(t) \quad (4)$$

The continuous system in (4) can be transformed to a discrete-time (k) with a scanning interval, $k+1 = k + \Delta t$, and, Δt is the length of the sampling interval. The inputs $u(k)$ are held constant during the time interval $(k+1)$ and (k). The symbols of $x_k = x(k)$ and $u_k = u(k)$ are also used:

$$\begin{aligned} \tilde{X}(k+1) &= A(k)\tilde{X}(k) + B(k)\tilde{u}(k) \\ \tilde{Y}(k) &= C(k)\tilde{X}(k) \end{aligned} \quad (5)$$

In this discretized model, the two control inputs are the difference in the actual and the desired velocity, $u_1(k) - u_{r1}(k)$, and, $u_2(k) - u_{r2}(k)$. The four outputs, $y(k) = \tilde{Y}(k) = C(k)\tilde{X}(k)$, are assumed totally to be measured and updated in real-time scanning interval from the GPS map. It is noted that the vehicle discretized model in (5) is a time variant system and its transfer function is depending on its positions and the scanning speeds. Linearized equations (5) are used to develop MPC algorithms in the next part.

3. MODEL PREDICTIVE CONTROL

MPC algorithms are now developed to control the two inputs of the vehicle driving velocity, $u_1(k)$, and, the vehicle steering velocity, $u_2(k)$, in order to achieve the four desired outputs of the vehicle coordinate positions, $x_1(k) = x(k)$, and $x_2(k) = y(k)$; the vehicle orientation body angle with respect to the x axis, $x_3(k) = \theta(k)$; and the steering angle, $x_4(k) = \varphi(k)$.

Then, a tracking setpoints MPC objective function with hard constraints can be developed:

$$\min_{U \in \{\Delta u_k, \ldots, \Delta u_{k+N_u-1}\}} \left\{ \begin{array}{l} J(U, x(k)) = \\ \sum_{i=0}^{N_y-1} \left[\begin{array}{l} (y_{k+i|k} - r_{k+i|k})' Q (y_{k+i|k} - r_{k+i|k}) \\ + \Delta u'_{k+i|k} R \Delta u_{k+i|k} \end{array} \right] \end{array} \right\} \quad (6)$$

where $x(k)$ denotes the state variables at the current discrete time (k): $U \in \{\Delta u_k, \ldots, \Delta u_{k+N_u-1}\}$ is the solution of input increments, N_u is the inputs predictive horizon; N_y is the outputs predictive horizon; $y_{k+i|k}$ are the predictive outputs at the current discrete time (k), $r_{k+i|k}$ are the corresponding reference output setpoints; $\Delta u_{k+i|k}$ are the input increments prediction with $\Delta u_{k+i|k} = u_{k+i|k} - u_{k+i-1|k}$; $Q = Q' \geq 0$, $R = R' > 0$ are the weighting penalty matrices for predicted outputs and input increments, respectively (Minh V.T. *et al.*, 2012) [8].

The MPC regulator computes the optimal solution, $U^* \in \{\Delta u_k^*, \ldots, \Delta u_{k+N_u-1}^*\}$ and generates the new inputs $u_{k+i|k} = u_{k+i-1|k} + \Delta u_{k+i|k}$, from the objective function (6), then applies only the first element of the current inputs increment, Δu_k^*, to the current optimal inputs, $u^*(k) = u_{k-1} + \Delta u_k^*$. After having inserted the current optimal inputs, the MPC regulator repeats the optimization, $u^*(k+1)$, for the next interval time, $k+1$, based on the new update state variables $x(k+1)$. This way, the closed loop control strategy is obtained by solving on-line the open loop optimization problem.

By substituting

$$x_{k+N_y|k} = A^{N_y}(k)x(k) + \sum_{i=0}^{N_y-1} A^i(k)B(k)u_{k+N_y-1-i},$$

equation (6) can be rewritten as a function of only the current state $x(k)$ and the current setpoints $r(k)$:

$$\begin{aligned} \Psi\left(x(k), r(k)\right) &= \frac{1}{2} x'(k) Y x(k) \\ &+ \min_U \left\{ \frac{1}{2} U' H U + x'(k) r(k) F U \right\} \end{aligned} \quad (7)$$

As only the optimizer U is needed, the term involving Y is usually removed from (7). Then, the optimization problem in (7) is a quadratic program and depends only on

the current state $x(k)$ and the current setpoints $r(k)$ subject to the hard combined constraints. The implementation of MPC requires an on-line solution of this quadratic program at each time interval (k). Since MPC is designed for on-line implementation, any infeasible solution of the online optimization problem in (7) cannot be allowed. Normally the input constraints are based on the physical limits of the vehicle (Minh V.T. *et. al.* 2012) [10]. If the outputs constraints are on tracking position errors, they are not very strictly imposed and can be violated somewhat during the evolution of the performance. To guarantee the system stability once the outputs violate the constraints, the hard constrained optimization in (6) can be modified to a new MPC objective function with some softened constraints as:

$$\min_{U\square\{\Delta u_k,\ldots,\Delta u_{k+N_u-1}\}}\left\{\begin{array}{l} J(U,x(k))= \\ \sum_{i=0}^{N_y-1}\left[\begin{array}{l}(y_{k+i|k}-r_{k+i|k})'Q(y_{k+i|k}-r_{k+i|k}) \\ +\Delta u'_{k+i|k}R\Delta u_{k+i|k}+\varepsilon_i'(k)\Lambda\varepsilon_i(k)\end{array}\right]\end{array}\right\} \quad (8)$$

The robustness of MPC can be also increased if some setpoints can be relaxed into regions rather than put in some specific values. Then, another new MPC algorithm can be developed if the setpoints $r(k)$ can be changed into regions. An output region is defined by the minimum and maximum values of a desired range. The minimum value is the lower limit, and the maximum value is the upper limit and satisfied $y_{lower} \le y_{k+i|k} \le y_{upper}$. The modified objective function for this MPC with output regions is:

$$\min_{U\square\{\Delta u_k,\ldots,\Delta u_{k+N_u-1}\}}\left\{\begin{array}{l} J(U,x(k))= \\ \sum_{i=0}^{N_y-1}\left[z'_{k+i|k}Qz_{k+i|k}+\Delta u'_{k+i|k}R\Delta u_{k+i|k}\right]\end{array}\right\}, \quad (9)$$

As long as the outputs still lie inside the desired regions, no control actions are taken because none of the control objectives have been violated, all $z_{k+i|k}=0$ (Minh V.T & Afzulpurkar N., 2006) [4]. But when an output violates the desired region, the MPC regulator will be activated and push them back to the desired regions. This modified MPC objective function can help to make the vehicle tracking smoother and the controller tasks can be reduced. Simulations for the MPC application are presented in the following part.

4. MPC FOR TRACKING SETPOINTS

For the trajectory tracking, a reference trajectory is generated by solving the vehicle differential equations in (1). The difference of the reference trajectory setpoints and the actual current vehicle positions is provided at the real time to the MPC regulator. The MPC regulator calculates the optimized control inputs and only the first element of this optimal solution is fed into system to generate the next outputs. The updated outputs are now compared with the updated setpoints for the next MPC regulator calculation. The diagram of the MPC control system is shown in figure 2.

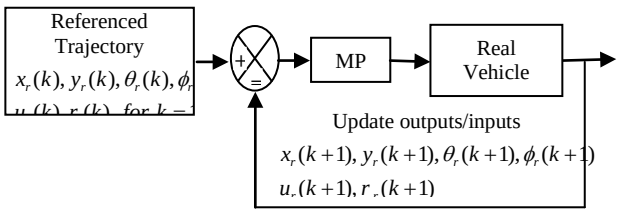

Fig. 2. MPC control system

We implement this MPC system to track a full circle trajectory. For generating online this full circle trajectory, the reference desired inputs are set at $u_1 = r\omega$ and $u_2 = 0$. The initial reference positions are set at $\left[x_{r0} \quad y_{r0} \quad \theta_{r0} \quad \varphi_{r0}\right]' = \left[0 \quad 0 \quad 0 \quad \arctan\frac{r}{l}\right]'$.

If the MPC prediction horizon is shortened, the online calculation burden will be considerably reduced but it will lead to faster incremental changes of the inputs and then, bad performance of the outputs. With shortened horizon predictions, the controller may become instable. Figure 4 shows the MPC performance with shortened predictive horizons to $N_u = 4$ and $N_y = 4$.

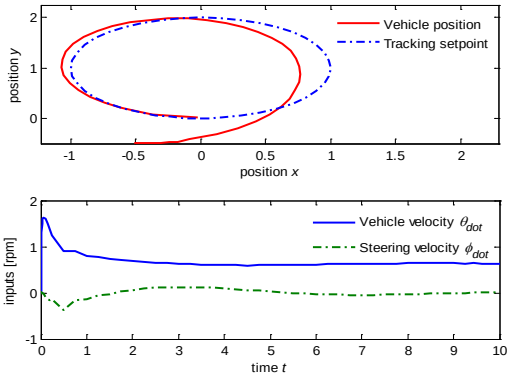

Fig. 3. Tracking MPC linearized model

Sufficient long prediction horizon will increase the MPC performance and its stability. However, the calculation burden of this system will be dramatically increased. The next MPC simulation runs with $N_u = 20$ and $N_y = 20$ shown in Figure 5. Performance of these tracking outputs is much improved as well as the inputs become smoother or easier to be regulated.

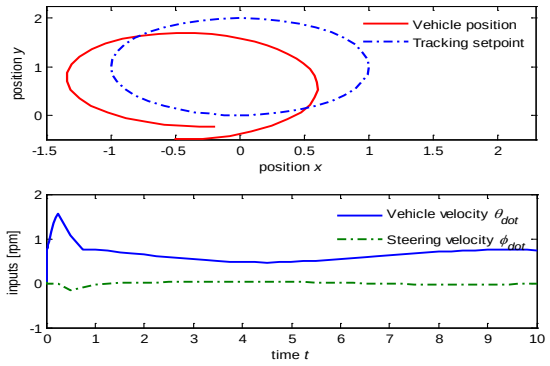

Fig.4. MPC linearized with short horizon

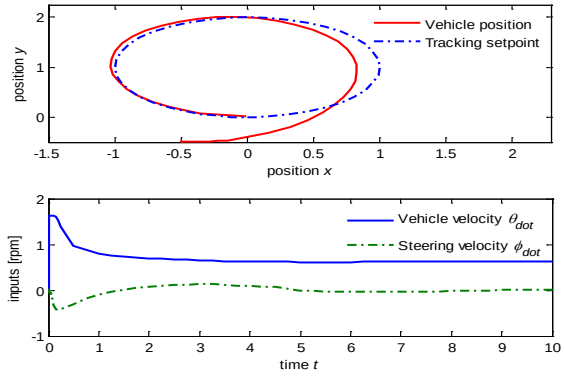

Fig.5. MPC linearized with long horizon

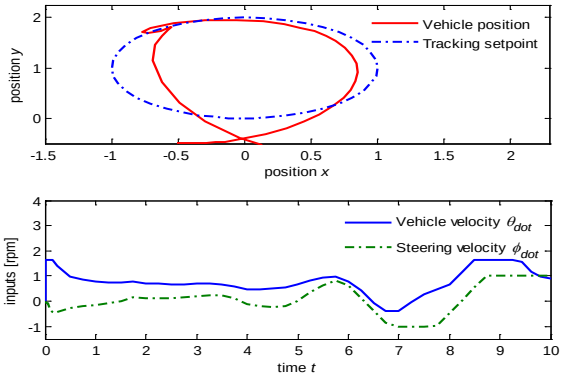

Fig.6. MPC with too long horizon

However with too long horizon length, MPC will result too slow control increments and therefore deteriorate the outputs performance. The MPC system becomes instable as shown in Figure 6 with too long prediction horizon of $N_u = 23$ and $N_y = 23$.

Regulation of the penalty matrices can also help to change the MPC performance. The next simulation shown in Figure 7 runs with $N_u = 6$, $N_y = 6$, $Q = diag\{1,1,1,1\}$, and $R = diag\{10,10\}$. Figure 7 shows that the inputs become smoother but the outputs tracking errors become considerably larger.

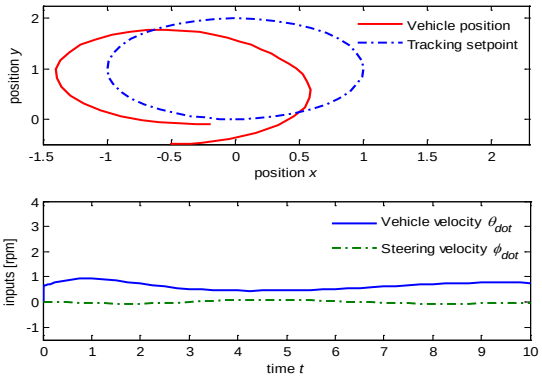

Fig.7. MPC linearized model with Q R

Inversely, we set now $N_u = 6$, $N_y = 6$, $Q = diag\{10,10,10,10\}$, and $R = diag\{1,1\}$. Figure 8 shows that the system becomes very sensitive to the input changes. These faster input changes can be seen in the triangular shape. These inputs shape is unrealistic or we cannot control the vehicle

velocity on that shape. And consequently, the system becomes instability.

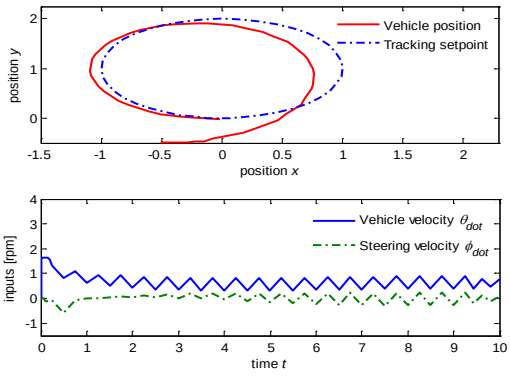

Fig.8. MPC linearized model with Q R

The MPC regulator can gradually eliminate these errors during its evolution and drive the vehicle closer to the reference setpoints.

5. CONCLUSION

Simulations show that MPC can control very well the tracking setpoints subject to constraints. The MPC performance, stabilization as well as the robustness can be regulated and improved by varying the MPC parameters as well as modifying its objective functions to softened constraints or to output regions. MPC schemes are able to guarantee the system stability even when the initial conditions lead to violations of some constraints.

6. REFERENCES

1. Bahadorian M., Savkovic B., Eston R., & Hesketh T., Toward a Robust Model Predictive Controller Applied to Mobile Vehicle Trajectory Tracking Control, In *Proceeding of 18th IFAC World Congress*, Milano, Italia, vol. 18(1), pp. 552-557, September 2011, DOI: 10.3182/20110828-6-IT-1002.01786.

2. Falcone P., Borrelli F., Tseng H., Asgari J., & Hrovat D., A Hierarchical Model Predictive Control Framework for Autonomous Ground Vehicles, In *American Control Conference* (ACC), Seattle, USA, pp. 3719-3724, June 2008. DOI: 10.1109/ACC.2008.4587072.

3. Lei L., Zhurong J., Tingting C., and Xinchung J., Optimal Model Predictive Control for Path Tracking of Autonomous Vehicle, In *3rd International Conference on Measuring Technology and Mechatronics Automation* (ICMTMA), February 2011, Shanghai, China, vol. 2, pp. 791-794, DOI: 10.1109/ICMTMA.2011.481.

4. Minh V.T & Afzulpurkar N., A Comparative Study on Computational Schemes for Nonlinear Model Predictive Control, *Asian Journal of Control*, 2006, vol 8(4) pp. 324-331, DOI: 10.1111/j.1934-6093.2006.tb00284.x.

5. Minh V.T and Afzulpurkar N., Robust Model Predictive Control for Input Saturated and Softened State Constraints, *Asian Journal of Control*, 2005, vol 7(3), pp. 323-329, DOI: 10.1111/j.1934-6093.2005.tb00241.x.

6. Minh V.T and Hashim F.B., Tracking setpoint robust model predictive control for input saturated and softened state constraints, *International Journal of Control, Automation and Systems*, 2011; vol 9(5): 958–965, DOI: 10.1007/s12555-011-0517-4.

7. Minh V.T, Awang M, & Parman S., Conditions for Stabilizability of Linear Switched Systems, *International Journal of Control Automation and Systems*, 2011, vol. 9 (1), pp. 139-144, DOI: 10.1007/s12555-011-0118-2.

8. Minh V.T, Hashim F. B, & Awang M., Development of a Real-time Clutch Transition Strategy for a Parallel Hybrid Electric Vehicle, *Proceedings of the Institution of Mechanical Engineers Part I – Journal of Systems and Control Engineering*, 2012, vol. 226 (2), pp. 188-203, DOI: 10.1177/0959651811414760.

9. Minh V.T. & Rashid A.A., Automatic Control of Clutches and Simulations for Parallel Hybrid Vehicles, *International Journal of Automotive Technology*, 2012, vol. 13(4), pp. 645-651, DOI: 10.1007/s12239-012-0063-y.

10. Minh V.T, Afzulpurkar N., & Mansor W, Fault Detection Model-Based Controller for Process Systems, *Asian Journal of Control*, 2011, vol. 13(3), pp. 382-397, DOI: 10.1002/asjc.346.

11. Wang J., Lu Z., Chen W., & Wu X., An Adaptive Trajectory Tracking Control of Wheeled Mobile Robots, In *Industrial Electronics and Applications* (*ICIEA*), June 2011, Beijing, China, pp. 1156-1160, DOI: 10.1109/ICIEA.2011.5975761.

ABOUT AUTHORS

Author: **Vu Trieu Minh**, PhD., Professor, Head of Chair of Mechanosystem Components.
Title of Manuscript: **Predictive Control for Controlling and Driving Autonomous Vehicles**.
Address: Department of Mechatronics, Tallinn University of Technology, Ehitajate tee 5, 19086, Tallinn, Estonia, email: trieu.vu@ttu.ee

9th International DAAAM Baltic Conference
"INDUSTRIAL ENGINEERING"
24-26 April 2014, Tallinn, Estonia

ADDITIVE MANUFACTURING WITH UV LIGHT CURED RESIN

Vuorio, J.; Nikkilä, V.; Teivastenaho, V.; Peltola, J.; Partanen, J.; Kiviluoma, P. & Kuosmanen P.

Abstract: *This paper introduces a method of additive manufacturing by injection of light-cured material. A fabrication system to produce three-dimensional parts by extruding multiple layers of photosensitive resin was constructed. The polymerization of the resin is achieved in a curing process that utilizes ultraviolet light-emitting diodes. The device is able to manufacture basic three-dimensional shapes. Curing time of the photopolymer was discovered to be the dominating parameter with the used manufacturing method.*
Keywords: Additive manufacturing; photosensitive materials; UV-LEDs; Rapid prototyping

1. INTRODUCTION

Additive manufacturing is a subject of intensive study. Additive manufacturing by injection of light-cured material is a manufacturing process for producing three-dimensional objects by extruding multiple layers of photosensitive materials. The process utilizes ultraviolet light to cure materials upon completion. Recent studies in radiant power of ultraviolet light-emitting diodes (UV-LEDs) suggest that mercury-vapour lamps may be substituted for UV-LEDs [1]. However, the use of high power UV LEDs as a curing light source has not been thoroughly investigated in the application of additive manufacturing, especially with regard to the method of injection of the photopolymer. In this study a prototype printer was constructed and tested.

Photopolymer is cured with UV light. The formula of the resin enables hardening process with UV light. When curing photopolymer by applying UV light, the cured layer absorbs light [2]. Curing process is halted when exposure subsides below threshold value. This restricts the thickness of one printed layer. The depth of cured layer can be expressed by Beer's law [2]:

$$C = \begin{cases} D_p \ln(E/E_c) & , E > E_c \\ 0 & , E \leq E_c \end{cases} \quad (1)$$

Where C expresses the curing depth, E refers to UV light exposure and D_p states the penetration depth of the resin, which is unique for each resin. Finally, E_c indicates the critical exposure of the resin. Curing process will not happen if this threshold is not exceeded.

Resin is extruded in liquid form. Initial curing is applied by focused UV-LEDs. These LEDs are attached to the extruder unit. However, to complete the process, additional UV light source is needed since the penetration depths of these LEDs are limited.

2. METHODS

Advantages of LED lights are their high durability and longer lifespan. Also, LED lights can be controlled with a very short response time. However, led lights alone are insufficient to finalize the curing of the resin. The effect of the radiation area was analysed. Different amounts of radiation of light and its effects to the quality were analysed. Developed device was tested with several resins and the effects of material properties to manufacturing

quality were compared. Common shapes such as cubes and cones were used to compare the accuracy of the developed method against existing additive manufacturing systems.

2.1 Mechanical design of constructed printer

The structural components of the printer are shown in Figure 1. The printer consists of the following subassemblies.
Extruder unit syringes the resin by applying pressure with piston to the resin container. Stepper motor controls the piston by rotating gear which pushes a screw down and force syringe's piston to extrude material through nozzle. Unit is controlled by RAMPS (RepRap Arduino Mega Pololu Shield) [3]. Extruder moves along y- and z-axis. Also the LEDs responsible for the primary curing are located in the extruder unit. A detailed assembly of the extruder unit can be seen in Figure 2.
Printbed functions as a platform for the printable object. This platform moves parallel to x-axis and thus has one degree of freedom. Movement is achieved with stepper motor controlling a belt drive. Print object can be moved in all three dimensions with printbed and extruder.
Printer body is made of polycarbonate which provides mechanical strength while still being easy to manufacture. The polycarbonate sheets are connected to each other with fixit blocks and threaded rods to achieve easy and rigid assembly.

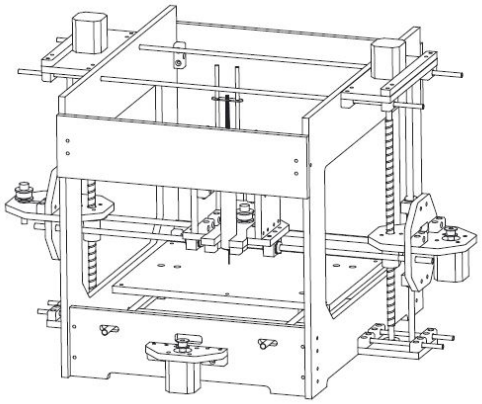

Figure 1: Structure of the printer

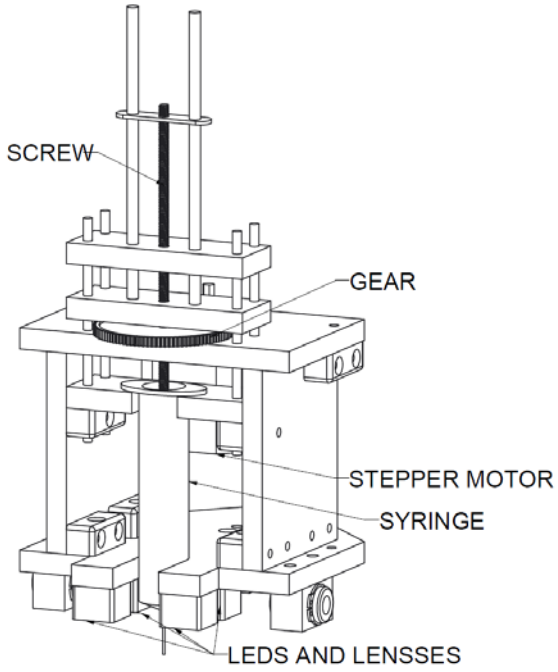

Figure 2: Extruder unit.

2.2 Curing with UV-LEDs

Four UV-LEDs were mounted to the extruder. Intensity of these LEDs stays constant but it can also be controlled by RAMPS unit. However, maximum intensity is generally desired at all times during the printing process. Properties of these LEDs are listed in Table 1.

Manufacturer	Tecled Lightning Co.
Model	XL5050UVC355
Peak wavelength	355 nm
Spectrum radiation bandwidth	28 nm
DC forward current	60 mA
Power dissipation	200 mW
Luminous intensity	4.5 mW
Life	30 000 h
Size	5 x 5 mm

Table 1. Extruder LEDs for primary curing of the resin

2.3 Beam steering

The alignment of the LEDs and lenses relative to the plane of the printbed is crucial. By overlapping the focused beams of UV light that are coming through the lenses will be concentrating the effective radiation of the UV light into a fixed area [6]. The optical properties of the lenses that were used for are shown in Table 2.
The resin will be extruded in such way that it will be completely exposed to the fixed area. This will have the most beneficial effect to the overall irradiance efficiency of the LEDs and thus in this case accelerate the polymerization process of the resin. The LED and lens alignment is shown in the Figure 3.

Type	FCA10911 NIS33U-SS
Optic Material	Cyclic Olefin Polymer (COP)
Holder Material	Polycarbonate
Fastening	Tape
Viewing Angle(FWHM)	10 degrees

Table 2. Lenses for concentrating the beam of light.

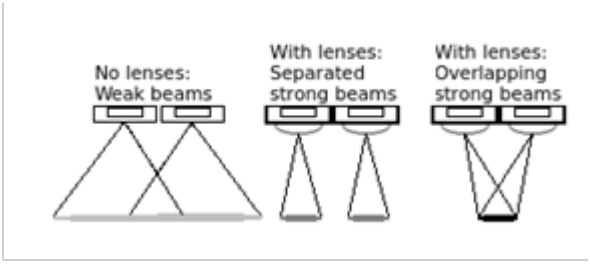

Figure 3: LED alignment and steering of the beam.

2.4 Evaluation of resins

We compared two different resins: Somos ProtoGen O-XT 18420 and Somos WaterShed XC 11122. Both of these resins are used in additive manufacturing processes, e.g., stereolithography. These both photopolymers resemble traditional engineering plastics, such as acrylonitrile butadiene styrene (ABS), and these materials were selected to this study due their mechanical properties, which makes it possible to create durable and functional parts. Properties of both resins are listed in Table 3.

	ProtoGen O-XT 18420	WaterShed XC 11122
Colour	White	Optically clear, near colorless
Viscosity at 30 °C	350	260
Density (g/ cm^2)	1.13	1.12
Critical exposure ($mJ/cm^{2)}$	6.73	11.5
$D_{p,}$ Slope of cure-depth vs. ln(E) curve (mm)	0.11	0.16

Table 3: Properties of the resins. [7,8]

3. RESULTS

This study demonstrated that photopolymer can be solidified with LED lights. Critical exposure was exceeded and with proper calibration of printing parameters, it is possible to manufacture solid objects.
In the photopolymerisation process the radiation of the UV light will be partially absorbed by the cured layer. This follows the Beer's law of absorbance which states that the exposure will decrease exponentially with the curing depth.
Calculated values of cure depth for both used resins are less than 1 mm. This and practical experiments with LEDs and resins indicate that limiting factor with minimum layer thickness is the accuracy of the extruder. While the maximum layer thickness is limited by the curing depth.
The ability of the light sources to cure sample lines of resin was also tested in practice. This test provided how long it takes for the LEDs to cure the resin. From the curing time it is possible to predict the

speed that the extruder can be moved while extruding material. These curing tests were executed with and without lenses and with variable number of LEDs. It was discovered that with one LED, curing process takes too long to be used in AM even with a lens focusing the beam. Although it also proved that the lens provided a remarkable improvement to the curing speed of the resin. In final construction, four LEDs with lenses were found to be good compromise between curing speed and keeping the size of the LED module small enough to fit in to the extruder.

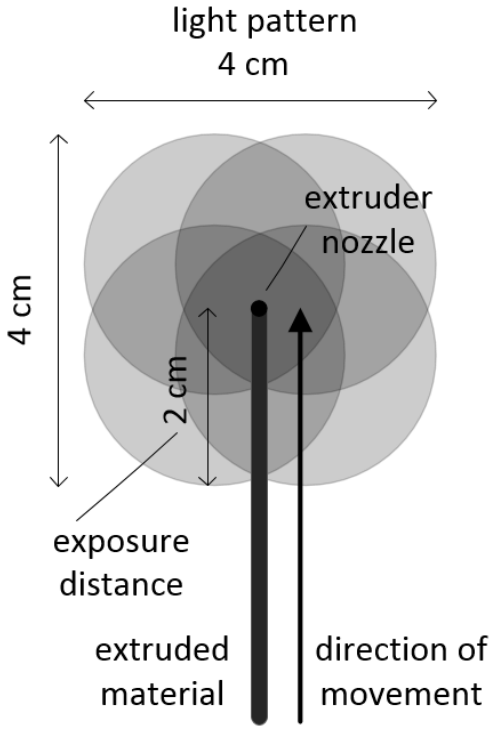

Figure 4: Topside view of the light pattern and printing process.

The reason the light sources were placed approximately 30 mm from the printbed was to get the most beneficial effect of overall irradiance efficiency of LEDs and thus get the most effective polymerization process. This distance was evaluated empirically by changing the distance from the LED lenses relative to the printbed and by changing the alignment of the angle of the UV-light beam from LEDs. The alignment of the LEDs needs to be done so that the beams are overlapping each other's enough to create a concentrated hotspot near the head of the syringe. At the same time combined beam needs to cover as large area as possible, so that the extruded resin is exposed to the UV-light long time enough for it to cure completely.

However even with optimized light source the curing time achieved with the developed prototype is 5 – 10 s, under the UV-light exposure, depending on the layer thickness. This means that curing time of the resin is the limiting factor of the printing speed the device is able to achieve. The aforementioned also means that the shape and size of the printed object have huge impact on final printing speed reached. Figure 4 illustrates the light pattern and how long is the exposure distance in a case when straight line is printed. From the figure it can be seen that if the outlines of the manufactured object can be fitted in the 40x40 mm area, the extruded resin is constantly exposed to the UV-light and therefore faster printing speed can be used. However the optimized printing speed versus the dimensions of the printed object was not in the scope of this study and the overall printing speed achieved with the built prototype is poor compared to modern thermoplastic printers.

4. DISCUSSION

The constructed prototype is able to provide an alternative method to additive manufacturing that is able to compete with more common layer manufacturing (LM) methods (e.g., fused deposition modelling). It has many advantages: increased accuracy, efficiency, controllability, response and safety. The developed method does not require heating of the printbed and extruder whereas it is required in normal thermoplastic printing. Therefore, the device consumes less power and does not require initialization time for the components to reach the desired temperature. In addition, cold printing process increases the safety and efficiency

of the system. Moreover the manufactured objects does not suffer from distortion caused by the shrinkage of material cooling down which is a common problem in most AM methods.

Because the extruded material has rather low viscosity and the material flow is controlled with syringe, an increased controllability can be reached compared to AM methods using more viscous materials. On the other hand, the low viscosity of extruded resins limits the overhanging features that can be manufactured.

It was originally thought that the manufacturing process with photopolymer would be faster than what was achieved in this study. It is crucial that built layer is solid enough to support the layers that will be extruded on top of it. Therefore, LEDs needs to be focused to the extruded resin long enough to be cured almost completely thus liming the speed of the printer.

Compared to other radiation sources, LEDs advantage is the emission of radiation of required wavelength. Therefore, LED light will cure the resin with high efficiency. The current problem of LED lights is their small power output, which will result in slow print speed. Lack of irradiation will also limit the layer thickness. Higher wavelength would allow deeper penetration depth. [1]

Future technology will provide us more efficient, higher power LEDs with lower price. As a result, we will likely see faster, cheaper and more power efficient photopolymer printers that can be used for rapid prototyping.

5. CONCLUSION

This study demonstrates that UV LED technology can be successfully applied to rapid prototyping and LM applications. The study demonstrated LED's capability to cure photopolymer. A prototype printer was built and simple objects were successfully created with it and numerous advantages compared to more common LM methods were discovered. However the achieved printing speed of the prototype printer was low due to the slow curing speed of the resin.

6. CORRESPONDING ADDRESS

Panu Kiviluoma, D.Sc. (Tech.)
Aalto University School of Engineering, Department of Engineering Design and Production
P.O. Box 14100
00076 Aalto, Finland
Phone: +358 50 433 8661
E-mail: panu.kiviluoma@aalto.fi
http://edp.aalto.fi/en/

7. REFERENCES

1. S.L. McDermott; J.E. Walsh and R.G. Howard. A comparison of the emission characteristics of uv-leds and fluorescent lamps for polymerisation applications. Optics and Laser Technology, 40(3), 2008.

2. Kim, J.S.; Kim, D-S and Lee, M-C. 3d printing method of multi piezo head using a photopolymer resin. International Conference on Control, Automation and Systems, 2007.

3. RepRapWiki. Ramps 1.4. http:// www.reprap.org/wiki/RAMPS_1.4/, 2014.

4. Tecled Lighting Co. 5050 355nm smd uv led reference. http://www.alibaba.com/ product-detail/5050-355nm-SMD-UV-LED_532109575.html, 2013.

5. LEDiL. Fca10911 nis033u-ss reference. www.ledil.fi/luopdf4.php?s=54&t=3194, 2013.

6. PhD Richard Sahara. Uv led 3 lens technology. http://www.clearstonetech.com/files/lens_array_paper_080225.pdf, 2008.

7. DSM Somos Materials. Somos ProtoGen O-XT 18420 reference.

http://www.quickparts.com/UserFiles/File/SLA_Somos_18420.pdf, 2007.

8. DSM Somos Materials. Somos WaterShed XC 11122. http://panashape.com/wp-content/uploads/2013/07/Somos-WaterShed_XC_11122_Datasheet.pdf, 2012.

8. ADDITIONAL DATA ABOUT AUTHORS

Vuorio, Jaakko, B.Sc. (Tech.)
Phone: +358 50 494 4651
E-mail: jaakko.vuorio@aalto.fi

Teivastenaho, Ville
Phone: +358 40 839 7931
E-mail: ville.teivastenaho@aalto.fi

Peltola, Jukka
Phone: +358 40 591 1278
E-mail: jukka.j.peltola@aalto.fi

Nikkilä, Vesa
Phone: +358 440 282 800
E-mail: vesa.s.nikkila@aalto.fi

Kuosmanen, Petri, D.Sc. (Tech.), Professor
Phone: +358 500 448 481
E-mail: petri.kuosmanen@aalto.fi

Partanen, Jouni, Ph. D. (Tech.), Professor
Phone: +358 50 5769 804
E-mail: jouni.partanen@aalto.fi

IV MATERIALS ENGINEERING

9th International DAAAM Baltic Conference
"INDUSTRIAL ENGINEERING -
24-26 April 2014, Tallinn, Estonia

PARTICLE SIZE AND PROPORTION INFLUENCE TO IMPACT PROPERTIES OF PARTICULATE POLYMER COMPOSITE

Aruniit, A.; Kers, J.; Krumme, A. & Peetsalu, P.

Abstract: *Current research concentrates on the impact properties of a particle reinforced polymer matrix composite material. The composite material consists of unsaturated polyester resin that is reinforced with aluminium hydroxide. Aluminium hydroxide acts as the hard phase and polyester as the binding agent. The aim of the work was to understand how the particle size and the filler material's mass fraction influence the impact resistance of the composite. Additionally was studied the effect of post-curing to the impact toughness of the matrix. The testing was done according to the ISO 179 Determination of Charpy impact properties. Smaller particle size increased the impact strength. Filler caused embrittlement of the matrix as did also post-curing.*
Key words: polyester composite, aluminium hydroxide filler, particle size, particulate reinforcement mass fraction, ISO 179 Charpy impact toughness

1. INTRODUCTION

Particulate polymer composite material consisting of unsaturated polyester resin and aluminium hydroxide powder is used in many interior design applications. It is known as engineered stone and produced in sheets or casted into shapes. The applications are culinary bench tops, sanitary ware and wall cladding.
The area of application dictates the properties. To perform well in service the material must have good impact toughness.

Fillers are used in polymers because of technical and economic reasons [1] [2] [3]. Aluminium hydroxide particles add many favourable properties to the polymer composite. It has flame retardant and smoke suppression quality. Moreover, it is non-toxic and chemically inert. Aluminium hydroxides low sorptive power makes it also economical as it has low liquid resin demand [1] [4].
Fillers reduce shrinkage of thermosetting polymers during the polymerisation process [1] [5]. This helps to avoid warpage or cracking that may occur with large moulded products. Moreover, the inclusion of mineral filler enhances the thermal conductivity of the composite and helps to bring down the exothermic temperature of the part and cool it faster [1]. This speeds up the cycle time and thus reduces cost.
Inorganic particulate fillers have much higher stiffness than polymers thus these improve the stiffness or Young's modulus of the composite [1] [6] [7].
There are also some unfavourable properties that particulate fillers add. The addition of a particulate filler reduces the elongation at brake of the polymer thus decreasing toughness or impact resistance [1]. Fracture toughness of a particle filled polymer composite depends mainly from the toughness of the matrix [8]. In composites with ductile matrix particulate filler causes brittleness [8]. Fracture toughness of ductile thermoplastics shows a significant decrease with particulate reinforcement [8] [9]. On the other hand, in composites with brittle matrix like thermosetting epoxy the brittleness is reduced with the addition of particulate

filler [2] [8] [10]. Generally, the thermosetting resins have a poor crack growth resistance compared to thermoplastics [7].

There are three properties of a particle that are considered to have the greatest effect on particulate composites properties: particle size, loading and adhesion with matrix.

There is strong evidence that particle size has direct impact on particulate composites toughness. Singh et al. [11] found that smaller particles give higher strength and higher fracture toughness at a given proportion in a thermosetting polyester. On the other hand, Radford [12] found that with a constant volume fraction of 0,295 the particle size increase improved the fracture energy of an epoxy-aluminium hydroxide particulate composite.

Particle loading is the second important factor that affects the mechanical properties of a particulate composite. The influence is varying to different properties and depends from the mass fraction of the filler. Surface hardness and flexural modulus of thermosetting polyester composite increases monotonically with increasing load of aluminium hydroxide [6]. On the other hand, fracture toughness increases till filler mass fraction of 10 – 20 % but decreases with higher loading in an epoxy composite [7]. In a thermoplastic the introduction of filler can dramatically decrease the fracture toughness compared to neat resin [7].

Third contributor to the mechanical properties of a particulate composite is the reinforcement-matrix interface adhesion [7]. Better adhesion improves the strength [7]. The adhesion is often enhanced with coupling agents. Aluminium hydroxide used in current research is treated with silane coupling agent. The effect of presence or absence of the coupling agent was not given heed to.

There is not any straightforward formula to define what particle size and mass fraction (wt.%) of the reinforcement gives optimal impact toughness to a composite material.

Besides the composition the mechanical properties of the composite depend from technological processes like elevated temperature post curing [13]. Moreover, one has to consider also other properties of the material when tuning the impact toughness to achieve a well-balanced entirety.

The composite has to have good wear and chemical resistance, surface hardness and it has to be economical to produce.

Since hardness and toughness are inversely related increased impact resistance is accompanied by reduced wear resistance [14].

A lot of research has been done on particulate composites with thermoplastic or epoxy matrix. Moreover, most of the research investigates low level filler loading of 1 – 10 %. Current research studies the particulate reinforcing of the most widely used and economic thermosetting matrix – polyester. Moreover, filler loading in the range of 50 – 65 % is studied as this would have considerable economical effect on the composites price.

The aim of the research was to find the particle size and proportion that gives good impact toughness to the composite without sacrificing other properties.

The tests were done as a completely randomized experiment with four levels of filler weight percentage (0 %, 50 %, 60 % and 65%) with ten replicates and three treatments of particle size (7 μm, 20 μm and 35 μm) with ten replicates. The specimens with different particle size had 60 wt.% of filler. The randomized test sequence is necessary to prevent the effect of unknown nuisance variables from contaminating the results [15].

2. EXPERIMENTAL

2.1 Materials

The matrix was an isophthalic acid and neopentyl glycol based unsaturated polyester resin with density of 1100 kg m^{-3}. Reinforcing aluminium hydroxide had density of 2400 kg m^{-3} and Mohs' hardness

index of 2,5 – 3,5 [4]. The aluminium hydroxide particles were pre-treated with silane.

2.2 Methods

The test specimens were fabricated with a vacuum assisted mixer. The dispersion was injected into a closed silicone mould having 12 cavities. The test specimen's dimensions were 80x10x4 mm (LxWxH). After room temperature cure the specimens were post cured 12 h at 40 °C.

The indentation hardness of the material was measured with a GYZJ 934-1 Barcol Impressor. The indentation hardness test was conducted according to ASTM D2583. The Barcol Impressor is developed for testing fabricated parts and test specimens. It is well suited for reinforced plastics. It enables quick and simple ranking of materials by surface hardness [16]. Surface hardness is a signal of percentage of cure of a polymer composite but also depends from the mass fraction and type of the filler material [13].

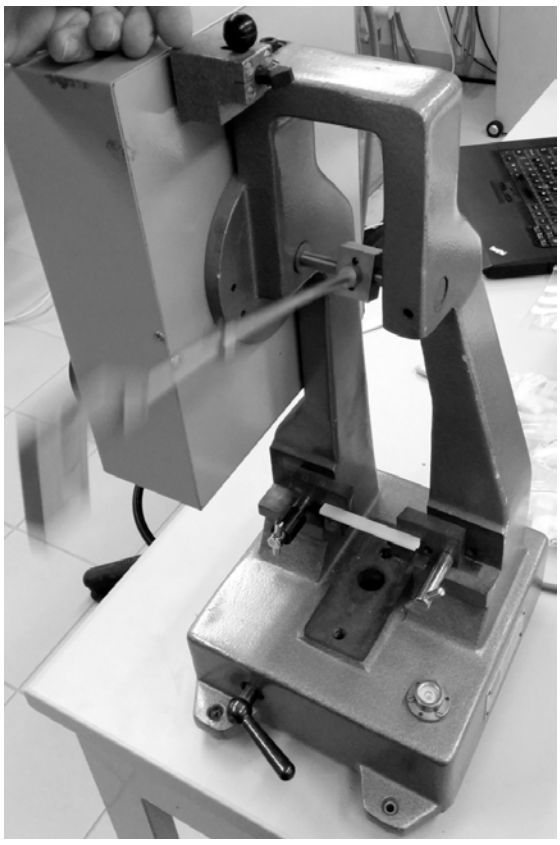

Fig. 1. Zwick/Roell 5102 Pendulum Impact Tester

Impact tests were conducted according to ISO 179-1 Plastics – Determination of Charpy impact properties [17]. The main value of this test method is the relative ranking of materials.

The tests were conducted with Zwick/Roell 5102 Pendulum Impact Tester (Fig. 1). The span between specimen supports was 40 mm. A velocity of impact of 2,92 m s^{-1} and pendulums of 0,5 J and 1 J were used.

3. RESULTS & DISCUSSION

3.1 Particle size

The first part of the research was to examine the influence of particle size to the impact properties of the composite. The results are presented on Fig. 2.

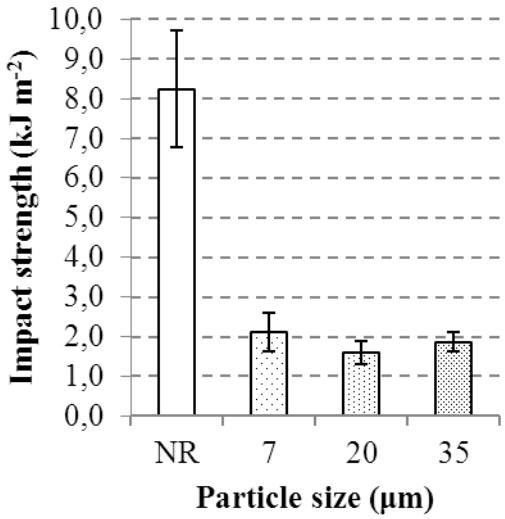

Fig. 2. Particle size influence to Charpy impact strength and comparison with neat resin (NR)

There is not a clear trend that with particle size reduction the impact strength increases. Nevertheless, composite with 7 µm particles differentiated from the rest and showed 24 % better impact strength than composite with 20 µm particles and 11 % better impact strength than composite with 35 µm particles. The 20 µm particles had 15 % lower strength than the 35 µm particles.

Smaller particles have a greater total surface area. This implies that the impact

strength increases with smaller particles through a better stress transfer between the matrix and the reinforcement. [7]
None of the reinforced test specimens could compete with neat resin (NR). The latter showed 4 times higher impact strength than the specimen reinforced with 60 wt. % of 7 μm particles. At this level of loading the properties of reinforcement dominate and cause brittleness.

3.2 Mass fraction

The second part of the study was done with 7 μm particles as these showed highest impact strength.
The impact strength peaked at 60 wt.% of filler. Further loading reduced the strength by 13 % and half-and-half mix showed 5 % lower values.
As in the first part of the research the results are incomparable to the neat resin (NR). The pure matrix is much tougher than the composite at different levels of loading as can be seen on Fig. 3.

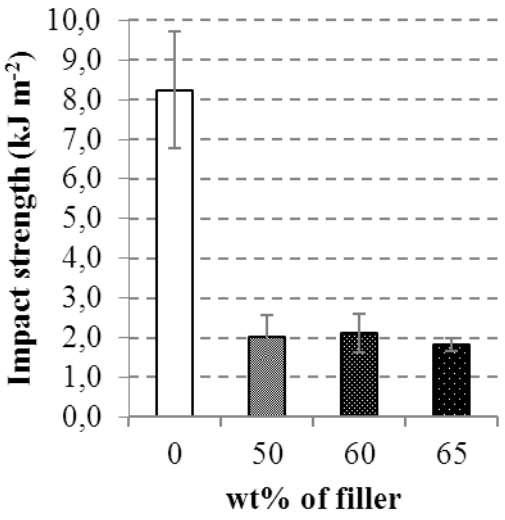

Fig. 3. Particle loading influence to Charpy impact strength

This confirms the fact that the crack growth resistance of a polymer – filler interface is considerably lower than that of pure polymer which deforms plastically and absorbs part of the impact energy. The impact strength is proportional to the rate at which the crack grows. The crack does not halve the hard particles but propagates through the relatively weak particle – matrix interface that is ruled by the adhesion forces between the two. [9] [18]

3.3 Post-curing

Thermosetting polymer composites are post cured at elevated temperature to increase the amount of cross linking to achieve better chemical and heat resistance and mechanical properties [13].
A correlation exists between the content of unpolymerised material and the mechanical and physical properties of the material. Unpolymerised material is residual styrene and phlegmatizers. The unpolymerised material has negative effect on hardness, flexural modulus and chemical resistance. [13] [19] [20]

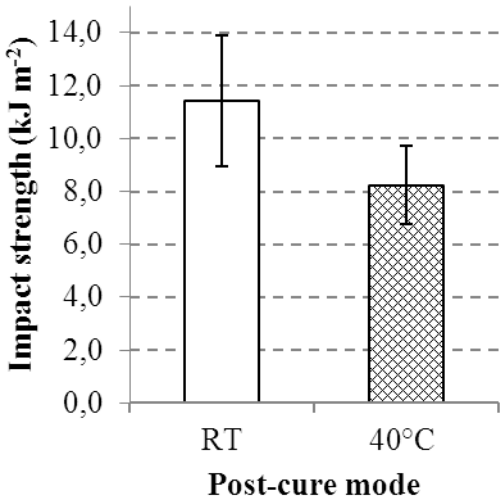

Fig. 4. Influence of post-curing (12 h @ 40 °C) to Charpy impact strength. RT – room temperature cured sample.

Fig. 4 depicts vividly how post-curing decreases toughness of the unsaturated polyester. The impact strength is 1/3 lower compared to the room temperature cured sample (RT).

3.4 Indentation hardness

Fig. 5 depicts the dilemma that is faced with highly filled particulate composites.

Some of the favourable properties increase with filler loading while others decrease. In this case higher filler loading improves indentation hardness but lowers toughness. The figure also demonstrates well the essence of a composite – filler improves a property that the matrix lacks.

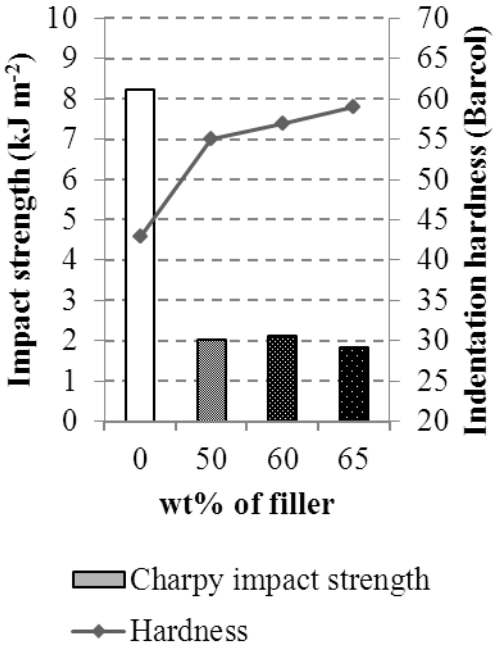

Fig. 5. Influence of filler loading to Barcol indentation hardness compared to Charpy impact strength

4. CONCLUSION

The composite with smallest particles had highest impact strength. Nevertheless, there was not a linear trend between particle size reduction and toughness increase.

The optimal matrix – reinforcement ratio from the point of strength was 40:60.

The tests demonstrated that the toughness of the particulate composite comes from the matrix and the filler makes the composite material brittle.

The brittleness is even further increased with post–curing. Post-curing is desirable when one wants to improve properties like indentation hardness, stain resistance or flexural modulus but it works concurrently with impact strength.

Since composite is a compromise between different properties the material has to be designed considering all the requirements.

Acknowledgment

The authors wish to acknowledge the support provided by TUT and European Social Fund's Doctoral Studies and Internationalisation Programme DoRa.

5. REFERENCES

1. Peters, S.T. *Handbook of Composites*. Chapman & Hall, 1998.

2. Spanoudakis, J., Young, R.J. Crack propagation in a glass particle-filled epoxy resin. *Journal of Materials Science*, 1984, **19**, 487–496.

3. Aruniit, A., Kers, J., Majak, J., Krumme, A., Tall, K. Influence of hollow glass microspheres on the mechanical and physical properties and cost of particle reinforced polymer composites. *Proceedings of the Estonian Academy of Sciences*, 2012, **61**, 160.

4. Ash, I. *Handbook of Fillers, Extenders, and Diluents*. Synapse Info Resources, Endicott, 2007.

5. Schneider, L.F.J., Cavalcante, L.M., Silikas, N. Shrinkage Stresses Generated during Resin-Composite Applications: A Review. *Journal of dental biomechanics*, 2010, **2010**,

6. Aruniit, A., Kers, J., Tall, K. Influence of filler proportion on mechanical and physical properties of particulate composite. *Agronomy Research*, 2011, **5**, 23–29.

7. Fu, S.-Y., Feng, X.-Q., Lauke, B., Mai, Y.-W. Effects of particle size, particle/matrix interface adhesion and particle loading on mechanical properties of particulate–polymer composites. *Composites Part B: Engineering*, 2008, **39**, 933–961.

8. Lauke, B., Fu, S.-Y. Aspects of fracture toughness modelling of particle filled polymer composites. *Composites Part B: Engineering*, 2013, **45**, 1569–1574.

9. Fu, S.-Y., Lauke, B. Fracture resistance of unfilled and calcite-particle-

filled ABS composites reinforced by short glass fibers (SGF) under impact load. *Composites Part A: Applied Science and Manufacturing*, 1998, **29**, 631–641.
10. Gao, J., Li, J., Benicewicz, B.C., Zhao, S., Hillborg, H., Schadler, L.S. The Mechanical Properties of Epoxy Composites Filled with Rubbery Copolymer Grafted SiO2. *Polymers*, 2012, **4**, 187–210.
11. Singh, R.P., Zhang, M., Chan, D. Toughening of a brittle thermosetting polymer : Effects of reinforcement.2002, **7**, 781–788.
12. Radford, K.C. The mechanical properties of an epoxy resin with a second phase dispersion. *Journal of Materials Science*, 1971, **6**, 1286–1291.
13. Aruniit, A., Kers, J., Krumme, A., Poltimäe, T., Tall, K. Preliminary Study of the Influence of Post Curing Parameters to the Particle Reinforced Composite ' s Mechanical and Physical Properties. *Materials Science*, 2012, **18**, 256–261.
14. Foley, A.G., Lawton, P.J., Barker, A.W., Mclees, V.A. The Use of Alumina Ceramic to Reduce Wear of Soil-engaging Components. *J. agric. Engng Res.*, 1984, **30**, 37–46.
15. Montgomery, D.C. *Design and Analysis of Experiments*. John Wiley & Sons, Inc., New York, 2011.
16. ASTM D2583-95 Indentation Hardness of Rigid Plastics by Means of Barcol Impressor. 2001.
17. ISO 179-1 Plastics - Determination of Charpy impact properties. 2010.
18. Brostow, W., Hagg Lobland, H.E. Brittleness of materials: implications for composites and a relation to impact strength. *Journal of Materials Science*, 2009, **45**, 242–250.
19. Lipovsky, K. Overcoming Vitrification of Polyester Solid Surface Resin for the Kitchen Environment using Postcure. *COMPOSITES*, 2006, 1–8.
20. *Composite Materials Handbook*. SP Systems, Isle of Wight, 1998.

6. CORRESPONDING AUTHOR

Mr. Aare Aruniit, PhD student
TUT, Department of Materials Engineering
Ehitajate tee 5, 19086, Tallinn, Estonia
Phone: +372 56 227 537
E-mail: aare.aruniit@ttu.ee

9th International DAAAM Baltic Conference
INDUSTRIAL ENGINEERING
24-26 April 2014, Tallinn, Estonia

ANALYSIS OF THE TWISTED AND FLUTED BIRCH DOWEL JOINTS

Dobris, J.; Luts, A.; Meier, P. & Kers, J.

The aim of the experiment is to find out the strength of both the twisted birch dowel and the fluted birch dowel joints. In order to gain accurate and precise results, one dowel at a time was used, and both the fluted and the twisted dowels were used in joints. In this case, it is important to ensure combining strength and durability of various components forces. Important parameters which are influencing the test results were determined during the experiments. The strength of tested joints was influenced by exact diameter of the dowel and accurate connection with dowel hole which should be drilled in the best possible fit. The methodology for analysing withdrawal and shear strength tests results was improved and the influence of external factors to the test results was minimized.
Key words: wooden dowel, glued joint birch, withdrawal strength, shear strength

1. INTRODUCTION

The aim of the experiment is to find out the strength of both the twisted birch dowel and the fluted birch dowel joints. Dowel is called a cylindrical stick, which is used to connect various pieces of wood. It's expected for forces to act upon various pieces of construction, thus, to ensure the durability of the object; certain measures have to be taken. For example, the accurate placement of the dowel hole, its size, and the overall tightness. All are necessary so that the wooden dowel would not be weakened under such force. The idea was given by the furniture company. The company is specialized in wooden chairs, especially made out of birch. Connecting different details in a chair the company uses wooden dowels. In the chair construction, it is very important that the cross rails can withstand different kinds of forces. This is why the company has taken to use twisted wooden dowels, (Fig. 1) because the technology of making twisted dowels is based on by pressing those rails.


Fig. 1. Twisted dowel [1]


Fig. 2. Fluted dowel [2]

In this case, it is important to ensure combining strength and durability of various components forces. [3]

2. MATERIALS AND METHODS

As there were no current standards for the experiment, the method for testing was worked out using IMAL IB 600 (Fig. 3) universal testing system. Firstly, test blocks (Fig. 6 and Fig. 7) were cut into desired shape to use special grips for withdrawal and shear strength tests. Test machine technical parameters are presented in **Table 1.** Test blocks were made using birch wood because this is the common wood making chair parts. When the test blocks were ready the next important step was drilling the dowel holes. [4]

Fig. 3. Test machine IMAL IB 600

Table 1: Test machine technical parameters

Minimum detail thickness	2 mm
Minimum working speed	0.001 mm/min
Maximum working speed	999 mm/min
Maximum variation	180 mm
Weighting accuracy	1/100 g
Accuracy	± 0.1 %
Engine power	1 kW
Air pressure	3 bar

2.1 Drilling holes

Several tests were made with variable length of dowels and two different diameters, 8 mm and 10 mm. To avoid spreading the glue and to get the accurate test results plastic film sheet was used (Fig. 4) between the wooden test pieces. It is important to avoid assembly of wooden test blocks surfaces with glue used in dowel joint preparation.

Fig. 4. Plastic film sheet between details

In order to connect wooden parts using wooden dowels, it is recommended that the hole in the top of the detail is supposed to be 0.6 of the dowel length and the hole in the side of the detail is 0.4 of the dowel length. A calibrated calliper gauge was used to control.

2.2 Gluing the blocks

The glue used in the tests was polyvinyl acetate based, *DORUS DD 060*, characterized as having a high viscosity and recommended specially for wooden dowels. The combination of the glue and wooden dowel help strengthen the bond between the two details, against the shear strength and withdrawal forces. The parameters for gluing are presented in **Table 2**.

Table 2: Parameters for gluing

Room temperature	18-23 °C
The room relative humidity	40-60 %
Moisture content of wood	8±2 %

In order to assembly the test pieces, the list of manufacturing conditions set by the glue *DORUS DD 060* producer was followed. [5]

The viscometer VISCO STAR L (Fig. 5) was used to determine the viscosity properties of the glue. The viscosity of the glue was 294 mPa·s.

Fig. 5. Viscometer VISCO STAR L

Table 3: Description of tools used

Tool	Description
Syringe	Used to place the glue with the same sized drops
Pencil	Used to spread the glue around in the dowel hole
Toothbrush	Used to spread the glue around the dowel
Plastic Film	Placed between the blocks in order to stop the details from gluing to each other
Hammer	Used to strike the dowel
Calliper	To measure the dowel

Cut-and-try method was used to determine suitable amount of glue to be inserted in the dowel hole (see Figs. 6 and 7). Using a dowel with a diameter of 8 mm and length of 40 mm, the determined amount of PVA glue for the hole was 0.47 g (12 drops). Using a dowel with a diameter of 10 mm and length of 40 mm, the amount for the hole was 0.8 g (18 drops).

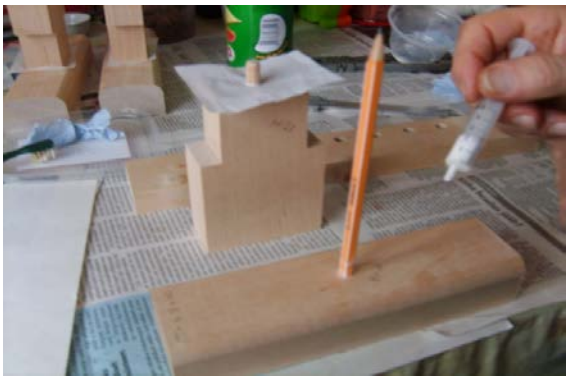
Fig. 6. Gluing of the withdrawal test block

Fig. 7. Gluing of the shear strength test block

3. RESULTS AND DISCUSSION

3.1 Testing withdrawal and shear strength of joints

For withdrawal strength determination, the resistance in Newtons was measured between fluted dowels and the wood (Fig. 8) as well as twisted dowels and the wood. The withdrawal strength for the glued surface of the dowel joint in N/mm² was calculated. Shear strength is very important to calculate for different kinds of wooden joints [6]. The test results showed the exact resistance to shear stresses and the differences of twisted and fluted dowel joints were examined (Fig. 9).

Fig. 8: Testing withdrawal strength

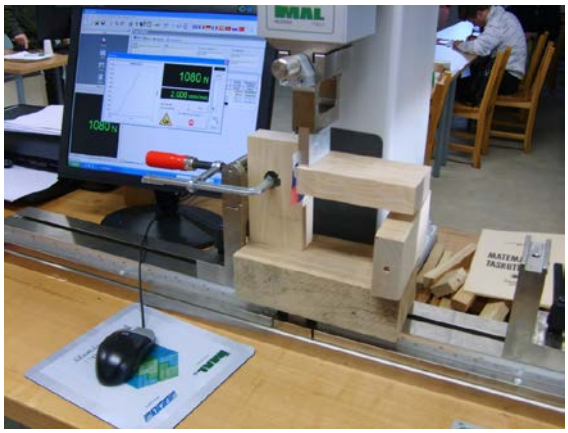

Fig. 9. Testing shear strength

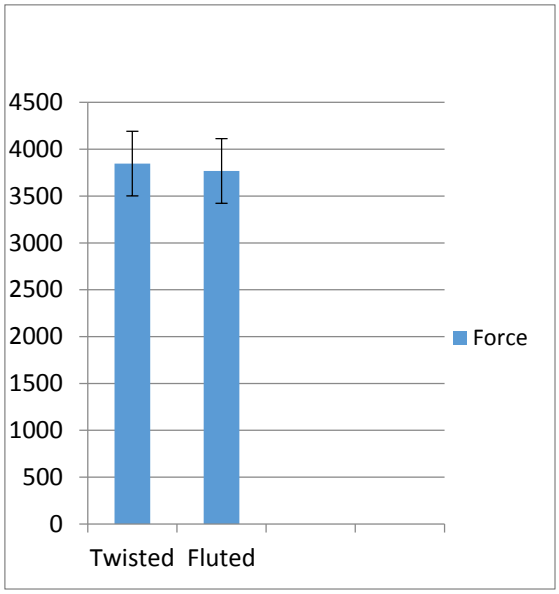

Fig. 10. Maximum load of withdrawal test

To get stronger joints:

-Increase the diameter of the dowel plugs a and use twisted dowel if the structure allows [7]

-Increase the number of dowels (3 or more) if the structure allows. This solution increases the shear stability

-Use twisted dowels [8]

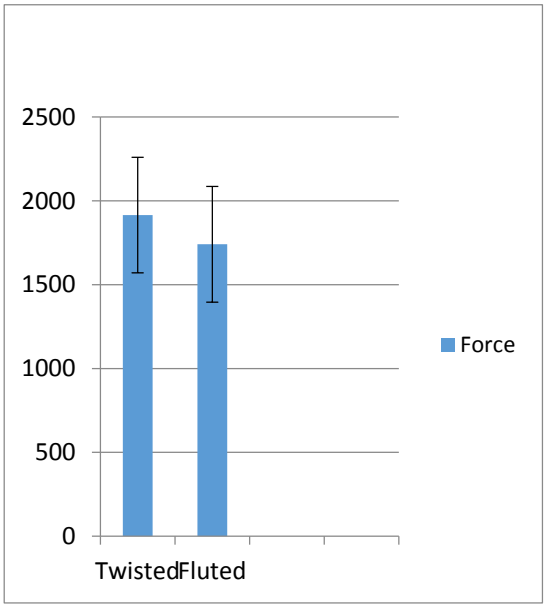

Fig. 11. Maximum load of shear strength test

4. CONCLUSION

In this work the main objective was achieved. Differences of withdrawal and shear strength of the twisted and fluted dowel joints were determined. The test method for withdrawal and shear strength test was developed. Withdrawal tests showed that the strength was higher with twisted dowels (Fig. 10). Amount of used adhesive in all joints and in all testing conditions were the same and also carry out the tests. Before the tests the hypothesis was made that, if the dowel diameter is smaller (e.g. Ø7.9 mm instead of Ø 8 mm dowel) the withdrawal strength of the joint increases due to thicker layer of glue. The test results showed, that there is no big difference. The difference between fluted and twisted dowels is caused by the technology how the dowels are made. The grooves on twisted dowel are pressed and the angle of the grooves had no influence to withdrawal strength. Shear strength test results showed that twisted dowel was stronger compared with the difference of up to 10% (Fig. 11). As in the manufacture of plug twisted dowel pressing the appropriate size, it gets more dense and therefore the resistance is greater than the fluted dowels.

Table 4: Withdrawal strength (P) and glued surface (Q) in dowel with diameter 8 mm

Test nr	Dowel type	Hole depth, By the side	On the top	P N	Q N/mm²
1	Twisted Ø 7,9 x 40 mm	21 mm	21 mm	3076	6.2
2	Twisted Ø 7,9 x 40 mm	21 mm	21 mm	3540	7.13
1	Twisted Ø 8 x 40 mm	21 mm	21 mm	3186	6.34
2	Twisted Ø 8 x 40 mm	21 mm	21 mm	3630	7.23
1	Fluted Ø 8 x 40 mm	21 mm	21 mm	3941	7.84
2	Fluted Ø 8 x 40 mm	21 mm	21 mm	3596	7.16
1	Twisted Ø 7,9 x 40 mm	16 mm	26 mm	3606	9.69
2	Twisted Ø 7,9 x 40 mm	16 mm	26 mm	2657	7.14
1	Twisted Ø 8 x 40 mm	16 mm	26 mm	2774	7.36
2	Twisted Ø 8 x 40 mm	16 mm	26 mm	3150	8.36
1	Fluted Ø 8 x 40 mm	16 mm	26 mm	4057	10.77
2	Fluted Ø 8 x 40 mm	16 mm	26 mm	3605	9.57

Table 5: Shear strength (P) and glued surface (Q) in dowel with diameter 8 mm

Test nr	Dowel type	Hole depth, By the side	On the top	P N	Q N/mm²
1	Twisted Ø 7,9 x 40 mm	21 mm	21 mm	1529	31.21
2	Twisted Ø 7,9 x 40 mm	21 mm	21 mm	1506	30.74
1	Twisted Ø 8 x 40 mm	21 mm	21 mm	1547	30.79
2	Twisted Ø 8 x 40 mm	21 mm	21 mm	1935	38.52
1	Fluted Ø 8 x 40 mm	21 mm	21 mm	1981	39.43
2	Fluted Ø 8 x 40 mm	21 mm	21 mm	1547	30.79
1	Twisted Ø 7,9 x 40 mm	16 mm	26 mm	1683	34.35
1	Twisted Ø 8 x 40 mm	16 mm	26 mm	1579	31.43
1	Fluted Ø 8 x 40 mm	16 mm	26 mm	1309	26.05

5. REFERENCES

1. Hapval homepage. [WWW] www.hapval.ee (09.03.2014)
2. Anro PT homepage. [WWW] www.anro.ee (09.03.2014)
3. Mustafa Altinok Effects of combined usage of traditional glue joint methods in box construction on strength of furniture. *Materials and Design*. 2009, **30**
4. Tering, T. (2005). Construction of timber.Väimela
5. The Institution of Structural Engineers 1998 „The strctural use of adhesives“
6. Noll, T. (2007). Pible of wooden joints. Tallinn
7. Saarman, E. (2006). Wood science. Tartu
8. Structural joints with glued-in hardwood dowels, http://eprints.lib.hokudai.ac.jp/dspace/bitstream/2115/22104/5/RILEM.pdf

6. ADDITIONAL DATA ABOUT THE AUTHORS

MSc. Jörgen Dobris
Chair of Woodworking
Department of Polymer Materials
Tallinn University of Technology
Teaduspargi 5, 12618, Tallinn, Estonia
Phone: +372 52 218 69
E-mail: jorgen.dobris@gmail.com

Andrus Luts
Head of Chair of Wood Processing Technology
Võru County Vocational Training Centre
Väimela, Võru vald
Võru maakond, 65566
Phone: +372 5554 8007
E-mail: luts@vkhk.ee

PhD. Pille Meier
Head of the Wood processing and Furniture Production Competence Centre
Võru County Vocational Training Centre
Väimela, Võru vald
Võru maakond, 65566
Phone: +372 7850821
E-mail: pille.meier@vkhk.ee

PhD. Jaan Kers
Professor
Chair of Woodworking
Department of Polymer Materials
Tallinn University of Technology
Teaduspargi 5, 12618, Tallinn, Estonia
Phone: +372 620 2909
Fax: +372 620 2903
E-mail: jaan.kers@ttu.ee

9th International DAAAM Baltic Conference
"INDUSTRIAL ENGINEERING -
24-26 April 2014, Tallinn, Estonia

FABRICATION OF ALUMINA NANOCOMPOSITES REINFORCED BY A NOVEL TYPE OF ALUMINA NANOFIBER AND GRAPHENE COATED ALUMINA NANOFIBER

Maria Drozdova, Roman Ivanov, Marina Aghayan, Irina Hussainova, Minje Dong, Miguel Angel Rodríguez

Abstract: *A novel type of alumina nanofibers (ANF) and alumina nanofibers covered with graphene (ANFC) has been used for fabrication of alumina composites with improved mechanical properties. Al_2O_3–1.5 wt. % ANF and Al_2O_3– 1,9 wt. % ANFC composites were consolidated by sinter/HIP technology at 1400 ºC in argon atmosphere under 20 bar pressure. It was demonstrated that the theoretical density of the obtained material strongly depends on the material of reinforcement. The structural homogeneity of the specimens was studied by SEM. The macro-hardness was measured by Vickers method.*
Key words: Ceramic composite; fibers; graphene; sintering

1. INTRODUCTION

Alumina (Al_2O_3) is one of the most well-known advanced ceramic materials that is widely used for its high strength, corrosion- and wear-resistance as well as good biocompatibility [1]. However, application of this material is somewhat limited by its brittleness. In comparison with traditional alumina ceramics, the reinforced alumina nanocomposites have proved to show better mechanical properties such as fracture toughness, for example [2-7]. Particularly, carbon nanofillers, such as carbon nanotubes (CNTs) and graphene platelets (GPLs), have recently attracted considerable attention as they demonstrate high tensile strength, stiffness, good flexibility and low density combined with a potential to improve electrical and thermal properties of the material. Presence of CNTs or GPLs inhibits the alumina grain growth [4-10] and can improve fracture toughness up to 53 % [9], whereas hardness remains uneffected or insignificantly decreased. Nowadays, the main challenge is producing composites with uniform distribution of reinforcing media throughout the matrix.

The objective of the present study is to produce alumina composites reinforced by Alumina Nano-Fibres (ANF) and Alumina Nano-Fibres covered with graphene (ANFC) which represent a novel type of nanostructured fillers. The effect of the reinforcements on the sintering behaviour, microstructure and mechanical properties of the ceramic composites are studied.

2. MATERIALS AND EXPERIMENTAL PROCEDURE

Commercially available α-alumina nanosized powder TAIMICRON TM-DAR with average particle size of 100 nm (TAIMEI CHEMICALS Co., Ltd., Japan) was used as a matrix material. Bundled ANFs described in detail in [11] with 50 mm in length and average single fibre diameter of 7 nm as well as ANFs covered with 20 wt.% graphene (ANFC) were used as reinforcing materials. The mixtures of Al_2O_3 powder with additions of 1,5 wt.% ANF and with 1,9 wt.% ANFC (which contains 20 wt.% of graphene deposited on the same volume of ANF) were prepared. As reference, a sample of

	Green density (%)	Density (%)	Hardness (GPa)
Al2O3	54	94	20.9 ± 1.0
Al2O3 + 1.5wt.%ANF	55	93	21.6 ± 1.8
Al2O3 + 2 wt.% ANFC	54	90	19.6 ± 1.0

Table 1. The results of density, hardness and fracture toughness for the obtained samples

Al_2O_3 without any additions was sintered. ANFs and ANFCs were ground intensively in a mortar and then mixed with alumina nanopowder. The obtained mixture was subjected to dry ball milling during 24 hours with ZrO_2 balls of 6 mm in diameter. Pure alumina nanopowder was used as a reference to study the effect of ANFs and ANFCs on the mechanical properties of alumina. The resulting mixtures as well as pure Al_2O_3 powder were uniaxially pressed in 12 mm diameter discs at 1000 kg. The pressed samples were compacted by sinter-HIP routine as following: (1) heating up to 700 ºC at heating rate of 3 ºC/min in vacuum; and then continued by (2) heating up to 1400 ºC with heating rate of 7 ºC/min under pressure of 20 bar in argon. A dwell time at the maximum temperature was 1 hour. A cooling rate was 10 ºC/min.

The density of the samples before and after sintering was measured by a conventional geometric method. The samples were polished to 3 µm with diamond paste. Structures of the sintered samples were characterised by scanning electron microscopy EVO MA 15. Hardness was measured by Vickers tester (Indentec 5030 SKV) under the load of 500 N. Room-temperature electrical properties were studied by impedance analysis meter HP 4294A.

3. RESULTS AND DISCUSSIONS

SEM micrographs of the surfaces of the sintered composites are shown in Fig.1. The microstructure of the sintered pure alumina with initial size of 100 nm was inhomogeneous with presence of irregular and abnormally grown grains as shown in Fig.1(a, c). There were plenty of large and small pores distributed all over the samples. The relative density of the sintered samples was 94% (Table 1), while the green density was 54%. As the reference sample exhibits quite low bulk density and high pore profusion, it can be concluded that sintering routine was not well ajusted and needs correction for achieving fully dense ceramics (99% or higher). Excessive porosity implies low mechanical reliability of materials and therefore, the sintered material possesses lower hardness (20.9 GPa) than it could be expected for nanostructured alumina. Hardness of about 21 GPa just slightly outperforms the hardness of alumina commonly produced from micro-sized powders (18.0-19.5 GPa) and is noticeably lower than hardness of poreless alumina obtained with SPS technique from the same type of nanopowder (26-27 GPa) [10]. Incorporation of ANFs reinforcements into alumina matrix does not result in significant changes in microstructure of the sintered composite (Fig.1d). Also, no fibres were detected in the composite. It is believed that the ANFs were broken down to the very short whiskers or particulates during milling and heating to 1400 ºC. The parts of the fibres could easily fill a space between the larger particles of commercial alumina and, therefore, lead to the slightly higher density of the pre-sintered sample (55%). This results in higher density of the sintered composite (95%). The presence of ANF also improves composite hardness to the value of 21.6 GPa.

However, for the composite containing graphene coated alumina nanofibers the microstructure differs visibly. The grain sizes are quite uniform throughout the specimen and close to the particle size of the precursor alumina particles. It can be demonstrated that there was no evident particle clustering and/or growing during

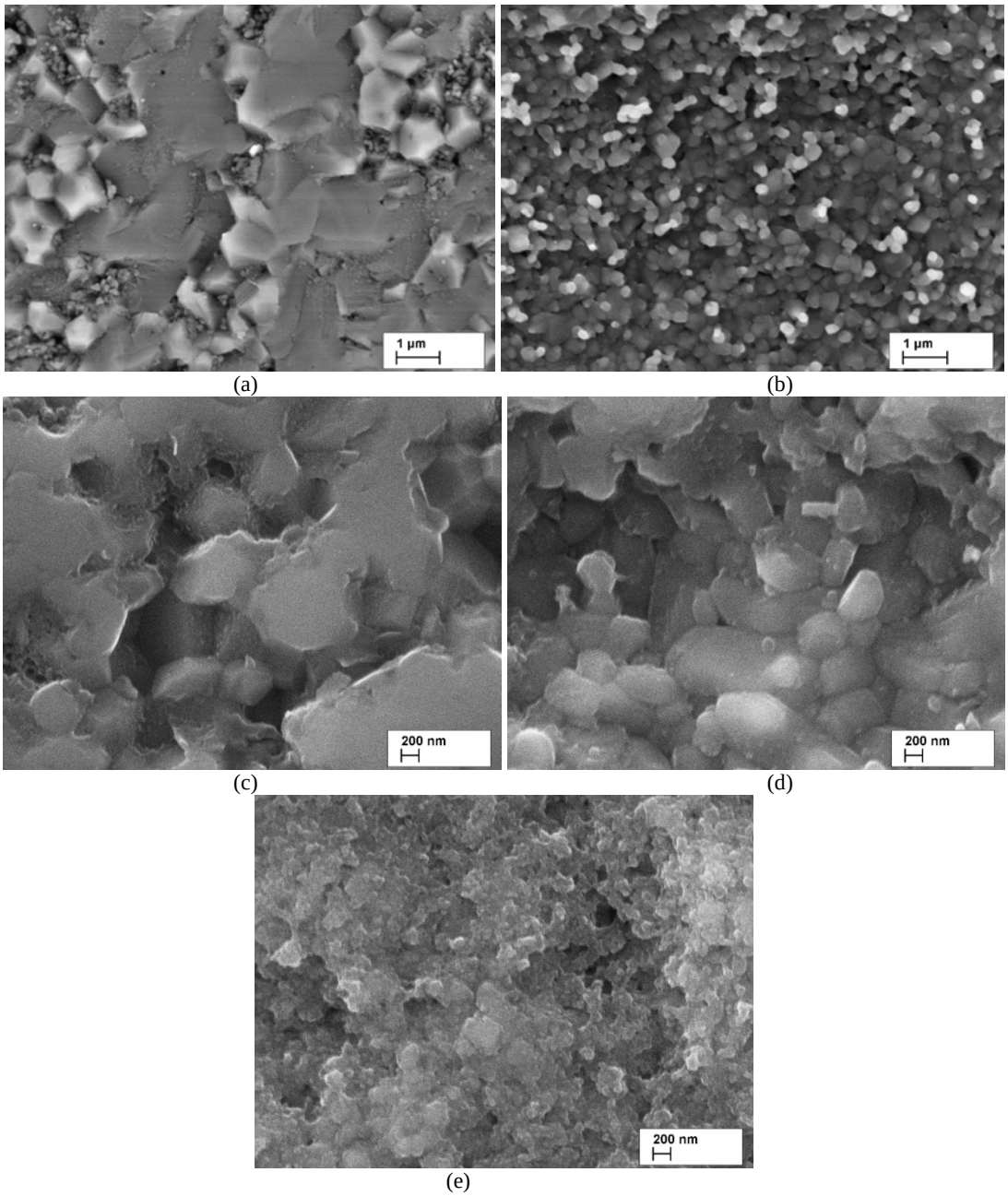

Fig. 1. SEM images of sintered monolithic Al_2O_3 sample (a, c), Al_2O_3 with ANF (d) and Al_2O_3 with ANFC (b, e)

sintering process. The grains were much finer than that of the alumina and alumina reinforced with ANF. This should be attributed to the presence of carbon (0.35%), which could be distributed along the grain boundaries and preventing rapid grain growth. Although the green density of the ANFCs containing composite was of the same level as for pure Al_2O_3, the relative density of the sintered sample decreased to 90%. With lower density the hardness of the composite dropped to 19.6 GPa as the result of higher amount of intergranular defects.

The room-temperature electrical conductivity measurements of the Al_2O_3-ANFC sample showed that the composite is dielectric. The impedance is high in all the frequency range and the phase angle is very close to -90 degrees according to dielectrical material (Fig. 2).

4. CONCLUSIONS

Addition of alumina nanofibers to alumina ceramics does not significantly affect the

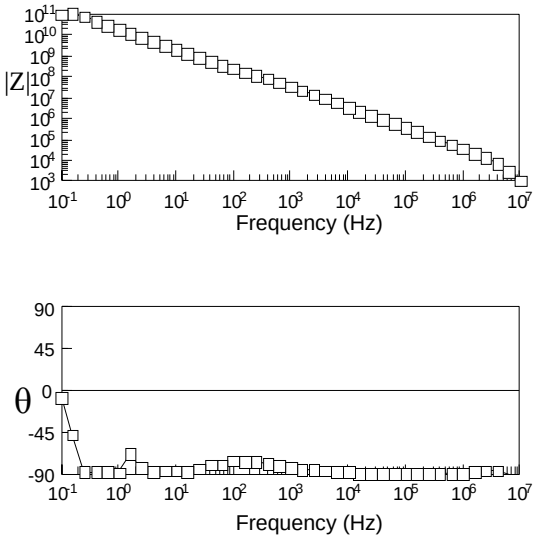

Fig. 2. Electrical properties of Al_2O_3-ANFC composite

mechanical properties and sinterability of the composites because of severe loss of fibres integrity during milling and following heat treatment. However, fibres covered by graphene significantly influence composites microstructure serving as grain growth inhibitors while decrease sinterability of alumina due to low affinity of carbon and oxides. The presence of graphene as well as a carbon polymorph in the sintered materials should be thoroughly studied in the nearest future.

5. ACKNOWLEDGEMENTS

Estonian Ministry of Education and Research (targeted project IUT 19-29) and Archimedes targeted grant AR12133 (NanoCom) is gratefully acknowledged for supporting this research.

6. REFERENCES

1. De Aza, a H., Chevalier, J., Fantozzi, G., Schehl, M. & Torrecillas, R. Crack growth resistance of alumina, zirconia and zirconia toughened alumina ceramics for joint prostheses. *Biomaterials*, 2002, **23,** 937–45.

2. Maensiri, S., Laokul, P., Klinkaewnarong, J. & Amornkitbamrung, V. Carbon nanofiber-reinforced alumina nanocomposites: Fabrication and mechanical properties. *Mater. Sci. Eng. A* , 2007, **447,** 44–50.

3. Voltsihhin, N., Rodriguez, M., Hussainova, I., Aghayan, M. Low temperature, spark plasma sintering behavior of zirconia added by a novel type of alumina nanofibers. *Ceramics International*, 2014, **40(5)**, 7235-7244

4. Liu, J., Yan, H., Reece, M. J. & Jiang, K. Toughening of zirconia/alumina composites by the addition of graphene platelets. *J. Eur. Ceram. Soc.*, 2012, **32,** 4185–4193.

5. Porwal, H. *et al.* Graphene reinforced alumina nano-composites. *Carbon N. Y.*, 2013, **64,** 359–369.

6. Liu, J., Yan, H. & Jiang, K. Mechanical properties of graphene platelet-reinforced alumina ceramic composites. *Ceram. Int.*, 2013, **39,** 6215–6221.

7. Centeno, a. *et al.* Graphene for tough and electroconductive alumina ceramics. *J. Eur. Ceram. Soc.*, 2013, **33,** 3201–3210.

8. Fan, Y. *et al.* Preparation and electrical properties of graphene nanosheet/Al2O3 composites. *Carbon N. Y.*, 2010, **48,** 1743–1749.

9. Wang, K., Wang, Y., Fan, Z., Yan, J. & Wei, T. Preparation of graphene nanosheet/alumina composites by spark plasma sintering. *Mater. Res. Bull.*, 2011, **46,** 315–318.

10. Fan, Y., Estili, M., Igarashi, G., Jiang, W. & Kawasaki, A. The effect of homogeneously dispersed few-layer graphene on microstructure and mechanical properties of Al2O3 nanocomposites. *J. Eur. Ceram. Soc.*, 2014, **34,** 443–451.

11. Aghayan, M., Hussainova, I., Gasik, M., Kutuzov, M. & Friman, M. Coupled thermal analysis of novel alumina

nanofibers with ultrahigh aspect ratio. *Thermochimica Acta*, 2013, **574,** 140–144.

6. ADDITIONAL DATA ABOUT AUTHORS

1. Maria Drozdova
Tallinn University of Technology,
Department of Materials Engineering,
Ehitajate tee 5, 19180 Tallinn, Estonia
maria.drozdova@ttu.ee

2. Marina Aghayan
Tallinn University of Technology,
Department of Materials Engineering,
Ehitajate tee 5, 19180 Tallinn, Estonia
marina.aghayan@ttu.ee

4. Roman Ivanov
Tallinn University of Technology,
Department of Materials Engineering,
Ehitajate tee 5, 19180 Tallinn, Estonia
roman.ivanov@ttu.ee

5. Minje Dong
Tallinn University of Technology,
Materials Research Center,
Ehitajate tee 5, 19180 Tallinn, Estonia
minje.dong@ttu.ee

6. Dr. Miguel Angel Rodríguez
Instituto de Cerámica y Vídrio (CSIC),
Campus Cantoblanco, 28049 Madrid,
Spain / mar@icv.csic.es

7. CORRESPONDING ADDRESS

Dr. Irina Hussainova
TUT, Department of Materials Engineering
Ehitajate tee 5, 19086 Tallinn, Estonia
Phone: 372+620 3371,
Fax: 372+620 3250,
E-mail: irhus@staff.ttu.ee

9th International DAAAM Baltic Conference
"INDUSTRIAL ENGINEERING"
24-26 April 2014, Tallinn, Estonia

THEORETICAL AND EXPERIMENTAL STUDIES OF STIFFNESS PROPERTIES OF LAMINATED ELASTOMERIC STRUCTURES

Gonca, V.; Polukoshko, S.

Abstract: *The technique of "force-displacement" stiffness characteristics calculation for thin-layer rubber-metal damping devices is presented in this work. It is proposed to take into account adhesive layers and deformation of non-elastomeric layers working under tension and compression. A variational method of linear theory of elasticity for weakly compressible materials is used for calculations. The received dependences allow explaining nonlinearity of "force - displacement" stiffness characteristics and various behavior of glued rubber-metal device under tension and compression, observed in experimental investigations.*
Key words: elastomeric, stiffness, multilayer devices, variational method

1. INTRODUCTION

Rubber and rubberlike materials (elastomers) are unique family of materials which offer many engineering advantages because of their small volume compressibility and ability to maintain large elastic deformation [1, 2,]. Reinforced elastomeric structures (laminated elastomer) consist of alternating thin layers of rubber and adhesive-bonded reinforcing layers of much more rigid material (usually metal). This allows to obtain the structures, which axial compression stiffness is in several orders greater than shear stiffness. Packages of thin-layered rubber-metal elements (further - TRME) are successfully used as bearing, joints, compensating devices, shock-absorbers etc. [1,2,3]. In practice TRME packages of different geometric shapes are used: flat, cylindrical, conical etc; number of layers may be different, at least three (Fig. 1).

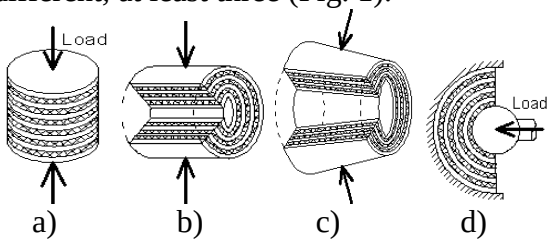

Fig. 1 Multilayer elastomeric structures examples: a) flat circular, b) cylindrical, c) conical, d) spherical

Elastomeric layer is considered as thin if its width/thickness ratio is much more than ten. For fastening of rubber layer to metal layer a rubber adhesive with vulcanization is used, during which the adhesive partially dissolves the elastomeric material on contact surface, forming bonding layer of some thickness. Mechanical properties of bonding layer may substantially differ from the mechanical properties of elastomeric layer. For very thin rubber elements thickness of elastomeric and bonding layer become comparable and the bonding layer influence on TRME stiffness becomes significant. Stiffness characteristics (relationship between imposed external forces and displacement) is very important for TRME practical applications and must be considered carefully.

In this paper analytical model taking into account effect of the adhesive layer and allowing to describe different behavior of TRME packet under compression and tension is proposed for flat rectangular TREM. Variational method of linear theory of elasticity for weakly compressible materials was used.

2. PROBLEM STATEMENT

The authors performing tension and compression tests of laminated elastomeric elements noted their features: influence of elastomeric layers weak compressibility on tension – compression stiffness properties; noticeable nonlinearity of "force - displacement" dependence even in small deformations domain (ε <10÷15%) under considerable specific loading; two-modularity of "force - displacement" dependence at tension and compression ("rigid" under compression and "soft"under tension) [5]. For optimal design and efficient operation of such TRME it is necessary to develop the analytical model taking into account the above listed features. Some authors propose to describe the effect of high specific loading by taking into account shear and bulk modules dependence on hydrostatic pressure [4,5]. Experiments show that at high specific loading these dependences are of "rigid" type for compression and "soft" for tension. The obtained results should be treat with a caution, since experiments were fulfilled with multilayered TRME packages, not with "clean" rubber elements, which do not exclude influence of the constructive nature on the results. In [5] it is shown that "force - displacement" dependence is much more nonlinear for TRME elements, produced by vulcanizing, than for "pure" rubber elements under the same high levels of specific compressive load. Processing of the experimental data, using the known "force - displacement" dependence [3] shows that disregarding of the deformation of nonelastomeric layers of thin TRME packages leads to the fact, that compressive stiffness characteristics may differ significantly from the experimental data, even at small levels of specific loading at which dependence of the share module G and volume module K on compressive loading value isn't yet observed.

Rubber adhesive using in manufacturing of laminated structures partially dissolves a contact surface of elastomeric (with initial thickness h_e) during vulcanization, forming a transitional layer of h_c thickness with mechanical characteristics different from the characteristics of the adhesive and elastomeric. Analysis of rubber adhesives composition shows that the mechanical characteristics of the transitional layer (shear modulus G_c, bulk modulus K_c and Poisson's ratio μ_c) may significantly differ from the mechanical characteristics G, K and μ of elastomeric element [5]. For bulk modules this difference may be more than an order of magnitude ($K_c << K$). Technologically, for the same curing techniques, regardless of elastomeric layer "finesse" α and β ($\alpha = a/h$, $\beta = b/h$, a, b – width and length of layer, h –its thickness), transitional layer thickness h_c will be approximately constant. If $h>>h_c$ the contribution of transitional layer work in response stiffness properties will be negligible. For very thin elastomeric layer h and h_c may be of the same order (but structurally it is always $h > h_c$) and neglecting of transitional layer deformation may lead to quantitative and qualitative errors in its design. Calculation show, that under compression influence of volume deformation may be on order of magnitude (and possibly, more) greater than form change deformation even if Poisson's ratio of elastomer $\mu \rightarrow 0{,}5$ [4,7,9]. It a fortiori will be fair for a transitional layer, as soon as $\alpha_c = a/h_c > \alpha = a/h$, $\beta_c = b/h_c > \beta = b/h >> 10$ and $K_c << K$.

In TRME packages metallic layers are generally used as intermediate non-elastomeric layer. Since compressive stiffness prorerties of metallic layers are much greater than of elastomeric layers, nonelastomeric layers deformation influence on TRME may be only if these layers are very thin (such as a metal foil). Such layers undergo only a tensile strain in plane of layer under the influence of forces transmitted through tangential stresses.

In this paper variant of analytical model allowing to describe the "rigid" response under compression and "soft" under tension

is developed. Influence of transitional and non-elastomeric layers deformation on stiffness characteristics is considered by the example of flat rectangular TRME package (Fig.2).

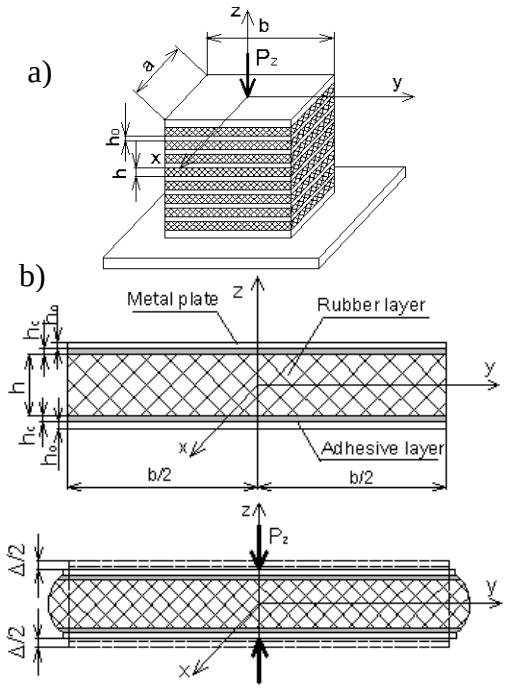

Figure 2. Scheme of designed object:
a) flat prismatic TRME packet; b) one TRME layer compressive deformation

3. ANALYTICAL SOLUTION

Problem is solved by means of variational method, using principle of a minimum of total potential energy Π:

$$\Pi = U + U_c + U_o - P\Delta_\Sigma, \qquad (1)$$

where: U - potential energy of deformation of elastomeric layer (taking into account weak compressibility of elastomeric);

U_c - potential energy of deformation of a transitional layer (taking into account the shear and volume deformations);

U_o - potential energy of deformation of thin nonelastomeric layer, which thickness allows to consider only energy of tension of this layer;

$\Delta_\Sigma=\Delta+2\Delta_c$ – one TRME element deformation, Δ –elastomeric layer deformation, Δ_c – transitional layer deformation.

$$U = G\int_V \left[\frac{1}{2}\left(u_{i,j}\, u_{j,i} + u_{i,j}\, u_{j,i} \right) + \frac{3\mu}{1+\mu}\, s u_{i,i} - \frac{9(1-2\mu)}{4(1+\mu)^2}\, s^2 \right] dV,$$

$$U = G_c\int_V \left[\frac{1}{2}\left(u^c{}_{i,j}\, u^c{}_{j,i} + u^c{}_{i,j}\, u^c{}_{j,i} \right) + \frac{3\mu_c}{1+\mu_c}\, s_c u^c{}_{i,i} - \frac{9(1-2\mu_c)}{4(1+\mu_c)^2}\, s_c{}^2 \right] dV_c,$$

$$U_o = 2(1+\mu_o)G_o \int_{V_o} \left(u^o_{x,x}{}^2 + u^o_{y,y}{}^2 + 2\mu_0 u^o_{x,x} u^o_{y,y} \right) dV_o,$$

where for elastomeric, transitional and nonelastomeric layers respectively: G, G_c, G_o – shear modules; μ, μ_c, μ_o – Poisson's ratio; s, s_c, s_o - relative hydrostatic pressure; u_i, $u^c{}_i$, $u^o{}_i$ – displacement functions; V, V_c, V_o – layers volume; i, j – coordinates x, y, z of rectangular coordinate system; on repeating subindexes summation is carried out, and the comma in subscripts indicate a partial derivative. Using functional (1) requires the mandatory fulfilment of the geometric boundary conditions and continuity conditions (joining conditions) of displacement on the borders between elastomeric, transitional and non-elastomeric layers. For one TRME element the centre of gravity is chosen as the origin of coordinates (Fig. 2b). Then we have: geometrical boundary conditions:

$$u_z(x,y,\pm 0.5h) = \mp 0.5\Delta, \qquad (2)$$
$$u^c_z(x,y,\pm 0.5(h+2h_c)) = \mp 0.5(\Delta+2\Delta_c);$$

conditions of displacement continuity on the surfaces of joining of layers:

$$u_x(x,y,\pm 0.5h) = u^c_x(x,y,\pm 0.5h);$$
$$u_y(x,y,\pm 0.5h) = u^c_y(x,y,\pm 0.5h); \qquad (3)$$
$$u_z(x,y,\pm 0.5h) = u^c_z(x,y,\pm 0.5h);$$
$$u^c_x(x,y,\pm(0.5h+h_c)) = K_{1_0}\, x;$$
$$u^c_y(x,y,\pm(0.5h+h_c)) = K_{2_0}\, y;$$

Considering the expected deformed state and boundary conditions (2), (3) and using a plane section hypothesis, functions of displacement and hydrostatic pressure is choosen for elastomeric layer:

$$u_x = C_1 x\left(4\frac{z^2}{h^2}-1\right)+K_1 x;$$

$$u_y = C_2 y\left(4\frac{z^2}{h^2}-1\right)+K_2 y; \qquad (4)$$

$$u_z = 6\Delta\left(\frac{z^3}{3h^3}-\frac{z}{4h}\right);\ s\approx C;$$

for transitional layer:

$$u_x^c = (K_{1o}-K_1)x\left(4\frac{z^2}{h^2}-1\right)\frac{1}{2\gamma+\gamma^2}+K_1 x;$$

$$u_y^c = (K_{2o}-K_2)y\left(4\frac{z^2}{h^2}-1\right)\frac{1}{2\gamma+\gamma^2}+K_2 y;$$

$$\gamma = 2\frac{h_c}{h};\ u_z^c = -4\Delta\frac{z^3}{h^3}+2B\frac{z}{h}\left(4\frac{z^2}{h^2}-1\right);$$

$$B=\frac{0.5\Delta\left((1+\gamma)^3-1\right)-\Delta_c}{(1+\gamma)\left(2\gamma+\gamma^2\right)};\ s\approx C; \qquad (5)$$

for non-elastomeric layer:

$$u_{ox} = K_{1o}x;\ u_{oy} = K_{2o}y. \qquad (6)$$

Force - displacement dependence is found from a condition of minimum of functional (1):

$$\frac{\partial\Pi\left(\Delta,\Delta_c,C,C_1,C_2,K_1,K_2,K_{1o},K_{2o}\right)}{\partial\left(\Delta,\Delta_c,C,C_1,C_2,K_1,K_2,K_{1o},K_{2o}\right)}=0.(7)$$

Influence of intermediate and non-elastomeric layers deformation on force-dependence will be noticeable only for a very thin elastomeric layers ($\alpha = a/h >>10$, $\beta = b/h >>10$). For this geometry the system of the equations (7) may be simplified, leaving in multipliers and summands only terms proportional α^2, α_c^2, β^2 and β_c^2 and the system (7) falls into two poorly connected subsystems of the equations for deformation Δ and Δ_c. definition.

For TRME package consisting of n one-type layers having identical geometry and physical and mechanical properties, "force - displacement" dependence is written:

$$\Delta_\Sigma = \Sigma(\Delta+2\Delta_c)=0.4\frac{Pn}{F}\left(\frac{hB}{G}+2\frac{h_c B_c}{G_c}\right);$$

$$D=\frac{a^2b^2}{h^2\left(a^2+b^2\right)(1+\gamma)^2};\ \gamma=\frac{2h_c}{h}; \qquad (8)$$

$$B=\frac{1+\frac{25}{48}\frac{D}{\chi}}{1+\frac{2.5D}{6+5(1-2\mu)D}};\ \chi=\frac{G_o h_o}{Gh(1-\gamma)};$$

$$B_c=\frac{1}{1+\frac{2.5D_c}{6+5(1-2\mu_c)D_c}};$$

$$D_c=\frac{a^2b^2}{h_c^2\left(a^2+b^2\right)};\quad F=ab.$$

If $h_c << h$ and $G_o h_o >> Gh$, deformation of transitional and nonelastomeric layers in TRME may be neglected. Equation for TRME displacement definition derived from (8) for very thin elastomeric layers coincides with results of work [6].

If $\alpha >> 10$ and $\beta >> 10$, elastomeric layer thickness h is commensurable with transitional layer thickness h_c and Poisson's ratio of transitional layer material is $\mu_c \approx 0{,}470\div0{,}485$ [9], displacement of transitional layer Δ_c will be defined only by its volumetric deformation, and influence of distortion strain energy may be neglected:

$$\Delta_c=\frac{Ph_c}{FK_c};\quad K_c=\frac{2(1+\mu_c)G_c}{1-2\mu_c}. \qquad (9)$$

In this case for displacement of elastomeric layer Δ from (8) we receive:

$$\Delta=\frac{0.4PhB_1}{FG};\quad B_1=\frac{1+\frac{25}{48}\frac{D_1}{\chi_1}}{1+\frac{2.5D_1}{6+5(1-2\mu)D_1}};$$

$$\chi_1=\frac{G_o h_o}{Gh};\ D_1=\frac{\alpha^2\beta^2}{\alpha^2+\beta^2}. \qquad (10)$$

Displacement of one TRME layer:

$$\Delta_\Sigma=\Delta+2\Delta_c=0.4\frac{PhB_1}{FG}+\frac{2Ph_c}{FK_c}. \qquad (11)$$

Dependences (8)÷(11) are applicable if displacement of TRME doesn't exceed 10 ÷ 15%. From formulas (9) and (10) it follows that, depending on values G/G_c and K/K_c under condition of $h > h_c$ no more than an order of magnitude, in the elastomeric layer will be small deformations, and in a transitional layer -

average deformations (Δ_c/h_c > 0,2) and formula (9) is not applicable. In works [5] it is shown that using a delta method, after simple transformations, on the basis of a formula (9) it is possible to receive dependence "force-displacement" for average deformations in a transitional layer and required dependences force displacement for glued TRME under compression Δ_Σ^{comp} and tension Δ_Σ^{tens} will be as follows:

$$\Delta_\Sigma^{comp} = \Delta + 2\Delta_c = 0.4\frac{PhB_1}{FG} + 2h_c\left(1 - e^{-\frac{P}{K_c F}}\right),$$

$$\Delta_\Sigma^{tens} = \Delta + 2\Delta_c = 0.4\frac{PhB_1}{FG} + 2h_c\left(-1 + e^{\frac{P}{K_c F}}\right). \quad (12)$$

The results of thin TRME compression experiments (up to 10%÷15%), when compression load per unit surface can reach 200 MPa, show that the graphics "force - displacement" are essentially nonlinear; it is not possible to describe by the relation (8) ÷ (11) obtained for small deformation [3,4]. In experimental studies it is shown that shear and bulk modulus of elastomeric depend on intensity of the specific loading if $s = P/F$ is more than 5 MPa [6, 8]. For taking into account of load intensity influence on "force-displacement" dependence it is proposed in [5] as an approximate solution to take the linear solution (11)÷(13), in which instead of modules G and K to substitute the values $G(s)$ and $K(s)$ which correspond to the average hydrostatic pressure values $s\ (x, y, z)$. For thin flat elastomeric layers it can be assumed with sufficient accuracy that $s \approx P/F$ (F – the area of plane layer). This approximation will be the better, the less form changing energy of a thin elastomeric layer specific contribution into "force-displacement" dependence. This approach allows calculating of $G(s)$ and $K(s)$ from the volumetric tension – compression experiments. Due to lack of experimental data it is proposed in [5] at first approximation to assume that the dependence of $G(s)$ and $K(s)$ has the same type:

$$G(s)/G \approx K(s)/K = 1 + \varphi \cdot s, \quad (13)$$

where factor φ is defined from experiment on pure volumetric compression.

4. NUMERICAL ANALYSIS AND EXPERIMENTAL RESULTS

The results of compression tests of rectangular TRME packages of different dimensions, commonly used in technical applications, are discuss in this chapter. Experimental investigation was performed at the Moscow Institute of Thermal Technology for TRME devices: PRM-60 (a=b=60mm, h=0.28mm), PRM-35 (a=b=35mm, h=0.1mm) and PRM-210 (a=b=35mm, h=0.44mm). For all structures metal layer thickness is equal h_o=0.1 mm, G=0.45 MPa, G_o=8.7·10^4 MPa, μ = 0.4981.Test pressure reached 200 MPa, which confirms the high efficiency of such elements. Fig. 3 shows the relative deformation of a single layer. As can be seen from the graphs, the relative deformation of elastomeric layers do not exceed 15%, i.e. may be considered as small, and force - deformation dependence may be calculated according to formulas (8) or (11).

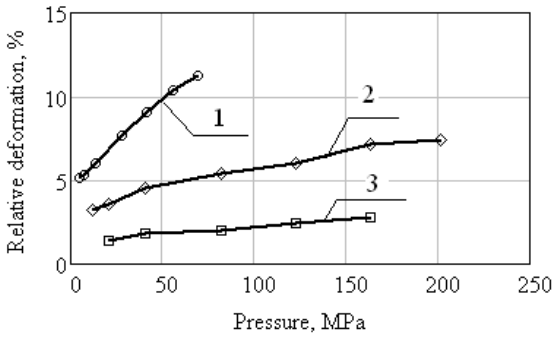

Fig. 3 Plots of dependence of relative deformation on pressure: 1- PRM-60, 2- PRM-35, 3- PRM-210

Since thickness of elastomeric layer is small, the influence of the transition layer must be taken into consideration; as soon as pressure is more than 5 MPa, the physical non-linearity of the elastomeric material also isn't be neglected.

In Fig. 4 force-displacement characteristics for PRM-60 element is presented. Calculations were performed using the formulas (11) and (13).Because of accurate experimental data lack, for calculation the shear and bulk modules in accordance with equation (13) factor φ = 0,04 is taken as constant [9,10]. Total elastic layer and glue bonded layers thickness is 0.28mm, it is assumed that thickness of glue bonding layer is h_c = 0.003 mm, then h = 0.28- $2h_c$ = 0.22 mm, G_c = 8 MPa, μ_c = 0.475.

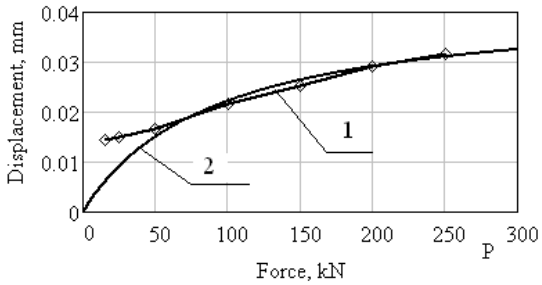

Fig. 4 Plot of PRM-60 force –displacement dependence: 1- experimental data,
2- analytical curve

Analytical calculation with accounting of adhesive layer deformation and materials nonlinearity show good agreement with experiment.

5. CONCLUSION

The improved analytical model of flat shape TRME is developed in this work based on variational principle of theory of elasticity for weakly compressible materials. The developed model and calculation method allows to take into account all the structural features of such elements (collaboration of elastomeric, transitional adhesive and rigid metal layers, physical nonlinearity of elastomeric material). In accordance with model "force-displacement" dependence is constructed, which is a necessary stiffness characteristic for optimal design of TRME products for all technical applications. This methodology permits to get a good results, the validity of the model is confirmed by the coincidence of calculation results with experimental data of other researchers.

6. REFERENCES

1. Frolov, N. N., Moldovanov, S. J. and Lozovoy, S. B. *Mechanics of thin rubber elements, monograph*. Kuban StateTechnological University, Jug, Krasnodar, 2011, (in Russian).
2. Gent, A. N. *Engineering with Rubber:How to Design Rubber Components.* CarlHanser Verlag, Munich, 2001.
3. Gusyatinskaya, N. S. *Application of Thin Layer Rubber-Metal Elements in Machine-Tools and Other Engines*. Mashinostroenie, Moscow, 1978. (in Russian).
4. Leykand, N. A., Lavendel, E. E., Lvov S. V. Experimental Research of Volume
Change of Rubber under Compression and Tension.In *Problems of Dynamics and Strength*, Riga, 1981, **38**, 49-54.
5. Dimnikov, S. I. *Design of Rubber Elements of Structures*. Zinatne, Riga, 1991, (in Russian).
6. Kardashov, D. A. *Synthetic glues*. Chemistry, Moscow, 1982, (in Russian).
7. Gonca, V. F. Influence of Weak Compressibility on Solution of Theory of Elasticity Problems for Incompressible
Material. In *Problems of Dynamics and Strength*, Riga, 1970, **20**, 185-189.
8. Wood, L. A. Values of Physical Constants of Different Rubbers. In *Smith. Phys. Tables*, 9-th rev.ed. Washington, 1956.
9. Leykand, N. A., Lavendel E.E.and Hrichikova, V. A. Calculation of Compression Rigidity of Thinlayer Rubber-Metal Elements. In *Problems of Dynamics and Strength*, Riga,1981, **38**, 57-63.
10. Dechwayukul, C., Thongruang, W. *Compressive modulus of adhesive bonded rubber block.* Songklanakarin J. Sci. Technol., 2008, 30, (**2**), 221-225. http://www.sjst.psu.ac.th

CORRESPONDING AUTHOR:
Svetlana Polukoshko
E-mail: pol.svet@inbo

9th International DAAAM Baltic Conference
INDUSTRIAL ENGINEERING
24-26 April 2014, Tallinn, Estonia

GRAPHENE COATED ALUMINA NANOFIBERS AS ZIRCONIA REINFORCEMENT

Roman Ivanov, Irina Hussainova, Marina Aghayan, Mihhail Petrov

Abstract: *Effect of alumina nanofibers covered with graphene (ANF-C) on zirconia sinterability and properties was studied in the present work. The nanofibres of aspect ratio of 10^7 were covered with several nanolayers of graphene by thermal chemical vapor deposition technique and were used as reinforcements in zirconia matrix. ANF-Cs were shown to be the promising reinforcements in ceramic matrix.*
Key words: Nanofibers; zirconia; sintering; microstructure; graphene

1. INTRODUCTION

Zirconium dioxide ceramics are one of the most known and widely used ceramics. Alumina toughened zirconia is a composite that combines the characteristics of zirconium and alumina to create a versatile material with an array of applications. Engineering ceramics such as Al_2O_3 and ZrO_2 usually have high stiffness, excellent thermostability and relatively low density, but extreme brittle nature restricted their structural applications [1,2]. Fibres are most often studied as the reinforcing additives for increasing fracture toughness and turning dielectric materials to electrically conductive ones. Nanofibers possess high-surface-to-volume ratio leading to activation in interactions between the fibers and targeted substrates. Therefore exploitation of nanofibers could be a promising approach for a wide range of advanced applications. Recently developed technology of controlled liquid phase oxidation of aluminum for manufacturing of the alumina nano-fibers (ANF) [8] with extremely high aspect ratio of more than 10^7 and fiber diameter ranged from 5 to 50 nm gives a possibility to develop new types of ceramic-based products with enhanced mechanical properties and excellent sinterability. The SEM image of the alumina nano-fibers bundle is shown in Fig. 1.

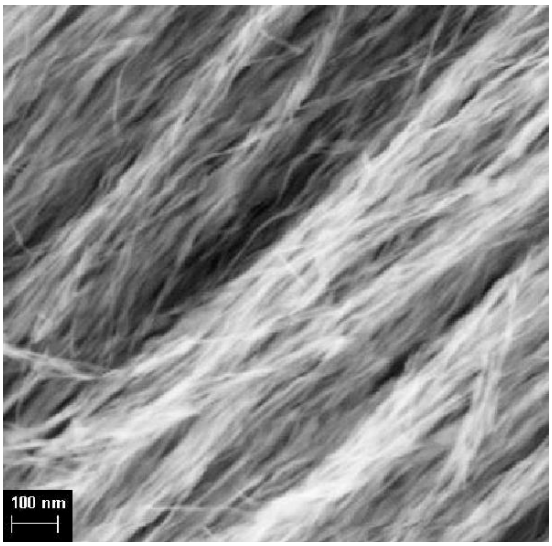

Fig.1. SEM image of uncoated ANFs

Because of graphene's exceptional thermal, mechanical, and electronic properties, it stands out as the most promising candidate to be a major filling agent for composite applications [3]. Recently, researchers have focused on the carbon nanomaterials, in particular carbon nanotubes (CNT) and graphene [3-6] to produce tough and electro-conductive ceramic based composites. It is well recognized that main difficulty in producing such kind of materials is inhomogeneous dispersion of CNTs or graphene in the ceramic matrix. Carbon structures are well known for poor

solubilization, which leads to phase segregation in the composite owing to the van der Waals attractive force. Agglomeration has a negative effect on the physical and mechanical properties of the final product [7]. Therefore, uniform distribution within the matrix is essential structural requirements for the hard and tough fibers reinforced composites.

In the present work, a technique for growing few layers of graphene films on the surface of γ-alumina nanofibers with the help of chemical vapour deposition (CVD) was developed and an attempt to produce zirconia reinforced with ANF-C is performed.

2. EXPERIMENTAL DETAILS

2.1. Materials and processing

The nanofibers of γ-alumina with diameters of 7 nm and specific surface area 155 m^2g^{-1} (BET method, [8]) represent well aligned bundles of several thousand fibers as shown in Fig. 1. To cover ANF by graphene, a thermal hot wall chemical vapour deposition technique was used. CVD is a technique of thin solid film deposition on substrates from the vapour species through chemical reactions. A principle scheme of the laboratory set-up is sketched in Fig. 2. It consists of a custom made tube furnace with working maximum temperature of 1200 °C and a quartz tube with wall thickness of 2 mm.

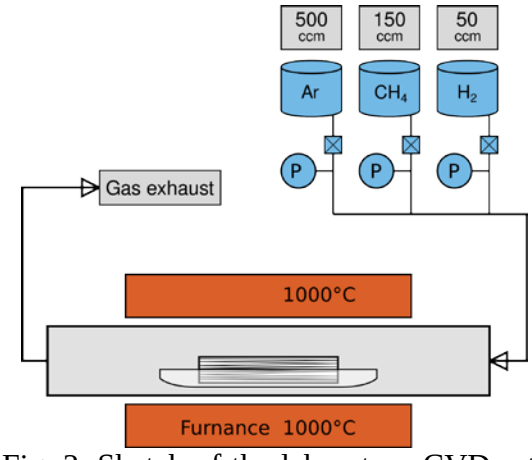

Fig. 2. Sketch of the laboratory CVD set-up.

The alumina bundles contain some amount of chemically bounded water and/or physically adsorbed water. To avoid the influence of admixtures and to reach the precise control of the carbon weight, samples have been annealed at the air atmosphere under normal pressure and temperature of 1000 °C for 3 minutes. The total mass loss for the specimen during heat treatment was about 3-7 % of weight depending on conditions of preliminary storage. For graphene growth, the ANFs bundle was loaded into a home-made CVD reactor with argon inert atmosphere in a chamber. As a catalyst, ferrocene ($C_{10}H_{10}Fe$, Aldrich) was evaporated at a temperature of 300 °C in argon atmosphere and transferred into the sample as Fe nanoparticles. Mix of hydrogen (H_2) and methane (CH_4) gases were introduced into the flow at 50 sccm and 150 sccm, respectively, and the CVD chamber was heated to 1000 °C. The process of graphene growth has been performed for 40 min. The covered alumina fibers were cooled down for 5 min in argon flow at room temperature. The deposition parameters control was carried out by varying of the ratio between a carbon source (methane) and a carrier gas agent preventing of the amorphous carbon formation (hydrogen).

Then 1g of graphene covered ANF (ANF-C) has been dispersed in 100 ml of deionized water by stick ultrasound (Hielscher Ultrasonic Homogenizer UP200Ht) for 5 min at 100 watt and under a pulse mode of 3 sec work and 1 sec pause. The obtained sol was mixed in different amount of partially stabilized zirconia (PSZ) nanosized powder (grain size of about 25 nm; produced by TOSOH, Japan) and ANF-C using magnetic stirrer. The percentage of the added ANF-C varies from 5 up to 20 %. The mixture has been vigorously stirred (1200 rpm) for 10 minutes and the obtained slurry was dried in a preheated furnace at 600 °C. After 15 min of heat treatment in the furnace, the dried mass was grinded, uniaxially pressed

at 1000 kg and sintered with the help of sinter/HIP routine as following: heating from room temperature to 600 °C with heating rate of 5 °C/min in vacuum that is followed by heating in argon (P=20 bar) up to 1450 °C with heating rate of 7 °C/min and dwell time of 1 hour.
Pure partially stabilized zirconia was sintered at the identical conditions as a reference material.

2.2. Characterization

The morphology of the graphene covered nanofibers after CVD treatment was examined by high-resolution transmission electron microscopy (HRTEM, JEOL 2200-S, Japan) with lattice resolution of 0.1 nm. Microstructural analysis of the powders and sintered composites was performed by scanning electron microscopy (SEM Zeiss EVO MA 15, Germany). To determine the degree structural perfection of sp^2 carbon and the presence of single-walled carbon nanotubes Raman spectroscopy was used. The Raman spectroscopy measurements were carried out using a Horiba Jobin Yvon LabRAM 300 spectrometer equipped with a 633 nm laser.
The sintered density was measured by the Archimedes technique using water as the immersion medium.
Hardness measurements were conducted according to EN ISO 14577 on a ZWICK tester (ZWICK, Ulm, Germany) applying an indentation load of 10 kg. The Vickers hardness value for each composition was taken as the average of 7 indents [15].

3. RESULTS AND DISCUSSION

The TEM image of the alumina nanofibers covered by several layers of graphene is presented in Fig. 3. It was shown that the carbon formed on the surface of the nanofiber is rolled over the fibers with some admixture of the opened graphene layers from one to several tens of atomic layers. The yield of graphene-like product was found to be linear at the certain temperature.

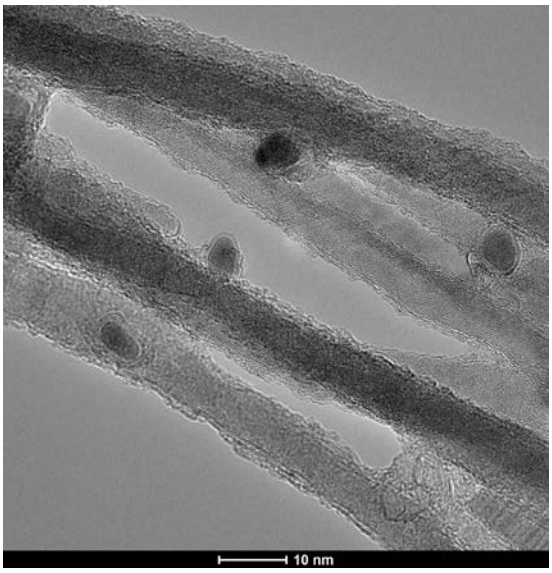

Fig. 3. TEM micrograph of ANFs covered by graphene and Fe nanoparticles.

Raman spectroscopy is a high-resolution tool for obtaining structural and electronic information about carbon-based structures. Raman techniques are particularly useful for graphene [9] because the absence of a band gap makes all wavelengths of incident radiation resonant, thus the Raman spectrum contains information about both atomic structure and electronic properties [10]. The Raman spectra of the specimen is presented in Fig. 4. The two most intense features are the G peak at 1580 cm^{-1}; D peak at around 1350 cm^{-1} and a 2D (or G') band at about 2650 cm^{-1}. The D peak is related to the breathing modes of the six atom rings and requires a defect for its activation. The G band, related to the C–C bond stretching, is the main Raman signature for all sp^2 carbons or graphene [10]. The 2D band depends on the number of graphene layers. The ratio of the G and 2D peaks intensity pointed to existence of several graphene layers deposited onto the surface of nanofibers. Carbon in such state may represent an intermediate state between graphene and graphite or, by the other words, multi-layered graphene with layers number between 5 and 10.

The D band intensity can be used to quantify disorder [10]. Significant increase in D peak' intensity at 1320 cm^{-1} suggests a large amount of edges or damages in the graphene sheets. It is worth mentioning that the very similar Raman spectra has been obtained for graphene irradiated by He^{+} ions at 30 kV and dose more than $1{,}3 \cdot 10^{14}$ ions/cm^2 [11] and damaged graphene [12,13]. Therefore, the deposition of the small and differently oriented sheets of graphene on ANF can be concluded. In all probability, this coating is non-uniform in thickness and assembled by 2 – 5 layers. Size of the sheets is comparable with dimension of ANF, i.e. some nanometers. In general, the structure is very similar to the structure of papier-mâché.

In principal, with the help of the proposed method, there is a possibility to enlarge the graphene sheets size and wrap the alumina substrate by the single layer of graphene, i.e. enclose the fiber inside a carbon nanotube.

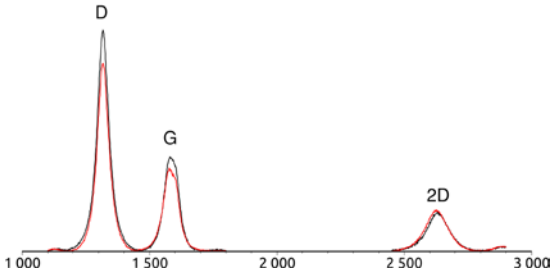

Fig.4. Raman spectroscopy of the ANF-C

The powder blend after mixing is shown on SEM image in Fig. 5. The image evidences the homogeneous distribution of the ANF-Cs throughout zirconia agglomerates.

The micrographs of the produced composites are shown in Fig. 6. The SEM images indicate the presence of rounded inclusions of carbonised species in the zirconia matrix. Dispersion of the carbonised alumina clusters is uniform throughout the composites.

As it is confirmed by TGA analysis [7], the transformation of γ-alumina into α-alumina polymorph at sintering temperature results in loss of structural integrity of the fibers and aggregation of the particles into fine clusters with average diameter of 0.5 μm.

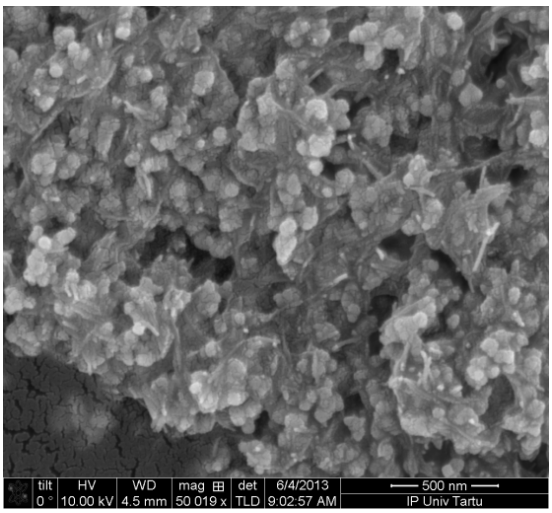

Fig.5. SEM micrograph of the blend of zirconia with 5 wt% ANF-Cs.

In Table 1 the basic properties such as the density, Vickers hardness and indentation toughness are presented for the zirconia and for zirconia reinforced with ANF-C. The density of the composite materials are lower than that is for zirconia. Increasing the amount of ANF-C, the density of the composites drastically decreases. The hardness of all of the composites is significantly lower as compared to the hardness of the monolithic material. Adding even small amount of ANF-C (5 %), the hardness of the composite decreases from 900 to 657. Moreover, the hardness sharply decreases from 605 to 159 when the amount of ANF-C increases from 10 % to 20 %. The indentation toughness also decreased after addition of ANF-C to the zirconia. The results of the present investigation are in a very good agreement with the results of Dusza et al. [4] and Sun et al. [14]. Sun et al. [5] studied the mechanical and fracture behaviour of MWCNT/3Y-TZP composites containing 0.1–1.0 wt.% MWCNTs and SWCNTs prepared by SPS. They found that the addition of CNTs had a negative influence on the hardness of the composites and no

influence (at 0.5 wt.%) or negative influence on the fracture toughness.

Composition	PSZ	A	B	C
% of ANF-C	0	5	10	20
Relative density	94	91	87	73
Hardness	900 ±12	657 ±20	605 ±42	-
Fracture toughness	5.0 ±0.7	4.7 ±2.4	4.4 ±0.7	-

Table 1. Properties of the composites.

According to them, the CNTs often agglomerate at the ZrO_2 boundaries, and the weak bonding between the CNTs and zirconia are the reason why the reinforcing effect of the CNTs is limited [6].
As regards the mechanical properties, our results show that even the use ANF-C that can intervene in zirconia particles relatively homogeneously is not effective in toughening the zirconia ceramic matrix. The reason for the relatively low indentation fracture toughness is probably the high agglomeration of ANF-C and low density/high porosity. More reliable technique has to be used for the measurement of the fracture toughness on fully dense composites to obtain information concerning the true effect of the ANF-C on the fracture toughness.

4. CONCLUSIONS

CVD technique developed in the present study allows deposition of the multi-layered graphene coating onto the surface of alumina nanofibers.
Thoroughly milled with matrix powder, the ANF-Cs can be uniformly distributed throughout the bulk specimen. Milled nanofibers of a large aspect ratio turn into the state of whiskers.
Alumina whiskers covered by graphene can be used as a promising reinforcement in ceramic composite materials in the case of perfectly designed manufacturing procedure.

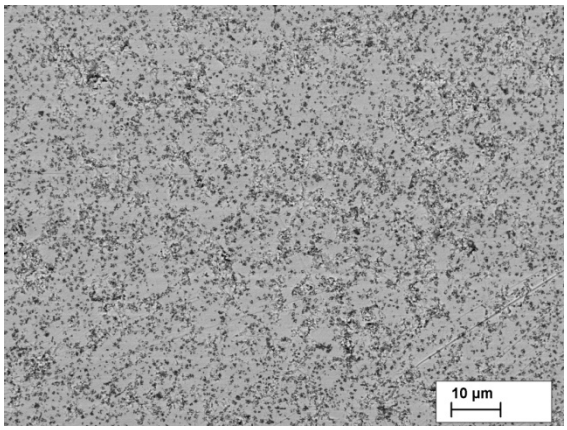

a

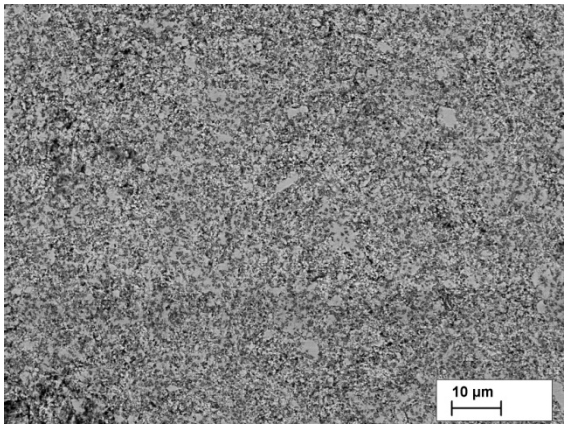

b

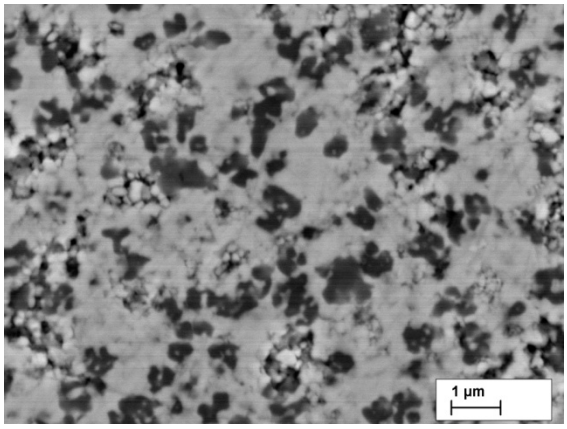

c

Fig. 6. SEM images of the PSZ - ANF-C composites with (a) 5 wt% of graphene covered fibers; (b) 20 wt% of graphene covered fibers; and (c) image of 10 wt% reinforced composite in higher magnification.

5. ACKNOWLEDGEMENTS

Estonian Ministry of Education and Research (targeted project IUT 19-29) and Archimedes targeted grant AR12133 (NanoCom) is gratefully acknowledged for supporting this research. The authors would like to thank Mr. M. Dong for the help with SEM imaging.

6. REFERENCES

1. A.H. De Azaa, J. Chevaliera, G. Fantozzia, M. Schehlb, R. Torrecillasb, Crack growth resistance of alumina, zirconia and zirconia toughened alumina ceramics for joint prostheses, *Biomater.*, 2002, **23**, 937–945.
2. O. Vasylkiv, Y. Sakka, V.V. Skorokhod, Low-Temperature Processing and Mechanical Properties of Zirconia and Zirconia–Alumina Nanoceramics, *J. Am. Ceram. Soc.*, 2003, **86**, 299–304.
3. T. Yang, X. Guo, Q. Kong, R. Yang, Q. Li, K. Jiao, Comparative studies on zirconia and graphene composites obtained by one-step and stepwise electrodeposition for deoxyribonucleicacid sensing, *Anal. Chim. Acta*, 2013, **786**, 29– 33.
4. J. Dusza, G. Blugan, J. Morgiel, J. Kuebler, F. Inam, T. Peijs, M.J. Reece, V. Puchy, Hot pressed and spark plasma sintered zirconia/carbon nanofiber composites, *J. Eur. Ceram. Soc.*, 2009, **29**, 3177–3184.
5. J. Liu, H. Yan, M.J. Reece, K. Jiang, Toughening of zirconia/alumina composites by the addition of graphene platelets, *J. Eur. Ceram. Soc.*, 2012, **32**, 4185–4193.
6. A. Duszova´, J. Dusza, K. Toma´sˇek, J. Morgiel, G. Blugand and J. Kuebler, Zirconia/carbon nanofiber composite, *Scr. Mater.*, 2008, **58**, 520–523
7. N. Voltsihhin, M. Rodríguez, I. Hussainova, M. Aghayan, Low temperature, spark plasma sintering behavior of zirconia added by a novel type of alumina nanofibers, *Ceram. Int.*, 2014, **40**, 7235–7244.
8. M. Aghayan, I. Hussainova, M. Gasik, M. Kutuzov, M. Friman, Coupled thermal analysis of novel alumina nanofibers with ultrahigh aspect ratio, *Thermochim. Acta*, 2013, **574**, 140–144.
9. M. Hulman. *Graphene: Properties, Preparation, Characterisation and Devices*, Woodhead Publishing Limited, Cambridge, 2014.
10. A.C. Ferrari and D.M. Basko, Raman spectroscopy as a versatile tool for studying the properties of graphene. *Nat. Nanotechnol.*, 2013, **8**, 235- 246.
11. S. Hang, Z. Moktadir, H. Mizuta, Raman study of damage extent in graphene nanostructures carved by high energy helium ion beam, *Carbon*, 2014, **72**, 233–241.
12. A. Jorio, Raman Spectroscopy in Graphene-Based Systems: Prototypes for Nanoscience and Nanometrology, *ISRN Nanotech.*, 2012.
13. S.D. Costaa, A. Righia, C. Fantinia, etc. Resonant Raman spectroscopy of graphene grown on copper substrates, *Solid State Commun.*, 2012, **152**, 1317–1320.
14. J. Sun, L. Gao, M. Iwasa, T. Nakayama, K. Niihara, Failure investigation of carbon nanotube/3Y-TZP nanocomposites, *Ceram. Int.*, 2005, **31**, 1131–1134.
15. I. Hussainova, M. Antonov, N. Voltsihhin, Assessment of zirconia doped hardmetals as tribomaterials. *Wear*, 2011, **271**, 1909–1915.

7. CORRESPONDING ADDRESS

Dr. Irina Hussainova
TUT, Department of Materials Engineering
Ehitajate tee 5, 19086 Tallinn, Estonia
Phone: 372+620 3371,
Fax: 372+620 3250,
E-mail: irhus@staff.ttu.ee

9th International DAAAM Baltic Conference
"INDUSTRIAL ENGINEERING"
24-26 April 2014, Tallinn, Estonia

MICROMECHANICAL PROPERTIES AND ELECTRICAL CONDUCTIVITY OF Cu AND Cu-0.7wt% Cr ALLOY

Kommel, L. Pardis, N. & Kimmari, E.

Abstract: *Microstructure, electrical conductivity and micromechanical properties of industrial Cu and Cu-0.7wt%Cr alloy after equal channel angular pressing, hard cyclic viscoplastic deformation and followed ageing treatment were studied. The tensile strength of 430 MPa and hardness of 195HV0.05 were arrived. The Young modulus was increased to 125 GPa and the maximal electrical conductivity for Cu was achieved 103% IACS after hard cyclic viscoplastic deformation and 94.5% IACS for Cu-0.7wt% Cr alloy after ageing at 450 °C for 1 h. The Cu-0.7% Cr alloy have high electrical conductivity at operation temperatures from 260 °C to 550 °C while the pure ultrafine grained Cu lost hardness, wear resistance and conductivity at 170 °C, respectively.*

Key words: Ultrafine grained microstructure, Electrical conductivity, Micromechanical properties, Young modulus, Copper.

1. INTRODUCTION

By using of severe plastic deformation (SPD) techniques like equal channel angular pressing (ECAP), parallel channel angular pressing (PCAP) or high pressure torsion (HPT) is possible to change the mechanical properties and microstructure of plastically deformable metals and alloys [1-3]. During the past two decades the microstructure, mechanical and physical properties stability of bulk ultrafine grained (UFG) and nanocrystalline (NC) materials are studied in large amount of papers [1-6]. The fields for further development related to UFG Cu and Cu-base alloys span a wide range of applications [7-9] in the different industries. Nevertheless, it is clear that for electrical conduction the Cu-based alloys with high electrical conduction properties, suitable high wear resistance (WR) and low coefficient of friction (COF) at increased temperatures will be used [10]. To date, the tribological properties of UFG Cu [11, 12] have been studied. Unfortunately, the results in [10-12] were inconsistent because the wear tests were conducted using different methods and as result the properties are not comparable. The Cu-Cr investigations are described alloys hardening by annealing and softening by deformation is studied [13-15]. In these articles also the different mechanisms of hardening via vacancy-assisted deformation are presented. The goal of this investigation is to study the mechanisms of UFG or NC microstructures, mechanical, physical and tribological properties forming in pure Cu and Cu-0.7wt% Cr alloy during ECAP and PCAP followed HCV deformation [16] and ageing treatment. In addition, we examine by tension, nanoindentation [17, 18] and wear testing the micromechanical properties in the sample body and/or inside of wear tracks.

2. EXPERIMENTAL

The commercially pure Cu and Cu-0.7wt% Cr alloy were selected as test materials for the study. The Cu samples were cut to diameter of 15.6 mm and in length of 120 mm, and samples from Cu-Cr alloy were

cut to square 12x12 mm and 120 mm in length, respectively. The samples from Cu were heat treated at 650 °C for 2h. The samples from Cu were processed in PCAP die with two intersection angles of 110° and step-by-step decrease of channel diameter from 16 to 15.5 and to 15 mm, respectively. The samples were routed by 90º and pressing direction was changed to 180º after each pressing. The 12 passes (ε_{vM} ~ 22) were conducted at room temperature. The Cu-0.7wt% Cr alloy was cold water quenching from 1000 ºC (for 2h), respectively. The samples from Cu-0.7wt% Cr alloy were subjected to ECAP by the B_c route with 6 passes (ε_{vM} = 6.9) at room temperature in the ECAP die with channel intersection angle of $\Phi = 90^{o}$ and $\Psi = 0^{o}$ in air with a pressing speed of 5 mm s^{-1} [3]. From received rods were cut off tension/compression test samples with test part of 8 mm in diameter and 12 mm in length. The extensometer base length was 10 mm. The samples were subjected to HCV deformation for 20 tension/compression cycles at strain amplitudes of ±0.05%, ±0.1%, ±0.5%, ±1%, ±1.5%, and ±2% at a low frequency of 0.5 Hz, respectively. The Young modulus was measured at least three-five times between each series for 20 cycles at constant strain amplitudes. These processed samples from Cu-Cr alloy were subjected to heat treatment at temperatures 250-750 ºC (with step of 100 ºC) for 1 h and some samples for 2h. The HCV deformation [16, 18] technique was conducted on the materials testing system Instron-8516. The microhardness was measured using a Mikromet-2001 tester after holding for 12 s at a load of 50 and 100 g. The obtained samples' microstructure was studied by optical (Nikon CX) and scanning electron (Zeiss EVO MA-15) microscopy. For SEM imaging a secondary (SE) and backscattered (BE) electrons were used. The accelerating voltage was 20 kV. The micromechanical properties were characterized using the nanoindentation device of the NanoTest NTX testing center (Micro Materials Ltd.). The nanoindentation was conducted for 49 indents on grinded and etched surface of sample under load of 100 mN. The tribological behavior under dry sliding conditions was investigated before and after ECAP, HCV deformation and heat treatment to provide a comparison over a range of material harness and to understand their influence on the electrical conductivity, COF and specific wear rate. The dry sliding wear was studied using a ball-on-plate tribometer (CETR, Bruker, and UMT2) with a counterface ball of alumina (Al_2O_3) with a ball diameter of 3 mm. The tribological tests were conducted at room temperature in air under normal compression load of 100 g. The sliding distance amplitude was 3 mm at a frequency of 5 Hz, velocity of 20 mm/s, testing time of 10 min and sliding distance of 12 m for all samples. For wear volume calculations, the cross-sectional area of the wear tracks was measured by the Mahr Pertohometer PGK 120 Concept 7.21. The electrical conductivity was determined by means of the Sigmatest 2.069 (Foerster), according to NPL standards. The measurements for different orientations at frequency of 60 and 480 kHz on a calibration area of 8 mm in diameter at room temperature of 23.0±0.5°C and humidity of 45±5 % with an uncertainty of 1% according to International Annealed Copper Standard (IACS) in the National Standard Laboratory for Electrical Quantities of Estonia were conducted.

3. RESULTS AND DISCUSSION

3.1. Microstructure

The SEM/EDS investigation of as-cast Cu-0.7wt% Cr alloy show that it contain porous and no-dissolved Cr particles with measures not higher then one micrometer (Fig 1a). During followed heat treatment at 1000 °C and ECAP for 6 passes by B_c route these inclusions measures were decreased (Fig 1b) and after followed HCV

deformation dissolved via Cr atoms diffusion into the Cu matrix.

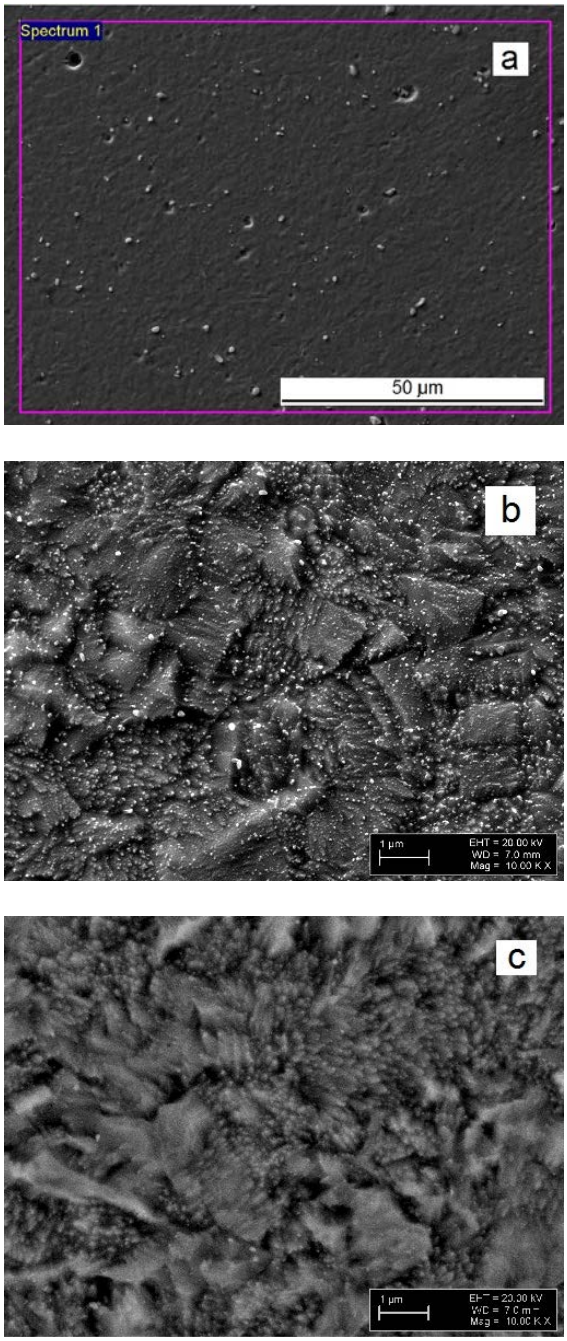

Fig 1. SEM/EDS micrograph of as-cast Cu-0.7wt% Cr alloy with not-dissolved Cr particles and porous (a), SEM (SE) microstructures on cross-section of ECAP processed by B_c route for 6 passes (b) and HCV deformed microstructure (c).

3.2. Mechanical and micromechanical properties correlation with electrical conductivity

The hardness of Cu-0.7wt% Cr alloy (in as-cast condition and after heat treatment at 1000 ºC for 2h) was ~75$HV_{0.1}$ and electrical conductivity was 40% IACS, respectively (Fig 2). During ECAP the hardness was increased up to 192$HV_{0.1}$ and electrical conductivity to 74.16% IACS, respectively. By this, during followed HCV deformation the hardness was decreased slightly to 187$HV_{0.1}$ and electrical conductivity increased to 75.52% IACS, respectively.

The optimal parameters of microhardness and electrical conductivity were choosing after heat treatment at temperatures in the interval from 250 to 750 ºC with step of 100 ºC. The optimal ageing temperatures in the interval of 250-500 °C for 1h were the mean microhardness of 120±10$HV_{0.1}$ and the mean electrical conductivity of 93.3±0.6% IACS. However, heating at temperatures higher than 650 °C leads to decreasing of the electrical conductivity due to the decomposition of the supersaturated solid solution [9]. The increasing of heat treatment temperature to 650 ºC and 750 ºC leads to decrease in the microhardness to 95$HV_{0.1}$ and to 78$HV_{0.1}$ and electrical conductivity to 87% IACS and to 77% IACS, respectively.

The electrical conductivity of pure Cu was decreased by increase of equivalent von Mieses strain higher then ~4 εvM (Fig 3). As is shown the electrical conductivity at ~11 εvM to ~14 εvM strain decrease sharply and by cumulative strain increase to ~22 εvM it was decreased to 58.95% IACS measured at frequency of 60 kHz and to 51.05% IACS measured at frequency of 480 kHz, respectively. At the frequency of 60 kHz the depth of measure is 3-3.5 mm and at frequency of 480 kHz it decreases to ~1 mm. This result shows that dislocation density has very large influence on the results of electrical conductivity measure as the dislocations have obstacle to electrons mowing in the material [6]. By this, in other works [7, 9, 10] is shown that the electrical resistivity/conductivity depends on hardness of material and the correlation is shown.

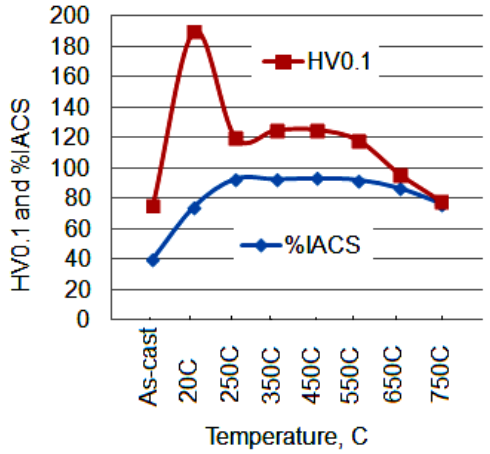

Fig 2. Electrical conductivity and microhardness of Cu-0.73wt% Cr alloy dependence from ageing temperature.

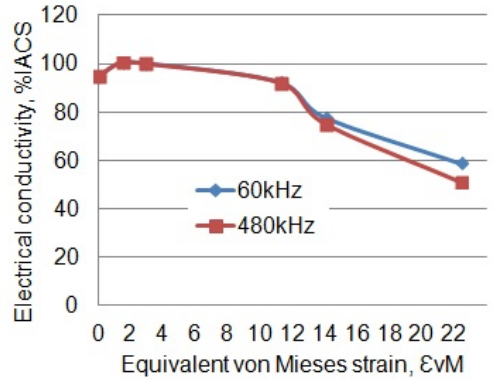

Fig 3. Electrical conductivity of pure Cu dependence from equivalent von Mieses strain and testing frequency.

3.3. Strength and thermal stability of UFG Cu and Cu-Cr alloy

The UFG pure Cu was lost your strength properties at temperature of 170ºC. After PCAP for 6 passes the strength was Rm = 430 MPa, after ageing treatment at temperature of 170 ºC the Rm = 355 MPa and at 200 ºC this parameter was decreased to 264 MPa.

The results of HCV deformation show that at strain amplitude increases (from ±0.1% to ~± 1%) the stress amplitude and Young module increase, respectively. At the increased strain amplitudes of ±2% (Fig 4a) the stress amplitude decrease at 15 cycle's from 339.7 MPa to 265.3 MPa and the Young modulus (Fig 4b) was sharply decreased from 130 GPa to ~100 GPa at these some strain amplitude. This result depend on the test material grain size before HCV deformation [16] and show the phenomena of NC metals [14] as softening by slight deformation. According to our speculative opinion the Young modulus was decreased (Fig 4b) as the interatomic interaction was decreased by cumulative strain or cycles number of HCV deformation increase (see Fig 4a). But these standpoints need detailed investigations in future.

The results of nanoindentation for UFG Cu-0.7wt% Cr are presented in Fig 5. The mean (from 49 indents measured under 100 mN load) nanohardness of sample N1 was HN = 3.84 GPa and indentation modulus Er = 538.5 GPA, respectively. The ageing time increase to 2h (sample N2) leads to decrease of hardness but increase of indentation modulus.

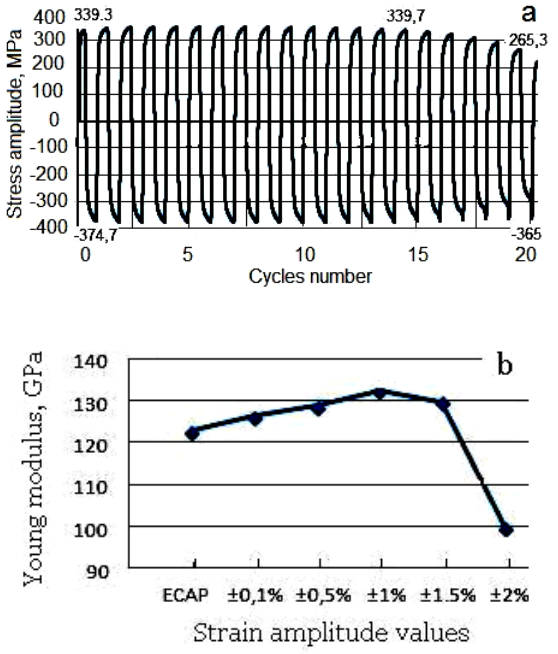

Fig 4. HCV deformation stress amplitude curves of Cu-0.7wt.% Cr alloy for ±2% of strain amplitude (a) and corresponding curve show the Young modulus increase to ~133 GPa at lowest (up to ±1%) strain amplitudes and decrease to ~100 GPa (b) by strain amplitude increase up to ±2%.

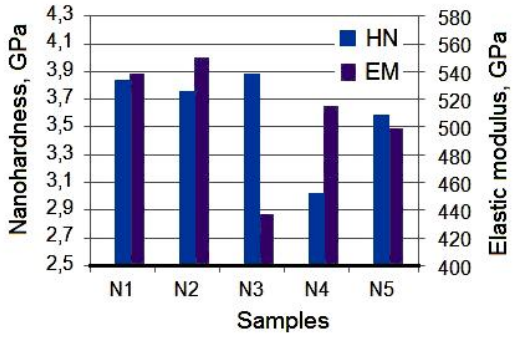

Fig 5. Nanohardness (HN) and Young/elastic modulus (EM) of Cu-0.7Cr alloy after 6 passes measured in cross-section of sample by nanoindentation. Definitions: N1 - ageing at 450 °C for 1 h; N2 – 450 °C for 2h; N3 – 450 °C for 2h+HCV; N4 – 550 °C for 1h; and N5 – 550 °C for 2h.

The minimal indentation modulus Er = 437 GPa was measured for hardest HN_{100}= 3.89 GPa Cu-0.7wt% Cr alloy (sample N3) after HCV deformation. The ageing time increase to 550 °C (sample N4 for 1h and sample N5 for 2h) leads to increase of hardness (from HN = 3.02 GPa to HV = 3.59 GPa) but decrease of indentation modulus.

The specific wear rate and COF measurements show their dependence from chemical composition of sample material, sample surface hardness as well material surface softening/hardening during wear testing. Results show that HCV deformed sample in surface was hardened from $77HV_{0.05}$ to $90HV_{0.05}$ and on the wear track surface from $115HV_{0.05}$ to $126HV_{0.05}$, respectively. In this case the wear track surface hardening was induced by cyclic straining as result of sliding. The specific wear rate was decrease from 0.3 to 0.07 mm^3min^{-1}, respectively. The minimal specific wear rate has sample with maximal hardness. By this, during cycling (Fig 4a) at strain amplitude of ±2% the stress amplitude and Young modulus (Fig. 4b) were sharply decreased as the interatomic interaction was lowered [18]. At that time the rate was increased. The results show that the pure Cu has lowest COF equal to 0.32 at the end of wear testing. By this at the first stage of testing the annealed Cu has slightly higher COF equal to 0.38 and Cu-0.7wt% Cr alloy COF was 0.57 at the end of wear testing. The COF was higher for Cu-0.7wt% Cr alloys as these have no dissolved hard Cr particles in soft Cu matrix. By this in our experiments the Cu-0.7wt% Cr alloys with higher hardness have highest COF but lowest specific wear rate.

4. CONCLUSIONS

In this study the pure Cu and Cu-0.7wt% Cr alloy the physical, mechanical and micromechanical properties, electrical conductivity, specific wear rate and COF were studied in dependence on cumulative strain and ageing temperature.

The UFG pure Cu (after ECAP+HCV deformation) have best electrical conductivity (~103% IACS) and low COF as well low specific wear rate but lowest thermal stability by temperature increase over 170 ºC.

The UFG Cu-0.7wt.% Cr alloy after ECAP show highest microhardness, good wear resistance but low electrical conductivity (74.16% IACS). During followed HCV deformation the electrical conductivity was lightly increased (75.52% IACS).

The ageing treated at 250-550 ºC UFG Cu-0.7wt% Cr alloy have highly stabile mechanical, tribological and electrical conduction (~94% IACS) properties and will be used as material for electrical energy industry.

5. ACKNOWLEDGEMENTS

The work was supported by the Ministry of Education and Science of the Estonia, Project No. IUT19-29 and EU ERA.Net RUS STPojects-219.

6. REFERENCES

1. Zehetbauer, M.J., Zhu, Y.T. *Bulk nanostructured materials.* Dresden, 2012.

2. Kommel, L., Hussainova, I. and Volobueva, O. Microstructure and properties development of copper during severe plastic deformation. *Mater. Design.,* 2007, **28,** 2121-2128.
3. Mathieu, J.P., Suwas, S., Eberhardt, A.., Tóth, L.S. and Moll, P. A new design for equal angular extrusion. *J. Mater. Proc. Techno.,* 2006, **173,** 20-33.
4. Dalla Torre, F., Lapovok, R., Sandlin. J., Thomson, P.F., Davies, C.H.J. and Pereloma, E.V. Microstructure and properties of copper processed by equal channel angular extrusion for 1-16 passes. *Acta Mater.,* 2004, **52,** 4819-4832.
5. Jiang, H., Zhu, Y.T., Butt, D.P., Alexandrov, I.V., Lowe, T.C. Microstructure evolution, microhardness and thermal stability of HPT-processed Cu. *Mater. Sci. Eng.*, 2000, **A290**, 128-138.
6. Kommel, L. Properties development of ultrafine-grained copper under hard cyclic viscoplastic deformation. *Mater. Lett.,* **64,** 2010, 1580-1582.
7. Wei, K.X., Wei, W., Wang, F., Du, Q.B., Alexandrov, I.V. and Hu, J. Microstructure, mechanical properties and electrical conductivity of industrial Cu-0.5%Cr alloy processed by severe plastic deformation. *Mater. Sci. Eng.,* 2011, **A528,** 478-1484.
8. Estrin Y, Vinogradov A Extreme grain refinement by severe plastic deformation: A wealth of challenging science *Acta Mater.,* 2013, **61,** 782-817.
9. Shangina D.V., Bochvar N.R., Dobatkin S.V. Structure and properties of Cu-Cr alloys subjected to shear under pressure and subsequent heating. *Russ Metal (Metally),* 2010, **11**, 1046-1052 (in Russian).
10. Zhilyaev, A.P., Shakhova, I., Belyakov, A., Kaibyshev, R. and Langdon, T.G. Effect of annealing on wear resistance and electroconductivity of copper processed by high-pressure torsion. *J. Mater. Sci.,* 2014, **49,** 2270-2278.
11. Yao, B., Han, Z. and Lu, K. Correlation between wear resistance and subsurface recrystallization structure in copper. *Wear,* 2012, **294-295,** 438-445.
12. Yao, B., Han, Z. and Lu, K. Dry sliding tribological properties and subsurface structure of nanostructured copper at liquid nitrogen temperature. *Wear*, 2013, **301**, 608-614.
13. Shangina, D.V., Bochvar, N.R., Dobatkin, S.V. The effect of alloying with hafnium on the thermal stability of chromium bronze after severe plastic deformation. *J. Mater. Sci*., 2012, DOI 10.1007/s10853-012-6525-9.
14. Su, L.H., Lu, C., Tieu, A.K., He, L.Z., Zhang, Y. and Wexler, D. Vacancy-assisted hardening in nanostructured metals. *Mater. Let.,* 2011, **65,** 514-516.
15. Lugo, N., Llorca, N., Suñol. J.J. and Cabrera, J.M. Thermal stability of ultrafine grains size of pure copper obtained by equal-channel angular pressing. *J. Mater. Sci.* 2010, **45,** 2264-2273.
16. Kommel, L., Veinthal, R. HCV deformation – method to study the viscoplastic behavior of nanocrystalline metallic materials. *Rev. Adv. Mater. Sci.,* 2005, **10,** 442-446.
17. Li, X., Bhushan, B. A review of nanoindentation continuous stiffness measurement technique and its applications. *Mater. Charact.,* 2002, **48**, 11-36.
18. Kommel, L., Saarna, M., Traksmaa, R., Kommel, I., Microstructure, properties and atomic level strain in severely deformed pure metal niobium. *Mater Sci (Medžiagotyra),* 2012, **18-4,** 330-335.

7. CORRESPONDING ADDRESS

PhD. Lembit Kommel
Department of Materials Engineering,
Tallinn Univ of Technology, Estonia
Phone: +372 52 365 13
E-mail: lembit.kommel@ttu.ee

9th International DAAAM Baltic Conference
"INDUSTRIAL ENGINEERING"
24-26 April 2014, Tallinn, Estonia

INVESTIGATION OF COMPOSITE REPAIR OF PIPELINES WITH VOLUMETRIC SURFACE DEFECT

Kovalska, A.; Eiduks, M.

Abstract: *The paper describes equivalent stress change of pipe with longitudinal volumetric form defect on pipe surface – approximated as half of ellipsoid. The optimal experiment design created to analyse that defect increase. For every size of modelled volumetric surface defect created different thickness of applied bandage. The equivalent stress for working pressure is numerically calculated using ANSYS software in pipe without defect, with defect and after composite repair with varying thickness of the bandage for different sizes of defect. All results are approximated and analysed.*
Key words: volumetric defect, composite repair, modelling

1. INTRODUCTION

There are different kinds of pipe defects resulting metal loss – such as scars, corrosions, pitting, abrasion, grinding off, rupture, puncture or leak etc. When areas of corrosion or other damage on operating pipelines are identified, there are significant economic and environmental incentives for performing repair without removing the pipeline from service. There are a variety of repair strategies available to pipeline operators for a given repair situation [1]. An application of composite materials for the repair of damaged pipelines considerably improved situation in the last time [2]. The goal of this paper is investigation of composite repair of pipelines modelling volumetric surface defect before and after advanced composite repair and the development of optimization methodology for advanced composite repair of pipelines with volumetric surface defects, which consists from several tasks.

2. PIPE DEFECT DESCRIPTION

2.1. Parameters of defect

There are different kind of pipe defects resulting metal loss – such as scars, corrosions, pitting, abrasion, grinding off, rupture, puncture or leak [3] etc. The paper describes defect, which has volumetric longitudinal form – approximately half of ellipsoid.

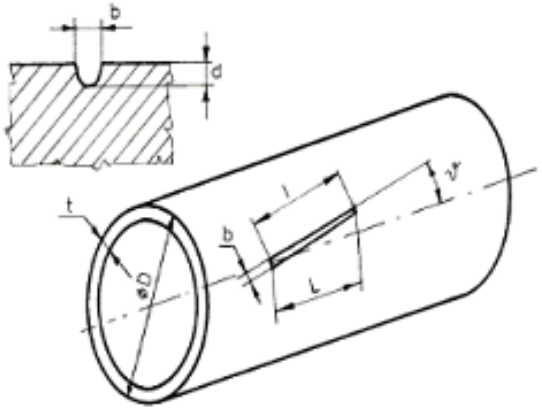

Fig. 1. Measures of longitudinal volumetric defect

The definition of pipe metal loss defect: groove like defect, which is nearly parallel with the centre line of the pipe having greater projected axial length than the triple of the nominal wall thickness and having a width, which is larger than the 30% of the nominal wall thickness [3]. Maximal depth of defect is close to 80% of pipe wall thickness.

Measures of longitudinal volumetric defect, see Fig.1.

- angle between the defect and the centre line of the pipe, υ[°];
- length, l [mm];
- projected axial length, L [mm];
- maximal width, b [mm];
- maximal or effective depth, d [mm],[2]

The constraints describing longitudinal volumetric defect is identified below (1, 2, 3, 4):

$$3t<L<10t \quad (1)$$
$$0.3t<b<3t \quad (2)$$
$$0.1t<d<0.8t \quad (3)$$
$$\upsilon = 0°, \quad (4)$$

where *t* is wall thickness of pipe, mm.

The geometrical and physical parameters of pipe and advanced composite repair materials are constant, except the thickness of bandage – *h, mm*. Thickness of bandage have to change in dependence of defect metal loss volume and it have to be less than pipe wall thickness.

The thickness of bandage defined as variable parameter – less is better, because of saving materials.

2.2. Description of VSD

For creation of optimal experiment design is used the model, which describes increase of longitudinal volumetric surface defect (VSD). Three parameters characterise increase of longitudinal volumetric surface defect (VSD) by mathematical linear expressions given below (5, 6, 7):

$$L_{n+1} = L_1 + 14n, \text{ where } L_1 = 3t \quad (5)$$
$$b_{n+1} = b_1 + 5.4n, \text{ where } b_1 = 0.3t \quad (6)$$
$$d_{n+1} = d_1 + 1.4n, \text{ where } d_1 = 0.1t \quad (7)$$
$$\text{and } n\epsilon(0,8)$$

The metal loss volume of longitudinal volumetric surface defect of pipe approximately is shown as a half of ellipsoid (8) by formula (9) [4]:

$$V = \frac{4}{3}\pi abc \quad (8)$$

$$V_n = \frac{1}{2} \times \frac{4}{3}\pi \frac{b_n}{2} d_n \frac{l_n}{2} = \frac{\pi b_n d_n l_n}{6} \quad (9)$$

Model of volumetric defect increase is given below, see Fig.2. That increase can consists of many different configurations of three parameters like axial length, maximal width and maximal depth, but in this research, they are given by expressions (5), (6) and (7).

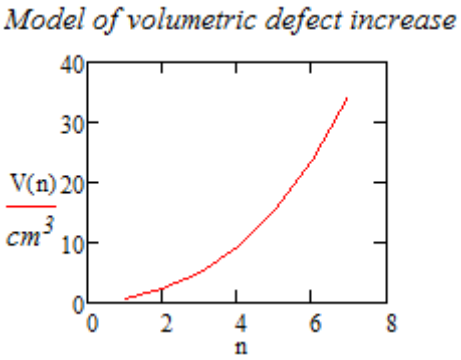

Fig.2. Model of volumetric surface defect increase for pipe with outside diameter is 1020 mm and wall thickness – 14 mm

3. EXPERIMENT DESIGN

3.1. Statement of the problem

Statement of the problem in this research is shown at Fig.3. Objective of optimization is to find a minimal stress *σ (MPa)* on the pipe surfaces after repair applying different thickness *h (mm)* of bandage on different size of chosen volumetric defect *V(L, b, d) (mm³)*[5].

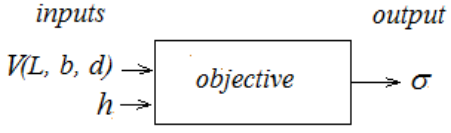

Fig. 3. Statement of the problem

$$\sigma = f(V(L, b, d), h) \quad (10)$$

As the result of experiment design is creating the output - σ functional dependence (10) of inputs – *V(L, b, d)* and *h*, which is necessary for optimization activities.

3.2. Experiment design

The experiment design [6] elaborated in the Table 1. Input data include:

- geometrical parameters of selected pipe; model of the defect defined by three increasing parameters – in this case (5), (6), (7);
- variable thickness of bandage;
- equivalent stress of the selected pipe without damage;
- equivalent stress of selected pipe with different size of defect (n=8 is number of different sizes of damage);
- equivalent stress of composite repaired pipe with different thickness of bandage.

Number of experiments	Outside diameter	Wall thickness	Axial length of defect:	Max width of defect:	Max depth of defect:	Equivalent stress	Equivalent stress with different bandage thickness (mm), Mpa							
#	D, mm	t, mm	l, mm	b, mm	d, mm	σ, MPa	1mm	3mm	5mm	7mm	9mm	11mm	13mm	15mm
			3t<l<10t	0.3t<b <3t	0.1t<d<0.8t									

Table 1. Experiment design

4. CREATION OF FEM MODELS

4.1. Constructive characteristics

According to elaborated experiment design plan FEM calculations were done. For calculations have been used parameters given below:

Pipe:

Geometry data:

outer radius R = 0.51m, wall thickness h_1 = 0.014m, half of length for calculations l_1 = 0.2m

Mechanical properties: E_1 = 200 GPa, υ_1 = 0.3, ρ_1 = 7850 kg/m^3

Filler:

Geometry data varies depending from size of VSD taken according to plan

Mechanical properties: E_2 = 20 GPa, υ_2 = 0.4, ρ_2 = 1250 kg/m^3

Bandage

Geometry data: inner radius equals pipes outer $R_3 = R_1$ = 0.51m, wall thickness h_2 = 0.014m, half of length for calculations l_2 = 0.1m

Mechanical properties: E_3 = 142 GPa, υ_3 = 0.3, ρ_3 = 1600 kg/m^3

For simplification glassfibre bandage considered as isotropic material.

Working pressure in the pipe 5.9 MPa.

As FEM element type is used Solid 95 and all three materials are connected with command *glue* (Ansys) and symmetry boundary conditions were applied.

At first, equivalent stress for pipe without any damage is founded. This numerical data is necessary for analysis of repaired system. From numerical calculations obtained, that in case for tube described above, the stress in undamaged pipe is very

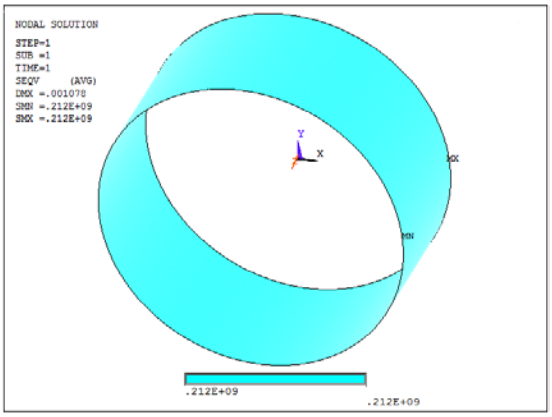

Fig.3. Equivalent stress in pipe without damage is 212 MPa

near to 200 MPa (see Fig.3) and it is more than half from Yield strength of material, factor of safety in statical loading case is more than 1, in this case is near or more than 2 (differs between used material properties). Stress 200 – 212 MPa will be

used for comparison with obtained stress in repaired pipe, for which in each VSD case will be changed thickness of glassfibre bandage, which will be wrapped around pipe and filler in damaged place.

4.2. Description of defect model

Second task is to create FEM models for growing volumetric surface defect (VSD). Metal loss in pipes outer surface is modelled by using ellipsoids and sizes are taken according to three parameters characterise increase of longitudinal VSD by mathematical linear expressions (5, 6, 7). Damage is created in ellipsoidal coordinate system in *Ansys*, relationship between dimensions of damage are used (it is determined by radius ratios, see Fig. 4) for curvature determination.

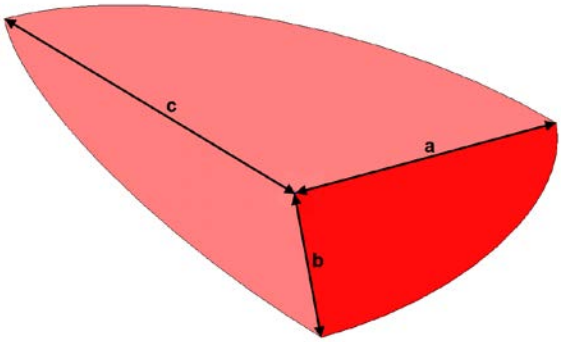

Fig. 4. ¼ of metal loss ellipsoid volume, letters correspond to dimensions

Totally is made eight different sizes of ellipsoidal volumetric surface defect using FEM, one model without defect with equivalent stress shown in Fig.3. A view of VSD is shown in Fig.5.

Figure 5 shows the VSD one model with wall thickness loss equivalent to 60% from pipe wall thickness.

Meshing is created so the smallest elements are in damage zone and farther elements grow by ratio (see in Fig. 6.), so it was possible to economy computing time, and for the same reason for modelling is

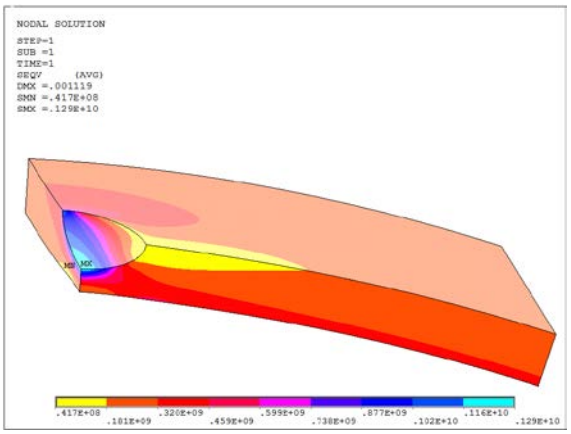

Fig. 5. Equivalent stress condition in case of one VSD size according to experiment plan

used only a sector of pipe with partial damage and for this symmetry boundary conditions were applied.

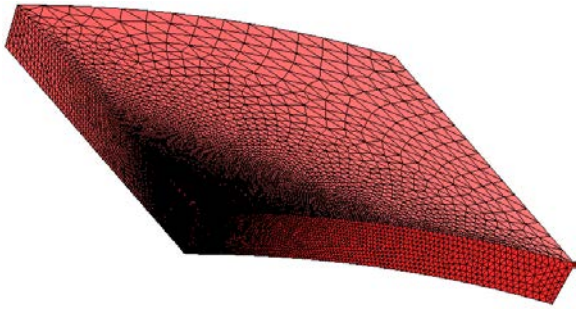

Fig. 6. Element map for pipe with damage

4.3. FEM models

In Fig. 7 and Fig. 8 is presented view on case 5 – 3 (number 5 means VSD size according to experiment design

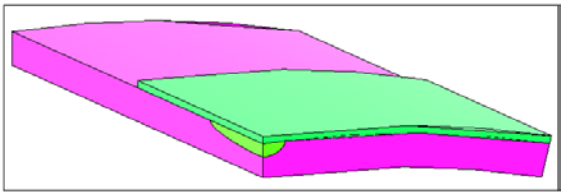

Fig.7. Model of sector of tube and bandage and filler in VSD cavern

expressions (5), (6), (7) and number 3 means thickness on bandage applied to pipe (3 mm)). Fig. 7 shows one sample without loading and in Fig. 8 is shown equivalent stress condition.

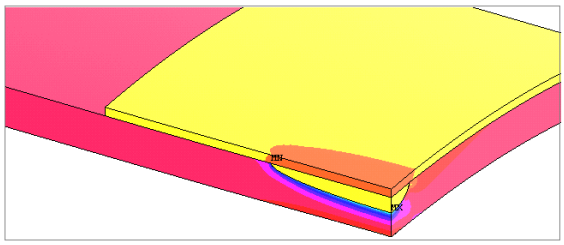

Fig.8. Equivalent stress condition for case 5 – 3

For several sizes of VSD is applied variable thickness of bandage, according to experiment design, for example, Fig.9.

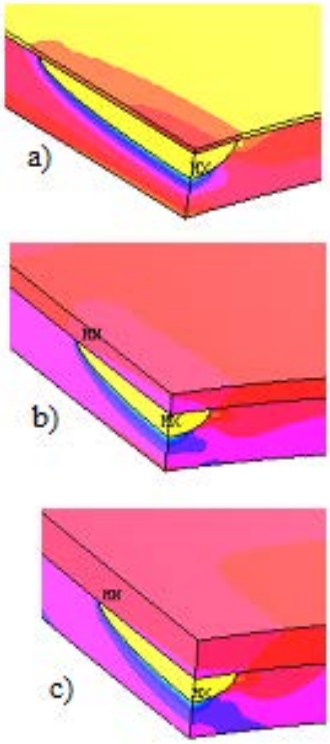

Fig. 9. Visualisation of increase of thickness of bandage layer for the one of VSD size, bandage thicknesses: a) 1 mm, b) 5 mm and c) 9 mm

Calculation results are collected. It shows that applying thicker layer of bandage, stress in damaged zone decreases. All results are useful for further research.

5. TREATMENT OF RESULTS

5.1. Equivalent stress

The results from Fig. 10 show how is changing the equivalent stress by applying composite repair materials for different size of volumetric defect if working pressure is constant. Different coloured lines characterize different size of modelled volumetric defect (VSD). The smallest VSD is defect Nr.1 and the largest – Nr. 9. The grey line shows the largest volumetric defect of the pipe being repaired, and blue line – the smallest volumetric defect of pipe being repaired. Coloured points shows numerically calculated Equivalent stress in pipe before and after composite repair depended on thickness of bandage

The horizontal axis is the thickness of bandage. The pipes with two smallest modelled volumetric damages according to expressions (5), (6), (7) and experiment design (Table 1) are crossing yield strength line when thickness of bandage of composite repair is less than 1mm, and the pipe with largest damage is crossing yield strength line when thickness of bandage of composite repair is more than 5 mm.

5.2. Equivalent stress approximation

For the analysis and optimization, the approximation curve was used. Fig. 10 shows approximated equivalent stress curve. The approximation with a logarithmic function gives very accurate approximations. The approximation with a logarithmic function used in the form:

$$\sigma(h) = \sigma_1 - C \cdot \ln(h) \qquad (11)$$

where $\sigma_1 = \sigma(h_1)$ is the equivalent stress of composite repaired pipe with a thickness of bandage of 1mm; C – is the constant, which depends on composite material properties and parameters of VSD. The constant for each sample is inside diapason (65; 83) in modelled configurations; h is the thickness of bandage.

Fig. 10 shows that the initial condition of equivalent stress of pipe after composite repair achieved in first two smallest modelled VSD. The largest modelled repaired VSD is Nr. 9 crossing yield stress with composite bandage thickness 5 mm. An impact of composite repair geometrical parameters and properties of its constituent

materials on stress state in VSD taken into consideration.

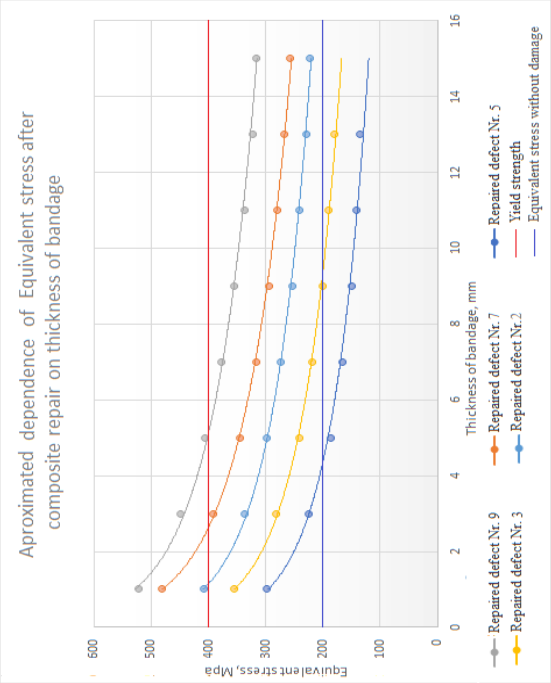

Fig. 10. Approximated Equivalent stress curves in pipe after composite repair depended on thickness of bandage

CONCLUSIONS

The optimal thickness of bandage for numerically modelled VSD depends on reserve ratio for working pipe, the total cost of applied composite materials and other external conditions, which shows the efficiency of repairing solution. Developed optimization methodology for the advanced composite repairs helps to engineer to make a decision about possibility of repair or not, and helps to find the necessary thickness of bandage for modelled VSD in this study. Approximated equivalent stress curves on Fig. 11 shows the impact of bandage thickness on repaired pipe.

The further model to analyse may include an angle between the defect and the centre line of the pipe.

ACKNOWLEDGEMENT

The authors gratefully acknowledge the support of the European Commission, Marie Curie programme, contract no. PIRSES-GA-2012-318874, project “Innovative Non-Destructive Testing and Advanced Composite Repair of Pipelines with Volumetric Surface Defects (INNOPIPES)” [5].

REFERENCES

1. Bruce B., Amend B., “Advantages of steel sleeves over composite materials for pipeline repair” Pipelines international, ISSUE 008 http://pipelinesinternational.com/news/advantages_of_steel_sleeves_over_composite_materials_for_pipeline_repair/061223/
2. itconsult-eu.de
3. Hashem El-Sayed A.A., PE 607: Oil & Gas Pipeline Design, Maintenance & Repair http://www.eng.cu.edu.eg/users/aelsayed/Part%209%20Pipeline%20defects.pdf
4. Olver F. W. J., Lozier D. W., Boisvert R. F., and Clark C. W., editors, 2010, NIST Handbook of Mathematical Functions, Cambridge University Press.
5. Kovalska A., Barkanov E., Eiduks M. “Development of experimental optimization methodology for the pipelines repairing by using advanced composite materials” VII Russian Conference on Solid Mechanics, Abstracts, 15-18 Oct 2013., Rostov-on-Don, SFU, 2013, p. 155.
6. Auzins J., Janusevskis A. (2007). Eksperimentu plānošana un analīze, Rīga, RTU, ISBN 97-9984-32-157-8

AUTHORS

1)Agrita Kovalska, Ezermalas Str. 6k, Riga, LV-1006, Latvia, Agrita.Kovalska@rtu.lv, +37127179587
2) Maris Eiduks, Ezermalas Str. 6k, Riga, LV-1006, Latvia, Maris.Eiduks@rtu.lv, +371261118

9th International DAAAM Baltic Conference
"INDUSTRIAL ENGINEERING -
24-26 April 2014, Tallinn, Estonia

THE EFFECT OF WOOD FLOUR FRACTION SIZE ON THE PROPERTIES OF WOOD-PLASTIC COMPOSITES

Kängsepp K., Poltimäe, T., Liimand K., Kallakas H., Süld, T.-M., Repeshova I., Goljandin D., Kers, J.

Abstract: *Wood-plastic composites are developing way of thought, sustainable and efficient. Most important question is how to enable recycling and to extend life-cycle of products. Plastic waste has long decomposition cycle. Wood particles in plastic matrix absorb water and enable more rapid decomposition. In this study different fractions of wood flour made from alder (Alnus) chips were used in composites with polypropylene and linear low-density polyethylene. Mechanical properties of composites were tested and additionally industrial experiments were carried out with the same mixture. Injection moulded forks were prepared and mechanical tests were performed.*
Key words: disintegrator, binding agent, mechanical properties, composites.

1. INTRODUCTION

Wood plastic composites (WPC) are composite materials that consist of either wood fibers or wood flour and different thermoplastic polymer matrix.
Wood plastic composites are the materials that combine the best performance and cost properties of both wood and thermoplastics. These composites are gathering bigger market share with every year because of their favorable properties, such as lower cost, improved stiffness, lower density, lower abrasiveness and better process ability compared to other fillers, for example inorganic fibers. [1-3]
Wood plastic composites mechanical properties depend on the properties of their components and the ratio of these components.
Wood component properties are affected largely by wood particle size. Previous studies have investigated wood particle size effects on WPC mechanical properties. These studies have examined the effects of small wood particles or fibers. The results of these studies showed that wood particle size influence on WPC mechanical properties was substantial. However, some studies showed that there was only slight effect to the WPC mechanical properties. Majority of the tested WPCs showed that increasing the wood fraction size also increases WPC mechanical properties. However, some of the tested WPCs, showed the reverse effect. [2-3]
It is difficult to give general explanations because there are many factors that are influencing the test results in these studies. For example, thermoplastic type, wood content, wood particle geometry, coupling agent type and content, and processing method influenced the results of the these studies. In conclusion, based on the previous studies, the influence of the wood particle size on WPC mechanical properties is not completely evident. More studies are needed to understand wood particle size importance on WPCs.
Wood particle dimensions can influence the strength properties in wood fiber based products. [4] Small wood particles (wood flour) are often used for manufacturing commercial WPCs. It is due that small particles are easy to use with manufacturing equipment. Small particles can be integrated easily into the process.

However, low length to diameter ratio can cause stress concentrations and therefore strength of the WPC is reduced lower than pure polymer. [5-6]. Some reports have stated, that when WPCs are formed with injection molding the using of longer wood fibers also increases the mechanical properties of WPCs. [7-8] Very few studies have shown beneficial influence of fiber length on mechanical properties when extrusion method was used. Other studies have stated that there was slight to none influence on mechanical properties. Therefore the effect of wood particle size on WPC strength properties varies with composites forming process. There are very few studies yet that explain the wood fiber size and their influence on the mechanical properties of WPC. [9-12]
The objective of this study was therefore to investigate the influence of wood component size to the WPC structure and mechanical properties. Three different wood particle sizes was used to find out what is the optimal wood particle size to be used in WPCs. Bending tests were done to investigate mechanical properties of WPCs. Also industrial products of WPCs were tested to investigate the influence of wood component size in industrially made forks of WPC.

2. MATERIALS AND METHODS

2.1 Wood particles

Alder chips were used as wood raw material for manufacturing WPCs. Wood chips were brought from sawmill and chips were undried and there were different sizes of wood particles: very small (smaller than 1 mm) and too big (ca 8 mm) particles. The moisture content of undried wood chips was 32 wt.%. The wood chips were dried in oven at 50 °C for 24 h. Then wood chips were mechanically refined with disintegrator DS – A into three fiber length classes. Particle length and distribution were measured using analytical sieve shaker method with Fritsch Analysette 3. Used sieve sizes were from 25 to 0.025 mm. Dimensions were measured and particle bulk density was also determined. Screening of the particles into three fiber length classes was done with screening mechanism SM-1.

Fraction	Fraction size, mm
I	1.25-2
II	0.63-1.25
III	Fine powder

Table 1. Measurements of wood flour fractions

The basic process consists of several steps:

- The material is placed from batcher to the boot.
- The material from the boot is sprinkled in different sieve sets.
- A large fraction is separated from the first sieve where then material goes into the collector.
- The rest of the small particle size fractions go to the sieves according to the particle size sieves.
- The process lasts until there are no more small particles in the bottom of the mechanism.

Three particle sizes were experimentally obtained, details are show in Table 1.

2.2 Polymers

For composite preparation pelletized polypropylene (PP) from Borealis Polymers and linear low-density polyethylene (LLDPE) Icorene 2550 were used. Polyethylene (PE) with maleic anhydride MAH was DuPont Fusabond M603 12% MAH and PE copolymer. Most important properties of polymers are shown in Table 2.

Polymer	Density g/cm³	MFI g/10 min
PP	0.95	2
LLDPE	0.92	1
PE-MAH	0.94	25

Table 2. Properties of polymers

2.3 Binding agents

For improving the adhesion between matrix and filler three different binding agent were used: triethoxyvinylsilane (TEVS), polyvinyl alcohol (PVA) and MAH. MAH was derivatised with PE pellets, DuPont Fusabond M603 12% MAH and polyethylene copolymer was used.

TEVS and PVA were added to wood flour. TEVS was mixed with ethanol-water 9:1 solution and sprayed over wood flour while mixing thoroughly. After mixing wood flour was kept at room temperature for 2h and then dried in oven at 110 °C.

From PVA a water solution was made and sprayed over wood flour while mixing thoroughly. After mixing wood flour was dried in oven at 110 °C.

2.4 Preparation of test specimens

All test specimens contained 65% polymer and 35% wood flour (WF). Properties of WPCs are shown in Table 3. Polymer and wood flour coupling agents amounts are weight% from wood flour. Wood flour and polymer were compounded in twin-screw extruder Brabender Plasti-Conder PLE 651 at 190 °C and 70-80 rpm. Test specimens for bending testing were made according to ISO 178:2003.

Injection moulding was done at Battenfeld BA 230 E device. Test specimen measurements were 60x10x4mm, cross-section area was 40 mm^2.

Sample	Polymer	Polymer coupling agent	Polymer coupling agent , wt%	WF fraction	WF coupling agent	WF coupling agent, wt%
1	PP	-	-	-	-	-
2	PP			II		
3	PP	MA	5	III	TEVS	5
4	PP			II	PVA	5
5	LLDPE	-	-	-	-	-
6	LLDPE			II		
7	LLDPE	MA	5	II		
8	LLDPE	MA	0.6	I	TEVS	5
9	LLDPE			I	PVA	5

Table 3. Properties of compounds

2.5 Bending testing

Three-point bending tests were carried out according to ISO 178:2003. For testing Instron 5866 tensile tester was used, testing temperature was 20 °C, test span 60 mm and speed 20 mm/min. From every mixture 10 test specimens were used.

3. RESULTS AND DISCUSSION

3.1 Mechanical testing

The results from the mechanical testing are shown in Table 4. Results show that the addition of wood flour makes the material more brittle - a deflection of test pieces was largest with pure polymers. From Table 3 and 4 it can be seen that the chemical pre-treatment affected the flexural properties positively: the composites with pretreated wood chips had better bending strength values than composites with untreated wood chips.

Sample	Deflection (mm)	Bending strength (MPa)	Deformation (%)	Modulus of elasticity (GPa)
1	11.5	33.0	7.7	4.3
2	5.0	32.0	3.4	9.5
3	8.0	34.1	5.3	6.4
4	6.3	37.2	4.2	8.9
5	16.7	8.8	11.1	0.8
6	10.7	20.4	7.1	2.9
7	12.6	22.9	8.4	2.7
8	12.4	20.7	8.3	2.5
9	10.3	16.4	6.9	2.4

Table 4. Results from mechanical testing

It is a noticeable increase in the bending strength of PP without additives transition to PP composite with additives, from 33.0 (pure PP) to 37.2 MPa (PP+WF+PVA).

In a view of bending strength and influence of additives, the wood flour processed with polyvinyl alcohol gives WPC the best physical resistance values. However, test results for specimens based on PP also showed that flexural properties increase gradually with increasing particle size from wood flour (less than 0.63 mm) to fraction (0.63-1.25 mm). These results correlate with other studies from the literature which show that increasing the fiber length and L/D ratio also increases the bending strength values. [13-15, 17] This can be explained as the fine powder acts more like a filler but larger wood particles show some mechanical strength and by choosing the right coupling agent the adhesion between filler and matrix is very good.

For the PE, best adhesion is achieved by adding maleic anhydride. Adding maleic anhydride gives WPCs good strength values as shown in Table 4. (PE+WF bending strength is 20.4 MPa compared to PE+WF+MA is 22.9 MPa) and also composites have smooth surface, material is tough and well workable. Compared to pure LLDPE samples the bending strength of composites is more than twice higher.

Comparing the bending results with other study [17] we see the difference in results: flexural strength differs in 8-24 % and modulus of elasticity differs in 47-79 % [13, 17]. Variation of the results may be due differences in dimensions of the test specimens, various polymers, using different manufacturing technologies and equipment and using different wood species. Also results from the other studies have been revised with series of experiments and test conditions were different from this work. WPCs are anisotropic materials and therefore large differences may occur in test results. [16, 18-19]

3.2 Industrial product testing

Forks were made with injection molding technology in the production test to explore the products made from low quality waste wood filler for use in the manufacture of the WPC product. The other interest was also to find out what fraction of wood particles is best to carry out injection molding technology experiments and compare the bending strength properties.

Forks were made of WPC using PP as matrix polymer in granule form and same wood flour made from Alder wood chips as filler material in laboratory tests. Composites were prepared with wood flour and polymer ratio of 1:1.

Four different mixtures were used to prepare test forks for bending testing. Bending testing of PP+WF composites was performed with three-point bending test using an Instron 5866 machine. A minimum of 3 specimens of each material were tested. Impact properties of the prepared composites were measured with a falling weight impact testing machine with the crosshead speed of 10 mm/min.

Forks made of WPC were tested to analyze if the forks made of WPC are competitive with pure PP forks, because the addition of wood flour can provide the cost reduction and combination of properties. To obtain high performance PP+WF composites, the influence of wood flour content on mechanical properties was investigated. Table 5 shows the effect of wood flour content on the mechanical properties of forks made of WPC.

Based on the results in Table 5, it is evident that flexural strength values of PP+WF composites are lower than those of pure PP which decrease with increased WF size. This may simply show that there is a poor interfacial interaction between reinforcing wood particles and polymer matrix because of the poor stress transformation across interphase. Another reason can be the design of a fork. Compared to laboratory test specimens which were made according to standard and have rectangular cross section the

Sample	Distance between supports (mm)	Crosshead speed (mm/min)	Flexural strenght (N)
Pure PP	32.00	10.00	40.1
PP+WF fr.III	32.00	10.00	37.32
PP+WF fr.II	32.00	10.00	35.4
PP+WF fr.I	32.00	10.00	32.61

Tabel 5. The effect of wood flour content on the mechanical properties.

forks have much thinner and more complicated cross section. This may explain why in forks the best results after pure PP were with finest wood flour.
External inspection revealed that failures occurred near the location of the wood particle as the particles were mainly parallel next to each other and perpendicular to the longitudinal axis of the fork stem. Tests showed that in these places were also fractures of bending forces.

4. CONCLUSION

In conclusion it can be said that alder wood is worth considering as source for wood fibers and particles for using in WPC. Most important is choosing the right binding agents as wood fibers are not compatible with polymers. Another important result of this study was that mixtures that gave good result in laboratory test were not working in industrial experiments as the design and area of a cross-section seem to have important role. With right ratios, particle size and processing parameters wood flour can be used in producing commodity products like forks and spoons and thus enabling faster degradation.

5. REFERENCES

1. Zimmermann, M.V.G., Turella, T. C., Santana, R. M.C., Zattera, A. J. The influence of wood flour particle size and content on the rheological, physical, mechanical and morphological properties of EVA/wood cellular composites. *Mat. and Design.* 2014, **57**, 660-666.
2. Kociszewski, M., Gozdecki, C., Wilczyński, A., Zajchowski, S., Mirowsk, J. Effect of industrial wood particle size on mechanical properties of wood-polyvinyl chloride composites. *Eur. J. Wood and Wood Prod.* 2012, **70**, 113-118.
3. Gibson, R. F. *Principles of composites material mechanics.* McGraw-Hill, New-York, 1994.
4. Bodig, J., Jayne, B. A. *Mechanics of wood and wood composites.* Krieger publishing company, Malabar, 1993.
5. Wolcott, M. P., Englund, K. A technology review of wood–plastic composites. In *Proceedings of the 33rd International Particleboard and Composite Materials Symposium*. Pullman WA, 1999.
6. Gamstedt, E. K., Nygård, P., Lindström, M. Transfer of knowledge from Papermaking to manufacture of composite materials. In *Proceedings of the 3rd Wood Fibre Polymer Composites International Symposium*. Bordeaux, 2007.
7. Stark, N. M., Rowlands, R. E. Effects of wood fiber characteristics on mechanical properties of wood/polypropylene composites. *Wood Fiber Sci,* 2003, **35**, 167–174.
8. Sanschagrin, B., Sean, S. T., Kokta, B. V. Mechanical properties of cellulose fibers reinforced thermoplastics. In: *Proceedings of the 43rd annual conference, Composites Institute. Soc. of Plastics Industry,* 1988, 5.
9. Leua, S. Y., Yang, T. H., Loc, S. F., Optimized material composition to improve the physical and mechanical properties of extruded wood–plastic composites (WPCs). *Construction and Building Mat.* 2012, **29**, 120–127.

10. Le Baillif, M., Oksman, K. The influence of the extrusion process on bleached pulp fiber and its composites. In: *Proceedings of the progress in wood and biofibreplastic composites conference*. Toronto, 2006, 9.
11. Yam, K. L., Gogoi, B. K., Lai, C. C., Selke, S. E. Composites from compounding wood fibers with recycled high density polyethylene. *Polym. Eng. Sci.* 1990, **30,** 693–699.
12. Migneault, S., Koubaa, A., Erchiqui F., Chaala, A., Englund, K., Wolcott M. P. Effects of processing method and fiber size on the structure and properties of wood–plastic composites. *Comp.: Part A.* 2009, **40**, 80–85.
13. Gwon, J. G., Lee, S. Y., Chun, J. S., Doh, H. G., Kim, J. H. Effects of chemical treatments of hybrid fillers on the physical and thermal properties of wood plastic composites. *Comp.: Part A.* 2010, **41**, 1491-1497
14. Hietala, M., Samuelsson, E., Niinimäki, J., Oksman, K. The effect of pre-softened wood chips on wood fibre aspect ratio and mechanical properties of wood-polymer composites. *Comp.: Part A.* 2011, **42**, 2110-2116
15. Faruk, O., Bledzki, A. K., Fink, A.-H., Sain, M. Biocompostes reinforced with natural fibers: 2000 – 2010. *Prog. Polym. Sci.* 2012, **37**, 1552-1596
16. Wang, Y., Qi, R., Xiong, C., Huang, M. Effects of coupling agent and interfacial modifiers on mechanical properties of poly(lactic acid) and wood flour biocomposites. *Iranian Polym. J.* 2011, **20** 281-294.
17. Ichazo, M. N., Albano, C., Gonzalez, J., Perera, R., Candal, M. V. Polypropylene/wood flour composites: treatments and properties. *Comp. Struct.* 2001, **54**, 207-214
18. Bhaskar, J., Haq, S., Yadaw, S. B. Evaluation and testing of mechanical properties of wood plastic composites. *J. Thermoplastic Comp. Mat.* 2012, **25**, 391-401.
19. Bhaskar, J., Haq, S., Pandey, A. K., Srivastava, N. Evaluation of properties of propylene-pine wood Plastic composite. *J. Mat. Environ. Sci.* 2012, **3**, 605-612.

9th International DAAAM Baltic Conference
"INDUSTRIAL ENGINEERING –
24-26 April 2014, Tallinn, Estonia

LIGNIN AND OUTER CELL WALL REMOVAL FROM ASPEN PULP FIBRES BY USING SUPERCRITICAL CO_2 EXTRACTION

Kärner, K.; Elomaa, M. & Kallavus, U.

Abstract: Supercritical carbon dioxide extraction ($scCO_2$) is chosen to a treatment to remove lignin and to peel off outer cell wall layers to expose S2 layer of aspen wood fibres. The aim is to find an effective and environmentally friendly method to advance the fibrillation of the BCTMP pulp. The effects of the treatment are analysed by using scanning electron microscopy (SEM). The chemicals used together with $scCO_2$ extraction include 1:1 ethanol: water co-solvent, isopropyl alcohol, and dimethyl sulfoxide (DMSO) with urea. The results show that supercritical CO_2 extraction helps to peel the fibres of mechanical pulp. Best results are gained with 1:1 ethanol: water co-solvent.

Key words: Cellulose; Lignin; Super-critical CO_2; Aspen; BCTMP, Microfibrils,

1. INTRODUCTION

Cellulose is one of the most abundant biopolymers on earth; it has attractive characteristics of being both recyclable and renewable. It consists of microfibrils that are bundles of elementary crystallites bridged by amorphous phases. Because a complete purification of cellulose demands a lot of energy and chemicals, there are many products in which cellulose is used only partly purified. For example, products like bleached chemi-thermo mechanical pulp (BCTMP) have been developed to be used as a component in paper making. A characteristic property of mechanical pulp is that it retains most of the wood lignin.

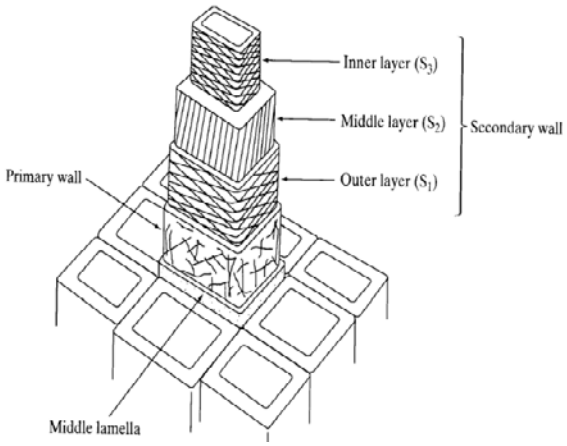

Fig.1. Wood cell wall layers

The structure of fibre consists of several different layers; three main layers are the middle lamella, the primary wall and the secondary wall. Secondary wall is divided into sub layers: S1, S2 and S3. Different cell wall layers can be identified by the orientation of cellulose microfibrils; it is specific to each layer, see Figure 1. Lignin and cellulose contents are also different in different layers; the lignin content is highest in the middle lamella and the primary wall, whereas cellulose content is highest in the S2 layer. Therefore, in order to get pure cellulose from wood fibre, it is necessary to remove outer cell wall layers. The proof of successful treatment is a clearly visible S2 layers with parallel orientation of cellulose microfibrils.

Lignin that is present on the surface of BCTMP forms a physical barrier against inter fibre bonding, moreover, it hinders the inter-fibre hydrogen bonding due to the hydrophobic nature of lignin [1]. Therefore, it is essential to remove the lignin-rich material in order to fibrillate fibres and to produce e.g. nanocellulose. The

hydrophobic lignin-rich material is also one of the main reasons for low inter-fibre bonding strength of mechanical pulp fibres [1]. On the contrary, when more cellulose fibrils are exposed, and more fibril separation takes place in the secondary wall, then inter-fibre bonding is enhanced. At the same time, by removing specifically the lignin-rich material on the fibre surface it will not reduce much the yield [1].

$ScCO_2$ is becoming an important commercial and industrial solvent due to its role in chemical extraction in addition to its low toxicity and environmental impact [2]. $ScCO_2$ is also non-flammable, chemically inert and inexpensive. $ScCO_2$ extraction under sub and supercritical conditions has been used to remove lignin and small molecular weight extractives from wood. Organic solvents (acetic acid, methanol, ethanol and butanol) have been used as co-solvents, they enhance the influence of sc CO_2 [3]. Organic solvents together with water are also used in organosolv pulping process. The use of $scCO_2$ extraction before pulping enhances the penetration of pulping chemicals [4]. One of the most effective modifiers in supercritical conditions might be isopropyl alcohol, it has been successfully used and it resulted delignification of 4 % [4]. Because 100% ethanol is not very nucleophilic it has been used as co-solvent with water (ethanol-water ratio 30-70%). The addition of water promotes the delignification reactions but reduces the ability of the solvent to dissolve the lignin separated by the process [7]. It has also been suggested that adding of co-solvent (ethanol-water 1:1 solution) to the extraction should dissolve lignin [7].

It is essential to use high pressures to permit the reaction of the solvent mixture (or fluid) with the lignin present in the wood [7]. Delignification effect of wood takes place under the pressure of 350 atmospheres. However, temperature does not affect the delignification rate so much, it can be between 80 and 140 °C [4]. The reaction temperature cannot be over 200°C, as the degradation of polysaccharides present in the wood starts around 200°C and is very significant over 250°C. Therefore, in order to preserve cellulosic fraction as much as possible, those limits must be considered [7]. 60-120 minutes treatment times for extraction have been reported [5]. However, most of the delignification takes place during the first 30 minutes [7]. In order to produce microcrystalline cellulose, dimethyl sulfoxide (DMSO) has been used together with urea. In this case urea helps the reaction agents to penetrate deeper into the fibre. Urea also dissolves well in DMSO [6].

The aim of this work is to examine if it is possible to use $scCO_2$ extraction, possibly intensified with co-solvents, to remove residual lignin and to peel off outer cell wall layers.

2. EXPERIMENTAL

2.1 Materials

Aspen BCTMP was obtained from Estonian Cell. All pulps were oven dried at 105ºC and grinded in a coffee-grinder. Commercially available technical grade CO_2 with a purity of 99.7% from AGA was used in the $scCO_2$ extraction process. Technical Acetone with 99.5% purity from APChemicals was used in the solvent exchange process. Isopropyl alcohol was from Sigma Aldrich with purity ≥99.7 % and with Mw=60.10. Ethanol and dimethyl sulfoxide (DMSO) were of laboratory grade and used without further purification. To enhance the influence of DMSO during the scCO2 treatment, urea was used; it was 99.0-100.5 % pure from Sigma Aldrich. Distilled water was readily used from laboratory's own distilled water system.

2.2 Equipment

A supercritical CO_2 experimental device SES-UK 1 from Norlab OÜ was used to carry out the $SCCO_2$ extraction experiments. Figure 2 depicts the reactor system.

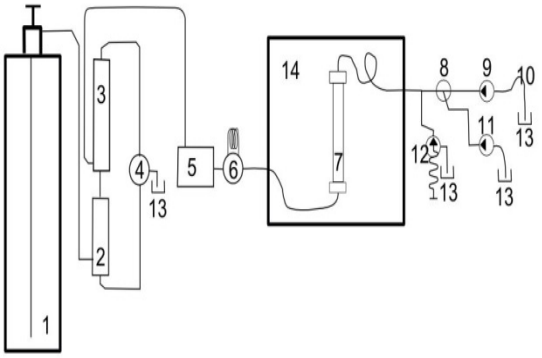

Fig.2. A set-up of the supercritical extraction system. CO_2 cylinder (1), liquid/gas outlet line (2,3,4) high pressure dual piston pump (5) six-way injector (6), reactor (7), three way joint (8), output vents (9) safety valve (12) flow outs (13), thermostat oven (14).

The Supercritical 24 constant flow-constant pressure dual piston pump was used the sufficient pressure to operate in the supercritical conditions of CO_2. The pump is built to operate in two distinct modes: constant pressure and constant flow regimes. Pressure is adjustable from 0 to 10000 Psi with an error of 1%. In the constant pressure mode a maximum value for the flow rate is set for the pump which is then one of the determining factors of pace at which the set constant pressure threshold is achieved.

Commercially available Carbolite PF30 convection oven is used as thermostat of the supercritical processing system. The maximum temperature of the system is 200°C. The reactor is placed inside the thermostat.

The two valves at the end of the system serve as the back-pressure regulator and a way to release the solvent from the reactor. The system allows for precise control of pressure and temperature that are the most important parameters defining the supercritical state. The processing time is also adjustable and variable at need. The system can operate under pressures up to 190 bars and temperatures up to 200°C.

The critical point drying was carried out in a commercially available Balzers CPD 030 device. The specimen chamber is incorporated into the body of the device. Heating and cooling of the specimen chamber are monitored with a digital temperature meter. Liquid CO_2 is used as the drying medium because of its low critical point values for temperature and pressure.

Blazer's critical point dryer was applied for drying wet samples before microscopy.

Fine Coat Ion Sputter JFC-1100 was applied for SEM samples.

All SEM analyses were carried out with a Zeiss EVO MA 15 scanning electron microscope; as it was used for imaging and morphological characterization, the secondary electron regime was used. The specific SEM allows for accelerating voltages ranging from 0.2 – 30 keV, magnifications up to 1 million and corresponding resolutions down to some nanometres. The field of view is defined to be 6 nm at the analytical working distance. The microscope allows for investigation of specimen with heights up to 145 mm.

2.3 Methods

For supercritical CO_2 extraction an accurately weighed dry sample (3 g) was put into stainless steel netting and placed inside the reactor. Stainless steel reactor was placed inside the thermostat (see Figure 1). Then thermostat was closed and pressure and temperature risen.

When solutions were used (ethanol: water co-solvent, isopropyl alcohol, DMSO with urea), samples were first mixed with 10 ml of solution and then placed to the reactor.

The extraction conditions were chosen close to the maximum parameters to ensure treatment throughout the wood fibre - 2900 psi and 120 °C. Treatment was set to 60 minutes starting from the point where pressure and temperature had reached their desired values.

Before SEM analysis, solvent exchange to acetone and critical point drying were performed. Solvent exchange is a method for shifting material from one solvent to another. Samples in water solutions were transformed into acetone via solvent

exchange using acetone-water solutions (30, 50, 70, 90, 100, 100w% of acetone).
A typical critical point drying was conducted in the Blazer's apparatus. The wood fibre mass in acetone was placed in the chamber which was cooled to 5 - 7 °C to ensure liquid CO_2, sealed, pressured from the CO_2 vessel and flushed with liquid CO_2 3 - 4 times. Finally the chamber was heated to 40 °C and gassed out.
For SEM studies, dry samples were placed with fine pipette to a metallic stub using a double-sided adhesive tape. Then the samples were placed into ion sputtering chamber for two minutes and coated with gold and platinum under vacuum to enhance electrical conductivity. Coating was carried out at 1.9 kV and 10 mA.
The SEM examination was carried out with EVO MA 15 at accelerating voltage of 12 to 15 keV. Two sets of images were taken for each sample: an overview image with 200 x magnification and close images of separate fibres with about 1000 x magnification. Specific points of interest were imaged with magnifications up to 4500 x.

3. RESULTS AND DISCUSSION

Our initial sample is bleached chemi-thermo mechanical aspen pulp (BCTMP). Emphasis is set to the fibres and changes on their surfaces caused by the $scCO_2$ extraction. The S2 layer of the cell wall is the thickest layer and contains the most of the cellulose. It is thus desirable to remove the middle lamella and two layers (P and S1) to open up the S2 layer for further treatment or processing. On the surface of BCTMP fibres, large pieces of non-fibrillar lignin-rich material can be seen, see Fig. 3. This is mainly because after mechanical pulping, outer cell wall layers (middle lamella and primary wall) are still on the surface of wood fibres. On Figure 3, the middle lamella is easily recognizable by its rectangular shape. It can be seen that outer cell wall layers are unbroken, no cracks can be seen in the middle lamella, layers are strongly attached to the fibre main body. Figure 3 also shows that there are non-fibrillar patches present and they derive from two adjacent fibres. This is the most lignin-rich area, which glues fibres together in wood (middle lamella contains about 70 % of lignin).

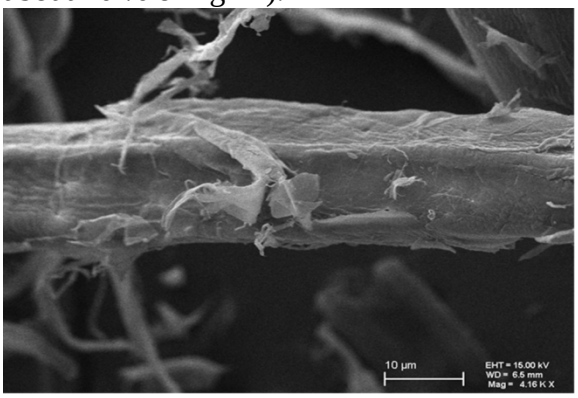

Fig. 3. Starting material-dried and grinded BCTMP.

After $scCO_2$ extraction, fibres look somewhat different than before the treatment. It can be seen from Figure 4 that outer cell wall layers, especially middle lamella, start to peel off from the wood fibre. It seems that outer cell wall is loosened. There are a lot of cracks in outer cell wall layers, splitting is likely to happen. It can be presumed, that after some mechanical treatment those almost loose patches come off completely.

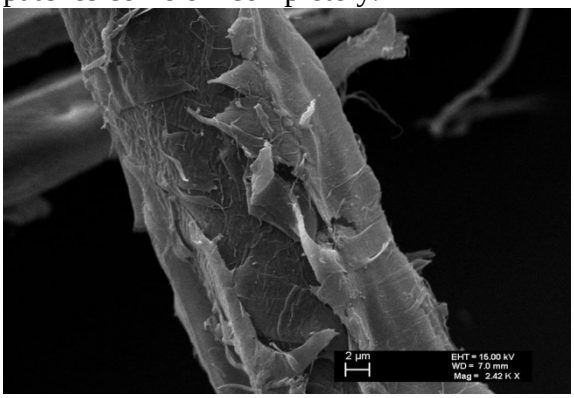

Fig. 4. Peeling effect after $scCO_2$ treatment.
The supercritical treatment is even more effective when ethanol is added to the reaction system. In our treatment 1:1 ethanol: water co-solvent was used and the pulp was moistened with this solution before the sc CO_2 extraction. As can be seen from Figure 5, middle lamella and

primary wall are both successfully removed from aspen pulp fibre. S2 layer is clearly visible and it can be easily identified by parallel orientation of cellulose microfibrils. It suggests that the addition of a co-solvent (1:1 ethanol-water solution) reacts with lignin and loosens the whole structure so that most lignin-rich layers split out from the main fibre.

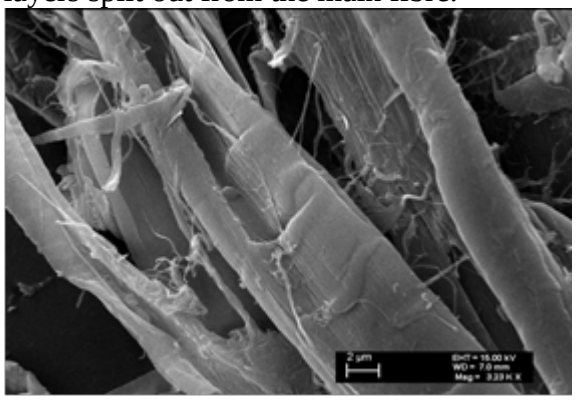

Fig. 5. Peeling effect after sc CO_2 treatment with ethanol: water cosolvent

The supercritical CO_2 extraction was not always very effective. For example treatments with isopropyl alcohol and dimethyl sulfoxide did not have very good effect on fibrillation and outer cell wall removal. The result is moderate after isopropyl alcohol (see Figure 6) as there is no sign of fibrillation. On the other hand, there is a little visible peeling. The whole fibres look quite unbroken. Thus isopropyl alcohol was not the best co-solvent to $scCO_2$ in the procedure used.

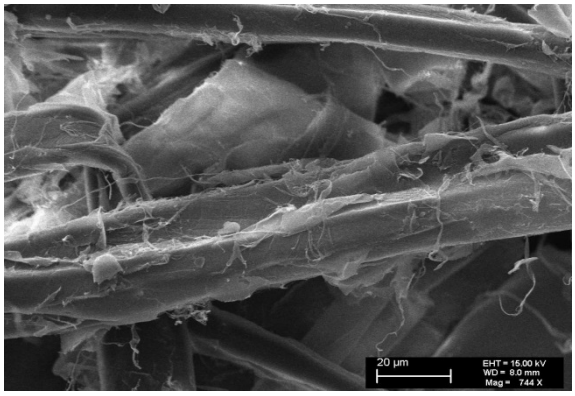

Fig. 6. Fibres looking almost the same as without treatment.

Supercritical CO_2 with DMSO and urea did not give any remarkable effect. On the contrary, it seemed that all residual lignin that was present in outer cell wall layers, has been "melted" on the fibre surface during the $scCO_2$ treatment, see Figure 7. Fibre surface looks quite smooth and there is no sign of peeling or fibrillation. It might be that DMSO and urea are not suitable for fibre fibrillation and lignin removal at higher temperatures. It is reasonable to assume that at high temperatures, lignin in the middle lamella melts and spreads over the fibre surface.

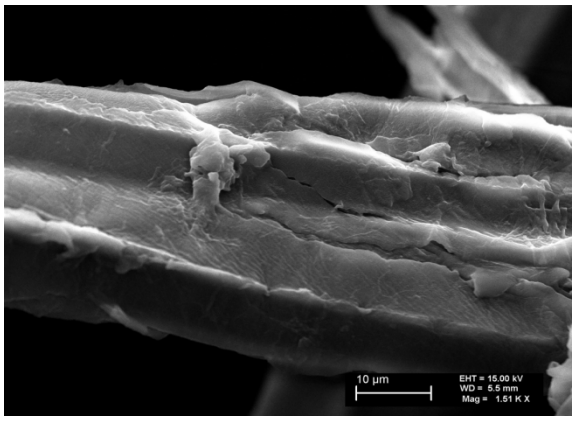

Fig. 7. DMSO with urea.

4. CONCLUSION

Results showed that supercritical CO_2 treatment has an influence on fibre peeling on mechanical pulp. It is possible to remove outer cell wall layers by using $scCO_2$ extraction. As the treatment loosens and in some cases even removes outer cell wall layers, it can be presumed that lignin content is also decreased as the lignin content is especially high in those removed layers. Best results were gained with 1:1 ethanol: water co-solvent. It was shown that $scCO_2$ extraction changes the appearance of wood fibres. Nevertheless, DMSO did not cause any residual lignin removal or peeling of the fibre outer cell walls. On the contrary, lignin was like a smooth film covering the fibre surface. Sc CO_2 treatment is a good starting point for fibre fibrillation; the process might be enhanced by further mechanical treatment.

5. ACKNOWLEDGEMENTS

The authors would like to acknowledge the financial support of SmaCell project AR12138.

6. REFERENCES

1. K. Li, L. Lei and C. Camm Surface Characterization and Surface Modification of Mechanical Pulp Fibres, *Pulp & Paper Canada*, 2010, January/February, 28-33
2. K. H. Kim, J. Hong, Supercritical CO2 Pretreatment of Lignocellulose enhances enzymatic cellulose hydrolysis, *Bioresources Technology*, **77** (2001), 139-144
3. D. Pasquini, M. T. B. Pimenta, L. H. Ferreira and A. A. De Silva Curvelo. Sugar Cane Bagasse Pulping Using Supercritical CO_2 Associated with Co-solvent 1-butanol/water, *J. of Supercritical Fluids*, 2005, **34**, 125-131
4. A.D. Ivahnov, T. E. Skrebete and K. G. Bogolitsyn, 2nd International IUPAC Conference on Green Chemistry, 2008, 14.
5. Li and E. Kiran. Interaction of Supercritical Fluids with Lignocellulosic Materials. *Industrial and Engineering Chemistry Research*, 1988, 42, 1301- 1312.
6. A. Selarka, R. Baney, S. Matthews, Processing of Microcrystalline Cellulose in Dimethyl Sulfoxide, Urea and Supercritical carbon dioxide, *Carbohydrate Polymers*, 2013, **93**, 698-708.
7. D. Pasquini, M. T. B. Pimenta, L. H. Ferreira and A. A. De Silva Curvelo. Extraction of Lignin from Sugar Cane Bagasse and Pinus Taeda Wood Chips Using Ethanol-Water Mixtures and Carbon Dioxide at High Pressures. *Journal of Supercritical Fluids*, 2005, **36**, 31-39.

9th International DAAAM Baltic Conference
"INDUSTRIAL ENGINEERING -
24-26 April 2014, Tallinn, Estonia

ON DETERMINATION OF RESIDUAL STRESSES IN SOME PVD COATINGS BY THE CURVATURE METHOD

Lille, H.; Ryabchikov, A.; Lind, L.; Sergejev, F.; Adoberg, E. & Peetsalu, P.

Abstract: *Hard thin coatings obtained by the process of physical vapour deposition (PVD) are gaining increasing importance in many industrial applications. One of the peculiar features of deposited layers is the presence of residual stresses therein. Residual stresses in coatings can be classified as follows: coating growth stresses and thermal stresses. In the presented experiments the values of the residual stress of three different PVD coatings, i.e. TiN, TiCN, AlCrSiN (commercially known as nACro®), were measured. Residual stresses were determined by the curvature method, based on the well-known Stoney's formula, where the substrate used was a nickel steel plate. The coatings were deposited on the substrate at two different angles with respect to the cathode axis. The residual stresses in the TiCN and AlCrSiN coatings were compressive and very large.*
Key words: PVD coatings, residual stress, curvature method

1. INTRODUCTION

Physical vapour deposition hard coatings have met wide application in tooling industry as compared with other technologies, the PVD process provides optimal sharp cutting edges [1, 2].
The typical fields of the application of different coatings are the following: cutting, punching, forming and moulding tools. PVD coatings reduce the coefficient of friction and increase the hardness of coated parts [3,4,5]. Residual stresses arise during coating deposition and play a considerable role in various applications as they may influence such characteristics as adhesion strength [6,7,8], wear resistance, fatigue crack propagation and damage development. For example, high tensile or compressive residual stress could cause spontaneous coating delamination. A balanced compressive residual stress state seems desirable to compensate for tensile stresses arising from the external load [6,8,9]. It is reported that large coating thickness could be a starting point for high residual stress [10,11]. Therefore, compressive coating stresses are beneficial to wear protection only if the coating thickness and edge radius of tools are optimized [2].
The level of residual stress is highly dependent on the process of manufacturing coatings. In thin hard coatings, there usually develop very high stresses. The main sources of residual stresses in hard PVD coatings are lattice mismatch epitaxial coating growth and phase transformations (intrinsic stresses) as well as the thermal stress produced by a mismatch between the thermal contractions of the coating and the substrate [4,12,13]. Therefore, accurate measurement and prediction of residual stresses is crucial in manufacturing PVD hard coatings.

2. EVALUATION OF RESIDUAL STRESSES IN THE COATING

In our experiments a nickel steel plate was used as the substrate (Fig. 1, Table 1).
As the coating is relatively thin $h_1/h_2 \geq 60$, then the well-known Stoney's formula was used where the biaxial state of stress is taken into consideration [14].

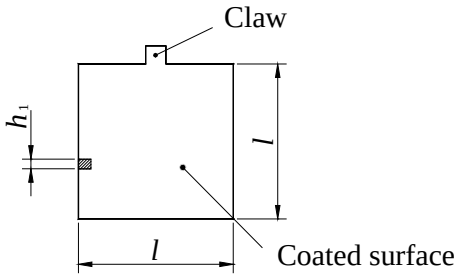

Fig. 1. Geometry of a specimen.

It was assumed that residual stresses are distributed uniformly throughout coating thickness; see the architecture of the coating system where most of layer thickness has a similar structure (Fig.4). When variation in the curvature and thickness are replaced with the variation in deflection and coating thickness, then the formula for the plate specimen will be [15]

$$\sigma = \frac{4E_1}{3(1-\mu_1)}\frac{h_1^2}{l^2 h_2} w \qquad (1)$$

where E_1 and μ_1 are the indentation modulus and the Poisson's ratio of the substrate respectively, h_1 is thickness of the substrate; h_2 is thickness of the coating; l is coated width; w is measured deflection in the middle of the plate (Fig.2).

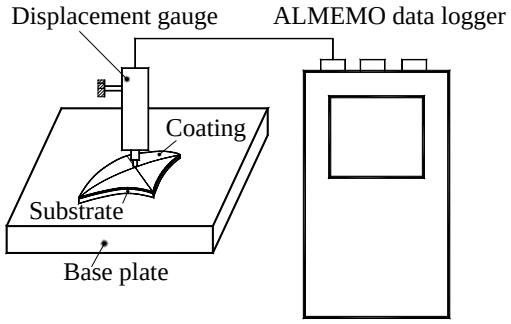

Fig. 2. A schematic representation of the experimental equipment for measuring deflection in the middle of the coated specimen.

Thermal stresses in thin coatings are calculated by the following equation [14]

$$\sigma_T = E_2^*(\alpha_2 - \alpha_1)(T_{dep} - T_{room}) \qquad (2)$$

where $E_2^* = E_2/(1-\mu_2)$; E_2 and μ_2 are the modulus of elasticity and the Poisson's ratio of the coating; α_1, α_1 are the coefficients of linear thermal expansion (CTE) of the substrate and coating; T_{dep} and T_{room} are deposition temperature and room temperature, respectively.

3. EXPERIMENTAL PROCEDURE

The studied PVD coatings were produced in the Laboratory of PVD Coatings at Tallinn University of Technology. PVD unit Platit π-80 with two rotating cathodes embedded in the door of the vacuum chamber was used for deposition.
Three different PVD coatings, i.e. TiN, TiCN, AlCrSiN, were studied. The coatings were deposited on nickel steel plates whose properties are presented in Table 1. The surfaces to be coated were polished. The specimens were placed in the box and fixed to the claw (Fig. 3). The exposed surfaces were coated in perpendicular and parallel orientations with respect to the axis of the rotating cathode. The deposition temperature was 450 °C for each coating.

Substrate material	Thickness, mm	Usable length, mm	
Nickel alloy plate	0.241–0.244	19.42 – 19.83	
Elastic Modulus, GPa	Poisson's ratio	CTE, $\alpha \cdot 10^{-5}$	Surface roughness *Ra*, μm
156.5	0.28	1.18	0.024 – 0.029

Table 1. The geometry and mechanical properties of the substrate material.

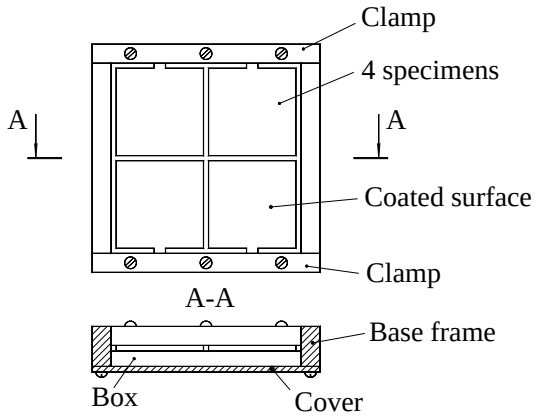

Fig. 3. The fixture of specimens for deposition.

For both orientations at least four specimens were coated. For calculation of residual stresses, the mean values of deflection were used. The deflections are presented in Table 3.
The moduli of elasticity and nanohardness of the coatings were measured by a MTS Nano Identer XP® and their thickness was measured using KaloMAX® (ballcrater method). A standard new Berkovich indenter was used in all experiments. Indentation was repeated at least 20 times for each coating at four different loads, 20, 30, 50, 70 mN. For calculation of residual stresses, the mean values of the moduli of elasticity were used.
Study was made of thermal stresses (Eq. 2) which appear due to temperature change between coating deposition at 450 °C and deflection measurement at 20 °C. The data of the calculation are presented in Table 3.

4. RESULTS AND DISCUSSION

The modulus of elasticity, and the hardness and thickness of the studied coatings are presented in Table 2. The calculated mean values of residual stresses are presented in Table 3.

For all coatings, the obtained mean values of residual stresses correspond to compressive stresses. These stresses were very high and fluctuated in different coatings more than three times and were markedly lower for the nACRo® specimens coated parallel with respect to the cathode axis. Residual stresses were not correlated with values of hardness.
Residual stresses in coatings depend strongly on deposition parameters, especially on bias voltage [16]. For all studied coating types, the main sources of residual stresses are the phenomena occurring during deposition, which are termed as growth stresses. In other words, residual stresses originate from ion bombardment and crystal growth by particles during coating deposition [12]. Thermal stresses were calculated only for TiN as the CTE and Poisson's ratios for TiCN and AlCrSiN were not determined. The obtained thermal stresses are comparable with relevant literature data [4]. Fig. 4 shows the cross-section of TiN and TiCN coatings where a columnar microstructure can be observed.

Coating	Type	Position	Elastic Modulus, GPa	Hardness, GPa	Poisson's ratio	CTE $[1/°C]\times10^{-5}$	Thickness, μm
TiN	Monolayer	parallel	527±33	24.1±0.84	0.22 [4]	0.74 [4]	3.3
TiCN	Gradient	parallel	494±24	31.9±1.43	-	-	2.2
		perpendicular					1.3
AlCrSiN (nACRo®)	Nano-composite, gradient	parallel	429±16	29.3±0.56	-	-	2.7
		perpendicular					1.6

Table 2. Mechanical properties of the studied coatings

Coating	Position of specimen	Deflection, mm	Compressive residual stresses, GPa			
			Calculation formula Eq.1	Literature data	Thermal component	Growth component
TiN	parallel	0.239 0.244	3.14 3.21	4.2 [3] 3.8 [4] 8-10 [12]	1.06 1.06	2.08 (2.9 [4]) 2.15
TiCN	parallel	0.535	11.45	4.6-5.9 [16]	not calculated	not calculated
	perpendicular	0.328	11.57	-	not calculated	not calculated
AlCrSiN (nACRo®)	parallel	0.264	4.55	-	not calculated	not calculated
	perpendicular	0.240	7.00	-	not calculated	not calculated

Table 3. Deformation parameters and mean residual stresses in the coatings

a b

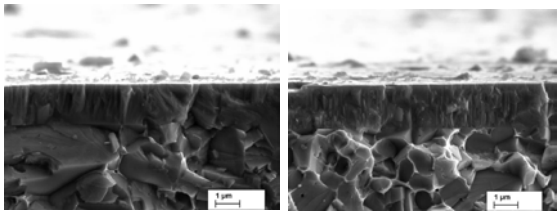

Fig. 4. SEM pictures of TiN (a) and TiCN (b) gradient coatings [17].

Furthermore, coatings under investigation were used on industrial fine-blanking punches. Discrete areas were found where the coating was detached (Fig. 5). Such failure may be connected with high residual stress inside coatings [2]. The results of our study showed that the failure was independent of the coating and more prevalent on punches with higher surface roughness. The revealed substrate increases the likeliness of the blanking material to adhere to the punch and cause alternating stress in the tool surface, which leads to fatigue and crack development [6, 18, 19, 20].

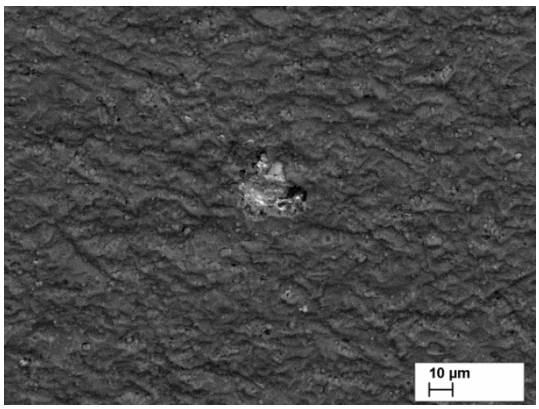

Fig. 5. Industrial fine-blanking punch showing discrete detachment of TiN coating.

The knowledge of the residual stresses induced by the manufacturing process in coating may be of importance in understanding the tendency for spalling and delamination of coatings, which is observed in coated parts working in presence of wear and contact fatigue conditions.

5. CONCLUSION

All residual stresses were compressive (negative) and very high and they fluctuated in different coatings many times. Residual stresses in coatings depend strongly on deposition parameters, especially on bias voltage. The state of residual stress is influenced less by thermal expansion than by layer growth which plays the predominant role. The values of residual stress in TiN coatings obtained by the curvature method were comparable with the correspond values presented in the literature [4].

6. ACKNOWLEDGEMENTS

This study was supported by the Estonian Ministry of Education and Reseach (SF0140091s08). Financial support from the R&D program „Materials technology" is acknowledged for supporting the project „Advanced thin hard coatings in tooling" No. AR12134.
Andre Gregor, PhD, prepared the specimens with TiN coatings.

6. REFERENCES

1. Soroka, O.B. Evaluation of residual stresses in PVD-coatings. Part 1.Review. *Strength of Materials*, 2010, **42**, 3, 287-296.

2. Gerth, J., Larsson, M., Wiklund, U., Riddar, F., Hogmark, S. On the wear of PVD-coated HSS hobs in dry gear cutting. *Wear*, 2009, 266, 444-452.

3. Dobrzanski, L.A., Lukaszkowicz, K. Mechanical properties of multilayer coatings deposited by PVD techniques. *Archives of Materials Science and Engineering*, 2007, **28** 9, 549-556.

4. Gunnars, J., Wiklund, U. Determination of growth-induced strain and thermo-elastic properties of coatings by curvature measurements. *Mater. Sci. and Eng.*, 2002, A336, 7-21.

5. Lind, L., Adoberg, E., Aarik, L., Kulu, P., Veinthal, R., Abdel Aal, A. Tribological properties of PVD coatings with lubricating films. *Estonian Journal of Engineering*, 2012, **18**, 3, 193-201.
6. Klocke, F., Raedt, H.-W. Formulation and testing of optimized coating properties with regard to tribological performance in cold forging and fine blanking applications. *International Journal of Refractory Metals & Hard Materials*, 2001, **19**, 495-505.
7. Ollendorf, H., Schneider, D. A comparative study of adhesion test methods for hard coatings. *Surface and Coatings Technology*, 1999, **113**, 86–102.
8. Holmberg, K., Ronkainen, H., Laukkanen, A., Wallin, K., Hogmark, S., Jacobson, S., Wiklund, U., Souza, R.M., Ståhle, P. Residual stresses in TiN, DLC and MoS2 coated surfaces with regard to their tribological fracture behavior. *Wear*, 2009, 267, 2142-2156.
9. Hogmark, S., Jacobson, S., Larsson, M. Design and evaluation of tribological coatings. *Wear*, 2000, **246**, 20-33.
10. Sergejev, F., Peetsalu, P., Sivitski, A., Saarna, M., Adoberg, E. Surface fatigue and wear of PVD coated punches during fine blanking operation. *Engineering Failure Analysis*, 2011, **18**, 1689-1697.
11. Cao, C., Zhang, X., Wang, H. Analysis on residual stress in TiN coating with different thicknesses. *Applied Mechanics and Materials*, 2012, **217-219**, 1306-1311.
12. Matsue, T., Hanabusa, T., Kusaka, K., Sakata, O. Effect of heating on the residual stresses in TiN films investigated using synchroradiation. 2009, *Vacuum*, **83**, 585 -588.
13. Soroka, O.B., Klymenko, S.A., Kopeikina, M.Yu. Evaluation of residual stresses in PVD-coatings. Part 2. *Strength of Materials*, 2010, **42**, 4, 450-458.
14. Kõo, J. *Determination of residual stresses in coatings and coated parts*. Thesis of Dr. Sc. Eng., Tallinn Technical University, Tallinn, 1994.
15. Kõo, J., Valgur, J. Residual stress measurement in coated plates using layer growing/removing methods: 100th anniversary of the publication of Stoney's paper "The tension of metallic films deposited by electrolysis". *Mater. Sci. Forum*, 2011, **681**, 165-170.
16. Murotani, T., Hirose, H., Sasaki, T., Okazaki, K. Study on stress measurement of PVD-coating layer. *Thin Solid Films*, 2000, **377-378**, 617-620.
17. Yaldiz, C.E., Veinthal, R., Gregor, A., Georgiadis, K. Mechanical properties of hard coatings on TiC-NiMo substrates. *Estonian Journal of Engineering*, 2009, **15**, 4, 329-339.
18. Cartier M., Neale, M. J., Polak, T. A., Priest, M. *Handbook of Surface Treatments and Coatings*. The Cromwell Press, England, 2003.
19. Anderson, A. *ASM Metals Handbook. Volume 18: Friction, Lubrication and Wear*. ASM International, USA, 1995.
20. Klocke, F., Maßmann, T., Gerschwiler, K. Combination of PVD tool coatings and biodegradable lubricants in metal forming and machining. *Wear*, 2005, 259, 1197-1206.

9. ADDITIONAL DATA ABOUT AUTHORS

Harri Lille, Assoc. Professor, Cand Sc (Phys-Math), Estonian University of Life Sciences, Institute of Forestry and Rural Engineering, Kreutzwaldi 5, Tartu 51014, Estonia, E-mail: harri.lille@emu.ee, Phone: +372 7313181, Fax: +372 7313156.

9th International DAAAM Baltic Conference
"INDUSTRIAL ENGINEERING
24-26 April 2014, Tallinn, Estonia

THE EFFECT OF VC, TiC AND Cr_3C_2 ON THE MICROSTRUCTURE AND PROPERTIES OF WC-15Co HARDMETALS FABRICATED BY THE REACTIVE SINTERING

Pirso, J.; Juhani, K.; Tarraste, M.; Viljus, M. & Letunovitš, S.

Abstract: *Effect of different grain growth inhibitors, such as VC, Cr_3C_2, TiC and mixtures of them, on the microstructure and mechanical properties of WC-15wt%Co hardmetals were investigated. Hardmetals grades were produced by the reactive sintering, where the synthesis reaction of the carbide phase is combined with the solid and liquid phase sintering and takes place in situ during the same heating cycle. The simplex-centroid design for experiments method was used in present investigation to specify the influence of grain growth inhibitors.*

Keywords: WC-Co, reactive sintering, microstructure, mechanical properties.

1. INTRODUCTION

WC-Co hardmetals are widely us as cutting tools and wear resistant parts. The hardness and wear resistance can be improved by decreasing the WC grain size. The attainment of fine grained structures is difficult due to coarsening trend of the WC grains during sintering. In order to control the grain growth in the hardmetals, one key factor is the proper selection of the second-phase additives as grain growth inhibitors [1,2] In hardmetals produced by conventional technology, the grain growth inhibitors usually used are VC, Cr_3C_2, TaC, NbC and TiC [3,4]. VC and Cr_3C_2 are by far the most effective grain growth inhibitors in the WC-Co hardmetals due to their high solubility and mobility in the cobalt phase at lower temperatures. VC is more effective than Cr_3C_2 in preventing anomalous grain growth [1, 4-6]. It is well known that VC interacts with WC to form (W,V)C solid solution, while Cr_3C_2 dissolves in the binder as chromium and carbon [7]. TiC is less effective grain growth inhibitor, but there is no information, how TiC behaves together with VC and Cr_3C_2. Nowadays there is not information how the grain growth inhibitors influence on the microstructure and mechanical properties of WC-Co alloys consolidated by the reactive sintering, where the synthesis reaction of the WC is combined with sintering [8].

The main objective of this work was to investigate the effect of VC, Cr_3C_2, TiC and their mixtures on the microstructure and mechanical properties of WC-15wt%Co hardmetals fabricated by reactive sintering.

2. MATERIALS AND EXPERIMENTALS

Elemental powder mixtures W, Co, carbon black and grain growth additives VC, Cr_3C_2 and TiC were used for preparation of 85WC-15Co hardmetals. The calculated amount of graphite powder in initial tungsten powder was 6.4 wt%. To powder mixtures were added the grain growth inhibitors VC, Cr_3C_2, TiC and these mix in summary 0.8 wt%. In our experiments, graphite and alloying elements was added during the ball milling directly. The chemical composition of initial mixtures is

given in Table 1. The milled powder was dried and cold compacted under pressure of 80 MPa and reactive sintered in vacuum at 1400 ^{o}C during 30 min.

Table 1. Chemical composition (wt%) of reactive sintered 85(93,6W-6,4C)-15Co – 0.8X hardmetals.

Grade	W - C		VC	Cr_3C_2	TiC
1	93.6	6.4	0.8	0	0
2	93.6	6.4	0	0.8	0
3	93.6	6.4	0	0	0.8
4	93.6	6.4	0.4	0.4	0
5	93.6	6.4	0.4	0	0.4
6	93.6	6.4	0	0.4	0.4
7	93.6	6.4	0.33	0.33	0.33
8*	93.6	6.4	0	0	0
9 **	85 WC		0	0	0

8* - undoped

9**– commercial 85WC-15Co (Element X)

Vickers hardness measurements were made on polished sections of hardmetals using a 10 kgf load and 15 s dwell time.

Transverse rupture strength was determined in accordance with the ASTM Standard B406-95 by three-point method using the device “Instron 8516”.

The fracture toughness (K_{1C}) was determined by measuring the crack length from the tip of the indentation made by Vicker´s indention load of 30 kG (Palmqvist method). The toughness is calculated by the following equation [9].

$K_{iC} = 0.0726\ P/\ C^{3/2}$,

where P is load, N and C is half of diagonal + crack length, mm.

Abrasive - erosion tests were conducted by means of a centrifugal accelerator [10]. Quartz sand with particle size 0.1-0.3 mm was used as abrasive. The particles velocity was fixed at 80 m/s and attact angle 30^{o} in all case. Before and after testing, each specimen was weighed to an accuracy of 0.1 mg. The loss in weight (mg) was converted into volume loss (mm^3). The erosion rate (mm^3/kg) was determined as the specific volumetric erosion in cubic millimeter per kilogram abrasive.

3. RESULTS AND DISCUSSION

3.1 Microstructure

The formation and grain growth during reactive sintering are of great interest. The carbide shape in undoped reactive sintered grade has approximately the same shape and size as commercial fine-grained WC-15wt%Co hardmetals (Fig.1).

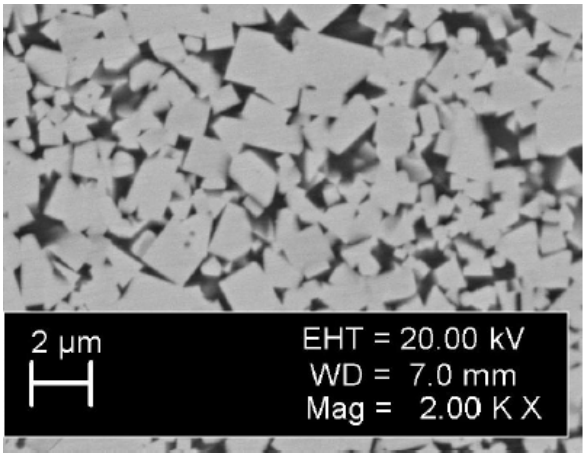

a)

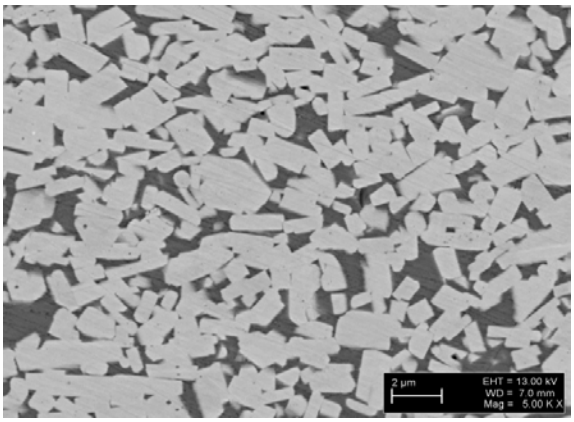

b)

Fig.1. Microstructure of WC-15w%Co hardmetals. a) Commercial, b) Reactive sintered.

The microstructures of doped hardmetals have a great contrast compared with undoped one (Fig.2a-g).

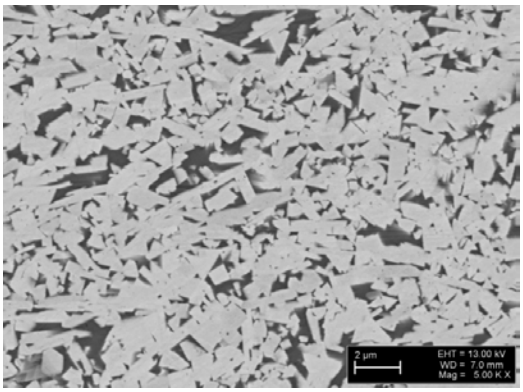

a)

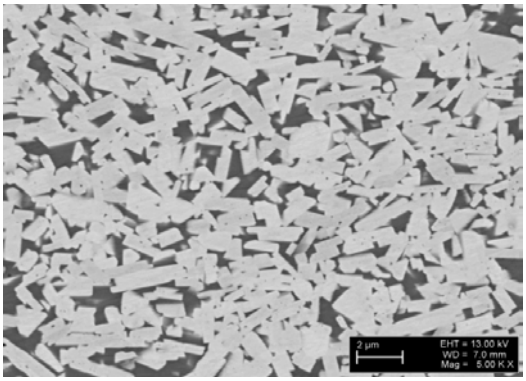

b)

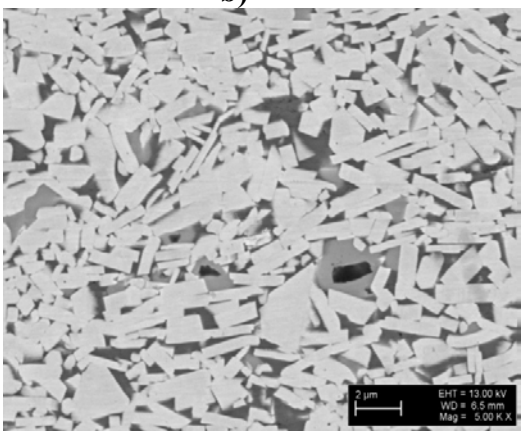

c)

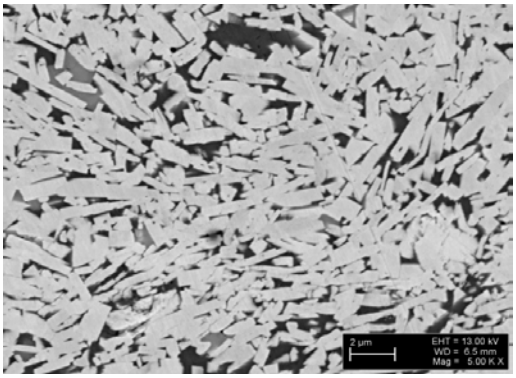

d)

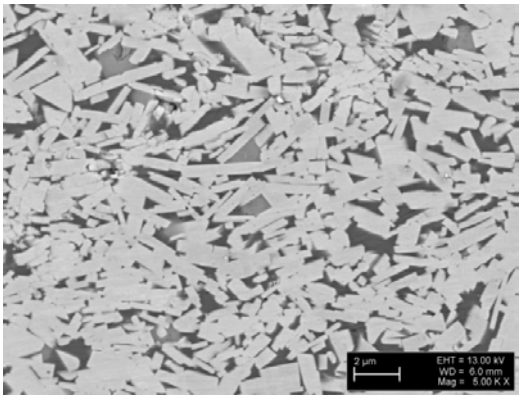

e)

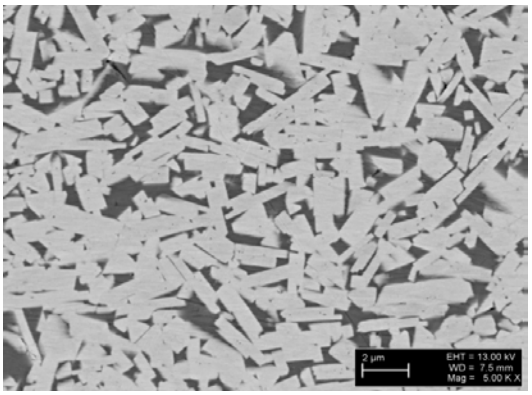

f)

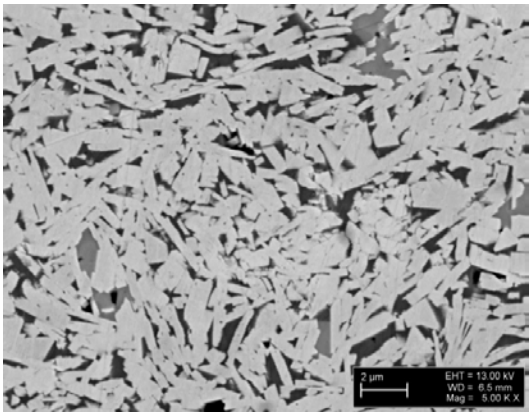

g)

Fig.2 Microstructure of doped reactive sintered 85WC – 15 wt%Co – X wt% hardmetals

a) 0.8 VC; b) 0.8Cr_3C_2; c) 0.8 TiC,

d) 0.4VC-0.4TiC; e) 0.4TiC-0.4Cr_3C_2;

f) 0.4VC-0.4Cr_3C_2; g) 0.33VC-0.33TiC-0.33Cr_3C_2.

The WC grain growth during vacuum sintering occurs by Ostwald ripening with dissolution of smaller WC grain and reprecitation on larger grains in liquid Co. Most of WC grains in the doped grades typically exhibit the shape of plate. The shape change and faceting of WC grains are indicative of rapid mass transport during sintering. As seen in Fig.2 the significant anisotropic WC grain growth occurred and large, thin trigonal plates were formed rather than equiaxed trigonal prisms. The formation of large WC crystals during sintering of ultrafine WC-Co alloys found also other authors [11-13].

3.2. Hardness´

Mechanical properties of doped and undoped reactive sintered WC-15wt%Co hardmetals are given in Table 2.

Table 2. Mechanical properties and erosion rate of undoped and doped WC-15wt%Co hardmetals.

Grade	HV10	TRS, MPa	Kic MPa $mm^{-1/2}$	E, mm^3/kg
1. VC	1457	1860	19.5	3.25
2. Cr_3C_2	1450	1290	13.1	2.14
3. TiC	1366	1190	15.0	3.3
4. VC/Cr_3C_2	1422	1250	18.1	1.25
5. VC/TiC	1488	2080	15.7	2.03
6. Cr_3C_2 /TiC	1492	2060	17.7	2.04
7. VC/TiC/Cr_3C_2	1473	1630	12.6	1.85
8. undoped	1420	2780	19.1	1.35
9. commercial	1264	2380	16.4	3.1

It is well-known that fine carbide grains hardmetals have a higher hardness compared to coarse grain ones with the same cobalt content. The hardness of reactive sintered undoped hardmetals is significantly higher than that commercial one (HV1420 and HV1264 respectively).It may be explain by somewhat finer microstructure of reactive sintered hardmetals and higher strength between carbide and binder phase.

The adding alloying carbide don´t change the hardness remarkably. Fig. 3 graphically summarizes the hardness in the WC-15wt%Co alloys with VC, TiC, Cr_3C_2 and their combination additions.

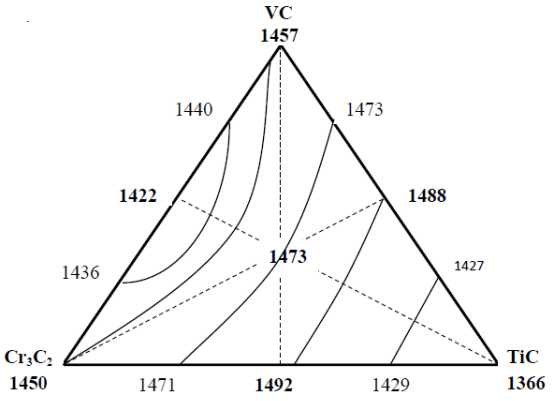

Fig.3. Vickers hardness (HV10) of doped reactive sintered WC-15wt%Co hardmetals Hardness of undoped reactive sintered hardmetal - HV1420 and commercial hardmetal - HV1264.

3.3 Transverse rupture strength (TRS)

When the grain growth inhibitors were added into the hardmetals, the TRS falls abruptly (Fig.4). It can be explained by

flatness structure of carbide grains.

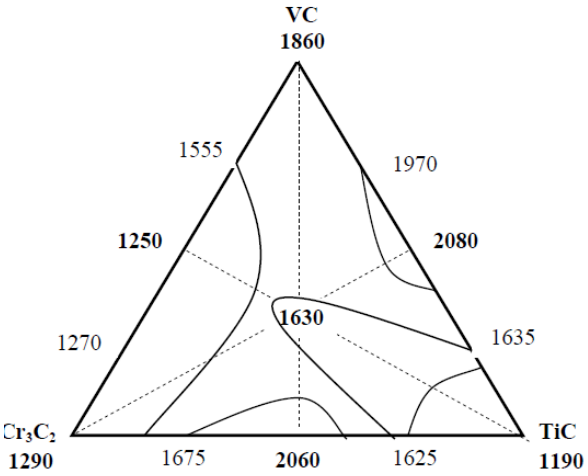

Fig.4.Transverse rupture strength of doped reactive sintered WC-15wt% Co hardmetals. TRS of undoped reactive sintered hardmetal - 2780 MPa and commercial hardmetal – 2380 MPa

3.4. Facture toughness

Fracture toughness of undoped reactive sintered hardmetals is higher than that of commercial one (19.1 and16.4 MPa $mm^{-3/2}$ respectively). The Kic of doped hardmetals is shown in Fig.5. As seen, K_{iC} of doped hardmetals as rule lower than that of undoped hardmetals. Most probably elongated WC grains fractured when the indenter intrude into the material.

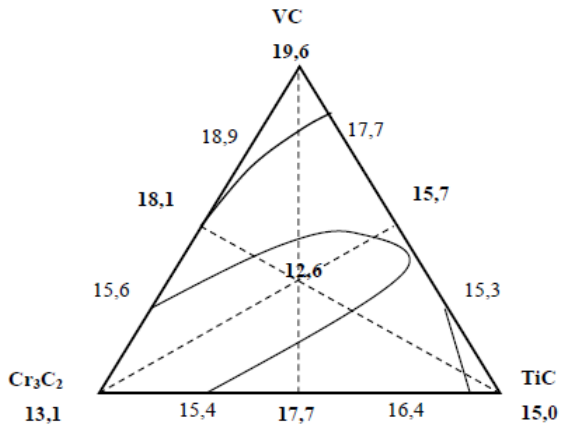

Fig.5. Fracture toughness of doped reactive sintered WC-15wt%Co hardmetals. K_{iC} of undoped reactive sintered hardmetal – 19.1 MPa $mm^{-3/2}$ and commercial hardmetal – 16.4 MPa $mm^{-3/2}$.

3.5. Abrasive erosion resistance

The abrasive erosion rate of undoped reactive sintered WC-15Co hardmetals was twice lower than that of commercial one (1.35 and 2.67 mm^3/ kg respectively). As seen in Fig.6, the erosion rate of doped hardmetals was higher than that of undoped hardmetals. Probably carbide grain shape give significant influence on the erosion rate. Elongated carbide grains break under abrasive particle impact priority compared with grains of equilateral shape.

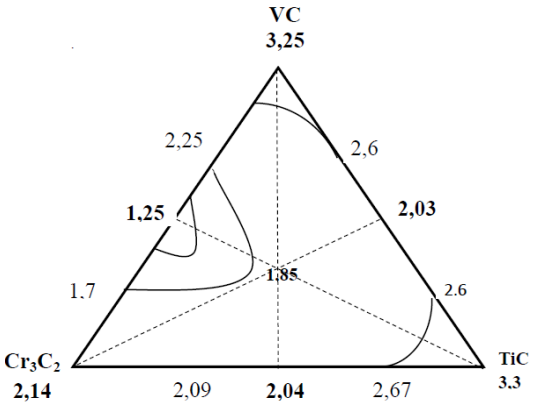

Fig.6. Abrasive erosion rate of doped reactive sintered WC-15wt%Co hardmetals. Erosion rate of undoped reactive sintered hardmetal – 1.35 mm^3/kg and commercial hardmetal –2.67 mm^3/kg.

4. CONCLUSIONS

A novel technology for production WC-Co hardmetals was under investigation, involving synthesis of WC during sintering *in situ*. The doped reactive sintered hardmetals carbide grains exhibits the shape plates.

The hardness, TRS and K_{iC} of undoped reactive sintered WC-15wt%Co hardmetals were 15-20% higher than commercial one. Transverse rupture strength and fracture toughness of doped reactive sintered

hardmetals is remarkably lower than that of undoped reactive sintered and commercial medium grade hardmetals. It may be explain by large WC grains plates in doped WC-Co alloys.

The erosion rate of undoped reactive sintered hardmetals is twice lower than that of the commercial hardmetals. It can be explain by somewhat finer microstructure and higher strength between carbide and binder phase. The erosion rate of doped reactive sintered hardmetals is same or higher compared with undoped one.

5. ACKNOWLEDGEMENT

This research was supported by the Estonian Ministry of Education and Estonian Science Foundation (T062 and IUT19-29).

6. REFERENCES

1 Sagandi, R.K.; McCandlish, LE.; Kerr, BH,.& Seegopaul.P. Grain growth inhibitors in liquid phase sintered nanophase WC/Co alloys. Int. J. Powder Met. 35 (1999) 27-33.

2. Huang, S.G.;.Li L,; Vanmeensel, K.; Van der Biest, O. & Vleuges, J. VC, Cr_3C_2, and NbC doped WC-Co cemented carbides prepared by pulsed electric current sintering. Int. J. of Refract. Met. & Hard Mater. 25 (2007) 417-422.

3. Luyckx, S. & Alli, M.Z. Comparison between V_8C_7 and Cr_3C_2 as grain refiners for WC-Co. Mater. Design 22(2001) 507-510.

4. Arenas, F.; de Arenas, I.B.;. Ochoa, J & Cho,S.-A. Influence of VC on the microstructure and mechanical properties of WC–Co sintered cemented carbides. Int. J. of Refract. Met.& Hard Mater.17(1999) 91-97.

5. Yamamoto T.; Ikuhara, Y. & Sakuma. T. High resolution transmission electron microscopy study in VC-doped WC-Co compound. Science and Tech. of Adv. Mater. 1 (2000) 97-104.

6. Zhu, L.H.; Huang,Q.W.& Zhao, H.F. Preparation of nanocrystalline WC-10Co-0.8VC by spark plasma sintering, J Mater Sci Lett 22 (2003) 1631-1633

6. Lin, C.; Kny, E.;Yuan, G. & Gjuricic, B. Microstructure and properties of ultrafine WC-0,6VC-10Co hardmetals densified by pressure-assisted critical liquid phase sintering. J.of Alloys and Compounds, 383 (2004) 98-102.

7. Upadhyaya, A.; Sarathy, D. & Wagner, G. Advances in alloy design aspects of cemented carbides. Materials and Design 22 (2001) 511-517.

8. Pirso, J.; Viljus,M.; Joost,R.,;Juhani,K. & Letunovitš,S. Microstructure Evolution in WC-Co Composites during Reactive Sintering From Nanocrystalline Powders. In the proceedings of the 2008 World Congress on Powder Metallurgy and Particulate Materials, June 8-12, Washington DC, USA;

9. Lawn, H.R. & Fuller, E.R. Equilibrium penny-like cracks in indentation fracture. J. Mater. Sci., 10 (1975) 2016-24.

10. Keis, I.& Kulu. P. Solid Particle Erosion. Occurrence, Prediction and Control, Springer 2008, 206 p.

11. Sommer,M.; Schubert, W.D.; Zobetz,E. &Warbichler, P. On the formation of very large WC crystals during sintering of ultrafine WC-Co alloys. Int.J. of Refrac. Met. & Hard Mater. 20 (2002) 41-50.

12. Allibert CH. Sintering feature of cemented carbides WC-Co processed from fine powders. Int. J. of Refrac. Met. & Hard Mater. 19 (2001) 53 – 61.

13. Wittmann B, Scubert W.D. Lux B. WC grain growth and grain growth inhibition in nickel and iron binder hardmetals. Int. J. Refract. Met. & Hard Mater. 20 (2002) 51-60.

7. CORRESPONDING ADDRESS

Kristjan Juhani. PhD.
Tallinn University of Technology.
Department of Materials Engineering
Ehitajate tee 5. 19086, Tallinn, Estonia
E-mail: kristjan.juhani@ttu.ee

9th International DAAAM Baltic Conference
"INDUSTRIAL ENGINEERING"-
24-26 April 2014, Tallinn, Estonia

INVESTIGATION OF BOILER MATERIALS WITH RELATION TO CORROSION AND WEAR: REVIEW

Priss, J.; Klevtsov, I. & Dedov, A., Antonov, M.

Abstract: *Elevated temperatures, oxidizing atmospheres and impacts by fluidized ash particles may cause significant degradation of some components in Circulating Fluidized Bed boilers [4]. The objective of presented research has been to investigate degradation process for some boiler steels in severe operation conditions and to rank investigated steel grades in these conditions. High temperature corrosion tests under impact of oil shale ash and tribotests have been used for research.*
Key words: boiler component, corrosion, wear, tribotests, analysis.

1. INTRODUCTION

Oil shale is the main energy source in Estonia. Around 90% of the electricity consumed in the country is produced from oil shale at the Narva Power Plants (NPP). The lower heating value (LHV) of oil shale used for electricity production is 8.3-8.4 MJ/kg [1]. Oil shale is a fuel with a high content of carbonate minerals. Burning that kind low-grade fuel is associated with several problems: dissociation of carbonate minerals, high CO_2 emission levels, ash handling and storing.

For minimizing the environmental impact of power production, the application of modern Circulating Fluidized Bed (CFB) technology at the NPP provides advantages in utilization of upgraded oil shale with the LHV at up to 11.0 MJ/kg [1].

Fluidized-bed combustion addresses to these challenges, like burning a wider range of fuels and generating power with improved thermal efficiency with low emissions compared to other existing combustion techniques.

However, conditions in fluidized-bed boilers (e.g., elevated temperatures, oxidizing atmospheres and impacts by fluidized sand and ash particles) may cause significant degradation of some boiler components, such as tubes of heating surfaces, by a combination of oxidative attack and erosive wear [4]. Scheme of CFB boiler in NPP is illustrated in Fig. 1.

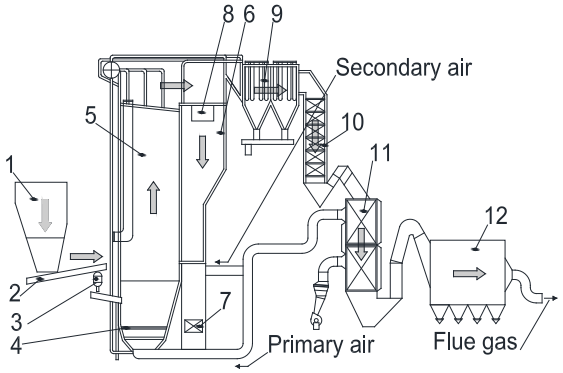

Fig. 1. Scheme of oil shale-fired CFB boiler (sample parts). 1-Raw fuel silo, 2-Fuel feeder, 3- Grate, 4- Secondary fuel crusher, 5- Furnace chamber, 6- Separating chamber, 7- Fluidized bed internal heat exchange (Intrex), 8- Separator of solids, 9- Convective superheater and reheater, 10- Economizer, 11- Air preheater, 12- Electrical precipitator [5].

2. MODES OF WEAR IN BOILER

According to previous studies it is well known that combustion products of Estonian oil shale highly accelerate the corrosion of the superheater tubes [17-19]. The main corroding ions are chlorides of alkaline metals, which cause the high corrosivity of combustion products of oil shale.

Erosion-corrosion process is a result of material wastage rates in waste incineration

systems and power generation industry. According to [2] convection pass tubes, such as superheater, reheater, and economizer tubes in fluidized bed boilers are suffering from fly-ash erosion (Fig.2). Major constitutes of the fly-ash are SiO_2, Al_2O_3, and Fe_2O_3. There is imposed limits for the flue gas velocities (12-13 ms^{-1} for erosive ash having high silica content and 18-20 ms^{-1} for less-erosive ash) to reduce the wear rates, but this also results in the drop of boiler efficiency.

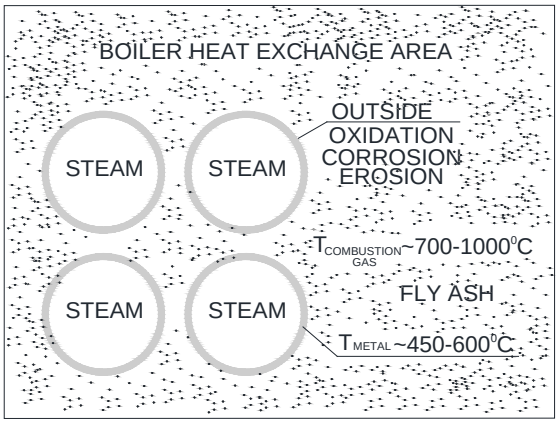

Fig. 2. Fireside corrosion and wear of boiler steels.

3. CORROSION AND TRIBOTESTS

In present research work high temperature corrosion (HTC) test and two tribotests: high temperature erosion (HTE) test, high temperature cyclic impact-abrasion (HT-CIA) test have been involved in process.
According to [3] tribotests could be classified by rising of the degree of realism (how closely they imitate the conditions of real application) as model test.
The model test usually involves standard test specimens and could be executed in short time (several minutes, hours). The test samples could be smaller than the real component and of simple geometry that makes higher the level of the conditions control. Model test enables to raise the level of tracking the corrosion- or tribosystem behaviour [3].

4. MATERIALS TESTED

In the present study, four different materials have been investigated in the HTE, HTC and HT-CIA tests. List of investigated steels is present in Table 1.

Grade	
(A) X12CrNiTi18-9	austenitic
(B) X10CrMoVNb9-1	martensitic
(C) 13CrMoV42	pearlitic
(D) TP347HFG	austenitic

Table 1. List of investigated steels.

Material A is an austenitic, heat-resistant steel 12X18H10T, equivalent grade is X12CrNiTi18-9 (DIN 17440). This steel has a high temperature resistant microstructure with a chromium content of 18% and additionally 10% of Ni, which improves the resistance against corrosion in reducing environments and stress corrosion cracking [9]. Additionally steel is alloyed by titanium (0.52%) to stabilize the carbon and the chromium in the matrix and increase the fracture toughness by precipitating intergranular TiC [10].
Material B is a chromium alloyed high strength martensitic steel 18Х12ВМБФР, equivalent grade is X10CrMoVNb9-1 (EN 10216-2) with increased creep resistance. At the chromium content of 9% and the added molybdenum (1.08%) the pitting and crevice corrosion resistance is increased [11-12].
Material C is a pearlitic steel 12Х1МФ, equivalent grade is 13CrMoV42 (DIN 17155) with a chromium content of 1.44%.
Material D is austenitic steel TP347HFG (ASTM 213). It has homogeneous structure in bimodal distribution of the grain size. In this material Nb is added to increase the strength and the resistance against different corrosive media [13].
The hardness have been measured at room temperature (RT), 100, 300, 500, 600, 700 and 800°C, respectively. Steels have an initial HV10 Vickers hardness of ~221(A);

235(B); 146(C); 180(D) at RT which is slowly declining with increasing temperature due to softening mechanisms, as seen in Fig. 3 [7].

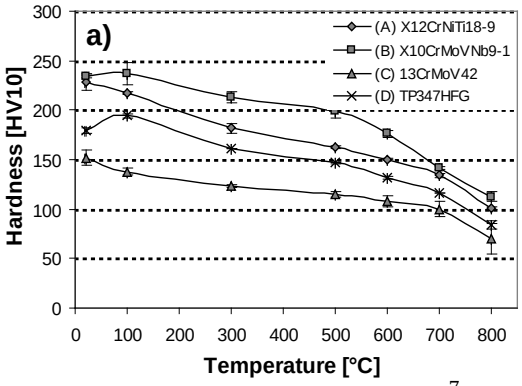

Fig. 3. Summary of hardness data [7].

5. EXPERIMENTALS AND RESULTS

5.1 High temperature corrosion test

Experiments have been performed at 500 °C and 600 °C with an exposure time of 24 h. The test conditions are presented in Fig.4. The samples were coated by manual brushing with a mixture of oil shale ash and ethanol for the optimal simulation of oil shale ash on-tube deposits for the corrosion tests. The tests have been carried out in the temperature-controlled horizontal tube furnace of the HTC test. For the experiments HCl was passed through the chamber at a velocity of 1.9 cm/s. The samples were positioned vertically and parallel to the flow direction. Before and after the test procedure the samples were weighed, determining the mass change for the calculation of the corrosion rates [6].

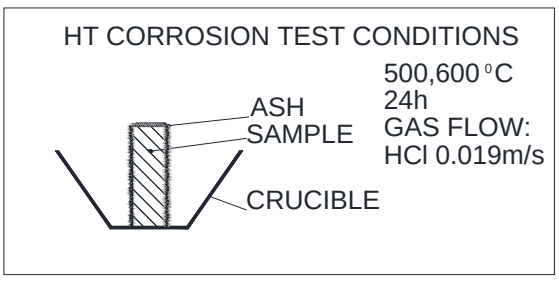

Fig. 4. The high temperature corrosion (HTC) test conditions.

Based on the test results following conclusions can be drawn, that the high temperature corrosion of different boiler steels is strongly dependent on the content of oxidation layer forming alloying elements, such as chromium and nickel.

The corrosion rate in presence of HCl in high temperature applications can be influenced by different other corroding anions, e.g. sulphate and potassium ions, presented in oil shale. Also oxidation cannot be neglected in corrosive environment at elevated temperatures [6].

Austenitic steel grades (materials A and D) and martensitic steel grade (material B) show better oxidation resistance against oxidation than the pearlitic steel grade (material C) [6].

Under HTC test conditions in HCl environment in presence of sulphur and potassium containing oil shale ash the best corrosion resistance shows austenitic steel grade X12CrNiTi18-9, then austenitic steel TP347HFG, pearlitic steel 13CrMoV42 and martensitic X10CrMoVNb9-1. That sequence represents the corrosion ranking of the tested steel grades for their application as high-temperature heating surfaces in boilers firing oil shale which contain chlorine, sulphur and potassium in outer deposits [6].

5.2 High temperature erosion test

Solid particle erosion tests have been performed in a conventional centrifugal four-channel accelerator (HTE) test. The abrasive particles used in this work were rounded silica particles.

"Investigation of steady state erosion rate was made as a function of the impact angle at the abrasive particles velocity of 80 m/s" [4]. Erosion tests were conducted at impact angles of 30° and 90°, respectively.

The duration of each erosive test was approximately 1 hour. In each test, 10 specimens of the size of 20x15x4.5mm were treated simultaneously. Parameters of the tests are presented in Fig. 5 [8].

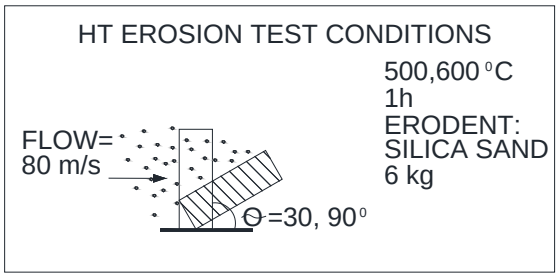

Fig. 5. The high temperature erosion test conditions.

The investigated materials show a change of the wear in the temperature range from 500 °C to 600 °C. Considering materials B, C and D volumetric wear rate for both tests increases with increasing temperature (Fig. 6, 7).

Opposite behavior can be detected for austenitic material A which exhibits better wear performance at higher testing temperature of 600 °C in test with impact angle of abrasive 30°. That may be explained by particle sticking [8].

Analyzing materials wear rate in respect to impact angle of abrasive particle influence, it should be mentioned that wear rate is lower with impact angle of 90° for materials investigated [8].

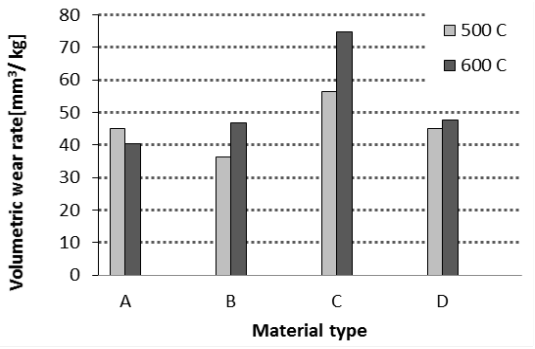

Fig. 6. Volumetric wear rate of materials at elevated temperatures under the impact angles of 30°, 80 m/s [8].

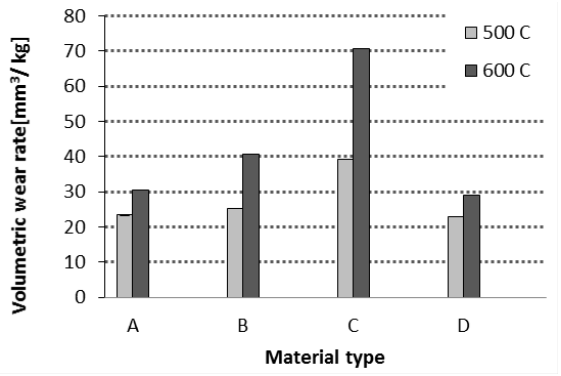

Fig. 7. Volumetric wear rate of materials at elevated temperatures under the impact angles of 90°, 80 m/s [8].

5.3 High temperature cyclic impact-abrasion test

Test principle is based on potential energy (0.8 J) which is cyclically turned into kinetic energy by free fall. Samples are fixed at 45° and are periodically hit by the plunger with 1.8-2.0 Hz frequency with a constant flow of abrasive (3 g/s, silica sand with particle size of 0.4-0.9 mm) between plunger and sample (Fig. 8) [14]. Tests were done at 500°C and 600°C. Wear was determined by mass loss and wear volume was calculated via materials density. The plunger material used for these tests was a Co-rich high-speed steel. Test duration was set constant to 1 h.

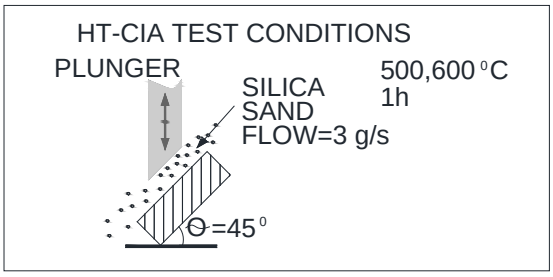

Fig. 8. The high temperature cyclic-impact abrasion test conditions.

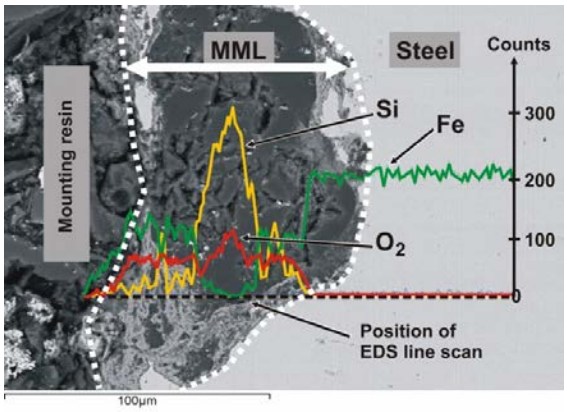

Fig. 9. SEM micrographs of typical worn surfaces of material B (martensitic X10CrMoVNb9-1) after cyclic impact/abrasion testing at 600 °C. Formation of mechanically mixed layer (MML) [7].

Wear under high temperature cyclic impact/abrasion strongly depends on the materials microstructure. Generally, the wear resistance decreases with increasing temperature due to different softening mechanisms for the investigated steels A, B and D.

Softer materials tend to incorporate abrasive particles in the surface and near-surface region by forming a mechanically mixed layer (MML) (Fig.9) [15-16] which can decrease the volumetric wear. Materials with higher initial hardness such as martensitic steels do not show this mentioned effect [7].

6. CONCLUDING REMARKS

Boiler steels ranking according to their resistance to high temperature corrosion does not agree with the ranking on the basis of tribotests.

Under HTC test conditions the best corrosion resistance shows austenitic steel grade (A) X12CrNiTi18-9, than are going austenitic steel (D) TP347HFG, pearlitic steel grade (C) 13CrMoV42 and martensitic (B) X10CrMoVNb9-1.

In order to compare the behaviour of steels the wear rate map was created (Fig.10, 11).

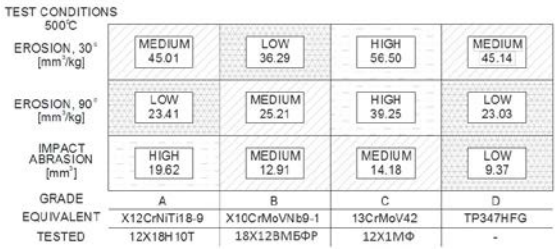

Fig. 10. Wear rate map of studied steels under at 500 °C.

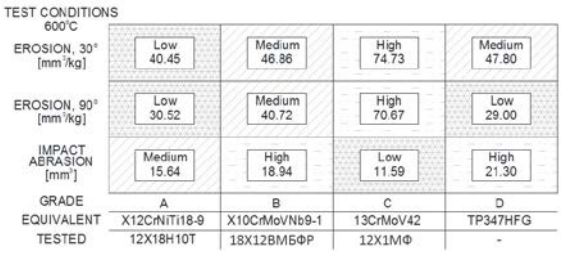

Fig. 11. Wear rate map of studied steels under at 600 °C.

7. REFERENCES

1. Plamus K., Ots, A., Pihu, T., Neshumayev, D. Firing Estonian oil shale in CFB boilers- ash balance and behavior of carbonate minerals. *Oil Shale*, 2011, vol. **28**, No.1, pp.58-67.

2. M.Antonov, M., Veinthal, R., Huttunen-Saarivirta, E., Hussainova, I., Vallikivi, A., Lelis, M., Priss, J. Effect of oxidation on erosive wear behaviour of boiler steels. *Tribo-Corrosion* 2013, **68**, 35-44.

3. Antonov, M., Michalczewki, D., Pasaribu, R., W.Piekoszewski, W. Comparison of tribological model and real component test methods for lubricated contacts. *Estonian Journal of Engineering*, 2009, **15**, 4-349-358.

4. Huttunen-Saarivirta, E., Antonov, M., Venthal, R., Tuiremo, J., Mäkelä, K., Siitonen, P. Influence of particle impact conditions and temperature on erosion-oxidation of steels at elevated temperatures. *Wear*, 2011, vol. **272**, pp.159-175.

5. Neshumayev, D., Ots, A., Parve, T., Pihu, T., Plamus, K., Prikk, A. Combustion

of Baltic oil shales in boilers with fluidized bed combustion. *Power technology and Engineering*, 2011, vol. **44**, No.5.

6. Priss, J., Rojacz, H., Klevtsov, I., Dedov, A., Winkelmann, H., Badisch, E. High temperature corrosion of boiler steels in hydrochloric atmosphere under oil shale ashes. *Corrosion Science*, 2014, vol. **82**, 36-44.

7. Priss, J., Klevtsov, I., Dedov, A., Antonov, M., Rojacz, H., Badisch, E. High temperature cyclic impact/abrasion testing of boiler steels. *Key Engineering, Materials*, 2014, vol. **604**, 289-292.

8. Priss, J., Klevtsov, I., Dedov, A., Antonov, M. Erosion wear testing of boiler steels at elevated temperatures. Proceeding of the 14th International Symposium *„Topical Problems in the Field of Electrical and Power Engineering"* Pärnu, Estonia, January 13-17, 2014, 248-250.

9. Bose, S. High Temperature Coatings, Butterworth-Heinemann, Oxford, 2007.

10. Kim, J.K., Kim, Y.H., Lee, J.S., Kim, K.Y. *Corros. Sci*., 2010, **52**, 1847-1852.

11. Ilevbare, G.O., Burstein, G.T. *Corros. Sci*., 2001, **43**, 485-513.

12. Wanklyn, J.N. *Corros. Sci*., 1981, **21**, 211-225.

13. Nam, N.D., Kim, J.G. *Corros. Sci*., 2010, **52**, 3377–3384.

14. Badisch, E., Katsich, C., Winkelmann, H., Franek, F., Manish, R. Wear behaviour of hardfaced Fe-Cr-C alloy and austenitic steel under 2-body and 3-body conditions at elevated temperature. *Tribology International*, 2010, **43**, 1234-1244.

15. Varga, M., Rojacz, H., Winkelmann, H., Mayer, H., Badisch, E. Wear reducing effects and temperature dependence of tribolayer formation in harsh environment. *Tribology International*, 2013, **65,** 190-199.

16. Antonov, M., Hussainova, I., Pirso, J., Volobueva, O. Assessment of mechanically mixed layer developed during high temperature erosion of cermets. *Wear*, 2007, **263**, 878–886.

17. Tallermo, H., Lausmaa, T., Klevtsov, I., Nuutre, M. The influence of chlorine in ash deposits on 12Cr1MoV alloy high temperature corrosion. - *Oil Shale*, 1997, vol. **14**, No. 3, pp. 307-316.

18. Klevtsov I., Tallermo H., Bojarinova T., Lausmaa T., High Temperature Corrosion Resistance of the Austenitic Steels in the Presence of Chlorine-Containing On-Tube Deposits. *Oil Shale*, 2003, vol. **20**, No. 4, pp. 501-509.

19. Tallermo H., Klevtsov I., Bojarinova T., Dedov A. Laboratory tests of high-temperature corrosion of steels B-407, X8CrNiNb1613 and X8CrNiMoNb1616 under impact of ash formed at pulverized firing of oil shale. *Oil Shale*, 2005, vol. **22**, No. 4, pp. 467-474.

6. ADDITIONAL DATA ABOUT AUTHORS

1) MSc. J. Priss, Prof. I.Klevtsov, Ph.D A. Dedov. Ph.D M.Antonov.
2) Compeering analysis of boiler materials according to tribotests.
3) Professor / Ivan Klevtsov
/klevtsov@staff.ttu.ee/
Ph.D / Andrei Dedov / dedov@staff.ttu.ee
Ph.D / Maksim Antonov /
maksim.antonov@ttu.ee
MS.C / Jelena Priss/
jelenapriss@gmail.com
4) Corresponding Author: (Jelena Priss, jelenapriss@gmail.com)

9th International DAAAM Baltic Conference
"INDUSTRIAL ENGINEERING -
24-26 April 2014, Tallinn, Estonia

EFFECT OF REDUCING ON THE MECHANICAL PROPERTIES OF COLD DRAWN TUBES

Ridzon, M.; Bilik, J. & Kosik, M.

Abstract: *The article describes the effect of reducing the mechanical properties of cold-drawn tubes. The aim of the experiment is to determine the mechanical properties of steel tubes cold drawn single-run three-draw technology. Tube drawing is without interpass recrystallization annealing. Recrystallization annealing serves for recovery of the plastic properties of materials. The experiment is part of the total experiment, which should show whether is possible economically take advantage of the technological process of tube drawing cold. Technological parameters are: finish temperature, deburring of tube ends, reduction determining dimensions of forming tools, optimal chemical treatment, speed of forming on draw benches, and the method of tube drawing. Mechanical properties of the formed material are also important when designing and construction of forming tools and in establishment of their useful life.*
Key words: reduction, recrystallization annealing, drawing of tube, mechanical properties

1. INTRODUCTION

Static tensile test is a basic mechanical test originally designed to become the most widespread and known testing method for evaluating the mechanical properties of metallic and non-metallic construction materials. It comes from observations that tensile stress can damage every kind of material (divided into an even number of friction areas), while pressure causes damage only by fragile materials. The law of geometrical similarity is kept with one-axis draw load for geometrically similar prismatic testing bodies with different sizes. The test is prescribed with the norm of STN EN 10002-1 [1].

A testing sample can help to determine four standard basic mechanical properties: tensile strength in draw, yield strength, ductility, and contraction. Data measured of testing machine, experimental diagram of tensile test, as well as the dimensions of the testing rod before and after the test are bases for evaluating the tests. The following stress characteristics are measured for the construction materials used in tube drawing: yield strength in draw R_e or yield strength in draw $R_{p0,2}$, tensile strength in draw R_m, ductility A_5 (1). *Tensile strength in draw* R_m is defined as a load when there is a loss of plastic deformation, and it is calculated as the rate of maximal load F_m [N], and the original cross-section of the testing bar in the middle part before the test S_0 [mm^2].

$$R_m = \frac{F_m}{S_0} \text{ [MPa]} \quad (1)$$

Yield strength in draw R_e is defined as the lowest load when there are permanent deformations. Where F_e is a force on a limit of yield strength [N] and S_0 is an original cross-section of the testing bar in the middle part before the test [mm^2]

$$R_e = \frac{F_e}{S_0} \text{ [MPa]} \quad (2)$$

Ductility A_5*:* is the permanent relative lengthening after breaking (expressed as a percentage). Where ΔL is the absolute lengthening [mm], L_u is the length after breaking of the testing bar [mm], and L_0 is

the original measured length of the testing bar before test [mm]

$$A = \frac{\Delta L}{L_0}.100 = \frac{L_u - L_0}{L_0}.100 \quad [\%] \qquad (3)$$

Vickers Hardness Test: The test is based on pressing of a diamond, regular four-sided pyramid with a top angle of 136° onto the tested material. The force effects are in the vertical direction on the surface of the tested body. Hardness, according to Vickers, is labelled HV and it is defined with a rate of force F to the surface of impress S. Vickers hardness is labelled as *HV* and it is calculated as:

$$HV = \frac{0{,}189F}{u^2} \qquad (4)$$

where F is the force *[N]* and u is the diagonal of impress *[mm]* expressed as a middle value [2].

2. DESCRIPTION OF THE EXPERIMENT

The experiment material was unalloyed construction steel of the class E235 (STN EN 11353) and E355 (STN EN 11523) used to produce tubes by warm rolling (with diameter ∅ 70 x 6.3). The properties of steels used for certain experiments are mentioned in Table 1. Drawing of tube ∅ 70 x 6.3mm to a new diameter ∅ 44 x 3mm was made in dependence on a three-draw single-run technology without application of interoperation recrystallization annealing. The resulting reduction of the three-draw single-run technology for both of materials is 69.35 %. Principle of tube drawing on mandrel is illustrated in Fig. 1 [2].

Table 1. Properties of steel STN 411353, E235 and STN 411523, E355

ČSN 411353 STN 411353	Non-alloyed structural fine grain steel		STEEL 11 353
Chemical composition [hm.]			
C [%]	P [%]	S [%]	P+S [%]
max. 0.18	max. 0.050	max. 0.050	max 0.090

ČSN 411523 STN 411523	Non-alloyed structural fine grain steel				STEEL 11 523
Chemical composition [hm.]					
C [%]	Mn [%]	Si [%]	P [%]	S [%]	N [%]
max 0.20	max 1.60	max 0.55	max 0.040	max 0.040	max 0.009

Fig. 1 Principle of tube drawing on mandrel

Drawn tubes can further be formed, for example. technological process - hydroforming. Hydroforming is a method of cold plastic deformation and refers to changes a semi-tubular shape, with the introduction of internal fluid pressure acting directly on the work piece. So, in this way, we can get to the desired shape in only one operation. [3,4]

3. EVALUATION OF THE EXPERIMENT

The basic norm which is decisive for mechanical test of tubes – a basic tensile test (STN EN 10002-1) – is STN EN 10305-1, and it defines the minimal value of tensile strength R_m and ductility A_5. The norm STN EN 10305-1 specifies the required mechanical values for material E235 +C (abbreviation +C means: no thermal treatment after the last cold forming) and these are: R_m minimum 480, MPa and A_5 minimum 6 %, for material E355 +C (abbreviation +C means: no thermal treatment after last cold forming), R_m is minimum 640MPa, and A_5 min 4 %. The final measured values of strength and

the ductility for materials E235 and E355 in dependence on a three-draw single-run technology, without interoperation annealing, are in accordance with the norm STN EN 10305-1. The input material E235 has tensile strength R_m=424MPa and ductility A_5=38.4 % and material E355 has tensile strength R_m=545MPa and ductility A_5=24.3 %. The biggest increase of tensile strength R_m and the biggest decrease of ductility A_5 are obvious after the first draw in a three-draw single-run technology. The reason is that the reduction was higher than in the first draws compared to the other following draws. In Table 2 there are mentioned the mechanical properties of drawn tubes of the formed experimental material E235 and E355 after the second and third draw. The norm STN EN 10305-1 does not show an appropriate value of hardness, so a final minimum hardness for material E235 150 HV and for material E355 200 HV was determined with an indirect method and with minimal tensile strength R_m. The application of this method helps to state that the final measured hardness after the third draw correlates with the required hardness. Based on ductility A_5, tensile strength R_m and hardness HV it can be said that the experiment material E235 and E355 fulfils the requirements of the norm STN EN 10305-1 for settled reductions R and for the suggested technology of tube drawing, and there was no destruction of experimental material from the visual side. The material E355 gained higher values of ductility A_5, tensile strength R_m, and hardness HV than material E235. It is caused by the chemical content of the material.

Table 2. Mechanical properties of drawn tubes experiment material E235 and E355 in dependence on a particular technology and reduction size after draws

Material E235			
	3-draw single-run technology Φ70x6.3 --> Φ44x3 mm		
	Resulting reduction = 69.35		
	Rm [MPa]	**A_5 [%]**	**hardness [HV]**
Rolled tube Φ70x 6.3 mm	424	38.4	108.3
1. draw	651	12.8	162.5
2. draw	736	9.93	182.2
3. draw	776	10.8	183.7
Material E355			
	3- draw single-run technology Φ70x6.3 --> Φ44x3 mm		
	Resulting reduction = 69.35		
	Rm [MPa]	**A_5 [%]**	**hardness [HV]**
Rolled tube Φ70x 6.3 mm	545	24.3	133.7
1. draw	763	8.16	190.3
2. draw	875	7.24	219.7
3. draw	928	5.9	222.3

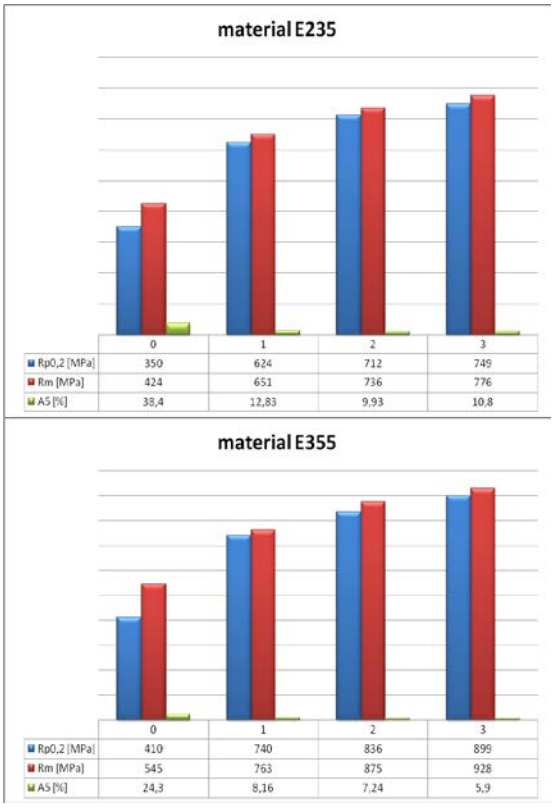

Fig. 3. Mechanical properties of drawn tubes according to the norm STN EN

10002-1 (basic tensile test), material E235 and E355

4. CONCLUSION

The main task here was research of the technological parameters influencing production and properties of steel tubes. The selected technological parameters must follow a product quality defined by ISO norms. These technological parameters are: finish temperature, deburring of tube ends, reduction determining dimensions of forming tools, optimal chemical treatment, speed of forming on draw benches, and the method of tube drawing. The mentioned parameters influence the mechanical as well as the structural properties of steel tubes. Therefore the basic part of the experimental evaluation is focused on the properties of steel tubes, concretely mechanical tests – basic tension test according to the STN EN 10002-1, Vickers hardness test STN EN ISO 6507-1. The measured mechanical values are up to the standard of requirements for the STN EN 10305-1 norm.

The experiment was based on testing of the drawing of a rolled tube with a three-draw single-run technology without interoperation recrystallization annealing. The experiment was processed with a rolled tube from materials E235 and E355, which is a standard non-alloy construction steel. The input dimension of the tube was ∅ 70 x 6 mm.

5. CORRESPONDING ADDRESS

[1,a] Martin Ridzoň, PhD., [2,b] Associate Professor Jozef Bílik, PhD., [3,c] MSc Miroslav Košík (PhD student), [1,2,3] Slovak University of Technology in Bratislava, Faculty of Material Sciences and Technologies in Trnava, Institute of Production Technologies, Bottova 25, 917 24, Trnava, Slovak Republic, www.mtf.stuba.sk

E-mails:
[a]martin.ridzon@stuba.sk,[b]jozef.bilik@stuba.sk, [c]miroslav.kosik@stuba.sk

6. REFERENCES

1. Martinkovic, M., Žubor, P. *Mechanical tests and materiology*. Bratislava: STU 2005. ISBN 80-227-2178-6

2. Ridzoň M., (2012), *The Effect of Technological Parameters Influencing the Properties of Seamless Cold-Drawn Tubes.* - 1. ed. – (Hochschule Anhalt, Köthen). 89 p. (Scientific monographs).

3. Ceclan, V.A., Grozav, S. D., Sabau, E., Popan, A.I., Borzan, C.S.: Structural analysis of tubes hydroforming. *Annals of MTeM for 2013 & Proceedings of the 11th International Conference Modern Technologies in Manufacturing*, ISBN 973-9087-53-1, s. 31-34. In: Academic Journal of Manufacturing Engineering. - ISSN 1583-7904. - Vol. 11, Iss. 3 (2013), s. 56-59.

4. Balážová, M., Matis, Ľ., Klenotičová, A., Brziak, P., Bílik, J.: Formability evaluation of bimetal using physical simulation. - registered: Web of Science. In: *METAL 2012: 21st International Conference on Metallurgy and Materials*. May 23rd-25th 2012, Brno Czech Republic. - Ostrava : TANGER s r.o, 2012. - ISBN 978-80-87294-29-1. - CD-ROM, s.[1-6]

9th International DAAAM Baltic Conference
INDUSTRIAL ENGINEERING
24-26 April 2014, Tallinn, Estonia

MECHANICAL PROPERTIES OF CONNECTING FITTINGS FOR PLYWOOD FURNITURE

Saar, K.; Kers, J.; Luga, Ü. & Reiska, A.

The main objective of the current study is to find the best detachable fitting for plywood furniture. In this study, connecting fittings of different type are tested under failure loads. Both tensile and bending test conditions were used. The test specimens are made from 21mm thick birch plywood. Different fittings like Lamello AG products Clamex P 10, Clamex P 15 and Invis Mx [1], and minifix [2] connectors were used in designing of joints in this study. The test results showed that the Invis Mx takes the highest average strength value in tensile and bending tests. Based on test results the best fitting for connecting plywood boards was selected.
Keywords: detachable furniture fittings, Clamex P, Invis Mx, mechanical properties, plywood

1. INTRODUCTION

Plywood is a common material to be used in the furniture industry. Estonian furniture manufacturers have widely adopted ready-to assemble (RTA) or manufacturing systems to increase their export of furniture to European countries. To export the product to abroad the assembly must be done by the client. Therefore glued joint is not an option, because the client may not have the tools for compressing as well as the knowledge and skills. The assembly has to be simple and handy, but also look aesthetically pleasing. The trend in the industry is towards the use of large proprietary minifixes (see Figure 1d) and dowels that have been specially designed for use with wood-based materials in point of assemble and disassemble [3]. But when using minifixes the cam part remains visible. The cam can be covered with a cap, but the cap may change the appearance of the furniture. Therefore the aim of this study is to test the bending and tensile strength of detachable furniture fittings that have no opening (Invis Mx – see Fig. 1c) or connection has small visible opening on inside face of furniture. Lamello AG products Clamex P10 (see Fig. 1a), Clamex P15 (see Fig. 1b) and Invis Mx fittings satisfy those requirements. Based on several recent studies [3, 4, 5, 6], bending and tensile test were conducted. The bending and tensile tests results of above mentioned fittings are compared with the most commonly used minifix fitting.

2. MATERIALS

2.1 Plywood

Plywood of 21mm thickness was used in tests. The bending test specimens were cut out from 1525x1525mm board. The bending tests specimens consisted of two 250x200mm plywood boards connected with two dowels on the side and the tested furniture fitting in the middle. No glue was added to the dowels in joint [4]. The joint was formed as a butt joint end to end without overlapping.
The tensile test specimens were cut of the remaining plywood from the bending test specimens. The tensile test specimens consisted of two plywood 200x98mm

boards and the connecting fitting. The joint formed was a flat end butt joint.

2.2 Fittings

In this study Lamello AG products Clamex P 10, Clamex P15 and Invis Mx, and minifix fittings were used (see Fig 1). In the bending test two multi-groove beech dowels 8 mm in diameter and 34 mm in length were used with the studied fitting.

Clamex P 10 (Fig. 1a) and Clamex P 15 (Fig. 1b) are oval biscuits shape connectors with a lateral ridge. The shell is made from fibreglass reinforced plastic and zinc die cast lever. Compared to Clamex P-15, Clamex P-10 possesses a shallower installation depth of just 10 mm and is therefore used for smaller material thicknesses. For Clamex P 10 the minimum material thickness is 13mm for corner joints and 16mm for mitre joints. For Clamex P 15 the minimum material thickness is 13mm for corner joints and 19mm for mitre joints. The insertion of the fitting to the groove is quick and tool-free. The connecting fittings can be removed from the profile groove for surface treatment without causing wear. The ridges on the sides of the fittings ensure that they stay in the groove, even when transporting parts with pre-fitted P-System fittings. Since the connectors are not secured with screws, they can move within the groove, allowing perfectly flush alignment of the work piece. P-System fittings can be used for virtually any angle. The groove is always positioned at a 90 degree angle to the joint. The positioning pins prevent twisting without the need for additional dowels. For closing a standard 4 mm hexagon key is needed to close the joint.

Invis Mx (Fig. 1c) is a magnet-driven connection fitting with no visible opening when the joint is connected. It consists of metal connector with a thread and a stud that is screwed into prepared 12mm holes of the joint. A rotating magnetic field is created with special jig (Fig.1e) that drives the connector thread just as one cogwheel drives another. The thread on the connector screws into the internal thread of the stud, driven by the contact-free magnetic field. The jig is then fixed to the cordless drill and rotated on the surface to close the connection. To open the connection, simply change the drill direction. The manufacturer offers multiple connector and stud lengths that can be combined. In this study 29mm length connector and 13.5 mm stud is used.

Minifix (Fig. 1d) joints consist of cam and bolt with a plastic plug. The bolt with

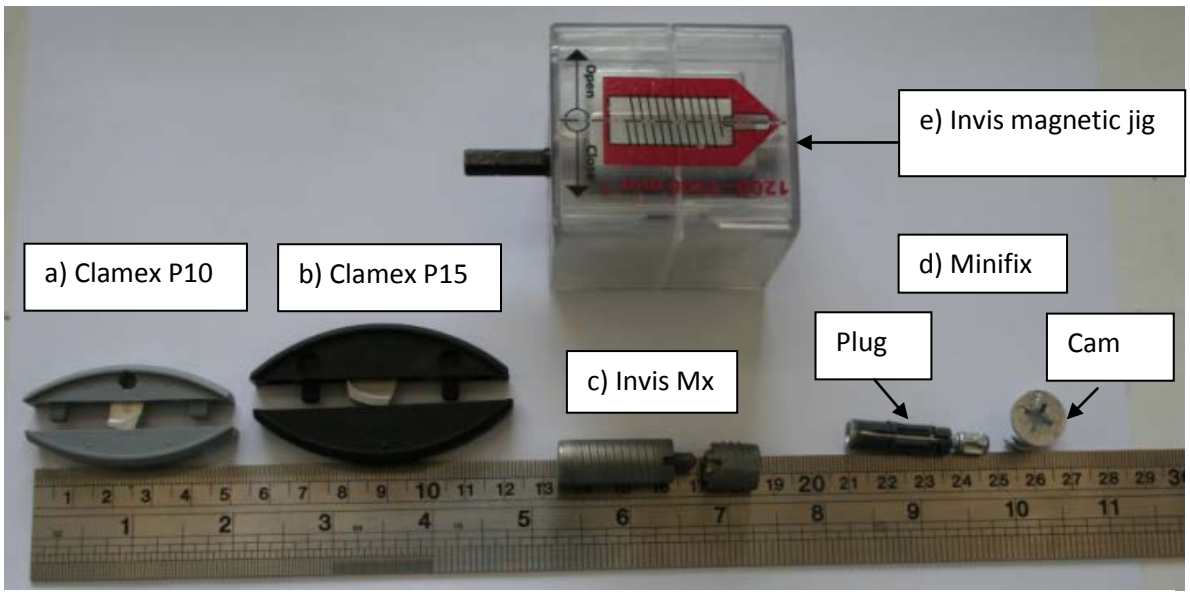

Figure 1. Furniture fittings.

a plastic plug was struck into the plug holes on the face member using a hammer. Cams were placed into holes on the butt member. Lastly, after face and butt members were placed in conjunction, cams were tightened using a screwdriver.

3. METHODS

3.1 Specimen preparation

For the bending test all the specimens were prepared with CNC machining. Into each specimen two Ø8mm diameter and 20mm depth holes were drilled with a Homag Weeke BHC280 CNC machine.
Both Clamex P 10 and Clamex P 15 fitting grooves were processed with Zeta P2 profile biscuit jointer [1]. The jointer has an oscillating motion that is seen on Figure 2.

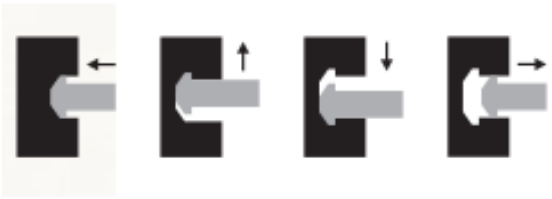

Figure 1. Oscillating motion [1]

As mentioned earlier the differents between the Clamex P 10 and Clamex P15 is the cutting depth. The cutting depth of Clamex P10 is 10mm and Clamex P 15 is 15mm. On one side of the specimen a Ø6mm hole is drilled for closing the joint.
For Invis Mx one Ø12mm hole is drilled on both sides of the specimen. The depth of the connector hole is 30mm and depth for the stud hole is 15mm. The holes are drilled with Homag Weeke BHC280 CNC machine to get accurate drilling. The dimensions are given in Figure 3a.
The minifix holes were drilled with Homag Weeke BHC280 CNC. The

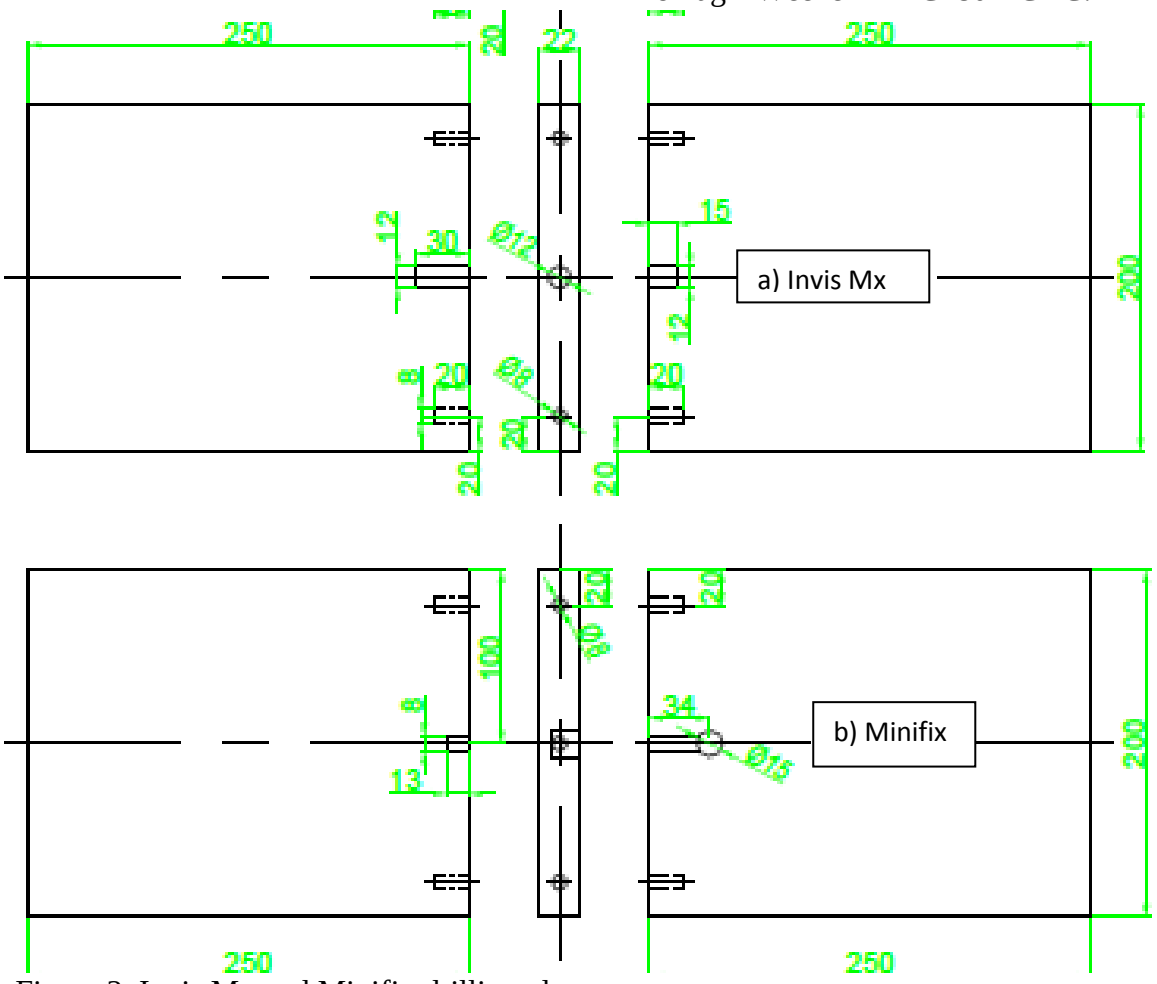

Figure 2. Invis Mx and Minifix drilling plans.

outside dimensions of the drilled holes and location are given in Figure 3b.

3.2 Testing procedures

A three point bending test was conducted. 3-point bending tests were performed by using electro-mechanical testing system Instron 5866 (PV005688) equipped with Bluehill software. The dimension of the bending test specimens are shown on Figure 3. Load was applied to each specimen until some separation occurred between face and butt members. The load and displacement graphs were plotted by a computer for all tests. The tests were carried out at room temperature of 20°C with a 10kN loading capacity on testing machine Instron at a speed of 50 mm/min.

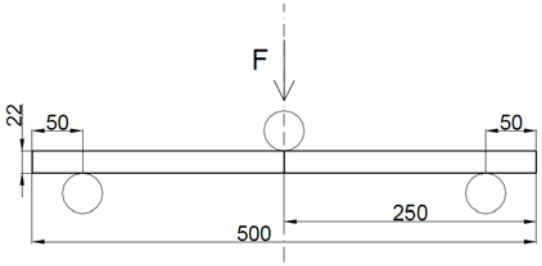

Figure 3. Bending test scheme

In the tensile test the specimens were fixed on the testing machine with two metal brackets. The specimens were connected to the brackets with a bolt on each bracket. Load was applied to each specimen until some separation occurred between face and butt members. The load and displacement graphs were plotted by a computer for all tests. The tests were carried out at room temperature of 20°C with a 10kN loading capacity Titus Olsen testing machine at a speed of 2mm/min.

4. RESULTS AND DISCUSSION

4.1 Failure load

The failure load obtained from bending and tensile test are given in Tables 1-2. The tension failure load was greater than the bending failure load of all joints. The standard deviation was higher in tensile tests. In bending test Invis Mx obtained the highest maximum test load. On the other hand Minifix had the lowest strength in both cases. Invis Mx compared to Minifix can bear 48% less bending load. Although the standard deviation was lower than that of Invis Mx. Clamex P 15 has better mechanical properties than Clamex P10. In the bending test Clamex P 15 can withstand 24% more force and the standard deviation of test results was 3 times smaller.

In the tensile test Invis Mx was withstanding the highest tensile force. Invis Mx also achieved the lowest standard deviation. In the tensile test Clamex P 15 can bear 50% more load and the standard deviation was twice lower, compared to Clamex P 10. Minifix resisted indisputably the lowest tensile load. Minifix´s average tensile load was 141N which was only 7% of Invis Mx strength. The standard deviation was lower than Clamex P10 and P 15 but higher than Invis Mx.

Bending [N]				
	Clamex P10	Clamex P15	INVIS	Minifix
1	196	262	254	147
2	179	248	322	165
3	195	267	295	158
4	221	257	316	162
5	148	259	318	156

Tabel 1. Bending test results at maximum loads.

Tension [N]				
	Clamex P10	Clamex P15	INVIS	Minifix
1	928	1812	1870	138
2	898	1748	1912	78
3	919	1844	1934	106
4	958	1880	1864	157
5	587	1656	1934	228

Tabel 2. Tensile test results at maximum loads.

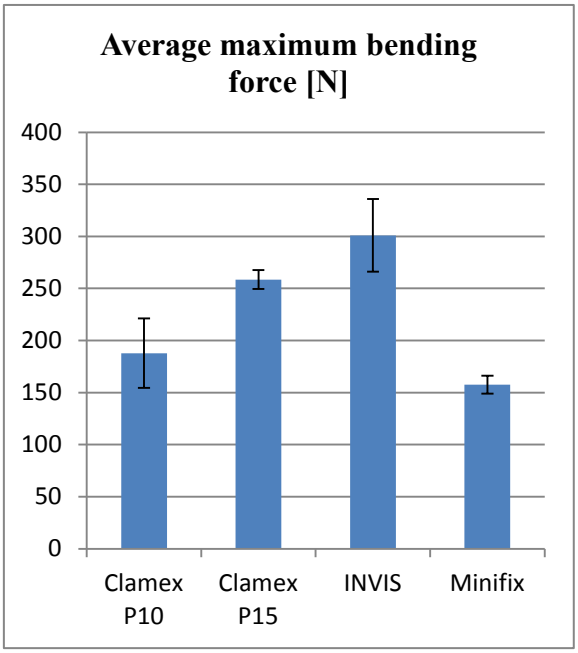

Figure 4. Maximum load of bending test.

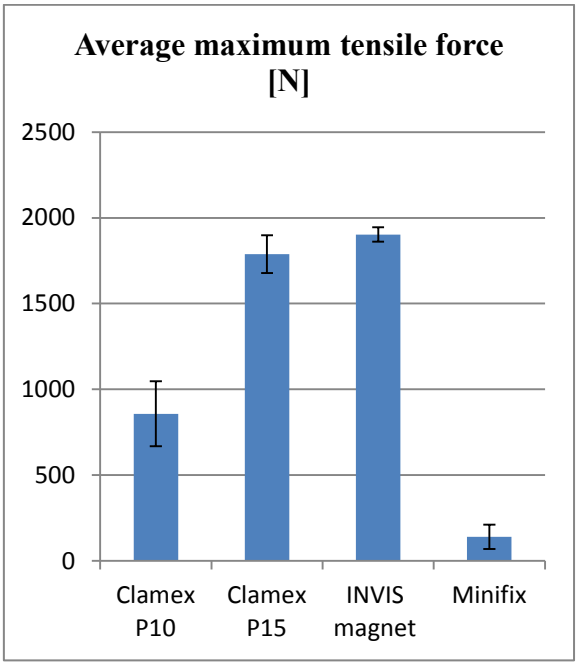

Figure 5. Maximum load of tensile test.

4.2 Failure modes

Both Clamex P fittings failed from the fibre reinforce plastic anchorage. In the bending test the anchorage broke entirely from one or both sides (Fig. 7).


Figure 6. Failed Clamex P 15 specimen after bending test.

In the tensile test the anchorage distorted or broke. The zinc die lever was pulled out from the anchorage.


Figure 7. Failed Clamex P 10 specimen after tensile test

Invis fitting did not break, but the plywood was delaminated from the centre layers. Minifix showed lowest load caring test values because the plug could not expand. The Minifix fitting did not break. When turning the cam, the bolt moves towards the cam by pushing the plug wider. Plywood is denser than MDF or particle board. The plug is softer, so it does not expand enough. The plug has no grip; it can be pulled out easily.

5. CONCLUSIONS

Testing procedure was worked out for testing different fixtures. Mechanical tests of different fittings were made in tensile and bending conditions. The tension failure load was greater than the bending failure load of all joints. The standard deviation was higher in tensile tests. In both cases Invis Mx had the highest maximum load. Also in the tensile test Invis Mx had the lowest standard deviation. The Invis fitting did not break; the plywood specimen

delaminated from the centre layers. Comparing Clamex P 10 and Clamex P 15, the tests showed that Clamex P15 can bear higher loads in both tests. The standard deviation of Clamex P15 was lower in bending and tensile test. Both Clamex P fittings were broken or distorted from the fibre reinforce plastic anchorage.
According to the tests Invis Mx is the best fitting. The situation can be changed by introducing new additional objective – cost of the fitting.

6. ACKNOWLEDGEMENT

This study was supported by the Enterprise Estonia Innovation voucher grant project "Bended laminates and plywood connection technology".

7. REFERENCES

1. Lamello AG homepage. [WWW] www.lamello.com (12.03.2014)
2. Häfele homepage [WWW] http://www.hafele.com/us/products/Minifix_Connecting_Bolt_Cam_Hafele.asp (12.03.2014)
3. Nurdan Çetin Yerlikaya. Enhancement of load-carrying capacity of corner joints in case-type furniture. *Materials and Design*. 2002, **37**, 393-401
4. Dobris, J., Luts, A,. Meier, P. Testing tensile and bending strength on twisted and fluted birch dowels. *Northern European network for wood science and engineering*. 2012, **8**, 163-168.
5. Piirlaid, M., Matsi, M., Kers, J., Rohumaa, A., Meier, P. Effect of birch veneer processing factors on adhesive bond shear strength. *8th International DAAAM Baltic Conference*. 2012, **8**.
6. Siim, K., Kask, R., Lille, H., Täkker, E. Study of physical and mechanical properties of birch plywood depending on moisture content. 8th International DAAAM Baltic Conference. 2012, **8**.

8. ADDITIONAL DATA ABOUT THE AUTHORS

Kaarel Saar, BSc.
Master student
Chair of Woodworking
Department of Polymer Materials
Tallinn University of Technology
Teaduspargi 5, 12618, Tallinn, Estonia
Phone: 372 581822509
E-mail: kaarelsaar@hotmail.com

Jaan Kers, PhD.
Professor
Chair of Woodworking
Department of Polymer Materials
Tallinn University of Technology
Teaduspargi 5, 12618, Tallinn, Estonia
Phone:+372 6202 910
E-mail: jaan.kers@ttu.ee

Üllar Luga, MSc
Lecturer
Chair of Woodworking
Department of Polymer Materials
Tallinn University of Technology
Teaduspargi 5, 12618, Tallinn, Estonia
E-mail: ullar.luga@ttu.ee

Ahto Reiska
Technician
Chair of Woodworking
Department of Polymer Materials
Tallinn University of Technology
Teaduspargi 5, 12618, Tallinn, Estonia
E-mail: ahto.reiska@ttu.ee

9th International DAAAM Baltic Conference
"INDUSTRIAL ENGINEERING
24-26 April 2014, Tallinn, Estonia

DESIGN FOR MANUFACTURABILITY AND QUALITY IN FIBRE OPTIC PRODUCTS

Temerbulatova, A.; Powell, L. & Tähemaa, T.

Abstract: *To find the right design approach for a particular product can take engineers several years, due to the fact that nowadays, a lot of products require knowledge and experience in a wide range of different areas. That is why engineers and researchers explore algorithms which can help to find weak links in the product design earlier in the design stage. However, design can not be explored as a separate unit, as it is only a base part of huge process.*

To work out efficient design and invent beneficial method of preventing errors on early design stages can save time and money. An engineering methodology for fibre optic products design improvements will be of great interest for engineers.

The workflow or algorithm, which gives a possibility and help to drive design process and check design for reliability, can bring a lot of benefits. The method described in this article contains synergy of empirical knowledge and theory. Information obtained from technical literature (articles, research papers, theory books, etc.) were used in order to develop logic algorithm and improve approach. Evidence received from real design projects improves structure of new formula.

We believe that a performed logic diagram could be further used in a PDM and PLM environment in order to improve efficiency by eliminating waste. Algorithm could be used to help to improve design principles, scope and constrains during invention, and give a direction for design rules and criteria.

Key words: Fibre Optic Product, Design for Quality, Design for Manufacturability, Innovation.

1. INTRODUCTION

There are different approaches on how to reach a success in business, a lot of it depends on company goals, strategy and values. Some companies tend to work on price, others on quality, but they are all pursuing the same goal. Increasing profit by acquiring, converting and retaining their most valuables asset: customers. [1], [2]

It is not a secret that it is high competition between companies which produce fibre optic products. Thus, it is in great importance to know how to sustain leadership in this market. Product is one important thing, which can give a significant advantage. We can observe and find, that fibre optic field is developing significantly fast, and new innovative products appear on a market. Competitors struggle, in order to get better quality and low cost.

To get a low cost, companies conduct researches in order to find parameters, which influence on their product cost, and define approach which will help to reduce cost. It is obviously, that design methods are playing crucial role and impact on product cost variety. This article involves topics, as Design for Manufacturing and Assembly, Quality, Test and Service which can help minimize waste and improve quality, and maximize income for fibre optic product.

2. DESIGN REQUIREMENTS

The design process cannot be started before a large amount of work is initially done, in order to specify all requirements for the product. Requirements create favorable environment for the designing team and clarify their working approach. Under requirements could be implied different aspects: customer needs, standards, material/component, cooperation with particular companies or research institutions, etc.

Success in the marketplace can be achieved only when company can accomplish all requirements and even 'more'. Company itself can change the requirements on a marketplace, bringing innovation and proving that the new approach (innovation) is more reliable, than it was before.

Market research, generation of new ideas, understanding customer need, improving design, these processes can help to generate requirement specification.

Fibre optic product requirements must be clarified in engineering documentation, that is why a lot of companies generate Product Design Specification, where engineers analyse requirements, standards, market, production/manufacturing, performance, tests, service requirements, scopes, strategy, and etc. for the new design. For a fibre optic product, that kind of document plays crucial role. All engineers, who are involved in the product design and researches, must clearly understand all requirements, goals and scopes in order to eliminate unnecessary work and errors. [3]

3. DESIGN METHODS AND DESIGN STEPS

3.1 TEAM

There is a large amount of fibre optic products, for instance, fibre optic amplifier. This product is used for boosting signal in fibre optic cable lines.

The first and most important aspect in design work is to create the design team. Dependant on the product, the fibre optic product team will consist of some or all of the followings: electrical and optical designers/researchers, mechanical designers, quality engineers, material engineer/researcher, component engineer/researcher, industrial engineer, product development engineer, test or service engineers, software engineers purchasing engineer, calibration, prototyping, packaging engineers, etc. It is important to have plan/algorithm for each project, in order not to miss or mix stages.

This algorithm could also be a guide for project planning and management departments. It is beneficial to use for work subsidiary software, which will minimize time, maximize efficiency and atomize process of team work.

Good relationship, collaboration and information flow can simplify the working process and generate favourable environment. All involved departments must recheck other departments work, and if they find errors/faults, feedback must be sent to other departments. The team must clearly understand member's responsibilities, in order to direct information to whom it must be concerned.

3.2 PRODUCT DESIGN: CAD, CAM, SOSTWARE

Nowadays we cannot represent product and design work without the use of drawings, CAD models, simulation files, calculation programs and etc. If we want to reduce time of generating all these files in order to make a high quality product, we need to know from the beginning how we are going to work and to take into account the thousand of factors, to know how implement engineering knowledge and to know all features and possibilities while using engineering programs. It is important, when engineers simplify their work and generate algorithm which reduce working time. CAD/CAM simplification

(defeaturing), using last innovative approaches and recent technologies/ software can bring to the project new ideas and opportunities. In order to reduce time of engineering documentation management modern companies use software support processes as Product Data Management (PDM), Manufacturing Process Management, Component Management, Product cost PM (Project management), for instance Epicor, Windchill, SAP, and other software can make engineering work easier and faster.

3.3 DESIGN FOR MANUFACTURING AND ASSEMBLY

Design for manufacturing means design for the ease of manufacturing product. Design for assembly means design for the ease of assembly. Design for manufacturing and assembly is a combination of two methods.
Throughout the 1960's and 1970's, a lot of internal research was done independently by many companies that realized the need to streamline their designs and processes for the evolving paradigm in manufacturing. By the 1980's the concept of design for manufacturing and assembly was being embraced by many companies. [4]
It is not a secret that during last decades humanity achieved a greate success in product development and production techniques have changed. The main target for engineers to ease design, manufacturing and assembly techniques. Thus, methods and techniques are not staying the same and constantly improving.
Nowadays most of the companies use DFMA main steps. Fig. 1 showing main steps of product design for manufacturing.
However these steps cannot be fully engaged for fibre optic product, as fibre optic product is multi-disciplinary product which has more relations and stages. [5]
Design for manufacturing and assembly is a very important method for fibre optic product. For this kind of product, the design engineer will be constantly researching and implementing new materials, components, assembly methods, production techniques. That is why design is divided into sub paragraphs: mechanical, optical, electrical, health and safety. But all this areas work in synergy with strong partnership and collaboration. [5]

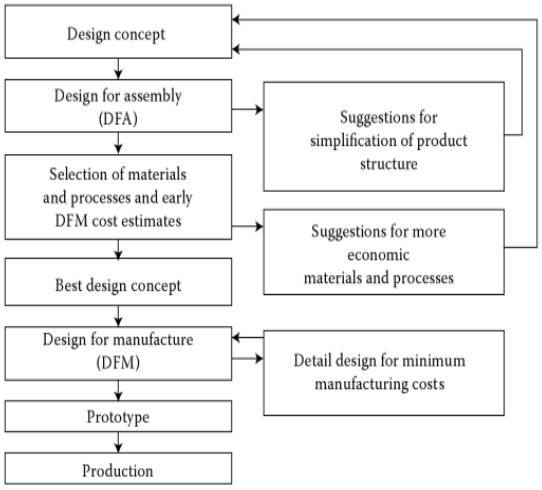

Fig. 1. Steps for DFMA
Mostly in fibre optic product design engineers use a modularity approach, which helps to reduce time and improve efficiency. [6]
If to take into more clause examination mechanical design, we can realize that this design must be divided into: parts, assemblies and components. For each stage the Design for Manufacture and Assembly (DFMA) approach must be applied. Material engineers and design engineers cooperate and research in order to select the right material. Manufacturing and purchase department must answer, could this material be machined and which manufacturing methods better to apply to this material. During the part and assembly design engineers make different calculations, analyses and researches: loads calculations/simulations, cost calculations, shape and material reductions, standardize parts, use symmetry principals, design for fixture, concurrent engineering of parts, machining processes (minimizing set ups, cutting tools, analysing tolerances, etc.).
For module design, engineers examine parts interaction within assembly, design

for assembly, and the relationship between mechanical design, electrical and optical designs, mechanical stress loading considerations.

3.4 DESIGN FOR QUALITY

Design for quality depends on manufacturing quality strategy. Nowadays, almost all companies implement term ”lean manufacturing”, but not all of them implement all concepts of this strategy and get valuable achievements.

Lean manufacturing is a concept of more value for less work. This concept, roots back to Frederick Winslow Taylor of Bethlehem Steel in the 1880s and 1890s. [7]

The Taylor approach starts with a clean slate- it designs the process to, as much as possible, only include steps that create value in the product. [8]

As fibre optic products require innovative approach, in order to hold customer’s interest, new product designs are required to be evaluated and checked. During the check must be examined, aspects, as material characteristics, interaction with other parts, sub assemblies, assemblies, electrical or optical components, methods of manufacture, methods of fixture, coating, handling criteria, stress loadings, performance indicators, etc. All these aspects needed to be researched and valued, with lean manufacturing point of view in focused on eliminating “Waste”. If waste is reduced, quality improves, production times are reduced and cost is minimized. Various methodologies are used as tools to achieve this including Value Stream Mapping, 6S, Kanban and error-proofing. [8]

In order to get maximum result, product must be manufactured and assembled in beneficial environment, that it is why it is in great importance when production adapts quality methods and systems. For instance, following 5 s/6 s method can minimize errors during assembly and manufacturing techniques. This system helps to find engineers faults and drawbacks in design. For example, if all tools are calibrated and under registration, during product tests/simulations faults which are discovered, the engineers can easily check was this an assembly error or was it a design fault, or something else, engineers can realise faster, the cause of the problem. Thus, using quality methods and systematic work, company can save time, quickly define problem and find the right solution. [8]

4. RESULT

The researched data was collected, examined and evaluated. Based on this data was generated design algorithm for fibre optic product, see Fig. 2.

This approach contains design goals of Design for Manufacturing and Assembly (DFMA), Design for Quality (DFQ), Design for Tolerance (DFT), Design for Modularity (DFM), Design for Test and Service.

It is impotent for this scheme to apply a quality approach: after each part of work inspections, checks and test must be carried on. All results must be documented and analysed. History should be saved for further projects.

It is essential to use quality management control documentation which will help to record and analyse data, for instance a Risk Review, Production Part Approval Process (PPAP) documentation, Failure Mode Effect Analysis (FMEA) or Taguchi evaluation, Engineering Change Note (ECO), Deviation Reports, etc.

Design, manufacturing and assembly processes are related to health and safety standards and requirements.

According to suggested method it is preferable to use 3 prototyping stages, after each stage product must be checked tested and sophisticated. Last third prototype must be closely approximated to production issue. It must be tested, passed qualification and performed to customer review.

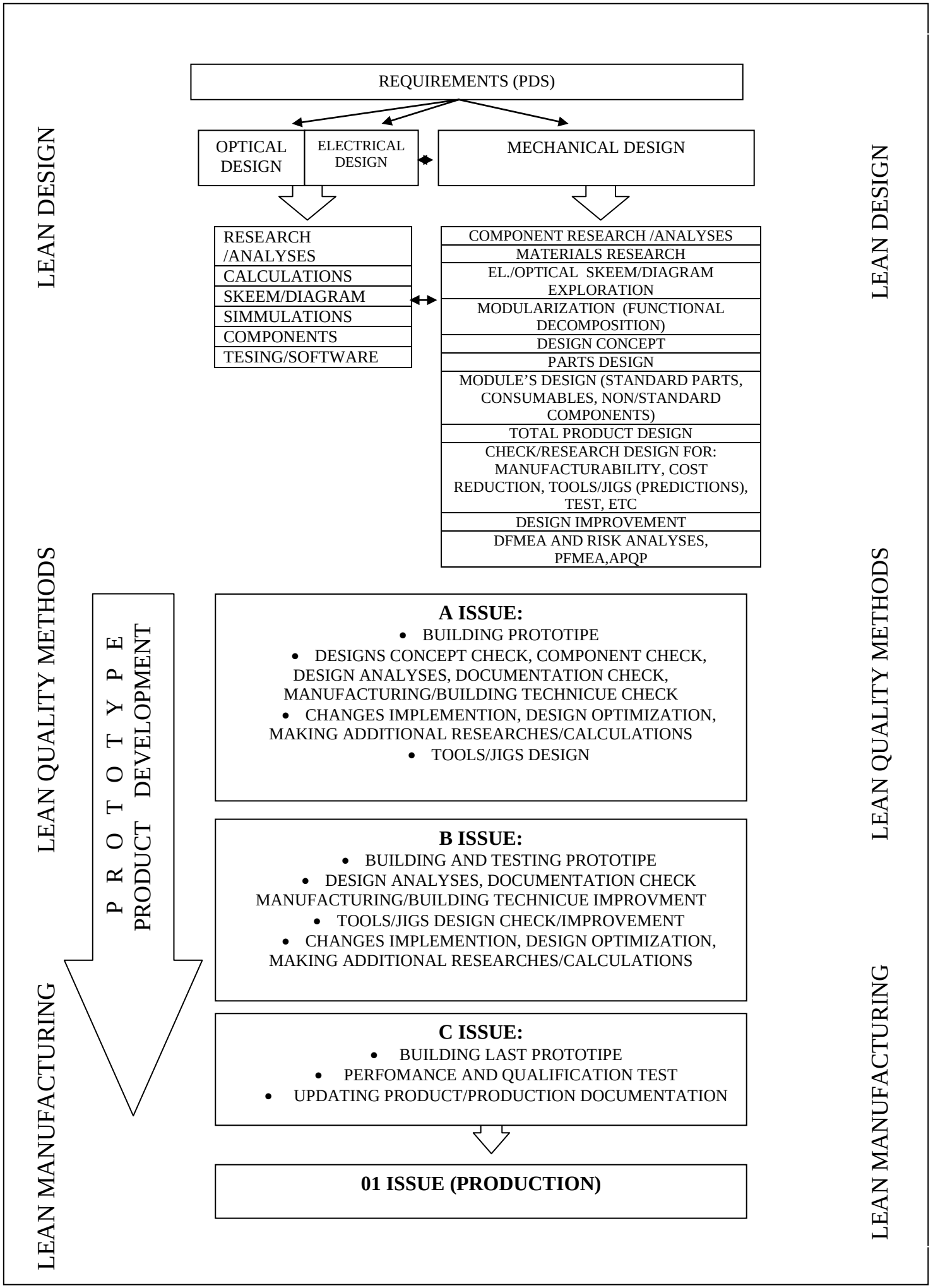
LEAN DESIGN
REQUIREMENTS (PDS)
OPTICAL DESIGN
ELECTRICAL DESIGN
MECHANICAL DESIGN
RESEARCH /ANALYSES
CALCULATIONS
SKEEM/DIAGRAM
SIMMULATIONS
COMPONENTS
TESING/SOFTWARE
COMPONENT RESEARCH /ANALYSES
MATERIALS RESEARCH
EL./OPTICAL SKEEM/DIAGRAM EXPLORATION
MODULARIZATION (FUNCTIONAL DECOMPOSITION)
DESIGN CONCEPT
PARTS DESIGN
MODULE'S DESIGN (STANDARD PARTS, CONSUMABLES, NON/STANDARD COMPONENTS)
TOTAL PRODUCT DESIGN
CHECK/RESEARCH DESIGN FOR: MANUFACTURABILITY, COST REDUCTION, TOOLS/JIGS (PREDICTIONS), TEST, ETC
DESIGN IMPROVEMENT
DFMEA AND RISK ANALYSES, PFMEA,APQP
LEAN DESIGN
LEAN QUALITY METHODS
LEAN MANUFACTURING
P R O T O T Y P E
PRODUCT DEVELOPMENT
A ISSUE:
BUILDING PROTOTIPE
DESIGNS CONCEPT CHECK, COMPONENT CHECK, DESIGN ANALYSES, DOCUMENTATION CHECK, MANUFACTURING/BUILDING TECHNICUE CHECK
CHANGES IMPLEMENTION, DESIGN OPTIMIZATION, MAKING ADDITIONAL RESEARCHES/CALCULATIONS
TOOLS/JIGS DESIGN
B ISSUE:
BUILDING AND TESTING PROTOTIPE
DESIGN ANALYSES, DOCUMENTATION CHECK MANUFACTURING/BUILDING TECHNICUE IMPROVMENT
TOOLS/JIGS DESIGN CHECK/IMPROVEMENT
CHANGES IMPLEMENTION, DESIGN OPTIMIZATION, MAKING ADDITIONAL RESEARCHES/CALCULATIONS
C ISSUE:
BUILDING LAST PROTOTIPE
PERFOMANCE AND QUALIFICATION TEST
UPDATING PRODUCT/PRODUCTION DOCUMENTATION
01 ISSUE (PRODUCTION)
LEAN DESIGN
LEAN QUALITY METHODS
LEAN MANUFACTURING

11. CONCLUSION

This paper describes the synergy of different design methods for improving design and quality of product. At the same time, it is discussed what could maximize production yields and quality of fibre optic product and minimize cost.
During the research it was discovered that design methods needed to be supported with propriety software and beneficial product data management system (PDM).
Very important to use this for research steps and the latest approaches for the work. Automation rate must be evaluated for each product. In order to reduce time it is suggestible to use software which will automatize process and minimize errors.
Proposed method could be used in further researches for fibre optic products.

11. REFERENCES

1. Wei D. The QoS of Web service for different service based on customer segments in CRM. University of Shanghai of Science and Technology, China, 2004.

2. Barac, N. Milovanovic, G. Andjelkovic, A. Lean Production and Six Sigma Quality in Lean Supply Chain Management. Economic and Organization Vol.7, 2010, pp. 319-334
3. Boothroyd, G. Dewhurst, P. Product Design for Manufacturing and Assembly, Third Edition. CRC Press Taylor and Francis Group 2011.
4. [WWW] http://dora.cwru.edu/gcc/dissertation/chap_4.pdf (25.02.14)
5. [WWW] http://www.ptc.com/product/windchill/engineering.htm (03.01.14)
6. Eggen, O. Modular product Department of Product Design. Norwegian University of Science and Technology
7. Marsh, R. Frederick W. Taylor: His Life, His Management Theory, His Legacy
8. [WWW] http://www.folkgroup.com/leanmanufacturing.pdf (28.01.14)
9. [WWW] http://www.boeing.com/commercial/aeromagazine/aero_08/human_textonly.html (25.02.14)
10. Quadros, W. R. Owen, S.J. Defeaturing CAD Models Using a Geometry-Based Size Field and Facet-Based Reduction Operators, Sandia National Laboratories, Albuquerque, New Mexico, U.S.A, 2009
11. Assimilalo, G. Goodfellow, L. Design For Manufacturing: Concept to Reality, 2012.
12. Kovac, M. Kovacova, L. Techniques and Tools for Quality Product Design, Technical University of Kosice, Slovak Republic, 2012.
13. David M. Anderson, Design for Manufacturability & Concurrent Engineering; How to Design for Low Cost, Design in High Quality, Design for Lean Manufacture, and Design Quickly for Fast Production, 2010.
14. Shetty, D. Kolko, A. Mechatronics System Design Second edition, 2011